EFCH2 2025

European Fuel Cells and Hydrogen

PIERO LUNGHI CONFERENCE

Book of Proceedings



September **17**th–**19**th 2025
Capri / Italy

ATENA FUTURE TECHNOLOGY

ENEA Italian National Agency for New Technologies, Energy and Sustainable Economic Development

Università degli Studi di Napoli Parthenope

CLEAN ENERGY INSTITUTE UNIVERSITY OF CALIFORNIA, IRVINE

EFCH2 2025

European Fuel Cells and Hydrogen

PIERO LUNGHI CONFERENCE

Proceedings

OF THE 11TH EUROPEAN FUEL CELL PIERO LUNGHI CONFERENCE

To Piero Lunghi. We miss you a lot. To you our gratitude for ever.

This book is dedicated to the memory of Piero Lunghi,
creator of the European Fuel Cell Technology and Applications Conference, dear friend and colleague, who prematurely passed away in a car accident on damned November 9, 2007.

Piero made significant contributions in the field of fuel cells in the course of his too short career. He was the leading figure in the formation of the fuel cell research group at the University of Perugia and several activities and research projects initiated by him are still ongoing.
This means that, thanks to Piero, many young people are working in this exciting research field and are coming to Naples to present their results. Therefore, Piero's memory is in the conference name but Piero's contribution is still in the contents of this book.
The memory of our friend Piero, his great personal generosity and energy, survives in our hearts, his contribution and his tenacity survive in the work of young people who carry on his vision throughout the world.

Give them your passion, your strength, and make all necessary effort to realize them. There is no greater satisfaction than seeing one's ideas become reality and become part of the future of our world.
Piero strongly desired this, and constantly followed this through with conviction, passion and dedication.

For a better future, we need young researchers of this kind.

European Fuel Cells and Hydrogen

EFCH2 2025

PIERO LUNGHI CONFERENCE

Capri, Gran Hotel Quisisana
17 > 19 September, 2025

edited by
Viviana Cigolotti, Alessia Piccolo, Gabriele Loreti
2025

ENEA
ITALIAN NATIONAL AGENCY FOR NEW TECHNOLOGIES, ENERGY AND SUSTAINABLE ECONOMIC DEVELOPMENT

Lungotevere Thaon di Revel, 76 / 00196 / Rome

ISBN 978-88-8286-527-6

ATENA FUTURE TECHNOLOGY

ENEA Italian National Agency for New Technologies, Energy and Sustainable Economic Development

Università degli Studi di Napoli Parthenope

CLEAN ENERGY INSTITUTE UNIVERSITY OF CALIFORNIA, IRVINE

EFCH2 2025

European Fuel Cells and Hydrogen

PIERO LUNGHI CONFERENCE

Organizers



Viviana CIGOLOTTI
Chairman of the Conference
ENEA



Jack BROUWER
Chairman of the Conference
University of California Irvine



Elio JANNELLI
University of Naples "Parthenope" / ATENA



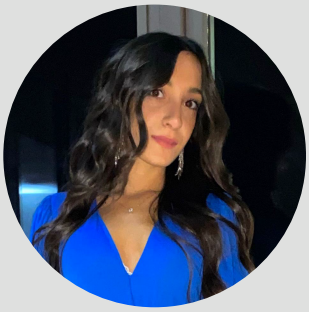
Adele PIANESE
ENEA/ATENA



Massimiliano DELLA PIETRA
ENEA



Gabriele LORETI
ENEA



Alessia PICCOLO
University of Naples "Parthenope"

European Fuel Cells and Hydrogen

PIERO LUNGHI CONFERENCE

Committee

Australia Rob Dickinson / Hydricity Systems and The University of Adelaide **Austria** Günter R. Simader / Austrian Energy Agency **Belgium** Alessandro Arrigoni / JRC **Bulgaria** Daria Vladikova / Institute of Electochemistry and Ebergy Systems - IEES **Chile** Ana María Ruz Frias / Chilean Economic Development Agency (CORFO) **Canada** Bruno Pollet / Université du Québec à Trois-Rivières **Finland** Marcus Rautanen / VTT Technical Research Center of Finland, Jari Kiviaho / VTT Technical Research Center of Finland **France** Deborah Jones / Université Montpellier **Germany** Can Remzi Samsun / Forschungszentrum Jülich (FZJ), Claudio Pistidda / Helmholtz-Zentrum Geesthacht, Nada Zamel / Fraunhofer Institute ISE **Greece** Panagiotis Tsiakaras / University of Thessaly **Italy** Marcello Baricco / Università di Torino, Domenico Borello / Sapienza Università di Roma, Luigi Crema / Fondazione Bruno Kessler, Mariagiovanna Minutillo / Università degli Studi di Salerno, Massimo Santarelli / Politecnico di Torino, Antonino Aricò / CNR ITAE, Bianca Maria Vaglieco / STEMS-CNR, Stefano Campanari / Politecnico di Milano, Giuseppe Spazzafumo / Università degli Studi di Cassino, Giulia Monteleone / ENEA, Giorgio Graditi / ENEA, Adolfo Iulianelli / CNR ITM, Stefano Ubertini / Università della Tuscia **Netherlands** P.V. Aravind / Groningen University **Norway** Marie-Laure Fontaine / SINTEF **Poland** Jakub Kupecki / Institute of Power Engineering - IPE **Portugal** Carmen Rangel / LNEG - National Laboratory of Energy and Geology **Spain** Emilio Nieto Gallego / Centro Nacional del Hidrógeno (CNH2) **Sweden** Martin Andersson / Lund University **Turkey** Cigdem Karadag / TUBITAK Marmara Research Center **United States of America** Wilson Chiu / University of Connecticut, Whitney G. Colella / Gaia Energy Research Institute LLC, Katrina Groth / University of Maryland, Kevin Huang / University of South Carolina, Luca Mastropasqua / University of Wisconsin - Madison, Yun Wang / University of California Irvine, Adam Weber / Lawrence Berkeley National Laboratory, Feng-Yuan Zhang / University of Tennesse, Knoxville, Xiao-Dong Zhou / University of Connecticut **United Kingdom** Shangfeng Du / University of Birmingham, Ioannis Ieropoulos / University of Soton

European Fuel Cells and Hydrogen

PIERO LUNGHI CONFERENCE

Capri, Gran Hotel Quisisana
17 > 19 September, 2025

TOPICS

HYDROGEN PRODUCTION

Electrolysis (PEM, Alkaline, AEM, SOEC, PCC, MCEC) / Thermochemical & Photochemical Processes / Biological Hydrogen Production / Low carbon hydrogen from Fossil Fuels (e.g., SMR, CCS) / Nuclear Hydrogen Production / Hydrogen from Biomass and Waste

HYDROGEN STORAGE AND DISTRIBUTION

Solid Hydrogen Storage (e.g. metal hydrides, MOFs) / Gaseous Hydrogen Storage / Liquid and Cryo-Compressed Hydrogen Storage / Hydrogen Infrastructure (Pipelines, Tankers, Trucks) / Hydrogen Blending in Natural Gas Grids / Natural Gas Grid Transformation / Hydrogen Derivatives and Carriers / Hydrogen Refilling Stations / Challenges in Hydrogen Delivery Systems

FUEL CELLS TECHNOLOGIES

Fuel Cells: components, stack, system (PEMFC, SOFC, AFC, MCFC) / Fuel Cells for Transportation (Cars, Buses, Trucks) / Fuel Cells for Heavy Duty & Freight Transport (Trains, Aircraft, Marine) / Fuel Cells for Stationary Power Generation / Portable and Backup Power Applications / Materials Handling Application

HYDROGEN END-USE APPLICATIONS

Hydrogen for Industrial Processes (Steel, Cement, Chemicals) / Hydrogen as Energy Storage Medium (e.g. Hybrid Systems with Renewable Energy) / Sector Coupling and Power-to-X / Next-Generation Hydrogen Fuels (Power-to-fuel) / Hydrogen as a Decarbonization Pathway

HYDROGEN ECONOMY AND SUSTAINABILITY

Life Cycle Assessment (LCA) and Social LCA / Techno-economic assessment (TEA) / Green Hydrogen and Carbon-Free Technologies / Water Use and Sustainability of Hydrogen Production / Hydrogen's Role in Achieving Climate Targets (Net-Zero Goals) / Hydrogen Hubs and International Trade / Hydrogen Valleys

HYDROGEN POLICY, MARKET, AND BUSINESS MODELS

National and Regional Hydrogen Strategies / Global Hydrogen Supply Chains / Economic Analysis and Market Forecasts / Public and Private Sector Investments / Hydrogen Pricing and Incentives / Hydrogen Safety Codes and Standards

HYDROGEN INNOVATION AND FUTURE TRENDS

Emerging Hydrogen Technologies / Breakthroughs in Catalysts, Electrodes, Membranes / Novel Systems Integration and Control / Digitalization and AI in Hydrogen Systems / Microbial and Bioelectrochemical Technologies

European Fuel Cells and Hydrogen

EFCH2 2025

PIERO LUNGHI CONFERENCE

SPONSORED BY

Duferco Engineering

NHP NEAHELIOPOLIS

YOKOGAWA

zabala INNOVATION

ALRIGH2T

CANTIERI del MEDITERRANEO

SUPPORTED BY

Clean Hydrogen Partnership

Ministero dell'Ambiente e della Sicurezza Energetica

H2IT ASSOCIAZIONE ITALIANA IDROGENO

ORGANIZED BY

ATENA FUTURE TECHNOLOGY

ENEA Italian National Agency for New Technologies, Energy and Sustainable Economic Development

Università degli Studi di Napoli Parthenope

CLEAN ENERGY INSTITUTE UNIVERSITY OF CALIFORNIA, IRVINE

EFCH2 2025

European Fuel Cells and Hydrogen

PIERO LUNGHI CONFERENCE

Contents

ATENA FUTURE TECHNOLOGY

ENEA Italian National Agency for New Technologies, Energy and Sustainable Economic Development

Università degli Studi di Napoli Parthenope

CLEAN ENERGY INSTITUTE UNIVERSITY OF CALIFORNIA, IRVINE



TABLE OF CONTENT

TOPIC 1: HYDROGEN PRODUCTION 8

Dynamic modeling of two-dimensional anion exchange membrane water electrolysis 9

Design of a fermentation system for the production of biological hydrogen by Thermotoga Neapolitana bacteria 12

Experimental investigation and 3D modelling of a planar SOEC 15

Optimising Green Hydrogen Production: How Renewable Energy Sources Shape Cost and Plant Design 18

Alkalinization of soecs with basic oxides nanoparticles for enhanced coelectrolysis of co_2-h_2o mixture 21

Long-term performance assessment of Single-Cell AEMWE configuration under Accelerated Stress Testing 25

Effect of operating conditions on proton exchange membrane electrolysis cell using computational fluid dynamics analysis 29

Numerical Analysis of Solid Oxide Electrolysis Cell (SOEC) System Combined with LOHC Hydrogenation System 32

Dual-Doping of Transition Metals into the Double-Perovskite $La_{0.3}Sr_{1.7}Fe_{1.5}Mo_{0.5}O_{6-\delta}$ for Potential Electrode Material in SOECs: Increased Stability in Hydrogen 35

On the effects of platinization of commercial titanium Porous Transport Layers in PEM water electrolysis cells 38

Hydrogen Production from Lignocellulosic Agro-Residues via Thermo-Catalytic Pathway 41

Development of a decision-oriented tool for operational management of a PEMWE 44

Seawater impact on Solid Oxide Cells materials: experimental methodology for laboratory characterization 48

Scalable development of 3D LDH gas diffusion electrodes for AEM water electrolysers 51

Impact of Porous Transport Layer Microstructure on Oxygen Transport in a PEM Electrolyzer 54

Residual biomass pyrolysis in fluidized-bed reactors: a data-driven approach for control and design 57

Systematic Investigation of Hydrogen Production Efficiency as a Function of Electrode Properties and Electrolyte Composition 60

On the development of doped cobaltite type electrocatalysts for OER in AMEWE 63

Biomass to methanol by Breakthrough SOEC-based Process 66

Anion Exchange Membrane Water Electrolysis with Poly(biphenyl piperidone co trifluoroacetophenone) random copolymers as Membranes 68

Advancing AEM Electrolysis: A Novel Single-Cell for Evaluating High-Performance Membranes and Electrodes 71

Matrices for Reversible Molten Carbonate Cells: Insights from Button Cell Testing 74

Electrochemical Impedance-Based Modeling of an Electrolyte- Supported SOEC Short Stack 78

Microkinetic Modeling of Surface Reactions and Charge Transfer Dynamics in Solid Oxide Electrolysis Cells under Electrothermal Balanced Operation 81

Electrochemical deposition of nife-layered double hydroxide layers for the anode catalyst in anion exchange membrane electrolyser 84

Gasifier and SOEC integration for enhanced fuel production 87

Integrated membrane & biogas electrified catalytic reformer for decarbonised h_2 production 90

One future of hydrogen production: Solar Heat Supported Solid Oxide Electrolysis Cell 93

High performance of a thin short-side-chain Aquivion® membrane for sustainable water electrolysis application 97
Recombination catalyst effect on AEM properties for AEMWE application ... 100
Redox-Mediated Electrolysis of Tar from Biomass Gasification for Hydrogen Production ... 103
Technical analysis of the current water electrolysis cell technologies by comparing plant design and requirements ... 106
Analysis of number of stacks and temperature on performance of large-scale pem electrolyser ... 109
Non-Precious Catalysts and Novel Membranes for High- Performance AEM Water Electrolysis ... 112
Optimization of hydrogen downstream treatment system for solid oxide electrolysis ... 115
High-Efficiency SOEC System Coupled with Renewable Sources: Modeling and Energy Analysis at Operating modes variation ... 118
Performance evaluation of anion exchange membrane water electrolysers using commercial membranes and non-precious metal catalysts. ... 121
TOPIC 2: HYDROGEN STORAGE AND DISTRIBUTION ... 124
No-vent LH_2 Transfer Processes using Top-Fill ... 125
Optimization of Hydrogen Refueling Infrastructure for Heavy-Duty Vehicles ... 128
Investigation of Pre-Cooling Systems for Hydrogen Refueling Stations Using Dynamic System Simulation: Design Requirements and Concept Comparison ... 131
Metal hydrides based hydrogen storage for fuel cell hybrid vehicles: Numerical evaluation in real-world operating conditions ... 134
Development of a numerical model for liquid hydrogen storage tanks for maritime sector ... 137
HASTA - Hydrogen Aircraft Sloshing Tank Advancement ... 140
Design of a Zero-Emission Metal Hydride-based Refueling Station for H2-powered L6e Light-Duty Hybrid Vehicles ... 143
Power vs. discharge efficiency of thermally controlled Metal Hydride hydrogen storage tanks: a revised analysis ... 146
Design and analysis of a thermal management system for a novel metal hydride tank for H2 storage in fuel cell vehicles ... 149
Evaluating Off-Grid and On-Grid Hydrogen Supply Scenarios for Refueling Infrastructure Deployment in Southern Italy ... 152
Multiphysics Numerical Modelling of Hydrogen-Refuelling-Station Components under Consecutive Dispensing Scenario ... 155
Technical and Economic Optimization Study of the Sizing and Operation of Key Components in Hydrogen Refueling Stations (HRS) ... 158
Development of Operational Optimization Models for Key Components in Hydrogen Refueling Stations (HRS) . 161
Cryogenic Storage Systems: state-of-the-art of Challenges and Preliminary Lab-Scale Numerical Model ... 164
Last-mile delivery of H2 to Airports: A Schiphol case study ... 167
Assessment of Hydrogen Integration into the Italian Gas Transmission Network: Blending vs. Pure Hydrogen Transport ... 170
Study of a PCM-hydride Reactor ... 173
Integrated Dynamic and Economic Modeling of Renewable Hydrogen Refueling Systems ... 176

Optimization of Hydrogen Refueling Infrastructure for Heavy-Duty Vehicles 179
Sizing of small on-site hydrogen refueling stations: a modeling approach 183
Fueling the Future: A University's Role in Advancing Hydrogen Mobility and International Collaboration 186
Techno-Economic Analysis of Hydrogen Storage Technologies for Different Real End-Use Demand Profiles and Sites 188
Hydrogen Storage for Renewable Energy Integration: A Techno-Economic Comparison with Ammonia as Hydrogen Carrier 191
Optimal Gas Flow Model for Evaluating the Fluid Dynamic Feasibility of Transporting Hydrogen-Natural Gas Blends in Gas Networks 194
Experimental Study on the Effects of Hydrogen in Gas Distribution Customer Service Lines: Stratification in Risers and Meter Aging 198
Effect of hydrogen blending on gas meters accuracy 201
TiFe-based alloys for solid-state hydrogen storage in industrial applications: the innovative REMEDHYS project towards a circular economy 204
TOPIC 3 : FUEL CELLS TECHNOLOGIES 207
Advanced Core-Shell Structured Electrocatalysts for Oxygen Reduction Reaction: Influence of Core Size, Nitrogen Doping, and Carbon Shell Engineering 208
Quantification and visualization of ionomer distribution in catalyst layers of PEMFCs 212
Thermal integration of pemfc and metal hydrides systems for maritime applications 215
Assessment of the performance of MEAs assembled with different polymers and catalysts for PEM Fuel Cells .. 218
Integrated Modeling of a Fuel Cell Stack and Thermal Management System in a Fuel Cell Electric Bus Using Metaheuristic Optimization 221
Fast and reliable parameterization of PEMFC models – sequential optimization for efficient parameter estimation 224
Gas Diffusion Electrode half cell: A Versatile Tool for Half-Cell PEMFC Characterization 227
Analysis of aging effects based on electrochemical characterisations within a durability test 229
Economic viability of sustainable railway propulsion systems: a decision- support framework 232
Impact of bio-syngas contaminants on SOFC performance: experimental characterization and degradation model 235
Experimental analysis and control of a SOFC-Battery hybrid for use as powertrain on seagoing vessels 238
Tailoring exsolved NP in Fe-doped Lanthanum Strontium Chromite: implications on H_2/CH_4 utilization in SOFCs241
Impact of Ammonia Decomposition on SOFC Performance: A DRT Study 244
Model-based Humidity Control of a Polymer Electrolyte Membrane Fuel Cell-based Electric Vehicle 247
Spatially and Temporally Resolved Stainless Steel Bipolar Plate Degradation Model for PEMFCs 250
Improved Local Description of the Capillary Pressure - Saturation Relation to Enhance Reliability of CFD Results 253
A simplified control strategy for optimal low-pressure operation of pemfc systems for aviation application 256
Degradation-Aware Design and Control of Fuel Cells for Hybrid Aeronautical Power Systems 259
Experimental validation of a PEMFC lumped dynamic model for on- board, diagnostic, prognostic and control

applications ... 262
Mathematical and numerical modelling of High-Temperature Solid Oxide Fuel Cells ... 265
3D Modelling of electrolyzer and fuel cells with NEOPARD-X framework: dimensionality effects ... 268
Investigation of an Auxiliary High-Temperature Refrigeration System to Increase Cooling Capacity in Fuel Cell Vehicles ... 271
CFD-Based Investigation of High Current Density Polarization Losses in PEM Fuel Cells ... 274
Performance evaluation of a copper interdigitated over- humidification sensor ... 277
Development of Advanced Conductive Bipolar Plates for Proton Exchange Membrane Fuel Cells: Synergistic Effects of Graphite Particle Size, Hybrid Systems, and Carbon-Based Additives. ... 279
Effect of water vapor content in MSR reformate on in-plane performance distribution of an HT-PEMFC ... 282
Impedance Modeling Framework for Proton Exchange Membrane Fuel Cells ... 285
Evaluating the combined effect of humidification, backpressure, and cathode stoichiometry on HT-PEMFC performance using DRT analysis ... 288
Application of the differential impedance analysis for deeper insight into solid oxide cells degradation ... 291
PEM Fuel Cell Stack with Dead-Ended Anode for Electric Aviation: Efficient Operating with Low Degradation ... 294
Development of composite sPEEK membranes containing zeolite imidazole frameworks as ionic cross-linkers for energy applications. ... 297
Towards Zero-Emission Shipping: SOFC-ICE Hybrid Propulsion for Maritime Decarbonization ... 300
Comparison of different fuel mixture for direct ammonia fuel cell ... 303
Enhancing Carbon Capture in the Steel Sector through MCFC and PEM Electrolyzer Integration ... 306
Innovative approaches to MCFC component development for industrial-scale implementation ... 309
Performance analysis of solid oxide fuel cell fed with simulated gas produced by biomass gasification process . 312
Sub-Optimal Control Strategy for Hydrogen Fuel Cell Heavy-Duty Trucks: A Fuzzy Logic Approach ... 315
Development and Optimization of a Solid Oxide Fuel Cell System for Combined Heat and Power: The SO-FREE Project ... 318
Quantifying the impact of nickel “shocking” in microbial fuel cells fed with synthetic fermentation broths ... 321
Study on experimental parameters of PEMFC stack under CO contamination with Machine Learning Technique ... 324
Electrospun polybenzimidazole: optimization of a novel proton exchange membrane for high temperature fuel cells ... 327
Numerical Performance Comparison of Battery and PEM Fuel Cell Models for Lightweight Aircraft Applications 330
Performance evaluation and durability analysis of pem fuel cells for sustainable energy applications ... 333
Techno-economic analysis of 10 MW SOFC powertrain system fed by hydrogen carriers in shipping ... 336
Microbial Fuel Cells Fed with Microbial Electrolysis Cell Effluent for Sustainable Energy Applications ... 339
Application of a Multiphysics Equivalent Stiffness Model of a PEMFC integrating the nonlinear mechanical behaviour of MEA components ... 342
An oriented green approach to the Matrix Fabrication for Molten Carbonate Cells (MCCs) ... 345
Membrane-Electrode Interactions in PEM Fuel Cells: The Role of Ionomers in Hydrocarbon-Based Membranes 349
Numerical analysis of an optimised serpentine HTPEM Fuel Cell with BP-integrated cooling channels ... 352

Dynamic modelling of sofc systems for hybrid maritime solutions 355
A multi-criteria approach to evaluate the use of solid oxide fuel cells (sofc) onboard vessels 358
Exploring the possibility of using hydrogen in po river inland waterways 361
Manufacturing Approaches for Proton-Conducting SOCs 364
Electrochemical Modelling of Dual-ion Effect in Molten Carbonate Fuel Cells 367
A Virtual H_2 Sensor for improved Fuel Cell Control 370
Techno-Economic Optimization of a SOFC-Based Biogas Power Plant Integrated with Green Hydrogen in a Local Energy System 375
Multi-modal porous microstructure for high temperature fuel cell application 378
A mechanistic interrogation of pgm-free oer catalyst for pem water electrolysis 381
Engineering Laboratory-Scale Multi-Stack Fuel Cell Systems 384
Experimental Investigation of High-Frequency,high-Amplitude Current Ripples on PEMFC Stack Degradation 387
Anomalous Diffusion of Water and Oxygen in Nafion Membrane 390
Enhanced Electrochemical Performance of PBA@CNF-rGO Cathodes for Sodium-Ion Batteries 393
Anode Purge Strategy Simulation for a Multi-Stack Fuel Cell System 396
Untreated vs. Treated Carbon Felt Anodes: Impacts on Power Generation in Microbial Fuel Cells 399
Innovative supported Pd@CeO_2-ZrO_2 catalysts for fuel cells applications 402
PVD and PECVD carbon based and nitride coatings for metallic bipolar plates 405
Development and Characterization of Electrospun PBI Membranes for Enhanced Acid Uptake in HTPEMFC Applications 408
The importance of modifying anode materials for use in sofc fuel cells in the methane reforming process 411
Dense electrolytes fabrication and innovative deposition technique for integration in Proton-conducting Fuel Cells 414
Bacterial cellulose-based ion exchange membranes for fuel cell applications 417
Machine learning based lifetime prediction of polymer electrolyte fuel cells for distributive power generation 421
The green transition of the Maritime Sector through Fuel Cell Systems: analysis of an Italian case study 424
Hydrogen Fuel Cell-Powered GPU for Zero-Emission Ground Power Supply in Aviation 428
Novel Dry Powder Processing Routes for Porous Anode Supports in Solid Oxide Electrochemical Cells 431
TOPIC 4 : HYDROGEN END-USE APPLICATIONS 434
Numerical Analysis of Natural Gas-Hydrogen blending in Pipelines 435
The impact of an economic green hydrogen supply on defossilized steelmaking and direct-reduced iron supply chains 438
A Region-Specific European Analysis of SOEC-Based Green Ammonia Cost Competitiveness 441
Preparation of European airports to operate with LH2 444
Comparative analysis of power-to-hydrogen energy storage system for residential applications 447
Green Hydrogen in Decarbonizing Hard-to-Abate Sectors: A Pathway for a Sustainable Steel Production 450
Hydrogen Valley Optimization: Integrating Sectoral Synergies for Decarbonization 453

Solar and wind energy integration with energy load and hydrogen production: the case of a large-scale airport in Italy 456
Impact of Subsidies on Hydrogen Refuelling Station Infrastructure Development 459
Hydrogen Integration in Commercial Aviation: Technical and Operational Analysis at Malpensa Airport 462
Experimental Evaluation of P2P for Long Duration Energy Storage 465
Effect of hydrogen blending on odorant measurement 468
Potential of retrofitting mgts to h2 and nh3: from combustion fundamentals to a techno economic prospective 472
$LaNiO_3$ perovskites for ammonia decomposition: Kinetic Analysis at low temperatures 475
TOPIC 5: HYDROGEN ECONOMY AND SUSTAINABILITY 478
Life cycle assessement and life cycle cost addressing in developing solid oxide fuel cells 479
Sustainability assessment of PEMFC 482
Hydrogen Ecosystem Development: A Case Study in California 485
A comprehensive assessment of hydrogen leakages along the entire supply chain: present and future scenarios 488
Robust design of green hydrogen production systems – Mitigating business risks from PPA power sourcing uncertainties 491
Green Hydrogen and Wastewater Synergies: Cost-Effective Integra- tion of Electrolysis Oxygen in Wastewater Treatment Plants 494
Pre-normative research on hydrogen release assessment 497
Techno-economic feasibility study of an innovative proton conducting ceramic electrolysis system for hydrogen generation 500
Electrosynthesis of Low-Carbon Olefins: A New Paradigm for Hard to Abate Industries 503
Techno-economic assessment of large-scale hydrogen production via solid oxide electrolysis systems 507
Blue hydrogen can be a low-carbon hydrogen 510
Driving Energy Transition in Ports: Hydrogen-Powered Heavy-Duty Vehicles in Port Logistics 513
Hydrogen's impact on the environment in a net-zero plastics industry 517
A Flexible Methodology for Renewable Energy Integration: A PyPSA-Based Optimization Approach Applied to Northern Canada 519
Scenarios for Operational and Techno-Economic Analysis of the Hydrogen Value Chain for Aviation 523
HyMantovalley – A Case Study from Italy 526
Techno-economic assessment of Methane, Methanol, Ethylene and Acetic Acid production from electrolytic hydrogen and recovered CO2 for one chemical industrial park in the Hesse region of Germany 529
H2Start Teaming Project "Green Innovations in Hydrogen for Sustainable Energy Transition" 532
Hybrid Renewable Energy Systems with Hydrogen Storage: A Sustainability-Driven Optimization Approach 535
Environmental and Circularity Insights for the Design of Sustainable TiFe-based Alloys for Hydrogen Storage 539
Techno-economic-environmental analysis of hydrogen production technologies using domestic wastewater 542
University–Business Collaboration in Transnational Hydrogen Valley 545
Cradle-To-Use Life Cycle Assessment of an Alkaline Electrolyzer 549

Spatial assessment of the impact of hydrogen production on European freshwater resources 552
Comparative life cycle analysis of green hydrogen production 555
TOPIC 6: HYDROGEN POLICY, MARKET AND BUSINESS MODELS 557
Techno-economic evaluation/analysis of different applications for the direct utilization of imported ammonia 558
HyAcademy.eu: Building a Pan-European Hydrogen Skills Ecosystem for Climate Neutrality 561
Business models and policy support for LH_2 supply infrastructure for H_2-powered aviation 564
The Impact of GH2 Infrastructure and Market Development on Optimal LH2 Supply Strategies for Aviation 567
An agent-based analysis of hydrogen penetration in the South Africa energy system 570
Exploring the role of hydrogen infrastructure in the energy transition 573
Global Deployment and Commercial Roll-Out of Electrolyzers and Co-Electrolyzers: Technology Pathways, Market Projections, and Industrial Integration Strategies 576
TOPIC 7: HYDROGEN INNOVATION AND FUTURE TRENDS 579
Design of Experiment (DOE) for Optimising Automated 3D Printing of Proton Exchange Membrane Fuel Cell (PEMFC) Electrodes 580
On the relevance of the para- to orthohydrogen conversion for the exergy utilisation of liquid hydrogen 583
Membrane engineering applications in hydrogen and CO_2 valorization under a greener energy scenario 586
A Simple and Field-Deployable Microbial Fuel Cell Architecture for Stable and Sustainable Energy Generation: A Comparative Study of Sediment- and Plant-based Systems 589
Microbial Fuel Cells working as transistors: addition of 3rd and 4th 592
N-integration in Ni-Fe-Cr-Ru-Mo High-Entropy Electrocatalytic Materials 595
Green Hydrogen Innovation: A Patent-Based Analysis of Critical and Strategic Resource Use 598
Techno-Economic and Environmental Assessment of Hydrogen Integration in Renewable Energy Communities in Italy 602
0D Modeling of Electrochemical Hydrogen Compressor 605
An optimization algorithm for the integration of hydrogen into multi-carrier energy systems 608

EFCH2 2025

European Fuel Cells and Hydrogen

PIERO LUNGHI CONFERENCE

Proceedings

OF THE 11TH EUROPEAN FUEL CELL PIERO LUNGHI CONFERENCE

ATENA FUTURE TECHNOLOGY

ENEA Italian National Agency for New Technologies, Energy and Sustainable Economic Development

Università degli Studi di Napoli Parthenope

CLEAN ENERGY INSTITUTE UNIVERSITY OF CALIFORNIA, IRVINE



TOPIC 1: HYDROGEN PRODUCTION

European Fuel Cells and Hydrogen
PIERO LUNGHI CONFERENCE
EFCH2 2025
September 17th–19th 2025
Capri / Italy

Dynamic modeling of two-dimensional anion exchange membrane water electrolysis

Kyoungjin Lee[a], Jinyoung Ham [a], Haeseong Shin[a], Juyeon Park[b], Sanggyu Kang*[a]

* corresponding author: sgkang@snu.ac.kr
[a] Department of Naval Architecture and Ocean Engineering, Seoul National University
[b] HD Hyundai Heavy Industries

Keywords: Anion Exchange Membrane Water Electrolysis (AEMWE), Dynamic modeling, Hydrogen production, Two-Dimensional (2D) Simulation

Abstract

Introduction: To prevent global warming, restrictions on greenhouse gas emissions have been implemented, and interest in new energy sources is growing. Among various energy sources, green hydrogen produced using renewable energy is gaining attention as a promising new energy source due to no carbon emissions. Also, green hydrogen can serve as energy storage to compensate for fluctuations in renewable energy such as wind or solar power. As a result, there is increasing research on water electrolysis that produces hydrogen. The AEMWE combines the strengths of other commercial water electrolysis types, alkaline water electrolysis and polymer electrolyte membrane water electrolysis. It is low cost due to use of non-noble metal catalysts, and it can produce high purity hydrogen [1].

Objectives: The technical readiness level of the AEMWE is low compared to the other commercial water electrolysis. Since it is in the demonstration stage, there is no study of detailed stack model and dynamic operation analysis. When the power is supplied from fluctuating renewable energy sources, it affects the operation and efficiency of the AEMWE stack. Therefore, it is necessary to analyze the response characteristics of the stack under the dynamic operating conditions. Additionally, by modeling the detailed stack and examining the changes in temperature, pressure, gas saturation, and crossover in each control volume, strategies for enhancing efficiency and extending lifespan of the AEMWE stack can be developed [2].

Material and methods: A two-dimensional dynamic model of the AEMWE stack was developed using AMESim®. The stack is modeled based on a numerical method that considers energy and mass transport. To account for the bubble effect resulting from the generation of oxygen and hydrogen gases, the model considers the impact of gas bubbles on mass transport and characteristics within the AEMWE cell [3]. The stack is divided into layers along the flow perpendicular direction to examine temperature and pressure variations from the inlet to the

outlet. These variations in temperature and pressure are used to adjust the concentration terms in the electrochemical equations. Additionally, the stack is divided along the flow parallel direction to determine the mass balance and implement dry cathode operation that water circulates only through the anode. To examine the dynamic response characteristics of the stack, the current density ups and downs at time intervals. Through this simulation, it is possible to analyze how each voltage such as Nernst voltage, activation overvoltage and ohmic overvoltage is affected.

Results: (a) 2D simulation results in steady state

The temperature inside the cell increases from inlet to outlet due to the accumulation of reaction heat. The current density increases in the flow direction of the water because internal resistance decreases. The pressure decreases according to the flow direction, and there is more pressure drop at the anode because the amount of flowing water at the anode is greater than the cathode.

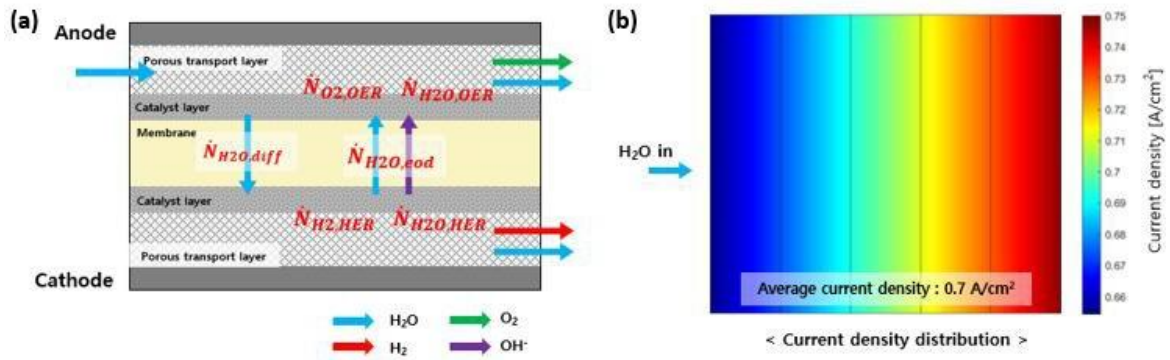


Figure 1: (a) Schematic diagram of the AEMWE stack (b) Current density distribution

(b) 2D simulation results in dynamic state

When the load changes, there is a delay to converge steady temperature. The voltage response graph shows that both overshoot and downshoot. As the load changes, temperature, pressure and gas production changes, as well. And, it affects Nernst voltage, activation overvoltage and ohmic overvoltage. When the AEMWE operates at high current density, diffusion and electro osmotic drag mass flow increase because they are dependent on the temperature and current density, respectively.

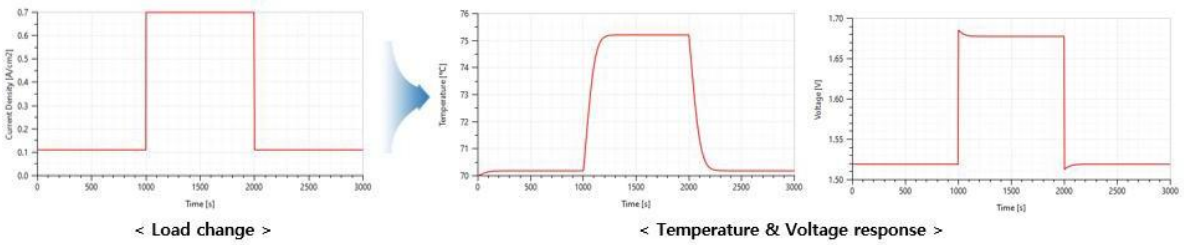


Figure 2: Dynamic response based on the load change

Conclusions: In this study, the two-dimensional AEMWE is developed to analyze physical phenomena and dynamic response characteristics based on the load change. The stack is modeled using energy and mass transport, including the effects of gas generation. With the detailed stack model, variations in temperature, pressure and concentration are analyzed. Additionally, by simulating the stack under the dynamic operating conditions, this study investigates the effects on the performance. Through this simulation, optimal operation conditions and control strategies can be identified to enhance the efficiency and the lifespan of the AEMWE stack.

Acknowledgment

This work was supported by the Korea Institute of Energy Technology Evaluation and Planning(KETEP) and the Ministry of Trade, Industry & Energy(MOTIE) of the Republic of Korea (No. RS-2024-00424923).

References

[1] El-Shafie, M. (2023). Hydrogen production by water electrolysis technologies: A review. Results in Engineering, 20, 101426.

[2] Jang, D., Cho, H. S., & Kang, S. (2021). Numerical modeling and analysis of the effect of pressure on the performance of an alkaline water electrolysis system. Applied Energy, 287, 116554.

[3] Chen, Q., Wang, Y., Yang, F., & Xu, H. (2020). Two-dimensional multi-physics modeling of porous transport layer in polymer electrolyte membrane electrolyzer for water splitting. International Journal of Hydrogen Energy, 45(58), 32984-32994.

European Fuel Cells and Hydrogen
PIERO LUNGHI CONFERENCE
September 17th–19th 2025
Capri / Italy

Design of a fermentation system for the production of biological hydrogen by Thermotoga Neapolitana bacteria

Giulia Crescente*[ab], Giuseppe Baiardo [b], Giuliana d'Ippolito[c], Gaetano Squadrito[b]

* corresponding author: giulia.crescente@studenti.unime.it / giulia.crescente@itae.cnr.it

[a] Università di Messina (UNIME) – Dipartimento di Ingegneria, C.da Di Dio (Vill.S.Agata), Messina – 98158, Italia

[b] Consiglio Nazionale delle Ricerche – Istituto di tecnologie Avanzate per l'Energia "Nicola Giordano (CNR-ITAE), via S. Lucia sopra Contesse 5, 98126 Messina - Italia

Keywords: Bio-Hydrogen, Fermentation, Thermoga Neapolitana, Wastes valorisation

Introduction

Clean hydrogen is proposed as a widely used commodity both as a fuel and as a raw material. In programs for de-carbonisation it appears to be one of the keys to sustainable development [1]. In addition to the traditional technologies that produce hydrogen, the biological and bio-electrochemical production of hydrogen from biomasses has begun to be evaluated in a circular economy perspective, trying to valorize wastes. In these processes microorganisms convert biomass into hydrogen by catalytic activity of enzymes as hydrogenase and nitrogenase, and different strains of bacteria applied to a wide range of substrates and by different methods, such as dark fermentation, has been proposed for this purpose [2].

Within these strain, the hyper-thermophilic (living over 60°C) Thermotogales showed a good activity in hydrogen production. In particular, Thermotoga neapolitana (DSM 4359, ATCC 49049) was largely studied at the Institute of Biomolecular Chemistry of the National Research Council (CNR-ICB). This bacterium is relatively easy to use in a single culture as the extreme temperature conditions reduce the risk of contamination by other strains. It has been reported that T. neapolitana reaches hydrogen yield values close to the theoretical 4 H_2 molecule per glucose molecule. These facts make T. neapolitana particularly promising for biotechnology and energy recovery, as well as for the sequestration of CO_2, while producing chemical compounds of industrial interest such as acetic acid and lactic acid, as well as biomass [3]. Consequently Thermotoga Neapolitana appears really interesting for scale up from laboratory to significant scale hydrogen production facility.

The objective of this work is the development of a prototype system for hydrogen production from waste water based on thermotoga strains. Here we report the first experimental results on a lab scale prototype running in continuous flow configuration.

Materials and methods

Starting from literature experimental data about thermotoga neapolitana hydrogen production in different operative conditions, and previous research on the capacity of thermotogales to grow attached to solid supports [3-4], was designed a fermenter and the model plant using the design approach sketched in Figure 1.

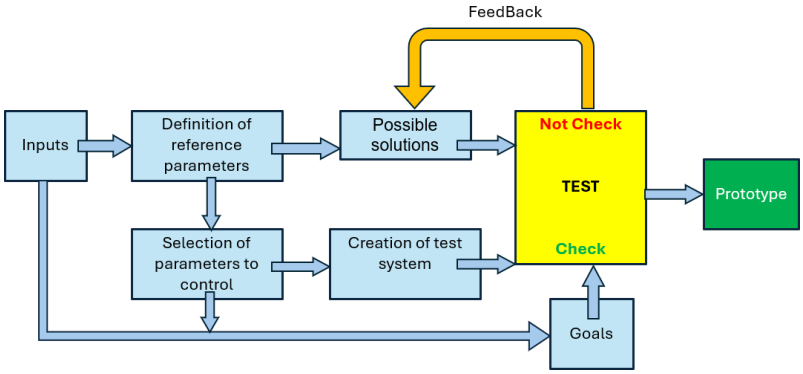


Figura 1: Operational cycle of prototype development

Results

Most of the experiments on Termotogales, including T. neapolitana, have been conducted in a batch configuration and on limited amounts of culture medium, usually between 100 mL and 1L. Moreover the nutrient concentrations reported in literature are relatively low (up to 10 g/L). Despite the good potential demonstrated by the batch approach, the scale-up is not easy both due to low production rate and the overall size of the system which is configured at low production density. One way to overcome this problem is to work with a higher concentration of bacteria and to achieve this an opportunity is done by moving from a batch configuration with floating bacteria to a configuration with supported bacteria and continuously flowing culture media. Because this allows to maintain a quite constant bacteria population and nutrients concentration optimising, in this way, the production rate of hydrogen and by-products. Among the various anaerobic fermentation systems proposed and implemented on an industrial scale, the internally circulating reactor (ICR) was identified in this work as the most suitable for working under continuous flow conditions, as shown in Figure 2, where the plant scheme is reported. Notably, in terms of the material used, stainless steel was chosen as the material for the construction of the bioreactor and whole plant because thermotogals have a low affinity for steel, ensuring easier maintenance of the plant, as well as for its excellent thermo-mechanical properties. Testing for evaluating the overall plant efficiency is running. Preliminary results are in line with literature data, and support confidence that these production rates could be excedeed by optimising the process operative conditions and controls.

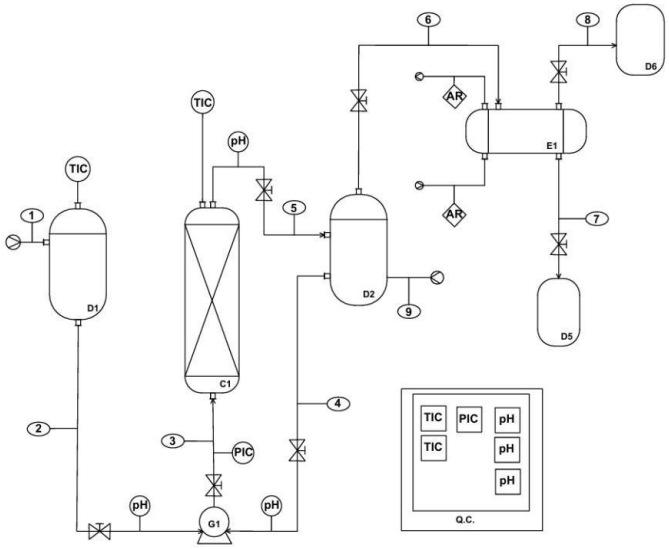


***Figure 2**: Prototype plant for bio-hydrogen production by bacteria T. Neapolitana (**Q.C.** Control panel, **TIC**, **PIC**, **pHC** are indicator and controller of T, P and pH, **AR** Cooling water, **C1** Bioreactor with filling, **D1** Thermostatted and insulated bacterial culture tank, **D2** Recirculation tank, **D3** Graduated tank for measuring hydrogen produced, **D4** Graduated free-flowing tank for measuring hydrogen produced, **D5** Condenser outlet , **D6** Hydrogen buffer, **E1** Condenser, **G1** Pump, **1** Input current, **2** Current input of T. Neapolitana bacteria, **3** Bioreactor power supply, **4** Recirculation current exiting the membrane reactor, **5** Outgoing current from the bioreactor, **6** Hydrogen saturated, **7** condensate, **8** Product hydrogen collection line, **9** Buffer solution supply to stabilize the pH of the bacterial solution)*

Conclusions

The possibility to scale up hydrogen production using thermotoga neapolitana attached on solid supports and in continuous flow has been demonstrated. The result was possible by the design of a plant based on ICR reactor configuration and by using a proprietary fermenter design. Future work will be centred on plant management optimisation and alternate bacteria batch testing.

Acknowledgement

“This research was funded by the European Union – NextGeneration EU from the Italian Ministry of Environment and Energy Security POR H2 AdP MMES/ENEA with involvement of CNR and RSE, PNRR - Mission 2, Component 2, Investment 3.5 "Ricerca e sviluppo sull’idrogeno", CUP: B93C22000630006”.

References

[1] Nicita A, Squadrito G, Maggio G – Int. J. Hydrogen Energy 44 (2019), pp 11371–84.
[2] Xianxian Xu, Quan Zhou, Dehai Yu - Int. J. Hydrogen Energy 47 (2022), 33677 - 33698.
[3] N Pradhan, L Dipasquale, G d’Ippolito, A Panico, P N L Lens, G Esposito and A Fontana- Int. J. Mol. Sci. 2015, 16, 12578-12600; doi:10.3390/ijms160612578
[4] G d'Ippolito, G Squadrito, M Tucci, N Esercizio, A Sardo, M Vastano, M Lanzilli, A Fontana, P Cristiani - Bioresource Technology 319 (2021) 124078

European Fuel Cells and Hydrogen
PIERO LUNGHI CONFERENCE
September 17th–19th 2025
Capri / Italy

Experimental investigation and 3D modelling of a planar SOEC

Valentina Biagioni*[a], Francesco Marino[b], Francesca Santoni[b], Luca Simonetti[b], Davide Pumiglia[b], Maria Anna Murmura[a]
* corresponding author: valentina.biagioni@uniroma1.it
[a] *DICMA Sapienza Università di Roma (Italy), Via Eudossiana 18, 00184 Rome, Italy*
[b] Department of Energy Technologies and Renewable Sources (TERIN) Laboratory for Hydrogen and new Energy Vectors (H2V), ENEA Italian National Agency for Energy, New Technologies and and Sustainable Economic Development, C.R. Casaccia, Rome, Italy;

Introduction: Solid oxide electrolysis cells (SOECs) represent an environmentally friendly alternative to produce H_2 fuel, reducing the CO_2 emissions [1]. One of the limiting factors to the widespread of this technology is the flow channel design, which has a significant impact on gas and temperature distribution, mass transfer, and electrochemical properties. In this regard, different designs of the flow channels, such as helical and serpentine [2], or triangular/trapezoidal shapes [3], have been studied to improve the H_2 yield efficiency and reduce the performance losses. Here, a planar SOEC cell has been investigated experimentally and theoretically to develop a more efficient and durable system of SOEC for energy conversion.

Objectives: This study aims to develop a three-dimensional model of the cathodic compartment of the cell that can capture the experimental gas composition along the flow direction obtained in a planar SOEC. The analysis assumes that the overall behavior of the SOEC is predominantly influenced by processes occurring at the fuel electrode. Therefore, the model considers the overpotential at the fuel electrode to be equal to the overall overpotential measured experimentally.

Materials and Methods: A planar SOEC cell has been investigated experimentally using an innovative setup based on 11 capillaries distributed across the fuel side and equipped with capillaries allowing the local measurement of temperature and gas composition in eleven points at seven coordinates along the flow direction. The geometry of the cell investigated is depicted in panel (A) of Figure 1, further details can be found in the literature [4]. A three-dimensional model of the cathodic channel has been developed to calculate cathode overpotentials and cathodic currents with the assumption of homogenous temperature distribution throughout the entire cathodic compartment. This assumption is corroborated by experimental data suggesting that the cell temperature is uniform throughout the cross section. The 3D model is based on: (i) the continuity equation, (ii) the momentum balance of the Navier-Stokes equation for compressible gases, and (iii) the mass balance, taking into account the transport of gaseous species by convection and diffusion, as well as the cathodic half-reaction, where the reaction rate is governed by the Butler-Volmer equation. The main equations are reported below:

(i) $$\nabla \cdot (\rho \boldsymbol{u}) = 0$$

(ii) $$\rho \boldsymbol{u} \cdot \nabla \boldsymbol{u} = \mu \nabla^2 \boldsymbol{u} + \frac{2}{3}\mu \nabla(\nabla \cdot \boldsymbol{u}) - \nabla p$$

(iii) $$\nabla \cdot j_i + \rho(\boldsymbol{u} \cdot \nabla)\omega_i = 0 \qquad j_i = -(\rho D_{ij} \nabla \omega_i)$$

Where $\boldsymbol{u}$ is the gas velocity field, ω_i is the mass fraction of component "i", p is the pressure gradient, and ρ, μ, D_{ij} are the gas density, the dynamic viscosity, and the binary diffusion coefficient, respectively. The 3D geometry of the compartment of the investigated SOEC cell is depicted in panel (B) of Figure 1.

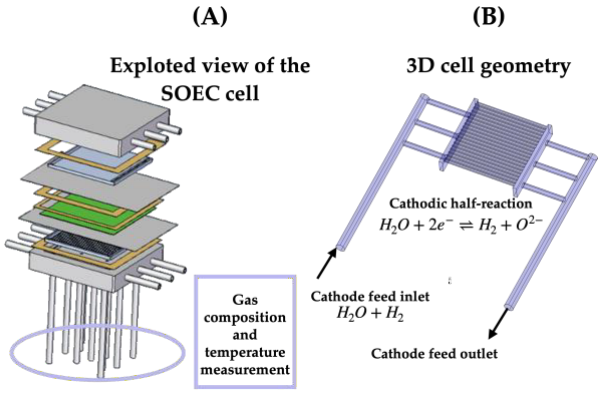


Figure 1: (A) Exploded view of the investigated planar SOEC cell. (B) Three-dimensional scheme of the computationally analyzed cathodic section of the SOEC cell.

Results: Panels (A)-(E) of Figure 2 show the comparison between calculated (squares) and experimental gas composition data (circles) recorded at seven coordinates along the direction of the flow for three different temperature conditions; T=725 °C, 750 °C, 775° C (left to right column). The main operating conditions have been reported in the caption of the figure. The results demonstrate excellent agreement between the experimental data and the values of the calculated hydrogen composition in all conditions except for those with high molar fraction of water at the inlet. In fact, in such conditions, the rate of the cathodic reaction is sufficient to reduce cathodic process resistance, which can make it no longer the most limiting resistance in the cell. Consequently, cathodic overpotential will be reduced, and ohmic or anodic resistances must be considered. In fact, high flow rates and low water content are conditions which unfavorably affect the cathodic processes.

Conclusions: The model proves that, under the investigated conditions, the cell performance is predominantly limited by fuel electrode processes, except when a gas mixture characterized by 70% H_2O and 30% H_2 is fed. This is because the increased cathodic reaction rate with high concentration of water results in lower cathodic resistance. To better characterize the planar cell under these conditions, the model should be extended to include the electrolyte and the anodic resistance. However, since the gas distribution within the cell has been verified as uniform, a two-dimensional model is sufficient for practical use.

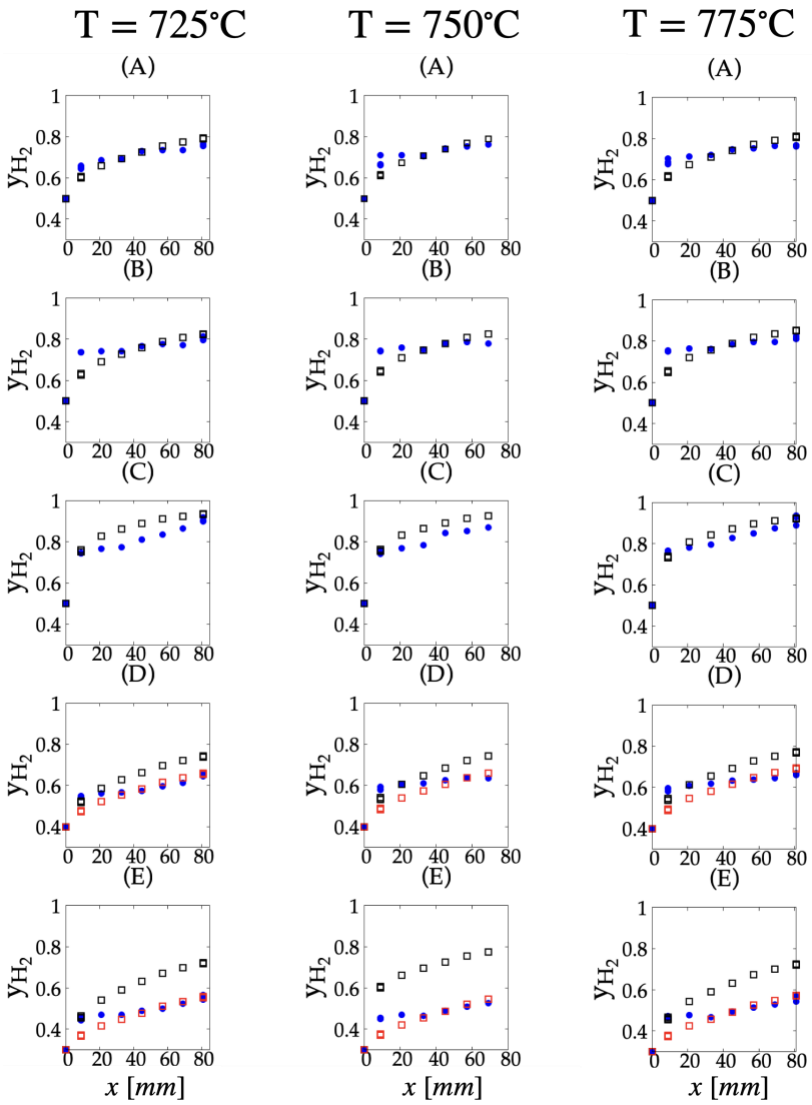


Figure 1: Hydrogen composition along the flow direction within the cathodic channel of the investigated SOEC cell. Panels (A)-(C) refer to the cases where a gas volumetric flowrate (Q) is set to Q=500, 400 and 300 $\frac{NmL}{min}$ with an inlet hydrogen molar fraction of $y_{H_2} = 0.5$. Panels (D) and (E) correspond to Q=500 $\frac{NmL}{min}$ and $y_{H_2} = 0.4$ and 0.3, respectively.

Acknowledge:

This research is funded by the European Union – NextGenerationEU from the Italian Ministry of Environment and Energy Security, POR H2 AdP MEES/ENEA with the involvement of the CNR and RSE, PNRR - Mission 2, Component 2, Investment 3.5 "Ricerca e sviluppo sull'idrogeno", CUP: I83C22001170006.

References

[1] Jolaoso, L. A., Bello, I. T., Ojelade, O. A., Yousuf, A., Duan, C., & Kazempoor, P. (2023). Operational and scaling-up barriers of SOEC and mitigation strategies to boost H2 production-a comprehensive review. *International Journal of Hydrogen Energy*, *48*(85), 33017-33041.
[2] Saied, M., Ahmed, K., Nemat-Alla, M., Ahmed, M., & El-Sebaie, M. (2018). Performance study of solid oxide fuel cell with various flow field designs: numerical study. *international journal of hydrogen energy*, *43*(45), 20931-20946.
[3] Xu, Y., Zhang, J., & Tu, Z. (2024). Numerical simulation of flow channel geometries optimization for the planar solid oxide electrolysis cell. *International Journal of Hydrogen Energy*, *52*, 288-301.
[4] F. Santoni, D. Silva Mosqueda, D. Pumiglia, E. Viceconti, B. Conti, C. BoiguesMuñoz, B. Bosio, S. Ulgiati and S. J. McPhail, In-situ study of the gas-phase composition and temperature of an intermediate-temperature solid oxide fuel cell anode surface fed by reformate natural gas. Journal of Power Sources, 2017, Volume 370, p. 36-44. doi: 10.1016/j.jpowsour.2017.09.078

Optimising Green Hydrogen Production: How Renewable Energy Sources Shape Cost and Plant Design

Paolo Marocco*[a], Marta Gandiglio [a], Massimo Santarelli[a]

* corresponding author: paolo.marocco@polito.it
[a] Department of Energy, Politecnico di Torino – C.so Duca degli Abruzzi 24, 10129 Turin, Italy

Keywords: Green hydrogen; optimal design; water electrolysis; renewable energy

Introduction:

Hydrogen is gaining strong momentum globally, driven by supportive policies and a growing number of projects aimed at accelerating its deployment as a clean energy carrier [1]. Its central role in decarbonising hard-to-electrify sectors is widely recognised, making it a key pillar in many net-zero strategies. However, producing hydrogen from renewable energy sources presents both technical and economic challenges, mainly due to the variable nature of solar and wind. Ensuring a reliable and cost-effective supply of green hydrogen requires careful system design capable of adapting to fluctuating resource availability. This study addresses these challenges at a European scale, demonstrating how advanced optimisation approaches can support the development of efficient and economically viable hydrogen production systems.

Objectives:

This study aims to develop a methodological framework based on mixed-integer linear programming (MILP) to identify the cost-optimal design of water electrolysis systems powered by solar and/or wind energy. A general layout of the power-to-hydrogen (PtH) system under investigation is shown in Figure 1. The proposed model is applied to all European countries, with the primary objective of assessing how varying renewable resource availability influence both the cost and optimal configuration of PtH plants. In addition, the analysis evaluates the impact of compliance with European Union (EU) regulatory frameworks – specifically the RED III directive – on system design and associated costs, with the goal of quantifying the potential cost burden introduced by regulatory constraints.

A key novelty of this work lies in its European-scale perspective, providing generalised guidelines by correlating renewable resource quality with key technical, energy and economic indicators.

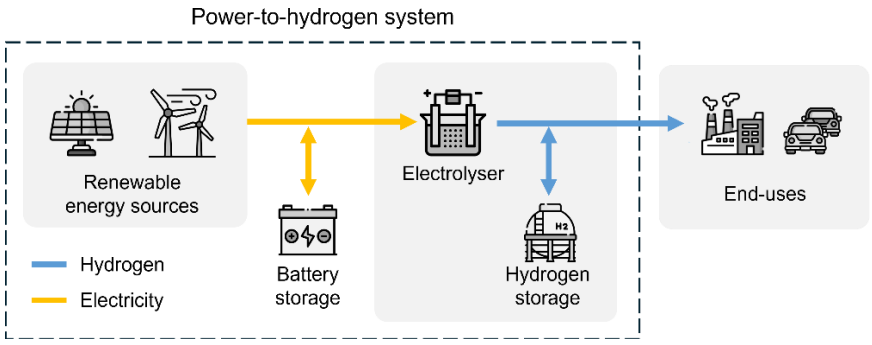


Figure 1. General layout of the power-to-hydrogen (PtH) system.

Material and methods:

Based on the authors' previous work [2,3], a MILP model is formulated to minimise the levelised cost of hydrogen (LCOH), accounting for capital, replacement, and operation and maintenance costs over a 20-year project horizon. As shown in Figure 2, both design variables (technology selection and sizing) and operational variables (hourly operating points for each technology) are included. Specifically, the framework determines the sizes for photovoltaic and wind generators, battery storage, electrolysers, and hydrogen storage, ensuring that hourly power and hydrogen balances are met while satisfying a specified hydrogen demand at the lowest possible cost. To ensure the robustness of the results, particular emphasis is placed on the accurate modelling of the hydrogen production process, including the integration of the electrolyser's real efficiency curve, modulation limits, and ramp rate constraints. The analysis is conducted for each European country based on local solar and wind capacity factor data, clustered through k-medoids from two decades of hourly records. A graphical representation of the MILP-based optimisation framework is shown in

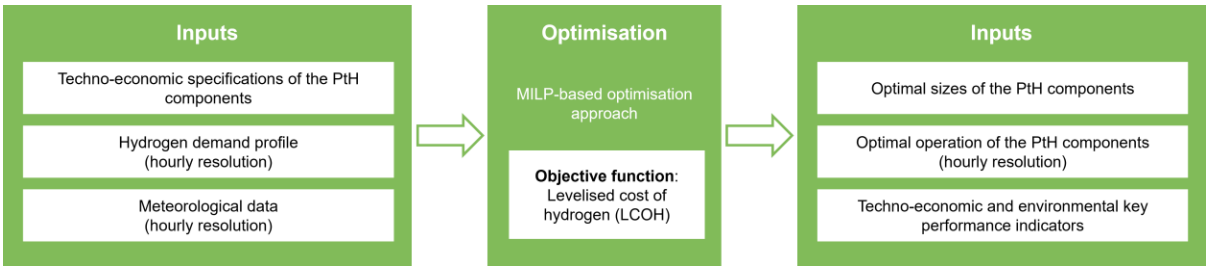


Figure 2. Optimisation framework for the optimal design and operation of PtH systems.

Results:

The results indicate that, depending on local renewable resource availability and the chosen system configuration, the LCOH varies significantly across Europe countries, ranging from about 4 to over 20 €/kg. Wind-only layouts typically achieve lower hydrogen production costs

than solar-only systems, reflecting more stable wind capacity factors and reduced oversizing requirements. However, hybrid solutions that combine photovoltaic and wind resources consistently offer the best performance, reducing the LCOH by an average of approximately 40% compared to single-generator setups. Additionally, although battery storage was evaluated, it rarely proved cost-effective under current cost assumptions, suggesting that hydrogen storage alone can provide sufficient flexibility. By correlating local resource conditions with key techno-economic indicators, this study provides practical guidelines to easily derive sizing and cost estimates, adaptable to any specific location.

Conclusions:

To comply with EU directives, hydrogen production must rely heavily on renewable energy sources, which are inherently variable. This leads to challenges in cost-effectively and reliably meeting a specified hydrogen demand profile. In this context, this study develops a flexible tool for the optimal design of hydrogen production systems, adaptable to any case study. The model takes as input the local availability of renewable resources, the hydrogen demand to be satisfied, and the techno-economic parameters of the PtH components.

An extensive, country-specific analysis reveals that hybridising solar and wind power is generally the most cost-effective and technically reliable solution to produce green hydrogen across Europe. Such systems effectively reduce LCOH disparities across different geographical regions. A set of techno-economic indicators is also defined, and their correlation with local resource conditions is presented to provide straightforward guidance on system design and expected LCOH for any location.

Future studies will extend this approach to other power-to-X pathways, including e-fuels production such as ammonia and methanol.

Acknowledgment

Funded by the European Union - NextGenerationEU, Mission 4 Component 1.5 - ECS00000036 - CUP E13B22000020001

References

[1] M. Gandiglio, P. Marocco, Mapping Hydrogen Initiatives in Italy: An Overview of Funding and Projects, Energies. 17 (2024). https://doi.org/10.3390/en17112614.

[2] P. Marocco, M. Gandiglio, M. Santarelli, Optimal design of PV-based grid-connected hydrogen production systems, J. Clean. Prod. 434 (2024) 140007. https://doi.org/10.1016/j.jclepro.2023.140007.

[3] P. Marocco, M. Gandiglio, D. Audisio, M. Santarelli, Assessment of the role of hydrogen to produce high-temperature heat in the steel industry, J. Clean. Prod. 388 (2023) 135969. https://doi.org/10.1016/j.jclepro.2023.135969.

Alkalinization of soecs with basic oxides nanoparticles for enhanced coelectrolysis of co_2-h_2o mixture

Patryk Błaszczak*[a], Agata Ducka [b], Imran Asghar [c], Sea-Fue Wang [d], Piotr Jasiński [a]

* corresponding author: patryk.blaszczak@pg.edu.pl

[a] Advanced Materials Center, Faculty of Electronics, Telecommunications and Informatics, Gdańsk University of Technology, ul. G. Narutowicza 11/12, 80-233 Gdańsk, Poland

[b] Advanced Materials Center, Faculty of Applied Physics and Mathematics, Gdańsk University of Technology, ul. G. Narutowicza 11/12, 80-233 Gdańsk, Poland

[c] Renewable Energy Technologies Group, Faculty of Engineering and Natural Sciences, Tampere University, FI-33014, Finland

[d] Department of Materials and Mineral Resources Engineering, National Taipei University of Technology, 1, Sec. 3, Zhongxiao E. Rd., Taipei, 106, Taiwan

Keywords: coelectrolysis, nanoparticles, SOEC, syngas

Abstract

Solid Oxide Electrolysis Cells (SOECs) offer a sustainable solution to reduce atmospheric CO_2 by generating 'green' hydrogen through simultaneous electrolysis of water vapor and CO_2. This process, known as coelectrolysis, produces valuable products (e.g. syngas) in a single step, making it a more environmentally friendly alternative to traditional methods.

The steam electrode, primarily composed of NiO and 8YSZ, faces challenges in atmospheres rich in CO/CO_2 and does not guarantee the highest possible efficiency in CO_2 reduction. To enhance performance, alkaline/alkaline earth metal oxides were incorporated into the steam electrode of the electrolyzer. These modifications significantly improved CO_2 conversion rates, H_2 yield and selectivity to CO, leading to increased electrical efficiency. In-situ characterization techniques provided insights into the formation of mixed compounds and the impact of these modifications on electrode behavior in CO_2-rich atmospheres.

Introduction:

The simultaneous increase in the need to retrieve the fossil fuels and an increasing consumption of energy led to a continuous increase in CO_2 emissions, contributing to the pressing issue of global warming driven by the greenhouse effect. Although low-carbon energy sources, such as nuclear plants and renewable energy sources (wind turbines, solar panels, tidal, geothermal, and biomass energy), have spurred development initiatives, they remain vulnerable to external environmental factors. Consequently, these cannot contribute significantly to fulfilling energy demands and lead to complete decarbonization[1].

To address this environmental challenge on the pathways for CO_2 conversion, electrochemical reduction has the potential to serve as a major carbon sink, paving the way for carbon

neutrality.

Solid Oxide Electrolysis Cell (SOEC) is a reversed operating mode of the Solid Oxide Fuel Cell that enables us to convert excess electrical energy into chemical energy by electrosplitting water vapor into H_2 and O_2. Electrochemical cells operate normally at quite high temperatures in the range between 600 and 1000 ^oC. It can be seen as an attitude of SOECs as the energy required for electrolysis decreases with increasing temperature[2].

Along with the water vapor, it is possible to supply the cell with another feedstock that can be reduced either electrochemically or chemically (e.g., CO_2). In that case, the whole process is called coelectrolysis and produces a mixture of CO and H2, which is called 'syngas'. Syngas can be utilized in the chemical synthesis of hydrocarbons.

The steam electrode within the electrolyzer is rich in metallic nickel, a well-known catalyst for various reactions. However, these electrodes may face rapid deactivation in a carbon-rich atmosphere, necessitating the incorporation of additional catalytic materials. Catalytic activity can be altered by adding another metal or oxide, which would affect the surface composition of the adsorbed species, change the route of the reaction, or increase the retention times of the intermediates[3].

Objectives:

The main objective of this work was to determine the influence of alkali/alkaline earth promoter oxides on the performance of HTCE-SOEC. The hypothesis was that the reaction rates of the reverse Water Gas Shift reaction (rWGS) can be increased as a result of increased basicity of the electrode and through nanometrization of the oxide scale distributed throughout the Ni-YSZ electrode.

Material and methods:

A series of modified SOECs was prepared by adding 5 mol.% alkaline/alkaline earth metal oxide (Na, K, Ca, Mg, Rb, Li, Sr, Cs) nanoparticles with respect to the metallic phase. SOEC 1-inch samples were fabricated by βCD-assisted wet impregnation method developed in our laboratory. The SOECs were tested for the coelectrolysis of CO_2/H_2O mixture with 5 vol.% H_2 (for protection of the electrode against the reoxidation). Electrical tests were conducted for various water vapor utilization factors, varying temperatures and under changing CO_2:H_2O ratio to better understand the mechanisms of syngas formation. The cells were subjected to EIS measurements under SOEC polarization accompanied by DRT technique to better understand the changes in the electrochemical performance. The interaction strength of CO_2 with the samples was measured by Temperature Programmed Desorption (TPD). X-ray Absorption Spectroscopy measurements were taken at the LISA beamline (ESRF, Grenoble) at

elevated temperatures to observe the changes in chemical surrounding of the Ni-YSZ electrode impregnated with the oxides.

Results:

The alkali/alkaline earth oxides were distributed uniformly throughout the electrode and formed a scale of various microstructures on Ni and YSZ grains. The addition of guest metal, in general, increased CO_2 conversion and selectivity toward CO production, as well as electrical efficiency, due to the alterations of basic acid sites and the introduction of active redox couples. Adsorption of CO_2 increased after the addition of promoter oxides due to the ease of carbonate formation. The selectivity toward CO could reach nearly 100%, with the yields varying according to the respective oxides. XAS studies revealed differences in electrode interaction with a CO_2 rich atmosphere (see Fig. 1). The most interesting was Li-impregnated samples, which came out as nearly fully resistant to oxidation even at 800 ºC. The DRT technique allowed to successfully disseminate the electrochemical processes occurring during the coelectrolysis.

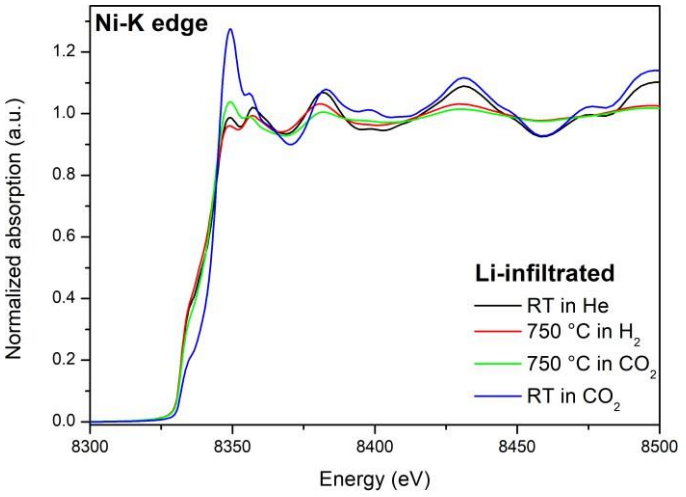


Figure 1. XAS spectra of Li-infiltrated Ni-YSZ measured at different conditions.

Conclusions:

It was possible to introduce homogeneously dispersed nanostructures of the I and II group metal oxides throughout the steam electrode of conventional AS-SOC using the simple impregnation method of the electrode. Promoter oxides altered the distribution of reactive sites on Ni-YSZ and influenced the interaction of the electrode with CO_2 as seen on TPD profiles. As a result, the electrochemical activity of the electrolysis process was altered depending on the oxide used. A lithium-enriched sample revealed an outstanding resistivity for Ni oxidation in contrast to the rest of the samples.

Acknowledgment

This work was supported by a project funded by National Science Centre Poland, based on decision UMO-2021/43/B/ST8/01831 (OPUS 22). The XAS experiments were supported by CERIC-ERIC consortium and performed at the European Synchrotron Radiation Facility (ESRF). The access to ESRF was financed by the Polish Ministry of Education and Science – decision number: 2021/WK/11.

References

1. David, M., Ocampo-Martínez, C. & Sánchez-Peña, R. Advances in alkaline water electrolyzers: A review. *J. Energy Storage* **23**, 392–403 (2019).
2. Min, G., Park, Y. J. & Hong, J. Thermodynamic analysis of a solid oxide co-electrolysis cell system for its optimal thermal integration with external heat supply. *Energy Convers. Manag.* **225**, 113381 (2020).
3. Carneiro, J. S. A., Williams, J., Gryko, A., Herrera, L. P. & Nikolla, E. Embracing the Complexity of Catalytic Structures: A Viewpoint on the Synthesis of Nonstoichiometric Mixed Metal Oxides for Catalysis. *ACS Catal.* **10**, 516–527 (2020).

Long-term performance assessment of Single-Cell AEMWE configuration under Accelerated Stress Testing

Carlotta Cosentini*[a], Gabriele Guglielmo Gagliardi[a], Domenico Borello[a]

* Corresponding author: carlotta.cosentini@uniroma1.it

[a] *Dept. of Mechanical and Aerospace Engineering, Sapienza University of Rome, Rome, Italy*

Keywords: AEM Water Electrolyser, Accelerated Stress Test, Durability, Electrochemical Impedance Spectroscopy (EIS), Single-Cell assembly

Abstract

This study investigates the long-term performances of AEMWEs in single-cell configuration under prolonged operation using an Accelerated Stress Test (AST) protocol. Over 100 hours of testing, variations in voltage, impedance, and electrolyte composition are analysed to assess degradation mechanisms. Scheduled shutdowns include polarization curves and Electrochemical Impedance Spectroscopy (EIS) analysis to monitor performance evolution. The study provides insights into AEMWE degradation under load cycling, addressing the necessity to support the optimization of system durability, which remain underexplored.

Introduction

The operational reliability of an electrolysis device is determined not only by its performance but also by its ability to maintain consistent functionality over time. This attribute, known as durability, is influenced by various factors, including cell design, manufacturing and assembly processes, and the operational conditions under which the system is subjected.

The durability of Anion Exchange Membrane Water Electrolysers (AEMWEs) remains a critical barrier to their widespread adoption, primarily due to membrane degradation, catalyst deactivation, and operational instability. Several studies have investigated these challenges, although research gaps still persist. Niaz et al. [1] demonstrated that frequent short rest periods increase ohmic resistance due to membrane dehydration, whereas longer operation cycles improve hydration and mitigate performance losses. However, their study did not address the chemical degradation of membrane functional groups. Li et al. [2] found that KOH-fed AEMWEs achieved superior durability, exceeding 12,000 hours at 1 A/cm² with minimal degradation (0.7 µV/h), while pure water-fed systems suffered rapid ionomer degradation while K_2CO_3-fed cells faced mechanical failure. The effect of dynamic operating conditions remains unexplored. Xing et al. [3] highlighted severe degradation in direct seawater electrolysis, with chloride infiltration and membrane thinning leading to rapid failure. While reinforced membranes extended operational life beyond 1000 hours, no effective mitigation strategies were proposed. Hyun et al. [4] identified weak ionomer-

catalyst adhesion as the cause of early-stage performance loss, mitigated by Nafion co-binders; however, long-term degradation mechanisms, such as catalysts dissolution, remain unaddressed. Ahmed et al. [5] optimized NiFeCoOx catalysts, showing that 5% Fe doping enhanced stability, but degradation beyond 1000 hours remains unverified. Thus, further research is required to elucidate the effects of load cycling on stability and durability of AEMWE. Furthermore, gaining a deeper understanding of long-term degradation phenomena in single-cell AEMWEs is essential to support the development of more stable and durable materials and operating strategies. Although significant advances have been made, the literature still lacks comprehensive insights into the impact of dynamic operating conditions and load cycling on performance and degradation mechanisms, especially in single-cell configurations using non-PGM catalysts.

Since the expected service life of an electrolyser extends over several years, it is essential to assess its degradation rate within a significantly shorter timeframe. To achieve this, Accelerated Stress Tests (ASTs) are implemented as part of the experimental campaign. These tests expose materials and components to operating conditions that exceed their standard functional range, inducing degradation mechanisms similar to those encountered under real- world conditions but at an accelerated rate. This approach significantly reduces the time required for durability evaluations.

Objectives

This study aims to investigate the durability of AEMWE in single cell configuration under prolonged operational conditions through the implementation of an Accelerated Stress Test (AST) protocol. Long-term testing is carried out to evaluate variations in cell voltage and impedance, as well as changes in the composition of the electrolyte solution over time, providing a comprehensive assessment of the degradation mechanisms.

Material and methods

Experimental set-up/test-bench

A dedicated test bench has been designed and implemented for the performance evaluation of a 5 cm^2 single-cell AEM electrolyser.

1M KOH potassium hydroxide aqueous solution is supplied to the cell via a peristaltic pump, ensuring controlled and continuous flow. The operating temperature is increased to the desired setpoint through two heating plates attached to the end plates of the cell, while a PID temperature controller continuously monitors and regulates the temperature to maintain stable operating conditions.

The electronic power supply used in the system features integrated communication capabilities, enabling direct interfacing with a PC. A customized control code is developed using LabVIEW software, allowing for real-time acquisition and monitoring of current (A) and voltage (V) values, ensuring precise control over the experimental conditions.

The cell hardware includes commercially available components, which have been tested and validated for performance. The flow field plates for both the anode and cathode adopt a single-serpentine configuration. The Membrane Electrode Assembly (MEA), with an active area of 5 cm², consists of a Fumasep® FM-FAA-3-50 Anion Exchange Membrane (AEM) a cathode Gas Diffusion Electrode (GDE) composed by 2 mg/cm2 NiFeCo nanoparticles catalyst deposited on a carbon paper Gas Diffusion Layer (Sigracet 39BC GDL) and an anode Gas Diffusion Electrode (GDE) composed by 2 mg/cm2 of NiFe2O4 particles catalyst on a 316L sintered stainless steel fiber felt Gas Diffusion Layer (Bekaert). To ensure proper sealing, a Teflon gasket is employed, securing the MEA within the Nickel 200 cell blocks. The assembly is mechanically fastened using bolts, which are tightened to a torque of 15 in-lb, ensuring uniform compression and structural integrity.

Experimental Methodology

For durability assessment of single-cell AEMWE, the EU harmonized protocols for testing of low-temperature water electrolysers [6] are considered as reference standardized procedure for performance evaluation. The AST protocol prescribes the application of a ramped load profile. The operating current is increased by 25% relative to the nominal value, following a predefined ramp rate, and maintained at this level for 15 minutes. This process is repeated until the current reaches 100% of the nominal operating value. The current is then reduced by 25% using a reverse ramp profile and held constant for 15 minutes. The ramp rate is defined as the variation of 25% of the maximum design operating current per second. Each complete ramp cycle has a total duration of two hours, and it is iterated up to 100 hours of operation.

In accordance with the experimental protocol, the dilute KOH electrolyte solution is replaced every two weeks to ensure the stability of its chemical and physical properties, preventing variations in electrolyte concentration and the accumulation of impurities that could compromise cell performance and test accuracy.

During the experimental campaign, scheduled shutdown and startup sequences are systematically executed. These phases include polarization tests and Electrochemical Impedance Spectroscopy (EIS) analyses, which are essential to monitor the evolution of the electrolytic cell's overall performance and assessing the degradation of its individual components over time. Polarization curves are acquired in triplicate using a programmable power supply (TDK-Lambda GEN H-20-38) to enhance measurement reliability and reproducibility. The current-voltage (I-V) curve is recorded by averaging the voltage values at each current step, ensuring a stabilization period of 120 seconds under constant current conditions. Furthermore, Electrochemical Impedance Spectroscopy (EIS) is conducted using an Ivium Vertex potentiostat/galvanostat in galvanostatic mode. Impedance measurements are performed by applying an alternating current perturbation corresponding to 5% of the peak-to-peak current over a frequency range spanning from 0.1 Hz to 100 kHz.

Expected Results

The ongoing experimental campaign is expected to provide a comprehensive evaluation of the durability of AEM water electrolysers in single-cell configuration under prolonged operational conditions. Over 100 hours of testing, variations in voltage, impedance, and electrolyte composition will be analysed to identify key degradation mechanisms. The application of an Accelerated Stress Test (AST) protocol will enable the assessment of load cycling effects on system stability and performance retention, addressing a critical gap in the existing literature.

Conclusions

In the present work, single cell AEM water electrolyser performances are tested, aiming at assessing the durability of the technology and investigating the degradation mechanisms the mostly affect the AEMWE cell components. These findings will contribute to a deeper understanding of degradation pathways and support the development of mitigation strategies to enhance the long-term viability of AEMWE technology.

References

[1] Niaz AK, Akhtar A, Park JY, Lim HT. Effects of the operation mode on the degradation behavior of anion exchange membrane water electrolyzers. J Power Sources 2021;481:229093. https://doi.org/10.1016/J.JPOWSOUR.2020.229093.

[2] Li D, Motz AR, Bae C, Fujimoto C, Yang G, Zhang FY, et al. Durability of anion exchange membrane water electrolyzers. Energy Environ Sci 2021;14:3393–419. https://doi.org/10.1039/D0EE04086J.

[3] Xing J, Zeng Z, Best W, Liu Z, Bonville L, Maric R, et al. Long-term durability test of highly efficient membrane electrode assemblies for anion exchange membrane seawater electrolyzers. J Power Sources 2023;558:232564. https://doi.org/10.1016/J.JPOWSOUR.2022.232564.

[4] Hyun J, Hwan Yang S, Wook Lee D, Oh E, Bae H, Suc Cha M, et al. Impact of the binding ability of anion exchange ionomer on the initial performance degradation of anion exchange membrane water electrolyzers. Chemical Engineering Journal 2023;469:143919. https://doi.org/10.1016/J.CEJ.2023.143919.

[5] Ahmed KW, Fowler M. Performance Evaluation and Durability Analysis of NiFeCoOx Catalysts for Alkaline Water Electrolysis in Anion Exchange Membrane Electrolyzers. Catalysts 2024;14:322. https://doi.org/10.3390/CATAL14050322/S1.

[6] Tsotridis G, Pilenga A. EU harmonised protocols for testing of low temperature water electrolysers, 2021. https://doi.org/10.2760/58880.

Effect of operating conditions on proton exchange membrane electrolysis cell using computational fluid dynamics analysis

SIHWAN YOON[a], SEUNGHUN OH[a], HAESEONG SHIN[a], SANGGYU KANG*[a]

* corresponding author: sgkang@snu.ac.kr

[a] Department of Naval Architecture and Ocean Engineering, Seoul National University

Keywords: Computational Fluid Dynamics, Electrochemistry, Multi-phase modeling, Proton Exchange Membrane Water Electrolysis

Introduction:

After the Paris Agreement, the world has been striving toward Net Zero targets to combat climate change, prompting various industries to establish sustainable energy systems. Among these efforts, hydrogen is expected to play a crucial role in the upcoming energy transition era and is gradually emerging as a mainstream energy source. However, the current cost of hydrogen remains high, leading to extensive research on various hydrogen production methods to reduce costs. Among these methods, water electrolysis has garnered significant attention due to its ability to produce hydrogen solely using electricity. In particular, Proton Exchange Membrane (PEM) water electrolysis offers high efficiency, compact system design, and fast response times, making it a promising solution for large-scale hydrogen production.

Objectives:

This study conducts Computational Fluid Dynamics (CFD) analysis on a PEM electrolysis cell, focusing on detailed flow behavior and reaction characteristics within the system. Since PEM electrolysis involves the transition of liquid water into gaseous hydrogen and oxygen, it is essential to consider multiphase flow and electrochemical reactions simultaneously. The formation of bubbles during this process reduces the effective reaction area, directly impacting performance. Therefore, analyzing multiphase flow behavior is crucial as it significantly affects electrochemical efficiency and overall system stability. To gain deeper insights into these complex interactions and optimize performance, CFD analysis plays a crucial role in accurately predicting the physical and electrochemical behavior of PEM electrolysis cells and stacks.

Material and methods:

A CFD model of a PEM water electrolysis cell was developed using ANSYS Fluent, incorporating User-Defined Functions (UDF) to enhance the accuracy of electrochemical reaction modeling. The model simulates flow behavior, electrochemical reactions, and

thermal characteristics under various operating conditions. In this study, the Mixture model was used to represent gas-liquid interactions within the electrolysis cell more efficiently. The computational domain consists of key components such as bipolar plates (BPPs), porous transport layers (PTLs), catalyst layers, and the polymer electrolyte membrane (PEM). The governing equations include mass conservation for water and gas transport, energy conservation for heat generation and dissipation, and momentum conservation for analyzing flow distribution within the cell. The electrochemical reaction model was implemented using UDF, allowing for a more detailed representation of the reaction kinetics and hydrogen generation process. To ensure realistic operating conditions, the water flow rate is set at 500 times the amount of water required for the electrolysis reaction, ensuring sufficient reactant supply and minimizing concentration losses. The simulation is conducted for a current density range of 0.5–2.5 A/cm², with operating temperatures varying between 60 °C and 80 °C. Additionally, the outlet pressure is varied from 1 bar to 10 bar to analyze its impact on performance. A fine adaptive mesh was used to capture the detailed gas-liquid interactions and physical behaviors in the reaction zone, particularly near the catalyst layers. Through this method, the distribution of hydrogen bubbles, local overpotentials, and thermal gradients, which are critical factors in analyzing PEM electrolysis performance, was identified.

Results:

The study reveals that as current density increases, the amount of hydrogen and oxygen bubbles generated within the catalyst layers and porous transport layers (PTLs) increases accordingly. At higher temperatures, the current density increases at the same voltage, resulting in a greater amount of bubble formation. Additionally, as the current density increases, the internal pressure loss within the cell also rises, affecting the overall transport of reactants and products. Additionally, the internal pressure loss within the cell increases with higher current densities, affecting the overall transport of reactants and products. This pressure drop is particularly significant in the flow channels and porous layers, where increased gas generation leads to higher resistance in fluid movement.

The thickness of the membrane also plays a critical role in determining cell performance and bubble formation. Thinner membranes have lower ohmic resistance, improving cell voltage efficiency, while thicker membranes introduce higher resistance, which affects overall performance. The I-V curve under different operating conditions is shown in Figure. 1. The analysis of the I-V curve under different conditions provides insight into how temperature, membrane thickness, and internal pressure loss influence electrochemical performance. By evaluating bubble formation, pressure loss, and their impact on electrochemical

characteristics, this study offers valuable insights into the operational conditions of PEM water electrolysis systems. The findings highlight the importance of optimized cell design and parameter selection to achieve stable and efficient hydrogen production.

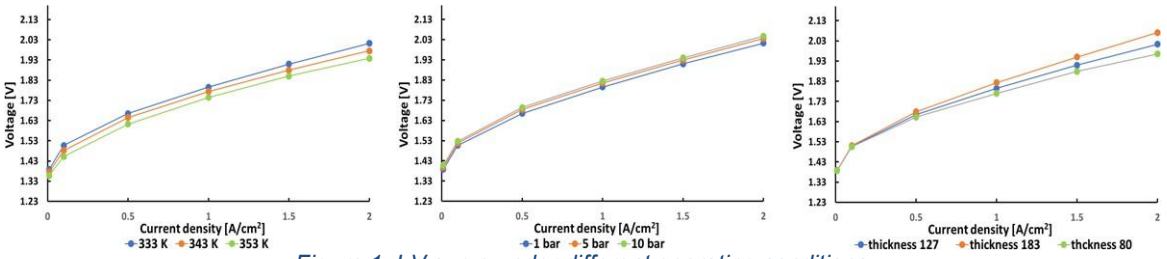


Figure 1. I-V curve under different operating conditions

Conclusions:

In this study, CFD analysis of a PEM electrolysis cell was conducted, incorporating User-Defined Functions to enhance the accuracy of electrochemical reaction modeling. The results provided insights into the complex interactions between flow characteristics, electrochemical reactions, and heat transfer mechanisms, confirming that temperature, membrane thickness, and internal pressure loss significantly affect the overall performance. By analyzing the performance variations and internal physical reactions of the cell under different conditions, the findings are expected to contribute to cell design optimization. Furthermore, future research will focus on further developing UDF-based models to enable more precise analysis of electrochemical reaction kinetics and transient conditions, ultimately improving the predictive capability of PEM electrolysis simulations.

Acknowledgment References

[1]S. Toghyani, E. Afshari, E. Baniasadi, S.A. Atyabi, Thermal and electrochemical analysis of different flow field patterns in a PEM electrolyzer, Electrochimica Acta 2018;234;245.

[2] Bo Han, Jingke Mo, Zhenye Kang, Gaoqiang Yang, William Barnhill, Feng-Yuan Zhang, Modeling of two-phase transport in proton exchange membrane electrolyzer cells for hydrogen energy, international journal of hydrogen energy, 2017;4478;4489

[3] Chao Hao, Qinghao Meng, Bowen Yan, Jia Liu, Bin Yang, Ligang Feng, Pei Kang Shen, Zhi Qun Tian, Efficient catalyst layer with ultra-low Pt loading for proton exchange membrane fuel cell, Chemical Engineering Jourcal, 2023;144945

EFCH2 2025 European Fuel Cells and Hydrogen
PIERO LUNGHI CONFERENCE
September 17th–19th 2025
Capri / Italy

Numerical Analysis of Solid Oxide Electrolysis Cell (SOEC) System Combined with LOHC Hydrogenation System

Geon Lee[a], Jongyun Jung[a], Seunghun Oh[a], Siwoong Kim[a], Minseok Kwon[a], Sanggyu Kang *[a]

* corresponding author: sgkang@snu.ac.kr

[a] Department of Naval Architecture and Ocean Engineering Seoul Nat'l Univ.

Keywords: SOEC, LOHC, Hydrogenation, Numerical Model, DBT

Abstract

Introduction: To achieve the 2050 Net Zero Emissions scenario, hydrogen production projects are expected to increase significantly. Both hydrogen supply and demand are projected to grow substantially. This trend is driving active development in hydrogen production, storage, and transportation technologies. Among these, Solid Oxide Electrolysis Cells (SOEC) are gaining attention as a promising production method, While Liquid Organic Hydrogen Carriers (LOHC) are emerging as a notable storage solution. SOEC operate at high temperatures, yielding high hydrogen production efficiency. They can be integrated with external heat sources, such as industrial waste heat, enhancing overall system efficiency. LOHC offer high hydrogen storage capacity by volume and weight. With hydrogen chemically bonded to organic liquid compounds, LOHC provide a safer storage and transportation method, minimizing hydrogen leakage risk. While SOEC system modeling is well-established, research on integrated models including post-production storage and transportation is limited. Laboratory-scale LOHC experiments are ongoing, but research on plant-scale LOHC reactors and systems is still limited. This research gap highlights the need for comprehensive studies that integrate production, storage, and transportation aspects of hydrogen technology at industrial scales.

Objectives: The objective of the research is to develop a numerical model of an SOEC-LOHC system. The research confirmed changes in stack, reactor, and overall system efficiencies in response to variations in SOEC operating temperature and current density, as well as reactor temperature and pressure in the LOHC hydrogenation system. We confirmed optimal operating conditions for both SOEC and LOHC hydrogenation systems and calculated system efficiencies for each condition.

Material and methods: In this study, Numerical Model of SOEC System with LOHC Hydrogenation System is developed using Aspen Plus® V14. Peng–Robinson (PR) is selected for the system as the equation of state (EOS). The model is developed using numerical methods for the SOEC (Solid Oxide Electrolysis Cell) and LOHC-Hydrogenation systems. Since Aspen Plus cannot simulate electrochemical reactions, these is developed using Fortran code. For the SOEC, the required voltage is calculated based on Nernst Voltage and overpotentials (activation, ohmic, and concentration) under specific operating conditions. This voltage determines power consumption, which is combined with the Balance of Plant (BOP) power usage to calculate overall system efficiency. The LOHC-Hydrogenation system uses a semi-batch reactor with Dibenzyltoluene (DBT) as the hydrogen carrier. The exothermic reaction generates heat, which is recovered through internal heat exchangers to improve efficiency. Total system efficiency is calculated by combining reactor performance with BOP power consumption.

Results: The developed SOEC-LOHC hydrogenation system simulated the effects of SOEC temperature and operating current density, as well as LOHC hydrogenation reactor temperature and pressure. The system calculated the hydrogen production rate, heat generation, and total power consumption required for storing hydrogenated LOHC under various operating conditions. This analysis enabled the identification of optimal operating conditions for maximizing system efficiency for both the SOEC and LOHC systems individually, as well as when the two systems were integrated. Temperature and pressure were found to be dominant operating parameters for both systems. Higher temperatures and pressures improved the efficiency of the SOEC stack and the LOHC reactor but increased power consumption in other Balance of Plant (BOP) components, resulting in reduced overall system efficiency. Furthermore, integrating the two systems increased overall system efficiency by approximately 40% compared to operating them separately.

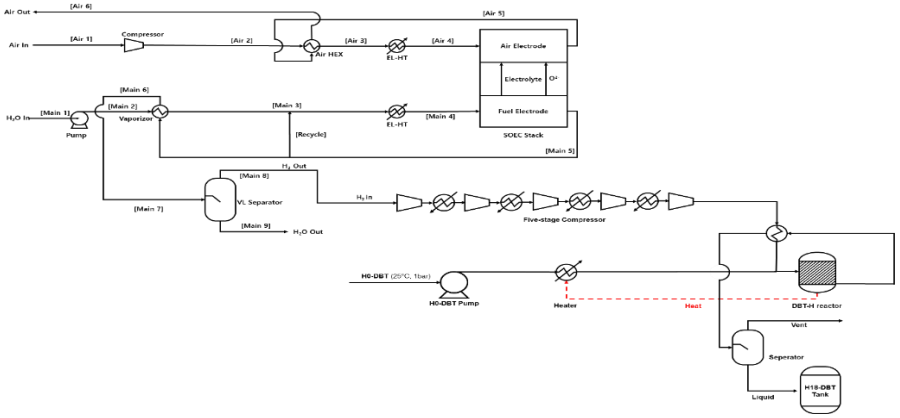


Figure 1: Schematic of SOEC combined with LOHC Hydrogenation system

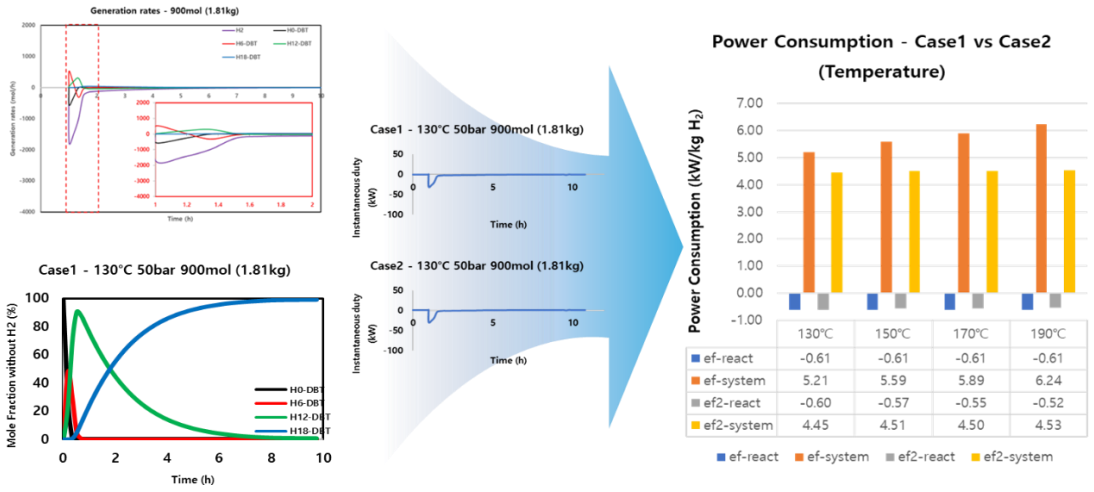


Figure 2: Schematic of SOEC combined with LOHC Hydrogenation system

Conclusions: In this study, an SOEC-LOHC hydrogenation system model was developed and validated by comparing it with experimental data, resulting in a highly reliable model. Optimal operating conditions for each system as well as for the integrated operation of the two systems were identified. These findings are expected to contribute to the integration of hydrogen production and storage systems in the future.

Acknowledgment References

[1] Kim, S., Kim, T., Oh, S., Ham, J., & Kang, S. (2023). Numerical analysis of a solid oxide fuel cell system integrated with a hybrid desiccant cooling system. Energy Conversion and Management, 296, 117699.

[2] Park, S., Abdullah, M. M., Seong, K., & Lee, S. (2023). Kinetic analysis of dibenzyltoluene hydrogenation on commercial Ru/Al2O3 catalyst for liquid organic hydrogen carrier. Chemical Engineering Journal, 474, 145743.

European Fuel Cells and Hydrogen
PIERO LUNGHI CONFERENCE
September 17th–19th 2025
Capri / Italy

Dual-Doping of Transition Metals into the Double-Perovskite $La_{0.3}Sr_{1.7}Fe_{1.5}Mo_{0.5}O_{6-\delta}$ for Potential Electrode Material in SOECs: Increased Stability in Hydrogen

Agata Ducka*[a], Patryk Błaszczak [b], Beata Bochentyn [a], Piotr Jasiński [b]
* corresponding author: agata.ducka@pg.edu.pl
[a] Advanced Materials Center, Faculty of Applied Physics and Mathematics, Gdańsk University of Technology, ul. G. Narutowicza 11/12, 80-233 Gdańsk, Poland
[b] Advanced Materials Center, Faculty of Electronics, Telecommunications and Informatics, Gdańsk University of Technology, ul. G. Narutowicza 11/12, 80-233 Gdańsk, Poland
Keywords: doping, phase transition, double perovskite, Ruddlesden-Popper perovskite

Abstract

$Sr_2Fe_{1.5}Mo_{0.5}O_{6-\delta}$ (SFM) is a promising material for electrodes in the SOCs due to its high electrical conductivity in oxidizing and reducing atmospheres. However, the double perovskite structure transforms into Ruddlesden-Popper layered perovskite under highly reducing atmospheres, limiting its potential use as a hydrogen electrode. Thus, efforts need to be put to enhance the redox stability of those compounds. In this work, the materials based on La-doped SFM with two additional transition metals at B-site: copper and cobalt or nickel are presented. It was found that the stability benefited from the synergistic effect of both dopants, while the catalytic performance was enhanced due to the exsolution of well-dispersed nanoparticles when compared to the non-doped SFM material.

Introduction:

One of the objectives of the European Green Deal is to reach neutrality for the climate until 2050. To achieve this, new technologies for electricity production have to be developed and implemented. Among others, hydrogen-based devices such as Solid Oxide Cells (SOCs) may be found. In SOFC configuration, they can convert the chemical energy of the fuel into electrical energy. The advantage of this setup is that it can operate with fuels other than hydrogen only or in a reverse mode known as an electrolyte setup (SOEC). Currently, the focus is on developing new electrode materials that can withstand the carbon-rich atmospheres with sufficiently high catalytic performance. Among many materials studied, double perovskites $A_2BB'O_6$ can be found. One of the representatives of this family is the strontium ferrite molybdate with a general formula $Sr_2Fe_{1.5}Mo_{0.5}O_{6-\delta}$ (SFM), which is commonly known to have a high ionic and electronic conductivity [1] in both oxidizing and reducing atmospheres. There is no clear agreement on the stability of this compound in hydrogen, because several studies, i.e. [2] claimed that it tends to transform into Ruddlesden-Popper (RP) layered perovskite, which is a serious drawback from its potential use as a hydrogen electrode.

In our previous work [3], we have found that the addition of La at the A-site not only increases the electrical conductivity but also stabilizes the structure to some extent. To perform exsolution, transition metals are incorporated at B-site during synthesis. Previously, we studied the monodoped SFM with Ni, Co, or Cu. For nickel and cobalt, the phase transition was observed. Also, the higher the doping level, the more RP was found. At the same time, an enormous number of bimetallic nanoparticles were formed on the surface, which may work as a catalytic centres for various reactions. Interestingly, no such phase change was found in the case of Cu doping, but less nanoparticles were visible. This observation led to the idea that dual doping of Cu with Co or Ni would benefit from the synergistic effect of both dopants.

Objectives:

The main objective of the presented study was to synthesise a single-phase material based on double perovskite and to analyse its stability in the reducing atmosphere. The hypothesis was stated that dual doping with copper and another transition metal (nickel or cobalt) would suppress the formation of the RP phase (due to the presence of Cu) and at the same time promote the formation of the well-dispersed nanoparticles on the surface (due to the Ni- or Co-doping).). Finally, materials were characterized for potential use in SOCs and the most promising composition was determined.

Materials and methods:

A series of compounds with a composition $La_{0.3}Sr_{1.7}Fe_{1.35}Mo_{0.45}(MCu)_{0.2}O_{6-\delta}$ (LSFM, where M=Ni or Co) were synthesised by the Pechini method. The ratio of M:Cu was changing to find the composition with the most promising properties, but the number of dopants did not exceed 0.2. Furthermore, the Fe:Mo ratio was fixed at 3 to suppress the formation of Mo- or Fe-rich phases. The obtained materials underwent structural analysis by means of XRD technique. After confirming the initial phase purity, the powders were reduced in hydrogen in a tube furnace at 700, 750 and 800 °C. Then, the possible structural changes were examined again by the XRD method with most of the focus being on the possible phase transition to Ruddlesden-Popper layered perovskite. The TPR technique was implemented to study the reducibility of the compounds and the impact of different doping ratios. Electrical conductivity was measured on dense rectangular bars using the DC4W method. The morphology was studied using a SEM microscope coupled with an EDX spectrometer. The selected, most promising samples also underwent XPS measurements to reveal the oxidation state of transition metals before and after reduction. In order to determine the thermal expansion coefficients and compare them with conventionally used electrolytes, dilatometry was used. Finally, the selected material was applied as a layer for SOECs.

Results:

The reduction of a single-phase materials in the range between 700-800 °C resulted in a slight formation of a Ruddlesden-Popper phase only at high temperatures (800 °C); otherwise the

structure remained stable. Fig. 1 presents XRD patterns of LSFM-CoCu with an equal amount of Co and Cu in the as-prepared state (initial) and reduced at 700 and 800 °C, respectively. Furthermore, after reduction at 800 °C, significant amount of exsolved nanoparticles formed on the surface. The exemplary microstructure revealed by SEM imaging is shown on the right in Fig.1. The TPR profiles show that the incorporation of additional dopants resulted in a shift in the reduction temperatures. The electrical conductivity of the compounds in both air and hydrogen is sufficient for use as electrode materials.

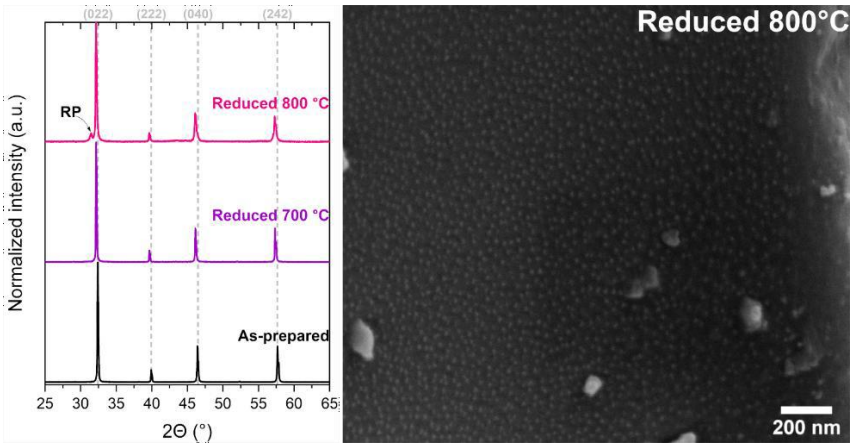


Fig. 1. XRD patterns of LSFM-CoCu before and after reduction (left); SEM micrograph of LSFM-CoCu reduced at 800 °C in hydrogen (right).

Conclusions: Dual-doping with copper and other transition metals, such as nickel or cobalt, significantly enhances the stability of the SFM-based compounds. The exsolution phenomenon occurring in the hydrogen makes them interesting from a catalytic point of view. Overall electrical performance makes these materials promising candidates for hydrogen electrodes in SOECs.

Acknowledgment

This work was supported by a project funded by National Science Centre Poland, based on decision UMO-2022/45/N/ST5/02933 (PRELUDIUM).

References

[1] Skutina et al. Undoped Sr_2MMoO_6 Double Perovskite Molybdates (M = Ni, Mg, Fe) as Promising Anode Materials for Solid Oxide Fuel Cells. Materials 2021;14. https://doi.org/10.3390/MA14071715.

[2] Lv et al. In Situ Investigation of Reversible Exsolution/Dissolution of CoFe Alloy Nanoparticles in a Co-Doped $Sr_2Fe_{1.5}Mo_{0.5}O_{6-\delta}$ Cathode for CO_2 Electrolysis. Advanced Materials 2020;32. https://doi.org/10.1002/ADMA.201906193.

[3] Ducka et al. Investigation of the phase transition to the Ruddlesden-Popper phase in La- or Nb-doped $Sr_2Fe_{1.5}Mo_{0.5}O_{6-\delta}$ double perovskites. Impact of lanthanum or niobium doping. Nanoscale, accepted for publication

On the effects of platinization of commercial titanium Porous Transport Layers in PEM water electrolysis cells

Elena Crespi*, Giulia Di Gregorio, Takwa Cheraiet, Matteo Testi
*corresponding author: ecrespi@fbk.eu
Fondazione Bruno Kessler (FBK), Center for Sustainable Energy (SE), Trento, Italy

Keywords: Pt coating, PTL, testing, characterization

Abstract:

Given the need of improving PEM electrolysis cell performances, this study investigates the role played by a thin Pt coating deposited on Ti PTL. The testing activity shows that, with some innovative commercial CCM with low Ir loading, the Pt coating allows to notably increase the performance at beginning of test, as well as the cell durability.

Introduction: Reducing the cost of producing hydrogen through water electrolysis powered by renewable electricity is fundamental in making renewable hydrogen economically competitive, thus allowing it to play a role in the decarbonization process. In this framework, improving the performance of the electrolysis systems is essential. For this reason, the Clean Hydrogen Joint Undertaking has set targets on the performance of each electrolysis technology in the Strategic Research and Innovation Agenda 2021-2027 [1]. For Proton Exchange Membrane (PEM) water electrolyzers, the 2030 target for the nominal system specific consumption is 48 kWh_e/kg_{H2}, to be reached with a nominal current density equal to 3 A/cm^2 and maximum use of critical raw materials as catalysts equal to 0.25 mg/W. To reach these targets, research efforts are mainly focused on the improvement of the Membrane Electrode Assembly (MEA), including the proton conducting membrane, anodic and cathodic catalyst layers, and Porous Transport Layers (PTL). Regarding catalysts, research mainly focuses on reducing the loading of noble metals while guaranteeing high performance by innovative production methods [2].

Objectives: This work focuses on assessing the impact that the deposition of a thin Pt coating on anodic Ti PTLs has on the performance of a PEM electrolysis cell adopting state-of-art commercial Catalyst Coated Membrane (CCM), with reduced catalyst loading.

Material and methods: An in-house developed sample holder is used to perform the test. The sample holder is optimized to test CCMs with an active area equal to 25 cm^2 with cathodic pressure up to 30 bar. The cell is assembled by applying a force of 24 kN on the total area, resulting in a uniform pressure of approximately 2.5 MPa on the active area (measured with pressure sensitive films, Fujifilm Prescale LW). The applied clamping force is defined according to the results of preliminary tests, where the electrochemical cell performances were

observed to increase while increasing the clamping force from a minimum value of 10 kN, reaching an asymptotic behavior at 24 kN. On the cathode side, a 1.7 mm thick graphite felt is used as PTL (SIGRACET® ECM 250, by SGL Carbon) while, on the anode side, a 1.7 mm thick platinum coated titanium mesh (by Saveions) is used for water distribution and a 0.28 mm thick sintered metal powder titanium plate (by Mott) is used as PTL. To investigate the effect of platinization of the Ti PTL, a platinum coating has been deposited through electrodeposition by a third-party company. Three commercial CCMs from different suppliers (named A, B and C in the following) have been tested, whose production process is not disclosed, with the same catalyst loading: 1 mg_{Ir}/cm^2 at anode and 0.4 mg_{Pt}/cm^2 at cathode.

An in-house developed test bench is used to perform the electrochemical tests. The cell is operated with dry cathode, while anode is supplied with 0.2 L/min of ultra-pure water (conductivity below 0.03 µS) at 65°C. Produced gases leave the cell at ambient pressure. The testing protocol includes a preliminary hydration phase, where hot water is circulated through the cell for 2 hours, followed by cell polarization. An initial characterization phase is followed by 17 hours of operation at constant voltage (2.0 V) and by a second characterization phase. The characterization includes current-voltage polarization curves (from 1.4 V to 2.0 V and backward, voltage variations 0.005 V/s) and Electrochemical Impedance Spectroscopy (EIS, performed at 1.6 V, 1.8 V, 2.0 V – amplitude 10 mV, 10^{-2}-10^5 Hz - and, when possible, at 50 A – amplitude 2 A, 10^{-2}-10^5 Hz). Additionally, SEM-EDS analysis of bare and Pt-coated PTL is performed before and after electrochemical testing to track changes in morphology and elemental composition.

Results: Figure 1 compares the polarization curves obtained with CCM samples A, B and C. For all tested CCMs, a substantial increase in electrochemical performance with the use of Pt-coated PTL is evident, although the gain value is strongly dependent on the CCM sample: at beginning of test the current at 2 V increases of 22, 2 and 7 times for sample A, B and C, respectively. Additionally, comparing curves obtained at beginning of test and after 17 hours of operation at constant voltage, it can be said that Pt-coated PTL guarantees a lower performance drop over time.

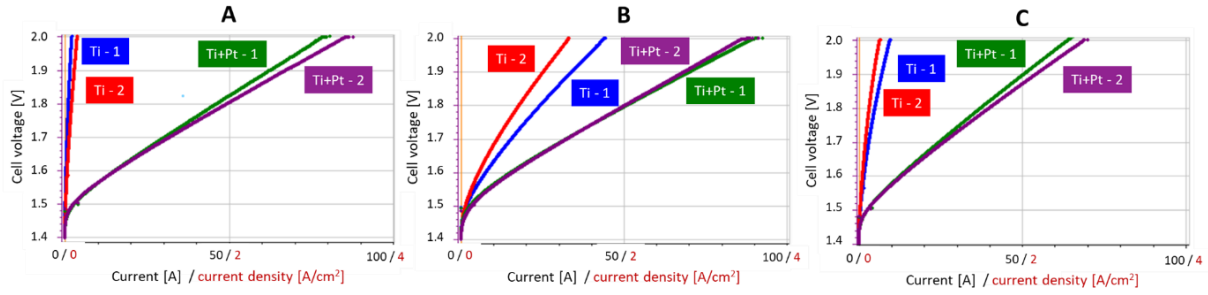


Figure 1 – Comparison of polarization curves at beginning of test (1) and after 17 h of operation (2) with bare PTL (Ti) and coated PTL (Ti + Pt), for 3 different commercial CCMs: sample A, B and C.

The higher performances obtained with Pt-coated PTLs can be explained by a reduction in the contact resistance, as shown in Figure 2 for CCM sample B, where EIS curves at 50 A and at 1.8 V highlight the positive role of the platinum coating in reducing high frequency resistance

(HFR), representing the overall ohmic resistance of the cell, mainly due to resistance to proton transfer through the membrane and contact resistance between the cell components. Additionally, for sample B, the HFR shows negligible variation with Pt-coated PTL (+2%) after constant voltage operation, which is not the case with bare PTL (+12% at 50A).

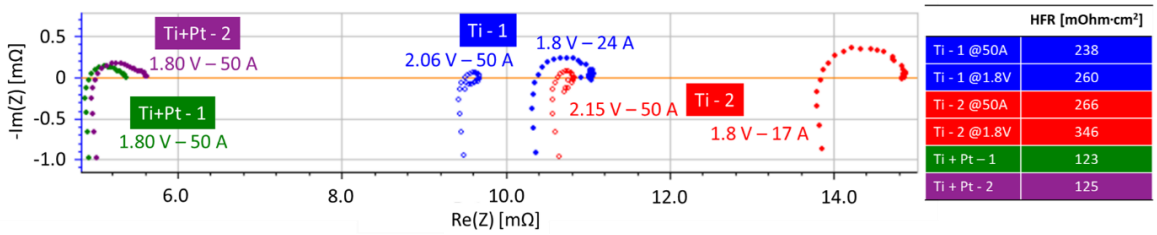


Figure 2 –EIS curves at beginning of test (1) and after 17 h of operation (2) with bare PTL (Ti) and coated PTL (Ti + Pt), at 1.8V and at 50A.

Figure 3 shows SEM-EDS mapping analyses of bare and Pt-coated PTLs before and after electrolysis. Prior to electrolysis, the bare PTL exhibits a relatively smooth surface with no detectable Pt, while the Pt-coated PTL displays a more textured morphology due to the Pt coating, which contributes to reducing interfacial contact resistance from the beginning of operation. After electrolysis, elemental analysis reveals notable differences in composition: Ir and F are detected on the bare PTL, whereas no trace of these elements is found on the Pt-coated PTL. This suggests that the Pt coating may enhance stability by minimizing Ir dissolution (well-known to occur under high anodic potential and acidic conditions of PEM electrolyzers) and limiting ionomer degradation (to whom F presence is often associated) [3]. These findings indicate that the Pt coating plays a crucial role in mitigating degradation phenomena at the anode, likely due to its impact on the local electrochemical conditions.

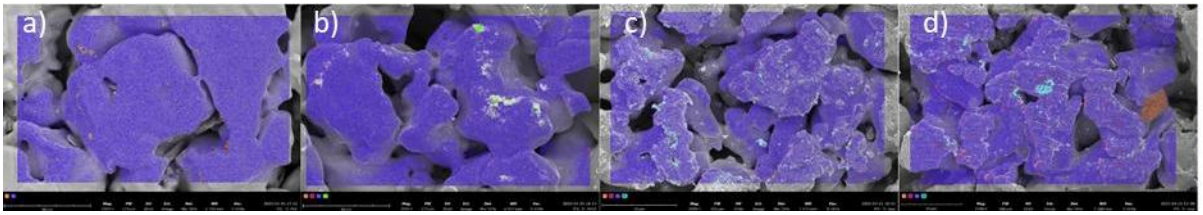


*Figure 3 –SEM-EDS of **a)** bare PTL before and **b)** after electrolysis and of **c)** Pt-coated PTL before and **d)** after electrolysis.*

Conclusions: The experimental activity highlighted the strong impact that a thin Pt coating deposited on Ti PTL has on the performance of PEM electrolysis cells when commercial innovative CCM with low Ir loading are adopted, increasing not only the durability, as already investigated in scientific literature, but also the performance at beginning of test. The effects of Pt coating will be further investigated in the following months, studying the effect of the coating thickness with in-house sputtering of Pt, and comparing PTLs with different structures (e.g., fibers) and CCMs with different catalyst loading. Material characterization will be expanded with XPS, XRD, and contact angle analysis.

References

[1] Strategic Research and Innovation Agenda 2021-2027, Clean Hydrogen Joint Undertaking (Clean Hydrogen JU), 2022
[2] Sustainable Energy Fuels, 2023, 7, 3560, doi: 10.1039/d3se00336a
[3] D2.1 – Degradation phenomena compendium, Project Electrolife, Clean Hydrogen Partnership GA No. 101137802

Hydrogen Production from Lignocellulosic Agro-Residues via Thermo-Catalytic Pathway

N. Cerone[a], M. Nacken[b], F. Zimbardi *[a], L. Contuzzi[a], U. Calice[c], T. Pecirep[b], C. Florio[a], G. Santilli[a], M.O. Carnevale[a], C. Ragone[a], V. Valerio[a], A. Villone[a]

* corresponding author: francesco.zimbardi@enea.it

[a] ENEA, Dipartimento Tecnologie Energetiche e Fonti Rinnovabili, SS 106, 75026 Rotondella (MT), Italy

[b] C&CS catalysts and chemical specialties GmbH, Georg-Wimmer-Ring 25, D-85604 Zorneding, Germany

[c] Università degli Studi della Basilicata, Via dell'Ateneo Lucano 10, 85100 Potenza, Italy

Keywords: biomass, catalysis, gasification, hydrogen

Abstract

Introduction: Hydrogen production from lignocellulosic biomass, particularly agricultural, agro-industrial, and forestry residues, is a sustainable and efficient route to clean energy. This approach offers several benefits, including lower GHG emissions—since biomass absorbs CO_2 during its growth—and enhanced circularity in the bioeconomy through the valorization of waste feedstocks. Thermo-catalytic and biochemical pathways are available, they differ fundamentally in their processes, reaction conditions, and efficiency. Biochemical pathway relies on microbial fermentation or enzymatic hydrolysis to convert biomass into biohydrogen, it operates at lower temperatures, making it more energy-efficient, but has slower reaction rates, lower yields, and is sensitive to feedstock composition and microbial performance. Thermal processes are fast, allow continuous operation, and achieve high hydrogen yields but requires advanced gas cleaning and catalyst stability at elevated temperatures. Gasification, often combined with catalytic processes, is the most widely used thermal process to convert biomass. The gasification process occurs at a sub-stoichiometric supply of oxygen, leading to the thermal decomposition of biomass into synthesis gas (syngas), primarily composed of CO, H_2, CO_2, and small fractions of CH_4 and other light hydrocarbons. The resulting syngas requires extensive purification to remove condensable organic compounds, which can otherwise constitute a significant fraction of the byproducts. To enhance H_2 yield and syngas quality, catalytic steam reforming plays a crucial role by converting complex organic molecules and CO into additional H_2. The development of

innovative catalysts with high stability and efficiency at lower temperatures is essential for optimizing this process. Furthermore, testing these catalysts in large-scale, representative systems, is critical to assessing their performance and long-term durability, ensuring their practical applicability in industrial H_2 production.

Objectives: This study evaluated the effectiveness of a two-stage catalytic system for tar reforming to purify syngas and enhance H_2 content at pilot scale using a stream of syngas from a updraft gasifier fed with hazelnut shells [1]. The steam reforming of tar contained in the syngas involved an initial treatment with dolomite, a cost-effective catalyst known for tar conversion efficiency. Then the partially cleaned syngas underwent further treatment by a novel fixed-bed catalyst, which already demonstrated superior performance in catalytic hot gas purification when model compounds were used to simulate tar [2]. In this work this catalysts was tested as catalytic fixed bed to treat syngas with high level of tar obtained from updraft gasifier.

Material and methods: The experiments utilized a side stream from the PRAGA gasification plant, which operates with a nominal feedstock input of 20–30 kg/h [1]. A syngas flow was drawn from the reaction bed. The raw syngas was transported via a thermally insulated pipeline at 250°C to a cracking section consisting of two reactors in series, each measuring 60 cm in length and 5 cm in diameter, with an effective volume of 980 cm^3. The system was housed in a vertical electric furnace. This setup enabled dolomite to function not only as a catalyst but also as a chemical scavenger for sulfur and chlorine contaminants. In the second stage the novel the catalyst C&CS #1050 B was used, it is a new class of Ni-based catalysts, initially developed form methane reforming in a Sorption Enhanced Reforming (SER) process [3], then tested for more complex organic molecules typical of tar. This catalyst features an high specific surface area, efficient Ni dispersion within the particle, and mechanical strength. Catalytic reforming was conducted at different temperatures in the range 650°C - 750°C, and different gas hourly space velocities (GHSV). The entire pilot system, including both the gasification and catalytic sections, was equipped with an online gas chromatography (GC) system for real-time monitoring of non-condensable gases (N_2, H_2, CO, CO_2, CH_4, O_2). Additionally, syngas samples were collected at the gasifier outlet and after the catalytic unit for offline analysis of water and organic volatiles, following the CEN/TS 15439:2006 standard HPLC and GC-MS characterization. Conversion efficiency of tar and hydrogen yields were calculated from analytical data and mass balance based on N_2 balance [4].

Results: The BET surface area of the catalyst was measured as 58.3 m2/g, that is 3.9 fold higher compared to the average value of surface areas of typical $MgO\text{-}Al_2O_3$ or $CaO\text{-}Al_2O_3$ supported Nickel steam reforming catalysts. The high surface area of tha catalyst was

generated on the basis of a synthesized high surface area support by impregnating the porous support with a high NiO amount at a high dispersion. The relatively high surface area at high temperature is responsible for the observed high performance of this catalyst. The tar contained in stream of syngas was efficiently reformed with conversion higher than 99%, as determined by the GC-MS and HPLC quantitative analysis. After the treatment, the H_2 production increased from the steam tar reforming and part from the conversion of CO by WGS. The treatment resulted in gain of energy for each cubic meter of syngas draft from the gasifier.

Conclusions: In this study, we demonstrated the effectiveness of biomass tar conversion by catalytic steam reforming while simultaneously increasing the H_2 content in the upstream, at pilot scale. This distinct increase in the real tar abatement capacity was confirmed, besides its previous testing with model compounds [2]. Using two catalysts, one cheap and moderately performant, the other more expensive and complex to produce, is an effective strategy to clean up syngas from tar and increasing the hydrogen production from biomass. This is a valuable option for the gasification occurring at low temperature characterized high energy efficiency, simple and robust operation, but also producing relatively large quantity of organic volatiles.

Acknowledgment

Work funded by the Italian Ministry of the Environment and Energy Security, program agreement MiTE_ENEA, PNRR - Hydrogen Research - Mission M2-C4 - Investment 3.5: Research and development on hydrogen.

References

[1] Cerone, N., & Zimbardi, F. (2018). Gasification of Agroresidues for syngas production. Energies, 11(5), 1280. https://doi.org/10.1016/j.fuproc.2017.07.027

[2] Nacken, M., Papa, A. A., & Di Carlo, A. (2024). Novel High Performance Catalyst for Complete and Energy Efficient Tar Reforming in Biomass Derived Syngas. Chemical Engineering Transactions, 109, 103-108. https://doi.org/10.3303/CET24109018

[3] Nacken, M. (2023) Novel steam-reforming catalyst for H_2 production with reduced CO_2 emisissions. Specialty Chemicals Magazine GEN/FEB 2023, pp 14-16 (joomag.com)

[4] Cerone, Nadia, et al. "Production of hydrogen-rich syngas from biomass gasification by double step steam catalytic tar reforming." International Journal of Hydrogen Energy 95 (2024): 1215-1221. https://doi.org/10.1016/j.ijhydene.2024.07.290

European Fuel Cells and Hydrogen
PIERO LUNGHI CONFERENCE
September 17th–19th 2025
Capri / Italy

Development of a decision-oriented tool for operational management of a PEMWE

Federico Del Mondo[a], Marco Russo Cirillo [a], Davide Pivetta [a], Marco Bogar[a], Rodolfo Taccani*[a]

* corresponding author: taccani@units.it

[a] Department of Engineering and Architecture, University of Trieste, 34127 Trieste, Italy

Keywords: #PEMWE #numerical model #electrolysis management #dynamic operation

Introduction: The hydrogen production via electrolysis represents a key pathway for decarbonizing shipping and contributing to carbon neutrality goals, as it enables the generation of green hydrogen with potential zero emissions. The electrolysers system management directly impacts on the cost-effectiveness of green hydrogen production and thus enhancing the overall competitiveness of the electrolysis technology.

In the context of Hydrogen Valleys development hydrogen production via Proton Exchange Membrane Water Electrolysis (PEMWE) is gaining increasing attention, with approximately 20% more facilities adopting PEM technology compared to alkaline ones [1], especially in renewable energy sources (RES) powered plants [2].

However, in large-scale industrial applications, for a determined market demand and in the case of coupling PEMWE with RES, optimal management strategies for hydrogen production are required to ensure effective operation under dynamic power supply conditions. In [3], it is highlighted that in order to ensure the economic viability of hydrogen production, a holistic approach that consider all interconnected variables of PEMWE under dynamic operation should be considered. In this context, data-driven approaches, such as Machine Learning and Digital Twins models, will play a key role in managing electrolysis systems under dynamic power conditions, enabling strategic decisions to be made for electrolyser operation.

Objectives: This research is to develop a comprehensive numerical model of a PEMWE offering insights into system management under variable load conditions driven by RES availability, electricity market price, and weekly hydrogen demand, while avoiding operational conditions that could lead to increase the energy intensity of the process. The work it is placed in a wider framework in which the resulting datasets, obtained through the model numerical simulation, are used to train a physics-based Digital Twin.

Materials and methods: The reference scenario features on a 5 MW PEMWE connected to a 5 MW_P photovoltaic (PV) plant and supported by a 5 MWh battery energy storage system for an yearly hydrogen production of 390 tons. At nominal power conditions, the system achieves a hydrogen production rate of 90 kg/h with an efficiency of about 56 kWh/kg, in line with the technical specifications in the datasheet [4].

the electrolytic cell voltage as sum of the reversible, activation and ohmic overvoltage through the relationships introduced in [5]. A voltage increase of 0.19 %/1000h at 2.2 A/cm^2 [6], corresponding to nominal load operation, is assumed. Below this threshold, the voltage increase is reduced linearly, and an additional contribution of 0.147 mV per cycle is considered for on-off operations. [7]. The system numerical simulation, following a bottom-up approach, is applied to the system: the hydrogen demand by the market ($H2_{dem}$) and the availability of stored hydrogen ($H2_S$) schedules the production of hydrogen, and the energy (E_{PEMWE}) requested by the PEMWE is provided based on RES availability from the PV plant, or electric grid. The model evaluates the economic and lifetime impact trade-off of hydrogen production accounting for different energy management strategies and enabling decision-informed system control for electrolyser operation.

Figure 1 introduces the considered hydrogen production system of this study, including the data flows employed for its modelling.

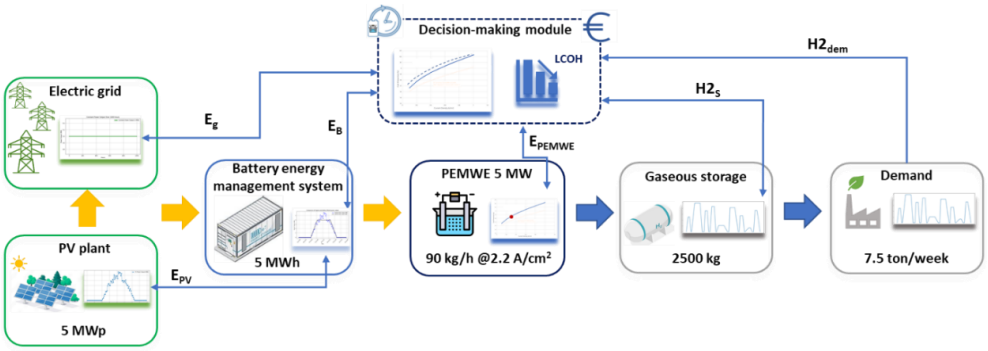


Figure 1: Schematic workflow of the hydrogen production system including the data flow exchange with the decision-making module.

Results: A weekly hydrogen demand—and corresponding production target—of 7.5 tons has been evaluated, assuming a fixed daily photovoltaic power generation of approximately 34 MWh and different PEMWE operational strategies (e.g. constant operation at 1A/cm^2). The weekly capacity factor (Cf_w) indicates the fraction of hours of PEMWE operation over the entire week. Table 1 summarizes the energy cost for each scenario considered in the analysis; the green scenario assumes that the surplus energy generated by the PV plant is used on-site while the blue and light blue scenarios consider the sale of surplus energy to the grid. Figure

2 presents the results of the economic analysis resulting from the different system management strategies. The diagonal stripes represent the impact of surplus energy—either sold or used on-site—on lowering the unit cost of hydrogen production.

Scenario	Energy from PV	Energy from grid	Energy sold to grid
Green	85	130	/
Blue	85	130	100
Light blue	70	130	100

Table 1: Scenarios considered in the analysis, the values are in [€/MWh].

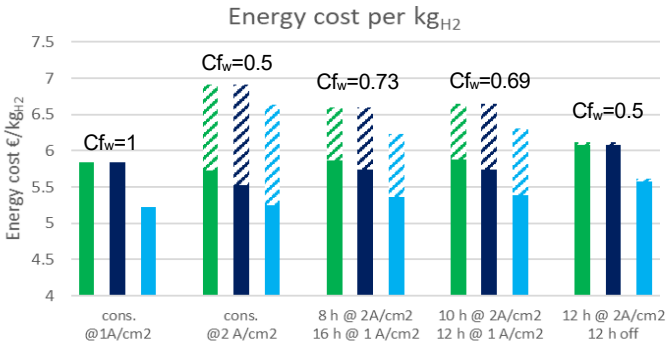


Figure 2: Energy cost per unit of produced hydrogen considering different operational strategies and market conditions.

Conclusions: The results highlight the significant impact of energy costs on the overall cost of hydrogen production. For example, under the considered management strategies, a 25% reduction in the energy cost per kilogram of produced hydrogen is achieved. However, addressing the complexities of real-world operations requires a system capable of adapting to variable hydrogen demand by selecting the optimal management strategy in real time. The increasing energy demand from hydrogen production systems during their lifetime is a critical factor to consider. However, currently, there is still a lot of uncertainty in the modelling of this phenomena but, at this stage, even simplified models can provide valuable support in introducing decision-making variables into systems modelling. Further developments of this study involve the analysis of monthly demand scenarios, supported by the implementation of an optimization tool. This tool will support decisions on the optimal management of the system with the aim of minimizing costs, taking into account the impact of operational strategies on the PEMWE lifetime.

Acknowledgements: The authors gratefully acknowledge the financial support provided by the sHYpS project (Sustainable HYdrogen powered Shipping), funded under the Horizon Europe call HORIZON-CL5-2021-D5-01, Grant Agreement No. 101056940.

References

[1] M. Bampaou and K. D. Panopoulos, “An overview of hydrogen valleys: Current status, challenges and their role in increased renewable energy penetration,” Renew. Sustain. Energy Rev., vol. 207, p. 114923, Jan. 2025, doi: 10.1016/j.rser.2024.114923.

[2] M. Carmo, D. L. Fritz, J. Mergel, and D. Stolten, “A comprehensive review on PEM water electrolysis,” Int. J. Hydrogen Energy, vol. 38, no. 12, pp. 4901–4934, Apr. 2013, doi: 10.1016/j.ijhydene.2013.01.151.

[3] H. Sayed-Ahmed, Á. . A. Toldy, and A. Santasalo-Aarnio, “Dynamic operation of proton exchange membrane electrolyzers— Critical review,” Renew. Sustain. Energy Rev., 2024, doi: https://doi.org/10.1016/j.rser.2023.113883.

[4] ITM power, “ITM Power Neptune V technical datasheet”, [Online]. Available: https://itm-power.com/products/neptune-5

[5] M. Chandesris, V. Médeau, N. Guillet, S. Chelghoum, D. Thoby, and F. Fouda-Onana,

"Membrane degradation in PEM water electrolyzer: Numerical modeling and experimental evidence of the influence of temperature and current density," Int. J. Hydrogen Energy, vol. 40, no. 3, pp. 1353–1366, Jan. 2015, doi: 10.1016/j.ijhydene.2014.11.111.

[6] CHJU undertaking, "Strategic Research and Innovation Agenda (SRIA) 2021 - 2027," 2022.

[7] A. Weiß, A. Siebel, M. Bernt, T.-H. Shen, V. Tileli, and H. A. Gasteiger, "Impact of Intermittent Operation on Lifetime and Performance of a PEM Water Electrolyzer," J. Electrochem. Soc., vol. 166, no. 8, pp. F487–F497, Apr. 2019, doi: 10.1149/2.0421908jes.

EFCH2 2025
European Fuel Cells and Hydrogen
PIERO LUNGHI CONFERENCE
September 17th–19th 2025
Capri / Italy

Seawater impact on Solid Oxide Cells materials: experimental methodology for laboratory characterization

Arianna Baldinelli*[a], Krystian Machaj[a,b,c], Anna Niemczyk[b], Marek Skrzypkiewicz[c], Michal Wierzbicki[b], Jakub Kupecki[b,c] , Alessandro Sorce[d], Marco Antonelli[a], Umberto Desideri[a]
* corresponding author: arianna.baldinelli@unipi.it

[a] University of Pisa, Department of Energy, Systems, Land and Construction Engineering - Pisa, Italy
[b] Institute of Power Engineering – National Research Institute - Warsaw, Poland
[c] Center for Hydrogen Technologies (CTH2) - Warsaw, Poland
[d] University of Genova, Department of Mechanical, Energy, Management and Transport Engineering, Genova, Italy

Keywords: hydrogen; seawater electrolysis; brackish water; solid oxide cells; experimental

Introduction: Hydrogen production via water electrolysis holds great promise, particularly for long-term renewable energy storage. Using seawater instead of fresh water could be essential for coastal and offshore applications, where large renewable generation capacity exhibits higher profitability [1], or in the event of islands [2]. Moreover, approximately 40% of the planned low-emission hydrogen production projects are located in regions experiencing water scarcity [1]. Therefore, it will be essential to utilize a variety of water sources and manage them sustainably from the point of view of the water-energy nexus [3]. Indirect seawater electrolysis entails water treatment and desalination upstream, the electrolysis process. In addition, recently a strong interest towards direct seawater electrolysis has risen [4]. However, this approach carries the risk of electrolyzer poisoning due to system failures or the presence of trace salts in inadequately treated water. This concern is especially critical for solid oxide cells (SOCs), which are highly susceptible to poisoning from chlorine and sulphur [5] — both abundant in seawater. If salts penetrate SOC stacks, they can significantly accelerate the degradation of both the stack materials and the cells themselves. Therefore, this paper shows an advanced methodological approach for the characterization of performance and durability of SOC stacks materials.

Objectives: develop an experimental methodology to address seawater effects both on solid oxide cell operation and stack materials.

Material and methods: This research focused on the microstructural and electrochemical evaluation of several materials constituting a SOC stack, namely the cell (ASC NiYSZ/YSZ/LSC), Crofer 22 APU, Stainless steel 430, and Schott GM31107 glass. Seawater was simulated with a solution of water and two model salts, simply pure NaCl and a synthetic Reef salt (Cl 19000-

19500 mg/l, Na 9720-11880 mg/l, Mg 1300-1360 mg/l, S 810-990 mg/l, Ca 410-430 mg/l, K – 360-380 mg/l, B 4,05 – 5,0 mg/l, Sr 7.2-8.8 mg/l, pH 8.0-8.2) [6]. In order to replicate different aquatic environments, two salinity levels were tested: 7 g/L (water salinity after partial treatment/brackish environment/Baltic sea) and 30 g/L (average seawater composition, like Mediterranean sea). A reference test in absence of salts is performed to compare results.

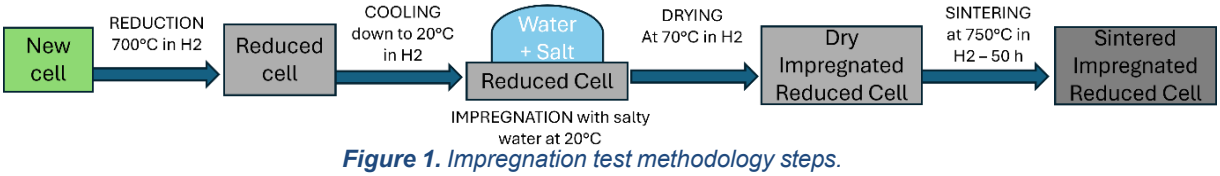


Figure 1. *Impregnation test methodology steps.*

The test protocol involves two stages: I) impregnation tests to reproduce the worst case (Figure 1) and II) operation test. Material impregnation is performed at ambient temperature on virgin material (Crofer 22 APU, NiYSZ/YSZ half cell, Schott GM31107 , Stainless Steel 430), then these undergo drying at 70°C and further sintering at 750°C for 50 hours, followed by cooling under hydrogen atmosphere down to ambient condition. Material characterization is then performed with SEM-EDS. Later, operation tests in real case involve experiments on single cells after exposure to 50:50% H_2:N_2 (fuel cell mode) and 50:50% H_2:H_2O (electrolysis mode) at the fuel electrode side, while ambient air is supplied at the air electrode. Procedures used are in-operando (electrochemical characterization of the SOCs involved linear voltammetry, long-term galvanostatic measurements, and EIS) and post-mortem (SEM-EDS).

Results: Figure 2 reports SEM pictures of SOC half cells after the application of the methodology described.

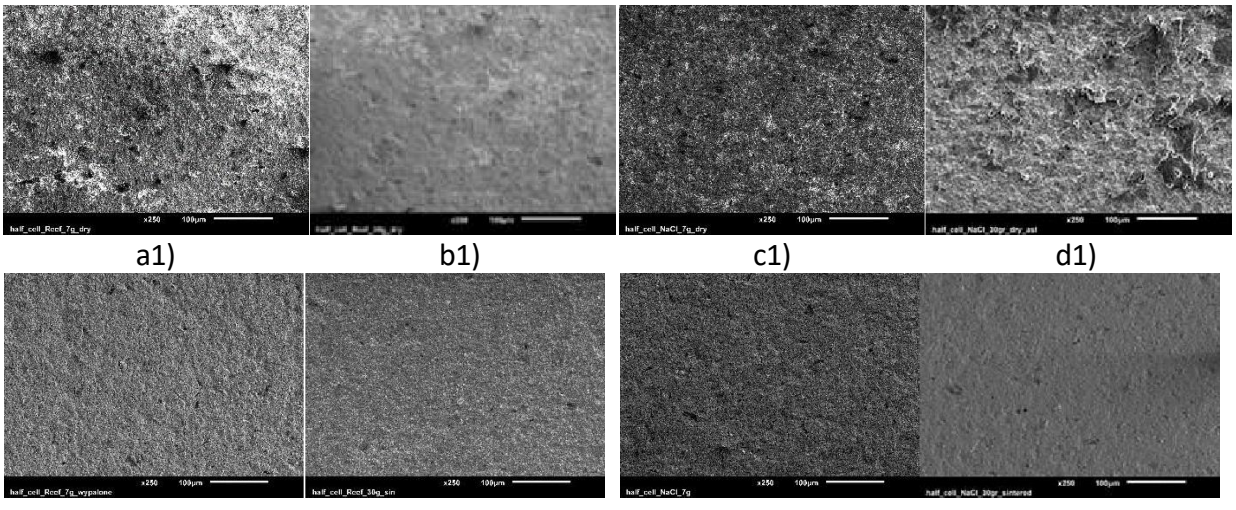


Figure 2*. Half cell dry samples SEM: a1) reef salt 7 g/L, b1) reef salt 30 g/L, c1) NaCl 7 g/L, d1) NaCl 30 g/L; Half cell sintered samples SEM: a2) reef salt 7 g/L, b2) reef salt 30 g/L, c2) NaCl 7 g/L, d2) NaCl 30 g/L*

Samples were exposed also to EDX analysis, revealing that after the sintering treatment the salt concentration on the surface of the sample decreased.The test on the half cell exposed to Reef Salt simulated seawater (30 g/l) reveled a decreased of Na concentration from 14% to 0.56% after sintering (Figure2 b1 vs. b2), while Cl fell below detection threshold. K and Ca were detectable on the sintered cell only with impregnation with higher salinity (Figure 2 b2) and are not detected on the low salinity test (Figure 2 a2). Test using a single salt compound (NaCl) confirm this trend (Figure 2 c1/C2, d1/d2) making a simple approach valid to test the effect of major salts components. However, the use of the synthetic reef salt mixture allow to investigate the presence of other elements which are typical of seawater feedstream. The same procedure was applied to the other materials constituting a SOC stack (Crofer APU, Stainelss Steel, Shott Glass sealing).

Conclusions: For the evidence collected in the impregnation test, it results that the model salts used (NaCl or the synthetic salts mixture called “Reef salt”) do not permanently bond with NiYSZ at typical SOC operating thermal conditions after 50 hours. This is deduced from the comparison of dry samples (carrying the entire salt load as er the design of experiments plan) with the same specimens after sintering. Therefore, seawater salt are desorbed and do not accumulate onto the electrode surface. Reef salts allow to investigate the impact of minor components - like K and Ca - which remain on the electrode surface at higher water salinity.

Acknowledgments

This study received funding from the European Union - Next-GenerationEU - National Recovery and Resilience Plan (NRRP) – MISSION 4 COMPONENT 2, INVESTMENT N. 1.1, CALL PRIN 2022 PNRR D.D. 1409 14-09-2022 – “POSEIDON - Photo-driven Optimal Seawater Electrolysis for energy-IslanDs OperatioN” P2022ER7KM –PE8, CUP I53D23006440001.

References

[1] International Energy Agency, Global Hydrogen Review 2024, www.iea.org
[2] Babaei R., Ting D., Carriveau R., Optimization of hydrogen-producing sustainable island microgrids, *Int. J. of Hydrogen Energy,* Vol. 47, Issue 32, 15 April 2022, Pages 14375-14392
[3] Jolaoso L.A., Asadi J., Duan C., Kazempoor P., A novel green hydrogen production using water-energy nexus framework, *Energy Conversion and Management*, Vol. 276, 2023
[4] Serafini, M., Weidner, E., Bolard, J., Hydrogen Production via Direct Seawater Electrolysis literature review, EU Commission Joint Research Center, 2025 ISSN 1831-9424
[5] Sasaki K, et al, Chemical durability of Solid Oxide Fuel Cells: Influence of impurities on long-term performance, J. of Power Sources, Vol. 196, Issue 22, 2011, 9130-9140
[6] Aquaforest Reef Salt – Product features https://aquaforest.eu/en/products/seawater/marine-salts/reef-salt/

EFCH2 2025
European Fuel Cells and Hydrogen
PIERO LUNGHI CONFERENCE
September 17th–19th 2025
Capri / Italy

Scalable development of 3D LDH gas diffusion electrodes for AEM water electrolysers

F. Basile[a*], F. Lisi[a], R. Viscardi[b], I. Gualandi[a], E. Scavetta[a], F. Mariani[a], A. Fasolini[a]

* f.basile@unibo.it

[a] University of Bologna Alma Mater Studiorum, Industrial Chemistry Department "Toso Montanari", Navile District, Via Pietro Gobetti 85, Bologna, 40129, Italy

[b] ENEA, Department of Energy Technologies and Renewable Sources, Casaccia research center, Via Anguillarese 301, 00123 Rome, Italy

Keywords: anion exchange membrane, hydrogen, layered double hydroxides, water electrolysis.

Abstract:

Anion Exchange Membrane (AEM) water electrolysis represents a cost-effective and sustainable alternative for hydrogen production. Leveraging a rapid and scalable electrodeposition procedure, the research addresses the industrial need for efficient and economically viable fabrication techniques. The tailored electrocatalysts exhibit excellent overpotential and reaction kinetics, optimizing the energy efficiency of the process. Metallic foams outperform carbon paper as gas diffusion layers (GDLs), achieving high current densities due to superior conductivity and capillary effects.

Introduction: In the last decade, AEM water electrolysis has emerged as promising technology for sustainable hydrogen production. Critical bottleneck in the process is the Oxygen evolution reaction (OER), as a multistep, four-electron transfer reaction that requires significant overpotential. Developing efficient and cost-effective catalysts for OER is thus a key challenge for improving the performance and viability of AEM water electrolysers. Layered double hydroxides (LDHs) are lamellar compounds consisting of positively charged metal hydroxide layers intercalated with charge-balancing anions and water molecules [1].

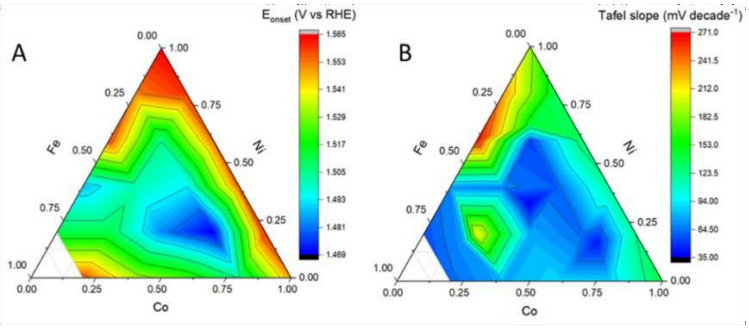


Fig. 1. *Ternary diagram of OER onset potential (A) and Tafel slope (B) as a function of the electrosynthesis bath composition [2]. Data are obtained from LSV recorded in 1.0 M KOH.*

Also known as hydrotalcite-like compounds, LDHs are characterized by high surface area and tunable composition. By incorporating various metal cations into the hydroxide layers, LDHs

offer excellent opportunities for tailoring their electronic and catalytic properties. Regarding OER performance, LDHs containing Ni, Co, and Fe showed low onset potential values and fast kinetics, therefore a huge appeal for electrocatalytic applications (Fig. 1) [2].

Objectives: The study focuses on the synthesis and optimization of Ni-based layered double hydroxides (LDHs) as electrocatalysts for AEM electrolysers. Surface modifications and doping strategies are investigated to enhance the catalytic activity and durability.

Material and methods: Electrodes fabrication occurred via potentiodynamic electrodeposition of LDHs on gas diffusion layers as carbon paper and Nickel foams [3]. Bare supports (geometric area: 6.25 cm^2) were immersed in an electrolytic bath containing catalysts precursors in form of nitrates, and two cycles of cyclic voltammetry (CV) were performed at cathodic potentials between 0 and -1.3 V vs SCE. The induced electrochemical reduction of nitrates generates an increase of the local pH at the electrode surface, leading to catalyst precipitation as LDHs. Nickel nitrate (>99%), cobalt nitrate (>98%), iron nitrate (>99%), and sodium hydroxide were purchased from Sigma–Aldrich (Germany). The deposition was carried out in a single compartment three-electrode cell (Amel, Italy), connected to a potentiostat Multi Autolab/M204 (Metrohm Italiana Srl, Italy). Characterization techniques such as X-ray diffraction (XRD), scanning electron microscopy (SEM), and electrochemical impedance spectroscopy (EIS) provided insights into the material properties and their correlation with electrochemical performance. The catalytic performance was evaluated in AEM flow cell operation (X-Cell, RedoxFlow), with key metrics including overpotential, current density, and long-term stability.

Results: The study provided an efficient and scalable solution for producing industrially viable electrodes for green hydrogen application. The physic-chemical characterization of the GDEs confirmed the accuracy of the synthetic method, providing stable and homogeneous catalyst deposition (Fig. 2). Catalyst composition was easily controlled by changing metals concentration in the deposition solution, and a wide range of transition metals was successfully placed in the LDH structure to optimize the structural and electronic properties. A quantitative SEM-EDS analysis on carbon paper electrodes confirmed the metals ratio of the precursors' solution, indicating excellent tunability of the synthesis (Table 1). The tailored electrocatalysts achieved excellent performance in terms of overpotential and reaction kinetics, minimizing the energy consumption of the process. Ni foams GDEs achieved current densities up to ten times higher than carbon paper electrodes, due to higher conductivity and capillary effect of the support, which led to a higher electrochemically active surface area.

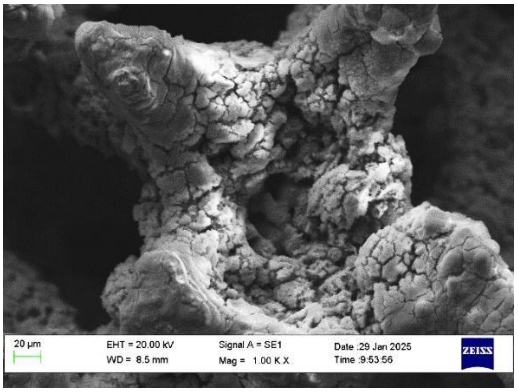


Fig. 4. SEM images of LDHs deposited on Ni foams.

Catalyst	Ni atomic ratio (%Ni)
Ni75Fe25	75 ± 2
Ni75Al25	78 ± 3
Ni67Al33	68 ± 2

Table 1. Catalyst composition obtained via SEM-EDS analysis.

The catalyst Ni75Fe25 LDH exhibited high OER activity, with an onset potential of 0.335 V vs SCE and Tafel slope of 70 mV dec^{-1} (Fig. 5). Finally, the selected OER and HER electrocatalysts were evaluated in flow cell, providing good overpotential values and stability over time.

Conclusions: The research provided an industrially viable solution for producing GDEs for AEM water electrolysers. The synthetic protocol adopted allowed stable, homogeneous, and controlled deposition of Ni-based LDHs on both carbon paper electrodes and Ni foams. The most promising electrocatalysts, tested in flow cell operation, showed low cell overpotential, good reaction kinetics, and long-term stability.

Acknowledgment

F.B. would like to acknowledge the NextGeneration EU from the Italian Ministry of Environment and Energy Security POR H2 AdP MMES/ENEA with involvement of CNR and RSE, PNRR – Mission 2, Component 2, Investment 3.5 “Ricerca e sviluppo sull’idrogeno” under the ENEA – UNIBO agreement (Procedure 1.1.3 PNRR POR H_2).

References

[1] Gualandi I, Monti M, Scavetta E, Tonelli D, Prevot V, and Mousty C. 2015. Electrodeposition of Layered Double Hydroxides on platinum: Insights into the reactions sequence. Electrochimica Acta 152:75-83.

[2] Gualandi I, Musella E, Costa G, Gazzano M, Scavetta E, Zappoli S, and Tonelli D. 2025. On the Quest for Oxygen Evolution Reaction Catalysts Based on Layered Double Hydroxides: An Electrochemical and Chemometric Combined Approach. Adv. Energy Sustainability Res. 6:2400233.

[3] Gualandi I, Vlamidis Y, Mazzei L, Musella E, Giorgietti M, Christian M, Morandi V, Scavetta E, and Tonelli D. 2019. Ni/Al Layered Double Hydroxide and Carbon Nanomaterial Composites for Glucose Sensing. ACS Applied Nano Materials 2:143-155.

EFCH2 2025
European Fuel Cells and Hydrogen
PIERO LUNGHI CONFERENCE
September 17th–19th 2025
Capri / Italy

Impact of Porous Transport Layer Microstructure on Oxygen Transport in a PEM Electrolyzer

Giuseppe Sassone*, Elena Crespi , Simone Zottele, Matteo Testi

* corresponding author: Giuseppe Sassone
Hydrogen Technologies and Resilient Energy Systems (HyRES) Unit, Sustainable Energy (SE) Centre, Fondazione Bruno Kessler (FBK), Via Sommarive 18, 38123, Trento, Italy.

Keywords: Electrolysis, Hydrogen, Multiphase Flow, Porous Transport Layer.

Abstract:

Proton Exchange Membrane (PEM) electrolyzers are promising technologies for decarbonizing energy systems through the production of renewable hydrogen. However, the performance and cost of PEM electrolyzers need to be improved and further efforts are required. A critical component affecting PEM performance is the porous transport layer (PTL), which plays an important role in the transport of species between channels and active sites for the electrochemical reaction. This work aims to evaluate the influence of PTL microstructure on pressure losses and oxygen distribution using Computational Fluid Dynamics (CFD). Both uniform porosity and gradient porosity are considered for the PTL. The CFD results will guide the next work on additive manufacturing via 3D printing.

Introduction: Nowadays, climate change and the depletion of non-renewable resources are the main reasons for developing more sustainable energy systems based on renewable energy sources (RES). In this context, Proton Exchange Membrane (PEM) electrolyzers can play a key role by using electricity from RES-based power systems to produce renewable hydrogen and decarbonize various sectors. A PEM cell is made of a Catalyst Coated Membrane (CCM) is a polymeric membrane coated with different catalysts on the two sides. The CCM is sandwiched between two Porous Transport Layers (PTL) and surrounded by a sealing system. The Bipolar Plates (BPP) are the most external components, which divide the anode and the cathode of two adjacent cells, avoiding mixing of hydrogen and oxygen, while providing mechanical support and electrical conduction. Finally, the BPPs generally host channels to supply the water to the cell and remove the gas generated. PTLs and BPPs are critical components that play a key role in ensuring efficient cell operation of the cell. The PTL has to ensure that a sufficient and uniform distribution of the water on the anodic catalyst, and that evolved hydrogen and oxygen bubbles are removed from the electrodes [1]. The high number of involved components and the required high precision make the assembly procedure of PEM electrolyzers a critical step. For this reason, it is important to simplify the process. In this

view, additive manufacturing allows to realize multifunctional electrodes that integrate the PTL and the BPP, reducing the complexity of state-of-the-art electrodes [2]. This simplifies the cell assembly, thus reducing the overall costs of the technology and the cost of producing renewable hydrogen. Additionally, 3D printing enable optimizing the design and improving the cell performance through a more precise control of PTL porosity, pore diameter, structure and morphology, as compared to sintered PTLs [3,4]. This work aims to study the impact of PTL microstructure by using Computational Fluid Dynamics (CFD) framework, considering two-phase flow through porous media. In this work the Eulerian method is considered, which is the most suitable multiphase method for simulating two phase flow with dispersed bubbles in low temperature electrolyzers [5].

Objectives: This work aims at developing a CFD framework to model a simplified PEM electrolyzer, including multiphase flow through porous media. Secondly, the impact of PTL microstructure on pressure drops is evaluated by changing the porosity in the PTL. Both uniform and gradient porosity are considered. The final objective of this study is to develop a tool aiming at supporting the planned work on the manufacturing of 3D printed PTL, by identifying the optimal microstructures.

Material and methods: CFD simulations are used to evaluate the impact of PTL microstructure on the pressure drops along the channel in a PEM electrolyzer. Numerical simulations are performed on small portions of the anode, including one single channel. Eulerian method is considered for describing the multiphase flow. Liquid water and gaseous oxygen are added for the two-phase flow. The PTL is modelled as a porous zone by introducing viscous resistance and porosity information. More specifically, both uniform homogeneous and non-homogeneous (i.e. gradient across the thickness of the PTL) porosities are considered, including three cases: uniform porosity equal to 0.4 (uniform), gradient porosity increasing towards the channel in the range 0.4-0.5 (gradient a), and gradient porosity increasing towards the membrane in same range (gradient b). A convergence study is performed to select the final mesh and to ensure the accuracy of the calculations. After that, a sensitivity analysis is performed by varying the microstructure of the PTL and considering transient simulations of 16s. Finally, the results are collected to assess the oxygen removal from the PTL towards the channel outlet.

Results: In this section the main results are summarized. The grid independence study, allowed to identify the best trade-off between computational cost and accuracy, with a total number of cells around 10^5., mass imbalance 0.9% and a relative error for oxygen volume fraction (VF) of 3%. Following the grid convergence that allowed identifying the best trade-off between accuracy and computational cost, the set of simulations have been launched for

the various PTL microstructures. Figure *1* depicts the results collected for the varied microstructures, including both homogeneous and gradient porosities.

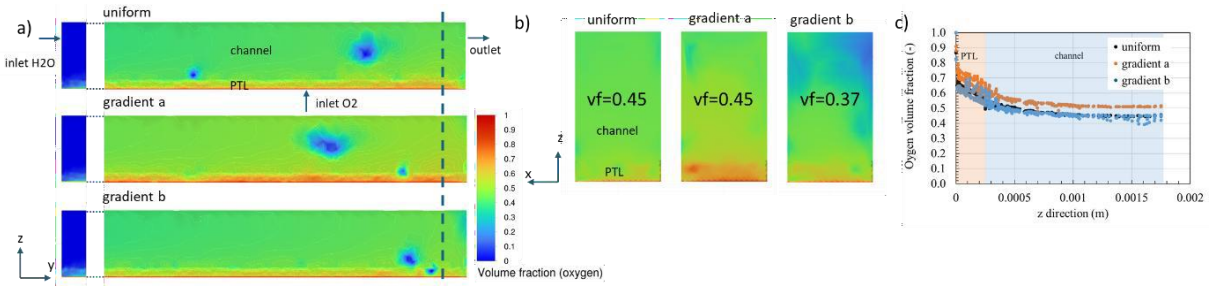


Figure 1. Oxygen volume fraction evaluated

a) along the YZ plane near the outlet, b) at the outlet, and c) near the outlet against the z-direction (see dashed lines in a).

These results underline the impact of PTL microstructure and enable the selection of the best option in terms of porosity. Considering the "gradient a" case, the VF is higher in both PTL and channel zones. This is also evident from the profile in Figure *1*c. It can be noted that in the "gradient b" case, the VF is lower at the outlet, while its value along the volume of the channel and PTL is comparable to the "uniform" case.

Conclusions

This work was devoted to the evaluation of the PTL microstructure on the pressure drops in a PEM electrolyzer. Different PTL porosities were considered for the CFD simulations. It resulted that the direction of gradient in PTL porosity affects the oxygen volume distribution within the PTL and towards the outlet of the channel. Further investigations are planned. This work paves the way for the next experimental campaign aimed at producing optimized PTL microstructure via metal powder additive manufacturing for improved PEM performance. This manufacturing technique enables precise control of the microstructural properties and eases the cell assembly procedure, limiting further post-processing and material waste, as well as providing design freedom to manufacture highly complex components.

References

[1] A. Bazarah et al., Int. J. Hydrog. Energy 47 (2022) 35976–35989.
[2] A. Baroutaji et al., Int. J. Hydrog. Energy 52 (2024) 561–584.
[3] J.K. Lee et al., J. Power Sources 559 (2023) 232606.
[4] C.-J. Tseng et S.-K. Lo, Energy Convers. Manag. 51 (2010) 677–684.
[5] M. Dreoni et al., J. Phys. Conf. Ser. 2385 (2022) 012040.

EFCH2 2025
European Fuel Cells and Hydrogen
PIERO LUNGHI CONFERENCE
September 17th–19th 2025
Capri / Italy

Residual biomass pyrolysis in fluidized-bed reactors: a data-driven approach for control and design

Matteo Baldelli*[a], Stefano Cordiner [a], Vincenzo Mulone[a]
* corresponding author: matteo.baldelli@uniroma2.it
[a] Department of Industrial Engineering, University Tor Vergata of Rome, via del Politecnico 1, 001333, Rome, Italy

Keywords: pyrolysis of biomass; fludized-bed reactor; machine learning, design and control, hydrogen production

Abstract

Introduction: The increasing global demand for sustainable and clean energy sources has driven significant interest in bio-fuel and bio-gas production. Among various renewable bio-fuel generation methods, biomass pyrolysis has emerged as a promising thermochemical approach for converting organic materials into, among others, hydrogen-rich syngas[1]. Fluidized bed reactors are widely used for biomass pyrolysis due to their efficient heat transfer, uniform temperature distribution, and ability to process various feedstocks. However, their design and control present significant challenges that impact process efficiency and product yields. Achieving optimal operating conditions requires precise control over fluidization velocity, temperature profiles, and catalyst distribution to enhance product selectivity and minimize undesired byproducts[2]. Machine learning (ML) techniques have significant potential as powerful tools for the design and control of fluidized bed reactors used in biomass pyrolysis. By leveraging large datasets from experiments and simulations, ML models can identify complex patterns in multiphase flow dynamics, optimize operating conditions, and predict reactor performance with high accuracy.[3], [4]

Objectives: In this work, the integration of ML techniques to develop a reduced order model for fluidized-bed reactors used for the pyrolysis of residual lignocellulosic biomass , is proposed. In particular, the proposed methodology serves as a demonstration platform for the potential of ROMs to simulate complex systems, enabling the development of reliable tools for real-time control and the design of pyrolysis fluidized-bed reactors for bio-fuel and bio-gas production[5].

Material and methods: Developing ROMs based on ML techniques, requires a large quantity of data for the training phase. In this work, the primary data source are CFD simulations of fluidizing-bed reactors. In this study, an Euler-Euler model is used to simulate the fluidized-bed reactors for biomass pyrolysis. The reactor geometry is simplified as a 2D domain and it is parameterized by its height H (up to 1.5 m) and diameter D (up to 0.35 cm), allowing for a systematic exploration of different design configurations. The reactor walls are maintained at a constant temperature T_w, equal to the pyrolysis temperature T_p (up to 873 K). The biomass mass flow rate remains fixed, while the outlet pressure is set at 1 bar. At the reactor inlet, a constant carrier gas velocity, v, is imposed (up to 0.4 m/s) to maintain stable fluidization conditions. The kinetics mechanism of the biomass follows the model proposed by Ranzi *et al* [6]. To investigate the influence of operating and design parameters, the Latin

Hypercube Sampling (LHS) technique is employed. This method enables an efficient selection of parameter variations, ensuring a broad and statistically meaningful exploration of the design space. The sampled parameters include pyrolysis temperature, carrier gas velocity, reactor height, and reactor diameter. By varying these factors, a total of 26 simulations are generated, each characterized by a unique combination of process and design conditions, hereinafter called design points (dps). This approach provides a robust dataset for analysing the effects of different operating conditions on reactor performance .Detail about the geometry and boundary conditions are summarized in Fig.1(a). Simulations results were then used to train two different NNs. The first NN, named NN_y, aims to predict the pyrolysis yield given design and process parameters. The second one, named NN_p, is dedicated to provide design and process information given a range of the desired products divided in the three macro-categories char, bio-oil and bio-gas.

Results:

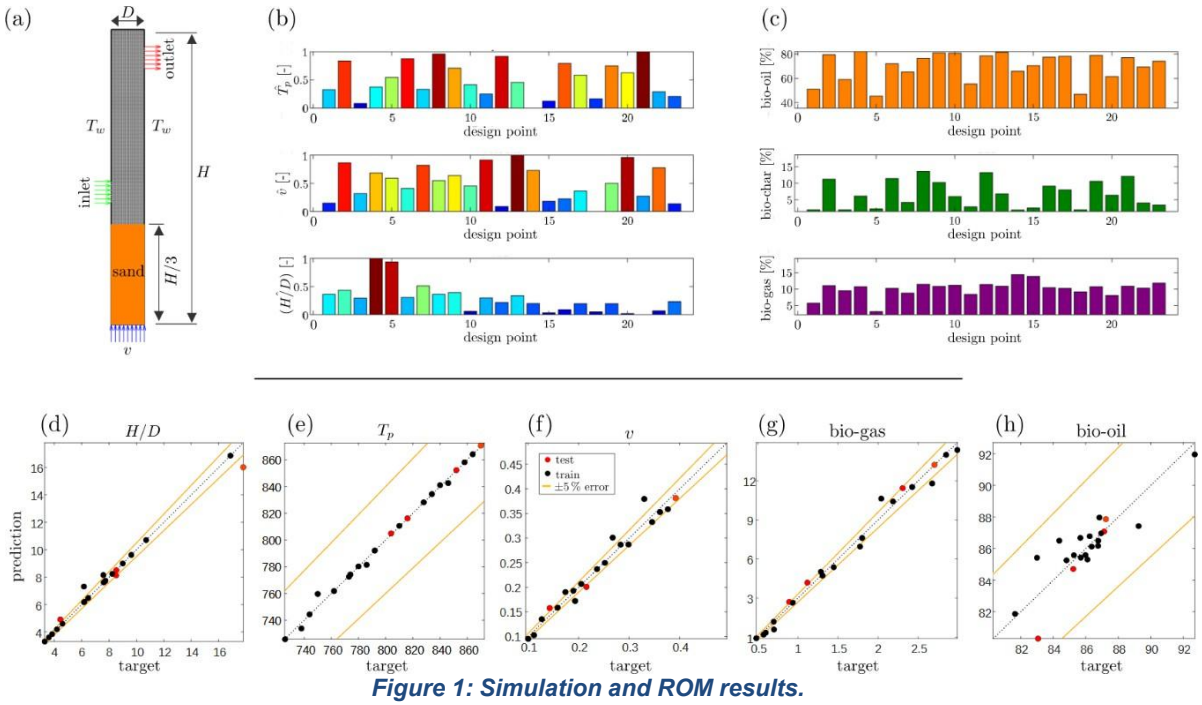


Figure 1: Simulation and ROM results.

(a) 2D CFD simulation domain sketch. (b) Normalized parameter values for each design point (simulation). (c) Percentage with respect to the total mass of the product yield for each simulation (weighted). (d, e, f) Parity plot, predictions vs. actual values, for the NN_y. (h, h) Parity plot for NN_p, for bio-gas and bio-oil.

The simulation results, summarized in Fig.1(b, c), indicate that design points characterized by moderate to high temperatures, relatively short residence times, or reactors with a low aspect ratio H/D, maximize oil production, thereby enhancing biofuel yield. To optimize the production of gaseous products such as methane and hydrogen, it is necessary to operate at high temperatures and low residence times. Despite the different reactor configurations analyzed, the bio-gas yield remains consistently stable, ranging between 12% and 15% of the total mass. A significant reduction in bio-gas production is observed only in configurations with low temperatures, low gas velocities, and high aspect ratios. This behavior can be attributed to the relatively long residence times, which tend to decrease the formation of gas and oil while increasing char production.

The simulation data are therefore used to train the two NNs (NN_y and NN_p). For both the NNs, the training was carried out using the 70% of the data for the actual training, while the remaining 30% was equally divided between the test and validation set. The number of training epochs is determined automatically based on the validation set error. Specifically, training is considered successful when the error on the validation set, evaluated using the RMSE, falls below 10^{-4}. As shown in the Fig. 1, the network performance results are presented using parity plots. In these plots, the predicted values of a given quantity are compared to their actual values, where a perfect prediction aligns with the diagonal bisector of the quadrant. As illustrated in Fig.1 (g, h), the prediction of product yields, given the design parameters , H/D, v, and T_p, consistently remains within a 5% error margin (indicated by the area enclosed within the orange lines). This confirms that the quality of training has led to the development of a reliable ROM. The trained network can therefore be employed as a real-time control tool. By predicting system outputs, it provides insights into how process parameters should be adjusted to achieve the desired output for a given feedstock composition. Fig.1 (d, f) display the parity plots for the NN_p, designed to predict optimal design parameters such as the aspect ratio H/D. In this case as well, the error remains consistently close to or below 5%, validating the network's applicability as a design tool to determine reactor dimensions based on target product yields for a given biomass feed rate.

Conclusions: Among the key challenges in pyrolysis systems, particularly in fluidized-bed reactors, control and design remain among the most critical. This work aims to demonstrate the effectiveness of predictive reduced-order models based on neural networks (NNs) in addressing these issues. Specifically, two NNs have been trained to independently perform these tasks. The first network, NN_y, is trained to predict pyrolysis product yields based on process parameters, making it suitable for control applications. The second network, NN_p, is designed to provide optimal reactor design parameters for a given feedstock, given the desired product distribution. Both networks, trained using data from CFD simulations of various fluidized-bed reactor configurations, have shown high reliability, with prediction errors consistently close to or below 5%.

Acknowledgment

The authors acknowledge support from Project ECS 0000024 Rome Technopole- CUP: E83C22003240001, NRP Mission 4 Component 2 Investment 1.5, Funded by the European UnionNextGenerationEU.

References

[1] A. K. Vuppaladadiyam *et al.*, “Biomass pyrolysis: A review on recent advancements and green hydrogen production,” *Bioresour Technol*, vol. 364, p. 128087, 2022.

[2] S. R. A. Kersten, X. Wang, W. Prins, and W. P. M. Van Swaaij, “Biomass pyrolysis in a fluidized bed reactor. Part 1: Literature review and model simulations,” Nov. 09, 2005. doi: 10.1021/ie0504856.

[3] T. Duriez, S. L. Brunton, and B. R. Noack, *Machine learning control-taming nonlinear dynamics and turbulence*, vol. 116. Springer, 2017.

[4] R. Nian, J. Liu, and B. Huang, “A review on reinforcement learning: Introduction and applications in industrial process control,” *Comput Chem Eng*, vol. 139, p. 106886, 2020.

[5] M. Baldelli, L. Bartolucci, S. Cordiner, and V. Mulone, “Fluidized Bed Reactors for energy recovery from biomass and wastes: a data-driven approach towards the development of digital twins for real time control and monitoring,” in *Journal of Physics: Conference Series*, IOP Publishing, 2024, p. 012014.

[6] E. Ranzi, P. E. A. Debiagi, and A. Frassoldati, “Mathematical modeling of fast biomass pyrolysis and bio-oil formation. Note I: kinetic mechanism of biomass pyrolysis,” *ACS Sustain Chem Eng*, vol. 5, no. 4, pp. 2867–2881, 2017.

EFCH2 2025 European Fuel Cells and Hydrogen
PIERO LUNGHI CONFERENCE
September 17th–19th 2025
Capri / Italy

Systematic Investigation of Hydrogen Production Efficiency as a Function of Electrode Properties and Electrolyte Composition

Jayesh P. Ruparelia[a]*, Jayvir Atodariya[a], Manav Agrawal[a], Ansh Singh[a]
* corresponding author: Jayesh P. Ruparelia
[a] Institute of Technology, Nirma University

Keywords: Alkaline water, Coated Electrodes, Green Hydrogen Generation, electrolyzer with an impermeable membrane

Abstract

The increasing concerns over climate change and the depletion of fossil fuel reserves have necessitated a transition toward sustainable and renewable energy sources. Among these, hydrogen emerges as a promising energy carrier due to its high energy density and environmentally benign combustion products. This study investigates hydrogen production via water electrolysis, specifically optimizing electrode and electrolyte configurations to enhance system performance. The experimental work utilizes alkaline water electrolysis, employing an alkaline electrolyte. The study systematically evaluates the hydrogen generation rate using various metallic electrodes, including variations in surface modifications achieved through the Standard Thermal Decomposition (STD) method. Additionally, the influence of electrolyte concentration on hydrogen production efficiency is examined. SS321 stainless steel electrodes demonstrated superior performance in coated and uncoated forms among the tested materials. Furthermore, an increase in electrode thickness correlated with enhanced efficiency. All the experiments were conducted to explore the effects of parameters in an electrolyzer with an impermeable membrane. The findings of this research contribute to two critical aspects of hydrogen production systems: (i) the enhancement of hydrogen yield, which is vital for the broader adoption of green hydrogen technologies, and (ii) the optimization of operational parameters to achieve higher output with minimal energy input, thereby improving overall system efficiency. These results hold significant potential for scaling up to industrial hydrogen production applications.

Objectives:

1. To investigate the impact of electrode material (SS321, Nickel, Titanium) and its thickness on hydrogen production efficiency during alkaline water electrolysis.
2. To assess the influence of electrolyte concentration (1N, 3N, 5N KOH) on the rate and efficiency of hydrogen generation.
3. To examine the role of surface coatings (cobalt and titanium dioxide) on different electrode materials in enhancing corrosion resistance, conductivity, and overall performance in hydrogen production.

Material and methods:

The alkaline water electrolyzer with an impermeable membrane was assembled using a custom-fabricated electrolyzer with internal dimensions of 11 cm × 9 cm × 17.5 cm, corresponding to a volume of 1 L. The system was powered by a direct current (DC) supply,

with the applied voltage maintained between 4.02 V and 4.18 V across all experimental runs. Later, the same electrolyzer is connected with a solar panel to generate hydrogen through a green route. The electrolyzer was designed to allow variation in electrode spacing, ranging from 10 mm to 50 mm, to assess the influence of ohmic resistance on electrochemical performance. Three different electrode materials were selected based on conductivity, chemical stability, and literature precedence, i.e., Stainless Steel 321 (SS321), Nickel (Ni), and Titanium (Ti). Each electrode material was tested in 1 mm and 2 mm thicknesses. Anode and cathode were constructed from the same material for each configuration to eliminate inter-material variability [1]. Further, the electrolyte employed was potassium hydroxide (KOH), prepared in three distinct molar concentrations: 1 N, 3 N, and 5 N. The electrolyte facilitated ionic conductivity and maintained charge neutrality during electrolysis. Electrode coatings were applied using the Standard Thermal Decomposition Method (STD), which was selected for its simplicity, reproducibility, and cost-effectiveness [2]. All the experiments were conducted to explore the effects of parameters in a membraneless electrolysis system.

Results:

The study evaluated hydrogen generation efficiency through alkaline electrolysis by varying four key parameters: electrode material, electrode thickness, electrolyte concentration, and electrode coatings. The results are summarized as follows:



Figure 1: Experimental Setup with 80 W Solar Panel, 10 kW Electrolyzer, and Gas Collection System

1. Effect of Electrode Material

- SS321 stainless steel consistently exhibited the highest efficiency among the tested materials.
- Nickel showed moderate efficiency, but performance decreased with increased thickness.
- Titanium electrodes failed to produce hydrogen under the given voltage range, likely due to forming a passive oxide layer, indicating a higher threshold voltage is needed [3].

2. Effect of Electrolyte Concentration

- Electrolyte concentration (1 N, 3 N, 5 N KOH) significantly affected hydrogen yield.

SS321 (uncoated, 1 mm) at 1 N concentration achieved maximum efficiency (32.95%).

- Higher concentrations (3 N and 5 N) increased conductivity but also promoted corrosion in uncoated electrodes, reducing performance.

3. Effect of Electrode Thickness

- Increasing the electrode thickness from 1 mm to 2 mm in SS321 significantly improved efficiency (up to 283.13% at 1 N).
- For nickel, increasing thickness reduces efficiency due to increased internal resistance and lower active surface area.

4. Effect of Electrode Coatings

- Cobalt-coated SS321 improved performance at higher concentrations (3N and 5N), mitigating corrosion effects [2].
  - Efficiency increased by 148.56% at 3 N and 40.81% at 5 N compared to uncoated SS321.
- Titanium dioxide-coated Nickel electrodes also improved performance for 1 mm electrodes:
  - Efficiency increased by 70.57% at 3 N and 51.55% at 5 N compared to uncoated Nickel.

5. Key Performance Metrics

- Maximum overall efficiency: 32.95% (SS321, uncoated, 1 mm, 1 N KOH)
- Coated electrodes generally improved performance in higher electrolyte concentrations.
- The STD coating method proved to be an effective and scalable technique.
-

Conclusions:

This study presents a comprehensive evaluation of the performance of green hydrogen production through alkaline water electrolysis, focusing on the effects of electrode material, electrode thickness, electrolyte concentration, and surface coatings. SS321 stainless steel electrodes demonstrated the highest efficiency among the tested parameters under coated and uncoated conditions. Notably, increasing the electrode thickness of SS321 significantly enhanced efficiency, particularly at lower electrolyte concentrations. Electrode surface coatings, especially cobalt on SS321 and titanium dioxide on Nickel, were effective in improving efficiency under higher electrolyte concentrations, likely due to enhanced corrosion resistance and catalytic activity. Conversely, Titanium electrodes were ineffective under the applied voltage range, indicating the formation of passivating oxide layers or the need for a higher activation voltage. The research underscores the importance of optimizing electrode characteristics and operating conditions to improve the electrochemical efficiency of green hydrogen production. Additionally, using a cost-effective, membraneless electrolyzer design combined with thermal decomposition coating techniques demonstrates the potential for scalable and affordable green hydrogen technologies. These findings offer practical insights for advancing sustainable hydrogen production systems and pave the way for future studies to optimize further material selection, reactor design, and process parameters.

Acknowledgment

The authors gratefully acknowledge the financial support received from Innovation Hub (i-Hub) under the Student Startup Innovation Program (SSIP) Startup Srujan Seed Support (S4), Government of Gujarat, INDIA, for a grant of ₹10,00,000 to facilitate this research on green hydrogen technologies.

References

[1] A. E. Karaca and I. Dincer, “Development of a new photoelectrochemical system for clean hydrogen production and a comparative environmental impact assessment with other production methods,” Chemosphere, vol. 337, p. 139367, 2023.

[2] B. D. Soni, U. D. Patel, A. Agrawal, and J. P. Ruparelia, “A comparative study for degradation of RB5 dye using Ti/Ir0.15–Ru0.15–Sn0.6–Sb0.1 electrodes fabricated by employing two different thermal decomposition methods,” SN Applied Sciences, vol. 2, no. 11, Oct. 2020, doi: https://doi.org/10.1007/s42452-020-03657-3.

[3] A. Gabler et al., “Ultrashort-pulse laser structured titanium surfaces with sputter-coated platinum catalyst as hydrogen evolution electrodes for alkaline water electrolysis,” International Journal of Hydrogen Energy, vol. 43, no. 15, pp. 7216–7226, Apr. 2018, doi: https://doi.org/10.1016/j.ijhydene.2018.02.130.

European Fuel Cells and Hydrogen
PIERO LUNGHI CONFERENCE
EFCH2 2025
September 17th–19th 2025
Capri / Italy

On the development of doped cobaltite type electrocatalysts for OER in AMEWE

Miryam Gulino[1], Marco Martino[2], Livia Della Seta[2], Ottavio Longo[3], Davide Principe[1], Marta Feroci*[1], Valentina Naticchioni*[2]

[1]*Department of Basic and Applied Sciences for Engineering (SBAI), University of Rome La Sapienza, Rome, Italy*
[2]*ENEA, Italian Agency for New Technologies, Energy and the Environment Department of Renewable Energies, Via Anguillarese, 301-00123 Rome, Italy*
[3]*Department of Mechanical, Energy and Management Engineering (DIMEG), University of Calabria, Rende (CS), Italy*

**Corresponding author: marta.feroci@uniroma1.it, valentina.naticchioni@enea.it*

Keywords: Electrocatalysts, electrolysis, anionic exchange membrane, oxygen evolution reaction

Abstract:

Perovskite-type oxides have attracted much attention for oxygen evolution reaction in anion exchange membrane water electrolysis, due their stability and catalytic activity. In this study we examined different transition metals doped lanthanum cobaltite performances. The electrocatalysts were preparate by a simple sol-gel route, and their structure, morphology and electrochemical activity were investigated by several analytical and electrochemical techniques. The obtained results showed that doping and combining different metals increase the catalytic activity.

Introduction:

Hydrogen is an energetic vector, and it is one of the most important alternatives, sustainable and clean way to produce zero emission energy avoiding fossil fuels. Currently, technologies associated with the production, storage, and transportation of hydrogen energy have seen rapid advancements worldwide. Among hydrogen production technologies, water splitting is one of the most interesting way to obtain pure hydrogen. In this field, alkaline anion exchange membrane water electrolysis (AEMWE) is a promising way because it combines the benefits of both the well-known alkaline electrolysis and the proton exchange membrane processes drawing inspiration from PEM technology.. AEMWE consists of two reactions, respectively hydrogen evolution at cathode and oxygen evolution at anode. This last reaction has slower

kinetics and require a high overpotential to start the reaction. For this reason, is important developing electrocatalysts which show better performance to reduce the overpotential.

Objectives:

This work aims to research and study in a homologous series of catalysts with different dopants which is the best one to improve the oxygen evolution reaction. Specifically, lanthanum cobaltite, $LaCoO_3$, was doped to elaborate a series of perovskite-type oxide electrocatalysts for application in alkaline exchange membrane water electrolyzers.

Material and methods:

In this study $LaCo_{0.9}Zn_{0.1}O_3$ and $LaCo_{0.9}Fe_{0.1}O_3$ were prepared by a simple sol-gel route where metal nitrates were used as precursors. They were first progressively dissolved in ethanol, and then citric acid were added to the solution with a 1:1:2 molar ratio of La:Co-Me:CA (Me= Zn, Fe). The solution was heated to 70 °C under continuous stirring overnight. Finally, the samples were ground and calcined in air at 1100 °C for 6 hours. The previous prepared electrocatalysts were characterized by TGA, XRD, SEM, EDS, to evaluate their structure, morphology and by RDE to study their electrochemical properties. Electrochemical performances of synthetised catalysts and a commercial cobaltite were studied by linear and cyclic voltammetry at RDE (stainless steel disk, diameter: 1 cm) at different value of rotating velocity.

Results:

An optimal catalytic ink composition and deposition procedure on RDE were defined: the smoothest deposit was reached by using a catalyst/ionomer ratio of 1:0.15.

The TGA of the pre-calcinated samples confirms the effective thermal treatment used during synthesis while XRD analyses showed the actual formation of the crystalline microstructure of the catalysts, a symptom of the effective success of the synthesis. In addition, from the SEM and EDS analyses it is possible to observe the homogeneous distribution of the elements present in the samples.

The analysed electrocatalysts showed promising applications in anion exchange membrane water electrolyzers. From the cyclic voltammograms, as reported in *Figure 1*, is possible to observe how the substitution of Co by Fe as doping improve the electrocatalytic activity for OER. In particular, the curve of $LaCo_{0.9}Fe_{0.1}O_3$ reaches higher current than $LaCo_{0.9}Zn_{0.1}O_3$, showing a best catalytic activity.

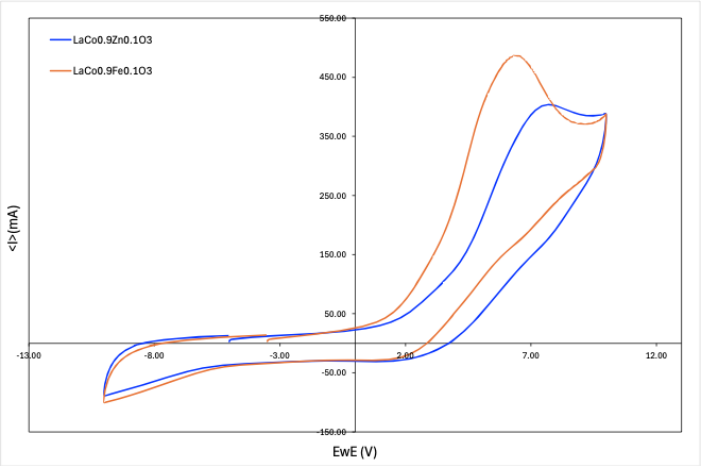


Figure 1: Cyclic voltammograms of two electrocatalysts investigated.

Conclusions:

The synthetised electrocatalysts showed promising applications in anion exchange membrane water electrolyzers. The data obtained from the different characterizations have shown how the doping with a different metal, even in small amount, improve the catalytic performance of the starting catalyst $LaCoO_3$. The future perspective of this work is to expand the study to other metals belonging to the fourth period of the periodic table, even mixing them in different ratios, to evaluate which is the best doping composition in lanthanum cobaltite structure.

Acknowledgment

ENEA - Italian National Agency for New Technologies, Energy and Sustainable Economic Development for funding (PNRR POR H_2 WP3.1 LA3.1.3 “Sviluppo di elettrocatalizzatori basati su metalli e leghe di metalli M/C a elevata area superficiale”).

References

[1] S. Perumal *et al.*, “Recent Advances in Electrochemical Water Splitting Electrocatalysts: Categorization by Parameters and Catalyst Types,” *American Chemical Society*, Aug. 05, 2024.

[2] F. Hadji, M. Omari, and M. Mebarki, “Boosting the electrocatalytic activity of lanthanum cobaltite ceramic through Zn doping for the oxygen evolution reaction,” *Ceramics International*, vol. 49, no. 15, pp. 25405–25413, Aug. 2023.

[3] X. Liang *et al.*, “Perovskite-Type Water Oxidation Electrocatalysts,” *Chinese Chemical Society*, Sep. 28, 2022.

EFCH2 2025 European Fuel Cells and Hydrogen PIERO LUNGHI CONFERENCE
September 17th–19th 2025 Capri / Italy

Biomass to methanol by Breakthrough SOEC-based Process

Asia Vedovi, Martina Marasi, Giulio Guandalini, Alessandro Donazzi*
*corresponding author: alessandro.donazzi@polimi.it
Politecnico di Milano, Milan, Italy

Keywords: syngas, co-electrolysis, Solid Oxide Cells

Abstract

This study explores the integration of solid oxide electrolysis cells (SOECs) in the process of methanol production, focusing on their performance with various fuel mixtures, which include water (H_2O), hydrogen (H_2), carbon dioxide (CO_2), carbon monoxide (CO), and methane (CH_4). The objective is to evaluate the cell's ability to operate at least at 500 mA/cm², enabling key reactions like water gas shift (WGS), steam methane reforming (SMR), and H_2O/CO_2 co-electrolysis. 25 cm^2 SOEC supplied by Elcogen were tested longer than 1000 h. The experimental results confirmed the SOEC's capability to meet the target requirements, although slow but steady degradation was observed.

Introduction: To enhance the contribution of renewables in the synthesis of methanol, an innovative cycle is proposed, wherein wood biomasses are gasified, and a SOEC stack is integrated downstream to tune the H_2/CO ratio of the reformate and achieve the optimal ratio of 2 [1, 2]. As SOECs are based on oxide ions transport, co-electrolysis of H_2O and CO_2 can be activated in parallel to high-temperature reactions such as SMR and WGS. The key challenge of the SOEC stack is the direct supply of a complex gas mixture whose target composition contains 4% CH_4, 15% H_2, 56% H_2O, 15% CO, and 10% CO_2. This raises critical questions regarding the cell's degradation, the extent to which various reactions take place, and the optimal operating point on the electrolysis curve, as the methanol synthesis line presents multiple waste heat streams that could be utilized by the SOEC if operated under endothermic conditions.

Objectives: The experimental investigation aims at understanding the kinetic and diffusive phenomena taking place in the electrodes, verify the SOEC's durability under target operating conditions, and assess how closely the system performs with respect to the expected conditions.

Material and methods: Single 5x5 cm^2 anode-supported cells (Elcogen) were tested, which featured a 290 µm Ni-YSZ fuel electrode, a 20 µm LSC ($La_{0.6}Sr_{0.4}CoO_{3-\delta}$) oxygen electrode, and a 7 µm YSZ electrolyte, with an additional 2 µm GDC ($Gd_{0.1}Ce_{0.9}O_{2+\delta}$) interlayer. Performance

and durability experiments were conducted at 700°C with a Horiba-FuelCon C50 Evaluator test station. Polarization curves (I/V) were collected between Open Circuit Voltage (OCV) and 1.4 V in electrolysis mode, and from OCV to 0.7 V in fuel cell mode. Electrochemical impedance spectra were measured at OCV. The durability experiments were performed for over 1000 h with the target mixture, at different voltage levels (thermoneutral and below).

Results: The cell's performance was first evaluated in electrolysis mode with an 42/58 H_2/H_2O mixture fed to the fuel electrode, and air to the oxygen electrode. The fuel composition was then adjusted step by step to assess kinetics, until reaching the target mixture: CO_2 was introduced (10% vol), showing no impact as OCV remained near the Nernst potential of pure H_2O electrolysis. The introduction of CO (15% vol) slightly shifted OCV towards the WGS thermodynamic equilibrium. Further addition of CH_4 (4% vol), with 56% H_2O and 15% H_2 allowed to achieve the required target composition, and activating the SMR reaction. The ability to sustain the 500 mA/cm² current density required by the project was validated (Fig. 1A). A over 350 h durability study at thermoneutral voltage with the target composition (Fig. 1B) revealed slow, but steady degradation. Modification of the operative voltage allowed to achieve stable performance.

Conclusions: The experiments confirmed that the SOC can operate at 500 mA/cm² with the cycle's target mixture. The I/V curve indicates that WGS, SMR, and water electrolysis characterize the SOEC's reactivity. Regarding durability, the SOEC degraded at thermoneutral voltage, but remained stable below.

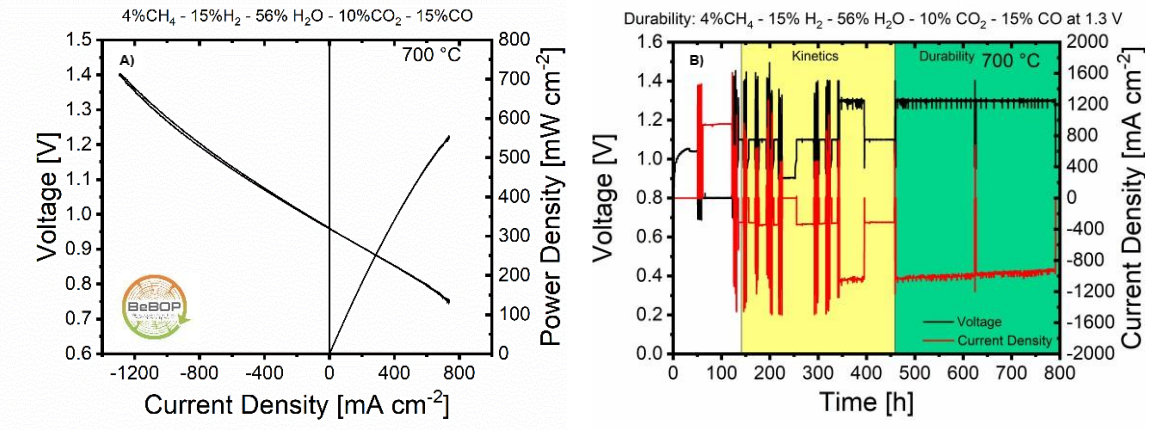


***Figure 1** – A) I/V curve 0.6 Nl/min F.E. and 1.50 Nl/min O.E. B) Durability experiment*

Funded by the European Union. This project has received funding from the European Union's Horizon Europe research and innovation programme under the Grant Agreement no. 101178117.

References

[1] A. Poluzzi et al. *Biomass Bioenergy*, 142, (2020)
[2] F. Rajaee et al. *Energy Convers Manag*, 301, (2024)

EFCH2 2025 European Fuel Cells and Hydrogen
PIERO LUNGHI CONFERENCE
September 17th–19th 2025 Capri / Italy

Anion Exchange Membrane Water Electrolysis with Poly(biphenyl piperidone co trifluoroacetophenone) random copolymers as Membranes

Valentina Prusakova*[a],
Giulia Di Gregorio[a], Matteo Testi[a], Tommaso Caielli[b], Alessandro Ferrari[b], Simone Zottele[a], Takwa Cheraiet[a], Sara Ferrari[c], and Piercarlo Mustarelli[b]

* corresponding author: prusakova@fbk.eu
[a] Hydrogen Technologies and Resilient Energy Systems, *Center for Sustainable Energy,* Fondazione Bruno Kessler, Via Sommarive 18, 38123 Povo (TN), Italy
[b] Department of Materials Science, University of Milano Bicocca, Via Cozzi 55, 20125, Milano, Italy
[c] Micro Nano Facility, Center for Sensors and Devices, Fondazione Bruno Kessler, Via Sommarive 18, 38123 Povo (TN), Italy

Keywords: anion exchange membrane water electrolysis, poly(aryl piperidinium).

Abstract

When coupled with renewable energy, Anion Exchange Membrane Water Electrolysis (AEMWE) offers a promising and low-cost route to green hydrogen production using platinum group metal-free catalysts. A critical component of AEMWE is the membrane, which must combine high anion conductivity with chemical and mechanical stability. However, many current materials fall short in long-term durability.

This study investigates Poly(biphenyl piperidone co trifluoroacetophenone) (PBPF), a random copolymer with a stable aromatic backbone and piperidinium cations. PBPF membranes showed 120 mS cm^{-1} conductivity at 80 °C, 20% water uptake, and a 14% swelling ratio. Electrochemical testing of these promising membranes against Versogen's PiperION® and using platinum group metal-free catalysts is ongoing. PBPF shows strong potential to advance AEMWE membrane electrode assemblies toward higher technology readiness.

Introduction: The development of the hydrogen sector is a prospective strategy to ensure decarbonization, improve economy and environment [1]. Hydrogen may be produced in a variety of techniques, including electrolytic processes that employ electrolyzers that use electricity to split water into hydrogen and oxygen [2]. Most importantly, electrolyzers produce "green hydrogen" with close to zero greenhouse gas emissions when coupled with renewable energy sources (e.g., electrolysis powered by wind/solar). Several electrochemical technologies are available in a wide range of technology readiness levels: alkaline electrolyzers, anion exchange membrane electrolyzers, proton exchange membrane electrolyzers, operating at low temperature; and high-temperature electrolyzers (solid

oxide, molten carbonate, proton conducting electrolyzers) [2].

Despite the pros and cons of all the technologies, there is no real competition among them, and each technology has its niche, depending on its unique specifications. Additionally, the demand for fast decarbonization and carbon dioxide reduction requires that the effort comes from all the available sources and technologies.

Anionic Exchange Membrane Water Electrolyzers AEMWE is a promising technology and has multiple strengths [3]:

- ✓ platinum group metals-free catalysts
- ✓ Titanium-free materials
- ✓ zero-gap electrolysis
- ✓ solid organic polymer electrolyte
- ✓ fast oxygen evolution reaction kinetics
- ✓ enabling swap approach to the more diffuse alkaline system.

The heart of this technology is a solid polymeric membrane that transports hydroxide anions from cathode to anode with high selectivity. Apart from the ion conduction, the membrane insulates electrodes and ensures the gas separation: oxygen from hydrogen. This is essential for efficient and safe operation. Unfortunately, despite all the benefits of the technology, the membrane itself suffers chemical and mechanical stability issues that result in low durability. Therefore, the search for the novel mechanically and chemically stable membranes with low gas-permeability and high anion conductivity is necessary to achieve higher technology readiness levels of membrane electrode assemblies, MEA, for AEMWE. Recently, a promising class of Poly(aryl piperidinium)s was extensively studied [4]. These membranes owe their stability to a combination of heteroatom-free aromatic backbone and piperidinium cation. The AEMWE tests using Poly(biphenyl piperidone co trifluoroacetophenone) random copolymer, PBPF, confirmed the excellent stability of the PBPF for 1500 h at 1.8 V. Therefore, this promising material should be further investigated against the testbench existing commercial materials and with platinum group metal -free catalysts.

Objectives: The aim is to incorporate the emerging promising poly(aryl piperidinium)-based membranes developed in academia into membrane electrode assemblies, MEA, to bring MEAs for AEMWE to a higher technology readiness level. Therefore, the most stable Poly(biphenyl piperidone co trifluoroacetophenone) random copolymers, PBPF, will be tested in AEMWE experiments against the Versogen's PiperION® benchmark material. Additionally, the performance of PBPF will be tested with platinum group metals-free electrocatalysts.

Material and methods: Full characterization of the PBPF (ion exchange capacity, conductivity, water uptake and swelling ratio, etc.) is published elsewhere [4]. Three PBPF membranes of about 6.5x6.5 cm^2 were prepared from solutions of PBPF in DMSO. The solutions were filtered with a 2 µm syringe filter, poured in a petri dish, and dried in an oven at 50 °C for 5

hours and then at 80 °C for 24 hours. Prior to the AEMWE testing, PBPF membranes will be immersed in abundant 1 M KOH for 24 to exchange AEMs in the OH^- form.

Results: Three PBPF membranes are in chlorinated form and display the following characteristics:
OH^- conductivity (80 °C in water): 120 mS cm^{-2}
Water uptake (OH^- form, 80°C): 20 %
Swelling ratio (OH^- form, 80°C): 14 %
The membranes are inhomogeneous with a thickness of 50 +/- 20 µm; however, the irregular structure is pronounced close to the borders of the films.
The electrochemical characterization in the AEM single-cell electrolyzer using platinum group metal-free electrocatalysts and against Versogen's PiperION® benchmark material is in progress.
Conclusions: Poly(biphenyl piperidone co trifluoroacetophenone) random copolymer, PBPF, is a promising stable material for AEMWE membrane. Therefore, it should be further investigated against the testbench existing commercial materials (Versogen's PiperION®), and with platinum group metal-free catalysts to bring MEA based on these polymers to higher technology readiness levels.

Acknowledgment

The authors thank PNRR NEST Project, Spoke 4 Partnership, for the financial support.

References

[1] The European Green Deal. https://eur-lex.europa.eu/legal-content/EN/TXT/?qid=1576150542719&uri=COM%3A2019%3A640%3AFIN
[2] Marian Chatenet, Bruno G. Pollet, Dario R. Dekel, Fabio Dionigi, Jonathan Deseure, Pierre Millet, Richard D. Braatz, Martin Z. Bazant, Michael Eikerling, Iain Staffell, Paul Balcombe, Yang Shao-Horn and Helmut Schafer "Water electrolysis: from textbook knowledge to the latest scientific strategies and industrial developments" ***Chem. Soc. Rev.***, 2022, **51**, 4583-4762.
[3] Carlo Santoro, Alessandro Lavacchi, Piercarlo Mustarelli, Vito Di Noto, Lior Elbaz, Dario R. Dekel, Frédéric Jaouen "What is Next in Anion-Exchange Membrane Water Electrolyzers? Bottlenecks, Benefits, and Future" *ChemSusChem* **2022**, *15*, e202200027.
[4] Tommaso Caielli, Alessandro Raffaele Ferrari, Diego Stucchi, Chiara Ferrara, Angela Caprì, Irene Gatto, Vincenzo Baglio, Alice Pancaldi, Adele Sassella, Stefania Zappia, Alberto Giacometti Schieroni, Piercarlo Mustarelli, "Poly(biphenyl-piperidinium)/poly(biphenyl-trifluoroacetophenone) random and block copolymers enabling highly stable anion exchange membranes for water electrolysis", Chemical Engineering Journal, *508*, 2025, 160825, ISSN 1385-8947, https://doi.org/10.1016/j.cej.2025.160825.

European Fuel Cells and Hydrogen
PIERO LUNGHI CONFERENCE
EFCH2 2025
September 17th–19th 2025
Capri / Italy

Advancing AEM Electrolysis: A Novel Single-Cell for Evaluating High-Performance Membranes and Electrodes

Giulia Di Gregorio*[a], Matteo Testi [a], Giovanni Cufalo[b], Nicholas Loi[b]

* corresponding author: gdigregorio@fbk.eu

[a] Fondazione Bruno Kessler, Center on Sustainable Energy, Povo, 38123 - Trento,
[b] Arco Technologies Inc, Quarto Inferiore, 40057 - Bologna

Keywords: AEM electrolysis, electrochemical characterization, membrane-electrode assembly

Abstract:

Introduction: Anion exchange membrane electrolysis (AEMEL) is increasingly emerging as a promising low-temperature water electrolysis technology, due to its potential to combine the key advantages of both alkaline and proton exchange membrane electrolysis. Operating under mild alkaline conditions, AEMEL enables the use of non-precious metal-based electrocatalysts and cost-effective cell components, thereby offering a compelling pathway toward sustainable and economically viable hydrogen production. Despite these advantages, the widespread adoption of AEMEL remains hindered by several challenges, particularly related to membrane stability and electrode degradation at high current densities. According to the *Strategic Research and Innovation Agenda 2021-2027* of the Clean Hydrogen Joint Undertaking [1], addressing these issues will require an integrated approach encompassing advanced material development, optimized cell architecture, and improved electrolyte and gas management strategies. In particular, the design and configuration of the membrane-electrode assembly (MEA) play a central role in minimizing ohmic losses and mass transport limitations, thereby enabling high performance and long-term durability.

Objectives: This work presents the design, fabrication, and electrochemical validation of a novel AEMEL single-cell system with an active area of 25 cm^2. The cell has been specifically engineered as a versatile testing platform for the screening of MEA components. Initial validation was performed using commercial materials to establish a reliable baseline for performance comparison. Current research activities are focused on the electrochemical characterization of advanced membranes and electrodes developed by Arco, with the goal of identifying highly stable and efficient materials for integration into future AEMEL stacks. In parallel, morphological and compositional changes induced by electrolysis are assessed using Scanning Electron Microscopy (SEM) with Energy Dispersive Spectroscopy (EDS), providing insights into degradation phenomena and material stability.

Material and methods: The custom-designed AEMEL single-cell (*Figure 1*) consists of AISI 316 stainless steel end plates, PTFE insulating layers, gold-sputtered copper current collectors with a branch for the electrical connection, and titanium-based bipolar plates. Electrolyte and gas distribution is managed through diametrically opposed holes, sealed with EPDM O-rings to ensure leak-free operation. The MEA components are housed within precision-machined PEEK frames, which provide uniform compression and accurate alignment. On the cathode side, a 1.7 mm thick graphite felt (SIGRACET® ECM 250, SGL Carbon) serves as the porous transport later, while the anode side includes a 1.7 mm thick platinum-coated titanium mesh (Saveions) and a 0.28 mm thick sintered metal powder titanium plate (Mott Corporation).

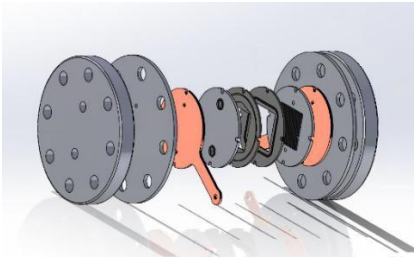


Figure 1 – Custom-designed AEMEL cell setup.

Electrochemical validation was performed using a 0.5 mg/cm^2 Platinum/Carbon Cloth (FuelCellStore) as the cathode electrode, a $NiFeO_4$/Stainless Steel (Dioxide Materials) as the anode electrode, and Sustainion® X37-50 Grade RT (Dioxide Materials) as the anion exchange membrane. The cell was operated with dry cathode, while anode was supplied with 0.2 L/min of 1 M KOH at 65°C. The test protocol included a preliminary 2-hour hydration phase, followed by cell polarization. Electrochemical characterization of Arco's components includes current-voltage polarization curves (from 1.4 V to 2.1 V, voltage variations 5 mV/s), Electrochemical Impedance Spectroscopy (EIS) performed at 1.8 V and 2.0 V (amplitude 10 mV, 10^{-2}-10^5 Hz), and chronopotentiometric test at 1 A/cm^2 for 7 days.

Results: The AEMEL single-cell has been systematically optimized to ensure effective sealing, uniform electrolyte distribution, and high mechanical robustness, allowing for reliable electrochemical testing under controlled operating conditions.

The polarization curve obtained using the benchmark MEA (*Figure 2*) demonstrates a current density exceeding 1.4 A/cm² at 2.1 V. These results are in line with expectations for state-of-

the-art AEMEL systems [2] and serve as a reliable baseline for the comparative evaluation of Arco materials.

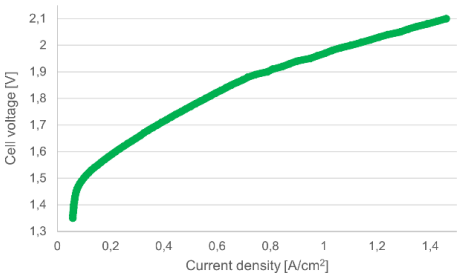


Figure 2 – Polarization curve for the benchmark MEA.

EIS results at 1.8 V and 2.0 V are shown in *Figure 3*. At 1.8 V, the Nyquist plot indicates a high-frequency resistance (HFR) of approximately 12.4 mΩ, and an area-specific resistance (ASR) of approximately 25 mΩ. Upon increasing the cell voltage to 2.0 V, a notable decrease in both the HFR and ASR values (10.2 mΩ and 4 mΩ, respectively) was observed.

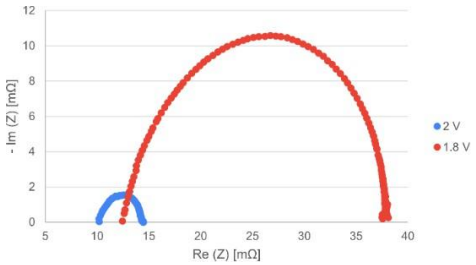


Figure 3 – EIS curves collected at 1.8 V and 2.0 V for the benchmark MEA.

The low overall impedance observed across the operating range supports the effectiveness of the cell architecture in minimizing ohmic losses. In particular, the stable contact interface between the membrane and electrodes, the homogeneous pressure distribution, and the optimized flow field design all contribute to maintaining low resistance and reproducible performance.

Conclusions: This study contributes to the advancement of AEMEL technology, supporting its progression toward commercial deployment. The developed AEMEL single-cell provides a reliable and versatile platform for the systematic evaluation of next-generation cell components. Ongoing work is focused on the electrochemical characterization of membranes and electrodes developed by Arco. The most promising results will be presented, together with the strategies adopted to optimize performance and durability.

Acknowledgment

The authors thank PNRR NEST Project, Spoke 4 Partnership, for the financial support.

References

[1] Clean Hydrogen Joint Undertaking, “Strategic Research and Innovation Agenda 2021-2027”, 2022
[2] Q. Xu, L. Zhang, J. Zhang, J. Wang, Y. Hu, H. Jiang, and C. Li, “Anion exchange membrane water electrolyzer: Electrode design, lab-scaled testing system and performance evaluation”, Energy Chemistry, vol. 4, p. 100087, Aug. 2022, doi: 10.1016/j.enchem.2022.100087

EFCH2 2025 European Fuel Cells and Hydrogen
PIERO LUNGHI CONFERENCE
September 17th–19th 2025
Capri / Italy

Matrices for Reversible Molten Carbonate Cells: Insights from Button Cell Testing

Silvia Lo Conte*[a], Massimiliano Della Pietra[b], Simone Mataloni[b,c], Alessia Gwis[c], Alfredo Zingone[b], Irfan[d], Stefano Frangini[b], Elio Jannelli[a]

* corresponding author: silvia.loconte@uniroma1.it

[a] Department of Engineering, University of Naples "Parthenope", Italy.
[b] Department of Energy Technologies and Renewable Sources, Laboratory for Hydrogen and new Energy Vectors (TERIN-DEC-H2V), ENEA Italian National Agency for Energy, New Technologies and Sustainable Economic Development, C.R. Casaccia, Rome, Italy.
[c] Department of Chemical Engineering Materials and Environment, University of Rome "La Sapienza", Rome, Italy.
[d] Department of Astronautical Electrical and Energy Engineering, University of Rome "La Sapienza", Rome, Italy.

Keywords: differential resistance analysis, electrolysis, matrix, molten carbonate cells

Abstract:

This work investigates the performance of various matrix samples for Molten Carbonate Cells (MCC), developed in-house at ENEA Casaccia using tape casting with γ-$LiAlO_2$ powder. The matrix plays a critical role in MCC operation by retaining the molten carbonate electrolyte, enabling ionic conduction, and ensuring gas separation. Although lithium aluminate is widely adopted due to its compatibility and stability, long-term performance challenges persist, prompting further material optimization. Button cells with a 3 cm^2 active area were assembled to test matrices of varying thicknesses (300–650 µm), while maintaining identical cell components (electrodes and electrolyte) from KIST. A standardized protocol was adopted: cells were operated first in fuel cell mode and then in electrolysis mode under controlled gas compositions and temperatures. Additional tests included flow rate variation at the air electrode to assess sealing, and thermal variation to evaluate matrix stability. Results demonstrated stable cell operation across all samples. Electrochemical impedance spectroscopy and polarization curves, analyzed via Differential Resistance Analysis (DRA), revealed the influence of matrix thickness on overall cell resistance. Intermediate-thickness matrices achieved the best trade-off between mechanical integrity and ionic conductivity, showing the lowest polarization resistance. These findings confirm the matrix's central role in determining ohmic losses and underscore the importance of optimizing its structure and dimensions for improved reversible MCC performance.

Introduction: Molten Carbonate Cells (MCC) are high-temperature electrochemical devices operating typically around 650 °C, originally developed as fuel cells (MCFCs) for combined heat and power applications [1]. Their ability to directly convert chemical energy into electricity using reformate gases has made them attractive for integration in distributed

generation systems and integrated gasification combined cycles. Beyond energy generation, MCFCs have gained attention as an innovative carbon capture solution, capable of separating CO_2 from low-concentration streams while simultaneously producing power [2]. Recent advances have pushed the development of reversible configurations, where the same cell can operate in electrolysis mode (MCEC) to produce H_2 and syngas from H_2O and CO_2 [3]. This dual capability represents a promising pathway for energy storage and synthetic fuel production, especially when coupled with carbon utilization strategies.

MCCs are composed of two porous electrodes separated by a ceramic matrix that holds the molten carbonate electrolyte, typically a eutectic mixture of lithium and potassium carbonates. This matrix is a key component for MCC operation: it must retain the electrolyte while ensuring electronic insulation, ionic conductivity between the electrodes, and effective gas separation. Its porous structure, with typical porosity between 50% and 70% [4], must combine mechanical strength with high wettability to guarantee the capillary retention of the electrolyte. Optimal performance is achieved when the matrix pores are filled with electrolyte, while the electrode pores are only partially saturated to avoid flooding. Although significant technological improvements have been achieved, the matrix remains one of the most critical and limiting elements, as its degradation over time directly affects cell performance in both fuel cell and electrolysis modes. Lithium aluminate ($LiAlO_2$) is the most widely adopted material for the matrix due to its chemical compatibility with molten carbonates and suitable structural properties [4]. Despite various modifications and extensive studies aimed at improving its properties—through dopants, reinforcements, and structural optimization—lithium aluminate-based matrices still face challenges related to particle coarsening, phase transitions, and chemical instability. These unresolved issues highlight the need for continued research to develop more stable, high-performance matrix materials capable of supporting long-term operation in molten carbonate cells.

Objectives: This work aims to evaluate the performance of different matrix samples synthesized in-house at ENEA Casaccia (Rome) Research Center through tape casting technique. The main objectives are to assess the mechanical integrity and sealing capability of each matrix by testing them in button cells, and to investigate their contribution to the overall polarization behavior. Particular attention will be given to identifying the optimal matrix thickness that ensures a balance between ionic conductivity, mechanical stability, and gas separation efficiency.

Material and methods: The matrix samples were prepared using commercial high-surface-area γ-$LiAlO_2$ ceramic powder as the primary material. An eco-friendly and low-cost solvent, commercial ethanol, was employed to dissolve the binder and plasticizer, forming a homogeneous slurry. The slurry was manually cast using a tabletop laboratory mini tape caster equipped with a single doctor blade. To enhance surface flatness, a warm rolling step was applied as post-processing. The thickness of the matrix tested range from 300 µm to 650 µm. The prepared matrices were subsequently used for the assembly of button cells with a geometric active area of 3 cm^2. All cell components, except for the matrix under investigation, were state-of-the-art materials provided by the Korean Institute of Science and Technology (KIST), including electrodes and electrolyte. A thorough description of the laboratory setup used along with a schematic representation is provided in [5]. Each matrix sample was tested under a defined protocol listed in Table 1. Initially, the cell was operated in fuel cell mode under a standard gas composition, commonly used to validate MCFC operation. Subsequently, tests in electrolysis mode were performed, during which the total flow rate at the air electrode was varied to induce differential pressure across the cell for evaluating the sealing performance. Finally, tests at different operating temperatures were carried out under fixed flow rate and gas composition to evaluate the thermal and mechanical stability of the matrices. For each testing condition, electrochemical impedance spectroscopy (EIS) and polarization curves were recorded to analyze the electrochemical performance of the cell. The polarization curves obtained for each matrix were further analyzed and compared using the Differential Resistance Analysis (DRA) [6], a technique that evaluates the changes in the slope of the voltage–current curve to distinguish between activation and ohmic losses. Since in MCCs the matrix is primarily responsible for ohmic loss due to its function in retaining the electrolyte and enabling ionic conduction, DRA could help to clearly identify and quantify the ohmic region of the curve, allowing for direct comparison of the resistive behavior of each matrix sample.

Table 1. Experimental protocol adopted for each matrix sample tested in the button cell setup.

		Fuel electrode		Oxidant electrode		
		Composition, %	Flow rate mL·min^{-1}	Composition, %	Flow rate mL·min^{-1}	
Type	Run	$CO_2/H_2O/H_2/N_2$		$CO_2/O_2/N_2$		T, °C
Standard composition	1	16/20/64/0	150	30/15/55	200	650
Electrolysis composition	2	20/20/10/50	200	30/15/55	200	650
Flowrate variation	3	20/20/10/50	200	30/15/55	**400**	650
	4	20/20/10/50	200	30/15/55	**600**	650
	5	20/20/10/50	200	30/15/55	**800**	650
T variation	6	20/20/10/50	200	30/15/55	200	**620**
	7	20/20/10/50	200	30/15/55	200	**680**

Results: Across all samples, stable operation was maintained in both fuel cell and electrolysis modes, with no major degradation observed during the short-term tests. Electrochemical testing under both fuel cell and electrolysis modes revealed differences in performance among the matrix samples, particularly in terms of internal resistance. Variations in thickness led to different slopes for the ohmic region in the polarization curves. For each tested cell the Differential Resistance Analysis helped to quantify the contributions of the matrix to overall polarization. Electrochemical impedance spectroscopy showed that the cells assembled with intermediate-thickness matrices exhibited the lowest polarization resistance, suggesting an optimal balance between ionic conductivity and active sites distribution inside the cell.

Acknowledgment

This research was funded by the European Union – NextGenerationEU from the Italian Ministry of Environment and Energy Security, POR H2 AdP MEES/ENEA with involvement of CNR and RSE, PNRR – Mission 2, Component 2, Investment 3.5 “Ricerca e sviluppo sull’idrogeno”, CUP: I83C22001170006

References

[1] J. P. Perez Trujillo, F. Elizalde-Blancas, M. Della Pietra, D. M. Silva-Mosqueda, J. M. García Guendulain, and S. J. McPhail, ‘Thermoeconomic comparison of a molten carbonate fuel cell and a solid oxide fuel cell system coupled with a micro gas turbine as hybrid plants’, *Energy Convers Manag*, vol. 276, p. 116533, Jan. 2023, doi: 10.1016/J.ENCONMAN.2022.116533.

[2] E. Audasso, L. Barelli, G. Bidini, B. Bosio, and G. Discepoli, ‘Molten Carbonate Fuel Cell performance analysis varying cathode operating conditions for carbon capture applications’, *J Power Sources*, vol. 348, pp. 118–129, Apr. 2017, doi: 10.1016/J.JPOWSOUR.2017.02.081.

[3] M. A. Murmura, S. Lo Conte, F. Santoni, M. Della Pietra, L. Turchetti, and M. C. Annesini, ‘Two-dimensional modeling and experimental investigation of an inverse molten carbonate fuel cell’, *J Power Sources*, vol. 573, p. 233103, Jul. 2023, doi: 10.1016/J.JPOWSOUR.2023.233103.

[4] A. A. Sheikh, F. R. Bianchi, D. Bove, and B. Bosio, ‘A review on MCFC matrix: State-of-the-art, degradation mechanisms and technological improvements’, *Heliyon*, vol. 10, no. 4, p. e25847, Feb. 2024, doi: 10.1016/J.HELIYON.2024.E25847.

[5] S. Lo Conte, S. Mataloni, M. Della Pietra, L. Simonetti, Y. De Pra, and M. C. Annesini, ‘DRT-based electrochemical investigation on the fuel electrode in a Molten Carbonate Electrolysis Cell’, *J Power Sources*, vol. 631, p. 236197, Mar. 2025, doi: 10.1016/J.JPOWSOUR.2025.236197.

[6] Z. Stoynov *et al.*, ‘Differential analysis of SOFC current-voltage characteristics’, *Appl Energy*, vol. 228, pp. 1584–1590, Oct. 2018, doi: 10.1016/J.APENERGY.2018.06.138.

European Fuel Cells and Hydrogen
PIERO LUNGHI CONFERENCE
September 17th–19th 2025
Capri / Italy

Electrochemical Impedance-Based Modeling of an Electrolyte- Supported SOEC Short Stack

Luca Riccio*[1,2], Francesca Santoni[1], Giuseppina Roviello[2], Alfredo Zingone[1], Davide Pumiglia[1], Giulia Monteleone[1]

* corresponding author

[1] Department of Energy Technologies and Renewable Sources Laboratory for Hydrogen and new Energy Vectors (TERIN-DEC-H2V) ENEA - Italian National Agency for New Technologies, Energy and Sustainable Economic Development), C.R. Casaccia, Via Anguillarese 301, 00123, Rome, Italy.
[2] Dipartimento di Ingegneria, Università degli Studi di Napoli Parthenope, Centro Direzionale, Isola C4, 80143 Napoli, Italy.

Keywords: *electrolysis, equivalent circuit, hydrogen, short stack.*

Abstract

This work investigates the electrochemical behavior of an electrolyte-supported SOEC short stack under electrolysis conditions using Electrochemical Impedance Spectroscopy in which four equivalent circuit models were simulated in MATLAB to identify the one that best fits the experimental data. After IV characterization and stabilization, EIS measurements are performed and validated. Results shown best fit was obtained with a circuit composed of a series resistance, two R–CPE branches for anodic and cathodic processes, and a Warburg diffusion element on the cathode side.

Introduction

Equivalent circuit modelling is a widely used method for interpreting impedance data from Solid Oxide Electrolysis Cells, especially when using Electrochemical Impedance Spectroscopy as a diagnostic tool. In this approach, the complex impedance response is represented by a network of lumped elements such as resistors, capacitors, and constant-phase elements, each associated with specific electrochemical phenomena in the cell. Typically, the high-frequency intercept in a Nyquist plot corresponds to a series resistance, reflecting the ohmic contributions of the electrolyte and interconnects, while lower-frequency arcs are modeled with R–CPE pairs to describe processes like charge transfer and mass transport [1]. Resistors indicate polarization losses from activation or concentration effects, while constant-phase elements capture non-ideal capacitive behavior related to double-layer capacitance or reaction kinetics [2]. Once an appropriate equivalent circuit is chosen, its parameters are obtained through nonlinear least-squares fitting, providing both quantitative estimates and statistical indicators of fit quality. This approach transforms raw EIS data into meaningful electrochemical information, helping identifiyng limiting factors such as electrolyte

conductivity or electrode kinetics and linking experimental observations to theoretical understanding [3].

Objectives

Objective of this work is to study the electrochemical behaviour occurring in an electrolyte-supported solid oxide short stack operating in electrolysis mode. To achieve this, four different equivalent circuit models were developed and simulated using MATLAB, to determine which best fit to the experimental EIS data, representing the most accurate equivalent circuit for the system internal processes.

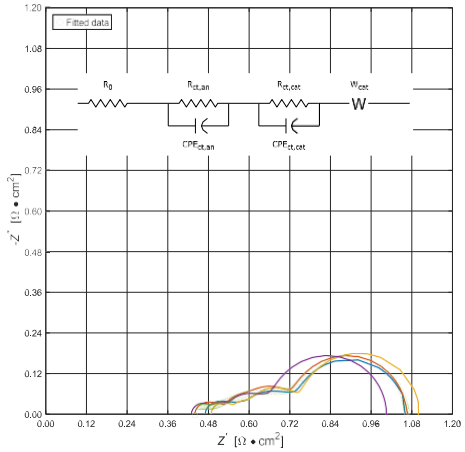
Material and methods

The experimental setup consists of a solid oxide electrolysis short stack supported by an electrolyte, operated under controlled conditions to assess its electrochemical behavior through EIS analysis. After validation of the setup through benchmark performance tests, the short stack is subjected to a sequence of experiments under different operating conditions, including variations in temperature, fuel composition, and current density. Each experiment begins under open circuit voltage, where a single operating parameter is modified compared to the previous test, and an IV curve is recorded at a constant ramp rate of 17 mA/s until the target current density is achieved. The system is then maintained at nominal load for 30 minutes to allow stabilization before performing Electrochemical Impedance Spectroscopy measurements. Once the impedance data are acquired, the system is returned to open circuit conditions and configured for the next test, with all EIS spectra subsequently validated using Kramers-Kronig relations and analyzed through MATLAB simulation.

Results

The impedance spectra were fitted using four different equivalent circuit models, each incorporating combinations of resistive and capacitive elements to reflect the electrochemical processes within the SOEC. Among these, the first model provided the best agreement with the experimental data in which different temperature experiment are made, as shown in Figure 1, which consists of a series polarization resistance (R_0), followed by a parallel combination of an anodic resistance and a constant-phase element ($CPE_{an}(R_1, CPE_1, P_1)$), a second parallel branch representing the cathodic resistance and constant-phase element ($CPE_{cat}(R_2, CPE_2, P_2)$), and finally a Warburg diffusion element ($W_{cat}(RW_1, CW_1, v_1)$) associated with the cathode layer.

A more detailed data will be show at the conference.



$R_0 = 0.260 \pm 2\%$
$R_1 = 0.258 \pm 2\%$
$R_2 = 0.292 \pm 2\%$
$RW_1 = 0.255 \pm 2\%$
$CPE_1 = 0.204 \pm 2\%$
$CPE_2 = 1.20 \pm 2\%$
$CW_1 = 3.05e-06 \pm 2\%$
$P_1 = 0.550 \pm 2\%$
$P_2 = 1.02 \pm 2\%$
$v_1 = 0.152 \pm 2\%$

Figure 1. Partially results of the equivalent circuit fitting (left) and respective fitting results (right).

Conclusions

This work investigates the electrochemical behaviour of an electrolyte-supported SOEC short stack using Electrochemical Impedance Spectroscopy, with four equivalent circuit models simulated in MATLAB to identify the configuration that best fits the experimental data. The most accurate representation was achieved with a model consisting of a series resistance, two R–CPE branches corresponding to anodic and cathodic processes, and a Warburg element capturing cathodic diffusion. Future developments will aim to integrate this circuit fitting approach with Distribution of Relaxation Times (DRT) analysis to obtain a more comprehensive understanding of the electrochemical phenomena occurring within the solid oxide electrolyte-supported short stack.

Acknowledgment

This research was funded by the European Union – NextGenerationEU from the Italian Ministry of Environment and Energy Security, POR H2 AdP MEES/ENEA with the involvement of the CNR and RSE, PNRR - Mission 2, Component 2, Investment 3.5 "Ricerca e sviluppo sull'idrogeno", CUP: I83C22001170006.

References

[1] Bianchi, F.R.; Spotorno, R.; Piccardo, P.; Bosio, B. "Solid Oxide Fuel Cell Performance Analysis through Local Modelling". *Catalysts*. **2020**, 10, pp. 519. https://doi.org/10.3390/catal10050519.

[2] Boaro, M.; Aricò, A. S. "Advances in Medium and High Temperature Solid Oxide Fuel Cell Technology". *Springer*. **2017**, 574, pp. 31-76. https://doi.org/10.1007/978-3-319-46146-5_2.

[3] Zhao, L.; Dai, H.; Pei, F.; Ming, P.; Wei, X.; Zhou, J. "A Comparative Study of Equivalent Circuit Models for Electro-Chemical Impedance Spectroscopy Analysis of Proton Exchange Membrane Fuel Cells". *Energies*. **2022**, 15, pp. 386. https://doi.org/10.3390/en15010386.

EFCH2 2025 European Fuel Cells and Hydrogen
PIERO LUNGHI CONFERENCE
September 17th–19th 2025
Capri / Italy

Microkinetic Modeling of Surface Reactions and Charge Transfer Dynamics in Solid Oxide Electrolysis Cells under Electrothermal Balanced Operation

Ifrah Akhtar*[a], Søren Hojgaard Jensen [a], Vincezo Liso[a], Henrik Lund Frandsen[b]

* corresponding author: ifak@energy.aau.dk
[a] Aalborg University, Department of Energy
[b] Technical University of Denmark, Energy

Keywords: Microkinetic, Solid oxide electrolysis cells, Transient, Water electrolysis

Abstract

Introduction: Solid oxide cells have been the most promising in terms of efficiency. They operate at a fairly high temperature that means their product streams are high energy which can be utilized in a process system that provides energy optimization. They can be operated in both electrolysis and fuel cell mode swiftly. However, widescale application of SOC is limited due to temperature fluctuations and degradation phenomenon such as Nickel migration. This considerably reduces the lifetime of Solid Oxide Electrolyzer cells (SOECs). A novel operation method by the name of Electrothermal balanced operation (also referred to as AC:DC) has been patented by DynElectro (1). In this operation the SOECs are operated 90% of the time in electrolysis mode with brief rapid reverse pulses in fuel cell mode. This operation method has been shown to considerably reduce Nickel migration phenomenon and makes the temperature profile flat across cell stack reducing degradation and improving cell life. This work investigates the impact of Electrothermal Balanced Operation (AC:DC) on the reaction pathways, surface species evolution, and charge transfer dynamics during high-temperature water electrolysis. This allows us to better understand the phenomenon that occurs during this operation that causes reduced degradation and allows us to optimize the frequency of AC:DC operation for desirable product efficiency. To do this we need to better understand transient and asymmetric operating regimes that deviate from traditional steady-state approaches. The current scientific challenge SOECs is to improve durability and enhance dynamic operation to upscale SOEC applications. This research will contribute towards the long road of upscaling solid oxide electrolysis cells by improving stability and economic viability of technology. Mitigating problems associated with SOEC long-term durable operation and towards economic operation of SOECs.

Work description:

This study develops a rigorous microkinetic model to investigate the electrochemical kinetics of a solid oxide electrolyzer cell (SOEC) under alternating current–direct current (AC:DC) operation. [1] Building upon a mechanism adapted from Luo et al [2] for reversible hydrogen-water systems, the model focuses on water electrolysis over Ni/YSZ cermet fuel electrodes. It incorporates thermodynamically consistent surface reaction kinetics coupled with a Butler-Volmer-based charge transfer formulation. Reaction rate constants are derived from literature, Arrhenius relations, and estimated sticking probabilities. The approach isolates intrinsic kinetics by neglecting transport phenomena and captures transient species evolution using a stiff differential equation solver (Radua) in Python. Scaling strategies account for surface roughness, triple-phase boundary (TPB) lengths, and unit consistency across surface and bulk interactions, enabling coupling between microscopic surface behaviour and macroscopic observables.

A surface reaction model for water electrolysis on Ni/YSZ cermet was developed, showing that water adsorbs onto Ni and YSZ, dissociating into Hydrogen, Hydroxide and Oxygen covered Ni and YSZ surfaces. This agrees with high-temperature electrolysis behavior proposed by Dasari et al [3]. The AC:DC simulations reveal significant modulation in surface species—particularly a decline in adsorbed hydrogen under periodic operation, offering potential for methane suppression in co-electrolysis. However, assumptions regarding dominant adsorption sites may require refinement for water-rich conditions. Voltage-dependent simulations reveal sensitivity in OH and O intermediate coverages and identify kinetic limitations linked to bulk oxygen accumulation. A pseudo-oxygen evolution reaction on the air side is introduced to resolve this bottleneck. The model reproduces coverage behavior trends with different cell potentials consistent with literature model proposed by Menon et al [4]. Enabling tuning factors, such as exchange current density, rate constants and charge transfer coefficients, sensitivity will allow us to further establish consistency between microkinetic rates and macroscale trends.

This work introduces the first microkinetic framework to simulate time-dependent AC:DC voltage profiles in SOECs, capturing non-equilibrium surface dynamics and TPB-limited charge transfer under transient conditions without relying on full-scale transport models. The framework is extensible and scalable, enabling future integration with Multiphysics simulations and spatially resolved domains. Ultimately, this model provides a foundational tool for understanding and optimizing dynamic SOEC operations, addressing a critical gap in the modelling of transient electrochemical processes.

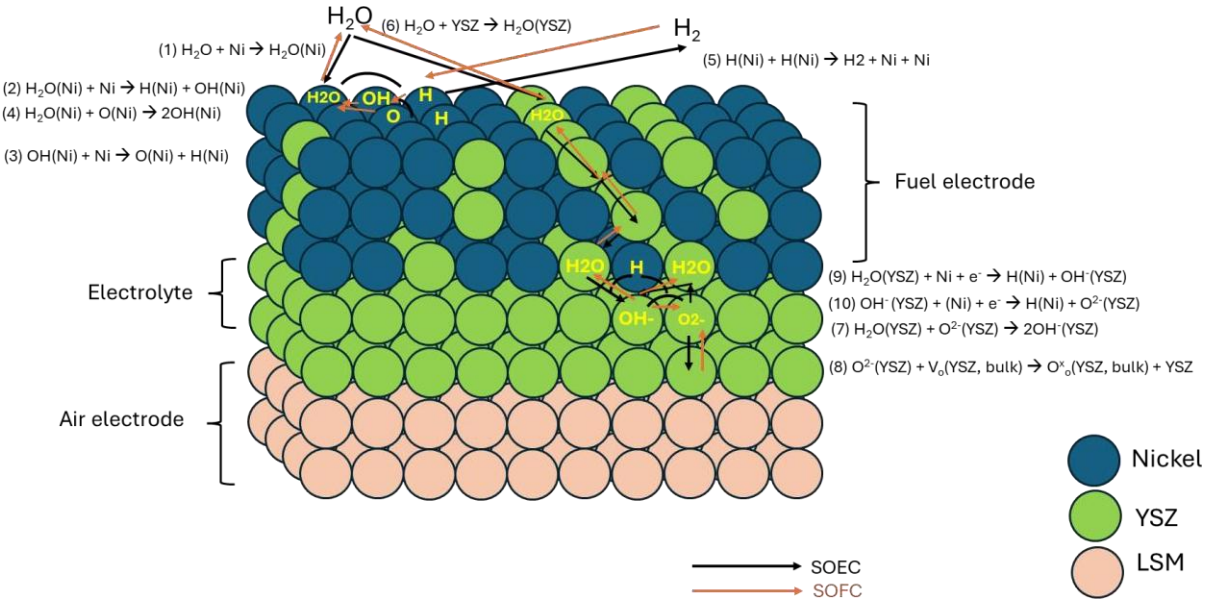


Fig.1 Schematic for elementary reactions for H2/H20 system operating in AC:DC mode

References

1. SKAFTE, Theis L., et al. *Electrothermally Balanced Operation of Solid Oxide Electrolysis Cells.* Elsevier BV, -01-25, 2022. ISBN 0378-7753.

2. LUO, Yu, et al. Mechanism of Rate-Limiting Step Switchover for Reversible Solid Oxide Cells in H2/H2O Atmosphere. *Electrochimica Acta*, 2019, vol. 326. pp. 135003. Available from <https://www.sciencedirect.com/science/article/pii/S0013468619318742>. ISSN 0013-4686.

3. DASARI, Hari Prasad, et al. Electrochemical Characterization of Ni–yttria Stabilized Zirconia Electrode for Hydrogen Production in Solid Oxide Electrolysis Cells. *Journal of Power Sources*, 2013, vol. 240. pp. 721–728. Available from <https://www.sciencedirect.com/science/article/pii/S0378775313008112>. ISSN 0378-7753.

4. MENON, Vikram; JANARDHANAN, Vinod M.and DEUTSCHMANN, Olaf. A Mathematical Model to Analyze Solid Oxide Electrolyzer Cells (SOECs) for Hydrogen Production. *Chemical Engineering Science*, 2014, vol. 110. pp. 83–93. Available from <https://www.sciencedirect.com/science/article/pii/S0009250913007124>. ISSN 0009-2509.

EFCH2 2025 European Fuel Cells and Hydrogen
PIERO LUNGHI CONFERENCE
September 17th–19th 2025
Capri / Italy

Electrochemical deposition of nife-layered double hydroxide layers for the anode catalyst in anion exchange membrane electrolyser

Stefan Edinger, Janine Lichtenberger, Marin Krammer, Rachmat Adhi Wibowo*

* corresponding author: rachmat.wibowoåit.ac.at
AIT Austrian Institute of Technology GmbH, Power and Renewable Gas Systems
Giefinggasse 2, 1210 Vienna, Austria

Keywords: anion exchange membrane electrolyser, electrochemical deposition, Nickel-alloy, oxygen catalyst.

Abstract

Introduction: Ni has been implemented as a catalyst for the oxygen evolution reaction (OER) in the emerging anion exchange membrane electrolyser (AEMEL) technology due to its characteristics of superior corrosion resistance in alkaline environments and low overpotential [1,2]. These characteristics enable the OER at the anode side without a need to use critical raw materials. In this contribution, an improved, low-overpotential OER catalyst based on the Ni alloy of NiFe-Layered Double Hydroxide (NiFe-LDH) was introduced to be implemented as an anode in AEMEL. A high-throughput electrochemical deposition was employed to prepare NiFe-LDH films.

Objectives: The contribution aims to improve the electrocatalytic behaviour of AEMEL's anode by providing a low overpotential OER catalyst based on electrochemically deposited NiFe-LDH films.

Material and methods: The NiFe-LDH films were prepared by a two-electrode electrochemical cell from electrolytes consisting of various Nickel nitrate hexahydrate and iron sulfate heptahydrate (Sigma Aldrich, Austria) mole ratios. The home-made glass with a stack of AZO/Au layers with a 25 x 25 mm^2 area was used as the substrate and was placed as the working electrode in the electrochemical cell. The counter electrode employed a platinumized Titanium mesh (IGW Plating, Austria). The electrochemical deposition and testing were carried out using an Autolab electrochemical station (Metrohm, Austria) at room temperature without any mechanical agitation. The electrochemical deposition was deliberately done at a current density of 50 µA/cm^2 in 2250 seconds, yielding an approximately 65 nm Ni-Fe deposit film thickness. For AEMEL testing, an electrolyte (1 M

KOH) is fed to both compartments (anode and cathode) via peristaltic pumps at a rate of ~4 ml/min. The electrolyzer is kept at a constant temperature of 60 °C. The experiments were carried out using a Vionic potentiostat (Metrohm, Austria). The flow rate of H_2 was measured using a manual bubble flow meter. A commercial electrolyzer with Ti flow fields and an active surface area of 5 cm_2 (Dioxide Materials, USA) was utilized.

Results: The as-deposited NiFe films' morphologies on glass/AZO/Au substrates are presented in Figure 1. The Ni deposit on the substrate resembles a nanoporous lamellae-like surface morphology. From the surface feature of the deposit, a Ni-oxide hydroxide is expected instead of a Ni metal deposit. The subsequent effect of Fe content in the NIFe deposits is apparent; it enhances the growth of fibrous or lamellae-like morphology. The growth enhancement by Fe becomes pronounced as the Fe content is larger than 50 at.%, determined by energy dispersive X-ray (EDX). This results in a bigger film porosity along with thicker lamellae walls. X-ray diffraction (XRD) experiments confirm that the NiFe deposits crystallise as NiFe layered double hydroxide with a typical $Ni(OH)_2$-like reflection (not shown).

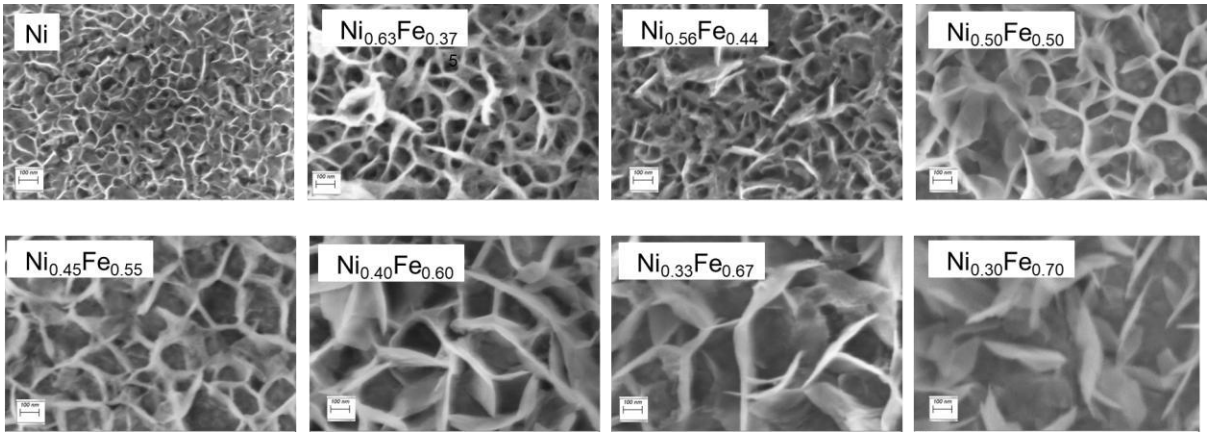


Figure 1. *As-deposited NiFe films surface morphology on planar glass/AZO/Au substrates as a function of Ni and Fe atomic contents.*

In Figure 2 (Left), the cyclic voltammetry experiments reveal the oxidation wave, followed by oxygen evolution current. The visibility of the NiFe-LDH oxidation wave is found to depend on the Fe content. Its magnitude is at the highest on Ni, followed by NiFe-LDH with Fe/(Ni+Fe) atomic ratio ~ 0.37. This anodic wave disappears as the Fe content in NiFe-LDH beyond Fe/(Ni+Fe) ~ 0.44. It is suggested that the disappearance of the anodic wave as Fe content increases is due to the overlapping of the anodic wave with oxygen evolution [2]. Fe in the NiFe-LDH tends to shift both oxidation and reduction waves to the higher overpotential. However, this is also accompanied by the shift of the oxygen evolution towards lower overpotential, which leads to the disappearance of the oxidation wave. From the viewpoint

of catalytic behaviour of NiFe-LDH, this shift is an indicator of the higher catalytic activity for oxygen evolution reaction (OER) since the oxygen evolution current takes place much earlier on NiFe-LDH with Fe/(Ni+Fe) ~ 0.37. A plot of Fe/(Ni+Fe) content vs overpotential at 10 mA/cm^2 is drawn and the result is presented in Figure 2 (Middle). The addition of Fe reduces the as-deposited layer's overpotential as low as 275 mV (NiFe-LDH layer with Fe/(Ni+Fe) 0.37 – 0.44 at. % Fe), measured at 10 mA/cm^2. The implementation of NiFe-LDH for AEMEL's anode was carried out by electrochemically depositing NiFe-LDH films with an Fe/(Ni+Fe) ratio of 0.37 on Ni felts. The AEM electrolyser employing NiFe-LDH anode demonstrates ~2.15 V at 5 A (or 2.15 V at 1 A/cm^2), showing a promising application of the NiFe-LDH in AEM electrolyser.

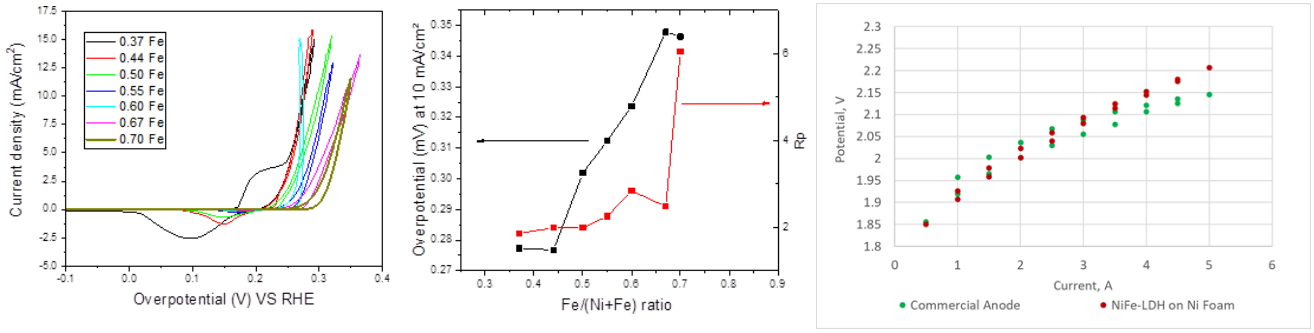


Figure 2. *(Left) Cyclic voltammograms of the as-deposited NiFe-LDH films on glass/AZO/Au substrates, (Center) and (Right), the current-voltage characteristics of the AEMEL using the NiFe-LDH as the anode.*

Conclusions: NiFe-LDH films with various Fe/(Ni+Fe) atomic ratios have been prepared by using electrochemical deposition from Ni and Fe-containing electrolytes. The deposits' surface morphological analysis reveals that the NiFe-LDH forms lamella-like and fibrous structures. Electrochemical behaviour of the deposits demonstrates the dynamic oxidation and reduction waves as a function of Fe content. The NiFe-LDHs with 0.37 – 0.44 Fe content exhibit an overpotential of ~275 mV at 10 mA/cm^2. An implementation of the NIFe-LDH as an anode in AEMEL was demonstrated, leading to 2.15 V at 1 A/cm^2.

Acknowledgment

This work is financially supported by the Austrian Promotion Research Agency (FFG) under the OxyCAT project with a project number FO999896670.

References

[1] W. Jiang et al., Adv. Funct. Mater. 2022, 32, 2203520

[2] Mary W. Louie and Alexis T. Bell, J. Am. Chem. Soc. 2013, 135, 12329−12337.

European Fuel Cells and Hydrogen
PIERO LUNGHI CONFERENCE
EFCH2 2025
September 17th–19th 2025
Capri / Italy

Gasifier and SOEC integration for enhanced fuel production

Elisabetta Orfei[a] Filippo Suzzi[b], Nicola Baraldi [d], Nikolaos Dimitratos[a], Andrea Fasolini[a], Angela Gondolini[b], Jacopo Maron[a], Elisa Mercadelli[b], Alessandra Sanson[b], Francesco Basile*[a]

* corresponding author: Francesco Basile, f.basile@unibo.it

[a] *Department of Industrial Chemistry "Toso Montanari", University of Bologna, Bologna (BO), Italy*
[b] *CNR-ISSMC, Institute of Science, Technology and Sustainability for Ceramics, CNR, Faenza (RA), Italy*
[c] *Solydera SpA Via Trento, 115/117, 38017 Mezzolombardo (TN).*
[c] *IRIDENERGY S.R.L.; Indirizzo: STRADA MADONNA DELL AIUTO 7/A - 43126 - PARMA (PR).*

Keywords: *gasifier soec integration, energy vector production, structured catalyst, tar and hydrocarbon reforming, electrodes stability*

Abstract:

The efficiency improvement, the technical feasibility and the main challenge of the integration of oxygen gasification with a soec is analysed in the soec and in the gasifier section. Tests have been carried on with structural catalyst to perform O2/H2O/CO2 trireforming process of hydrocarbons. The tests on methane results in higher performances with respect to powder catalyst even if the amount of catalyst was ten times lower.

Introduction: While main European regulations divide among Bio-H2 and RFNBO H2 groundbreaking solution can be obtained by combining biological origin feedstock and electrolysis. One of the most promising way is the use of an enhanced high temperature solid oxide electrolysis (SOEC) process in combination with a biomass gasification process, exploiting the oxygen co-produced by the electrolyser as an alternative oxidant to air or pure oxygen produced by expensive air separation units. The hydrogen produced by electrolysis is increasing the Hydrogen productivity and can be used to increase the H2/CO ratio at the exit of the gasifier, avoiding the need for a water gas shift reaction (WGSR) step and maximizing the overall efficiency of carbon conversion to fuel. The use of oxygen reach feed (eventually in combination with other gasification agents such as H2O and steam) in gasification is implemented on a highly flexible. The upgrading of the gases from gasifier will use oxygen reach mixture coming from electrolyser (nitrogen free) and will be implemented using structured catalyst promoting tri-reforming of tar and hydrocarbons inside a gasifier. This process allow to increase the quality and yields of the syngas and to increase the temperature of the exit gas up to 900°C which can be used to heat up the steam and the sweep gas fed to the SOEC, thus reducing its balance of plant (BOP) energy and costs.

Objectives:. Two project are working in the perspective of updraft and soec integration (H2 synergy and Genius fuel) with 6 main technical challenges: 1) prove the operability of the updraft gasifier (build by Iridinergy SRL) in oxygen reach atmosphere, 2) develop a foam based

system for tar and hydrocarbon upgrading by oxygen/CO2/steam, 3) tests the stability of the soec component and oxygen evolution electrodes in oxygen, CO2 and steam atmosphere, 4) Increase SOEC performance at 700°C or lower and 5) production of renewable fuel with high efficiency and high carbon utilization 6) char valorization . In this abstract the focus will be on proven the technical feasibility of the process and mainly on carried out a preliminary evaluation of the potential efficiency, highlights the main challenges related to SOEC and describe the performances in the structure catalyst development obtained in H2 synergy

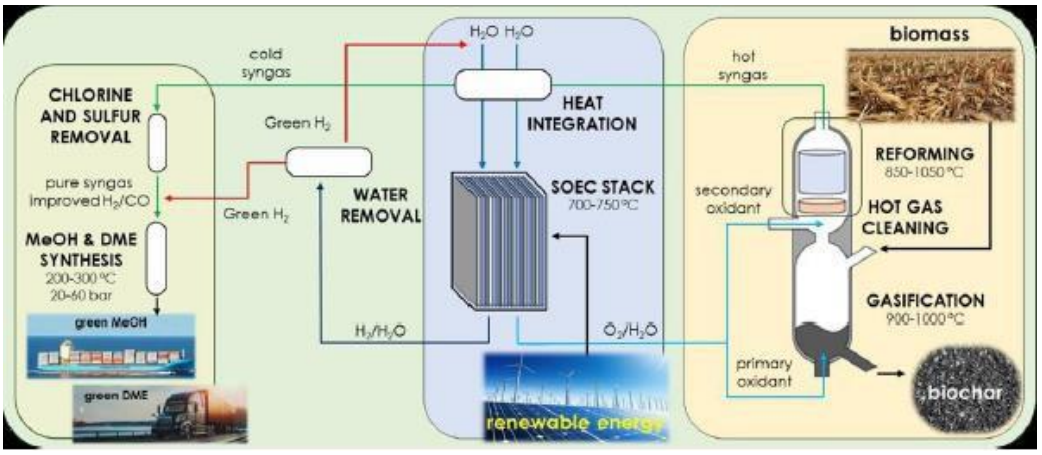


Figure 1 : scheme of the process integration between gasifier and SOEC.

Materials and methods. A preliminary analysis of the efficiency of the system was based on literature study and mass and energy balance while the effect of $O_2/H_20/CO_2$ atmosphere on the soec materials and components have been analysed identifying challenges in terms of materials stability and power density change. Finally the NiMgAl LDH have been synthetized by coprecipitation and calcined to mixed oxides[1,2]. Catalysts were pelletized or coated on a NiCrAl foam by dip-coating. The reduction (10%vH_2) and tri-reforming catalytic tests were carried out in a plug flow reactor feeding CH_4, CO_2, H_2O and O_2.

Results and discussion. The process use a 50 Kg/h biomass patented gasifier based on an updraft system and a two-stage oxidant injection system (one at the bottom of the gasifier for biomass gasification and one at the top to upgrade the produced gases). In air configuration the concentration of the resulting syngas (CO + H2) is 58-60% (H_2O and N_2 free bases) and it still contains 8 % methane and other unconverted hydrocarbons. The use of oxygen and the conversion of hydrocarbons to CO and H2 increases the efficiency to MeOH+H2 e from 16.5 to 42.6 % and the carbon conversion to fuel from 12.8 to 32.2 %. For this purpose two type of catalyst based on NiMgAl powder have been tested. In specific to prepare the catalyst on metallic foam the powder was suspended in water and the effect of different deflocculants, binders and surfactant was studied to obtain a stable suspension with reological properties and wetting ability adequate for the dip coating. The optimized suspension was used in dip-coating repeated up to four times. The catalysts were analyzed by XRD and SEM analysis, which showed a micrometric NiMgAl coating homogenously

distributed over the foam. The final catalytic system was obtained by stacking 7 foams layers with a thermos-press. (Figure 2). In past autothermal reforming tests hot spot are reduced and catalyst performances have shown to be crucial. The NiMgAl pelletised catalyst showed high performances converting more than 90% of CH_4 and 75% of CO_2 in the best conditions while the comparison of the pellets and coated foams showed that an increase in the conversion to 97% and 80% for CH_4 and CO_2 respectively is given by the structured catalyst with stable performance under reaction conditions. Interestingly, the amount of catalyst deposited over the foam was almost one order of magnitude lower than the one charged as pellets, even if a side effect on thermal profile is present an increase of the effectiveness in the use of catalyst is the main factor due to an increase of external area and active phase exposed and a decrease of the intrapore diffusion limitation in oxygen conversion reactions. Furthermrore the scale up of the structure catalyst have been carried out in 1*1 inch foam.

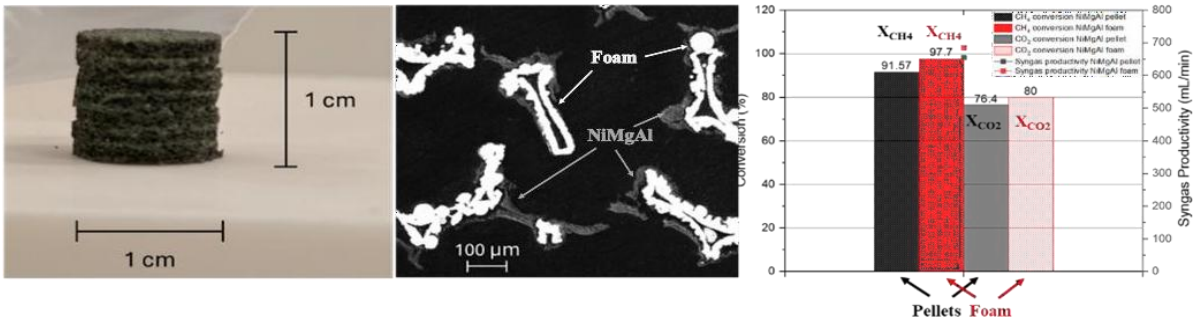


Figure 2: coated foam (left) SEM analysis of the coated foam (middle), tri-reforming performances (right) at 800°C, 1 atm, CH_4/CO_2 1.5; O_2/CH_4 0.21, S/CH_4 0.2, GHSV 40000 h^{-1}

Process efficiency can be improved by integrating a high temperature solid oxide electrolyser (SOEC) to i) supply the H2 required to adjust the H2/CO ratio of the syngas and to ii) provide the O2 needed for the gasification and the partial oxidation of hydrocarbons iii) the use of heat (from reaction) for steam generation for SOEC. In this perspective the use of pure oxygen in the oxygen evolution side can cause corrosion while dilution with CO2 and water can respectively decrease the power supply or increase the energy cost due to steam production.

Conclusion: The integration of SOEC and gasifier in the best scenario allow to increase the efficiency to CH_3OH and the carbon conversion to fuel at 55.6% and 47.6%, respectively.

Acknowledgments

European funding from the Emilia-Romagna Region, H2-Synergy - PR FESR 2021-2027 ACTION 1.1.2 Call for strategic industrial research projects targetting the priorities of the smart specialization strategy referred to in DGR 2097/2022 – S3 Area: Clean, safe and affordable energy; (PN° PG/2023/311159). CETP project Genius Fuels is also aknoledged.

References

[1] Basile, F., et al., Biomass and Bioenergy, **2011**, *32*, s116-S122.
[2] Fasolini, A., et al. *Catal Today* **2023** *423* 114271.

EFCH2 2025 European Fuel Cells and Hydrogen
PIERO LUNGHI CONFERENCE
September 17th–19th 2025
Capri / Italy

Integrated membrane & biogas electrified catalytic reformer for decarbonised h_2 production

Vincenzo Palma [a], Eugenio Meloni [a], Concetta Ruocco [a], Antonio Vita [b], Cristina Italiano [b], Adolfo Iulianelli [c]

* corresponding author: V. Palma
[a] Department of Industrial Engineering, University of Salerno, Via Giovanni Paolo II 132, 84084 Fisciano, SA, Italy
[b] Advanced Energy Technology Institute, National Research Council of Italy (CNR-ITAE), Salita Santa Lucia Sopra Contesse 5, 98126 Messina, ME, Italy
[c] National Research Council - Institute on Membrane Technology (CNR-ITM), via P. Bucci 17C, Rende, (CS), 87036, Italy

Keywords: Biogas Reforming, Electrified Catalytic Reactor, Hydrogen Production Efficiency, Pd-Based Membrane

Introduction:

The decarbonised production of hydrogen from renewable feedstocks is a strategic goal in the context of the energy transition. Biogas, due to its availability and carbon-neutral footprint, is a promising candidate for hydrogen production via catalytic reforming. Integrating Joule-electrification of structured catalysts and membrane separation in a single intensified unit may overcome traditional reforming limitations in terms of energy efficiency and purity of H_2.

Objectives:

This study aims to develop and test an electrified catalytic reformer equipped with a hydrogen-selective Pd-based membrane, using synthetic biogas as feedstock. The objective is to evaluate the potential of the direct Joule heating of structured catalysts and the integrated membrane separation for enhancing hydrogen yield as well as energy efficiency.

Material and methods:

A structured metallic foam coated with a Ni-based catalyst was directly heated via the Joule effect to reach reforming temperatures. The catalyst was properly shaped in order to be perfectly integrated with a tubular dense Pd-Ag membrane to continuously separate hydrogen during operation. Tests were performed at temperatures between 400–550 °C, at pressures up to 4 bar, and varying WHSVs. The energy efficiency was calculated considering the total electrical power input, the overall ideal enthalpy changes, and the H_2 produced.

The experimental plant employed for membrane permeation tests as well as catalyst activity measurements consists of a feed, reaction and analysis section. The CH_4/CO_2/Ar stream (45%-45%-10%) can be admitted to the catalytic membrane reactor by means of mass-flow controllers. Before dry reforming tests, the Ni/La_2O_3-CeO_2 catalyst is activated under a 5% H_2/Ar stream at 600°C for 1h at 10°C/min.

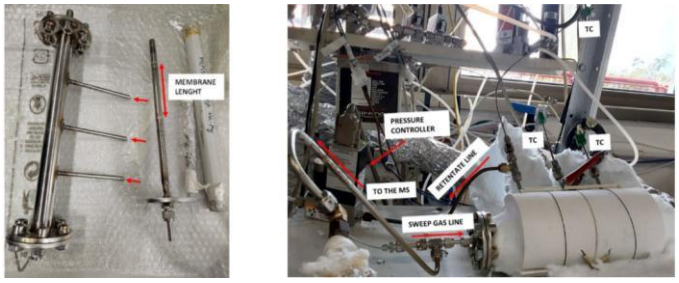


Figure 1 displays the reactor employed, the reaction section including the heating system, and the pressure controller.

Once completed the membrane activation procedure, the membrane permeation tests were carried out by feeding H_2-N_2 streams with an H_2 concentration ranging from 10 to 100%; a flowrate of 300 $Ncm^3 \cdot min^{-1}$ of Ar was fed in the permeate side, while the outlet permeate stream can be monitored on-line by means of a Hiden mass spectrometer.

The results of permeation tests were compared in terms of H_2 purity (P_{H2}) and H_2 selectivity (S_{H2}), defined, respectively, in Eq. 1 and Eq. 2 (Q refers to the normal flowrate).

$$P_{H_2} = \frac{Q_{H_{2,permeate}}}{Q_{H_{2,permeate}} + Q_{N_{2,permeate}}} \cdot 100 \qquad \text{Eq. 1}$$

$$S_{H_2} = \frac{Q_{H_{2,permeate}}}{Q_{N_{2,permeate}}} \cdot 100 \qquad \text{Eq. 2}$$

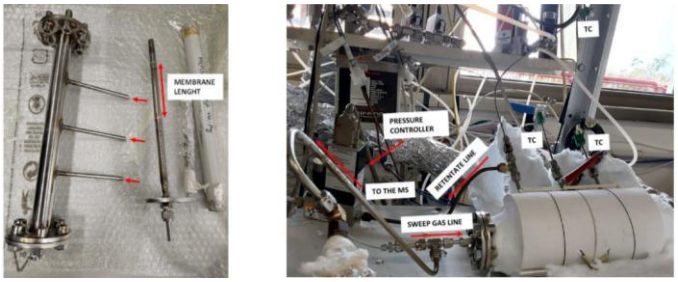


Figure 1. Membrane reactor (left) and reaction section (right) during H_2-permeation tests.

Results:

The system demonstrated stable operation under all the tested conditions. An increase in the operating pressure from 3 to 4 bar significantly enhanced the hydrogen flux through the membrane, reaching up to 15,600 $Ncm^3 \cdot min^{-1} \cdot m^{-2}$. The reactor achieved energy efficiencies

as high as 90%, surpassing those reported in literature for electrified reformers without membranes, such as ~80% at 720 °C [1] and ~60% at 550 °C [2,3].

Conclusions:

The results obtained demonstrate the strong potential of electrified membrane reformers as a disruptive (oppure bursting) technology for low-carbon hydrogen production from biogas. The direct Joule heating of the structured catalyst enabled outstanding energy efficiency, reaching values up to 90%, significantly higher than those typically reported for conventional or non-integrated electrified systems. This high performance, combined with the use of green electricity, results in a nearly fully decarbonised hydrogen pathway. Furthermore, this work represents one of the first experimental demonstrations of a catalytic reformer that integrates a hydrogen-selective Pd membrane with a Joule-heated structured catalyst, confirming the feasibility of this innovative configuration and its relevance for modular and decentralised H_2 production in a renewable context.

Acknowledgment

The authors would like to thank the MIUR for funding this work as part of the project “PLUG-IN” - Process for Low-carbon blUe & green hydrogen Generation via Intensified electrified reforming of Natural gas/biogas (PRIN 2020)

References

[1] Meloni, E. et al. (2024). Highly-efficient hydrogen production through the electrification of OB-SiC nickel structured catalyst: Methane steam reforming and ammonia cracking as case studies, 65, 42 – 49. DOI: 10.1016/j.ijhydene.2024.03.349
[2] Meloni, E. et al. (2023). SiC-based structured catalysts for a high-efficiency electrified dry reforming of methane. Renewable Energy, 211, 336–346.
[3] Zheng, L. et al.(2023). Direct electrification of Rh/Al2O3 washcoated SiSiC foams for methane steam reforming: An experimental and modelling study. International Journal of Hydrogen Energy, 48(39), 14681–14696Z

European Fuel Cells and Hydrogen
PIERO LUNGHI CONFERENCE
September 17th–19th 2025
Capri / Italy

One future of hydrogen production: Solar Heat Supported Solid Oxide Electrolysis Cell

Nathalie Monnerie*[a], Yasuki Kadohiro [a,c], Timo Roeder [a,b], Kai Risthaus [a], Enric Prats-Salvado [a,b], Christian Sattler [a,b]

* corresponding author: nathalie.monnerie@dlr.de

[a] Deutsches Zentrum für Luft- und Raumfahrt – DLR/German Aerospace Center, Institute of Future Fuels, Linder Höhe, 51147 Cologne, Germany

[b] RWTH Aachen University, Faculty of Mechanical Engineering, Chair for Solar Fuel Production, 52062 Aachen, Germany

[c] Dresden University of Technology, Faculty of Mechanical Science and Engineering, Chair of Hydrogen and Nuclear Energy, 01069 Dresden, Germany

Keywords: Concentrated solar energy, Hydrogen, High temperature electrolysis

Abstract:

An energy economy focused on hydrogen begins to be developed in order to reduce CO_2 emissions, and non-fossil hydrogen production is now more important than ever. High temperature steam electrolysis has the potential to have the highest electric efficiency among the several electrolysis techniques for producing sustainable hydrogen based on electricity from renewable sources. The required high-temperature heat can be produced and delivered by concentrated solar thermal technology. This solar-driven technology has been evaluated through simulation and experimental research, paving thus the way for energy systems in the MW_e range.

Introduction:

Combining solar thermal energy with high temperature electrolysis is one promising pathway to produce green hydrogen and to go towards hydrogen economy. On one hand the high-temperature electrolysis operates indeed with the highest electrical efficiency as a part of the required energy is supplied by high temperature heat [1] and on the other hand solar tower systems are able to supply the thermal energy needed for high-temperature electrolysis [2]. Different receiver reactors have been tested in order to produce either steam required [1] or hot air, used for removing excess oxygen [3] and first simulations were carried out [4]. However, in order to produce green hydrogen in large quantities in the future, different

scenarios still needed to be analysed and a receiver concept that can produce high-temperature steam and air at the same time larger than laboratory scale is still required.

Objectives:

The aim of this work is to assess the future potential of coupling concentrated solar energy with a solid oxide electrolysis cell (SOEC), including heat storage, in order to produce green hydrogen.

This evaluation is done not only through process simulation but also with experimental research which validate the models, paving thus the way for energy systems in the MW_e range.

Material and methods:

Different scenarios have been developed for the integration of concentrated solar energy in hydrogen production via high temperature electrolysis wherein the subsystems are coupled and integrated with each other, including heat storage. Process flowsheets have been elaborated in accordance with these scenarios and process simulations have been done.

To validate this technology development through experimental investigations, a solar reactor for coupling concentrated solar energy to the SOEC has been designed, optimized and scale-up for the first time to 70 kW_{th} nominal power scale for the experiments, based on previous experience [1] and has been tested.

Results:

Simulations of the processes have been carried out first in steady state with Aspen Plus software for MW-scale hydrogen production plants. A transient process simulation was then conducted using Python, considering the unique solar resource data of various locations, in order to assess the coupling of concentrated solar energy with SOEC. At the studied sites, a process utilization of up to 7900 full load hours is achievable.

Regarding the new concepted reactor, it enables not only to deliver high temperature steam but can also heat air in the same time to increase the electric efficiency and decrease temperature gradients in the SOEC thus potentially increasing lifetime. It has been successfully tested in the DLR solar simulator Synlight [5], and both hot air and steam at the target temperatures above 800°C and stable conditions required by the SOEC to produce green hydrogen has been produced for several hours [6] as shown on figure 1.

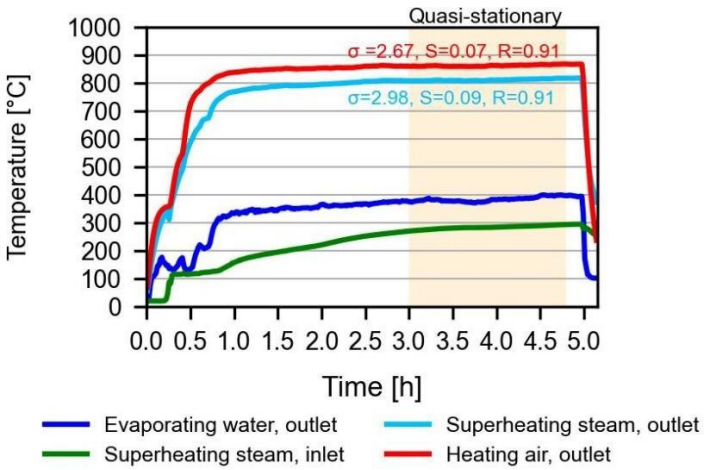


***Figure 1**. Fluid temperature results of a new concepted solar reactor during the experiment. "σ", "S", and "R" represent standard deviation, slope, and correlation coefficient, respectively.*

The target temperature above 800°C is also beneficial for co-electrolysis to produce synthesis gas which can be e.g. further converted into liquid fuel by the Fischer-Tropsch synthesis process.

Conclusions:

To evaluate the solar-driven high temperature electrolysis, process simulations have been conducted for several scenarios, considering different solar resources. Moreover, from an experimental point of view, the solar components have been improved and scaled-up in comparison to earlier experiments for the coupling of concentrated solar energy with the high temperature electrolyser and have been successfully tested for simultaneously direct steam generation, superheating of steam, and preheating of air.

Acknowledgment

The authors of this paper gratefully acknowledge the financial support from DLR's basic funding of the projects Solar Heat Supported Solid Oxide Cell Electrolysis, NeoFuels and HybrEEen.

References

[1] G. Schiller, M. Lang, P. Szabo, N. Monnerie, H. von Storch, J.-P. Reinhold, P. Sundarraj. (2019) Solar heat integrated solid oxide steam electrolysis for highly efficient hydrogen production. Journal of Power Sources, 416, 72-78. Elsevier. doi: 10.1016/j.jpowsour.2019.01.059. ISSN 0378-7753.

[2] M. J. Blanco, S. Miller. (2017). Introduction to concentrating solar thermal (CST) technologies. In: M.J. Blanco, L.R. Santigosa (eds) Advances in Concentrating Solar Thermal Research and Technology: Woodhead Publishing Series in Energy. Woodhead Publishing, 3–25.

[3] S. Chu, F. Bai, X. Zhang et al. (2018) Experimental study and thermal analysis of a tubular pressurized air receiver. Renewable Energy 125:413–424. https://doi.org/10.1016/j.renene.2018.02.125

[4] N. Monnerie, H. von Storch, A. Houaijia, M. Roeb, C. Sattler. (2017). Hydrogen production by coupling pressurized high temperature electrolyser with solar tower technology. Int. J. Hydrogen Energy, 42, 13498–13509

[5] K. Wieghardt, D. Laaber, P. Hilger, V. Dohmen, K.-H. Funken, B. Hoffschmidt. (2016) Engineering and Erection of a 300kW High-Flux Solar Simulator. In: AIP Conference Proceedings, 1850 (130013). American Institute of Physics. 22nd SolarPACES Conference, 2016-10-11 - 2016-10-14, Abu Dhabi, VAE. doi: 10.1063/1.4984507.

[6] Y. Kadohiro, T. Roeder, K. Risthaus, D. Laaber, N. Monnerie, C. Sattler. (2024) Experimental demonstration and validation of tubular solar cavity receivers for simultaneous generation of superheated steam and hot air. Applied Energy. Elsevier. doi: 10.1016/j.apenergy.2024.125042.

European Fuel Cells and Hydrogen
PIERO LUNGHI CONFERENCE
September 17th–19th 2025
Capri / Italy

High performance of a thin short-side-chain Aquivion® membrane for sustainable water electrolysis application

Antonino Salvatore Aricò*[a]

* Corresponding author: arico@itae.cnr.it
[a] CNR-ITAE Institute of Advanced Energy Technologies, National Research Council, Via Salita S. Lucia Sopra Contesse 5, 98126, Messina, Italy

Keywords: green hydrogen production, sustainable energy supply, water electrolysis, proton exchange membrane

Abstract

A perfluorosulfonic acid (PFSA) Aquivion® membrane (C98 05S-RSP) based on Ce-radical scavenger technology was developed and evaluated for use in polymer electrolyte membrane (PEM) electrolyzers. Manufactured by Solvay Specialty Polymers, the membrane had an equivalent weight (EW) of 980 g/eq and a thickness of 50 µm to minimize ohmic losses at high current densities. The electrochemical properties and gas crossover were assessed after creating a membrane-electrode assembly (MEA) over a temperature range of 30 to 90°C and under varying differential pressures (ambient, 10, and 20 bars). For comparison, bare extruded (E98 05S) and reinforced (R98 05S) PFSA Aquivion® membranes with similar EWs and thicknesses were tested under the same conditions to evaluate their performance, stability, and hydrogen crossover. The membrane manufacturing method had a notable impact on the interfacial properties, with the electrodes influencing polarization resistance, H_2 permeation in the oxygen stream, and the degradation rate, as indicated by the durability tests.

Introduction:

Green hydrogen is crucial for combating climate change, with PEM electrolysers offering high efficiency, reduced energy consumption, and improved safety at high pressures. [1] To enhance efficiency, strategies include minimizing precious metals and using coated stainless steel in bipolar plates, along with thinner membranes and recombination catalysts. Short-side-chain PFSA Aquivion® membranes provide better ionic conductivity and lower gas crossover compared to Nafion®. [2] Incorporating Pt nanoparticles and radical scavengers like Ce or Mn nanoparticles can improve stability and reduce degradation. The study shows that Aquivion® membranes with Ce-radical scavenger powder (C98-05S-RSP) significantly improve stability and performance over standard Aquivion® membranes.

Objectives:

The present work shows how the properties of a thin short-side-chain Aquivion® membrane with a thickness of 50 µm, containing Ce-radical scavenger powder (C98-05S-RSP), assessed in a differential pressure PEM electrolyser, can considerably affect the performance and stability with respect to bare Aquivion® membranes, extruded and reinforced (E98 05S and R98 05S, respectively).

The electrochemical properties and gas crossover of the membrane under study were evaluated in a range of temperatures between 30 and 90 °C and at various differential pressure (pressurised H_2; non-pressurised O_2) values (ambient, 10 and 20 bars). The electrocatalytic layers, which were deposited onto the membrane to form the MEA, consisted of Pt/C for the cathode and IrRuOx for the anode in combination with Aquivion® ionomer dispersion to enhance the electronic percolation within the catalytic layers.

Material and methods:

A catalyst-coated membrane (CCM) method was employed for the preparation of membrane–electrode assemblies. The catalyst loading was 0.1 Pt and 0.37 Ir/Ru mg cm^{-2} at the cathode and anode, respectively. The anodic and cathodic catalyst–ionomer inks were prepared by mixing the respective catalyst with Solvay ionomer in the defined ratios, with ethanol, and were deposited on membrane by spray deposition technique. The Galvanostatic polarization curves and electrochemical impedance spectroscopy (EIS) measurements were carried out at 1.5V, 1.8V at different temperatures, in a range of 30–90 ◦C, and at different pressure conditions (ambient, 10 and 20 bars). The stability and the degradation of the MEAs were investigated by a galvanostatic durability test at 1 A/cm^2.

Results:

For comparison, bare extruded (E98 05S) and reinforced (R98 05S) PFSA Aquivion® membranes, with similar equivalent weights (EWs) and thicknesses, were electrochemical tested in a single electrolysis cell under identical conditions of pressures and temperatures to assess their performance, stability, and hydrogen crossover.

In the durability test, C98 05S-RSP membrane demonstrated better kinetic performance, particularly after an initial reduction phase of 3000 hours. After the durability test, C98 05S-RSP membrane showed a higher ohmic resistance, which resulted in a lower slope in polarization curves at high current densities compared to the extruded and reinforced membranes.

Hydrogen concentration in the oxygen stream was measured at constant temperatures of 55°C and 90°C under differential pressure conditions, varying with current density. When differential pressure was applied, hydrogen concentration in the oxygen stream increased at

low current densities. The extruded membrane shows a lower capability to mitigate the hydrogen crossover as a function of the temperature.

Conclusions:

This study demonstrates that both membrane fabrication and the incorporation of a Ce nanofiller have a significant impact on the properties at the interface with the electrodes in a PEM water electrolysis cell. In particular, the Ce-based radical scavenger perfluorosulfonic acid Aquivion® membrane exhibited significant resistance to degradation and reduced H_2 content in the oxygen. The enhanced performance observed during a 3500-hour durability test suggests that the nanofiller effectively improves the system's stability.

Acknowledgment

The authors acknowledge the financial support from the ADVANCEPEM project. This project is supported by the Clean Hydrogen Partnership and its members including top-up funding by the UK Research and innovation under grant agreement No 101101318. This Joint Undertaking receives support from the European Union's Horizon Europe research and innovation programme, Hydrogen Europe and Hydrogen Europe research.

References

[1] Capurso, T.; Stefanizzi, M.; Torresi, M.; Camporeale, S.M. Perspective of the role of hydrogen in the 21st century energy transition. Energy Convers. Manag. 2022, 251, 114898.
[2] Siracusano, S.; Pantò, F.; Tonella, S.; Oldani, C.; Aricò, A.S. Reinforced short-side-chain Aquivion® membrane for proton exchange membrane water electrolysis. Int. J. Hydrog. Energy 2022, 47, 15557–15570.

European Fuel Cells and Hydrogen
PIERO LUNGHI CONFERENCE
EFCH2 2025
September 17th–19th 2025
Capri / Italy

Recombination catalyst effect on AEM properties for AEMWE application

A. Carbone*[a], S. C. Zignani[a], I. Gatto [a], M. Pascale [a], M. Fazio [a], Z. Moreno Botello [a], A. Aricò [a]

* corresponding author: Alessandra Carbone
[a] CNR - Istituto di Tecnologie Avanzate per l'Energia (ITAE)

Keywords: Anion Exchange Membrane (AEM), Recombination Catalyst, Anion conductivity, Anion Exchange Membrane Water Electrolyzer (AEMWE)

Introduction:

Anion Exchange Membrane Water electrolysis (AEMWE) is an emerging technology alternative to traditional Alkaline Water Electroysis (AWE), due to the advantage to operate with cheap non-platinum or non-precious group metal catalysts while concentrated KOH can be replaced by diluted alkaline solutions. AEMWE is not yet as durable as AWE, as catalysts, membranes and electrodes tend to degrade under the desired operating conditions. In particular, thinner membranes can increase cross-over of H_2 into the O_2 stream, creating a safety risk. In situ radical generation is the main cause of membrane chemical degradation. [1]

Different strategies have been developed to improve the electrolysers safety characteristics, among these, recombination catalyst (RC) for the hydrogen permeated to oxygen site are most investigated.[2] The approach is generally based on the use of a hydrogen oxidation catalyst at the interface with the membrane and an anode catalyst layer. In this work the approach is the development of membranes containing Pt recombination catalyst dispersed in the polymer matrix for reducing the anodic hydrogen content.

Objectives:

The objective of this work is to develop recast membranes containing recombination catalysts to limit the effect of the H_2 crossover at the oxygen site of AEMWE.

Material and methods: Membranes preparation and characterization

FAA3 solid ionomer (shredded film by Fumatech) was solubilized in dimethylsulfoxide (DMSO) (10 wt%) at 60 °C, under magnetic stirring. Different loadings of RC were added to the polymer dispersion, and the solvent was evaporated to obtain a suitable viscosity to be cast with a doctor-blade. The membranes were characterized in terms of ion-exchange capacity (IEC), water uptake (Wup%), creep tests and anion conductivity. Used RC are 40 % Pt/C ALFA AESAR and 50 % Pt/C Tanaka.

In-situ electrochemical tests were carried out in a 5 cm^2 single cell in AEMWE configuration. Tests were carried out in the temperature range 50-90 °C flowing 0.5 M KOH at the anode side. Electrodes were prepared by spray-coating process, using NiFe catalyst deposited on a Ni felt at the anode side and Ni felt at the cathode.

Results:

The effect of RC properties was evaluated, in fact two different commercial catalysts were used in different percentages. In particular, Pt/C Alfa AESAR and Tanaka catalysts were adopted for composite membrane development. In table 1 are reported the developed membranes and physico-chemical results.

Table 1 Membrane composition and physico-chemical properties

MEMBRANE	Catalyst	Loading, wt %	Thickness, μm	IEC_{OH}, meq/g	Wu 30°C, %	Wu 60°C, %
FAA3-50	-	-	50	1.13	20	45
FAA3-11 S	-	-	30	2.74	23	29
FAA3-12 S	40% Pt/C AA	0.5	28	2.66	36	41
FAA3-14 S	50% Pt/C Tanaka	0.21	28	2.38	22	30
FAA3-16 S	50% Pt/C Tanaka	0.5	32	2.03	22	31

It is evident that the addition of different RCs produces different properties in terms of IEC and wu. In fact, the loading of 50 wt % produces membranes with different IEC and water uptake at both 30 °C and 60 °C. The IEC was reduced respect the recast membrane (FAA3-11S) and the highest reduction is obtained with Tanaka catalyst. This means that there could be hypothesized an interaction between the surface groups of the Carbon and the functional groups of the polymer. In addition, the water uptake is higher for FAA3-12 S respect FAA3-16 S and FAA3-11 S recast membrane, meaning that the water sorption properties are increased in accordance to the RC hydrophilic properties.

Preliminary electrochemical single cell tests and EIS measurements at 2 V are reported in Figure 1 at 60 °C.

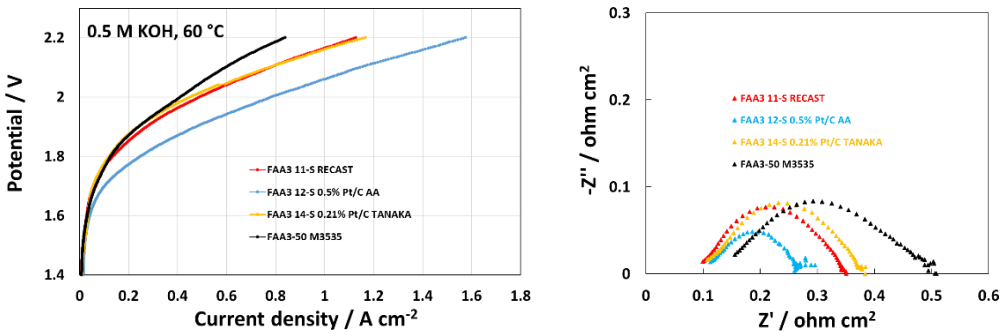


Figure 1 I-V curves and EIS spectra at 2 V of developed MEAs at 60 °C.

The I-V curves of the tested samples are in accordance with the water uptake data. In fact, membranes with higher water uptake, shown better performance reaching 2.06 V @ 1 A/cm^2. The EIS confirm this behaviour, with similar Rs value for all samples. FAA3-12 S sample shows also lower Rct, in accordance with best I-V curve and higher water transport.

Conclusions:

The introduction of RC into the polymer matrix, affects the properties of the final membrane. The properties of the carbon used a s a support influence the physico-chemical properties, in terms of IEC but in particular the water uptake.

The membrane with the highest water uptake show the best performance and reduced charge transfer resistance.

Acknowledgment

The authors acknowledge the financial support provided by the Clean Hydrogen Partnership Horizon Europe “AEMELIA” project Grant Agreement number: 101137912

References

[1] Naiying Du, Claudie Roy, Retha Peach, Matthew Turnbull, Simon Thiele, Christina Bock, Anion-Exchange Membrane Water Electrolyzers, Chemical Reviews 2022, 122, 11830−11895

[2] N. Briguglio, F. Pantò, S. Siracusano, A.S. Aricò, Enhanced performance of a PtCo recombination catalyst for reducing the H 2 concentration in the O 2 stream of a PEM electrolysis cell in the presence of a thin membrane and a high differential pressure, Electrochimica Acta, 344(16):136153

EFCH2 2025 European Fuel Cells and Hydrogen
PIERO LUNGHI CONFERENCE
September 17th–19th 2025
Capri / Italy

Redox-Mediated Electrolysis of Tar from Biomass Gasification for Hydrogen Production

F. Zimbardi*[a], U. Calice[ab], N. Cerone[a], A. Romanelli [a], V. Valerio[a]

* corresponding author: francesco.zimbardi@enea.it

[a] ENEA, Dipartimento Tecnologie Energetiche e Fonti Rinnovabili, SS 106, 75026 Rotondella (MT), Italy

[b] Università degli Studi della Basilicata, Via dell'Ateneo Lucano 10, 85100 Potenza, Italy

Keywords: Biomass gasification, hydrogen, redox mediator, waste

Introduction:

Biomass electrolysis is a sustainable and energy-efficient alternative to conventional water electrolysis. Unlike water electrolysis, which requires high cell voltages (>1.8 V) and energy input (~4.8 kWh/Nm³ H_2), biomass electrolysis utilizes organic feedstocks such as ethanol, glycerol, lignocellulosic biomass derivatives, to generate hydrogen at significantly lower voltages (~0.6 V), reducing energy consumption by up to three times [1]. Unlike traditional electrolysis, where the oxygen evolution reaction (OER) dominates at the anode, biomass electrolysis can selectively oxidize organic feedstocks, yielding organic molecules alongside hydrogen. This process can be designed to co-produce value-added chemicals alongside hydrogen, significantly improving economic viability. Different biomass-derived feedstocks offer distinct advantages in hydrogen production. The most interesting feedstock is lignocellulosic biomass, which includes agricultural and forestry residues. It is an abundant and renewable hydrogen source. However, its complex polymeric structure, made of cellulose, hemicellulose, and lignin, requires pretreatment to release fermentable sugars for electrolysis. The general process is:

$$\text{Biomass feedstock} + H_2O \rightarrow CO_2 + H_2 + \text{Chemicals}$$

To optimize efficiency, various electrocatalysts have been investigated, including Ni-based catalysts, which improve biomass oxidation at the anode. Recently, polyoxometalates (POMs) have emerged as promising electrocatalysts due to their high redox activity, tuneable electronic structure, and ability to facilitate multi-electron transfer reactions. POMs have shown potential in improving catalytic efficiency for both HER and OER, thereby enhancing overall H_2 production efficiency from biomass-derived feedstocks. Another promising approach involves the use of $FeCl_3$ as a redox mediator in biomass electrolysis. $FeCl_3$ can

effectively facilitate electron transfer in oxidation reactions, improving the efficiency of lignocellulosic biomass breakdown. It acts by forming Fe^{2+}/Fe^{3+} redox couple, which enhance the conversion of biomass intermediates into hydrogen and chemicals. This approach is particularly useful in combination with Ni- or POM-based catalysts, creating synergistic effects that improves overall process efficiency. On another side, biomass gasification offers a route for H_2 generation, utilizing renewable feedstock and minimizing waste. In thermochemical conversions the formation of tar poses significant operational challenges, necessitating effective mitigation strategies to enhance efficiency and sustainability.
By appropriately coupling the thermochemical and electrochemical technologies it is possible to maximise the production of H_2 from biomass and establishing a more sustainable process, both from the energetic and environmental point of view. In particular, the smart use of renewable power will increase the yield of hydrogen which in turn is a form or energy storage to stabilise the energy grid [2].

Objectives: The study focused on H_2 production using as feedstock the tar obtained from biomass gasification in a pilot updraft reactor. The organic compounds recoverable in the aqueous phase of a scrubbing system underwent a redox-mediated electrochemical treatment using separately $FeCl_x$ and PMA. The proposed integration allows simultaneous organic waste treatment and H_2 production.

Material and methods: Tar was obtained from the pilot plant PRAGA after gasification of hazelnut shells, the aqueous phase was sampled from the scrubber of the plant after gasification campaigns [3]. Heating tar 100°C for 5 hours enabled its oxidation and the reduction of the redox mediators, PMA hydrate and $FeCl_3$. The electrochemical experiments were conducted in an H-cell made of borosilicate glass, equipped with a perfluorinated cation exchange membrane (Nafion 117). The anode consisted of a graphite electrode, while the cathode was a platinum electrode. A standard Ag/AgCl reference electrode was used to monitor the cell potentials. The electrolyte in the cathodic compartment consisted of demineralized water and 1M H_3PO_3. Chronoamperometry, chronopotentiometry, and electrolysis experiments were performed to evaluate electron transfer and hydrogen production. The H_2 was quantified from the produced current at the cathode. The composition of tar, before and after oxidation, was determined using HPLC and GC-MS.

Results: The oxidation of tar was successfully achieved. When PMA was used as the redox mediator, complete oxidation to CO_2 was observed. In contrast, oxidation with the Fe^{2+}/Fe^{3+} system resulted in partial oxidation, with CO_2 as primary product. The degree of oxidation of PMA following tar treatment was verified through chronopotentiometric analysis. HPLC and GC-MS analyses confirmed a substantial degradation of tar components post-oxidation. The

Fe^{2+}/Fe^{3+} oxidation system led to a significant reduction of several tar components. Notably, phenol and its derivatives were almost eliminated, with reductions exceeding 95% for compounds such as phenol, phenol, 3-ethoxy, and vanillin. Other oxygenated organic compounds, such as 1-hydroxy-2-butanone and 2-propanone, 1-(acetyloxy)-, also exhibited a drastic decrease. Other molecules, such as 2(5H)-furanone and 2-cyclopenten-1-one, 2-hydroxy-3-methyl-, showed partial degradation, with reductions of 27.4% and 63.8%, respectively. Overall the yield of H_2 was on average 0.35 cm^3 (STP) per gram of treated tar. The energetic cost was assessed by comparing the oxidation potential of different mediators after tar pretreatment, using the same conditions each time. In the best-performing experiment—oxidizing the PMA redox mediator after biomass pretreatment—the anodic oxidation processes in water showed a decrease in energy consumption, from an anodic contribution of 30.6 kWh per kg of H_2 (1.15V) for OER, to 14.7 kWh per kg of H_2 (0.55V), resulting in a theoretical 52% energy savings. These results demonstrate the feasibility of coupling tar oxidation with hydrogen production through a mediated electrochemical process, offering an effective approach for waste valorisation and sustainable energy generation.

Conclusions: This study confirms the potential of redox-mediated oxidation for converting tar into CO_2 and reducing the aromatic content while generating H_2 through electrolysis with significant lower energy cost. Current works are addressing the optimization of the pretreatment process to further reduce energy consumption and recycling of the mediators [4].

Acknowledgment

Work funded by the Italian Ministry of the Environment and Energy Security, program agreement MiTE_ENEA, PNRR - Hydrogen Research - Mission M2-C4 - Investment 3.5: Research and development on hydrogen.

References

[1] https://doi.org/10.1002/aenm.202101180
[2] https://doi.org/10.1016/j.ijhydene.2022.09.191
[3] https://doi.org/10.3390/en11051280
[4] https://doi.org/10.1021/cm0487977

EFCH2 2025 European Fuel Cells and Hydrogen
PIERO LUNGHI CONFERENCE
September 17th–19th 2025
Capri / Italy

Technical analysis of the current water electrolysis cell technologies by comparing plant design and requirements

Fiammetta Rita Bianchi*[a], Dario Bove [a], Barbara Bosio [a]

* corresponding author: fiammettarita.bianchi@unige.it
[a] Department of Civil, Chemical and Environmental Engineering
University of Genova
Via Opera Pia 15, 16145 Genova, Italy

Keywords: Water Electrolysis, Green Hydrogen, Energy Transition, Process simulation

Abstract

Green hydrogen production through water electrolysis is a challenging solution to move to a clean energy economy. H_2 can be used as a renewable energy vector as well as an alternative fuel, but technical issues due to operation management and system stability are still limiting a large-scale commercial application. Referring to under study technologies, a feasibility analysis is proposed to show the current state-of-the-art by evaluating plant requirements and energy consumption for four configurations: proton exchange membrane and solid oxide electrolysis cells characterised by a quite high technological readiness level, anion exchange membrane and, above all, molten carbonate electrolysis cells at initial stages of development. Process simulation performed in DWSIM allows for the flowsheet design of each case, considering the cell peculiarities in terms of working conditions and water supply.

Introduction: Hydrogen has a long-lasting application as a chemical in several processes, such as ammonia and methanol synthesis, petroleum refining, metalworking and electronic manufacturing. In recent years hydrogen has been one of the main leading actors in the framework of energy transition due to low emissions when oxidised and high energy density (~120 kJ/kg (LHV)), resulting in an alternative green fuel for mobility and stationary applications as well as a renewable energy vector. Indeed, electrolysis allows for hydrogen synthesis by water dissociation, exploiting the electricity derived from renewables. Alkaline electrolysers are the only long-term proven technology at MW scale, with more than 80,000 stable working hours. Nevertheless, they are characterised by several drawbacks due to limited applicable current densities (<0.5 A/cm^2), high plant size, limited hydrogen outlet pressures (<30 bar), high risk of gas crossover and electrolyte corrosion [1], [2]. Different

alternative technologies are being tested based on both low-temperature and high-temperature cell technologies with the aim of lowering the energy consumption and increasing the operation flexibility.

Objectives: The research activity consists of a feasibility analysis of water electrolysis coupled to renewables, focusing on two low-temperature cell technologies, Proton Exchange Membrane Electrolysis Cell (PEMEC) and Anion Exchange Membrane Electrolysis Cell (AEMEC), compared to two high-temperature cell ones, Solid Oxide Electrolysis Cell (SOEC) and Molten Carbonate Electrolysis Cell (MCEC). The green hydrogen production process is schematised in Figure 1, where the electrolysis stack is connected to batteries to allow continuous operation despite renewable fluctuations and a compression train to store hydrogen under pressure suitable for variable possible uses. The main evaluated key factors are energy consumption, in terms of heat and electricity at both stack and plant level, reactant requirement and sizing of different unit operations.

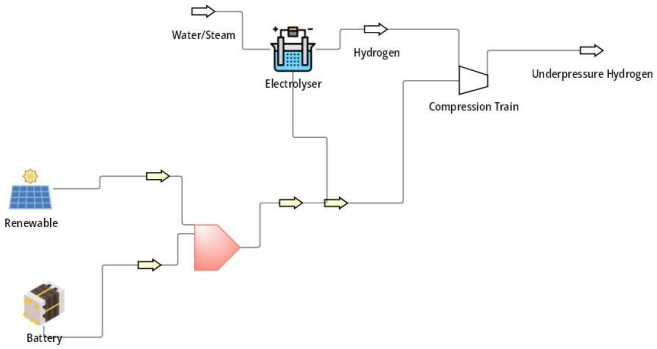


Figure 1: Green hydrogen production plant.

Methods: Process simulation has been performed by DWSIM, an open-source software [3], where specific plant layouts have been designed for all considered electrolysis configurations. Cell operation has been modelled by in-home-built Python codes implemented in the DWSIM flowsheet. They consist of solving simple balances to evaluate the hydrogen production by Faraday's law and knowing cell efficiency in view of the semi-reactions that characterise each electrode, as reported in Table 1.

Table 1: Reaction paths of considered electrolysis cell technologies.

	Anode	*Cathode*
PEMEC	$H_2O \rightarrow 2H^+ + 0.5O_2 + 2e^-$	$2H^+ + 2e^- \rightarrow H_2$
AEMEC	$2OH^- \rightarrow H_2O + 0.5O_2 + 2e^-$	$2H_2O + 2e^- \rightarrow H_2 + 2OH^-$
SOEC	$O^{2-} \rightarrow 0.5O_2 + 2e^-$	$H_2O + 2e^- \rightarrow H_2 + O^{2-}$
MCEC	$CO_3^{2-} \rightarrow CO_2 + 2e^- + 0.5O_2$	$H_2O + CO_2 + 2e^- \rightarrow H_2 + CO^{2-}_3$

Results: A feasibility analysis of water electrolysis operation considering different technologies has been performed. Figure 2 shows the stack energy consumption and the active area requirement as preliminary results. Quite similar performances characterise high-temperature cells and low-temperature cells. Indeed, SOEC and MCEC result in ~3.5 kWh_{el}/Nm^3 compared to ~4.7 kWh_{el}/Nm^3 of AEMEC and PEMEC, since a fraction of the required energy can be provided as heat. Nevertheless, the active area per hydrogen produced is different, showing PEMEC and SOEC with a lower space requirement due to high applicable loads at the current technology level.

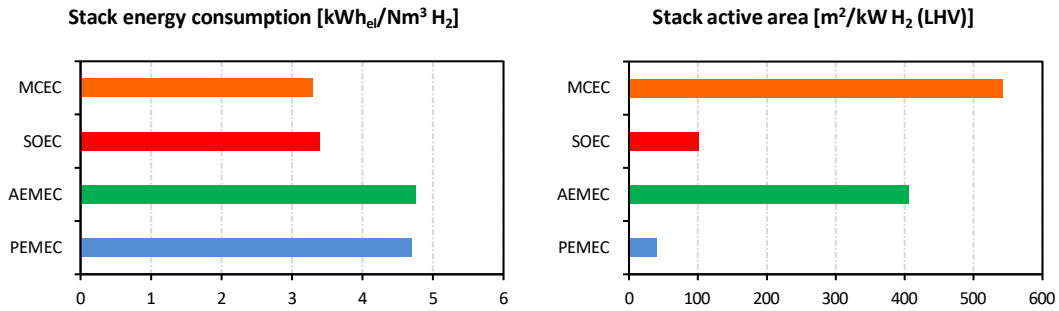


Figure 2: Feasability analysis of electrolysis cells referring to stack features.

Conclusions: Current electrolysis cell performances have been evaluated for different configurations, referring to both stack and plant levels. Peculiar working operations in terms of temperature, pressure, feed composition and load influence energy consumption, thermal management, plant complexity and needed spaces.

Acknowledgment

Funded by the European Union - NextGenerationEU and by the Ministry of University and Research (MUR), National Recovery and Resilience Plan (NRRP), Mission 4, Component 2, Investment 1.5, project "RAISE - Robotics and AI for Socio-economic Empowerment" (ECS00000035).

References

[1] S. Sebbahi *et al.*, 'A comprehensive review of recent advances in alkaline water electrolysis for hydrogen production', *International Journal of Hydrogen Energy*, 82, 583–599, 2024, doi: 10.1016/j.ijhydene.2024.07.428.

[2] O. Schmidt *et al.*, 'Future cost and performance of water electrolysis: An expert elicitation study', *International Journal of Hydrogen Energy*, 42(52), 30470–30492, 2017, doi: 10.1016/j.ijhydene.2017.10.045.

[3] *DWSIM*. Available: https://dwsim.org/ (accessed on 30/03/2025).

European Fuel Cells and Hydrogen
PIERO LUNGHI CONFERENCE
September 17th-19th 2025
Capri / Italy

Analysis of number of stacks and temperature on performance of large-scale pem electrolyser

Anis Ahmad Sher*[a], Domenico Ferrero[a], Leonardo Catalano[a], Massimo Santarelli[a]

* corresponding author: anis.sher@polito.it
[a] Department of Energy, Politecnico di Torino, Corso Duca degli Abruzzi 24, Torino, Italy

Keywords: Aspen plus, electrolysis, PEM electrolyser, stack

Introduction:

Proton Exchange Membrane (PEM) electrolysis is an emerging technology with significant potential to meet the growing demand for zero-emission and renewable hydrogen energy. PEM electrolysers offer several advantages over alkaline electrolysers, for instance, their hydrogen electrode (cathode) can operate across a wide range of pressures, eliminating the need for a separate compressor to compress hydrogen gas into storage tanks [1,2]*, the only limitation is the influence of cathode pressure on the gas cross over. PEM electrolysers can operate at relatively low temperatures and achieve current densities of up to 2 A/cm², while consistently producing hydrogen of high purity* [3,4].

However, the performance of a PEM electrolyser is influenced by a range of parameters, including cathode pressure, current density, voltage, temperature, electrode thickness, and electrode cell area. Despite extensive ongoing research on PEM electrolysis, there remains much to be explored.

This article provides a systematic analysis of how the number of stacks in a PEM electrolyser impacts its performance also from the economic perspective in terms of Levelized Cost of Hydrogen (LCOH). Key insights from the study reveal that variations in the number of stacks directly affect current density, which in turn influences voltage. Additionally, the impact of temperature on performance is also thoroughly examined.

Objectives:

To assess the impact of stack number on the performance of the PEM electrolyser, including its effects on current density and system voltage, as well as to examine how temperature influences overall performance.

Material and methods: *This article primarily utilizes Aspen Plus for the modelling and simulation of an 18.2 MW PEM electrolyser system. In this system, most parameters taken from Tijani et .al.* [5] *are kept constant, with the number of stacks and temperature being the*

variable. Figure 1 presents the schematic of the system, which includes the main stack and various auxiliary components. The cathode pressure is set to 1 bar, with 300 cells per stack. Two temperature conditions, 343.15 K and 353.15 K, are considered, and the number of stacks is varied from 25 to 1500.

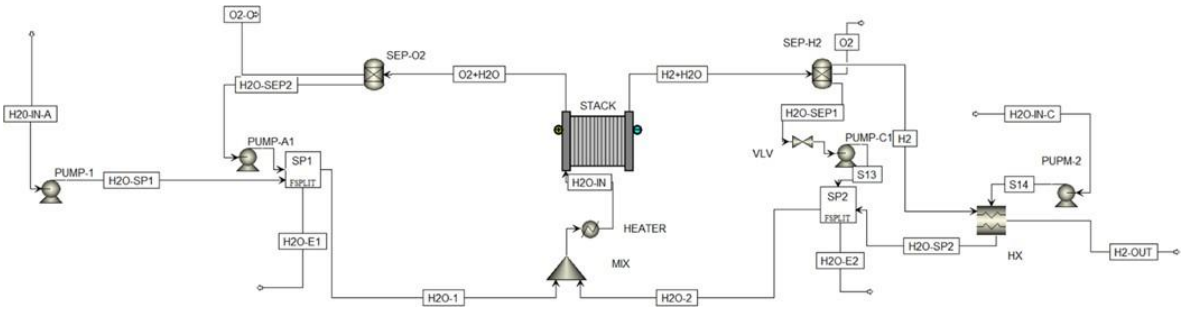


Figure 1. PEM along with other auxiliaries

Results: *Figure 2 clearly demonstrates that as the number of stacks increases, the current density decreases, which in turn affects the voltage. In Figure 3, it is observed that the Lower Heating Value (LHV) efficiency increases as the current density decreases, reaching a maximum value of 0.77 when 610 stacks are used at a temperature of 353.15 K, which ultimately results lower overall LCOH. At this point, the corresponding current density is 0.215 A/cm², and the voltage is 1.52 V. However, beyond this point, further increases in the number of stacks lead to a decline in all of these parameters. On the other hand, the effect of temperature on current density is minimal, it does have a noticeable impact on voltage, following a similar trend. At a temperature of 343.15 K, the maximum LHV efficiency observed is 0.74, with a corresponding current density of 0.24 A/cm² and a cell voltage of 1.54 V.*

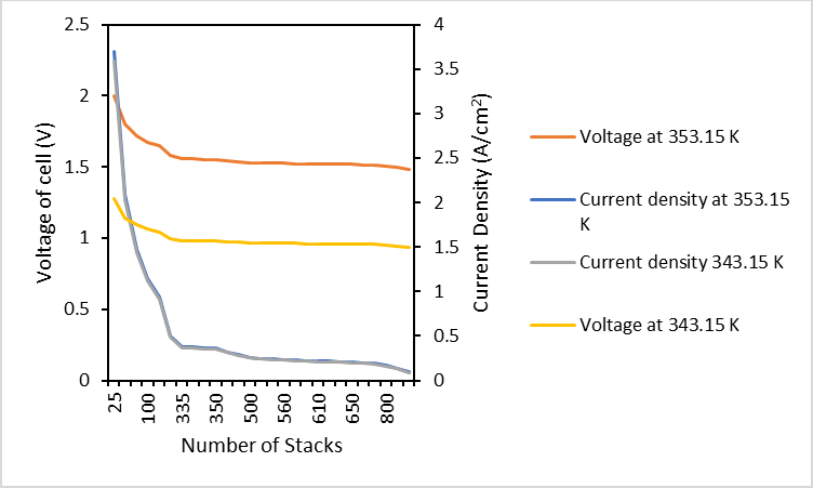


Figure 2. Current and voltage curve of the PEM electrolyser

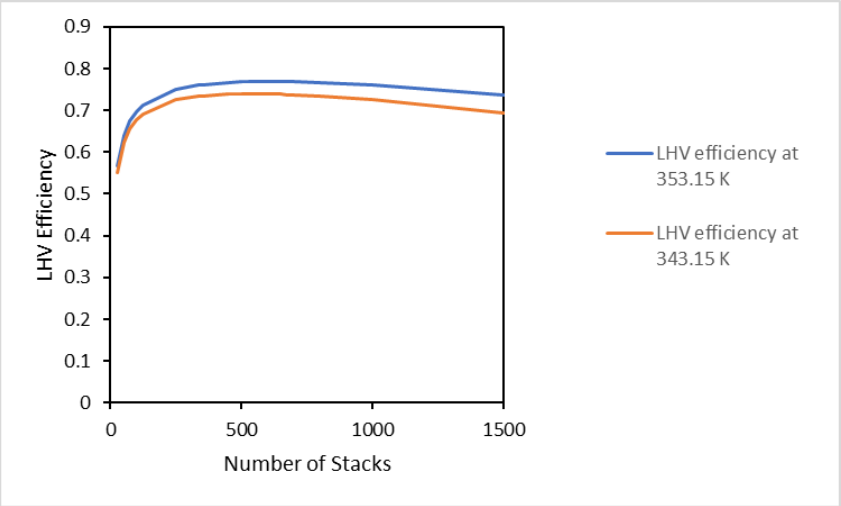


Figure 3 Performance curve of the PEM electrolyser

Conclusions: *Based on this study, we can confidently conclude that the number of stacks positively influences the performance of the PEM electrolyser up to a certain threshold, beyond which the effect becomes negative. The highest LHV efficiency along with lowest LCOH observed at 610 stacks, corresponding to voltage 1.5 V, current density 0.215 A/cm², and temperature 353.15 K. However, this optimal performance varies with different parameters, which remain consistent throughout this study.*

Acknowledgment

We acknowledge the Polito for providing the Aspen Plus software and financial support.

References

[1] Ni GP, Xu LP, He KY. Important trait and application of time-frequency to traceable source link. Astron Res Technol 2006;3:13–20.

[2] Ni M, Leung MKH, Sumathy K, Leung DYC. Potential of renewable hydrogen production for energy supply in Hong Kong. Int J Hydrogen Energy 2006;31:1401–12. https://doi.org/https://doi.org/10.1016/j.ijhydene.2005.11.005.

[3] Carmo M, Fritz DL, Mergel J, Stolten D. A comprehensive review on PEM water electrolysis. Int J Hydrogen Energy 2013;38:4901–34. https://doi.org/https://doi.org/10.1016/j.ijhydene.2013.01.151.

[4] Barbir F. PEM electrolysis for production of hydrogen from renewable energy sources. Sol Energy 2005;78:661–9. https://doi.org/https://doi.org/10.1016/j.solener.2004.09.003.

[5] Tijani AS, Ghani MFA, Rahim AHA, Muritala IK, Binti Mazlan FA. Electrochemical characteristics of (PEM) electrolyzer under influence of charge transfer coefficient. Int J Hydrogen Energy 2019;44:27177–89. https://doi.org/https://doi.org/10.1016/j.ijhydene.2019.08.188.

European Fuel Cells and Hydrogen
PIERO LUNGHI CONFERENCE
September 17th–19th 2025
Capri / Italy

Non-Precious Catalysts and Novel Membranes for High- Performance AEM Water Electrolysis

Lo Vecchio C.*, Bucca G., Modica E., Patti A., Bottari M., Gatto I., Baglio V.

* corresponding author: carmelo.lovecchio@cnr.it
Consiglio Nazionale delle Ricerche, Istituto di Tecnologie Avanzate per l'Energia "Nicola Giordano", CNR-ITAE, Via Salita Santa Lucia sopra Contesse 5, 98126, Messina, Italy

Keywords: Cost-effective catalysts, AEM (Anion Exchange Membrane), alkaline water electrolysis

Abstract

In this study, membrane electrode assemblies (MEAs) were developed by incorporating mixed transition metal oxide catalysts into the anode layer and coupling them with newly synthesized anion exchange membranes (AEMs). The performance of these MEAs was systematically evaluated in a laboratory-scale anion exchange membrane water electrolyzer (AEMWE). For benchmarking purposes, reference MEAs utilizing commercial membranes and platinum group metal (PGM)-based catalysts were tested under identical operating conditions. This comparative analysis highlights the potential of non-precious metal catalysts and novel membrane materials for cost-effective and efficient AEMWE systems.

Introduction: Anion exchange membrane water electrolysis (AEMWE) is emerging as a promising next-generation technology for sustainable hydrogen production [1]. By combining the advantages of conventional alkaline electrolysis with the high-performance characteristics of proton exchange membrane (PEM) systems, AEMWE enables the use of non-precious, earth-abundant catalysts while supporting high current densities and dynamic load-following capabilities. This hybrid approach positions AEMWE as a cost-effective and scalable solution for clean hydrogen generation at the industrial level [2].

A key challenge in water electrolysis lies in the development of efficient and stable electrocatalysts, particularly for the oxygen evolution reaction (OER) at the anode. The OER is inherently sluggish, requiring significant overpotentials and thus demanding highly active catalysts. While noble metal oxides such as IrO_2 and RuO_2 remain benchmarks due to their excellent catalytic activity, their high cost and limited availability present significant barriers to widespread adoption. In contrast, transition metal-based catalysts—particularly those

based on nickel, cobalt, iron, and manganese—have shown considerable promise in alkaline environments. These materials, often synthesized as mixed oxides with spinel or perovskite structures, offer a viable path toward precious-metal-free OER catalysis [3].
Equally critical to the performance and durability of AEMWE systems is the anion exchange membrane (AEM) itself. The AEM must facilitate efficient hydroxide ion conductivity and water management while maintaining chemical, thermal, and mechanical integrity under highly alkaline and oxidative conditions [4]. Although recent advances have led to significant improvements in membrane chemistry and cell architecture, the development of robust, high-conductivity AEMs remains a central bottleneck. Ongoing research into innovative polymer backbones, crosslinking strategies, composite formulations, and ionomer integration is essential to overcome current limitations and enable the commercial viability of AEMWE technologies.

Objectives: This study underscores the critical role of integrating efficient, low-cost electrocatalysts and chemically durable anion exchange membranes in advancing AEM water electrolysis (AEMWE) toward practical, large-scale hydrogen production.

Materials and methods: Membrane electrode assemblies (MEAs) were fabricated by incorporating mixed transition metal oxide catalysts into the anode layer and assembling them with newly developed anion exchange membranes (AEMs). These MEAs were assembled into a laboratory-scale AEM water electrolyzer (AEMWE) system for performance evaluation. For benchmarking purposes, reference MEAs employing commercial AEMs and platinum group metal (PGM)-based catalysts were tested under identical operating conditions, enabling a direct comparison of activity and efficiency.

Results: Experimental results revealed that MEAs incorporating the newly developed non-PGM catalysts delivered competitive performance, with notable enhancements in oxygen evolution reaction (OER) activity relative to reported values in the literature. In particular, Ni–Fe oxide-based catalysts demonstrated superior electrocatalytic behavior, attributed to synergistic interactions between the metal components and improved electron transfer kinetics. Additionally, the integration of the novel anion exchange membranes contributed to overall cell performance by providing high hydroxide ion conductivity and robust mechanical stability under alkaline operating conditions.

Conclusions: The encouraging performance of mixed transition metal oxide catalysts, combined with the enhanced properties of the novel AEMs, demonstrates a viable strategy for addressing key challenges in catalyst activity and membrane stability. These findings provide a solid foundation for further development of cost-effective and high-performance

AEMWE systems. Moving forward, continued efforts in material optimization and membrane electrode assembly (MEA) design will be pivotal in unlocking the full potential of this sustainable hydrogen production technology for industrial applications.

Acknowledgment

This work was supported by Ministero degli Affari Esteri e della Cooperazione Internazionale (MAECI) within the framework of the Italian-German joint research initiative "Green Hydrogen Research: A Collaboration to Empower Tomorrow's Energy", under the project DURALYS (DURAble, Scalable, and Recyclable Components and Cell Designs for Next Generation Alkaline Exchange Membrane Water Electrolysis).

References

[1] C. Santoro, A. Lavacchi, P. Mustarelli, V. Di Noto, L. Elbaz, D.R. Dekel, F. Jaouen, What is Next in Anion-Exchange Membrane Water Electrolyzers? Bottlenecks, Benefits, and Future, ChemSusChem 15 (2022) e202200027 https://doi.org/ 10.1002/cssc.202200027.

[2] M. Chatenet, B.G. Pollet, D.R. Dekel, F. Dionigi, J. Deseure, P. Millet, R.D. Braatz, M.Z. Bazant, M. Eikerling, I. Staffell, P. Balcombe, Y. Shao-Horn, H. Schäfer, Water electrolysis: from textbook knowledge to the latest scientific strategies and industrial developments, Chem. Soc. Rev. 51 (2022) 4583–4762, https://doi.org/ 10.1039/D0CS01079K.

[3] M. Montalto, W. da Silva Freitas, E. Mastronardo, V.C.A. Ficca, E. Placidi, V. Baglio, E. Mosca, C. Lo Vecchio, I. Gatto, B. Mecheri, A. D'Epifanio, Spinel-type high-entropy oxides for enhanced oxygen evolution reaction activity in anion exchange membrane water electrolyzers, Chemical Engineering Journal, 507 (2025), 160641, https://doi.org/10.1016/j.cej.2025.160641.

[4] N. Carboni, L. Mazzapioda, A. Caprì, I. Gatto, A. Carbone, V. Baglio, M. A. Navarra, Composite anion exchange membranes based on graphene oxide for water electrolyzer applications, Electrochim. Acta 486 (2024) 144090, https:// doi.org/10.1016/j.electacta.2024.144090.

European Fuel Cells and Hydrogen
PIERO LUNGHI CONFERENCE
EFCH2 2025
September 17th–19th 2025
Capri / Italy

Optimization of hydrogen downstream treatment system for solid oxide electrolysis

Massimiliano Della Pietra [a], Yuri De Pra * [a], Carla Menale [a]

* corresponding author: yuri.depra@enea.it

[a] ENEA - Department of Energy Technologies and Renewable Sources

Keywords: SOE, hydrogen purification, compression, BoP

Abstract

Solid oxide electrolysis is well known to be the most efficient process for electrochemical conversion of water into hydrogen and oxygen via electrical power. Nevertheless, the exploitation of hydrogen produced via SOE needs a certain amount of purification steps to be used for commercial purpose (e.g. mobility) and the correct assessment of this step is crucial for the deployment of the technology itself. This work focus on the investigation of the most efficient solution for the downstream purification and compression process of a 25kW class SOE, taking in consideration the correct functioning of the electrolyser and the different operation point.

Introduction:

In the context of the ongoing research and development initiatives being conducted within both the scientific and industrial domains, aimed at enabling the short- to medium-term deployment of large-scale electrolyzer systems (on the order of megawatts), advanced high-temperature solid oxide electrolyzer cells (SOEC) are increasingly recognized as a promising technological solution. These systems have the potential to significantly enhance the overall energy efficiency of hydrogen production processes, primarily owing to their superior thermodynamic and electrochemical performance compared to conventional low-temperature electrolysis technologies. Despite these promising features, the technological maturity of SOEC systems remains limited and, to date, has been fully demonstrated only in a restricted number of pilot- scale case studies. The industrial scalability and integration of SOEC technology into existing hydrogen value chains thus still face several technical and engineering challenges that must be thoroughly addressed to unlock their full potential.[1]

In this context, the research activity under consideration specifically aims to investigate and address a set of critical issues associated with the integration of high-temperature solid oxide electrolysis modules with downstream processes for the distribution, conditioning, and utilization of the hydrogen produced. The ultimate objective is to define optimized system architectures and operating strategies capable of ensuring the technical, economic, and

environmental viability of these integrated solutions. From a technological standpoint, SOEC systems are characterized by three principal criticalities that may limit their industrial deployment if not properly managed. These include: (i) the relatively low operating pressure of the hydrogen stream at the cathode outlet, which is typically close to atmospheric levels; (ii) the purity of the hydrogen produced, which, while free from oxygen contamination, still presents challenges due to the residual water content arising from the co-existence of steam and hydrogen in the cathode off-gas; and (iii) the high temperature of the output gas mixture, which can exceed 700°C under nominal operating conditions. In contrast to more established electrolytic technologies, such as alkaline water electrolysis (AWE), where the process design inherently allows for the production of pressurized hydrogen suitable for direct utilization in various industrial processes, SOEC systems require additional downstream compression stages to bring the hydrogen to the pressures necessary for storage, transport, or end-use applications. Moreover, while the absence of oxygen in the cathode stream is an advantageous feature from a safety and product quality standpoint, the presence of significant water vapor fractions necessitates the design and implementation of efficient gas separation and purification systems to achieve hydrogen purity specifications compliant with industrial standards, particularly when the hydrogen is intended for use in sensitive applications such as fuel cells or chemical synthesis processes. [2] Finally, the elevated temperature of the produced hydrogen offers both opportunities and challenges: on one hand, it allows for potential integration with high- temperature industrial processes, providing valuable thermal energy recovery options; on the other hand, it imposes additional constraints on the materials, components, and safety measures required for gas handling, compression, and conditioning systems, which must be specifically designed to withstand such extreme operating conditions.

Objectives:

The primary objective of this work is to characterize and optimize the post-electrolysis treatment of hydrogen produced via a 25 kW class SOE, with the aim of making it compatible with downstream applications, including transportation and end-use in mobility sectors. Specifically, the study focuses on developing and assessing strategies to condition the hydrogen downstream to meet operational requirements in terms of pressure and purity, while minimizing the cost of such process. Optimal hydrogen target specifications include outlet pressures in the range of 24 to 30 bar and purity levels that comply with regulatory standards for fuel cell electric vehicle (FCEV) refuelling, such as those defined in ISO 14687.

Material and methods:

To evaluate and define a suitable downstream treatment configuration for hydrogen produced by Solid Oxide Electrolyzer Cells (SOEC), a comprehensive modeling and simulation approach was employed. The analysis was conducted using a simulation environment, which allowed for the dynamic representation of the hydrogen processing chain, from the outlet of the SOEC stack to the final conditions required for storage, transport, or end-use. The model includes modules for compression, purification (including

water separation), and thermal conditioning of the hydrogen stream, taking into account the specific thermodynamic and physical characteristics of SOEC-produced gas, namely, near-atmospheric pressure and outlet temperatures exceeding 700°C. The simulation framework was designed to support both system-level configuration and operational analysis. Multiple process configurations were evaluated to determine the most effective architecture for achieving target outlet conditions (pressure in the 24–30 bar range, and hydrogen purity in accordance with ISO 14687 for vehicular use). The model was also used to assess system behaviour under varying SOEC operating conditions, specifically contrasting full-load and partial-load operation scenarios. These scenarios were critical in capturing the effect of fluctuating hydrogen production rates on downstream component performance and energy requirements. A key operational constraint imposed throughout the simulations was the pressure differential between the oxygen (anode) and hydrogen (cathode) compartments within the SOEC stack. In accordance with safety and performance standards, this differential was maintained at a nominal value of 50 mbar, with an allowable deviation of ±10%. This constraint was integrated into the model to ensure realistic and safe boundary conditions during all operational scenarios. The simulation outputs included different steady-state profiles of system parameters such as outlet pressure, hydrogen purity, energy consumption of compression stages, water removal efficiency, and temperature profiles across the gas conditioning stages. These results provided quantitative insight into the optimal configuration and control strategies required for effective integration of SOEC systems into hydrogen distribution infrastructures and mobility-related applications.

Results and Conclusions:

Experimental activities highlighted the possibility of integrate the down stream treatment process with SOEC electrolizers considering coherent CAPEX and OPEX values. In particular, the treatment of the downstream offers also the possibility to re-design the BOP of the electolizer optimizing the features of some key equipment like the chiller unit and the reciculation unit for the anodic gases. The challenges in the design of the down stream treatment includes the specifications of the BOP in accordance with the availability of commercial products and the development of requirements for new products.

Acknowledgment

This research was funded by the European Union – NextGenerationEU from the Italian Ministry of Environment and Energy Security , POR H2 AdP MEES/ENEA with involvement of CNR and RSE, PNRR – Mission 2, Component 2, Investment 3.5 "Ricerca e sviluppo sull'idrogeno", CUP: I83C22001170006.

References

[1] A. Hauch et al. "Recent advances in solid oxide cell technology for electrolysis", Science (2020).

[2] kròl et al. "Hydrogen Purification Technologies in the Context of Its Utilization", Energies (2024)

European Fuel Cells and Hydrogen
PIERO LUNGHI CONFERENCE
September 17th–19th 2025
Capri / Italy

High-Efficiency SOEC System Coupled with Renewable Sources: Modeling and Energy Analysis at Operating modes variation

M. Minutillo[ac], E. Jannelli[bc], A. Giaconia[d], A. Altomonte[bc], G. D'Andrea[b]*

* Corresponding author: gianpaolo.d'andrea@collaboratore.uniparthenope.it
[a] Department of Industrial Engineering, University of Salerno, Fisciano, Italy
[b] Department of Engineering, University of Naples "Parthenope", Naples, Italy
[d]ENEA, Italian National Agency for New Technologies, Energy and Sustainable Economic Development, Casaccia Research Centre, Rome, Italy
[c] ATENA Scarl, Naples, Italy

Keywords: *electrolytic hydrogen production*, *SOEC system*, *Numerical model*, *energy assessment*

Abstract:

This study focuses on the analysis and steady-state simulations of different operating modes (night mode, hot standby, full and partial load) of a SOEC-based plant for green hydrogen production, developed within the framework of the European PROMETEO project.

Introduction: In recent years, green hydrogen production through water electrolysis powered by renewable sources has gained significant attention as a sustainable pathway for decarbonizing the energy and industrial sectors. In this context, Solid Oxide Electrolyzer Cells (SOEC) represent a highly promising technology for high-temperature electrolysis, due to their superior thermodynamic efficiency and the effective use of industrial or solar waste heat. The EU project PROMETEO aims to develop a high-efficiency green hydrogen production plant powered by a hybrid renewable energy configuration, combining photovoltaic electricity and solar thermal energy from Concentrated Solar Power (CSP) systems.

Objectives: The main objective of this study is to identify and analyze the process flows associated with the various operating modes of the SOEC system, as defined for the 25 kW SOEC stack and validated through over 200 hours of experimental testing on a 5 kW prototype recently carried out in laboratory during PROMETEO preliminary studies [1,2]. The study aims to define the effects of different operative process parameters such as air, steam, hydrogen and forming gas flows, as well as the related energy consumption and heat recovery for each mode, through the development of a model in Aspen Plus. These results will form the basis for the future optimization of the control system and balance of plant (BoP) management, helping to preserve stack integrity and reduce thermal stress or damage caused by uncontrolled transitions.

Material and methods: A simulation model was developed in Aspen Plus to analyze the behavior of the SOEC system under different operating conditions. Figure 1 shows the flow sheet of the model. This includes all the main subsystems, such as air handling, hydrogen recirculation, and water and

steam management, as well as the preheating and heat recovery systems. The heat supplied for water vaporization comes from diathermic oil, which is heated by a CST (concentrated solar thermal) system.

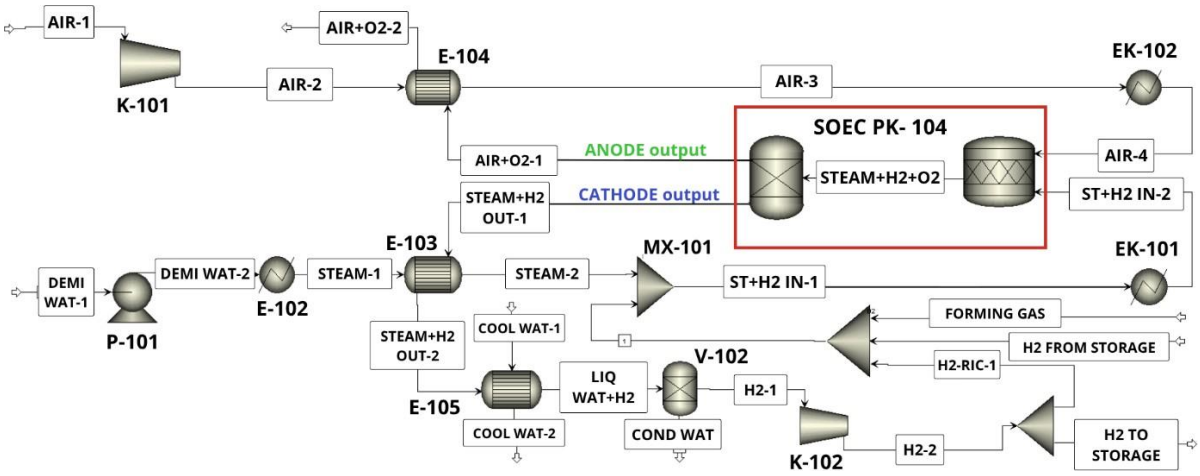


Figure 1 Aspen scheme of the soec plant

The SOEC was modeled in Aspen Plus using an RSTOIC reactor block, with separate treatment of the anodic and cathodic outlet streams. A fixed steam conversion of 0.695 was assumed. For the full load condition, the operating temperature was set at 733 °C and the pressure at 1.035 bar. The simulation was conducted under steady-state conditions, using the NRTL-RK (Non-Random Two-Liquid with Redlich-Kwong) property method, particularly suitable for non-ideal vapor–gas mixtures. The four operating modes (Figure 2) were simulated by properly adjusting flow rates, bypass configurations, and energy streams. In general, the following operation modes have been considered:

- **Full Load:** nominal operation of the electrolyzer with design electric and thermal power.
- **Partial Load**: the system produces hydrogen at reduced power, adapting to the available power input. All parameters operate at a fraction of their nominal values.
- **Hot Standby:** system not powered. It is kept hot through air flow at the anode and a steam-hydrogen mixture at the cathode, ready to resume operation.
- **Night Mode:** the stack remains hot with minimal energy consumption during long non-operational periods. This mode can be managed either with steam and H_2 or with forming gas.

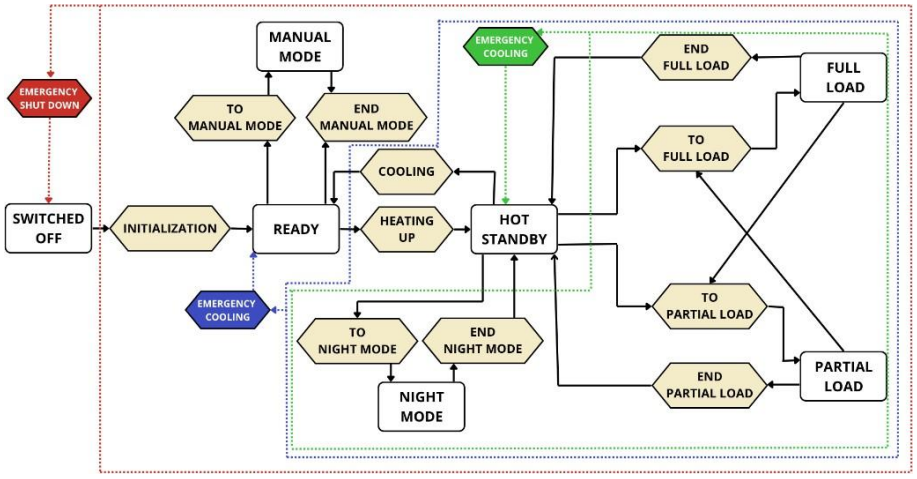


Figure 2 State machine diagram

Results: The main outcome of this work is the identification of process streams and energy balances for each analyzed operating mode. Table 1 summarizes the main streams in these operating modes.

Table 1 streams streams and the heat balances

Operating modes		FULL LOAD								PARTIAL LOAD							
Stream		AIR			STEAM				RIC H2	AIR			STEAM				RIC H2
From		K-101	E-104	PK104	P-101	E-102	MX-101	PK-104	V-102	K-101	E-104	PK104	P-101	E-102	MX-101	PK-104	V-102
to		E-104	EK-102	E-104	E-102	E-103	EK-101	E-103	MX-101	E-104	EK-102	E-104	E-102	E-103	EK-101	E-103	MX-101
Mass flowrate	[kg/hr]	28,0	28,0	33,4	8,7	8,7	8,791	3,41	0,091	28,0	28,0	30,6	4,1	4,1	4,17	1,614	0,075
Temperature	[°C]	29,7	576,9	715	10	130	620,83	714,9	20	29,7	576,9	683	10	130	571,6	683,8	20
Pressure	[bar]	1,07	1,051	1,04	3,11	1,07	1,055	1,038	1,06	1,07	1,051	1,04	3,11	1,07	1,055	1,038	1,06
Vapor phase fraction		1	1	1	0	1	1	1	1	1	1	1	0	1	1	1	1
H2O	[%mol]	0	0	0	100	100	90	27	2,2	0	0	0	100	100	90	27	2,2
H2	[%mol]	0	0	0	0	0	10	73	97,8	0	0	0	0	0	10	73	97,8
O2	[%mol]	22	22	33,6	0	0	0	0	0	22	22	33,6	0	0	0	0	0
N2	[%mol]	78	78	66,4	0	0	0	0	0	78	78	66,4	0	0	0	0	0
Operating modes		**HOT STANDBY**								**NIGHT MODE**							
Stream		AIR			STEAM				RIC H2	AIR			STEAM		RIC FORM GAS		
From		K-101	E-104	PK104	P-101	E-102	MX-101	PK-104	V-102	K-101	E-104	PK104	P-101	E-102	MX-101	PK-104	BL
to		E-104	EK-102	E-104	E-102	E-103	EK-101	E-103	MX-101	E-104	EK-102	E-104	E-102	E-103	EK-101	E-103	MX-101
Mass flowrate [kg/hr]	[kg/hr]	28,0	28,0	28,0	1,5	1,5	1,522	1,522	0,091	28,0	28,0	33,4	0	0	2,1	2,1	2,1
Temperature [°C]	[°C]	29,7	576,9	684	10	130	581,71	714,9	20	29,7	576,9	715	-	-	25	684	25
Pressure [bar]	[bar]	1,07	1,051	1,04	3,11	1,07	1,055	1,038	1,06	1,07	1,051	1,04	-	-	1,055	1,038	1,059
Vapor phase fraction		1	1	1	0	1	1	1	1	1	1	1	-	-	1	1	1
H2O [%mol]	[%mol]	0	0	0	100	100	90	90	2,2	0	0	0	-	-	0	0	0
H2 [%mol]	[%mol]	0	0	0	0	0	10	10	97,8	0	0	0	-	-	20	20	20
O2 [%mol]	[%mol]	22	22	22	0	0	0	0	0	22	22	33,6	-	-	80	80	80
N2 [%mol]	[%mol]	78	78	78	0	0	0	0	0	78	78	66,4	-	-	0	0	0

Conclusions: This work enabled the identification of the SOEC system's process flows and energy requirements under four different operating modes, highlighting the associated thermodynamic variations. These results provide a solid basis for developing efficient control strategies that ensure operational flexibility and preserve stack integrity. This information will be used to optimize the BoP design and support future experimental activities within the PROMETEO project.

Acknowledgment: This project has received funding from the Fuel Cells and Hydrogen 2 Joint Undertaking (now Clean Hydrogen Partnership) under Grant Agreement No 101007194. This Joint Undertaking receives support from the European Union's Horizon 2020 Research and Innovation program, Hydrogen Europe and Hydrogen Europe Research.

References:

[1] Crespi, E., Ragaglia, D., Panaccione, F., & Testi, M. (2023, June). Control of a Solid Oxide Electrolysis system for hydrogen generation from solar power and thermal energy storage. In *2023 International Conference on Clean Electrical Power (ICCEP)* (pp. 765-774). IEEE.

[2] Crespi, E., Panaccione, F., Ragaglia, D., & Testi, M. (2024). Integration of a solid oxide electrolysis system with solar thermal and electrical energy: A testing campaign for operation and control strategy definition. *IET Renewable Power Generation*, *18*, 4399-4413.

European Fuel Cells and Hydrogen
PIERO LUNGHI CONFERENCE
EFCH2 2025
September 17th–19th 2025
Capri / Italy

Performance evaluation of anion exchange membrane water electrolysers using commercial membranes and non-precious metal catalysts.

Shiva Kumar Sampangi*, Ramakrishna Siripalli, Betty Tietzmann, Mohamed Elasmar, Lars Röntzsch

Brandenburg University of Technology Cottbus-Senftenberg (BTU), Hydrogen Research Center, Siemens-Halske-Ring 13, Cottbus, Germany

E-mail: ShivaKumar.Sampangi@b-tu.de ; Lars.Roentzsch@b-tu.de

Keywords: Water electrolysis, Anion exchange membranes, Non-precious metal catalysts, Hydrogen production, Electrochemical performance.

Abstract

Anion exchange membrane (AEM) water electrolysis is gaining increasing attention as a cost-effective and environmentally friendly method for green hydrogen production [1], [3]. Unlike proton exchange membrane water electrolyser systems, AEM electrolysers enable the use of perfluorosulfonic acid (PFSA)-free membranes and abundant non-precious metal catalysts with alkaline operating conditions, making them attractive for large-scale deployment [2]. In this study, the performance of three different commercially available AEMs (AMVN, and Fumasep®FAA-3-50 and Fumasep®FAA-3-PK-130) was systematically tested using a 100 cm² single-cell electrolyser with 1 M KOH solution. Initially, the test operations were conducted without any catalyst materials to study membrane behaviour and thermal stability. The test operations were conducted across a temperature range of 30°C to 70°C to simulate varying operational environments and identify thermal effects on membrane behaviour and cell performance. Key electrochemical parameters including current density, cell voltages were recorded and analysed. The results revealed that, Fumasep®FAA-3-50 shows better cell performance of 120 mA/cm2 at 2.5 V. This comparative analysis highlights the importance of membrane selection and thermal optimization in achieving high-efficiency AEM electrolyser operation. Additionally, a systematic study on the effect of different electrolyte flow rates from 0.5 l/min to 3.0 l/min was conducted using the Fumasep®FAA-3-50 membrane using a single cell with 100 cm² active area. The aim was to evaluate the impact on membrane hydration, ionic conductivity, gas bubble removal, and overall system efficiency using the Fumasep®FAA-3-50 membrane. The results demonstrated that a flow rate of 1.0 l/min shows the better performance (Fig.1a) in terms of cell efficiency and gas purity of produced gases.

Furthermore, six deferent membrane electrode assemblies (MEAs) were fabricated using non-precious metal catalysts of NiFe2O4 and NiMoO4 for the anode and 30% Ni/C for the cathode. The MEAs were configured as follows: MEA-1 comprising an AMVN membrane with $NiFe_2O_4$ and Ni/C; MEA-2 using a Fumasep® FAA-3-130 membrane with $NiFe_2O_4$ and Ni/C; MEA-3incorporating a Fumasep® FAA-3-50 membrane with $NiFe_2O_4$ and Ni/C; MEA-4 consisting of a Fumasep® FAA-3-50 membrane with $NiMoO_4$ and Ni/C; MEA-5 employing a Fumasep® FAA-3-130 membrane with $NiMoO_4$ and Ni/C; and MEA-6 featuring an AMVN membrane with $NiMoO_4$ and Ni/C. These MEAs configurations involved all three different membranes such as

AMVN, Fumasep®FAA-3-50 and Fumasep® FAA-3-PK-130 and their performance was evaluated in the 100 cm² single cell using a 1 M KOH solution at various temperatures. Among all, MEA-4 demonstrated the better performance of 220 mA/cm2 at 2.0 V and 300 mA/cm2 at 2.08 V at 70oC. Following this, MEA-3, achieved 203 mA/cm2 at 2.0 V and 300 mA/cm2 at 2.1 V at 70oC (Fig.1b) under the same experimental conditions. Ongoing research efforts are focused on further improving cell performance through the optimization of operating parameters and the incorporation of various alternative catalyst compositions. Additionally, scale-up studies are underway, progressing from 100 cm² single-cell evaluations to a 360 cm2 single cell, with subsequent development of a 5-kW short stack.

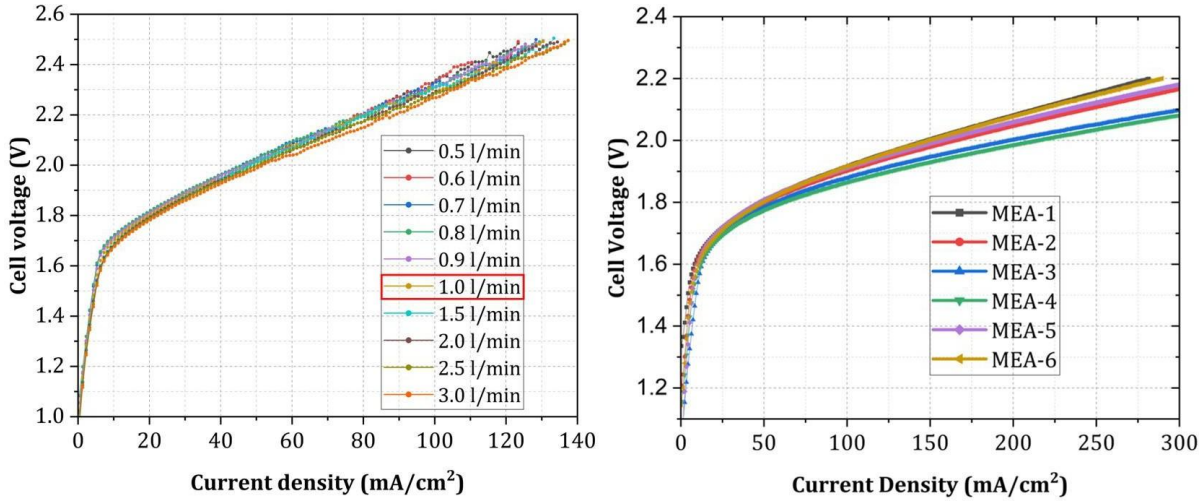


Fig. 1 *(a) Current–voltage polarization curves showing the effect of electrolyte flow rate on cell performance, with flow rates ranging from 0.5 l/min to 3.0 l/min.*

(b) Current–voltage polarization curves comparing different MEAs at a constant temperature of 70°C.

Acknowledgements:

The authors gratefully acknowledge the support of the Federal Ministry of Education and Research (BMBF) and the State of Brandenburg (ILB) within the framework of the joint project "EIZ – Energy Innovation Center" (Project Numbers: 85056897 and 03SF0693A), funded through the Structural Development Act for Coal-Mining Regions.

Reference:

[1] S. Shiva Kumar and H. Lim, 'An overview of water electrolysis technologies for green hydrogen production', *Energy Reports*, vol. 8, pp. 13793–13813, Nov. 2022, doi: 10.1016/j.egyr.2022.10.127.

[2] D. Henkensmeier, M. Najibah, C. Harms, J. Žitka, J. Hnát, and K. Bouzek, 'Overview: State-of-the Art Commercial Membranes for Anion Exchange Membrane Water Electrolysis', *J. Electrochem. En. Conv. Stor*, vol. 18, no. 2, May 2021, doi: 10.1115/1.4047963.

[3] S. Metz, T. Smolinka, L. Röntzsch, et al., Producing hydrogen through electrolysis and other processes, in: R. Neugebauer (Ed.), Hydrogen Technologies, Springer International

Publishing, Cham, 2023: pp. 203–252. https://doi.org/10.1007/978-3-031-22100-2_9.



TOPIC 2: HYDROGEN STORAGE AND DISTRIBUTION

EFCH2 2025
European Fuel Cells and Hydrogen
PIERO LUNGHI CONFERENCE
September 17th–19th 2025
Capri / Italy

No-vent LH_2 Transfer Processes using Top-Fill

Albert Gil-Esmendia*[a], Robert J. Flores [a], Jack Brouwer [a]
* corresponding author: agilesme@uci.edu
[a] Clean Energy Institute, University of California, Irvine, CA 92617

Keywords: Boil-off venting, Liquid hydrogen , No-vent transfer processes, Top-fill

Introduction:

The transfer of liquid hydrogen (LH_2) is a critical process in storage, transportation, and fueling applications of LH_2. Due to the extremely low boiling point for hydrogen (20.28 K at 1 atm), effective management of pressure, temperature, and boil-off is essential for system integrity and transfer efficiency [1]. A key challenge in LH_2transfer is balancing pressure buildup, boil-off, and venting, with the filling method—bottom-fill versus top-fill—significantly impacting these dynamics [2].

Objectives:

The choice between bottom-fill and top-fill methods presents different advantages: top-fill offers superior pressure and temperature control with minimized venting risks, while potentially resulting in warmer final LH_2 temperatures that reduce storage density and dormancy periods. This study examines these fundamental differences, quantifying their effects to determine optimal approaches for LH_2 transfer operations.

Material and methods:

The methodology for modeling top-fill LH_2 transfer builds upon previous bottom-fill models [3] while addressing additional complexities in thermal and fluid dynamics. These include interactions between cold LH_2 and warmer hydrogen gas, phase changes in both liquid and vapor phases, and potential nucleation and condensation phenomena.

Key modeling considerations include:

- Model Foundation: The core challenge involves capturing heat exchange between cold LH_2 and warmer hydrogen gas in the ullage space, accounting for convection, phase changes, and variable flow patterns.
- Phase Change and Conservation Laws: The model incorporates energy conservation principles to account for condensation of vapor due to cooling and potential warming of LH_2 leading to density reduction and boil-off.
- Parametric Analysis: The study examines two key parameters to understand how they affect pressure, temperature, and venting dynamics:

- Variation in top-fill convection coefficient
- Variation in inlet LH_2 temperature

Results:

The simulations reveal significant differences in process dynamics between bottom-fill and top-fill methods, with implications for pressure and temperature dynamics, boil-off venting and final LH_2 conditions.

- Bottom-fill and top-fill process dynamics

Bottom-fill processes show significant pressure buildup due to vapor displacement and compression. As illustrated in Figure 1, pressure increases steadily, eventually reaching the maximum allowable pressure of the tank. This triggers a venting phase with pressure oscillations, as H_2 gas is vented to avoid an overpressure event in the storage tank. In contrast, top-fill methods demonstrate superior pressure control, potentially eliminating venting requirements during transfers.

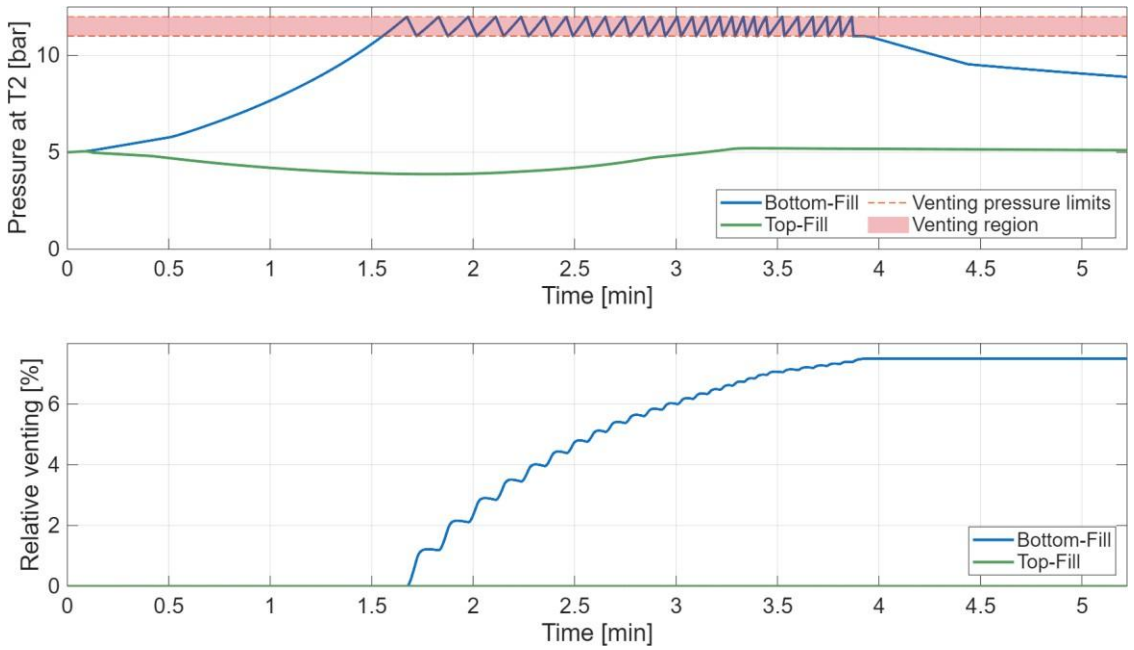


Figure 1. Pressure and relative venting evolution for a bottom-fill and a top-fill LH2 transfer process

- Effect of Different Top-fill Powers in relative venting, final temperature and transferred mass

Results show that top-fill power significantly affects transfer dynamics. For any specific transfer operation there is a minimum top-fill power—critical top-fill power—required to achieve a no-vent process, represented in blue in *Figure 2*. This power depends on many operational factors such as flowrate and inlet LH_2 temperature. Higher flowrates require greater top-fill powers, while lower inlet LH_2 temperatures reduce this requirement.

Applying excessive top-fill power ensures no-vent operation but causes unnecessary warming of the final LH_2, reducing storage density and efficiency. The convection coefficient, largely determined by nozzle configuration, is typically fixed after tank design, highlighting the importance of careful design considerations for optimal performance across various operating conditions.

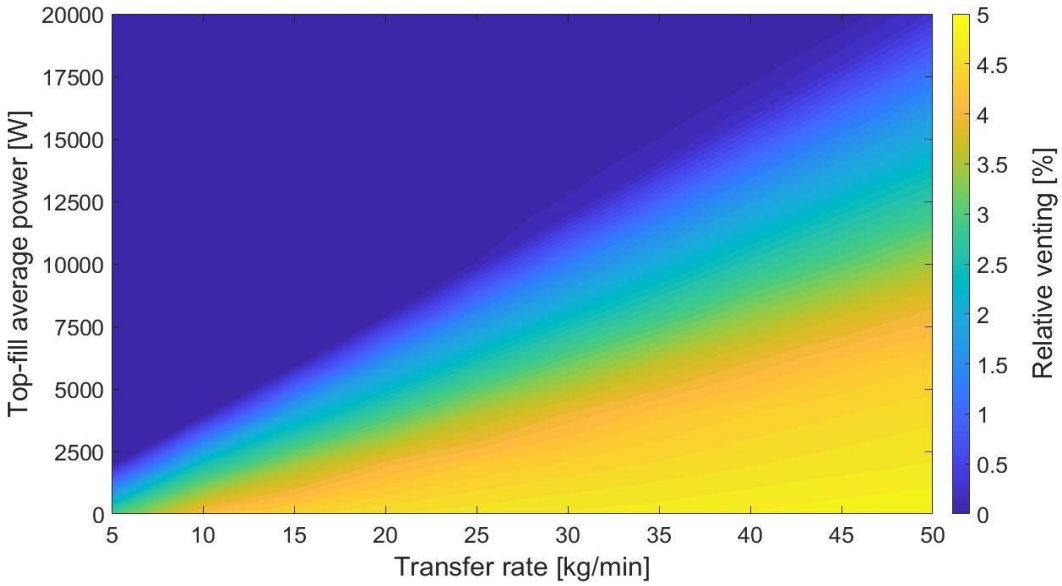


Figure 2. Relative venting dependence on LH2 transfer rate and top-fill average power.

Conclusions:

Top-fill methods offer better pressure control compared to bottom-fill, enabling reduced venting transfers, resulting though in warmer final LH_2 temperatures. Optimizing the cooling effect from a top-fill process depends on multiple operational parameters.

A hybrid bottom-top-fill approach shows promise as a flexible solution to achieve optimal transfer across diverse scenarios. By adjusting the balance between bottom and top filling, operators could potentially achieve optimal top-fill effects even with fixed nozzle configurations.

References

[1] Wang C, Li Y, Deng D, Wang R, Xie G. Performance Model of the Top Filling Configurations for No-Vent Fills. J Thermophys Heat Trans 2011;25:140–6. https://doi.org/10.2514/1.49564.

[2] Taylor WJ, Chato DJ. Comparing the results of an analytical model of the no-vent fill process with no-vent fill test results for a 4.96 cubic meters (175 cubic feet) tank. Joint Propulsion Conference and Exhibit , 1993.

[3] Gil-Esmendia A, Flores RJ, Brouwer J. Modeling and improving liquid hydrogen transfer processes. (*Manuscript submitted for publication at Applied Energy)*, 2025.

European Fuel Cells and Hydrogen
PIERO LUNGHI CONFERENCE
EFCH2 2025
September 17th–19th 2025
Capri / Italy

Optimization of Hydrogen Refueling Infrastructure for Heavy-Duty Vehicles

Minseok Kwon[a], Sanggyu Kang*[a]

* corresponding author: sgkang@snu.ac.kr

[a] Department of Naval Architecture and Ocean Engineering Seoul Nat'l Univ.

Keywords: Heavy duty, Heavy duty tank, Hydrogen, Hydrogen Refueling System(HRS)

Abstract :

This study presents the development of a dynamic model for a heavy-duty hydrogen refueling system using MATLAB-Simulink®. The proposed system comprises key components, including a high-pressure storage tank, pressure reduction valve, cooling unit, breakaway coupling, refueling hose, pipelines, nozzle/receptacle assembly, and an onboard vehicle tank designed for heavy-duty applications. The model simulates the transient thermodynamic behavior of the hydrogen refueling process, capturing key parameters such as pressure, temperature, and mass flow rate under real-world operating conditions. To ensure both safety and refueling efficiency, this study investigates the influence of pipeline geometry while adhering to standardized refueling protocols. Through a systematic analysis, an optimized refueling strategy is proposed, mitigating safety risks while enhancing the overall efficiency of hydrogen transfer. The findings contribute to the advancement of hydrogen refueling infrastructure for heavy-duty transportation, facilitating the widespread adoption of hydrogen-powered vehicles.

Introduction : Hydrogen fuel cell electric vehicles (FCEVs) are well-suited for heavy-duty applications due to their long driving range and fast refueling times. As the adoption of heavy-duty FCEVs continues to grow, the development of efficient and safe hydrogen refueling infrastructure is becoming increasingly critical [1]. Most hydrogen refueling systems operate under high-pressure conditions and adhere to established standards, with SAE J2601 being the most widely adopted protocol. However, SAE(Society of Automotive Engineers) J2601 does not provide sufficient guidance on refueling methods specifically for heavy-duty hydrogen tanks [2]. Despite the rising demand for heavy-duty refueling solutions, research on hydrogen refueling stations tailored for heavy-duty tanks remains insufficient, and optimized refueling methods for large-capacity storage systems have not been thoroughly investigated. Additionally, the lack of references and publicly available datasets on the design, operation, and performance of heavy-duty hydrogen refueling stations hinders the development of reliable models for refueling behavior and system efficiency, limiting accurate impact

assessments and the establishment of validated optimization strategies. To ensure both safety and efficiency, it is essential to develop optimized refueling strategies that comply with SAE J2601 while addressing the unique requirements of heavy-duty hydrogen storage systems.

Objectives:

This study aims to identify and analyze the optimal Average Pressure Ramp Rate (APRR) during hydrogen refueling by conducting a parameter study of key components, such as pipelines. Through this analysis, the research seeks to optimize hydrogen refueling stations and develop a safe and efficient refueling method. Additionally, to validate the reliability of the model, complementary experimental data between heavy-duty hydrogen tanks and refueling stations is incorporated.

Material and methods:

A. Real gas equation

To accurately describe the thermodynamic behavior of hydrogen gas during refueling, the compressibility factor Z is defined as:

$$Z = \frac{Pv}{R_g T} = (1 + \frac{\alpha P}{T}) \quad (1)$$

$R_g$is the specific gas constant for hydrogen, given as 4124.3 J/(kg·K), and α is constant coefficient with a value of 1.9155×10^{-6} K/Pa.

B. Energy conservation & mass conservation

The energy and mass conservation equations are applied to both the hydrogen tank and its components, allowing for the calculation of the thermodynamic state. These equations can be expressed as:

$$\frac{dm}{dt} = \dot{m}_{in} - \dot{m}_{out} \quad (2)$$

$$\frac{d(mu)}{dt} = \dot{m}\,(h_{in}(T,P) - h_{out}(T,P)) + Q \quad (3)$$

Results: The hydrogen refueling system consists of a storage tank, reduction valve, cooling system, breakaway coupling, hose, pipelines, nozzle/receptacle, and vehicle tank, as shown in Fig. 1(a). The hydrogen tank model was validated by comparing temperature variations in the tank during the filling process between simulation and experimental data, as shown in Fig. 1(b). The simulation results demonstrated high reliability, with a maximum deviation of 3 K from the experimental data. The system's optimal APRR was evaluated based on the pipe inlet diameter and operating conditions, as shown in Fig. 1(c). It was confirmed that the APRR of

the 2 mm pipe was the lowest at 7.1 MPa/min, while the 6 mm, 7 mm, and 8 mm pipes exhibited the same APRR of 13.3 MPa/min, indicating an optimal range for pipe diameters.

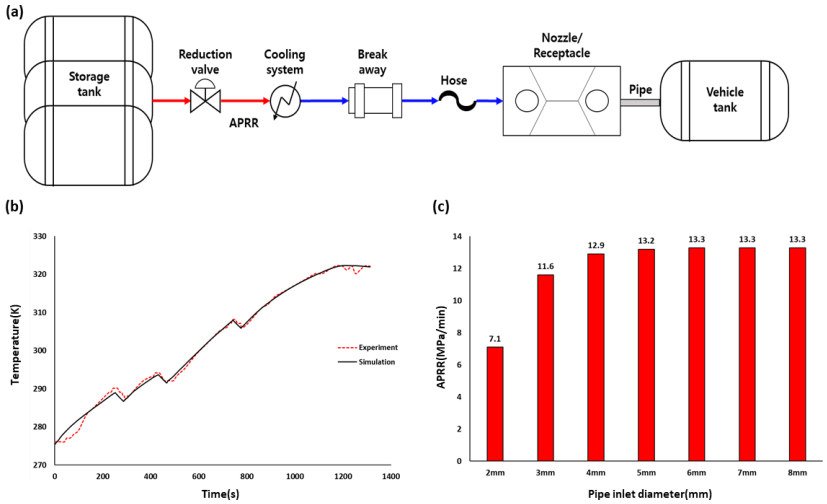


Fig. 1. (a) Schematic diagram of the hydrogen refueling system.

(b) Comparison of temperature variations in the tank between simulation and experimental data.

(c) Optimal APRR in the pipeline under different operational cases based on pipe diameter.

Conclusions: In this study, a dynamic model of a hydrogen refueling system was developed using MATLAB-Simulink®. The hydrogen tank and its components were validated by comparing them with experimental data. The optimal APRR of the hydrogen refueling system was evaluated under system configurations.

Acknowledgment

This work was supported by Korea Institute for Advancement of Technology(KIAT) grant funded by the Korea Government(MOTIE) (P0023684, HRD Program for Industrial Innovation)

References

[1] M. Genovese and P. Fragiacomo, Hydrogen refueling station: Overview of the technological status and research enhancement, *Journal of Energy Storage*, vol. 61, 106758, 2023.

[2] SAE International, *Fueling Protocols for Gaseous Hydrogen Powered Heavy Duty Vehicles*, Standard J2601/2_202307, 2023.

European Fuel Cells and Hydrogen
PIERO LUNGHI CONFERENCE
September 17th–19th 2025
Capri / Italy

Investigation of Pre-Cooling Systems for Hydrogen Refueling Stations Using Dynamic System Simulation: Design Requirements and Concept Comparison

Henrik Waßmuth*[a], Steffen Heinke[a], Lisa Busche[b], Wilhelm Tegethoff[a,b], Jürgen Köhler[a]

* corresponding author: h.wassmuth@tu-braunschweig.de

[a] Technische Universität Braunschweig, Institut für Thermodynamik,
Hans-Sommer-Str. 5, 38106 Braunschweig Germany

[b] TLK-Thermo GmbH, Rebenring 31, 38106 Braunschweig Germany

Keywords: Hydrogen Pre-Cooling, Hydrogen Refueling, Refrigeration System

Introduction:

In a typical gaseous hydrogen refueling station, hydrogen is compressed from a lower-pressure supply source (e.g., a tube trailer or pipeline) into high-pressure storage banks for temporary storage (see Figure 1). During refueling, pressure differences cause hydrogen to flow from these storage banks into the vehicle's storage system. Before dispensing, the hydrogen is cooled to a desired pre-cooling temperature. This is necessary for a fast and secure refueling process. Due to the Joule-Thomson effect and the compression of hydrogen within the vehicle tanks, the gas temperature rises significantly during refueling. Without pre-cooling the hydrogen to temperatures as low as -40 °C, it is not possible to maintain the operating limits of the vehicle tank (<85 °C) within acceptable refueling times. The standardized procedures to ensure that the vehicle tank is filled in a specified time while maintaining its operating limits are commonly known as refueling protocols.

Objectives:

In this study, the objective is to investigate pre-cooling systems for hydrogen refueling stations, focusing on efficient and environmentally friendly solutions for conditioning hydrogen to refuel light- and heavy-duty vehicles. Hence, different refrigeration system concepts are examined considering efficiency-enhancing refrigeration circuit layouts and the use of the natural refrigerant R744 (CO_2) as the working fluid. The utilization of thermal energy storage is also considered. Key design requirements for the refrigeration system are addressed and compared for the different concepts.

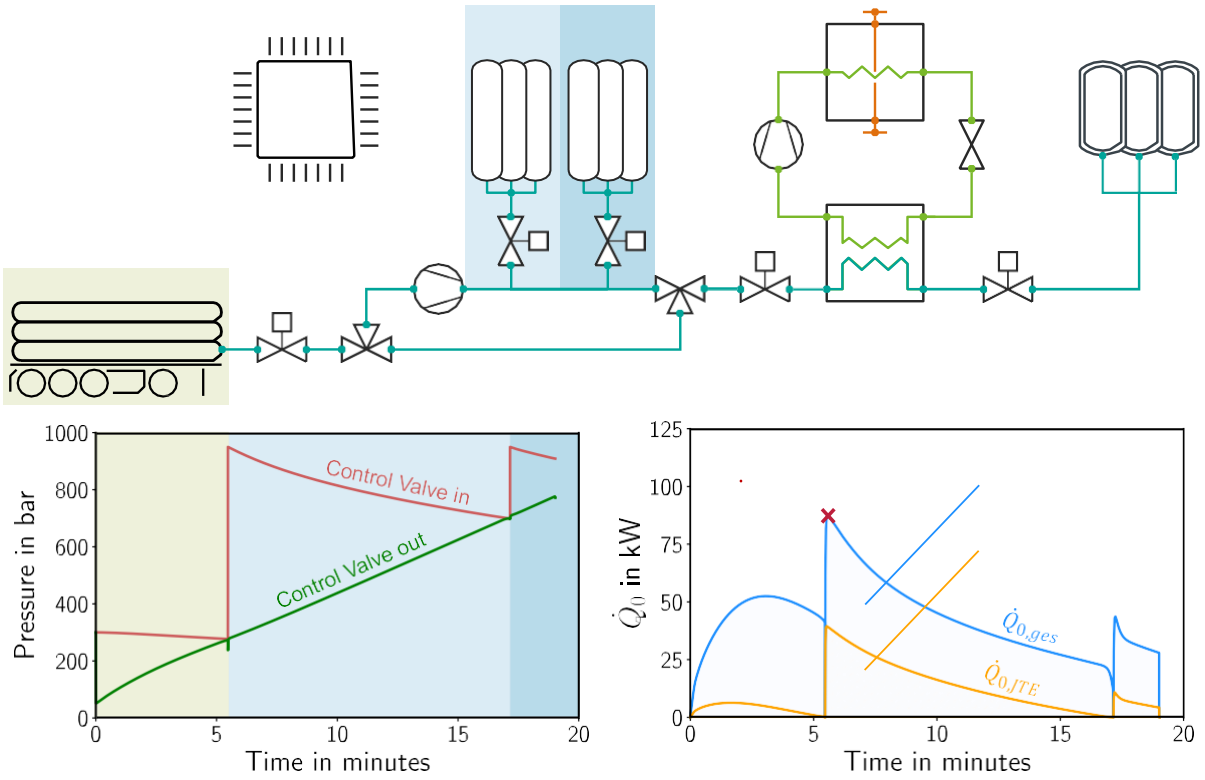


Figure 1: Thermodynamic model of the hydrogen refueling station and exemplary results from the dynamic system simulation for refueling the example fuel cell truck at one specific ambient temperature. On the left, the pressure levels of the refueling station's various storage tanks (highlighted in different colors), together with the pressure of the hydrogen after the control valve as it flows towards the vehicle's storage system during refueling. On the right is the required cooling capacity of the pre-cooling system during refueling, highlighting the portion caused by the Joule-Thomson effect and the integrated cooling load per kilogram of dispensed hydrogen.

Material and methods:

A thermodynamic model of the hydrogen refueling station was developed to simulate the dynamic refueling process. The model is built in the equation-based modeling language Modelica [1] using the TIL Suite library [2]. The model is divided into several sub-models (see Figure 1), such as the hydrogen supply, the hydrogen compressor unit, the high-pressure storage banks, the pre-cooling system, valves for controlling the hydrogen flow and the vehicle storage system. Through object-oriented modeling, each sub-model can be adjusted and modified, allowing variations in station parameters and layout, as well as the vehicle storage system. For this study, a hydrogen supply trailer with an initial pressure level of 300 bar and two storage banks with an initial pressure level of 950 bar are considered. For the vehicle storage system, a fuel cell passenger car with a total capacity of 5.5 kg hydrogen (divided into three 46 L Type IV tanks) and a long-haul transport fuel cell truck with a total capacity of 78 kg hydrogen (divided into eight 244 L Type IV tanks) are used as example vehicles. Each vehicle's storage system operates at a nominal working pressure of 700 bar. The vehicles are filled from an initial pressure of 50 bar to 97 % of their maximum filling capacity. Based on prescriptive SAE refueling protocols (SAE J2601 [3] and SAE J2601-5 [4]),

the fueling speed and the pre-cooling temperature are chosen. Using the dynamic system model of the hydrogen refueling station, simulations are conducted to refuel the example vehicles at various ambient conditions. Key design requirements of the pre-cooling system are specified by determining the integrated cooling load and the required cooling capacity. Influencing factors, such as the Joule-Thomson effect and the chosen refueling protocol, are systematically analyzed. The different refrigeration system concepts are examined focusing on system efficiency, energy consumption and the identification of optimization potentials.

Results and Conclusions:

For the investigated example vehicles, a design cooling capacity of 89 kW was determined for the pre-cooling system refueling the fuel cell truck, while the fuel cell car required 60 kW. The temperature rise caused by the Joule-Thomson effect resulted in a higher integrated cooling load and significantly increased the design cooling capacity (see Figure 1). Because the impact of the Joule-Thomson effect primarily depends on the pressure levels of the refueling station's various storage tanks, the specific station layout should be taken into account when designing the refrigeration system. If the hydrogen is cooled with a large temperature difference during heat exchange, there is considerable potential for optimization. Refrigeration cycle concepts that reduce these temperature differences can thus save energy, e.g., a two-stage evaporation cycle. Compared with a cycle concept with single-stage evaporation, energy savings between 25 % and 60 % were determined, depending on the ambient conditions. The model-based investigation of refueling a fuel cell truck and car highlights the complex design requirements of hydrogen pre-cooling, characterized by high and simultaneously varying cooling capacities during the refueling process (see Figure 1) and a relatively large temperature difference between the heat source (hydrogen) and the heat sink (ambient).

Acknowledgment

We would like to acknowledge the funding from the Ministry of Science and Culture of Lower Saxony (Germany) through "Niedersächsisches Vorab" as part of the research project THEWA (FKZ VWZN3769 and FKZ VWZN3821).

References

[1] Modelica Association, *Modelica – A Unified Object-Oriented Language for Systems Modeling Language Specification*. (Mar. 09, 2023). [Online]. Available: https://specification.modelica.org/maint/3.6/MLS.html
[2] TLK-Thermo GmbH, *TIL Suite*. (Jun. 05, 2024). [Online]. Available: https://www.tlk-thermo.com/en/software/til-suite
[3] SAE J2601: Surface Vehicle Standard, *Fueling Protocols for Light Duty Gaseous Hydrogen Surface Vehicles*, May 2020.
[4] SAE J2601: Surface Vehicle Technical Information Report, *High-Flow Prescriptive Fueling Protocols for Gaseous Hydrogen Powered Medium and Heavy-Duty Vehicles*, Feb. 2024.

European Fuel Cells and Hydrogen
PIERO LUNGHI CONFERENCE
September 17th–19th 2025
Capri / Italy

Metal hydrides based hydrogen storage for fuel cell hybrid vehicles: Numerical evaluation in real-world operating conditions

Lorenzo Bartolucci [a], *Edoardo* Cennamo *[a], *Stefano* Cordiner [a], *Vesselin Krassimirov* Krastev [b], *Vincenzo* Mulone [a], *Alessandro* Polimeni [a]

* corresponding author: edoardo.cennamo@uniroma2.it

[a] Department of Industrial Engineering, Tor Vergata University of Rome, via del Politecnico 1, 00133, Rome, Italy

[b] Enterprise Engineering Department, Tor Vergata University of Rome, via del Politecnico 1, 00133, Rome, Italy

Keywords: fuel cell vehicles, hydrogen storage, sustainable mobility, thermal management

Abstract

Introduction: In the context of transport sector decarbonization, hydrogen stands out as a promising energy carrier due to its clean production potential, as well as utilization, its integration with the Renewables and its high energy density [1]. However, several challenges must still be addressed to enable its full exploitation, such as its fossil-based production, the lack of adequate infrastructure for handling and refueling, and its storage [2]. Indeed, the state of the art relies on high pressurized tanks (350-700 bar), exhibiting low volumetric energy densities and requiring highly energy-intensive compression processes. Then, metal hydride-based storage systems present an attractive alternative, consisting of metallic powders capable of absorbing and releasing hydrogen through a desorption reaction. Their key advantages include compactness, due to their high gravimetric energy density, and enhanced safety, as they operate at low pressures (typically 10-30 bar, making them particularly suitable for mobile applications [2]-[3]. However, despite these benefits, the adoption of metal hydride storage systems remains limited, primarily due to the exothermic and endothermic nature of the hydrogen absorption and desorption reactions, respectively. Indeed, effective thermal management is crucial, since reaching critical thermodynamic conditions can compromise the operational continuity [1].

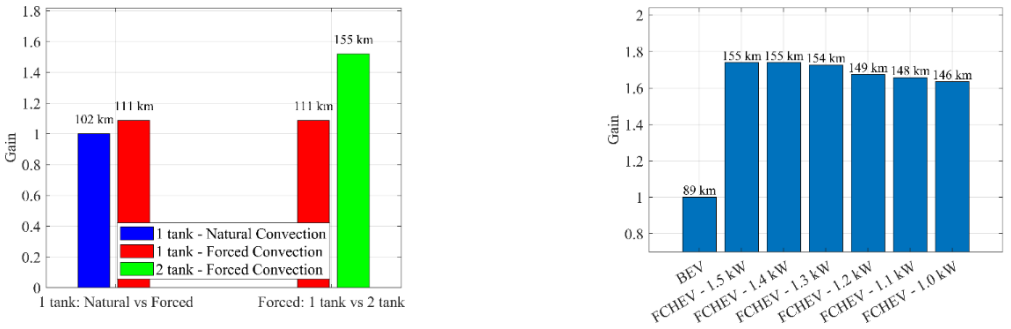
Objectives: This study focuses on the integration of a validated 1D numerical model of a metal hydride storage tank, based on an AB_2 alloy, into the simulation platform of a microcar equipped with a hybrid electric powertrain, comprising a fuel cell stack and a battery pack. First, the evaluation of the impact of the storage system configuration on its efficiency has been carried out; subsequently, the influence of the hybrid powertrain control strategy on hydrogen release capacity has been examined, through the assessment of the overall microcar performance in terms of driving range.

Material and methods: A 1D numerical model of a metal hydride storage tank has been implemented in the Matlab/Simulink platform based on Pressure-Composition Isotherms (PCI) curves to characterize the thermal behavior of the absorption and desorption processes. The system dynamics has been described through mass and energy conservation equations, incorporating the exothermic (or endothermic) term associated with the reaction. The model was initially validated for a $LaNi_5$ alloy, using data from Jemni et al. [4] and from Chung and Ho [5], to assess the accuracy of the modeling approach. Then, the analysis has been extended to a storage tank containing an AB_2 Hydralloy C5 alloy, while the tank specifications are based on the commercial MyH2 3000 cylinders from H2Planet. This system has been selected for its compatibility with the microcar's requirements in terms of hydrogen flow rates and total storable mass. The model has then been integrated into the hybrid microcar

simulation platform, developed in the Matlab/Simulink/Simscape framework. The powertrain consists of four in-wheel motors with a combined output of 6 kW, a lithium-ion battery pack with a nominal capacity of 5.1 kWh, a commercial PEM FC stack (Horizon H2000), and a custom-designed DC/DC converter. For a detailed explanation of the microcar model, including component validations, the reader is referred to previous studies [6],[7]. Concerning the powertrain control strategy, it has been designed to account for the system's ability to meet power demands: a thermostatic ON/OFF controller is implemented to operate the FC as a range extender for the battery pack, thereby increasing the vehicle's driving range. Specifically, the storage operating pressure is used as the control variable: when the pressure approaches the critical threshold (desorption stop), the fuel cell is deactivated, allowing thermodynamic conditions to relax before restarting operation. The tests have been conducted using the WMTC homologation driving cycle, starting from a 100% State of Charge (SOC) and terminating when either the onboard hydrogen is fully consumed or SOC reached 10%. Finally, the storage system configuration, integrated with the FC, has been varied to analyze its impact on the vehicle's overall performance. In particular, configurations with one and two tanks in parallel were tested with the aim of observing the effect of reduced hydrogen flow rates on mitigating thermodynamic constraints. Moreover, these configurations were analyzed under natural convection conditions (i.e., still air) and forced convection, assuming a passive thermal management system utilizing the hot air from the FC to heat up the tank walls. Additionally, the FC power level has been investigated as a key parameter, since it directly affects the hydrogen demand from the storage tanks.

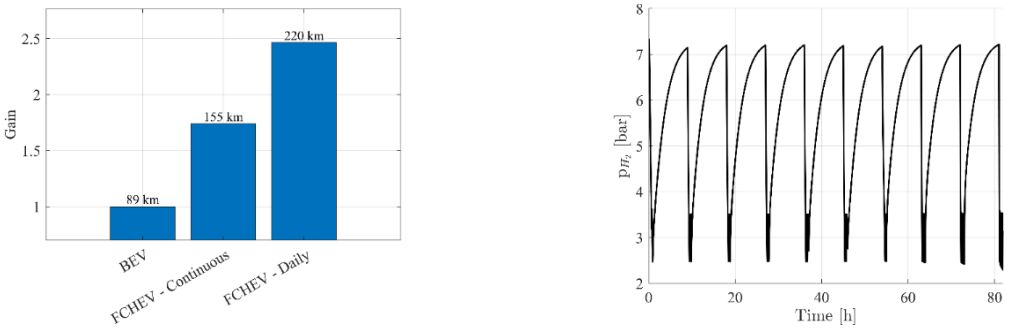
Results: The first analysis examines the impact of the storage system configuration (Figure 1 (a)) on the overall performance of the microcar. It is worth highlighting that implementing a passive thermal management system, where the hot air exiting the FC is directly used to heat up the tank walls (assuming air at the FC temperature with a heat transfer coefficient of $h = 25$ W/m²K), can increase the driving range by approximately 10% without any additional energy expenditure. Furthermore, significant improvement can be achieved by including an additional storage tank in parallel, which significantly mitigates the risk of reaching critical system conditions. This configuration results in an estimated range increase of approximately 40% (from 111 km to 155 km). On the contrary, the effect of FC power level, kept constant during operation, has been found not to have significant impact on vehicle performance (Figure 1 (b)), with a maximum variation of 6% when operating the FC between 1 and 1.5 kW. For the sake of clarity, it is worth noting that the estimated driving range is not constrained by the total amount of storable hydrogen, as none of the cases exceeded 49% of hydrogen utilization. Instead, the limiting factor is the continuous operation of the system, leading to continuous ON/OFF switches of the FC, finally depleting the battery pack ($SOC = 10\%$).

The previous tests are performed by continuously repeating the WMTC cycle until the battery discharged to 10%, assuming uninterrupted vehicle operation. However, the microcar is primarily designed for urban applications, where travel distances are typically shorter and distributed over time. A mixed operating scenario is finally considered to better represent realistic daily use, in which the vehicle is alternated between a nearly 20 km driving pattern (WMTC) and an 8-hour idle period (e.g., during work hours or overnight). This mixed usage significantly enhances the usage of the storage system, as the long idle periods allow for the stabilization of the metal hydrides (i.e., temperature and pressure), as shown in Figure 2 (b), before being used again during the subsequent driving session. Overall, the daily usage pattern increases the estimated vehicle range to approximately 220 km, representing a 40% improvement compared to continuous operation. This improvement is primarily due to the system's capacity to desorb a significantly greater fraction of the stored hydrogen, i.e. 527 g compared to 263 g in the continuous usage scenario.



(a) **(b)**

Figure 1. *Impact of storage system layout (a) and powertrain control (b) on the microcar estimated range.*



(a) **(b)**

Figure 2. *(a) Effect of daily use on the microcar range; (b) Hydrogen pressure profile into the metal hydride tank.*

Conclusions: This study presents an assessment of the feasibility of employing metal hydrides for onboard hydrogen storage. The results highlight that leveraging waste heat from the fuel cell can enhance system efficiency, as well as adopting a dual-tank configuration, significantly mitigates thermodynamic limitations, improving the microcar range by 10% and 40% respectively. Moreover, a realistic urban driving pattern allows for more effective hydrogen utilization (up to 220 km), demonstrating the potential viability of metal hydrides in automotive applications.

References

[1] Liu, J., et al. "A review of thermal coupling system of fuel cell-metal hydride tank: Classification, control strategies, and prospect in distributed energy system." International Journal of Hydrogen Energy 51 (2024): 274-289.

[2] Davids, M. W., et al. "Metal hydride hydrogen storage tank for light fuel cell vehicle." International Journal of Hydrogen Energy 44.55 (2019): 29263-29272.

[3] Tribioli, L., et al. “Fuel Cell/Battery Hybrid Lightweight Quadricycle with Metal Hydride Hydrogen Storage for Improved Performance. No. 2023-24-0137. SAE Technical Paper, 2023.

[4] Jemni, A., et al. "Experimental and theoretical study of ametal–hydrogen reactor." International journal of hydrogen energy 24.7 (1999): 631-644.

[5] Chung, C., et al. "Thermal–fluid behavior of the hydriding and dehydriding processes in a metal hydride hydrogen storage canister." international journal of hydrogen energy 34.10 (2009): 4351-4364.

[6] Bartolucci, L., et al. "Fuel Cell Hybrid Electric Vehicles: Fuel Cell experimental characterization and modeling towards the development of a Hardware-in-the-Loop platform for advanced powertrain design." Journal of Physics: Conference Series. Vol. 2648. No. 1. IOP Publishing, 2023.

[7] Bartolucci, L., et al. Fuel Cell Hybrid Electric Vehicle: Validated Fuel Cell and Battery Pack Model to Enhance Reliability in Performance Predictions. No. 2024-01-2188. SAE Technical Paper, 2024.

European Fuel Cells and Hydrogen
PIERO LUNGHI CONFERENCE
EFCH2 2025
September 17th–19th 2025
Capri / Italy

Development of a numerical model for liquid hydrogen storage tanks for maritime sector

Michela ZANELLI [a*], Diego MICHELI [b], Stefano MALABOTTI [a], Michele CAPOBIANCO [a], Rodolfo TACCANI[b]

* corresponding author: Michela ZANELLI, CENERGY S.r.l., Area Science Park, Basovizza SS14, Edificio Q1, 34149, Trieste (Italy) michela.zanelli@cenergy.it

[a] *CENERGY S.r.l., Trieste, Italy*

[b] *Department of Engineering and Architecture, University of Trieste, Italy*

Keywords: Cryogenic fluid storage, Liquid hydrogen, Numerical modelling, Self-pressurization.

Abstract

Introduction. A relevant technical challenge in liquid hydrogen (LH2) storage and transport to deal with is managing boil-off gas (BOG), which is formed by unavoidable heat leakage into cryogenic tanks. In closed systems, BOG is accumulated and this leads to pressure and temperature increase, requiring effective strategies to extend the holding time and ensure operational safety. For this reason, it is important to be able to accurately predict tank internal conditions so that operations can be carried out safely and the BOG can be properly managed.

Objectives. The aim of the work is to provide a tool able to help in managing LH2 tanks for the maritime transport sector, dealing with a generic navigation profile: self-pressurization phase at full tank, possible pressure setting through an evaporator, fuel withdrawal, BOG management, and self-pressurization phase at empty tank. The main objective of this paper is to investigate the self-pressurization phase of LH2 tanks, by simulating internal conditions and pressure trends thanks to the development of four numerical models. These models are compared to experimental data at two conditions where the tank is likely to be in self-pressurization phase: one at full tank (83% volume) and one at empty tank (29% volume).

Material and methods. The numerical models are developed in MatLab and are zero-dimensional (with 1, 2 or 3 zones, see Fig.1) in which no thermal gradient in single-phase volumes is considered. These models have been developed starting by the open scientific literature and they will be here referred to as: Homogeneous Model (HM) [1], Superheated Vapor and liquid in thermal equilibrium Model (SVM) [2], subcooled liquid and vapor in thermal equilibrium, or Surface Evaporation Model (SEM) [3], Subcooled Liquid and Superheated Vapor and interface in thermal equilibrium Model (SLSVM) [4].

Results. In general, results of the numerical models are in good agreement with those reported in the papers taken as reference, when reasonable values of the calibration parameters are applied.

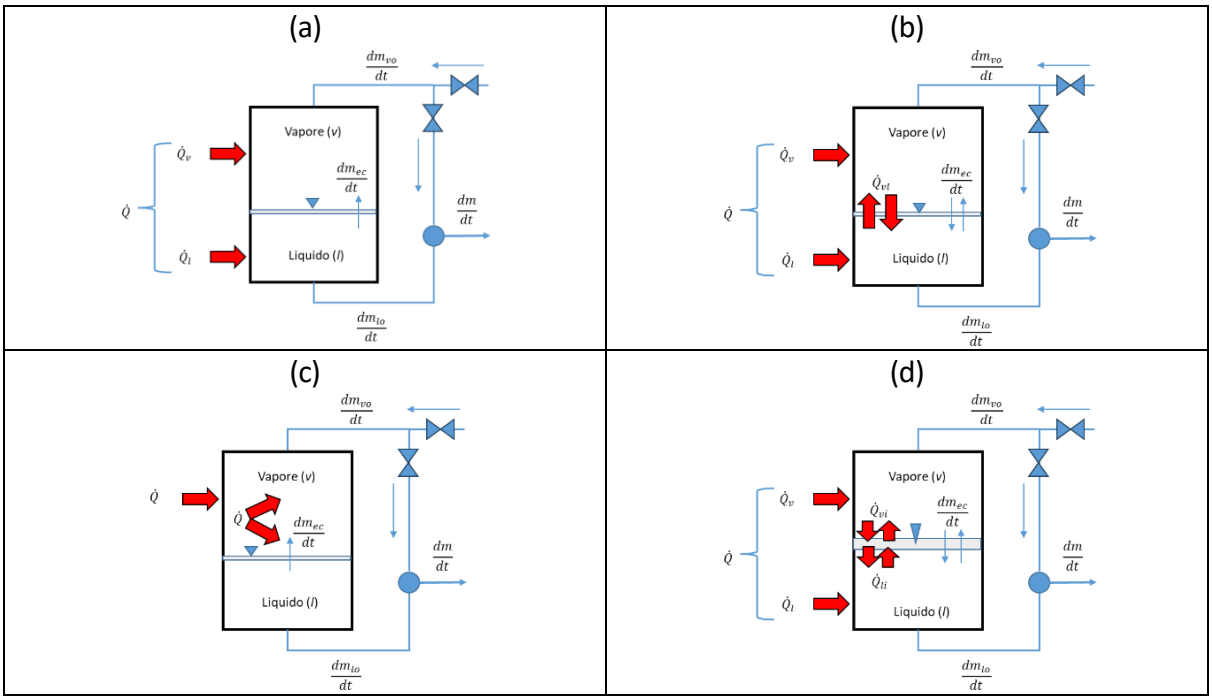


Figure 1 – Schematic of the tank models: (a) HM, (b) SVM, (c) SEM, (d) SLSVM.

In particular, in SLSVM the values of the heat exchange coefficients at the interface on both the vapor and liquid sides must be accurately chosen. Nonetheless, the developed models present some limitations. For instance, the SEM assumes that all the incoming heat is used to evaporate the fluid while the vapor phase is maintained at saturation condition. This condition limits the application of the model to pressure values below that at which, as the enthalpy increases due to the heat transmitted from the walls, the vapor shall be superheated; from the h-s diagram of para-hydrogen, this pressure limit is 3.38 bar.

Another example of limitation regards the SLSVM, which gives results highly sensitive to the initial tank temperature: going from an initial condition of phases equilibrium to one of vapor superheating of 1K and liquid subcooling of 1K, pressurization time results are quite different.

For the comparison among the models, the experimental data reported in [1] has been considered. The pressure trends are reported in Figure 2 for four cases: fill level of 29% and 83% with heat input of 2 W/m^2 and 3.5 W/m^2. From the summarized outcomes of the models' comparison, it results that the HM highly underestimates the pressure increase; the SVM also underestimates the pressure increase but its trend is slightly faster than the HM; the SEM, instead, overestimates the pressure increase; finally, the SLSVM can provide the closest trend to the experimental data.

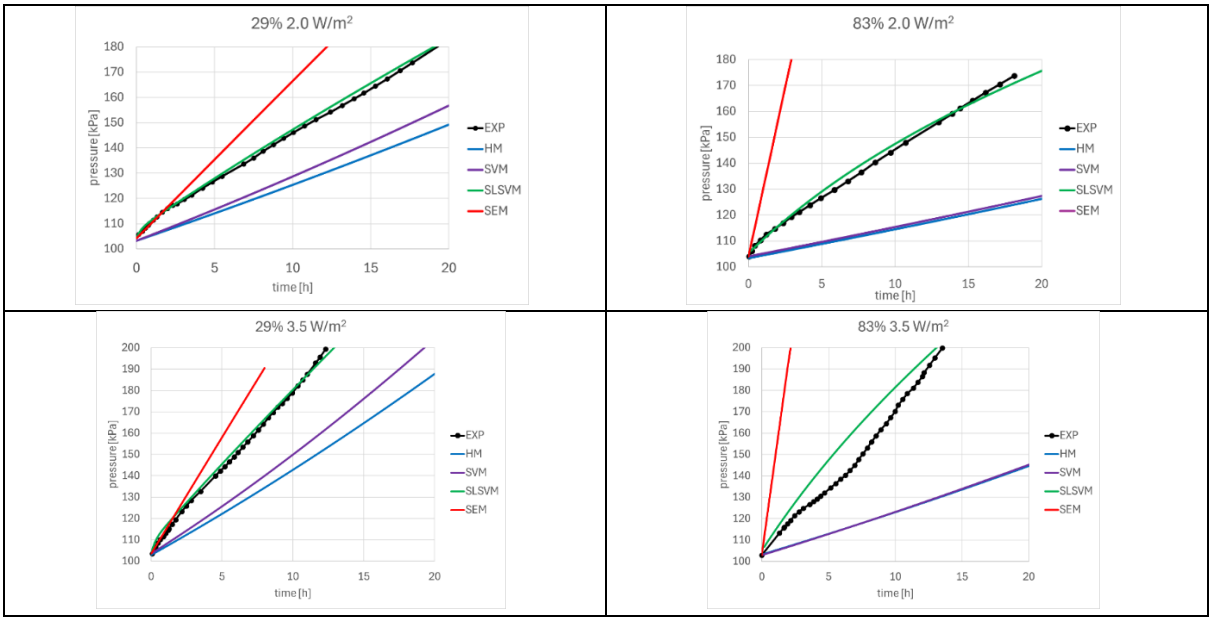


Figure 2 – Numerical vs. experimental results from [1].

Conclusions. The main focus of the paper stands in the comparison of different simulation approaches regarding the self-pressurization phase of LH2 storage tanks, as part of a more complex numerical model capable of simulating an entire navigation profile for tanks of different sizes and shapes.

Acknowledgment. This work has been partly funded by the Horizon Europe Project sHYpS – sustainable HYdrogen powered Shipping – Grant Agreement 101056940.

References

[1] *Van Dresar, N.T., Lin, C.S., Hasan, M.M., 1992. Self-Pressurization of a Flightweight Liquid Hydrogen Storage Tank: Effects of Fill Level at Low Wall Heat Flux. NASA Technical Memorandum 105411.*

[2] *Perez, F., Al Ghafri, S.Z.S., Gallagher, L., Siahvashi, A., Ryu, Y., Kim, S., Kim, S.G., Johns, M.L., May, E.F., 2021. Measurements of boil-off gas and stratification in cryogenic liquid nitrogen with implications for the storage and transport of liquefied natural gas, Energy 222 119853.*

[3] *Gursu, S., Sherif, S.A., Veziroglu, T.N., Sheffield, J.W.,1993. Analysis and Optimization of Thermal Stratification Effects in Liquid Hydrogen Storage Systems – Part 1: Model Development. Journal of Energy Resources Technology, Vol. 115, 221-227.*

[4] *Wang, H,R., Wang, B., Pan, Q.W., Wu, Y.Z., Jiang, L., Wang, Z.H., Gan, Z.H., 2022. Modeling and thermodynamic analysis of thermal performance in self-pressurized liquid hydrogen tanks. International Journal of Hydrogen Energy, 47, 30530-30545.*

European Fuel Cells and Hydrogen
PIERO LUNGHI CONFERENCE
September 17th–19th 2025
Capri / Italy

HASTA - Hydrogen Aircraft Sloshing Tank Advancement

A.Agresta*[m], L.M. Gonzalez-Gutierrez [a], R.A.Barca[b], M.Wellner[c], P.Behruzi[d], L.Constantin[e], M.Antuono[f], S.Zaleski[g], G.Coppotelli[h], M.T.Scelzo[i], A.Krieger[j], T.Pagliaroli[k], A. Malan[l], F.Gambioli[n], J.E.Cooper[o], W.Liu[p]

** Corresponding Author: Antonio Agresta*

[A] Universidad Politechica De Madrid, Madrid, Spain
[B] Airbus Operations Sl, Avenida John Lennon S/N, Getafe 28906, Spain
C Airbus Operations Gmbh, Kreetslag 10, Hamburg 21129, Germany
[D] Arianegroup, Airbus Allee 1, 28199 Bremen, Germany
[E] Academia Tehnica Militara "Ferdinand I, Bucuresti 050141, Romania
[F] Cnr-Inm, Via Di Vallerano 139, 00128 Rome, Italy
[G] Sorbonne Universite, Rue De L'ecole De Medecine, Paris 75006, France
[H] Universita La Sapienza, Via Eudossiana 18, 00184 Rome, Italy
[I] Von Karman Institute For Fluid Dynamics, Waterloose Steenweg, 72, Belgium
[J] Deutsches Zentrum Fur Luft Und Raumfahrt Ev, Lin Der Hohe, Koln 51147, Germany
[K] Universita Degli Studi Niccolo Cusano Telematica, Roma 00166, Italy
[L] University Of Cape Town, Rondebosch, Cape Town 7701, South Africa
[M] Enea - Agenzia Nazionale Per Le Nuove Tecnologie, L'energia E Lo Sviluppo Economico Sostenibile, Lungotevere Grande Ammiraglio Thaon Di Revel 76, Roma 00196, Italy
[N] Airbus Operations Ltd, Filton, Bristol Bs34 7pa, United Kingdom
[O] University Of Bristol, University Walk, Bristol, Bs8 1tr, United Kingdom
[P] Uk Research And Innovation Science And Technology Facilities Council, United Kingdom

Keywords: Liquid Hydrogen storage, Cryogenic Sloshing, Aircraft environmental impact, Thermal-Fluid-Structure-Interaction

Abstract

The Hydrogen Aircraft Sloshing Tank Advancement (HASTA) project focuses on the storage of liquid hydrogen (LH2) as aviation fuel, addressing key factors like tank size, placement, and connections. These factors are critical for aircraft range, payload, and size, influencing environmental impact. HASTA aims to develop design criteria for LH2 tanks based on experimental and computational models, particularly for cryogenic sloshing. The project extends current knowledge of fuel sloshing, adapting it for LH2's cryogenic temperatures. The goal is to create validated design tools for use in both conceptual and detailed aircraft design, with a focus on the complex thermo-fluid dynamics of LH2 and its interaction with the tank's thermo-mechanical behavior. The consortium combines expertise in fuel sloshing, cryogenics, and aerospace applications.

EFCH2 2025
European Fuel Cells and Hydrogen
PIERO LUNGHI CONFERENCE
September 17th–19th 2025
Capri / Italy

Introduction:



Figure 1: View of the flying Airbus A380 with LH2 tanks and detailed cut view of a LH2 tank.

The HASTA (Hydrogen Aircraft Sloshing Tank Advancement) project is a European Union-funded initiative aimed at studying and developing innovative solutions for the design of liquid hydrogen (LH2) tanks for civil aviation. The use of hydrogen as aircraft fuel is considered a key strategy to reduce greenhouse gas emissions in the aviation sector, but it presents several technical challenges.

The most critical aspect is the need to store hydrogen at cryogenic temperatures (-253°C) in lightweight, safe, and efficient tanks. A fundamental issue is the study of sloshing, i.e., the movement of the liquid inside the tank during flight, which can compromise the structural and thermodynamic stability of the system.

HASTA aims to tackle these problems by developing advanced numerical models, validated with experimental data, to provide reliable design criteria for future hydrogen-powered aircraft.

Objectives:

The objectives of the HASTA project focus on the development of advanced methodologies for the design of LH2 tanks, with particular attention to the following areas:

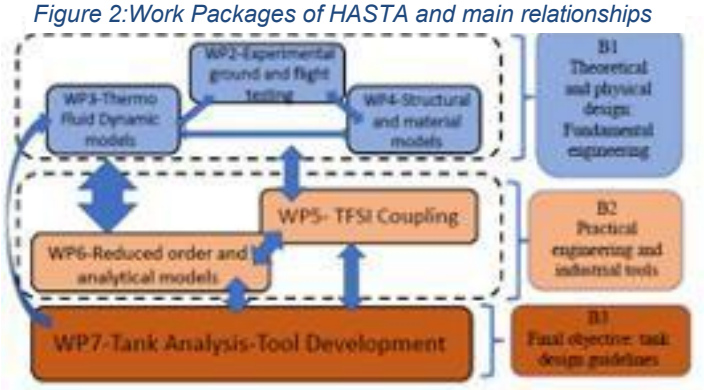
- Analysis of sloshing behavior: studying the effects of liquid motion on heat transfer, structural stresses, and operational stability of the tank ([1],[2]).
- Development of advanced numerical models: creating computational simulations to reproduce tank behavior under realistic flight conditions [3].
- Experimental validation: conducting tests with substitute liquids and liquid nitrogen (LN2) to verify the reliability of theoretical models [1].
- Design of an optimized system: defining guidelines for the design of safe and efficient aeronautical tanks, to be used by the aerospace industry.

The ultimate goal is to provide concrete tools to facilitate the adoption of hydrogen in aviation, contributing to the sector's environmental impact reduction.

Material and methods:

To achieve its objectives, the HASTA project adopts a multidisciplinary approach that combines experimentation, numerical modeling, and data validation. To meet the HASTA objectives, the proposed methodology for development of the technical guidelines and software tools for design of the LH2 tank goes from the bottom

Figure 2:Work Packages of HASTA and main relationships



up, in other words, from first engineering principles to the final tests during a complete flight mission. The structure of the work is divided into three blocks as in Fig.2.

Conclusions:

The HASTA project represents a crucial step in the search for technological solutions for hydrogen use in civil aviation. Through an approach based on experimentation and advanced simulation, HASTA will contribute to the creation of reliable design tools for LH2 tanks.
The expected outcomes include:
- A greater understanding of the thermodynamic behavior of liquid hydrogen in aeronautical tanks.
- The development of validated numerical models for simulating the sloshing phenomenon.
- The definition of design guidelines for safe and efficient tanks.

These developments will be essential for the aviation industry, supporting the transition towards more sustainable air mobility and contributing to reducing the sector's CO2 emissions.

Acknowledgment

This work was funded by the HASTA project (Grant No. 101138003) as part of the European Union Horizon research programme. Views and opinions expressed are however those of the authors only and do not necessarily reflect those of the European Union. Neither the European Union nor the granting authority can be held responsible for them.

References

[1] J.Martinez-Carrascal, L.M. Gonzalez-Gutierrez. Experimental study of the liquid damping effects on a SDOF vertical sloshing tank, Journal of Fluids and Structures, Vol.100, 2021,103172

[2] Michel, J., Durante, D., Colagrossi, A. & Marrone, S. (2022). Energy dissipation in violent three-dimensional sloshing flows induced by high-frequency vertical accelerations. Phys. Fluids, 34(10), 102114.

[3] Malan, L.C., A.G. Malan, S. Zaleski & P.G. Rousseau (2021) A geometric VOF method for interface-resolved phase change and conservative thermal energy advection. J. Comput. Phys., 426, 109920.

European Fuel Cells and Hydrogen
PIERO LUNGHI CONFERENCE
EFCH2 2025
September 17th–19th 2025
Capri / Italy

Design of a Zero-Emission Metal Hydride-based Refueling Station for H2-powered L6e Light-Duty Hybrid Vehicles

Marco Maggini[a], Stefano Ubertini[a], Lorenzo Bartolucci[b], Stefano Cordiner[b], Vincenzo Mulone[b], Cesare Pianese[c], Pierpaolo Polverino[c], Massimo Sicilia[c], Andrea Luigi Facci*[a]

* corresponding author: andrea.facci@unitus.it

[a] Department of Economics, Engineering, Society and Business Administration, University of Tuscia, 01100 Viterbo, Italy

[b] Department of Industrial Engineering, Tor Vergata University of Rome, 00133, Rome, Italy

[c] Department of Industrial Engineering, University of Salerno, Via Giovanni Paolo II 132, 84084 Fisciano (SA), Italy

Keywords: hydrogen, hybrid electric vehicles, zero-emission vehicles, metal hydrides

Abstract:

This paper investigates the potential of hydrogen as a sustainable alternative fuel to mitigate the environmental impact of the automotive industry. It presents the design of a hydrogen refueling station for L6e light vehicles, powered by a photovoltaic system. The study optimizes the capacity of the energy storage elements (buffer battery and hydrogen tank) and of the electrolyzer to minimize the levelized cost of hydrogen storage for a fleet of 8 vehicles in urban driving cycles. Key components such as the photovoltaic system, PEM electrolyzer, and hydrogen storage method are discussed.

Introduction: An ecologically sustainable mobility is necessary to reduce the environmental impact of this sector, in line with the 17 points of sustainable development set out by the UN **[1]**. Transport still accounts for 26.6% of total greenhouse gas emissions in the EU, falling far short of the objectives of the European Green Deal targets to reduce greenhouse gas emissions by 60% compared to the 1990 levels **[2]**. The characteristics that make hydrogen particularly interesting for its applications in the energy and automotive fields, namely in Fuel Cell-powered cars, are: absence of local emissions, high energy density, high driving range compared to battery electric vehicles, short refueling times **[3]**. In terms of on-board and stationary hydrogen storage solutions, Metal Hydrides (MH) are a promising alternative to traditional compression or liquefaction storage systems, insomuch the theoretical energy density is higher and the safety issues overcome **[4,5]**, thanks to a lower storage pressure.

Methodology: A hydrogen refueling station is powered by a PV system to produce green hydrogen, which is then stored in a MH storage system (see **Fig. 1**). A buffer battery decouples

energy generation and utilization in the PEM electrolyzer (PEM-EL). A 8-element fleet of L6e small quadricycles, with an individual daily mileage of 20 km and a driving range of 160 km is considered, for a total yearly hydrogen demand of $m_{H_2} = 144.2$ kg. The hydrogen demand was determined through the development of a detailed digital model of the quadricycle and an extensive experimental campaign conducted in previous studies within the framework of the HySum project **[7, 8]**. The digital model was then used to estimate the vehicle's range under various operating conditions, fuel sizings, and driving cycles, leading to an average specific consumption of about 0.35 kg/100 km for the vehicles **[9]**. The yearly energy demand is $E_e = \mathrm{LHV}_{H_2} \cdot m_{H_2} / \eta_{\mathrm{PEMEL}} = 6{,}860.6$ kWh, where LHV_{H_2} and η_{PEMEL} are the hydrogen lower heating value (33.3 kWh/kg) and the PEM-EL efficiency (70%). A seed Real Driving Emissions cycle in terms of speed, acceleration, and road slope is selected to generate a vehicle fleet driving mission **[6]**. From the original drive cycle, the cinematic inputs are discretized in a finite states number to define a comprehensive state variable. We treat the driving cycle as a Markovian chain process and we use a Montecarlo approach to generate several driving cycles with the same probabilistic features. An iterative optimization procedure is carried out on MatLab to minimize the Levelized Cost of Hydrogen (LCOH) taking battery and MH tank capacities, and the PEM-EL rated power as variables and assuming the formula defined in **[10]** for the LCOH. The hydrogen storage medium is $LaNi_5$, with a gravimetric density of 1.40%, whose dimensions are determined in previous works **[4,5]**. One module can store approximately 1 kWh of hydrogen and deliver a maximum rated power of 1 kW **[4]**. An external jacket of $LiNO_3 – 3H_2O$ facilitates the ab/desorption thermal cycle **[11]**.

Results: By selecting central Italy on the tool PVGIS **[12],** a photovoltaic plant of 4.85 kW_p is sized, which produces the needed amount of energy E_e each year, assuming a null yearly variability for simplicity. A PEM electrolyzer with a rated power of 3.75 kW and delivery pressure of 14 barg is employed. The Li-Ion buffer battery has a capacity of 1.5 kWh, whilst the MH tank comprises 570 modules in parallel for a total of approximately 17.1 kg of hydrogen. An estimated LCOH of 11.46€/kg is achieved. A total of 41,760 km driving range is covered in one year by the fleet. The on-board hydrogen is stored inside a MH tank of 600g H_2. The MH tank presents a decrease in fill level during wintertime, where less energy is produced by the PV plant, and an increase during summertime, where more energy is available (see Fig. 2). The small buffer battery aids during wintertime whilst it is almost unused

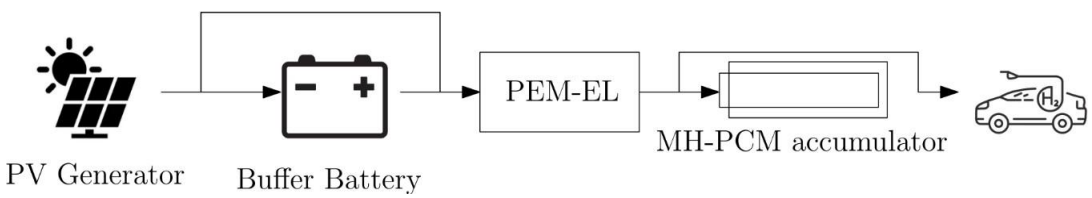


Figure 1: FCEV refueling station layout. PV panels and buffer battery work in parallel

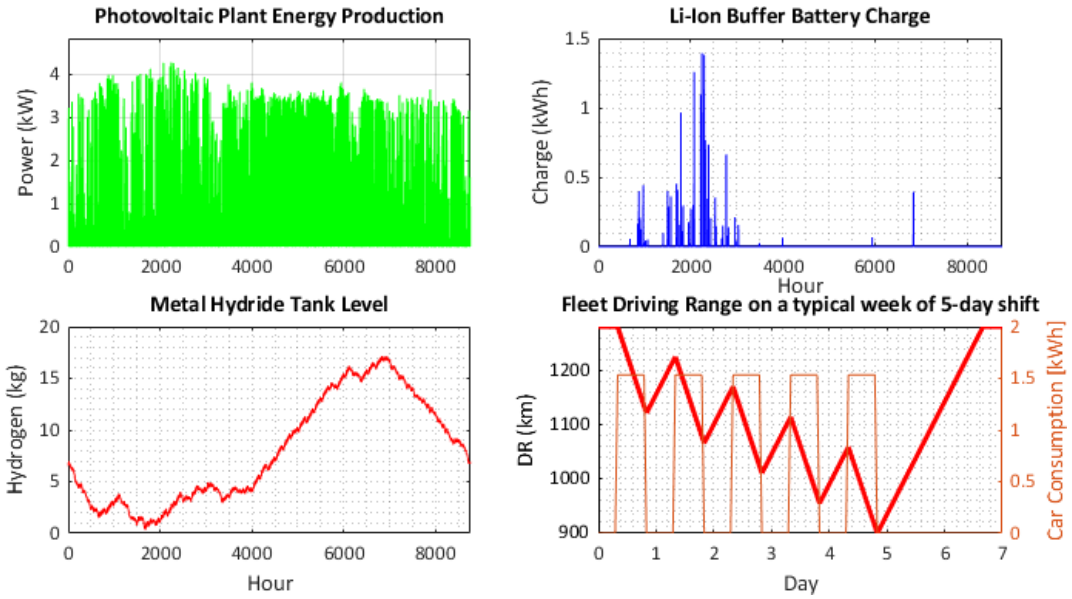


Figure 2. Results of the optimization procedure: **(top-left)** *Yearly PV production (4.85 kW$_p$);* **(top-right)** *buffer battery hourly charge;* **(bottom-left)** *hourly MH hydrogen tank level;* **(bottom-right)** *cumulative driving range of 8-car fleet on a typical week, along with the hourly car consumption in kWh.*

during summertime. Cars are recharged during night-time and weekends, thus the sawtooth profile.

Conclusions: The project demonstrates the feasibility of designing a hydrogen refueling station for 8 L6e light-duty vehicles powered by a photovoltaic system and a Metal Hydride-based H_2 accumulator, offering a sustainable alternative for urban transportation (daily mileage = 20 km). Future work should focus on optimizing the integration of the electrical system to enhance reliability and efficiency, as well as a sensitivity study on green hydrogen production costs and to battery/MH tank capacities.

Acknowledgment

This work is partially funded by the projects: (a) PRIN 2020BFX8JY- Hybrid Sustainable Mobility – HYSUM and (b) PRIN P20223JMB3 - Modeling and optimization of sustainable hydrogen refueling infrastructures – HyREFI. This work was performed as partial fulfillment for the final work of the Master "European Specialization School in Sustainable Energy - SkillBill" by Marco Maggini".

References

[1] United Nations, Sustainable Development Goals, https://sdgs.un.org/goals.
[2] EU Commission, The European Green Deal, https://eur-lex.europa.eu/legal-content/IT/TXT/, 2019.
[3] B.E. Lebrouhi, Y. Khattari, B. Lamrani, M. Maaroufi, Y. Zeraouli, T. Kousksou, **J. Energy St.**, (44) 2021, 103273.
[4] M. Maggini, G. Falcucci, A. Rosati, S. Ubertini, A. L. Facci, **Journal of Energy Storage**, (93) 2024, 112230.
[5] M. Maggini, A. L. Facci, G. Falcucci, S. Ubertini, **Applied Energy**, (378) 2025, 124725.
[6] D. Cervone, M. Sicilia, M. Romano, P. Polverino et al., **SAE Int. J. Adv. & Curr. Prac. in Mobility**, (4) 2024, 2087-2101.
[7] Bartolucci, L., Cennamo, E., Cordiner, S., Donnini, M. et al., **SAE Technical Paper** 2024-24-0006, 2024.
[8] Bartolucci, L., Cennamo, E., Cordiner, S., Donnini, M. et al., **SAE Technical Paper** 2024-01-2188, 2024.
[9] Lorenzo Bartolucci *et al* 2024 ***J. Phys.: Conf. Ser.***, 2893 012080
[10] Z. Abdin, K. Khalilpour, K. Catchpole, **Energy Conversion and Management**, (270) 2022, 116241
[11] M. Maggini, G. Falcucci, A. L. Facci, S. Ubertini, **Energy Proceedings**, (49) 2024
[12] Photovoltaic Geographical Information System, Photovoltaic Geographical Information System (PVGIS)

European Fuel Cells and Hydrogen
PIERO LUNGHI CONFERENCE
EFCH2 2025
September 17th–19th 2025
Capri / Italy

Power vs. discharge efficiency of thermally controlled Metal Hydride hydrogen storage tanks: a revised analysis

V. K. Krastev*[a], M. Baldelli [b], L. Bartolucci[b], S. Cordiner[b], G. Falcucci[a] and V. Mulone[b]

* Corresponding author: krastev@dii.uniroma2.it
[a] Enterprise Engineering Department, University of Rome "Tor Vergata"
[b] Industrial Engineering Department, University of Rome "Tor Vergata"

Keywords: Discharge Efficiency, Metal Hydrides, Phase Change Materials, Power

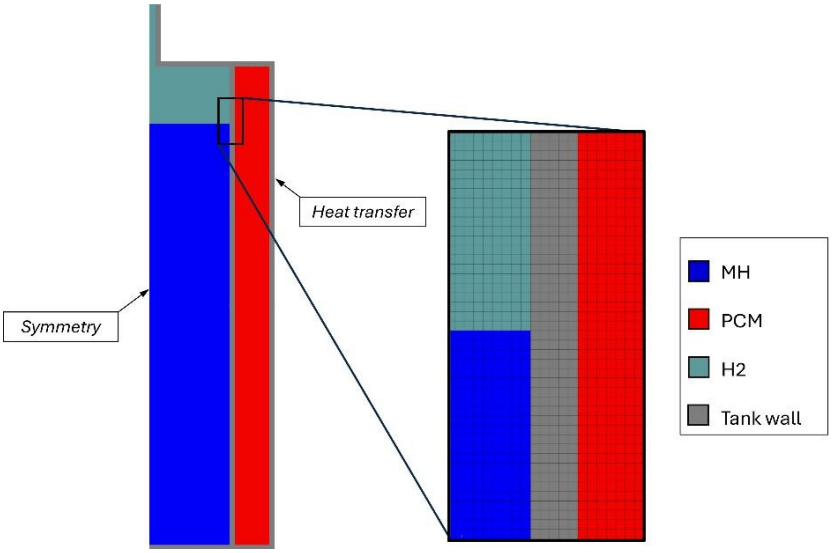
Abstract

Introduction: Metal Hydrides (MH) have been considered for at least three decades as a viable alternative for safe and efficient hydrogen storage, due to their intrinsically high volumetric storage density and favourable operating conditions [1,2]. The application of numerical modelling to analyse and improve the MH storage and discharge performances is almost as old [3], with a remarkable increase in the publication pace detected in the last ten years [4]. Regardless of the year of publication, most of the MH-related computational studies are comparative in nature and do not include a clear link with application-oriented performance parameters [4]. Furthermore, almost all the available results are obtained at constant charge/discharge pressure, which is not compliant with actual massflow-controlled operating conditions. A remarkable exception is the work of Niamsi and Tolj [5], where to the authors' knowledge a first-of-a-kind study is presented on the actual discharge power performance of a 1 kg_{H2} MH tank integrated with a Phase-Change Material (PCM) jacket for thermal control of the hydrogen release reaction.

Objectives: The present work aims at using CFD modelling to evaluate the discharge efficiency at rated power of cylindrical MH tanks with various thermal management strategies. Differently from a previous recent work from the authors [4], the analysis has been performed at constant rated power (constant hydrogen mass flow), rather than at constant discharge pressure. The main expected outcome is to derive insights and guidelines on the limiting factors that affect the MH discharge performances for a given application power envelope.

Material and methods: The analysis has been made on an axisymmetric cylindrical tank configuration (Fig. 1). The computational domain includes the MH and PCM (if present) tank volumes, a small exit nozzle and the tank solid walls, while the H/D ratio (MH tank) is equal to 3. Three different thermal management strategies are considered: 1) *NC* - the tank exchanges heat with the external environment through natural convection; 2) *FC_50* - forced convection with waste heat recovery at 50 °C; 3) *PCM* – PCM controlled. The domain is discretized using a uniform grid with a 1 mm spacing and

the fluid flow, energy and melting/solidification equations are solved numerically through the Ansys® Fluent commercial CFD code [6]. The MH discharge kinetics is implemented through user-coding within the software UDF programming framework.



MH ($LaNi_5$)	
ΔH_R (MJ/kg_{H2})	15.2
ρ_0 (kg/m^3)	7164
ρ_s (kg/m^3)	7259
w%	1.3
ε	0.5

PCM ($LiNO_3$-$3H_2O$)	
ρ (kg/m^3)	1960
C_p (J/kg·K)	2250
λ (W/m·K)	0.95
α (m^2/s)	$2.15 \cdot 10^{-7}$
L_f (J/kg)	296000

Figure 1 – *Schematics of the computational domain, with details on the mesh elements. When the PCM is not present, the external jacket is removed and the MH-PCM separation wall becomes the external heat transfer boundary.*

The PCM mass and volume account for the total heat of reaction of the maximum amount of hydrogen stored.

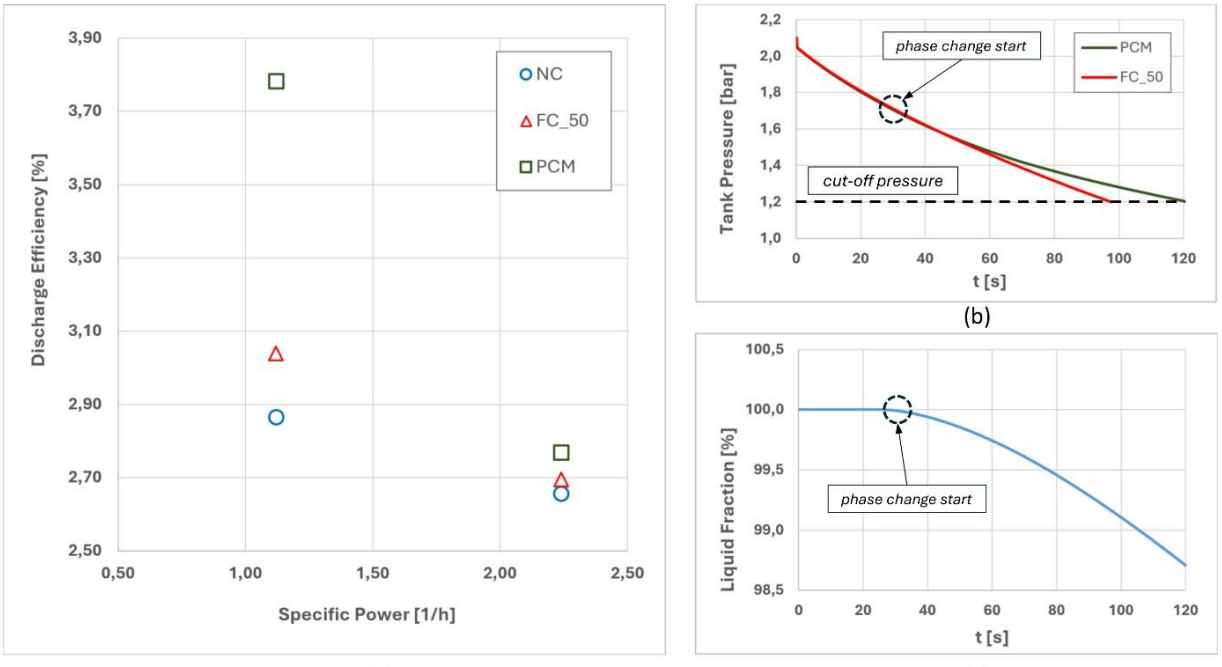


Figure 2 – *a) Discharge efficiency vs. specific power chart; b) tank internal pressure evolution; c) PCM liquid fraction evolution.*

Results: Figure 2a shows results from an initial simulation sweep. The discharge efficiency is defined as the percentage of released hydrogen mass compared to the initial fully-saturated tank capacity,

which is fixed at 270 g_{H2} (~ 9 kWh, based on the hydrogen LHV). The specific rated power is the ratio between the power delivered (LHV-based) and the initial capacity. All simulations begin with the tank elements at 1°C above the PCM solidus temperature, while the initial internal pressure is set at the corresponding MH equilibrium pressure (around 2.05 bar for the $LaNi_5$ MH). A cut-off pressure is set at 1.2 bar, assuming that below that threshold the MH tank is no longer capable of effectively feeding a FC-based conversion system. The *FC_50* strategy produces only marginal efficiency gains compared to *NC* (up to +6% at low-power conditions). Conversely, the PCM strategy increases efficiency up to +32% compared to *NC* and up to +24% compared to *FC_50* (low-power). This is apparently linked to the triggering of the phase-change mechanism (Figs. 2b and 2c).

Conclusions: The results shown above reveal that: i) the LaNi5 hydride has strong discharge efficiency limitations, mainly due to the low equilibrium pressure at ambient temperature; ii) using PCMs for thermal control seems convenient compared to forced air convection. Further results are in the process of being produced, considering more H/D ratios, better performing hydrides and other PCM types (organic-based).

Acknowledgments

The authors acknowledge partial support from the National Center for HPC, Big Data and Quantum Computing, Project CN_00000013 - CUP: E83C22003230001, Mission 4 Component 2 Investment 1.4, funded by the European Union - NextGenerationEU.
V. K. K. and G. F. wish to acknowledge support from Project PRIN 2022F422R2 - CUP: E53D23003210006, funded by the European Union - NextGenerationEU.

References

[1] C. Drawer, J. Lange, M. Kaltschmitt, Metal hydrides for hydrogen storage – Identification and evaluation of stationary and transportation applications, J Energy Storage 77 (2024). https://doi.org/10.1016/j.est.2023.109988.

[2] G. Scarpati, E. Frasci, G. Di Ilio, E. Jannelli, A comprehensive review on metal hydrides-based hydrogen storage systems for mobile applications, J Energy Storage 102 (2024). https://doi.org/10.1016/j.est.2024.113934.

[3] A. Jemni, S. Ben Nasrallah, Study of Two-Dimensional Heat and Mass Transfer During Absorption in a Metal-Hydrogen Reactor, Int. J. Hydrogen Energy 20 (1995) 43–52.

[4] V. Krastev, G. Bella, G. Falcucci, L. Bartolucci, S. Cordiner, V. Mulone, Power Vs. Capacity Performances of Thermally Integrated MH-PCM Hydrogen Storage Solutions: Current Status and Development Perspectives, in: 36th International Conference on Efficiency, Cost, Optimization, Simulation and Environmental Impact of Energy Systems, ECOS 2023, Las Palmas de Gran Canaria, 2023: pp. 2183–2193. https://doi.org/10.52202/069564-0197.

[5] S.N. Nyamsi, I. Tolj, Metal hydride reactors and phase change materials: Enhancing energy storage for medium-high power vehicles, J Energy Storage 104 (2024). https://doi.org/10.1016/j.est.2024.114545.

[6] Ansys Inc., ANSYS® Academic Research CFD, Release 2024 R1, Fluent User's Guide, 2024. http://www.ansys.com.

European Fuel Cells and Hydrogen
PIERO LUNGHI CONFERENCE
September 17th–19th 2025
Capri / Italy

Design and analysis of a thermal management system for a novel metal hydride tank for H2 storage in fuel cell vehicles

Jigarkumar Ghevariya*[a], Gabriele Scarpati [a], Giovanni Di Ilio [a], Elio Jannelli [a]

* corresponding author: jigarkumararjanbhai.ghevariya001@studenti.uniparthenope.it
[a] University of Naples Parthenope, Department of Engineering, Naples, Italy

Keywords: Metal hydrides, Hydrogen storage, Sustainable mobility, Fuel cell vehicles

Abstract

In this work, a novel metal hydrides-based tank design is proposed for the storage of hydrogen (H2) onboard of fuel cell electric vehicles. The storage system is conceived in a modular configuration, with each module consisting of an aluminum block containing cylindrical cavities for the MH material and integrated channels for the transport of the thermal fluid (i.e. water-glycol mixture) used for thermal management. A 3D numerical model is developed and the H2 refueling process of the tank is simulated under different operating conditions to investigate the thermal behavior and refueling performance of the system. The achieved compact design of the tank allows to store around 4.3 kg of H2. The results from the numerical analysis demonstrate that the refueling performance of the tank is close to that of more conventional H2 storage systems.

Introduction: Metal hydrides (MHs) are promising materials for H2 storage, due to their ability to absorb/desorb H2 at moderate pressures and temperatures [1]. This characteristic makes them inherently safer than high-pressure gas or cryogenic liquid storage methods. Moreover, MHs offer high volumetric energy density, this being a key advantage over other H2 storage alternatives, which make them an attractive option for fuel cell vehicle applications, where space is crucial [2]. In contrast, their use presents some critical drawbacks, including low gravimetric energy density and the need of an advanced thermal management system (TMS) to handle the exothermic/endothermic reaction occurring during the H2 absorption/desorption process. For these reasons, only a limited number of studies have explored the use of MHs in mobile applications, with very few prototypes developed, and further research is still necessary to overcome these challenges [3].

Objectives: This study focuses on the design and performance of a MH-based H2 storage tank for fuel cell vehicles, with particular emphasis on its TMS and the analysis of the refueling process. In fact, the refueling of the tank is the most critical aspect, as it is required achieving short times, comparable to those of conventional vehicles, which result in high heat transfer

rates. In contrast, the H2 release during vehicle operation occurs at much lower flow rates, aligned with the fuel cell supply needs, and therefore this can be effectively managed using the vehicle's existing onboard TMS.

Material and methods: The proposed MH storage system comprises 8 identical modules, each consisting of an aluminum block with 20 cylindrical cavities housing the MH material, along with 26 channels for the circulation of a 70:30 water-glycol mixture, which serves as the heat transfer fluid (HTF) for thermal management. A numerical model is setup to simulate the refueling process in a 3D finite element method (FEM) framework. The numerical model leverages on the symmetry of the system, hence only one-quarter of a single module is considered, to reduce the computational burden. The model takes into account heat and mass transfer phenomena, including H2 diffusion thorough the MH material, which is treated as a porous medium, as well as the kinetics associated with the absorption chemical reaction. The dynamics of the HTF instead is not simulated, rather a convection boundary condition is applied by setting the average temperature and velocity of the HTF along the channels.

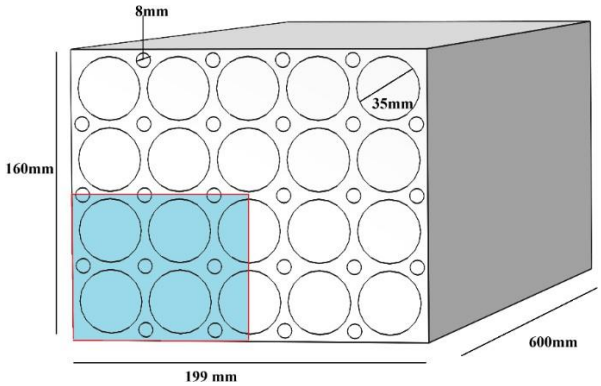


Figure 1 – Geometry of a single module of the designed MH storage system, with highlighted the computational domain

Results: A parametric analysis is conducted to explore a wide range of operating conditions. The refueling process is simulated by applying an inlet pressure ramp up to 30 bar in all cases. The pressure ramp rate (PRR) and the HTF temperature and velocity are varied to assess their impact on the refueling time, defined as the time duration required to reach 97% of the tank's capacity, starting from a nearly empty state (i.e. 10% full). Temperature, pressure and concentration fields are then analyzed and compared.

Effect of PRR and HTF velocity: The input PRR has a moderate impact on the results, as higher values of the ramp allowing only to slightly decrease the temperature in MHs while achieving comparable refueling times. In contrast, the HTF velocity exhibits a much more pronounced influence on the results, indicating that refueling performance are strongly related to this parameter, as expected. In fact, the HTF velocity is directly related to the heat transfer capabilities of the TMS and, for instance, doubling this value results in a reduction of the

refueling time of around 40% (i.e. 0.4 kgH2/min), with the average temperature at the end of the process reduced by 10°C.

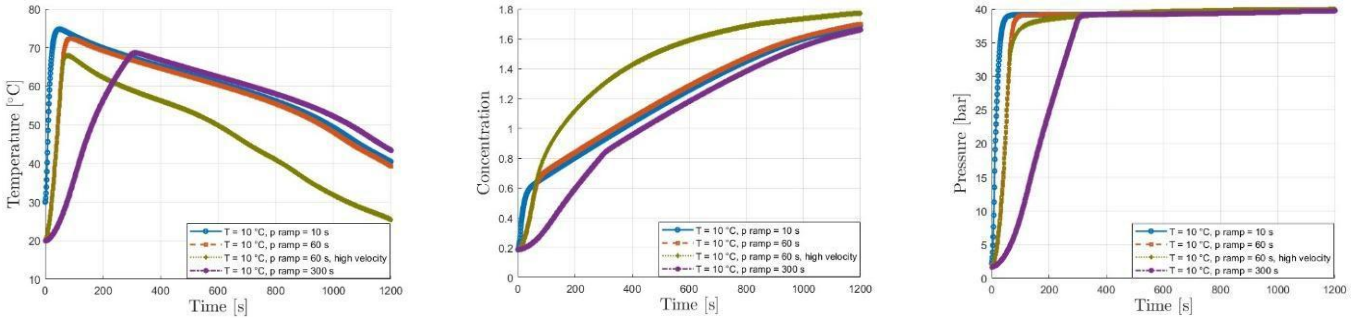


Figure 2 – Effect of PRR and HTF velocity on average temperature, concentration and pressure in the MH tank.

Effect of HTF temperature**:** This parameter significantly affects the refueling times, which stand at around 20 minutes when the average HTF temperature is set at 0 °C, i.e. 0.25 kgH2/min. Lower HTF temperatures allow to mitigate the temperature rise within the MH material caused by the exothermic absorption reaction. This results in a general reduction of the local equilibrium pressure, ultimately enhancing reaction kinetics and improving refueling performance. Conversely, the peak temperature reached during the process remains almost unchanged.

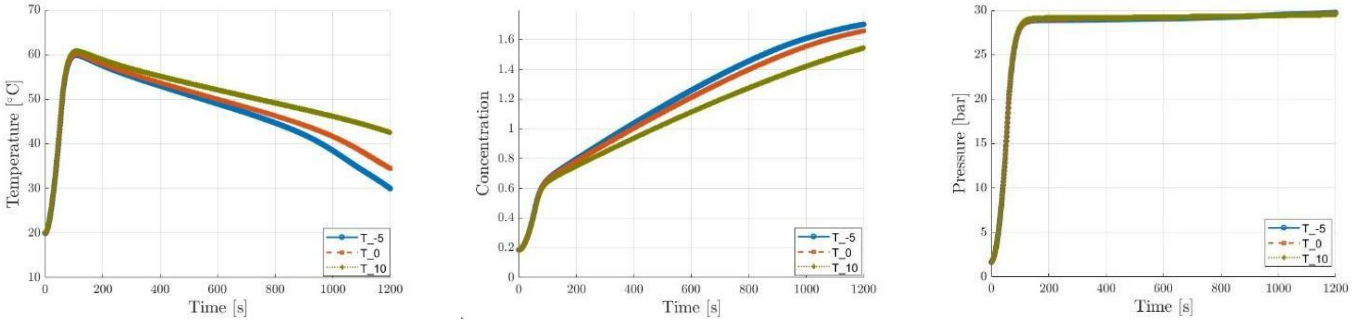


Figure 3 – Effect of HTF temperature on average temperature, concentration and pressure in the MH tank.

Conclusions: This study proposes an innovative design of MH tank tailored for mobile applications and its TMS is evaluated for the refueling process, with several refueling parameters systematically varied to assess their impact. The results demonstrate that the proposed system ensures an effective thermal control, which enables refueling times comparable to those of conventional H2 gas tanks.

Acknowledgment

This research has received funding from the Italian Ministry of University and Research through the Italian National Program PRIN – "Advanced Low-Pressure Hydrogen storage systems for Automotive applications" (ALPHA), Grant no. 2022KLJHZW.

References

[1] M.V. Lototskyy et al., Prog. Nat. Sci.: Mater. Int. 27 (2017) 3–20, http://dx.doi.org/10.1016/j.pnsc.2017.01.008

[2] G. Scarpati et al., J. Energy Storage 102 (2024) 113934, https://doi.org/10.1016/j.est.2024.113934

[3] V.A. Yartys et al., Int. J. Hydrogen Energy 46 (2021) 35896–35909, https://doi.org/10.1016/j.ijhydene.2021.01.190

European Fuel Cells and Hydrogen
PIERO LUNGHI CONFERENCE
September 17th–19th 2025
Capri / Italy

Evaluating Off-Grid and On-Grid Hydrogen Supply Scenarios for Refueling Infrastructure Deployment in Southern Italy

M. Minutillo[a], S. Di Micco*[b], V. Finamore[b], P. De Falco [b], A. Bracale [b], P. Caramia [b]

* corresponding author: simona.dimicco@uniparthenope.it

[a] Department of Industrial Engineering, University of Salerno, Fisciano, Italy
[b] Department of Engineering, University of Naples "Parthenope", Naples, Italy

Keywords: sustainable mobility, hydrogen refueling station, renewable source, hydrogen cost

Abstract:

The study is devoted at evaluating the techno-economic performance of hydrogen refueling stations (HRSs) in off-grid and on-grid configurations.

Introduction: Fuel Cell Electric Vehicles (FCEVs) represent a promising option for supporting the sustainable mobility. Their penetration in the market is limited by the lack of adequate infrastructures. Therefore, the development of HRSs plays a fundamental role in the potential transition towards the hydrogen mobility [1].

Objectives: This study is focused on the design and sizing of two HRSs, in off-grid and on-grid configurations, as well as on the assessment of the levelized cost of hydrogen (LCOH). The HRSs are designed to deliver 180 kg/day of H_2.

Material and methods: The analysis is performed by using a numerical algorithm developed in Matlab environment. The proposed HRS configurations are illustrated in Fig. 1.

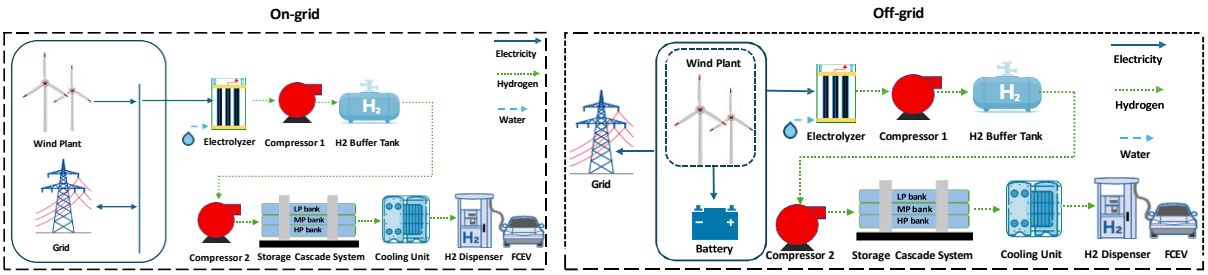


Figure 1: General layout of the HRS

In the off-grid configuration, H_2 is produced on-site by using an electrolysis unit powered by electricity from a Wind farm (WT) integrated with a battery system, while the grid connection is conceived just to discharge the energy excess. On the other hand, in the on-grid configuration, the electrolyzer is supplied by the electricity from WT and from the grid when

the WT power production is not enough to meet the H_2 daily demand. For both configurations, a sensitivity analysis is performed by analyzing several scenarios differing in terms of components' size and, as a consequence, in terms of energy share among WT, battery and grid. According to these scenarios, the optimal configuration is identified as the one that assures the minimum LCOH. This economic parameter is calculated as:

$$LCOH = \frac{CRF \cdot [CAPEX + \sum_{n=0}^{N-1}(C_{O\&M_an,n} + C_{rep_an,n=t} - R_{O_2_an,n} - R_{EL_an,n})]}{m_{H_2}} \quad (1)$$

Where $CAPEX$, $C_{O\&M}$, C_{rep} and R are the investment costs, the operating and maintenance costs, the replacement cost and the revenues (due to the oxygen and electricity selling), respectively and m_{H_2} is the annual hydrogen production. The subscript "an" means that the costs are calculated as annualized costs (they are calculated by considering the nominal discount rate and an inflation rate) [2]. The analysis considers a plant lifetime (N) of 20 years.

Results: Table 1 illustrates the results for the considered configurations. In the off-grid configuration, a 4.2 MW WT plant is needed, coupled with a battery system of 3.5 MWh and with a H_2 storage system of 1000 kg. As concern the on-grid configuration, a WT farm of 3 MW and a H_2 storage system of 490 kg are needed. Table 2 lists the cost items for each component of the HRSs. The prices for water and electricity purchase are assumed equal to 2 €/m³ and 150 €/MWh, respectively. For the revenues, 0.17 €/kg and 50 €/MWh are considered as the prices for oxygen and electricity. The WT sizes for both configurations are chosen for assuring the same annual electricity supplied to the electrolyzer. It is clearly depicted in Fig.2, in which the percentages of WT utilization for the HRS are almost the same (45% vs 40%). It is worth noticing that for the off-grid configuration, for assuring the daily H2 production compression and storage, an oversize of the WT system is needed, which involves having a higher percentage of electricity diverted to the grid compared to the amount used in the HRS (55% vs 45%); it implies, as a consequence, a higher investment cost that affects the LCOH, calculated equal to 9.10 €/kg. At the same way, for the on-grid configuration, the choice of using the same WT percentage utilization for the HRS, involves having an oversize of the WT system and, as a consequence, a higher percentage of electricity diverted to the grid (60%). In this case, the LCOH is equal to 5.2 €/kg.

Table 1: Technical results for the off-grid and on-grid configurations

Components	Off-grid	On-grid
WT[MW]	4.2	3.0
Electrolysis unit [MW]	1.3	0.95
Battery [MWh]	3.5	-
H2 storage [kg]	1000	490
Compressor 1, Compressor 2 [kW]	8.6; 3.7	8.6; 3.7
Cooling unit [kW]	16.3	16.3
WT electricity production [MWh/year]	9908.0	7044.0

Table 2: Costs items for each components of the HRSs

Components	Units	C_{FC}	$C_{O\&M}$	C_{rep}
Wind turbine	€/kW	1110	2.5% CFC	-
Electrolyzer	€/kW	1094	3.8% CFC	40% CFC
Battery	€/kWh	463	3% CFC	CFC
Compressor	€	$43872 \cdot (P_c)^{0.5861}$	2% CFC	CFC
H2 storage LP	€/kg	1360	-	-
H2 storage MP	€/kg	1632	-	-
H2 storage HP	€/kg	2448	-	-
Cooling unit	€/kW	6071	3% CFC	CFC
Dispenser	€/kg	$350 \cdot m_{H_2,daily}$	0.5% CFC	CFC

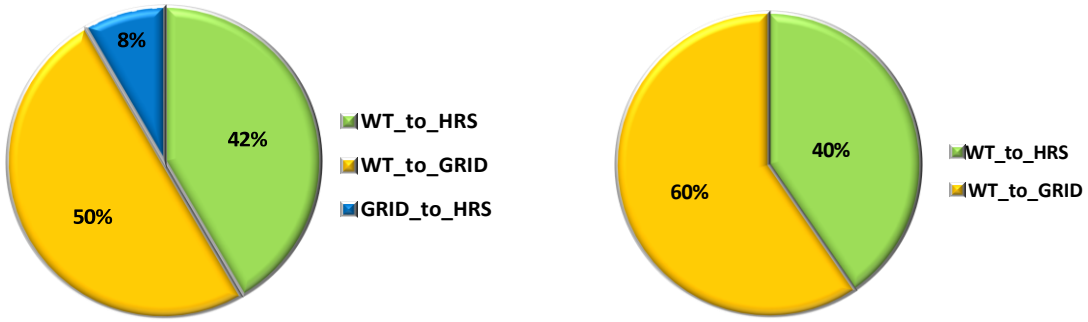


Figure 2: Electricity share in the HRS for the off-grid and on-grid configuration

Conclusions: As expected, the proposed off-grid HRS is less competitive with respect to the on-grid configuration. It is due to the lower investment cost and about the same revenues for the electricity sold. However, by applying a different strategy for the on grid configuration, considering to have, for example, the same annual amount of electricity purchase and sell to the grid, the LCOH increases to 6.27 €/kg. Therefore, with an incentive policy for the green H2 production, the LCOH for the off-grid configuration will decrease and so, become competitive with respect to the off-grid one.

Acknowledgment

This study was carried out within the MOST – Sustainable Mobility National Research Center and received funding from the European Union Next-Generation EU (PIANO NAZIONALE DI RIPRESA E RESILIENZA (PNRR) – MISSIONE 4 COMPONENTE 2, INVESTIMENTO 1.4 – D.D. 1033 17/06/2022, CN00000023). This manuscript reflects only the authors' views and opinions, neither the European Union nor the European Commission can be considered responsible for them.

References

[1] Cristina Blazquez-Diaz. Techno-economic modelling and analysis of hydrogen fuelling stations. International journal of hydrogen energy 44 (2019) 495-51

[2] A. Perna et al. "Designing, sizing and economic feasibility of a green hydrogen supply chain for maritime transportation," *Energy Convers Manag*, 278, 2023, doi: 10.1016/j.enconman.2023.116702.

European Fuel Cells and Hydrogen
PIERO LUNGHI CONFERENCE
EFCH2 2025
September 17th–19th 2025
Capri / Italy

Multiphysics Numerical Modelling of Hydrogen-Refuelling-Station Components under Consecutive Dispensing Scenario

M. Genovese[a], F. Piraino *[a], L. Andaloro [b], I. Belviso[b], N. Alessi[b], L. Pagnotta[a] , P. Fragiacomo[a]

* corresponding author: francesco.piraino@unical.it

[a] Department of Mechanical, Energy and Management Engineering, University of Calabria, Arcavacata di Rende, 87036 Cosenza, Italy

[b] National Research Council of Italy, Institute of Advanced Energy Technologies, Via Salita S. Lucia Sopra Contesse, 5, 98126, Messina, Italy

Keywords: dynamic simulation, hydrogen refuelling station, multiphysics modelling, validation

Abstract

Large road-freight operators are beginning to adopt fuel-cell electric trucks, yet the hydrogen refuelling infrastructure that exists today was optimised for light-duty passenger cars. Heavy-duty vehicles (HDVs) require 5- to 10-times higher mass flow-rates, longer duty-cycles and often different pressure paradigms (350 bar nominal delivery with buffers up to 500 bar). The Italian research project SaFE H2D addresses this gap through a multi-physics, dynamic simulation framework and an iterative validation campaign that links component-level models to full-station operation. This paper summarises the project rationale, modelling approach, validation results to date, and the implications for next-generation hydrogen refuelling stations (HRSs) that can safely deliver more than 100 g s^{-1} at acceptable temperature rise during back-to-back (B2B) truck fills.

Introduction

Hydrogen mobility is scaling from pilot fleets to nationwide deployment, making the reliability, safety and cost of HRS hardware pivotal. Experimental optimisation alone is costly; therefore, high-fidelity numerical models able to predict coupled thermo-fluid phenomena across the entire station are crucial. Early station studies focused on isolated vehicle tanks or simplified lumped-parameter lines. Ebne-Abbasi *et al. [1]* developed the first CFD model covering the complete dispenser line, yet validation was limited to a single light-duty fill. Zhao *et al.* extended the domain to include the pre-cooler, demonstrating the importance of conjugate heat-transfer coefficients [2]. Dynamic network models have since captured multi-component interactions with markedly lower computational cost, enabling parameter sweeps for compressor staging and storage cascade layouts [3]. More recently, Poudel *et al.* analysed techno-economic trade-offs in pre-cooling units for heavy-duty protocols [4], while He *et al.* modelled flash-boiling losses during rapid pressure ramps [5]. Although these studies

advance understanding, most cover single fills; few address consecutive, high-throughput scenarios that dominate commercial forecourt duty cycles. Standards provide only partial guidance. SAE J2601-3 [6] extends the well-known light-duty protocol to industrial trucks but still caps the *Category D* flow at 70 g s^{-1}, acknowledging the lack of validated precooling data beyond that threshold. European projects such as PRHYDE and a recent NREL campaign demonstrated controlled fills at 100 g s^{-1} into 80 kWh truck tanks, confirming the practical need for new control strategies [7–9]. Against this backdrop, SaFE H2D sets out to: (i) create high-fidelity digital twins of an HDV-capable HRS, (ii) design scalable station architectures that respect safety envelopes, and (iii) perform B2B refuelling at 350 bar and 500 bar storage levels.

Objectives

1. Develop a transient, multiphysics numerical model of the principal HRS subsystems (storage, compressor, chiller, dispenser).
2. Analyse pressure-management and thermal-control challenges during three consecutive vehicle fills.

Material and methods

One-dimensional network couples the conservation equations for mass, momentum and energy with an equation-of-state for high-pressure hydrogen. Compressors are represented by dynamic performance maps; the chiller is treated with a finite-volume wall model linking refrigerant and hydrogen streams. Real-gas viscosity and thermal conductivity correlations are implemented. Station parameters reflect a commercial facility: three ASME Type-IV storage banks (45 °C initial, 40 kg total), a three-stage diaphragm compressor (max 90 g s^{-1}), a -40 °C glycol pre-cooler and SAE J2601-compliant nozzle.

Results

Multiphysics and dynamic models of the main components of hydrogen refuelling stations (HRS) were developed, focusing on their interaction during refuelling processes. These models incorporate the thermodynamic, fluid dynamic, and heat transfer phenomena to simulate real-world refuelling scenarios accurately. The outcomes provide a foundation for simulating operational behaviors, ensuring safety, and investigating refuelling processes for both standard and heavy-duty vehicles.

Conclusions

Within the activity 3.1, the objective was to develop advanced numerical models that accurately simulate the dynamic behavior of key HRS components under various operational

conditions. This objective was fully realized through the creation of comprehensive multiphysics models, which incorporate thermodynamic, fluid dynamic, and heat transfer phenomena. These models enable detailed analysis of hydrogen cascading, compression, pre-cooling, and dispensing processes. The incorporation of real-gas behavior at high pressures, precise temperature rises predictions during compression, and an enhanced pre-cooling simulation contributed to achieving highly accurate and reliable models.

Acknowledgment

This work is part of the SaFE H2D: Safe, Fast and Efficient Hydrogen Refuelling for Heavy-Duty Vehicles; project, funded under the National Recovery and Resilience Plan (PNRR) - Mission 4 - Component 2 - Investment 1.1, within the framework of the National Research Program and Projects of Significant National Interest (PRIN) - PRIN 2022 PNRR, under project reference CUP H53D23008740001 P2022YHME9.

References

[1] Ebne-Abbasi H, Makarov D, Molkov V. CFD model of refuelling through the entire equipment of a hydrogen refuelling station. Int J Hydrogen Energy 2024;53:200–7. https://doi.org/https://doi.org/10.1016/j.ijhydene.2023.12.056.

[2] Zhao L, Liu Y, Yang J, Zhao Y, Zheng J, Bie H, et al. Numerical simulation of temperature rise within hydrogen vehicle cylinder during refueling. Int J Hydrogen Energy 2010;35:8092–100. https://doi.org/https://doi.org/10.1016/j.ijhydene.2010.01.027.

[3] Ren S, Jia X, Wang S, He P, Zhang S, Peng X. Creation and validation of a dynamic simulation method for the whole process of a hydrogen refueling station. J Energy Storage 2024;82:110508. https://doi.org/10.1016/j.est.2024.110508.

[4] Poudel S, Tun H, Reddi K, Elgowainy A. Investigation of precooling unit design options in hydrogen refueling station for heavy-duty fuel-cell electric vehicles. Int J Hydrogen Energy 2024;61:493–502. https://doi.org/10.1016/j.ijhydene.2024.02.197.

[5] Yang X, Wang W, Wang Z, Ma F. Simulation of pre-cooling in a high pressure hydrogen refueling station for operation optimization. Int J Hydrogen Energy 2024;86:434–44. https://doi.org/10.1016/j.ijhydene.2024.04.064.

[6] SAE MOBILUS. J2601/3_202209 Fueling Protocol for Gaseous Hydrogen Powered Industrial Trucks 2022.

[7] NREL. Fast Flow Future for Heavy-Duty Hydrogen Trucks 2022. https://www.nrel.gov/news/program/2022/fast-flow-future-heavy-duty-hydrogen-trucks.html?utm_source=chatgpt.com (accessed April 23, 2025).

[8] PRHYDE project on heavy-duty hydrogen refueling protocol. Fuel Cells Bulletin 2020;2020:8–9. https://doi.org/https://doi.org/10.1016/S1464-2859(20)30112-7.

[9] H2Mobility. Overview Hydrogen Refuelling For Heavy Duty Vehicles. 2022.

European Fuel Cells and Hydrogen
PIERO LUNGHI CONFERENCE
EFCH2 2025
September 17th–19th 2025
Capri / Italy

Technical and Economic Optimization Study of the Sizing and Operation of Key Components in Hydrogen Refueling Stations (HRS)

F. Piraino[a], M. Genovese*[a], M. Della Pietra[b], V. Cigolotti[b], O. Corigliano[a], M. Martorelli[a], G. Florio[a], P. Fragiacomo [a]

* corresponding author: matteo.genovese@unical.it

[a] Department of Mechanical, Energy and Management Engineering, University of Calabria, Arcavacata di Rende, 87036 Cosenza, Italy

[b] ENEA - Italian National Agency for New Technologies, Energy and Sustainable Economic Development, Via Anguillarese 301, Rome, 00123, Italy

Keywords: component sizing, energy efficiency, hydrogen refueling station, techno-economic optimization

Abstract

As hydrogen becomes a key vector in the decarbonization of mobility and industrial processes, Hydrogen Refueling Stations (HRS) must be designed to deliver fuel safely, efficiently, and at a competitive cost. Proper sizing and configuration of core components—electrolyzers, compressors, storage systems, and dispensers—directly affect the performance and cost-effectiveness of HRS infrastructure. This study, conducted within the scope of the POR H2 – ENEA project (WP2.4 – LA2.4.1_A), explores the techno-economic optimization of HRS component sizing to minimize hydrogen shortfall and energy consumption while evaluating investment and operational costs.

Introduction

Recent studies have examined the optimal design of hydrogen refueling stations (HRS) by balancing component sizing, capital costs, and energy efficiency. A key challenge is sizing electrolyzers and storage to meet demand at lowest cost. Caponi et al. (2024) developed an optimization algorithm for a scalable on-site HRS serving a fleet of fuel cell buses, focusing on minimizing LCOH by tuning electrolyzer capacity and utilization [1]. They found that increasing the hydrogen demand (from 2 to 30 buses) allows higher electrolyzer utilization, dropping LCOH from about 12 €/kg to 10.2 €/kg for the best-case configuration. However, even at ~10 €/kg, such on-site green hydrogen remained marginally cost-competitive; the study concluded that significant reductions in electricity price and electrolyzer capital cost (on the

order of 50%) would be needed to make fuel-cell bus refueling economically competitive at scale. This highlights the importance of both component cost reductions and smart sizing in improving HRS economics. Integrating renewable energy can further enhance HRS sustainability and reduce operating costs. Atabay and Devrim (2024) evaluated a solar-powered HRS with on-site photovoltaic (PV) generation supplying a dedicated electrolyzer [2]. Their techno-economic analysis demonstrated the feasibility of meeting a station's hydrogen demand with grid-connected PV, substantially reducing reliance on grid electricity. The solar-driven HRS achieved comparable refueling performance to conventional stations while lowering operational costs by leveraging free solar energy. The authors emphasize that careful dimensioning of PV capacity, electrolyzer, and storage is required to handle variability yet ensure refueling reliability. In a similar vein, Gökçek et al. (2024) explored optimal sizing of hybrid renewable power systems (wind+ PV) for on-site HRS in case studies from Turkey and Spain [3]. They used multi-parameter optimization to determine the ideal capacities of electrolyzers, storage tanks, and compressors that minimize hydrogen cost for given local wind/PV resource profiles. Their results show that an optimally sized hybrid system can produce hydrogen at a competitive cost (on the order of 5–8 €/kg, depending on location) while fully meeting daily refueling demands. These studies collectively highlight that proper dimensioning of each HRS component (production, compression, storage) in concert with renewable integration is crucial for maximizing energy efficiency and minimizing unit hydrogen cost. The literature indicates that techno-economic optimization of HRS design—spanning production method selection, component sizing, and energy management—can greatly improve performance. High efficiencies (over 70%) and LCOH below 7 €/kg are achievable in specific configurations today, and around 10 €/kg for green hydrogen at bus scales [1]. Further cost declines in electrolyzers and electricity (or increased use of on-site renewables) will be needed to approach parity with conventional fuels. Strategies like leveraging off-peak power and right-sizing equipment to match demand are consistently recommended to enhance HRS energy efficiency and economics.

Objectives

The main objectives of this work are:

- To model key HRS components using engineering and economic parameters.
- To simulate hydrogen production, storage, and refueling under realistic daily demand profiles.
- To identify optimal design parameters (electrolyzer capacity, tank volume, pressure rating) that minimize hydrogen shortage and maximize energy efficiency.
- To evaluate the impact of sizing decisions on the levelized cost of hydrogen (LCOH) and operational viability.

Results

A simulation environment was developed in MATLAB to replicate a 24-hour operational cycle of a modular HRS. Refueling profiles were derived for various use cases (public access, industrial fleets, transit buses) based on literature and field data. The system model includes electrolyzer performance curves, storage tank thermodynamics, and compressor energy consumption. An optimization function (fgoalattain) was applied to explore trade-offs between energy efficiency (kg/kWh) and hydrogen shortfall (kg/day). Multiple scenarios were tested by varying daily hydrogen demand, load factors, and energy prices. Component capital and operational costs were estimated using recent industry benchmarks.

Conclusions

Smart sizing of HRS components leads to improved energy performance and cost reductions without compromising service availability. The developed model proves effective for evaluating design trade-offs and supports decision-making in early-stage planning of HRS infrastructure. Integration with renewable energy and dynamic operation strategies can further enhance economic and environmental performance.

Acknowledgment

This research was funded by the European Union – NextGenerationEU through the Italian Ministry of Environment and Energy Security under the POR H2 project, in collaboration with ENEA, CNR, and RSE, within the PNRR – Mission 2, Component 2, Investment 3.5 "Research and Development on Hydrogen", CUP: I83C22001170006.

References

[1] Caponi, R., Bocci, E., & Del Zotto, L. (2024). On-site hydrogen refuelling station techno-economic model for a fleet of fuel cell buses. *International Journal of Hydrogen Energy, 71*, 691–700. https://doi.org/10.1016/j.ijhydene.2024.05.216

[2] Atabay, R., & Devrim, Y. (2024). Design and techno-economic analysis of solar energy based on-site hydrogen refueling station. *International Journal of Hydrogen Energy, 80*, 151–160. https://doi.org/10.1016/j.ijhydene.2024.07.166

[3] Gökçek, M., Paltrinieri, N., Liu, Y., Badia, E., Dokuz, A.Ş., Erdoğmuş, A., et al. (2024). Optimum sizing of hybrid renewable power systems for on-site hydrogen refuelling stations: Case studies from Türkiye and Spain. *International Journal of Hydrogen Energy, 59*, 715–729. https://doi.org/10.1016/j.ijhydene.2024.02.068

European Fuel Cells and Hydrogen
PIERO LUNGHI CONFERENCE
EFCH2 2025
September 17th–19th 2025
Capri / Italy

Development of Operational Optimization Models for Key Components in Hydrogen Refueling Stations (HRS)

M. Genovese[a], F. Piraino*[a], V. Cigolotti[b], M. Della Pietra[b],P. Fragiacomo [a]

* corresponding author: francesco.piraino@unical.it

[a] Department of Mechanical, Energy and Management Engineering, University of Calabria, Arcavacata di Rende, 87036 Cosenza, Italy

[b] ENEA - Italian National Agency for New Technologies, Energy and Sustainable Economic Development, Via Anguillarese 301, Rome, 00123, Italy

Keywords: hydrogen demand forecasting, HRS control, multi-objective optimization, refueling station operation

Abstract

As hydrogen infrastructure expands to meet transportation decarbonization targets, the efficient operation of Hydrogen Refueling Stations (HRS) becomes essential to maximize service reliability and minimize operational costs. Variability in hydrogen demand, electricity pricing, and component dynamics presents challenges that static scheduling cannot adequately address. This research, conducted within the scope of the POR H2 – ENEA project (WP2.4 – LA2.4.1_B), focuses on the development and validation of operational models for HRS, incorporating real-time control, demand profiling, and multi-objective optimization strategies.

Introduction

Beyond design, researchers have focused on optimizing the operation of HRS in real-time to handle dynamic demand and energy price fluctuations. One line of work uses predictive scheduling to minimize operating cost. Sun et al. (2022) formulated an optimized operation plan for an on-site HRS with electrolytic hydrogen production, aiming to produce hydrogen during low-cost electricity periods and store it for later use [1]. By coordinating electrolyzer and storage operation with time-of-use power tariffs, their model reduced overall hydrogen cost. Building on this, Lu et al. (2023) introduced a demand-responsive optimization algorithm for HRS operations that incorporates predictive modeling of hydrogen consumption [2]. The optimized strategy exploited peak–valley electricity price differences, cutting the unit hydrogen cost relative to a static operation. Notably, Lu et al. report that their approach allowed a smaller electrolyzer and storage size to suffice for the same demand, by smartly scheduling production when power is cheapest – effectively reducing required rated

capacities while still meeting all refueling needs [2]. Another important research direction is the development of advanced control strategies (often multi-objective and model-predictive) to manage HRS operations under uncertainty. Cardona et al. (2023) designed a model predictive control (MPC) system for a solar-powered HRS in Zaragoza that serves light-duty vehicles, buses, and trailer filling [3]. Their MPC approach performs a weighted multi-objective optimization in real time, managing power flows between a PV array, grid electricity, a battery, and hydrogen equipment (electrolyzer, compressors, buffers). The controller simultaneously satisfies hydrogen demand and operational constraints while optimizing economic objectives. Handling uncertainty in demand and energy markets is a key focus of modern HRS control strategies. Abdelghany et al. (2024) proposed a resilient stochastic scheduling approach for HRS operation under uncertain hydrogen demand and renewable output [4]. They considered an HRS powered by renewables and backed by grid hydrogen purchases or sales ("hydrogen market"), with multiple storage tanks to enable parallel refueling of vehicles. Using a scenario-based MPC framework with relaxed integer constraints, their controller optimizes hydrogen production, storage, and dispensing to minimize cost and maximize revenue while respecting all system. Simulations showed the strategy could meet all refueling needs and maintain safety constraints, all while substantially reducing operating costs [4]. Advanced control schemes, especially MPC-based, enable multi-objective optimization – for example, meeting fuel demand, minimizing energy cost, and limiting equipment wear simultaneously. These strategies improve resilience to uncertainty and can integrate HRS into energy networks (buying/selling hydrogen or providing grid services). As hydrogen infrastructure scales up, such dynamic and predictive operational optimizations will be as important as upfront station design in ensuring economic and reliable refueling service.

Objectives

The main goals of this study are:

- To implement dynamic modeling of electrolyzers, compressors, and storage units for hourly operations.
- To forecast hydrogen demand based on user behavior and refueling patterns.
- To design a simulation-based optimization routine capable of minimizing hydrogen shortfall and energy cost.
- To explore the benefits of predictive operation and control algorithms, including model predictive control (MPC) and demand-responsive dispatching.

Results

An HRS simulation environment was developed in MATLAB to emulate 24-hour operations. Hydrogen demand was modeled for different use cases (public access, fleet vehicles, logistics) using historical refueling data and statistical probability distributions. The system's core

components were represented by parameterized classes (electrolyzer, storage, compressors), allowing flexibility in operational scenarios.

A composite cost function, combining energy efficiency and hydrogen availability, was optimized using MATLAB's fgoalattain solver. Control strategies included static dispatch, price-based scheduling, and look-ahead predictive operation. Multiple configurations were simulated to evaluate trade-offs between equipment usage, energy consumption, and unmet hydrogen demand.

Conclusions

Predictive and demand-responsive operation significantly enhance the efficiency and economic performance of HRS. By forecasting usage and aligning production with electricity pricing, operators can reduce both energy cost and equipment wear. The use of model predictive control enables HRS to become more adaptive and grid-aware, particularly in contexts with variable renewable generation. These operational improvements complement physical sizing strategies and are vital for scalable hydrogen infrastructure deployment.

Acknowledgment

This research was funded by the European Union – NextGenerationEU through the Italian Ministry of Environment and Energy Security under the POR H2 project, in collaboration with ENEA, CNR, and RSE, within the PNRR – Mission 2, Component 2, Investment 3.5 "Research and Development on Hydrogen", CUP: I83C22001170006.

References

[1] Sun, J., Peng, Y., Lu, D., Chen, X., Xu, W., Weng, L., & Wu, J. (2022). Optimized configuration and operating plan for hydrogen refueling station with on-site electrolytic production. *Energies, 15*(7), 2348. https://doi.org/10.3390/en15072348

[2] Lu, D., Sun, J., Peng, Y., & Chen, X. (2023). Optimized operation plan for hydrogen refueling station with on-site electrolytic production. *Sustainability, 15*(1), 347. https://doi.org/10.3390/su15010347

[3] Cardona, P., Costa-Castelló, R., Roda, V., Carroquino, J., Valiño, L., & Serra, M. (2023). Model predictive control of an on-site green hydrogen production and refuelling station. *International Journal of Hydrogen Energy, 48*(47), 17995–18010. https://doi.org/10.1016/j.ijhydene.2023.01.191

[4] Abdelghany, M.B., Al-Durra, A., & Zeineldin, H. (2024). Optimizing resilient parallel refueling operations: Relaxed stochastic economic mobility scheduling for fuel cell vehicles with multiple hydrogen storage systems. *eTransportation*, 100393. https://doi.org/10.1016/j.etran.2024.100393

European Fuel Cells and Hydrogen
PIERO LUNGHI CONFERENCE
EFCH2 2025
September 17th–19th 2025
Capri / Italy

Cryogenic Storage Systems: state-of-the-art of Challenges and Preliminary Lab-Scale Numerical Model

Ronelly José De Souza[a], Mauro Reini[a], Rodolfo Taccani*[a]

*corresponding author: taccani@units.it
[a]*University of Trieste, Department of Engineering and Architecture, Trieste, Italy*

Keywords: Boil-Off Gas, Cryogenic Storage, Liquid Nitrogen, Numerical Modelling

Abstract:
Cryogenic fluids like LNG and renewable LH_2 play a key role in decarbonizing transport and hard-to-abate sectors, yet their use faces challenges such as Boil-Off Gas (BOG) losses during storage and transfer. Literature presents few studies addressing the modelling of these phenomena in lab-scale cryogenic storage systems. This work proposes a preliminary numerical model simulating BOG dynamics and liquid transfer in a lab-scale setup using liquid nitrogen (LN2). Initial results show good agreement with expected system behaviour. Future efforts will focus on experimentally validating the model through dedicated lab tests.

Introduction: The use of cryogenic fluids, such as Liquefied Natural Gas (LNG) and liquid hydrogen from renewable sources (LH2), is crucial in the decarbonisation pathway, particularly in hard-to-abate sectors and in the energy-intensive transport sector. However, the use of cryogenic fluids still involves significant critical issues: fluid transfer, tank filling, heat loss in systems and the resulting Boil-Off Gas (BOG) can lead to significant fuel loss [1,2]. A significant contribution to the improvement of these issues can come from the development of numerical simulation models validated by experimental data.
The main strategies for reducing BOG losses in cryogenic systems are normally the following [1,3]: (i) re-liquefaction, which involves converting the BOG back into the liquid phase using a refrigeration cycle, (ii) increasing the reservoir pressure, and (iii) improving thermal insulation through the use of advanced materials. Cryogenic fluid transport also presents critical issues in pipeline transfer, for example, in terms of heat transfer, pipeline cooling and flushing, and component selection [4].

Objectives: Providing a brief state-of-the-art about the main issues regarding cryogenic storage systems and presenting a preliminary thermodynamic numerical model of a lab-scale cryogenic plant to represent the processes involved in the BOG phenomenon and the liquid transfer between cryogenic storage tanks.

Material and methods: The model has been developed by using Aspen HYSYS software, version 11, and is based on the flowsheet presented in Figure 1. The initial boundary conditions that have been used are provided through Table 1.

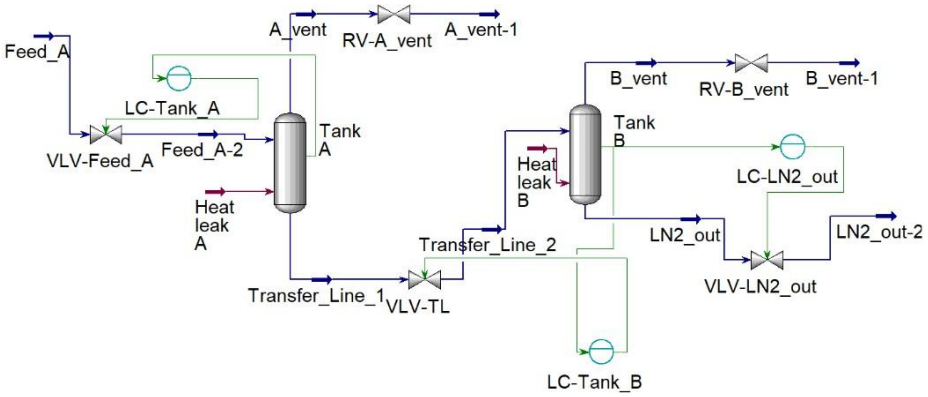
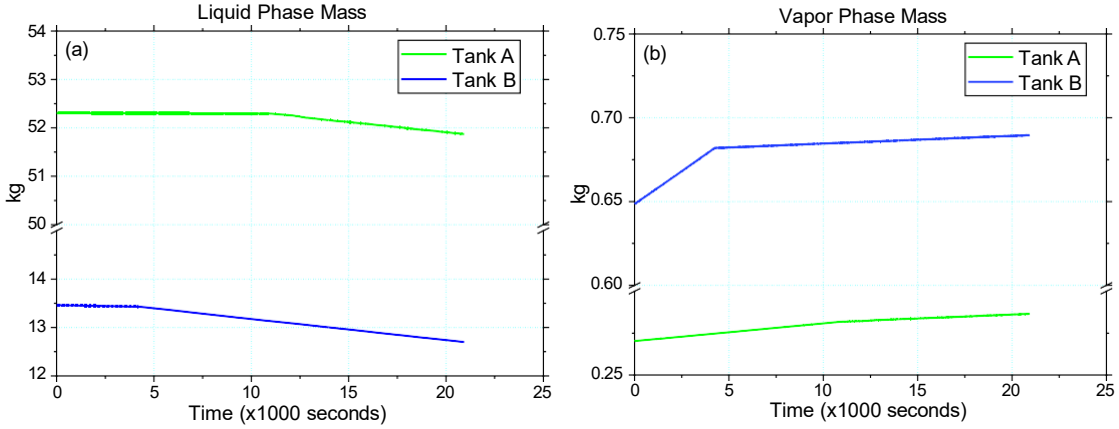


Figure 1. Flowsheet of the model in Aspen HYSYS V11.

Table 1. Initial boundary conditions defined in the Aspen model.

Stream	A_vent	B_vent	A_vent-1	B_vent-1	Transfer_Line_1	Transfer_Line_2	Feed_A	Feed_A-2	LN2_out	LN2_out-2
Vapour Fraction	1	1	1	1	0	0	0	0	0	1
Temper. [°C]	-187	-185	-180	-180	-195	-194	-196	-195	-194	-180
Pressure [kPa]	190	180	101.325	101.325	200	190	250	200	190	101.3

Results: According to the state-of-the-art, few studies in the literature combine numerical model development with experimental validation, particularly for lab-scale cryogenic storage systems. This work have addressed that gap by focusing on the preliminary phase of the study, i.e., developing a numerical model and evaluating its initial performance. Figure 2 presents some of the main results obtained through the simulation of the model presented on Figure 1. It is possible to observe a behaviour in agreement with it is expected from a typical cryogenic plant: relief valves start to open as soon as the cryogenic tanks reach the set pressure and the vapour phase mass starts rising while the liquid phase mass decreases, which is a consequence of the heat leakage into the tanks.



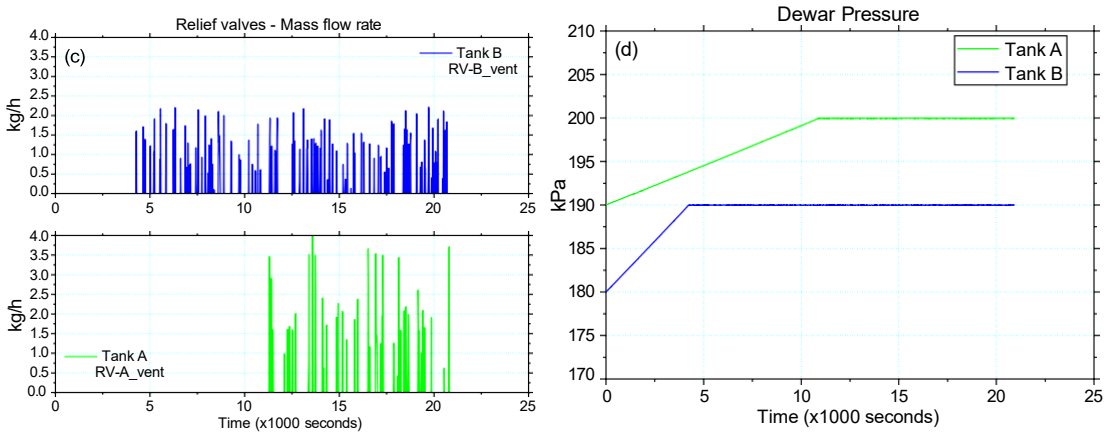


Figure 2. Preliminary results obtained from the cryogenic storage plant modelled in Aspen. Figures (a) and (b) present, respectively, the mass variation on the liquid and vapour phases.

Figure (c) shows the relief valves behaviour when the tanks reach the pressure set point, while figure (d) provides the tanks pressure variation.

Conclusions: This study presents a preliminary numerical model for simulating BOG dynamics and liquid transfer in lab-scale cryogenic systems. Initial results align with expected behaviour, supporting the model's validity. Future work will focus on experimental validation with liquid nitrogen to enhance accuracy and support practical applications in cryogenic system design.

Acknowledgment

This work has been developed within the CRYODESIGN project, which is funded by the PNRR project Mission 4, Component 2, Investment 1.3, Spoke 5 NEST Program – Network 4 Energy Sustainable Transition – CUP: D43C22003090001.

References

[1] Morales-Ospino R, Celzard A, Fierro V. Strategies to recover and minimize boil-off losses during liquid hydrogen storage. Renewable and Sustainable Energy Reviews 2023;182:113360. https://doi.org/10.1016/j.rser.2023.113360.

[2] Kalikatzarakis M, Theotokatos G, Coraddu A, Sayan P, Wong SY. Model based analysis of the boil-off gas management and control for LNG fuelled vessels. Energy 2022;251:123872. https://doi.org/10.1016/j.energy.2022.123872.

[3] Zuo Z, Zhu W, Huang Y, Wang L, Tong L. A review of cryogenic quasi-steady liquid-vapor phase change: Theories, models, and state-of-the-art applications. Int J Heat Mass Transf 2023;205:123916. https://doi.org/10.1016/j.ijheatmasstransfer.2023.123916.

[4] Deng BC, Yang SQ, Xie XJ, Wang YL, Pan W, Li Q, et al. Thermal performance assessment of cryogenic transfer line with support and multilayer insulation for cryogenic fluid. Appl Energy 2019;250:895–903. https://doi.org/10.1016/j.apenergy.2019.05.025.

European Fuel Cells and Hydrogen
PIERO LUNGHI CONFERENCE
September 17th–19th 2025
Capri / Italy

Last-mile delivery of H2 to Airports: A Schiphol case study

Espen Flo Bødal*[a], Ida Hjorth [a]

* corresponding author: Espen Flo Bødal
[a] SINTEF Energy Research

Keywords: Hydrogen supply-chain, Energy system modelling, liquefaction, truck transport

Abstract

Hydrogen may be incorporated at airports in moderate amounts (a few tonnes per day) in the near-to-medium term, and massive amounts (several hundred tonnes per day) [1] in the long term. The timescale and volumes of these scenarios puts airports in a follower-position when it comes to the supply of hydrogen. As the energy system and hydrogen market are at the start of a deep transformation, the planning of value chains for hydrogen supply to airports should be made in the context of the energy transition. To identify the suitable value chains in this uncertain landscape, we employ energy system modelling and optimization. Emphasis is put on development of truck transport representation in this framework, as truck transport is relevant in the near term. Preliminary results show how significant amounts of storage is needed both for liquid and gaseous hydrogen, when truck is the preferred mode of H_2-supply.

Introduction:

Many airports have committed to reaching zero emissions from own operations by 2030. Heavy duty ground operations are candidates for hydrogen-electric technologies. As several solutions are being demonstrated in the operational environment, airports are close to investment decisions and may incorporate hydrogen in the near term.

In the long term, aircraft may also be powered by hydrogen. Entry into service is disputed, but 2035 is the target for commercially relevant platforms. Scenario for hydrogen needs, particularly for direct use as an aviation fuel, vary significantly. Ground operations may require moderate amounts of hydrogen, at least compared to the hydrogen required for SAF-production, or as an aircraft fuel directly.

Policies/incentives and the total cost of ownership will determine the roll-out of hydrogen solutions in ground operations. This is strongly influenced by the cost and availability of hydrogen, which is strongly linked to the evolution in the European energy system.

Several studies have been performed to provide scenarios for scale and cost of the future of hydrogen systems. The first movers within green hydrogen end-use are refineries and industrial processes that currently use grey hydrogen. Aviation is likely to incorporate

hydrogen as a follower, piggybacking on emerging value chains [2]. Therefore, the study of hydrogen value chains for airports must be conducted within the context of the development of the energy system and merchant hydrogen market. Both are at the start of the deep transformation needed to reach climate targets, which causes great uncertainty in the planning of value chains.

For the Amsterdam Airport Schiphol (AMS), planning the hydrogen supply in the context if the energy system is particularly important, as the power demand at the airport is projected to grow from about 80 MW to 160 MW within ten years, and potentially 500 MW by 2050 or 2060, and the area has been identified as a "red zone" due to grid capacity limitation [3].

Objectives:

The objective of this study is to investigate the value chain for delivering hydrogen to an airport (AMS), both in liquid and gaseous form. An overall goal is improving the understanding of energy availability and scale effects on the value and distribution chain. To contextualize the value chain within a changing energy system, we employ energy system modelling for optimization of the last mile delivery. As last mile delivery of hydrogen, at least in initial phases, will rely of truck transport, this work will develop a new representation of truck transport that captures the dynamic characteristics of supply by truck, but is compliant with an energy system optimization model.

Material and methods:

We are developing an energy system model for the optimization of hydrogen value chains to Amsterdam airport. The energy system model is based on EnergyModelsX (EMX), a multi-energy-carrier model [4]. The model is modular and flexible which allows us to define new technologies without alteration to the fundamental model setup. Such modularity makes it easier to study the effect of new technology representations when modelling energy systems. This capability will be actively used to iterate the model set-up and boundary conditions.

The context of the energy system modelled is formulated with basis in the following:

- Scenario for investments in Dutch renewable energy and export capacity, as provided by the Ten-Year Network Development Plan [5]. We will dis-aggregate scenario to more granular regions, relevant for the AMS hydrogen value chains.
- Foreseen investments in hydrogen infrastructure, such as electrolysers and the European hydrogen backbone, as well as import capability. Value chain sensitivity to the availability of these facilities will be checked.

- Scenario for electricity and hydrogen prices as given by the ten-year network development plan. However, sensitivities and adjustments will be made to analyse potential local variations in production cost.

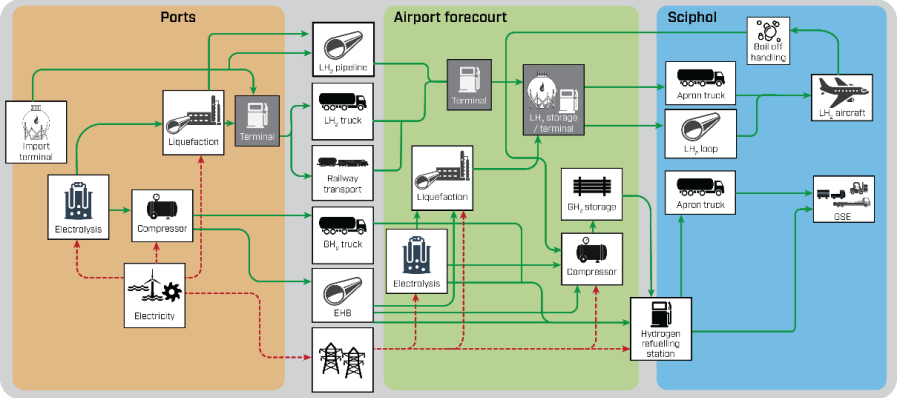


Figure 1: Technologies and value chains considered by the energy system model

New technology representations will be developed for the energy system model. In particular, truck-based transport of gaseous and liquid H_2: I) Trucks as mobile storages, II) dynamic supply as a function of transport-, loading- and unloading- durations. For truck transport of liquid hydrogen, we add the possibilities for boil-off.

Expected results and conclusions:

The work shall provide insight in future value chains, and understanding of sensitivities related to the energy system and other hydrogen demands. Preliminary results with simple truck models show how significant amounts of storage is needed both for liquid and gaseous hydrogen. We will investigate how a dynamic representation of truck transport within the energy system model impacts the value chain and potentially reduce the number of trucks required and needs for energy storage. The work will be used as input to the development of a roadmap for roll-out of hydrogen to airports.

Acknowledgment:

This work was supported by the TULIPS project (EU), Grant Agreement No. 101036996.

References:

[1] H. Krog, Y. Joos, H. Fyhn, P. Nekså, I. Hjorth, "Large-scale LH2 pipeline infrastructure concept for airports," [In *prep]*.

[2] D. van Dijk, H. Ebrahim, Y. Jooss, E. Bødal, I. Hjorth, "Integrating liquid hydrogen infrastructure at airports: Conclusions from an ecosystem approach at Rotterdam The Hague Airport," *J. Airpt. Manag.*, 2024.

[3] T. Baltus, "Schiphol, the energy transition, and the future of aviation," HyTEPS. Accessed: May 30, 2025. Available: https://hyteps.com/power-journal/schiphol-the-energy-transition-and-the-future-of-aviation/

[4] L. Hellemo, E. F. Bødal, S. E. Holm, D. Pinel, and J. Straus, "EnergyModelsX: Flexible Energy Systems Modelling withMultiple Dispatch," *J. Open Source Softw.*, vol. 9, no. 97, p. 6619, May 2024.

[5] ENTOG, "Download | ENTSOs TYNDP 2024 Scenarios." Accessed: May 30, 2025. [Online]. Available: https://2024.entsos-tyndp-scenarios.eu/download/

European Fuel Cells and Hydrogen
PIERO LUNGHI CONFERENCE
EFCH2 2025
September 17th–19th 2025
Capri / Italy

Assessment of Hydrogen Integration into the Italian Gas Transmission Network: Blending vs. Pure Hydrogen Transport

Marco Cavana*[a], Angelo Spadavecchia [a], Luisa Di Francesco [a], Pierluigi Leone [a]

* corresponding author: marco.cavana@polito.it
[a] Politecnico di Torino, Department of Energy "Galileo Ferraris"

Keywords: Decarbonization, Gas Network Simulation, Hydrogen Blending, Hydrogen Infrastructure

Abstract

Introduction: *The increasing demand for sustainable energy, combined with the gradual depletion of fossil fuel resources, is driving both the scientific community and the energy industry to seek environmentally friendly alternatives. In this scenario, hydrogen stands out as one of the most promising solutions for decarbonising sectors that are challenging to electrify. Its greenhouse gas mitigation characteristics and potential for long-term energy storage make it a key player in the transition toward a low-carbon future. However, establishing a large-scale hydrogen infrastructure requires thorough technical assessments, particularly regarding the potential role of pipeline transport solutions and the opportunities for repurposing the existing natural gas infrastructure.*

Objectives: *The central goal of this work is to analyse and support the transition of the Italian natural gas network to hydrogen, either through blending (mixing hydrogen with natural gas) or full hydrogen conversion. The study will focus on the Sicilian trunk of the transmission infrastructure as a main gate of the future SouthH2 Corridor. While most studies focus on material compatibility aspects, this study aims to evaluate the technical feasibility of blending and pure hydrogen transport, offering useful insights on operational performance and the strategic implications for a sustainable decarbonization of the energy system.*

Material and methods: *An own-developed fluidynamic multi-component and transient gas network model is used for the assessment of pipeline hydrogen transport under different scenarios. A commercial tool for energy network modelling and simulation is used to cross-validate results and ensure the robustness of the analysis* [1].

Results: *In the blending scenario, a gas mixture composed of 80% natural gas and 20% hydrogen (H_2) in volume was simulated, aiming to maintain the same energy transport capacity of approximately 1041 GWh/day. The objective was to evaluate the feasibility of integrating hydrogen into the existing natural gas infrastructure through partial blending.*
The simulation results highlighted several operational challenges. The most critical findings were:

- *Increased pressure drops across the network, resulting from the lower density and higher velocity of the gas mixture compared to natural gas only.*
- *Gas velocities reached approximately 21 m/s, which is close to the recommended operational limits for safe and stable pipeline operation.*

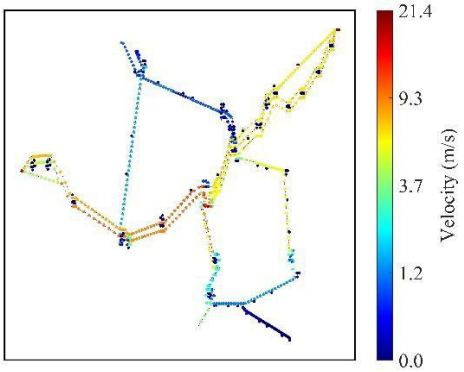


Figure 1 – Velocities in the Hydrogen Blending scenario

The pure hydrogen scenario assumes a configuration in which part of the existing pipeline infrastructure is repurposed for the transport of pure hydrogen. The hydrogen backbone simulation scenario is designed to carry 2.5 Mtpa, as defined in [2]. The system is developed in accordance with ASME B31.12, with a reduced operating pressure to mitigate the risk of hydrogen embrittlement, a critical safety concern in metallic pipelines under high pressure.
Meanwhile, the remaining natural gas network undergoes a reduction in imports via the Transmed pipeline in order to continue operating under the new system constraints.
Key findings include:

- *Due to hydrogen's lower density, flow velocities increase significantly, reaching up to 25 m/s, which introduces substantial challenges related to pipeline safety and vibrations.*
- *The reduced natural gas transmission system operates at its maximum allowable operating pressures, with gas inlet velocities at the Enna compression station reaching approximately 21 m/s, indicating high dynamic stress on the infrastructure. To limit the transmission capacity reduction, the system is also operated at the maximum allowable pressure.*

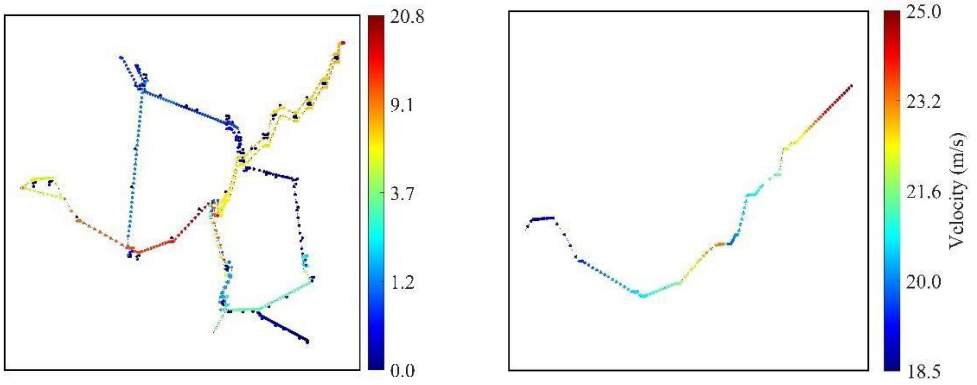


Figure 2 – Velocities in the Reduced Natural gas Network (left) and Hydrogen Backbone (right)

Conclusions: *Blending represents a promising approach to hydrogen integration, yet it brings notable operational challenges—particularly concerning pipeline velocity limits, which must be strictly controlled to ensure safe and efficient operation. Transitioning to a dedicated hydrogen backbone would require significant infrastructure modifications and thorough risk analysis to address issues such as material compatibility and pressure management. It is important to highlight that both options address different decarbonization needs: blending does not assume the presence of a specific demand for hydrogen, but rather serves to decarbonize the natural gas supply, promoting the starting up of green hydrogen production and supply. On the other hand, a hydrogen backbone is designed to meet a specific demand for hydrogen, whether it comes from the industrial sector and/or the transport sector, with a better valorization of the energy vector itself.*

Acknowledgments:

- *Part of this research has been carried out within the project funded under the National Recovery and Resilience Plan (NRRP), Mission 4 Component 2 Investment 1.3 - Call for tender No. 1561 of 11.10.2022 of Ministero dell'Università e della Ricerca (MUR) funded by the European Union – NextGenerationEU. Project code PE0000021, Concession Decree No. 1561 of 11.10.2022 adopted by Ministero dell'Università e della Ricerca (MUR), CUP E13C22001890001; Project title "Network 4 Energy Sustainable Transition – NEST".*
- *Part of this research has been developed the frame of SHIMMER. This project has received funding from the Clean Hydrogen Partnership under Grant Agreement No. 101111888. This partnership receives support from the European Union's Horizon Europe Research and Innovation program, Hydrogen Europe and Hydrogen Europe Research. Views and opinions expressed are however those of the authors only and do not necessarily reflect those of the European Union or the clean hydrogen joint undertaking.*

References

[1] Encoord, "SAInt - An Integrated Systems Modeling Platform," [Online]. Available: https://www.encoord.com/solutions/saint.

[2] https://www.south2corridor.net/

European Fuel Cells and Hydrogen
PIERO LUNGHI CONFERENCE
EFCH2 2025
September 17th–19th 2025
Capri / Italy

Study of a PCM-hydride Reactor

Paolo Proia*[a], Giovanni Erme [b], Mauro Sbragaglia [c] and Giacomo Falcucci [a, d]

* corresponding author: paolo.proia@uniroma2.it
[a] Dept. of Enterprise Engineering ''Mario Lucertini'', University of Rome ''Tor Vergata'', Via del Politecnico 1, 00133 Rome, Italy
[b] Dept. Civil and Mechanical Engineering, University of Cassino and Southern Lazio, Via di Biasio 43, 03043 Cassino, Italy
[c] Dept. of Physics & INFN, University of Rome ''Tor Vergata'', Via della Ricerca Scientifica 1, 00133, Rome, Italy.
[d] Dept. of Physics, Harvard University, 33 Oxford Street, 02138 Cambridge, Massachusetts, USA.

Keywords: Hydrides, Hydrogen, LBM, PCM

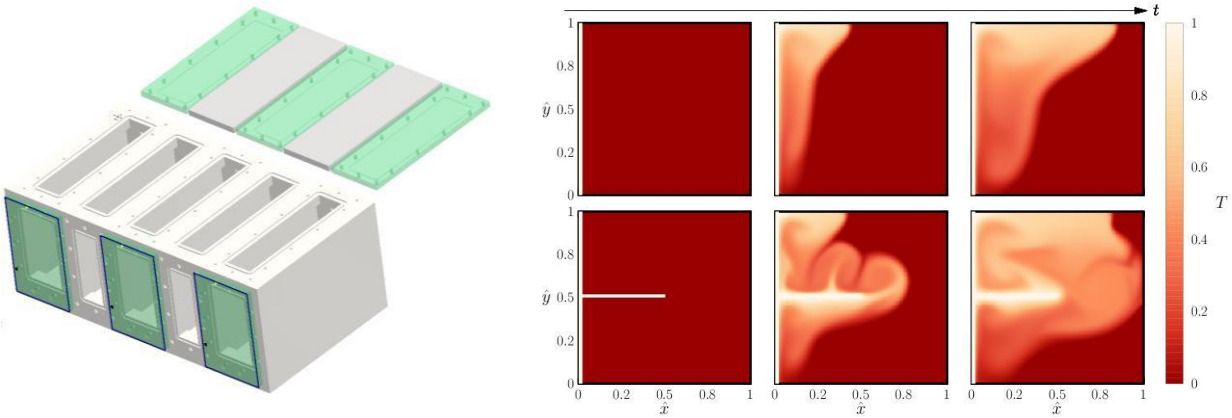
Abstract

Introduction: Metal Hydrides are one of the prominent ways of storing hydrogen in a space efficient and reliable manner [1]. They allow for easy operation, storing H_2 through an exothermic reversible adsorption reaction and releasing it via the inverse endothermic reaction. Thermal Energy Storage (TES) proves to be an effective tool for saving energy in the process, as the heat generated in the initial adsorption can be stored and then resupplied to the hydride to release the stored molecules. A promising approach is to use Phase Change Materials (PCMs) [2,3], thanks to their large latent heat can store heat at their phase change temperature, which remains constant and can be designed to be close to ambient temperature (Latent Thermal Energy Storage, LTES). This provides the benefits of simplifying system design and improving the efficiency of the hydride reactions by avoiding large temperature variations, while minimizing costs in upkeep and maintenance. The focus of this work is combining hydrides and PCMs to build a reactor prototype that can supply hydrogen to a small fuel cell, while validating and testing layouts with a coupled 3D thermal fluid dynamic simulation.

Objectives: The goal of this work is to discuss the results of a multi-dimensional model based on the Lattice Boltzmann Method (LBM) of an ad-hoc designed reactor for metal hydride H_2 storage. Such a reactor has been designed and realized in the LUCE (Laboratorio Universitario di Calcolo per l'Energia) Lab at the University of Rome ''Tor Vergata'' and it is characterized by the presence of multiple compartments, alternating metal hydride and PCM.

The simulations are realized with a Thermal LBM (TLBM) in-house developed platform: benchmark simulations are presented to validate the code. A digital copy of the reactor is imported in the solver, to study its performance in terms of hydrogen absorption/release, as well as the connected thermal fluxes. The TLBM platform ensures fast and reliable analyses, even in a fully 3D environment, allowing for parametric investigations to retrieve the best geometries.

Material and methods: A 3D render of the reactor layout is depicted in Figure 1a: the shell is divided in five parts, of which the outmost and central ones contain a PCM and the others contain a metal hydride. The system is outfitted with numerous sensors measuring temperature, pressure and hydrogen intake/outtake, as to measure its efficiency and relate it to the PCM TLBM simulation. The reactor is then connected to a fuel cell that produces electricity. The PCM shells are provided with heating units should the need to melt it arise. The TLBM simulation is a 3D code using the enthalpy formulation approach to model substance melting. TLBM allows for easy parallelization and trivial implementation of several boundary conditions [4], including metal meshes and fins of various shapes. This approach has already been tested by the authors in 2D cases [5,6], Figure 1b, and it has proven its viability. Moreover, it offers unique access to local measurements.



(a) (b)

Figure 1: (a), 3D rendering of the reactor; (b), Benchmark of a PCM, simple and with fin.

Results: The benchmarks correctly capture the melting dynamics of a PCM both with and without fin, as seen in Figure 1b. The insertion of the fin provides a speed up in the melting, aiding the small conductivity of the material.

Conclusions: The simulations capture PCM dynamics quite well and in the future their extension to import the geometry of the reactor will prove a useful tool to pre-test and validate layouts and to compare practical and theoretical results.

Acknowledgment

G.F. wishes to acknowledge the support of Italian Government Program PRIN, grant n. 2022F422R2, “Hydrogen Advanced solutions for Water eleCtrolysis and solid-state Storage (HAWCS)”, CUP E53D23003210006, Funded by the European Union – NextGenerationEU, the support of the Italian Government Program PRIN, grant n. P202298P25, "BIO-inspired Experimental and nuMerical BRidge pier Analysis for an innovative scour protection deviCE" (BIO-EMBRACE), CUP E53D23016990001, Funded by the European Union – NextGenerationEU, and the support of Project ECS 0000024 Rome Technopole, - CUP B83C22002820006, NRP Mission 4 Component 2 Investment 1.5, Funded by the European Union – NextGenerationEU.

G.F. and P.P. wish to acknowledge the support of the Office of Naval Research Global Grant N629092412072.

The authors acknowledge fruitful discussions with Prof. Vesselin K. Krastev.

References

[1] K. S. Nivedhitha et al., “Advances in hydrogen storage with metal hydrides: Mechanisms, materials, and challenges,” International Journal of Hydrogen Energy, vol. 61, pp. 1259–1273, Apr. 2024, doi: 10.1016/j.ijhydene.2024.02.335.

[2] J. Lin, X. Liu, S. Li, C. Zhang, and S. Yang, “A review on recent progress, challenges and perspective of battery thermal management system,” International Journal of Heat and Mass Transfer, vol. 167, p. 120834, Mar. 2021, doi: 10.1016/j.ijheatmasstransfer.2020.120834.

[3] A. L. Facci, M. Lauricella, S. Succi, V. Villani, and G. Falcucci, “Optimized Modeling and Design of a PCM-Enhanced H2 Storage,” Energies, vol. 14, no. 6, p. 1554, Mar. 2021, doi: 10.3390/en14061554.

[4] Q. Li, K. H. Luo, Q. J. Kang, Y. L. He, Q. Chen, and Q. Liu, “Lattice Boltzmann methods for multiphase flow and phase-change heat transfer,” Progress in Energy and Combustion Science, vol. 52, pp. 62–105, Feb. 2016, doi: 10.1016/j.pecs.2015.10.001.

[5] P. Proia, M. Sbragaglia, and G. Falcucci, “Melting with natural convection with heterogeneous heating sources,” Applied Thermal Engineering, vol. 257, p. 124089, Dec. 2024, doi: 10.1016/j.applthermaleng.2024.124089.

[6] P. Proia, M. Sbragaglia, and G. Falcucci, “Parametric study on the effect of the position and length of a fin in the melting of Phase Change Materials”, *in submission* 2025

EFCH2 2025
European Fuel Cells and Hydrogen
PIERO LUNGHI CONFERENCE
September 17th–19th 2025
Capri / Italy

Integrated Dynamic and Economic Modeling of Renewable Hydrogen Refueling Systems

Elio Simeoni*,[1], Jacob Brouwer[2], Elio Jannelli[1], Simona Di Micco[1]
*Corresponding author: Elio Simeoni
[1]University of Napoli Parthenope
[2]University of California Irvine

Introduction

Green hydrogen is emerging as a critical solution for decarbonizing the transportation sector, particularly via fuel cell electric vehicles (FCEVs). Despite their high efficiency and zero emissions, the adoption of FCEVs is constrained by limited refueling infrastructure and high hydrogen delivery costs. This study presents a comprehensive dynamic model of an on-site hydrogen refueling station (OS-HRS), integrating renewable energy sources and designed to minimize the Levelized Cost of Hydrogen (LCOH) [1, 2].

Methodology and Refueling phase

The OS-HRS model combines MATLAB and Python for detailed simulation and optimization. It includes:

- Dynamic weather-driven simulation of PV and wind energy production,
- Hydrogen generation from PEM Electrolysis [3],
- Cascade hydrogen storage (200 - 450 - 900 bar) [4, 5],
- Multistage intercooled hydrogen compression to 900 bar [6],
- Pre-cooling systems (-40°C) for compliance with SAE J2601 protocols,
- Economic analysis.

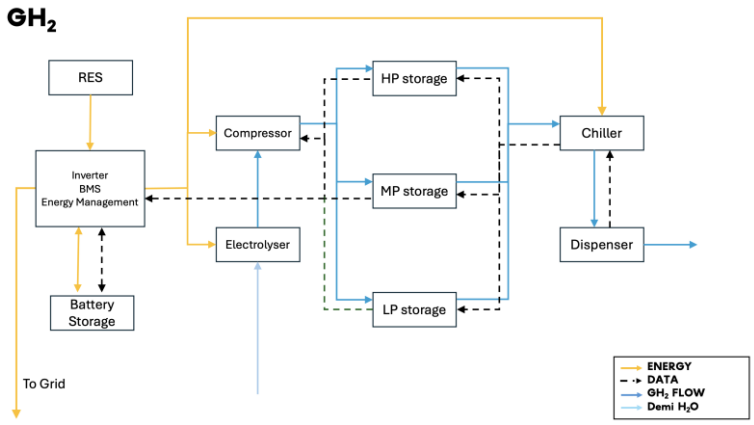


Figure 1: OS-HRS architecture schematic

The station dispenses and produces an average of 250 kg of hydrogen per day. The refueling processes in HRSs must complain to SAE J2601 protocols to ensure safety and tank integrity. The model implements realistic thermal and pressure dynamics during refueling using a zero-dimensional approach. Hydrogen temperature rise is evaluated using energy balances, considering convection with tank walls and heat of compression. Vehicle tanks and storage banks are simulated as adiabatic systems, and pressure evolution is modeled using mass and

energy conservation principles. The hydrogen is precooled to -40°C to minimize thermal stress and ensure rapid refueling within 3-5 minutes, in accordance with the Average Pressure Ramp Rate (APRR) method [7].

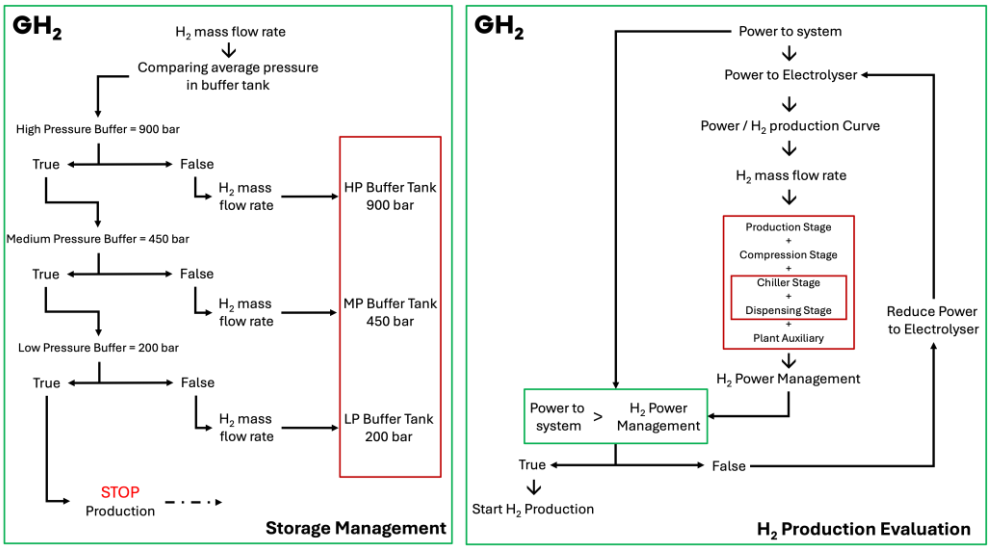
Results: Albuquerque Case Study

The analysis has been carried for different cities in different climate area. As a case study, I selected the city of Albuquerque, New Mexico. Albuquerque's high solar potential allows a well-optimized system. The best configuration resulted in:

- LCOH: 20 $/kg H_2
- Capital Investment: $16M

Key insights include:

- RES energy is mostly consumed for hydrogen production, with limited grid sales,
- The compressor and chiller stages significantly contribute to energy demand.



a b

Figure 2: a. Process flow diagram for storage management ; b. Modular process scheme showing interaction between hydrogen production and dispensing

Conclusion

This study confirms the feasibility of green OS-HRSs using integrated dynamic modeling. Accurate simulation of hydrogen thermal and pressure behavior ensures safety and performance under SAE J2601. Techno-economic modeling reveals that the most influential components for LCOH are hydrogen production, storage, and thermal management. Optimizing RES sizing relative to hydrogen demand is critical for cost control. While LCOH currently ranges between $20–28/kg H_2, reductions in RES and electrolyzer costs will significantly enhance economic viability.

References

1. Zhao, L., Brouwer, J. Dynamic operation and feasibility study of a self-sustainable hydrogen fueling station using renewable energy sources. Int J Hydrogen Energy, 2015.
2. Viktorsson, L. et al. Life Cycle Cost Analysis of A Hydrogen Refueling Station. Energies, 2017.

3. Fragiacomo, P., Genovese, M. Techno-economic analysis of a PEM electrolyzer powered by RES. Energy Convers Manag, 2020.
4. Rothuizen, E., Rokni, M. Optimization of cascade fueling stations for hydrogen vehicles. Int J Hydrogen Energy, 2014.
5. Talpacci, E. et al. Cascade storage system topology effects on cooling energy. Int J Hydrogen Energy, 2018.
6. Elgowainy, A. et al. Compression and storage optimization in HRS. ASME Conference, 2008.
7. Reddi, K. et al. Impact of SAE J2601 fueling methods on FCEV fueling time. Int J Hydrogen Energy, 2017.

EFCH2 2025 European Fuel Cells and Hydrogen PIERO LUNGHI CONFERENCE
September 17th–19th 2025 Capri / Italy

Optimization of Hydrogen Refueling Infrastructure for Heavy-Duty Vehicles

Minseok Kwon[a], Sanggyu Kang*[a]

* corresponding author: sgkang@snu.ac.kr

[a] Department of Naval Architecture and Ocean Engineering Seoul Nat'l Univ.

Keywords: Heavy duty, Heavy duty tank, Hydrogen, Hydrogen Refueling System(HRS)

Abstract :

This study presents the development of a dynamic model for a heavy-duty hydrogen refueling system using MATLAB-Simulink®. The proposed system comprises key components, including a high-pressure storage tank, pressure reduction valve, cooling unit, breakaway coupling, refueling hose, pipelines, nozzle/receptacle assembly, and an onboard vehicle tank designed for heavy-duty applications. The model simulates the transient thermodynamic behavior of the hydrogen refueling process, capturing key parameters such as pressure, temperature, and mass flow rate under real-world operating conditions. To ensure both safety and refueling efficiency, this study investigates the influence of pipeline geometry while adhering to standardized refueling protocols. Through a systematic analysis, an optimized refueling strategy is proposed, mitigating safety risks while enhancing the overall efficiency of hydrogen transfer. The findings contribute to the advancement of hydrogen refueling infrastructure for heavy-duty transportation, facilitating the widespread adoption of hydrogen-powered vehicles.

Introduction : Hydrogen fuel cell electric vehicles (FCEVs) are well-suited for heavy-duty applications due to their long driving range and fast refueling times. As the adoption of heavy-duty FCEVs continues to grow, the development of efficient and safe hydrogen refueling infrastructure is becoming increasingly critical [1]. Most hydrogen refueling systems operate under high-pressure conditions and adhere to established standards, with SAE J2601 being the most widely adopted protocol. However, SAE(Society of Automotive Engineers) J2601 does not provide sufficient guidance on refueling methods specifically for heavy-duty hydrogen tanks [2]. Despite the rising demand for heavy-duty refueling solutions, research on hydrogen refueling stations tailored for heavy-duty tanks remains insufficient, and optimized refueling methods for large-capacity storage systems have not been thoroughly investigated. Additionally, the lack of references and publicly available datasets on the design, operation, and performance of heavy-duty hydrogen refueling stations hinders the development of reliable models for refueling behavior and system efficiency, limiting accurate impact

assessments and the establishment of validated optimization strategies. To ensure both safety and efficiency, it is essential to develop optimized refueling strategies that comply with SAE J2601 while addressing the unique requirements of heavy-duty hydrogen storage systems.

Objectives:

This study aims to identify and analyze the optimal Average Pressure Ramp Rate (APRR) during hydrogen refueling by conducting a parameter study of key components, such as pipelines. Through this analysis, the research seeks to optimize hydrogen refueling stations and develop a safe and efficient refueling method. Additionally, to validate the reliability of the model, complementary experimental data between heavy-duty hydrogen tanks and refueling stations is incorporated.

Material and methods:

A. Real gas equation

To accurately describe the thermodynamic behavior of hydrogen gas during refueling, the compressibility factor Z is defined as:

$$Z = \frac{Pv}{R_g T} = (1 + \frac{\alpha P}{T}) \quad (1)$$

R_g is the specific gas constant for hydrogen, given as 4124.3 J/(kg·K), and α is constant coefficient with a value of 1.9155×10^{-6} K/Pa.

B. Energy conservation & mass conservation

The energy and mass conservation equations are applied to both the hydrogen tank and its components, allowing for the calculation of the thermodynamic state. These equations can be expressed as:

$$\frac{dm}{dt} = \dot{m}_{in} - \dot{m}_{out} \quad (2)$$

$$\frac{d(mu)}{dt} = \dot{m}\,(h_{in}(T,P) - h_{out}(T,P)) + Q \quad (3)$$

Results: The hydrogen refueling system consists of a storage tank, reduction valve, cooling system, breakaway coupling, hose, pipelines, nozzle/receptacle, and vehicle tank, as shown in Fig. 1(a). The hydrogen tank model was validated by comparing temperature variations in the tank during the filling process between simulation and experimental data, as shown in Fig. 1(b). The simulation results demonstrated high reliability, with a maximum deviation of 3 K from the experimental data. The system's optimal APRR was evaluated based on the pipe inlet diameter and operating conditions, as shown in Fig. 1(c). It was confirmed that the APRR of the 2 mm pipe was the lowest at 7.1 MPa/min, while the 6 mm, 7 mm, and 8 mm pipes exhibited the same APRR of 13.3 MPa/min, indicating an optimal range for pipe diameters.

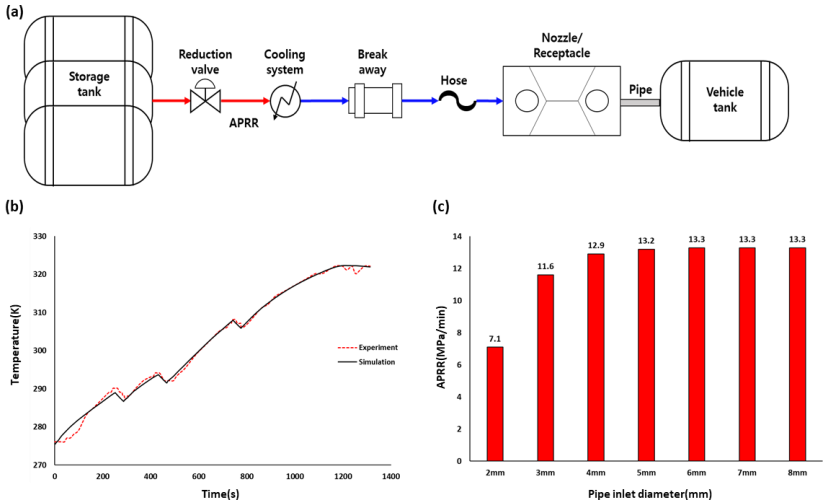


Fig. 1. (a) Schematic diagram of the hydrogen refueling system. (b) Comparison of temperature variations in the tank between simulation and experimental data.

(c) Optimal APRR in the pipeline under different operational cases based on pipe diameter.

Conclusions: In this study, a dynamic model of a hydrogen refueling system was developed using MATLAB-Simulink®. The hydrogen tank and its components were validated by comparing them with experimental data. The optimal APRR of the hydrogen refueling system was evaluated under system configurations.

Acknowledgment

This work was supported by Korea Institute for Advancement of Technology(KIAT) grant funded by the Korea Government(MOTIE) (P0023684, HRD Program for Industrial Innovation)

References

[1] M. Genovese and P. Fragiacomo, Hydrogen refueling station: Overview of the technological status and research enhancement, *Journal of Energy Storage*, vol. 61, 106758, 2023.

[2] SAE International, *Fueling Protocols for Gaseous Hydrogen Powered Heavy Duty Vehicles*,

Standard J2601/2_202307, 2023.

European Fuel Cells and Hydrogen
PIERO LUNGHI CONFERENCE
September 17th–19th 2025
Capri / Italy

Sizing of small on-site hydrogen refueling stations: a modeling approach

D. Lanni*[a], G. Di Cicco[a], A. Perna[a], A. Agresta[b], M. Della Pietra[b], V. Cigolotti[c]
* corresponding author: davide.lanni@unicas.it
[a] Department of Civil and Mechanical Engineering, University of Cassino and Southern Lazio, Cassino, Italy
[b] DTE-PCU-SPCT, ENEA R. C. Casaccia, Rome, Italy
[c] TERIN-PSU-ABI, ENEA Portici, Portici, Italy

Keywords: hydrogen refueling stations, modeling, on-site hydrogen production

Abstract

On-site hydrogen refueling stations (HRSs) play a key role in advancing sustainable mobility, providing greater flexibility and scalability than centralized hydrogen production. This research introduces a numerical approach for sizing a small on-site HRS, where hydrogen is produced via electrolysis units powered by a photovoltaic (PV) plant, utilizing a three-cascade storage system for refueling. The sizing of the refueling line is carried out considering two different recharge strategies of the cascade system.

Introduction

In response to climate change and fossil fuel depletion, interest in clean fuels like green hydrogen is rising [1]. CO_2 emissions from energy reached 37.8 Gt in 2024, largely driven by the transport sector [2]. Green hydrogen, produced from renewables, is seen as a long-term alternative to hydrocarbons [3], [4]. Its adoption in transport requires dedicated infrastructure, particularly on-site hydrogen refueling stations (HRSs), which offer greater flexibility than centralized systems [5]. These stations can operate in diverse settings, matching local demand and supporting fuel cell vehicle deployment [5], [6]. Several recent studies focus on their techno-economic feasibility.

Objectives

In this scenario, this study introduces a dynamic modeling strategy that is capable of sizing both the hydrogen production section (HPS) and the refueling line (RL) of a small on-site grid-connected HRS (Figure 1), taking into account two different recharge strategies of the three-cascade storage system.

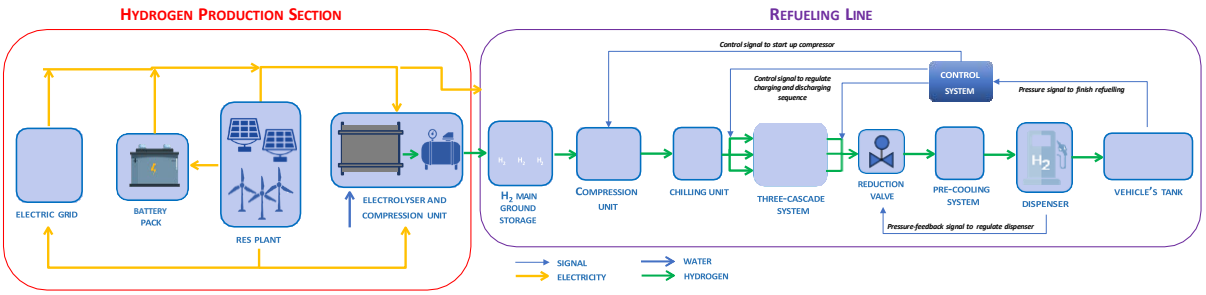


Figure 1. Schematic of the on-site HRS

Material and methods

The numerical approach is structured according to the following steps:

1. A semi-randomized algorithm is developed in order to generate realistic hourly hydrogen demand profiles based on the characterization of the vehicles' fleet, and a worst-case scenario (WCS) is identified. In this scenario, each incoming vehicle is assumed to have a tank at 10% state of charge, while each outgoing vehicle leaves with a fully filled tank at 100%. The tank capacity of the light-duty vehicles is assumed to be equal to 5.1 kg.
2. The RL is modeled considering its two principal subsystems: the three-cascade storage system and the dispenser. A mass balance between these subsystems is employed to schematize the refueling process. The cascade system consists of three banks: low-pressure (LP) bank, medium-pressure (MP) bank, and high-pressure (HP) bank. They operate at 900, 650, and 400 bar, respectively. During each refueling event, the process begins with the storage tank at the lowest pressure in the cascade system. As the dispenser pressure rises and approaches that of the active tank, the system switches to the next available tank, either from the same bank or from a higher-pressure unit. This sequence continues until the refueling is completed. The number of storage tanks (NN_{SSSS}) of the banks is chosen according to the following relationship: $NN_{SSSS,LLLL} = NN_{SSSS,MMLL}/2 = NN_{SSSS,HHLL}/3$. The H_2 main ground storage operates at 200 bar. For the small-scale HRS analyzed, a single dispenser is considered.
3. The HPS is sized by using an algorithm that takes into account: (i) renewable energy potential (RES load factor), (ii) RES technology performance, and (iii) hourly hydrogen demand. The electrolyzer is sized for the peak hourly demand, while the RES system is sized to meet the annual electricity needs of all units. The algorithm performs dynamic mass and energy balances and follows a priority-based energy management: RES power feeds the electrolyzer first, then the battery, and finally the grid. When RES is insufficient, power is drawn from the battery, then from the grid.
4. The modeling approach is applied to a specific case study. The analyzed small on-site HRS, located in Central Italy, is powered by a PV plant using Jinko Solar 560 W modules (20.5% efficiency, 19% capacity factor) and supported by a Tesla Megapack battery (88% round-trip efficiency). Hydrogen is produced via PEM electrolysis units (100 kW each), operating at 20 bar and 55 °C, with 1.68 kg/h output per module and 56.5% LHV efficiency.

Results

The identified WCS for the hydrogen demand profile is characterized by 38 daily refueling events, with a maximum hourly demand of 32.1 kg_{H2}/h, and a daily flow of hydrogen equal to 174.4 kg_{H2}/day. The refueling event lasts 5 minutes, during which an average hydrogen flow rate of 0.918 kg/min is delivered to the dispenser.

Two different recharge strategies have been considered for the three-cascade storage system of the RL during the daily operation: (i) the cascade system is recharged from the H_2 main ground storage at the end of the working day (single recharge, 1R); (ii) the cascade system is recharged three times at equal intervals throughout the workday (3 recharge events, 3R). The H_2 main ground storage is sized

to satisfy the required maximum capacity to supply the three-cascade storage system during the working day, increased by 20%.

For the HPS, the hourly hydrogen demand is assumed constant at 1/24 of the daily maximum. Consequently, the HPS is sized for a steady output of 7.27kg_{H2}/h. The PV plant covers the annual electricity needs of the HRS, while the battery is sized to run the electrolyzer at full load for 4 hours. Table 1 presents the sizing results of the analyzed HRS. The hydrogen utilization factor (HUF) of the three-cascade storage system is calculated as the ratio between the daily dispensed hydrogen mass and the maximum hydrogen mass contained in the cascade system.

Table 1. HRS sizing results

Parameter	**Unit**	**Value**	
Refueling Line		**1R**	**3R**
$NN_{SSSS,LLLL}$ / $NN_{SSSS,MMLL}$ / $NN_{SSSS,HHLL}$	-	3 / 6 / 9	2 / 4 / 6
Storage tank volume	m^3	0.7	
H_2 main ground storage size (200 bar)	kg (m^3)	418.6 (27.7)	355.6 (23.5)
HUF of the three-cascade storage system	%	33.9	50.9
Hydrogen Production Section			
PV plant size	MW	2.44	
Electrolysis unit size	kW	500	
Compression unit size	kW	10	
Battery pack size	MWh	2.3	

Conclusions

The proposed methodology allowed for the sizing of a small on-site HRS. The HPS consists of a 2.44 MW PV plant with a 2.3 MWh battery storage, a 500 kW electrolyzer, and a 10 kW compressor. Compared to the 1R, the 3R strategy allows a reduction of the cascade system size of about 33%, an increase of its HUF of about 50%, and also a decrease of the H_2 main ground storage size of about 15%.

Acknowledgment

This research was funded by the European Union - NextGenerationEU from the Italian Ministry of Environment and Energy Security, POR H2 AdP MEES/ENEA with involvement of CNR and RSE, PNRR - Mission 2, Component 2, Investment 3.5 "Ricerca e sviluppo sull'idrogeno", CUP: I83C22001170006.

References

[1] T.N. Chaudhary, A. Akbar, M. Usman, M.A. Mahmood, A.O.M. Maka, B. Chen, Energy Convers. Manag.: X 18, 100374 (2023)

[2] IEA, Global Energy Review 2025 (2025)

[3] P. Marocco, M. Gandiglio, M. Santarelli, J. Clean. Prod. 434, 140007 (2024)

[4] S. Ramakrishnan, M. Delpisheh, C. Convery, D. Niblett, M. Vinothkannan, M. Mamlouk, Renew. Sustain. Energy Rev. 195, 114320 (2024)

[5] T.L. Berg, D. Apostolou, P. Enevoldsen, Int. J. Hydrogen Energy 46, 146 (2021)

[6] P. Cardona et al., Int. J. Hydrogen Energy 52, 49 (2024)

European Fuel Cells and Hydrogen
PIERO LUNGHI CONFERENCE
September 17th–19th 2025
Capri / Italy

Fueling the Future: A University's Role in Advancing Hydrogen Mobility and International Collaboration

David Blekhman*[a]
Matteo Genovese [b]

* corresponding author: blekhman@calstatela.edu
[a] Cal State LA
[b] University of Calabria

Keywords: Fueling Protocol, Hydrogen Refueling Station, International Collaboration, Workforce

Abstract Introduction:

Since its establishment in 2011, the Hydrogen Research and Fueling Facility (HRFF) at Cal State LA has exemplified how academic institutions can play a transformative role in advancing hydrogen mobility and fostering international collaboration. As the world's largest university-based electrolysis hydrogen station at the time, the HRFF served as a real-world platform for innovation in hydrogen fueling technologies, offering workforce training, academic-industry partnerships, and long-term operational data.

Designed and operated according to SAE standards, the facility supported fueling for both light- to heavy-duty vehicles and became a cornerstone in hydrogen infrastructure research. Although decommissioned in October 2022, its mission continues through a major redevelopment supported by a $7.15 million award from the U.S. Department of Transportation's Charging and Fueling Infrastructure funding. The upgraded facility will enable high-capacity fueling for vehicles ranging from passenger cars to heavy-duty fleets and will integrate renewable electrolysis systems to ensure low-carbon hydrogen production.

The HRFF also enabled international academic exchange. In 2015, a partnership was initiated by Professor Petronilla Fragiacomo, the University of Calabria (Italy), fostering international research on hydrogen fueling infrastructure between the two institutions.

Objectives:

Over the years, three Italian PhD students have conducted research utilizing the data and experiments applied at the HRFF that included station performance optimization, system efficiency, and fueling data analysis. Their work contributed to scientific publications and

deeper understanding of hydrogen infrastructure operations. They also mentored undergraduate interns while at the station.

Results:

Several pioneering studies have been conducted contributing to the development of the HRS knowledge. A few summaries further underscore the significance of this cooperation.

First study addresses pressure pulsation issues in hydrogen fueling stations, where pressure oscillations up to 6.7 MPa were observed due to piston compressors during 70 MPa fueling without a buffer. A mathematical model was created to determine the minimum buffer volume needed to eliminate pulsations. By isolating four tanks one-by-one, experiments confirmed that one tank significantly reduced pulsations to 0.2 MPa. This provides valuable insight into designing efficient hydrogen delivery systems with minimal flow disturbances and enhances operational safety and efficiency in hydrogen infrastructure.

Another paper analyzes hydrogen leakage from production to dispensing at the station. Using data from reports and sensors, the team evaluated leakage sources and calculated inefficiencies. Initially, losses reached 30–35%, but improved practices and better understanding reduced this to 2–10%. Maintenance activities were found to be the most critical factor affecting hydrogen accounting. The study provides a guideline for operators to prevent leaks and data mismatches.

In 2022, the California Energy Commission awarded a $500,000 grant for the “California ZEV Engineering Workforce Pilot,” a joint initiative between Cal State LA and Cerritos College. This program strengthens the pipeline of skilled professionals entering the hydrogen and zero-emission vehicle sectors. As part of the initiative, two internship-based courses were developed.

Conclusions:

Cal State LA’s Hydrogen Research and Fueling Facility (HRFF) not only advanced hydrogen infrastructure research through the collaborations with the University of Calabria, but also became a vital educational platform.

Acknowledgment:

This material is based upon work supported by the National Science Foundation under Grant No. 2112554 and California Energy Commission under Grant No. ARV-21-062.



Techno-Economic Analysis of Hydrogen Storage Technologies for Different Real End-Use Demand Profiles and Sites

Andrea Ademollo*[a], Mattia Calabrese[a], Carlo Carcasci[a], Maurizio Vaccaro[b], Joshi Ipsita[b]

* Corresponding author: andrea.ademollo@unifi.it

[a] Università degli Studi di Firenze, Department of Industrial Engineering - DIEF, Via di Santa Marta 3, 50139 Firenze, Italy

[b] Baker Hughes – CTS, Via Felice Matteucci 2, 50127, Firenze (FI)

Keywords: hydrogen storage, metal hydrides, levelized cost of hydrogen

Abstract

This work presents a techno-economic analysis of hydrogen storage options—compressed tanks (Type I–IV), Underground Hydrogen Storage (UHS), and Metal Hydrides (MH)—for industrial and Hydrogen Refueling Station (HRS) demand profiles at diverse locations, subject to green-hydrogen emission limits. Hydrogen is generated from renewables (PV + wind) or grid power (if allowed), under site-specific electricity prices and carbon intensities. Different options were compared in terms of Levelized Cost of Hydrogen (LCOH), footprint, and GHG emissions. MH configurations address process heat integration via waste-heat recovery, electric heaters, or natural gas boilers—with or without Phase-Change Materials (PCM).

The resulting LCOH and Levelized Cost of Storage (LCOS) were evaluated, highlighting not only economic competitiveness but also the footprint and weight of the investigated storage solutions. Our findings show that: (i) hybrid off-grid systems (photovoltaic + wind) generally outperform single renewable energy source technology, (ii) UHS offers great advantages where high electricity prices are present, and (iii) for metal hydrides, leveraging on-site waste heat —as well as PCM adoption— reduces external energy needs and leads to competitive hydrogen production costs.

Introduction: *Green hydrogen deployment hinges on cost-competitive, scalable storage. While 700 bar compressed tanks are established, large-scale use demands lower-cost or higher-density solutions such as Underground Hydrogen Storage (UHS) or Metal Hydrides (MH). Likewise, each storage technology interacts differently with site constraints (grid emission intensity, renewable generation potential) and end-use demand (constant industrial load vs. fluctuating Hydrogen Refueling Station (HRS) profile) [1, 2].*

Metal hydrides (e.g., MgH_2) offer high volumetric density but need 200–350 °C heat for release. Integrating phase-change materials (PCM) in MH beds stores reaction heat, cutting external heat requirements [3, 4]. However, techno-economic trade-offs under real demand profiles and varied electricity/carbon costs remain underexplored.

Baker Hughes Confidential

Objectives:

- *Compare hydrogen storage technologies (compressed tanks, UHS, and MH) for two prototypical demand profiles (industrial vs. HRS) and identify the best-performing configurations by balancing capital cost, operational cost, and emissions compliance.*
- *Quantify how geography, renewable energy availability, grid carbon factors, and emissions thresholds affect the Levelized Cost of Hydrogen (LCOH).*
- *Assess MH systems' performance under different heat-supply scenarios (waste-heat reuse, electric boiler, natural gas boiler) and with or without PCM.*

Material and methods: *A Linear Programming optimization model has been developed to optimize the sizing of key components (PV, wind, electrolyzer, compressor and storage) as well as the hourly operation of the plant by minimizing LCOH over a 20-year horizon.*
Four representative sites—Bari (Italy), Bremen (Germany), Houston (USA), and Hajira (India)—were selected to capture varied conditions of renewable availability, grid electricity prices, and GHG limits. Two demand profiles —Industry: A constant 38 kg/h of hydrogen load at low delivery pressure (1 bar) and HRS: The same annual mean demand but exhibiting hourly peaks up to 85 kg/h and requiring final pressures up to 700 bar— were modelled in both off-grid (purely renewable) and grid-connected electrolyzer configurations. The latter one is subjected to location-specific GHG emission limits for green hydrogen certification.
Technical and economic data for PV, wind turbines, electrolyzers, compressors, tanks (Type I–IV, 30–700 bar), UHS, MH and PCM were drawn from literature and vendor information. MH systems were tested with six sub-variants, depending on the heat source (waste heat, electric boiler, or natural gas boiler) and on the presence of PCM to reduce external heat demand.

Results: *Industrial and HRS demand profiles gave similar results as the seasonality of HRS load profile —which is the one driving the storage size— is not really marked. The HRS experiences slightly higher LCOH because of extra compression requirements (up to 350–700 bar).*
In off-grid scenarios, a PV-wind hybrid typically outperformed single-source approaches by smoothing generation fluctuations, leading to lower overall LCOH. When grid electricity is available, cheap electricity purchase price (as in Hajira) combined with higher GHG thresholds greatly reduced system sizes and costs. In contrast, higher electricity prices (Bari, Bremen) often favoured enlarging hydrogen storage —especially if low-cost UHS is available— over purchasing electricity from the grid. The lowest LCOH (7,61€/kg) is obtained with UHS operating at 100 bar in Hajira in the grid-connected scenario when covering an industrial constant load profile (Figure 1), while the highest LCOH (12,36€/kg) is obtained with Tank Type IV operating at 700 bar in Houston in the off-grid scenario when covering the HRS load.
MH such as MgH_2-based systems proved economically advantageous whenever waste heat was readily available at sufficient temperature (300 °C) outperforming conventional tanks in

final LCOH (7,65€/kg) because of the absence of the compressor to reach extra-pressure or satisfy high pressure process needs, despite having a slightly higher storage CAPEX. Where no suitable heat source was present, a natural gas boiler or an electric boiler was required. Although that increased operational costs, the resulting LCOH still remained competitive in sites with low gas prices (Hajira and Houston). Integrating PCM reduce the external heat demand by 70%, but at the expense of higher storage CAPEX leading to a cost-effective adoption in case an electric heater is employed but not if a gas boiler is employed.

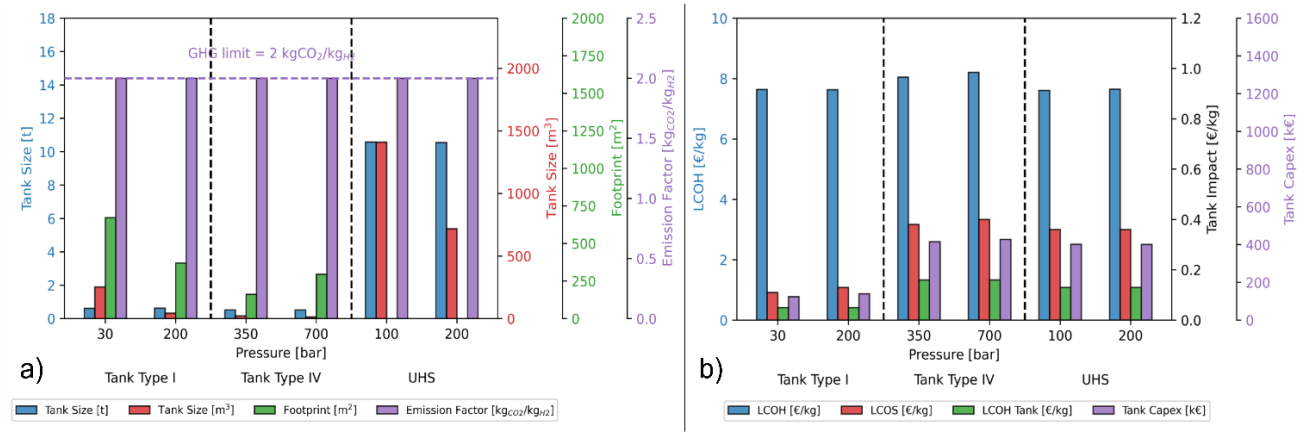


***Figure 1**: Optimal grid-connected PtH plant in Hajira (India) with different storage options for multiple pressure levels to satisfy a constant industrial hydrogen demand. a) Optimal storage configuration; b) Optimal economic KPIs.*

Conclusions: *This study demonstrates that no single hydrogen storage technology is universally optimal; rather, the best choice depends strongly on local renewable resources, electricity pricing, demand profile, and available heat sources and footprint requirements.*

References

[1] G. Karayel et al. "A comprehensive assessment of energy storage options for green hydrogen". Energy Conversion and Management 2023.

[2] M. Yang et al. "A Review of Hydrogen Storage and Transport Technologies". Clean Energy, 2023.

[3] Mellouli, M. et al. "Numerical analysis of metal hydride tank with phase change material." Int. J. Hydr. Energy 2015.

[4] Garrier, S. et al. "A new MgH_2 tank concept using a phase-change material to store the heat of reaction." Int. J. Hydr. Energy 2013.

European Fuel Cells and Hydrogen
PIERO LUNGHI CONFERENCE
September 17th–19th 2025
Capri / Italy

Hydrogen Storage for Renewable Energy Integration: A Techno-Economic Comparison with Ammonia as Hydrogen Carrier

Mattia Calabrese*[1], Valentina Veltroni[1], Marco Pagliai[2], Carlo Carcasci[1]

* corresponding author: mattia.calabrese@unifi.it

[1] University of Florence, Department of Industrial Engineering - DIEF, Via di Santa Marta 3, 50139 Firenze, Italy

[2] University of Florence, Department of Chemistry "Ugo Schiff" – DICUS, Via della Lastruccia 3, 50019 Sesto Fiorentino, Italy

Keywords: Ammonia as Hydrogen carrier, Hydrogen Storage, Renewable Energy Integration, Techno-economic analysis

Introduction: The global fight against climate change is tied to the development of energy policies, which have established ambitious targets to reduce greenhouse gas emissions and facilitate the transition to a sustainable energy system. Renewable energy sources are pivotal to this transition, but their intermittent nature poses significant challenges. In this regard, the development of long-term storage technologies is crucial to managing production fluctuations and reducing dependence on conventional plants. Moreover, energy storage has the potential to address not only temporal but also spatial challenges, helping to mitigate regional production imbalances. Currently, chemical storage using hydrogen appears to be the most promising solution to meet these requirements. Nevertheless, the technical and economic challenges associated with hydrogen storage and transportation necessitate the exploration of alternative solutions. One promising solution is using ammonia (NH_3) as a hydrogen carrier. The utilization of ammonia as a hydrogen carrier can offer several advantages [1]. Ammonia has a hydrogen content of 17.8% in weight, is very stable at ambient conditions and allows for much less severe storage conditions than compressed hydrogen. Moreover, the infrastructure for handling and transporting ammonia is already well-developed, facilitating its use as an energy carrier on an industrial scale.

Objectives: This study aims to evaluate how hydrogen storage in the form of ammonia could contribute to the development of the hydrogen supply chain. To this end, a comparative analysis is conducted between the direct storage of compressed hydrogen and its conversion to ammonia, followed by ammonia storage. The analysis is performed across various demand profiles to identify the scenarios in which each system exhibits an economic advantage. Finally, a parametric analysis was conducted, considering the costs associated with transportation. This analysis is aimed to evaluate whether the utilization of ammonia as a hydrogen carrier would confer an additional benefit regarding transportation.

Material and methods: The analysis is conducted using an in-house developed software called Multi Energy System Simulator (MESS). MESS is a modular, bottom-up, multi-node model that allows the simulation of energy systems with multiple energy carriers, multiple users, and adjustable spatial resolution. The simulations are based on a set of predefined priorities, allowing different control logics to be analysed and with accurate performance analysis of the various technologies, for which design and off-design models have been developed [2]. Within MESS, a realistic and detailed ammonia synthesis reactor model from green hydrogen was developed ad-hoc for this study, together with an ammonia storage and an ammonia decomposition model. The considered case study consists of the comprehensive modelling of the hydrogen supply chain to assess the feasibility of decarbonization of an electricity demand. The electricity demand is met with priority by Renewable Energy Sources (RES). If RES production exceeds demand, the surplus is supplied to a Proton-Exchange Membrane (PEM) electrolyser to produce green hydrogen, which is then stored and converted back into electricity through a PEM fuel cell when demand exceeds production. In the storage phase, the case of compressed hydrogen storage in tanks is compared with the use of ammonia as a storage carrier. In the latter scenario, the hydrogen is utilized to produce ammonia in a synthesis reactor, which is then reconverted in electricity. Since the reactor must operate at a minimum load of 30% for technical reasons, a hydrogen buffer is introduced before the synthesis reactor to guarantee uninterrupted operation. The economic viability of these two scenarios is compared using the Levelized Cost of Electricity (LCOE). Three distinct electricity demand profiles were considered in this study: one characterized by the absence of seasonality, one exhibiting heightened energy consumption during the summer months, and one during the winter months. The exclusive use of RES presents significant operational challenges and disadvantages from the perspective of component sizing. Specifically, storage systems must be capable of recovering the seasonal variability of RES production. A meta-heuristic optimization method is implemented to perform the sizing of the system. The algorithm chosen is the adaptive PSO proposed by Zhan et al. [3] and implemented through the Python library Pymoo [4]. A parametric analysis was then conducted to determine the impact of the production plant's location relative to the consumption site. This analysis incorporated transportation cost data from existing literature and examined the variation in costs as the distance between the production and consumption sites changed.

Results: It is observed that the demand profile has a significant impact on the selection of the optimal storage system. In particular, the demand profile with higher consumption in the summer months benefits direct hydrogen storage, while the “winter-intensive” demand profile makes ammonia very competitive and economically advantageous. In the absence of seasonality, direct hydrogen storage is favourable over ammonia if no control strategy is applied to the reactor with an LCOE respectively of 0.319 and 0.346 €/kWh. Conversely, when a control strategy is adopted, maintaining the reactor at minimum operational load when the

buffer level exceeds a specified threshold, the LCOE of ammonia-based storage decreases and at a minimum of 0.309 €/kWh with a 70% threshold. The introduction of transportation costs further enhances the competitiveness of ammonia-based storage, given ammonia's lower transportation costs relative to hydrogen. Figure 1 depicts the variation in component sizes and the consequent LCOE for the three scenarios outlined.

Conclusions: The utilization of ammonia as a hydrogen storage medium has the potential to accelerate the development of the hydrogen supply chain, particularly in scenarios where there is spatial and temporal decoupling between hydrogen production and utilization. The results of this study appear both generalizable and reproducible across various contexts where the adoption of renewable hydrogen is expected to play a crucial role in meeting increasingly urgent climate targets in the near future.

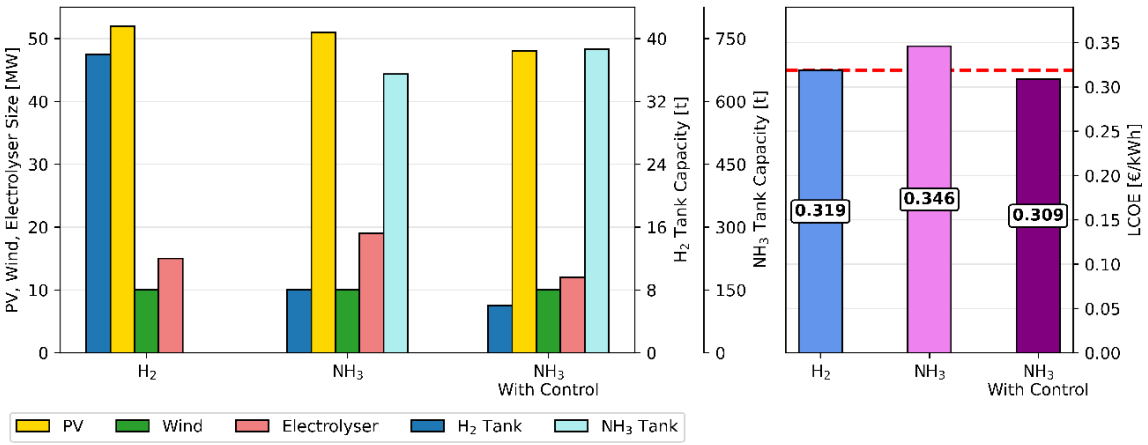


Figure 1: Variation in component sizes (left) and LCOE (right) for the hydrogen-based and ammonia-based storage (with and without control).

References

[1] Estevez R, López-Tenllado FJ, Aguado-Deblas L, Bautista FM, Romero AA, Luna D. Current Research on Green Ammonia (NH3) as a Potential Vector Energy for Power Storage and Engine Fuels: A Review. Energies 2023, Vol 16, Page 5451 2023;16:5451. https://doi.org/10.3390/EN16145451.

[2] Lubello P, Pasqui M, Mati A, Carcasci C. Assessment of hydrogen-based long term electrical energy storage in residential energy systems. Smart Energy 2022;8:100088. https://doi.org/10.1016/J.SEGY.2022.100088.

[3] Zhan ZH, Zhang J, Li Y, Chung HSH. Adaptive particle swarm optimization. IEEE Transactions on Systems, Man, and Cybernetics, Part B: Cybernetics 2009;39:1362–81. https://doi.org/10.1109/TSMCB.2009.2015956.

[4] Blank J, Deb K. Pymoo: Multi-Objective Optimization in Python. IEEE Access 2020;8:89497–509. https://doi.org/10.1109/ACCESS.2020.2990567.

European Fuel Cells and Hydrogen
PIERO LUNGHI CONFERENCE
EFCH2 2025
September 17th–19th 2025
Capri / Italy

Optimal Gas Flow Model for Evaluating the Fluid Dynamic Feasibility of Transporting Hydrogen-Natural Gas Blends in Gas Networks

Guzzo Gabriele[1]*, Carcasci Carlo[1]
* corresponding author: gabriele.guzzo@unifi.it
[1] University of Florence via Santa Marta, 3 50139 Florence (IT) Phone: +39 055 275 8783

Keywords: Hydrogen; Linepack; Natural Gas Pipeline; Optimal Gas Flow;

Abstract

Blending hydrogen in gas networks has the potential to support the development of the hydrogen economy and facilitate decarbonisation in the gas sector. However, due to the different properties of natural gas and hydrogen, fluid-dynamic models are needed to assess transport feasibility. This work introduces an optimal transient gas flow model for homogeneous NG-H_2 blends, incorporating linepack management to ensure system flexibility. A topologically simple case study highlights the main features of the model. A second case study, based on a real gas transmission network, evaluates the feasibility of transporting NG-H_2 blends with 20% mol H_2. The results confirm the robustness of the model and its effectiveness in conducting fluid dynamic feasibility studies to support the decarbonization of gas networks.

Introduction: Natural Gas (NG) is regarded as a transition fuel due to its comparatively lower carbon intensity in comparison with coal and oil. A significant number of countries have developed extensive NG infrastructure, including transmission pipelines and distribution networks [1]. Nevertheless, despite its advantages, NG is still a fossil fuel and is not considered a long-term sustainable solution to climate change. In the context of the ongoing energy transition, a shift towards electrification wherever feasible is being explored, complemented by the idea of repurposing existing gas infrastructure for H_2 transport. In fact, green H_2 is a clean energy vector that retains the advantage of being transported in gas form [2]. Consequently, the development of dedicated analytical tools to evaluate the fluid-dynamic feasibility of NG-H_2 transportation via large-scale gas networks is necessary [3].

Objectives: The work presents an optimization framework embedding a transient gas flow model for homogeneous NG-H_2 mixtures that also considers linepack constraints in the planning problem. The goal is to use the optimal gas flow (OGF) model developed to study

the feasibility of transporting homogeneous NG-H_2 blends in a large-scale gas transmission network considering a multi-day planning horizon.

Material and methods: The analysis includes two case studies. The first one is a simple but representative pipeline system with a demand node at the end of the pipeline and a compressor station at the supply point. The second case study is a real national gas transmission network. The length of the network is 7560 km network (including loops and laterals) containing 11 NG sources and 21 compressor stations.
A gas network can be modelled as a graph where elements such as nodes, pipes, and compressors are connected. The fluid-dynamic model adopted for the pipe is a 1-dimensional unsteady state isothermal model. The numerical scheme used to discretize the partial differential equations, namely the continuity and the momentum equation is the first-order backward discretization scheme in time and the first-order forward difference scheme in space. The unsteady state model is initialized with the fluid-dynamic solution obtained through a steady-state model. The gas properties are modelled by the SRK equation of state. The optimization function minimizes resource usage (gas supplied) while incorporating a penalty term for linepack consumption [4]. The resulting problem is a non-linear, non-convex problem implemented in an optimization framework and solved through an interior point optimizer named Ipopt [5].

Results: The first case study is used to demonstrate that by omitting the penalty term on linepack usage in the optimization function, the gas supply is interrupted for several hours. This phenomenon can be attributed to the fact that the model interprets linepack as a zero-cost NG source. This solution, although feasible, is not representative of real gas pipeline operation. The second case study is used to demonstrate the model capacity on a large-scale national gas network. The results demonstrate the fluid-dynamic feasibility of transporting blends of NG and H_2 containing 20% mol H_2. The pressure losses increase by up to 20% for blends containing 20% mol H_2 compared to pure NG and compressors offset these losses by operating with higher pressure ratios.

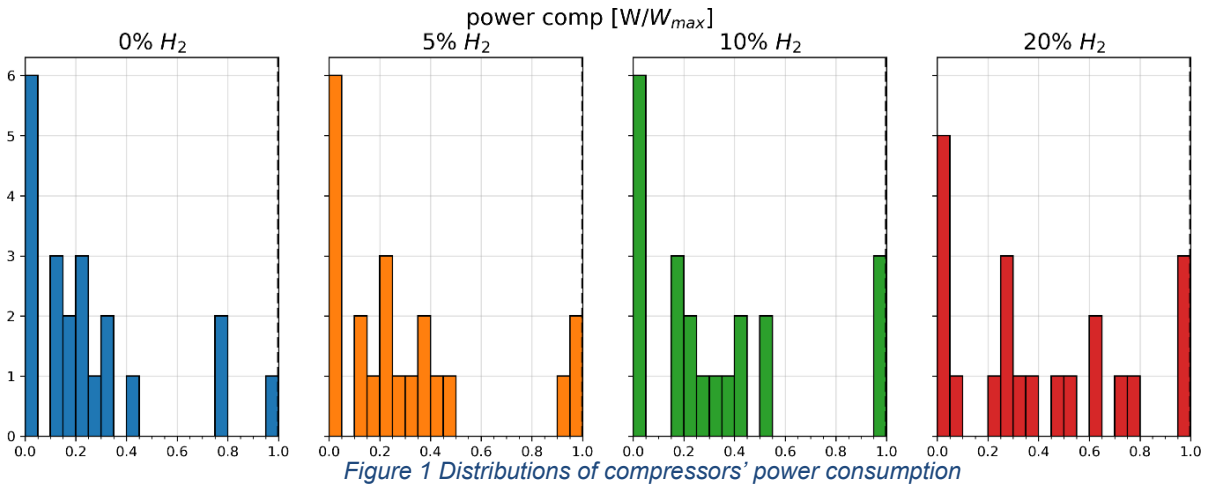


Figure 1 Distributions of compressors' power consumption

(relative to the maximum compressor power), at peak demand, for several NG-H2 blends

Conclusions: The OGF presented can effectively assess the fluid-dynamic feasibility of transporting NG-H_2 blends in large-scale networks.

Moreover, it was demonstrated that not including a linepack usage penalty term in the OGF formulation can yield misleading optimal solutions characterized by unacceptable progressive linepack reduction. OGF models must incorporate linepack management, as solutions showing a decrease in linepack indirectly diminish the pipeline's safety margin, thereby compromising the network's ability to manage unforeseen events. The model demonstrates the fluid-dynamic feasibility of transporting 20% mol H_2, decarbonizing 7.80% of the energy transported by the network.

Acknowledgment References

[1] Guzzo G, Cheli L, Carcasci C. Hydrogen blending in the Italian scenario: Effects on a real distribution network considering natural gas origin. Journal of Cleaner Production 2022;379:134682. https://doi.org/10.1016/j.jclepro.2022.134682.

[2] Cavana M, Leone P. Solar hydrogen from North Africa to Europe through greenstream: A simulation-based analysis of blending scenarios and production plant sizing. International Journal of Hydrogen Energy 2021;46:22618–37. https://doi.org/10.1016/j.ijhydene.2021.04.065.

[3] Arya AK, Katiyar R, Senthil Kumar P, Kapoor A, Pal DB, Rangasamy G. A multi-objective model for optimizing hydrogen injected-high pressure natural gas pipeline networks. International Journal of Hydrogen Energy 2023;48:29699–723. https://doi.org/10.1016/j.ijhydene.2023.04.133.

[4] Tran TH, French S, Ashman R, Kent E. Linepack planning models for gas transmission network under uncertainty. European Journal of Operational Research 2018;268:688–702. https://doi.org/10.1016/j.ejor.2018.01.033.

[5] Wächter A, Biegler LT. On the implementation of an interior-point filter line-search algorithm for large-scale nonlinear programming. Math Program 2006;106:25–57. https://doi.org/10.1007/s10107-004-0559-y.

European Fuel Cells and Hydrogen
PIERO LUNGHI CONFERENCE
September 17th–19th 2025
Capri / Italy

Experimental Study on the Effects of Hydrogen in Gas Distribution Customer Service Lines: Stratification in Risers and Meter Aging

Michele Francesconi*[a], Niccolò Taddeucci [a], Carlo Carcasci [a],
Lorenzo Busi[b], Michele Meazzini[b]
* Corresponding author email: michele.francesconi@unifi.it
[a] University of Florence, Department of Industrial Engineering, Via di Santa Marta 3, 50139 Firenze
[b] Centria S.r.l., via I. Cocchi, 14, 52100 Arezzo

Keywords: Gas Distribution Network, Gas Meter Accuracy, Hydrogen Blending, Stratification

Introduction: The injection of hydrogen into existing gas networks, known as hydrogen blending, has been widely proposed as a transitional solution to reduce carbon emissions while facilitating the rapid integration of hydrogen-based technologies. The existing gas grid can tolerate modest hydrogen volume concentrations ($c_{v,H2}$ <10%) without noticeable changes in thermo-fluid properties or gas quality. Nonetheless, several studies have reported functional limitations on components and equipment in high and medium-pressure infrastructure. Conversely, detailed research on the operational impact of hydrogen blending on low-pressure distribution network equipment, particularly in customer service lines, remains limited. This gap directly affects safety and billing accuracy, highlighting two critical aspects of hydrogen blending: (i) mixture stability in vertical risers, where hydrogen's low density may lead to stratification and localized enrichment during withdrawal. Existing studies offer conflicting results on hydrogen stratification, with some reporting significant separation in stagnant conditions, while others suggest the effect does not persist over long periods [1,2]; and (ii) the metrological integrity of domestic gas meters (GMs), as volumetric billing may result in significant composition-dependent errors, with several GM technologies showing accuracy deviations in hydrogen-rich blends [3].

Objectives: This study aims to expand the available dataset and validate it under real operational conditions, testing various blending levels up to $c_{v,H2}$=10%. Accordingly, this work:

- Investigates hydrogen stratification phenomena in vertical gas risers, under stagnation conditions, measuring the difference in concentration of hydrogen from the highest and lowest point in a vertical column over daily and weekly timescales.
- Assessing the accuracy drift of domestic GMs under prolonged exposure to several hydrogen blends, determining the average volumetric flow measurement error.

Material and methods: The experimental activity was carried out at CENTRIA S.r.l. test facility, which included two main modular, separately instrumented operational sections: the vertical riser section and the GMs Section. The experimental setup for the gas riser section consists

of an isolated vertical DN40 steel gas riser, 4 meters high (h_{max}). Gas sampling ports for chromatographic composition analysis are positioned at three sampling points: Pt.1, Pt.2, and Pt.3 (respectively at $h/h_{max}=0.05$, $h/h_{max}=0.5$, and $h/h_{max}=0.95$). Two tests were performed: a high-resolution daily short-term analysis with hourly measurements and a weekly long-term stability test with a 12-hour resolution (*Figure 1a*). Gas composition analysis was performed using an on-site gas chromatograph, which sampled gas at different heights using pure Helium and Argon as carrier gases. Instead, the meters under test (MUT) included two ultrasonic meters (US), one thermal mass meter (TM), and one diaphragm meter (D). Each meter applied temperature-compensated conversions in compliance with MID Directive 2014/32/EU [4]. The tests were conducted using natural gas along with hydrogen blends containing 2% and 10% hydrogen by volume. To simulate real-world conditions, a domestic boiler was operated for two weeks under continuous and 3-hour cycle modes. Metrological drift was assessed before and after through laboratory tests in pure methane at an accredited facility, involving meter removal, acclimatization, testing, and reinstallation.

Results: The results for gas risers confirm the long-term stability of the hydrogen-natural gas mixture. The daily test recorded a maximum concentration difference of less than 0.02% between the highest (Pt.3) and lowest (Pt.1) sampling points, while the weekly test showed differences ranging from -0.335% to 0.336% (*Figure 1b*). The Spearman correlation coefficient (ρ_{sp}= 0.924 - 0.989, p-value < 0.05) indicates a strong positive monotonic relationship.

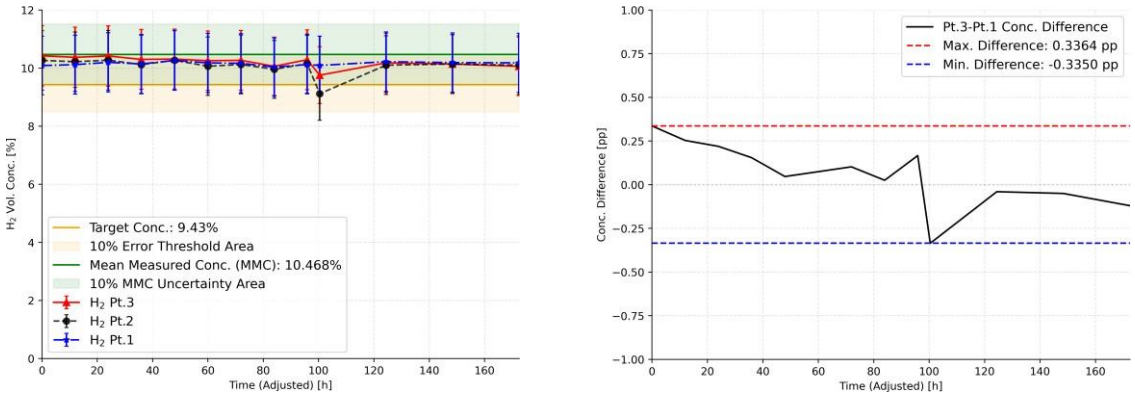


***Figure 1**. Weekly test: (a) concentration profile along the column; (b) end-point difference.*

Field trials show that the thermal-mass meter TM-G4 consistently under-registers, with the error increasing in proportion to $c_{v,H2}$ reaching −22.55 % at 10 vol% H_2, thereby introducing substantial billing inaccuracies (*Figure 2*).

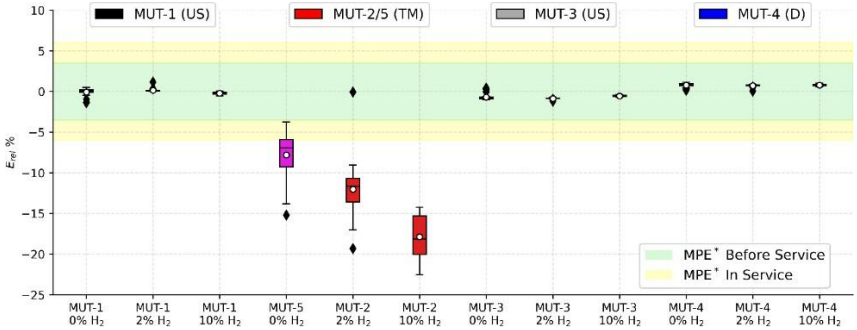


***Figure 2**. Operational metrological drift of various gas meters.*

Ultrasonic and diaphragm meters remain within ±1.5 % deviation and comply with regulatory limits [4]. Complementary laboratory tests before and after hydrogen exposure reveal these findings: the diaphragm meter MUT-4 exhibits pronounced low-flow drift, the thermal-mass MUT-2 stays within its Maximum Permissible Error (MPE), and the ultrasonic units MUT-1 and MUT-3 display a positive drift, with errors diminishing as hydrogen content rises.

Conclusions: Minimal concentration differences and strong monotonic correlation indicate negligible separation effects over time, supporting the feasibility of hydrogen blending in low-pressure networks. Where stratification is absent, proper mixing at injection points ensures uniform hydrogen distribution. Regarding MUTs, field measurement accuracy varies by meter type. Thermal mass meters tend to underestimate flow with higher hydrogen content, while ultrasonic and diaphragm meters maintain deviations within acceptable regulatory limits. However, laboratory tests show that exposure to hydrogen causes some metrological drift, but the impact on fiscal accuracy is limited. Enhancing metering reliability could be achieved with advanced meters that detect hydrogen.

Acknowledgment

This work was funded by the Italian Ministry of Environment and Energy Security through the Ricerca di Sistema Elettrico Nazionale (RdS) program, within the 2022-2024 Triennial Implementation Plan – Hydrogen Technologies Integrated Project.

References

[1] C. Liu et al., «Study on the stratification of the blended gas in the pipeline with hydrogen into natural gas», doi: 10.1016/j.ijhydene.2022.11.074.

[2] S. Peng et al., «Equilibrium distribution and diffusion of mixed hydrogen-methane gas in gravity field», doi.org/10.1016/j.fuel.2023.130193.

[3] G. Ficco, M. Dell'Isola, G. Cortellessa, G. Grossi, P. Kulaga, and J. Jaworski, «Effect of hydrogen blending on the accuracy of smart gas meters», doi: 10.1016/j.ijhydene.2024.03.101.

[4] «Directive 2014/32/EU of 26 February 2014».

European Fuel Cells and Hydrogen
PIERO LUNGHI CONFERENCE
September 17th–19th 2025
Capri / Italy

Effect of hydrogen blending on gas meters accuracy

P. Gislon *[a], V. Cigolotti [a], A. De Marco [a], A. Giaconia [a], G. Monteleone [a] A. Zingone [a],
G. Cortellessa [b], F. Arpino [b], M. Dell'Isola [b], G. Ficco [b], G. Grossi [b],
J. Jaworski [c], P. Kulaga [c], E. Kukulska–Zaja¸c [c], P. Tafani Alunno [d]
* corresponding author: Paola Gislon paola.gislon @enea.it
[a] Department of Energy Technologies and Renewable Sources, ENEA Casaccia, Italy
[b] DICEM, University of Cassino and Southern Lazio, Cassino, Italy
[c] Oil and Gas Institute—National Research Institute, 31-503 Kraków, Poland
[d] Tifernogas Srl Via Rodolfo Morandi, 44/D, 06012 Città di Castello (PG)

Keywords: gas meters; accuracy; natural gas; reliability; hydrogen blending;

Abstract

This study investigates the impact of blending green hydrogen with natural gas (NG) on the accuracy of domestic gas smart meters. Although this practice can reduce greenhouse gas emissions and improve the integration of renewable energy, it can also cause grid imbalances and consumer protection issues due to the possible decay of the meters' accuracy.

Introduction

Decarbonizing energy production and use is worldwide an impelling need to ensure the next generation survival and an equilibrate and long-lasting resources utilization. Among the different paths the European governments are following in a collaborative and synergic process to get this ambitious goal, green hydrogen is recognized to play a crucial role. Hydrogen, when produced in centralized large plants, needs to be stored, transported and distributed to the different end-users. Injecting it into the existing gas grid represents an immediate and cost-saving method to achieve its wide spreading, especially in countries, as Italy, that beneficiates of a capillary gas grid. However, several technological and normative issues need to be addressed to ensure a safe and fiscally correct utilization of the H_2 in natural gas (H2NG) mixture in the current residential appliances, heaters and industrial plants [1].

Objectives

Several research projects and scientific papers addressed the issue of investigating the metrological performance of gas meters with H2NG mixtures. However, available literature has not investigated volumetric and static meters simultaneously in laboratory conditions, with air, NG and NGH2 mixtures. To address this research gap, this study aims at investigating domestic gas meters of different technologies both new and removed for the network with H2NG up to H_2 content of 23% for the first time, as well as the so-called "H_2 ready" thermal-mass gas meters have been investigated for the first time. Finally, a new test facility for assessing gas meter meters performances also with H2NG mixtures was designed, installed and operated at ENEA Casaccia Labs. The newly developed test bench (see Fig.1) is capable to perform tests on gas meters up to 16 m^3/h in air, gas and H2NG with H_2 content up to 20%.

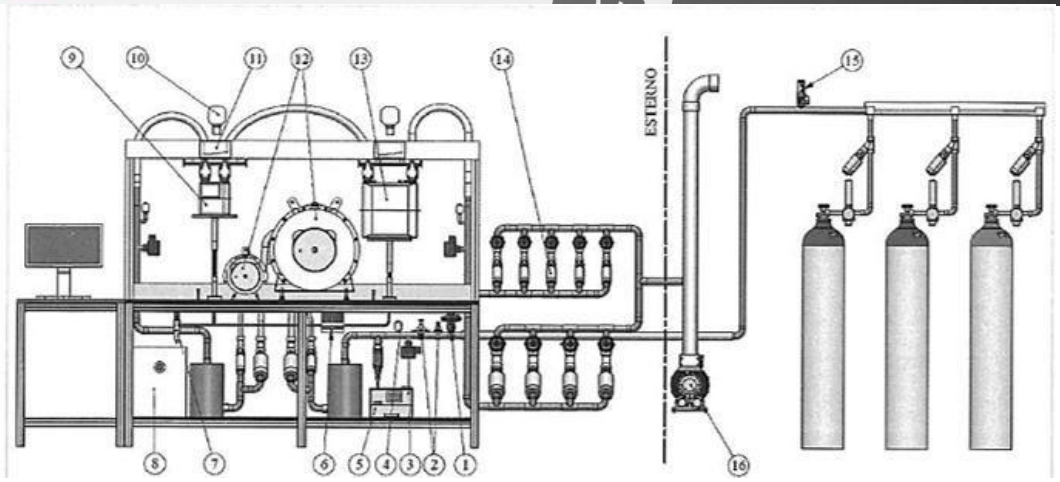


Figure1: Sketch of the gas meter test bench at ENEA Casaccia

Material and Methods

The test facility was realized with the support of BESSEL and TIFERNOGAS of Città di Castello (PG), leading companies in the gas sector for testing and calibration. The gas mixture, coming from the calibrated H2NG cylinders (currently available with H_2 in the range from 0% to 20% vol and odorized with THT=9.7ppmol) passes through the two pressure reduction valves (15 and 2 in the scheme) that reduce the gas pressure from the cylinder pressure (about 200 bar) firstly to 6 bar and subsequently to the typical distribution gas grid operative pressure of 30 mbar. The gas flows through the two meters under test (9 and 13) and then, by opening/closing pneumatic valves (6) in one of the two calibrated master meters (12) circuit branch: a) the Bessel BSM-0 in the range 0.02-0.2 m^3/h, b) the RITTER TG50/5 in the 0.2-16m^3/h range. Both reference master meters guarantee the test uncertainty of the meter under test is within 1/5 of the maximum permissible error (i.e., MPE=±3.0% in the range $Q_{min} < Q \leq Q_t$ and MPE=±1.5% in the range $Q_t < Q \leq Q_{max}$).

The actual gas flow rate is adjusted by setting one of the nine manual valves, the other eights being closed (14). Along the gas path several temperature (PT100) and pressure (capacitor Keller 41X) sensors (3, 4, 7) allow to measure thermo-dynamic conditions of the gas flow aiming at converting the volumes of both the meters under test and the master meter to the standard reference conditions. A dedicated software controls the valves during the run phases, acquires and stores the measurement data, converts the meter reading to the standard temperature and pressure conditions, and calculates errors and related uncertainties. Safety valve (15 and 1) along the gas circuit and an air diluting blower at the out-gas venting ensures safety conditions are kept during tests.

Experimental tests have been first developed at the Department of Flow Metrology of the Oil and Gas Institute in Krakow (PL) to assess how H_2 contents of 2%, 5%, 10% and 23% affect the measuring performances of domestic gas meters. The relative error of the meters was measured at 5 different flow-rates (i.e., Q_{min}, Q_t, 0.4 Q_{max}, 0.7 Q_{max} and Q_{max}), to investigate how MPEs are fulfilled. For gas meters removed from the network MPEs double of those for brand new meters apply. A two phases experimental campaign has been carried

out on three different gas meter types (i.e., diaphragm, ultrasonic and thermal mass: 5 brand-new gas meters [2]; ii) 3 gas meters removed from the network after 6-8 years [3].

Results and Conclusions

The obtained results show that H2NG up to 23% H_2 does not affect significantly the accuracy of both diaphragm and ultrasonic gas meters, being the measured errors within the limits at all tested flow-rate with all gas mixtures. Only, the underestimation at Q_{min} increases as the H_2 content increases, due to the high volatility of H_2. On the other hand, a good reliability of the first-generation thermal mass gas meters has been found only at H_2 content lower than 2%vol, which is the current admitted limit in the national grid. For higher H_2 contents, very large errors and exceeding the admitted limits were found (see Fig. 2). Furthermore, error increases as the H2 content in the mixture increases. A notable result is that the "H_2 ready" thermal mass gas meters equipped with a specific second- generation sensor exhibited accuracies within the admitted limits. On the other hand, WME always positive were found as well as the gas-air relationship (i.e., the difference between errors in gas and in air) was positive at all flowrates, with errors in gas always higher than those in air.

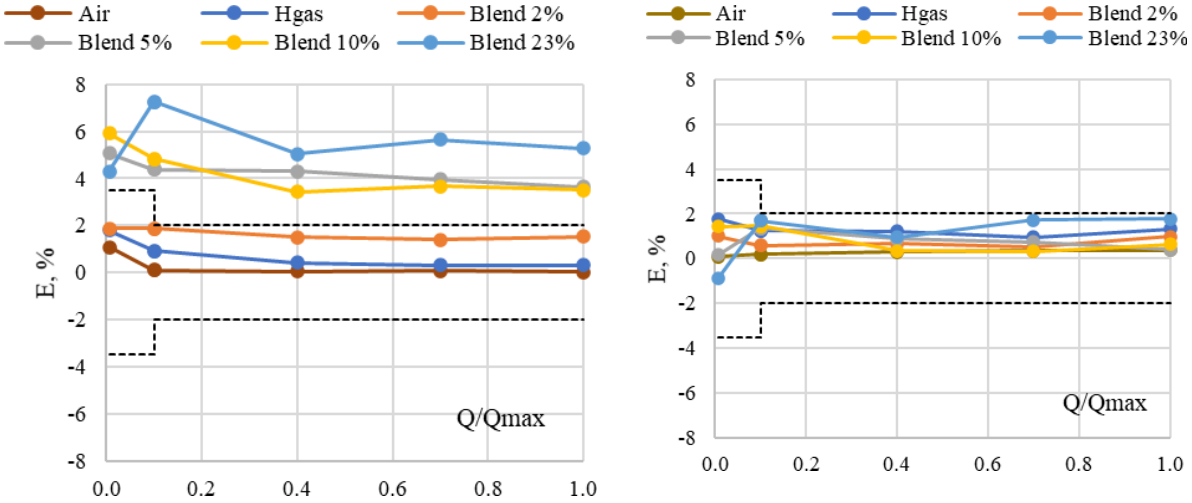


Figure 2: Error trend of thermal mass gas meters: a) I generation sensor; ii) II generation "H2 ready" sensor

Acknowledgements

This work was funded by the Italian Ministry of Environment and Energy Security through Ricerca di Sistema Elettrico (RdS), 2022-2024 Integrated project 1.3: Hydrogen Technologies.

References

[1] Dell'Isola, M.; Ficco, G.; Moretti, L.; Jaworski, J.; Kułaga, P.; Kukulska–Zaja¸c, E. Impact of Hydrogen Injection on Natural Gas Measurement. Energies 2021, 14, 8461.
[2] Ficco, G., Dell'Isola, M., Cortellessa, G., Grossi, G., Kulaga, P., Jaworski, J. Effect of hydrogen blending on the accuracy of smart gas meters (2024) International Journal of Hydrogen Energy, 62, pp. 892-903.
[3] Ficco, G.; Dell'Isola, M.; Graditi, G.; Monteleone, G.; Gislon, P.; Kulaga, P.; Jaworski, J. Reliability of Domestic Gas Flow Sensors with Hydrogen Admixtures. Sensors 2024, 24, 1455.

EFCH2 2025 European Fuel Cells and Hydrogen
PIERO LUNGHI CONFERENCE
September 17th–19th 2025 Capri / Italy

TiFe-based alloys for solid-state hydrogen storage in industrial applications: the innovative REMEDHYS project towards a circular economy

Alessandra Nico*[a], Francesca Garelli [a], Erika M. Dematteis[a], Marcello Baricco[a], Paola Rizzi[a]

* corresponding author: Alessandra Nico
[a] University of Turin

Keywords: metal hydrides, hydrogen, REMEDHYS project, TiFe-based alloys for solid-state hydrogen storage

Abstract

Introduction: The continuous growth of the global population necessitates an increasing energy demand to sustain modern life. To mitigate the environmental impact of fossil fuels, renewable energy sources, such as solar, wind, and biomasses, offer a clean, sustainable, and abundant alternative. However, many renewable sources are intermittent, requiring integration with complementary energy solutions and advanced storage systems to ensure a stable supply. Hydrogen has emerged as a promising energy carrier, due to its high gravimetric energy density and its exothermic reaction with oxygen to produce only water making it particularly suitable for fuel cell applications. With an energy-to-weight ratio surpassing that of methane and gasoline, hydrogen is increasingly considered for large-scale storage and distribution. Nonetheless, its widespread adoption faces challenges, particularly regarding efficient and cost-effective storage solutions. Among various storage methods, such as in liquid phase and compressed gas, solid-state hydrogen storage using metal hydrides demonstrates a very high potential in terms of safety and energy consumption [1]. Interstitial hydrides, infact, achieve volumetric capacities of 70 - 150 gH_2/L, significantly outperforming compressed (40 gH_2/L at 70 MPa) and liquid hydrogen (71 gH_2/L) storage. Additionally, metal hydrides store hydrogen at much lower pressures (3 - 30 bar) compared to compressed gas (up to 700 bar), enhancing safety and operational feasibility **[²]**. Their ability to reversibly store hydrogen under ambient conditions makes them particularly advantageous for stationary energy storage applications.

Objectives: In the context of growing environmental awareness, the **REMEDHYS** collaborative project started in 2025 (Horizon Europe grant agreement n°101192503, supported by Clean Hydrogen Partnership) has emerged with the objective of developing a modular hydrogen storage system with a capacity of 100 kg H_2. This initiative focuses on

utilizing solid-state hydrogen storage solutions based on metal hydrides (MHs) integrated with a 2 MW PEM electrolyser located in Cuxhaven, Germany, which supplies H_2 to vessels of the hydrogen-powered offshore service Coastal Liberty. The project will implement an innovative approach in the production of MHs, by employing recycled starting materials sourced in Europe, ensuring both cost efficiency and sustainability. As mentioned before REMEDHYS is a collaborative project that builds on a consortium of four Research Centres (*Institutt for Energiteknikk* [**IFE** the coordinator], *Helmholtz-Zentrum hereon GmbH* [**HEREON**], *Institut de Chimie et des Matériaux Paris Est* [**CNRS**], *Fondazione Bruno Kessler* [**FBK**]), two Universities (*Università degli Studi di Torino* [**UNITO**], *Université de Paris-Est Créteil* [**UPEC**]), and four partners from industry (Pometon SpA [**POM**], *Stühff Maschinen- und Anlagenbau GmbH* [**SMAB**], *Ingenion Hydrogen GmbH* [**ING**], *MetHydor srl* [**MET**]) covering a wide range of disciplines in chemistry, phisics, engineering, energy and the key aspects of the value chain. The project focuses on engaging industry, local authorities, citizens and other relevant stakeholders to promote the use of hydrogen as an energy carrier and to define suitable roadmaps to prepare the deployment of cost-efficient MH-based hydrogen storage solutions. In this study, a potential material based on TiFe alloys, suitable for the requirements of the REMEDHYS project, is presented. From a circular economy perspective, the primary challenge lies in utilizing recycled materials, while maintaining impurity levels that do not adversely affect the hydrogen sorption properties of the solid carrier, thereby ensuring the feasibility of this approach for sustainable hydrogen storage solutions. Therefore, the preliminary part of the study is dedicated to a survey of the possible scraps present in the market, taking into account compositions, prices and provenance. Various metal scraps were examined, originating from a lathe machining process that exhibited variations in shapes, size, and oxidation state.

Material and methods: The request specifically concerned Ti grade 2 or, at most, grade 4 (as higher oxygen levels could promote the formation of oxides that facilitate the activation mechanism [3]) and pure Fe. The primary objective was to conduct a preliminary analysis to assess material purity, verify the homogeneity of their composition within the received batch, and to determine impurity levels. The samples were analysed using *Scanning Electron Microscopy* (Tescan Vega), complemented by chemical composition analysis via *Energy Dispersive X-ray Spectrometry* (EDX) using *Aztec software* (Oxford Instruments).

Results: The results confirmed the presence of 100% Ti in square-shaped scraps, while the iron, identified as mild steel (S235) in spiral-shaped form, contained 0.4% Mn and 99.60% Fe, as expected for this type of steel. Despite originating from recycled materials, the high quality of these scraps enabled the synthesis of the TiFe alloy using the *arc melting* method. Subsequent SEM, SEM-EDX, and *Powder X-ray Diffraction* (XRD) analyses identified an optimal microstructure, with the presence of the β-Ti phase, which facilitates alloy activation **[4]**. *Pressure Composition Temperature* analysis (PCT-Pro by Setaram) confirmed that the alloy

exhibits favourable hydrogen absorption and desorption properties, supporting the potential of recycled metals as promising materials for synthesizing TiFe alloy.

Conclusions: The challenge was also to develop and evaluate different methods for melting metal scraps, using various techniques, including an *induction melting furnace* (TOPCAST), a *tube furnace* (Carbolite Gero), and *melt spinning*. These methods were compared with the conventional *arc melting* process, which is currently widely used for metal melting. The objective was to determine the most suitable methodology based on several key factors: achieving the best microstructure (analysed via SEM), optimizing the melting process to enhance the formation of secondary phases that could improve activation kinetics (evaluated through SEM-EDX and XRD analysis), and obtaining the best sorption properties (assessed using PCT analysis) for future industrial applications. By employing recycled materials and optimizing metal hydride-based storage solutions, the REMEDHYS project will open the way to a cleaner, more efficient energy future where hydrogen will become a key driver of the global transition toward sustainability.

Acknowledgment

This project has received funding from the European Union's Horizon Europe research and innovation program under grant agreement No 101192503. The project is supported by the Clean Hydrogen Partnership and its members. Funded by the European Union. Views and opinions expressed are however those of the author(s) only and do not necessarily reflect those of the European Union or CLEANH2. Neither the European Union nor the granting authority can be held responsible for them.

References

[1] Drawer, C.; Lange, J.; Kaltschmitt, M. Metal Hydrides for Hydrogen Storage – Identification and Evaluation of Stationary and Transportation Applications. *Journal of Energy Storage* **2024**, *77*, 109988. https://doi.org/10.1016/j.est.2023.109988.

[2] Sujan, G. K.; Pan, Z.; Li, H.; Liang, D.; Alam, N. An Overview on TiFe Intermetallic for Solid- State Hydrogen Storage: Microstructure, Hydrogenation and Fabrication Processes. *Critical Reviews in Solid State and Materials Sciences* **2020**, *45* (5), 410–427. https://doi.org/10.1080/10408436.2019.1652143.

[3] Davids, M. W.; Lototskyy, M. Influence of Oxygen Introduced in TiFe-Based Hydride Forming Alloy on Its Morphology, Structural and Hydrogen Sorption Properties. *International Journal of Hydrogen Energy* **2012**, *37* (23), 18155–18162. https://doi.org/10.1016/j.ijhydene.2012.09.106.

[4] Murray, J. L. The Fe–Ti (Iron-Titanium) System. *Bulletin of Alloy Phase Diagrams* **1981**, *2* (3), 320–334.

TOPIC 3 : FUEL CELLS TECHNOLOGIES

EFCH2 2025
European Fuel Cells and Hydrogen
PIERO LUNGHI CONFERENCE
September 17th–19th 2025
Capri / Italy

Advanced Core-Shell Structured Electrocatalysts for Oxygen Reduction Reaction: Influence of Core Size, Nitrogen Doping, and Carbon Shell Engineering

Yongmin Kwon [a,b], Eunjik Lee [a], Iksung Lim [a], Jiye Choi [a], Eunbi Park [a], Jungmin Han [a], and Gu-Gon Park *[a,b],

* corresponding author: Gu-Gon Park

[a] Hydrogen Fuel Cell Laboratory, Korea Institute of Energy Research (KIER), Daejeon 34129, Republic of Korea

[b] Task 31 Member, Advanced Fuel Cells Technology Collaboration Programme

Keywords: Core-shell structure, Fuel Cells, Nanocatalysts, Oxygen Reduction Reaction

Abstract:

Advancing the performance and durability of oxygen reduction reaction (ORR) catalysts is essential for the commercialization of proton exchange membrane fuel cells (PEMFCs). This study systematically investigates four strategies—core-shell structure optimization, nitrogen doping, carbon shell engineering, and carbon encapsulation—to enhance catalytic efficiency and stability. Pd@Pt catalysts revealed that increasing Pd core size improves Pt shell durability by mitigating leaching. FePt@Pt catalysts demonstrated that nitrogen doping effectively suppresses metal dissolution, surpassing DOE durability targets. Carbon shell optimization in Pt@C catalysts, particularly at 400 °C, minimized Pt aggregation and enhanced stability. Similarly, PtNi@C catalysts encapsulated with thin carbon layers exhibited superior durability even after 90k accelerated stress cycles. By integrating these approaches, this work presents a comprehensive design roadmap for robust and scalable ORR electrocatalysts suitable for next-generation PEMFC applications.

Introduction:

Fuel cells hold great potential as clean energy solutions, but their widespread adoption depends on overcoming performance and durability challenges in electrocatalysts. The oxygen reduction reaction (ORR) is particularly crucial, requiring catalysts that combine high activity with long-term stability. Several approaches have been explored to achieve this goal, including core-shell structures, alloying, and carbon encapsulation. This study investigates how these strategies—specifically, Pd core size optimization, nitrogen doping in FePt intermetallic catalysts, carbon shell engineering in Pt@C catalysts, and carbon encapsulation in PtNi@C catalysts—can be leveraged to enhance catalyst performance. By understanding the synergies among these techniques, we aim to provide a roadmap for the development of next-generation fuel cell catalysts.

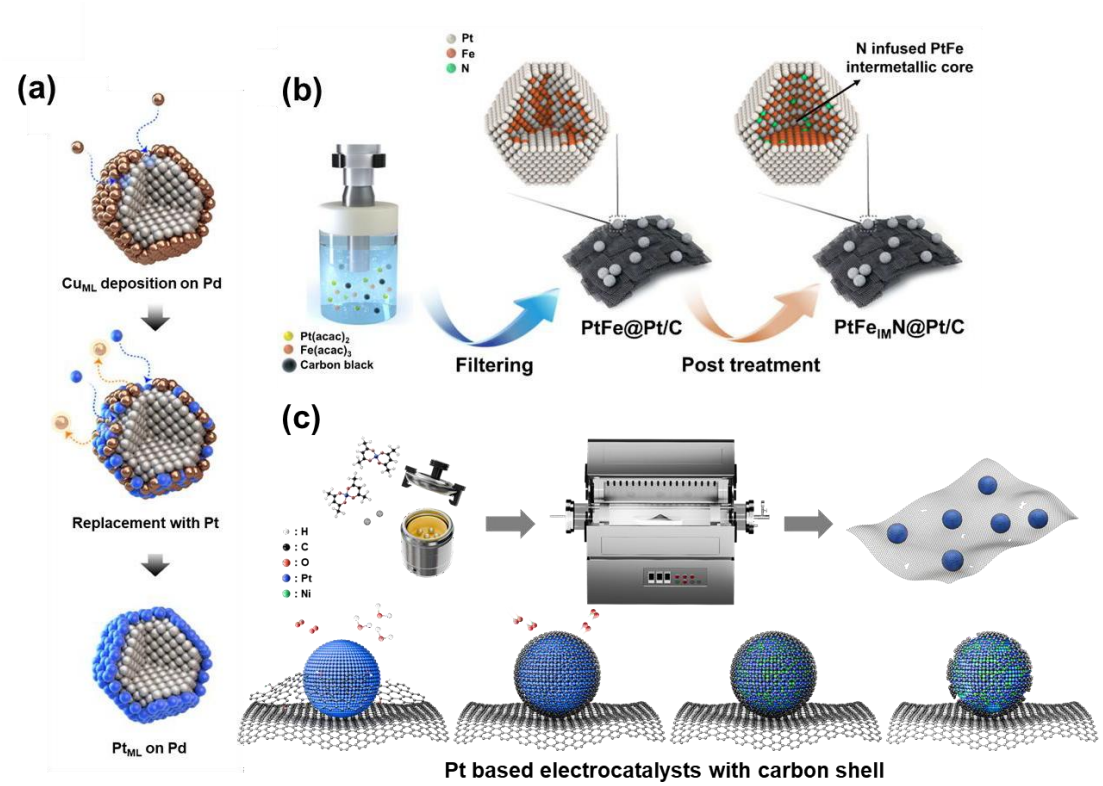


Figure. Schematic overview of catalyst design strategies for ORR enhancement. (a) Pd@Pt core–shell catalyst synthesis via Cu underpotential deposition and Pt monolayer replacement. (b) Preparation of nitrogen-doped FePt@Pt/C catalysts using precursor co-deposition, filtration, and NH_3-assisted heat treatment. (c) Carbon shell engineering of Pt-based catalysts through solid-state synthesis and thermal treatment to form stabilized carbon-encapsulated nanoparticles.

Objectives: The primary objective of this study is to improve ORR catalyst performance by fine-tuning structural and compositional parameters. The Pd@Pt system was analyzed to determine the effect of core size on Pt monolayer stability and catalytic efficiency. FePt@Pt catalysts were studied to assess how nitrogen doping influences metal dissolution resistance and durability. The Pt@C catalysts were evaluated to understand the role of carbon shell engineering in stabilizing Pt nanoparticles, while PtNi@C catalysts were developed to investigate how carbon encapsulation enhances alloy catalyst longevity. Through these investigations, we aim to establish a unified approach to designing robust and scalable PEMFC electrocatalysts.

Material and methods: Pd@Pt Core-Shell Catalysts: Pd nanoparticles of varying core sizes (3.8 nm and 4.9 nm) were synthesized via a CO-assisted reduction method, followed by Cu underpotential deposition (UPD) to form a Pt monolayer. FePt@Pt Core-Shell Catalysts: High-loading (>50 wt%) FePt intermetallic nanoparticles were synthesized via ultrasound-assisted polyol synthesis, with subsequent annealing, acid washing, and nitrogen infusion using NH_3 gas. Pt@C Catalysts: A dry synthesis process involving ball-milling Pt precursors with carbon black, followed by heat treatment (200–800 °C), was used to control carbon shell structure. PtNi@C Catalysts: A solid-state synthesis approach was used, in which PtNi nanoparticles (~3 nm) were encapsulated within carbon shells via high-temperature treatment to improve stability and performance. Electrochemical Characterization: All catalysts were analyzed using a rotating disk electrode (RDE) in a three-electrode setup. Cyclic voltammetry (CV) and linear sweep voltammetry (LSV) were performed in 0.1 M $HClO_4$ at room temperature to determine electrochemical surface area (ECSA), mass activity (MA), and specific activity (SA). Durability was assessed using an accelerated stress test (AST) involving 30k–90k cycles between 0.6 V and 0.95 V (vs. RHE).

Results: Achieving a balance between catalytic activity and long-term durability is crucial for advancing fuel cell technologies. The findings of this study illustrate how various material modifications can contribute to this goal.

For Pd@Pt core-shell catalysts, the results indicate that core size significantly affects catalyst stability. While smaller Pd cores (3.8 nm) initially exhibited higher ORR activity, they experienced greater Pt-shell degradation over time. Conversely, larger Pd cores (4.9 nm) provided improved durability by mitigating Pt leaching and preserving structural integrity. These findings underscore the importance of optimizing core-shell architectures for practical applications.

In FePt@Pt catalysts, nitrogen doping proved to be an effective strategy for improving catalyst stability. The PtFeIMN@Pt/C_600 °C catalyst, featuring a nitrogen-doped PtFe intermetallic core, exceeded the 2020 US DOE durability targets. The nitrogen infusion reinforced the structural stability of the catalyst, reducing metal dissolution and enhancing long-term performance.

The role of carbon shell engineering was examined in Pt@C catalysts, where a thermal treatment at 400 °C was found to yield the most stable configuration. This process effectively minimized Pt nanoparticle aggregation while maintaining catalytic efficiency, demonstrating how carbon structures can be tailored to improve catalyst performance.

For PtNi@C catalysts, carbon encapsulation emerged as a key factor in enhancing alloy catalyst longevity. The sub-3 nm PtNi nanoparticles, encased in thin carbon shells, displayed remarkable stability, with minimal loss of ECSA and MA even after 90k AST cycles. These

findings confirm that carbon encapsulation is a highly effective approach for improving catalyst durability and performance.

Ultimately, this study provides a comprehensive perspective on the interplay between core-shell design, nitrogen doping, and carbon encapsulation. By integrating these approaches, we offer a roadmap for the rational design of high-performance electrocatalysts that can meet the demanding requirements of PEMFC applications.

Conclusions: This study demonstrates the effectiveness of core-shell engineering, such as size-controlled core-shell, nitrogen doping, and carbon encapsulation in developing advanced ORR electrocatalysts. Optimizing the Pd core size has been shown to enhance catalyst durability by reducing Pt leaching and structural degradation. Nitrogen doping significantly improves the stability of FePt@Pt catalysts, allowing them to meet DOE durability standards. Carbon shell engineering plays a crucial role in preventing Pt nanoparticle aggregation, thereby enhancing the stability of Pt@C catalysts. Additionally, carbon encapsulation is a key factor in improving the long-term performance of PtNi@C catalysts, making them strong candidates for commercial PEMFC applications. By systematically analyzing these approaches, this study provides valuable insights into the rational design of electrocatalysts, contributing to the advancement of highly efficient and durable PEMFC systems capable of meeting future energy demands.

References

[1] Choi, J., Lee, E., Woo, S., Whang, Y., Kwon, Y., Seo, M., Cho, E., & Park, G.-G. (2025). Effect of palladium core size on the activity and durability of Pt-Monolayer electrocatalysts for oxygen reduction reaction. Applied Surface Science, 689, 162477. DOI: 10.1016/j.apsusc.2025.162477

[2] Lee, H., Kim, S., Lee, E., Lim, I., Yim, S.-D., Kang, Y.S., & Park, G.-G. (2025). Scalable synthesis of robust, high-loading nitrogen-infused intermetallic FePt@Pt (core@shell) catalyst for proton exchange membrane fuel cells. Journal of Power Sources, 625, 235652. DOI: 10.1016/j.jpowsour.2024.235652

[3] Park, E., Lee, E., Han, J., Whang, Y., Kwon, Y., Kim, N., An, B.-S., Jung, N., & Park, G.-G. (2025). Temperature-dependent carbon shell engineering for highly durable Pt@C catalysts in the oxygen reduction reaction. Applied Surface Science, 698, 163043. DOI: 10.1016/j.apsusc.2025.163043

[4] Han, J., Lee, E., Park, E., Whang, Y., Kwon, Y., Kim, N., An, B.-S., Jung, N., & Park, G.-G. (2025). Carbon encapsulation dynamics for the solid-state synthesis of high-loading sub-3 nm PtNi alloy electrocatalysts. Journal of Power Sources, 653, 237787. DOI: 10.1016/j.jpowsour.2025.237787

European Fuel Cells and Hydrogen
PIERO LUNGHI CONFERENCE
September 17th–19th 2025
Capri / Italy

Quantification and visualization of ionomer distribution in catalyst layers of PEMFCs

Q. Zhao[a,b], T. Morawietz[a], J. Sanchez Monreal[a], K. A. Friedrich[a,b], P. Gazdzicki*[a]

* corresponding author: pawel.gazdzicki@dlr.de
[a] DLR, Institute of Engineering Thermodynamics, Stuttgart, Germany
[b] University of Stuttgart, Institute of Building Energetics, Stuttgart, Germany

Keywords: AFM, catalyst layer, Ionomer, PEMFC

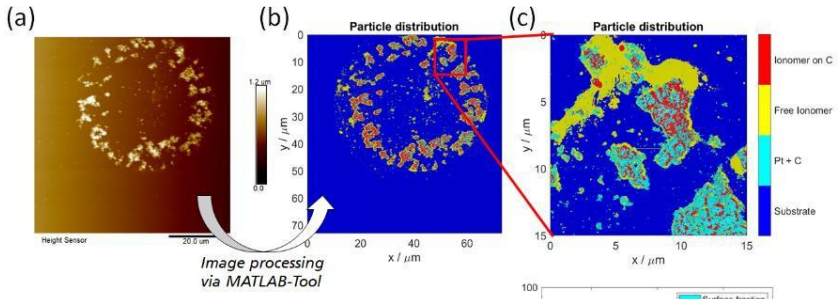
Abstract:
In this work, an approach for the differentiation and quantification of ionomer adsorbed on Pt/C and free ionomer in catalyst layers of PEMFCs is investigated. In order to determine the position of the ionomer in relation to Pt/C, a model system is introduced in which individual ink droplets are applied to a platinum substrate by inkjet printing. The results are compared with the analysis of the catalyst layers which are related to the electrochemical performance. The correlation between the IPA content used in the ink and the resulting CL ionomer coverage shows the potential of tuning the ionomer distribution when using inkjet printing as a deposition technique by adjusting the solvent composition.

Introduction: Ionomers play an important role in binding the catalysts and providing proton conduction pathways in the catalyst layers (CLs) of proton exchange membrane fuel cells (PEMFCs). Its specific adsorption on the Pt surface can lead to poisoning of the catalyst and thick ionomer films can hinder O_2 access to the catalyst surface at cathode CL. In this context, not only the choice of an appropriate ionomer-to-carbon ratio but also the choice of solvent composition in the ink is crucial for control of ionomer distribution, which influences the coverage of the catalyst and determines the electrochemical performance. To analyse ionomers in CLs with local resolution, AFM has proven to be a suitable method [1]. Nevertheless, it is still a challenge to separate non-adsorbed and adsorbed ionomers on Pt/C. To bridge this gap, an approach to distinguish ionomer adsorbed on Pt/C from free ionomer and to quantify their contents at different IPA/water ratio of the used ink is explored.

Objectives: The goal of this study is to demonstrate an approach to analyse the distribution of ionomer in CL and to determine fractions of ionomer not attached to Pt/C (free ionomer) and ionomer adsorbed to Pt/C (ionomer-Pt/C) by using atomic force microscopy (AFM) and data processing using a developed MATLAB tool.

Material and methods: CLs on membrane were prepared by inkjet printing technique with inks containing various IPA contents, and the impact of IPA contents on electrochemical performance was investigated in single cell. For more detailed analyses individual ink drops were printed onto a Pt substrate (15 nm Pt sputtered on Si-Wafer) using the same inks as for the catalyst layer and then characterized by AFM and evaluated using a developed MATLAB tool allowing to quantify the influence of varying IPA/H_2O on the ionomer distribution and ratio of free ionomers to adsorbed ionomers. This approach is possible due to using IJP which is a drop-on-demand method able to deposit individual ink drops or entire CLs using the same type of ink [2].

Results: Distribution of ionomer in catalyst and determination of free ionomer and ionomer-Pt/C was conducted using a combination of AFM measurements and data processing using a dedicated developed MATLAB tool; in Figure 1 (a) a typical AFM image of an ink drop on a Pt substrate is shown. The AFM data processed using MATLAB and applying selection rules based on selected AFM measuring channels (see Figure 1 (d) as an example) is shown in Figure 1 (b) and (c). In Figure 1 (e) an example of the quantification of components is provided. The results obtained in individual drops were compared with AFM analysis ink drops on Nafion and of CL cross-sections (not shown). Eventually, electrochemical characterisation of the corresponding MEAs was performed.



Parameter	Channel	Threshold
Particle	Height	≥5 nm
Conductivity	Peak current	>50 pA
	TUNA current	>5 pA
Large particle	Height	≥200 nm

Figure 1: Methodology to determine ionomer distribution in catalyst layers. (a) Height (topology) AFM image of an entire ink droplets deposited onto Pt film, (b) AFM topology and electrical conductivity data of the ink droplet processed via a MATLAB tool, (c) enlarged image showing regions containing ionomer-Pt/C, free ionomer, and uncovered Pt/C, (d) Example of selection rules to determine CL ink components, (f) quantification of volume and surface fractions of CL ink components.

While the CL ionomer coverage (from CL cross-sections, not shown) shows a strong linear correlation with the IPA content used for the ink during printing (Figure 2(a)), the surface fractions of free ionomer and ionomer-Pt/C (determined from individual drops) strongly depend on specific threshold values; in Figure 1(e) a height threshold of 200 nm was chosen as an example to determine free-ionomer. However, to adjust the threshold additional AFM measuring channels should be included into the analyses. Hence, a link between the results obtained from individual inks and results based in CL cross sections is not straight forward. In

this study, ECSA and performance increase with decreasing CL ionomer coverage in the CL until a coverage of 42% is reached; below that value, cell voltages and ECSA drop suddenly (Figure 2(c)). The behaviour of charge transfer resistance, Rct, is opposite (Figure 2(b)). On the other hand, increase of CL ionomer coverage from 41% to 53% leads to a 4-fold drop in proton transport resistance, R_{H+}, in the CL (Figure 2(c)).

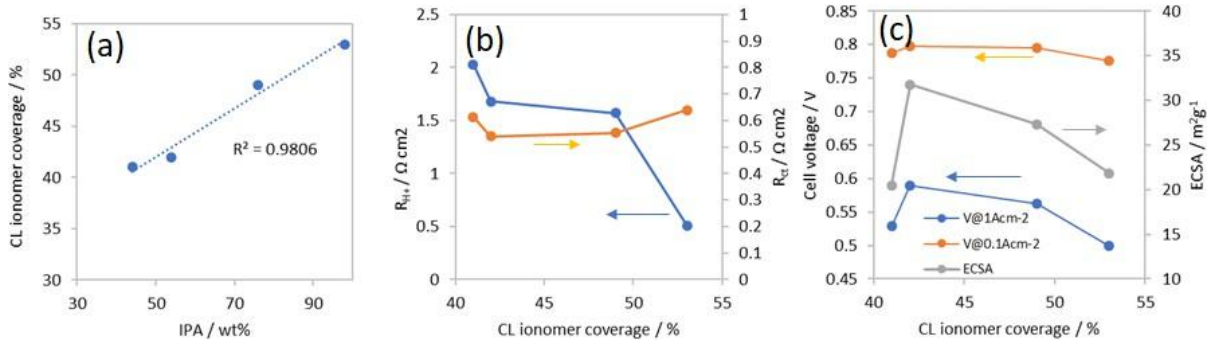


Figure 2: (a) Relationship between ionomer coverage in CLs (determined from CL cross section) and IPA content of the used ink. (b) protonic and mass transport resistance (measured at 0.1Acm-2) and (c) cell voltages and ECSA as a function of ionomer coverage in CL cross-sections.

Conclusions: The impact of water:alcohol ratio of deposited ink on ionomer distribution in the CL was quantitatively analysed via AFM and linked with electrochemical performance. The correlation between IPA content of the ink and the resulting CL ionomer coverage shows the potential of tuning ionomer distribution when using ink jet printing as deposition technique. A careful adjustment of ionomer CL coverage is needed to find the trade-off between proton conductivity and mass transport limitation and ECSA. While the overall ionomer coverage in CL cross section could be linked to cell performance, the quantitation of ionomer in individual ink droplets strongly depends on specific threshold values of involved AFM measuring channels. Apparently, height and conductivity are insufficient for a reliable quantification of ionomer. Hence, additional AFM measuring channel such as DMT modulus, adhesion or deformation, have to be considered for more detailed analyses.

Acknowledgment:

This work was financially supported by the DAAD-DLR scholarship. The research leading to these results was supported by the project PEMTASTIC (Grant Agreement No. 101101433), funded by the Clean Hydrogen Partnership and its members Hydrogen Europe and Hydrogen Europe Research.

References

[1] T. Morawietz, M. Handl, C. Oldani, K.A. Friedrich, R. Hiesgen, Fuel Cells 18 (2018) 239.

[2] Q. Zhao, T. Morawietz, P. Gazdzicki, K.A. Friedrich, Journal of Power Sources 625 (2025) 235624.

European Fuel Cells and Hydrogen
PIERO LUNGHI CONFERENCE
September 17th–19th 2025
Capri / Italy

Thermal integration of pemfc and metal hydrides systems for maritime applications

Stefano Barberis [a], Silvia Crosa [a], Federico Iester [a], Loredana Magistri [a], Massimo Rivarolo *,[a]
* corresponding author: massimo.rivarolo@unige.it
[a] Thermochemical Power Group (TPG)-DIME, via Montallegro 1, University of Genoa (IT)

Keywords: PEM Fuel Cell, Maritime Hybridization, Thermal Management, Metal Hydrides.

Abstract

This study explores the design and management of a hybrid system integrating Proton Exchange Membrane Fuel Cells (PEMFC) and diesel Internal Combustion Engines (ICE) for short-travel ferries. The system relies on hydrogen storage via metal hydrides (MH) and employs waste heat recovery from the ICE to heat a Thermal Energy Storage (TES) for efficient energy management. The system is simulated in different scenarios to understand the best control strategy, considering to heat the MH in the start-up condition via TES before reaching the self-sustaining condition in which the PEMFC heat is sent to the MH tanks.

Introduction: Research has focused on new solutions for reducing GHG emissions, especially in the maritime sector, to meet the challenging 2040 requirements [1]. This motivation suggests the possibility of adopting new technologies with alternative low-carbon fuels, i.e. H2 fuel cells. The focus of this work is on utilizing metal hydrides to supply PEMFC in port, aiming to reduce emissions [2].

Objectives: A dynamic model in MATLAB-Simulink was developed to simulate transient operations, demonstrating the performance and emission reduction benefits of the hybrid system in a real case study. The simulation considers different control logics and operational strategies to optimize thermal management between ICE and PEMFC, minimizing fuel consumption. The study analyses real operational data from ferries in coastal regions, focusing on power requirements and operational patterns. During port manoeuvres, power demand reaches almost 25% of nominal capacity (P_{el} = 640 kW out of 3.1 MW in navigation addressed by ICE) and, while cruise navigation spans from 20 minutes to 2 hours, port operations can last up to 50 minutes.

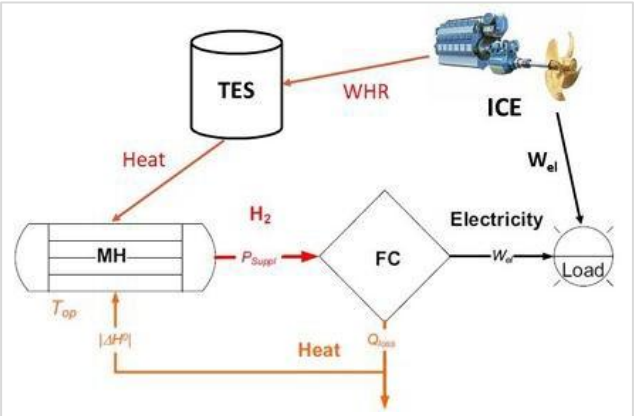


Figure 1. Schematic representation of the integrated system.

Material and methods: The model includes the main devices: MH, PEMFC, TES and auxiliary components such as heat exchangers and valves. The control logic uses the load profile and send the H_2 request to the MH, regulating the temperature according to its dynamics for start-up. Particular focus is placed on modelling the MH storage and the PEMFC systems, along with the thermal balance to assess waste heat utilization and overall system efficiency. The ICE is not considered in the model except for the heat input to the TES, assumed at 70 °C.

The MH model uses experimental Pressure-Composition-Temperature (PCT) curves of Fe-Ti powder system, provided by Methydor company [3], to evaluate H_2 absorption and desorption; the geometry for the heat exchange considers the heat flux to pass through the centre of the cylindrical MH divided in many racks. The H_2 flux released is evaluated with the orifice equation and the mass flow rate that is responsible of the input heat is controlled according to the hydrogen request. An additional control on the storage system is imposed to avoid not physically feasible behaviour in terms of minimum temperature for start supplying, set at 40 °C, and to meet the operational pressure of the fuel cell (2.5 bar). A preliminary study tested the required time for the storage to be ready, using as parameter the mass flow rate of water that comes from the TES (T_{out_TES} fixed at 60 °C) to preheat the tanks (Figure 2). The FC model was developed for previous work by the authors' research group [4] [5] and was calibrated on the datasheet values of commercial MARINE System 200 by PowerCell Group [6], assuming to install four modules and make it work at nominal voltage value of 0.7V.

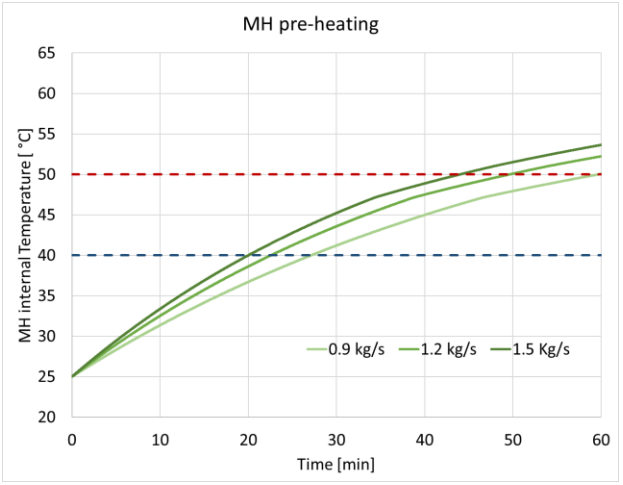


Figure 2. Pre-heating of MH with different mass flow rates from TES. At 40 °C the MH model is allowed to supply H_2.

Results: A real case study has been simulated, and the main outputs are presented in Figure 3. The MH model successfully meets the hydrogen demand by PEMFC, though it requires a certain amount of heat ($P_{th_TES} = P_{th_MH} + P_{th_FC}$). During the startup phase, this heat must be supplied by the TES; only afterward the PEMFC becomes self-sustaining and capable of generating heat, which can then be stored in the TES. Given the cold-startup duration, which requires a few minutes, plus the load ramp-up time (assumed to be 10 A/s) of nearly one minute, the control logic switch on the FC system in advance to match the port entering time. While the startup phase consumes a small amount of hydrogen, this approach ensures zero emissions in port.

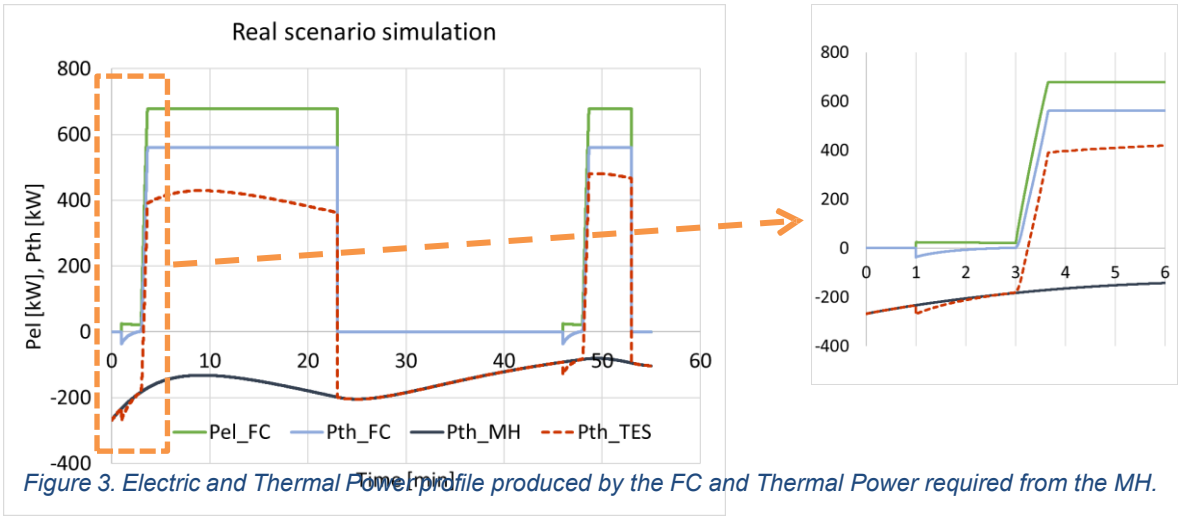


Figure 3. Electric and Thermal Power profile produced by the FC and Thermal Power required from the MH.

Conclusions: The study demonstrates the feasibility of a hybrid energy system integrating PEMFC and diesel ICE for short-travel ferries, adopting MH for H_2 storage (lower risk compared to pressurized H_2) and TES for efficient thermal management. The simulation results highlight the importance of optimizing the control strategy to ensure a correct startup while minimizing hydrogen consumption. The TES effectively supports the MH during startup, allowing the system to transition to a self-sustained state. By activating the fuel cell ahead of demand, the system achieves zero emissions during port operations.

Acknowledgments: The Authors acknowledge financial support under the National Recovery and Resilience Plan (NRRP), Mission 4, Component 2, Investment 1.1, Call for tender No. 1409 published on 14.9.2022 by the Italian Ministry of University and Research (MUR), funded by the European Union – NextGenerationEU– Project Title Novel hEat REcovery solutions on board of FC equipped vessels for metal HYDridES storage optimal management (NEREHYDES) – CUP B53D23006590006 - Grant Assignment Decree No. 961 adopted on 30/06/2023 by the Italian Ministry of Ministry of University and Research (MUR).

References

[1] International Maritime Organization official website, Accessed: Mar. 06, 2025. [Online]. Available: https://www.imo.org/

[2] E. Mata *et al.*, "Feasibility study and sizing of TES coupled with Metal Hydrides storage for H2 fuelled ships," *J Phys Conf Ser*, vol. 2893, no. 1, p. 012084, Nov. 2024, doi: 10.1088/1742-6596/2893/1/012084.

[3] "MetHydor official website, Accessed: Mar. 06, 2025. [Online]. Available: https://methydor.com/

[4] L. Mantelli, F. Iester, S. Crosa, M. Bozzolo, L. Magistri, and A. Massardo, "Dynamic Performance Analysis of a Turbocharged PEMFC System," *J Eng Gas Turbine Power*, vol. 147, no. 5, May 2025, doi: 10.1115/1.4066610

[5] M. Cavo, M. Rivarolo, L. Gini, L. Magistri, An advanced control method for fuel cells - metal hydrides thermal management on the first Italian hydrogen propulsion ship, International Journal of Hydrogen Energy, 46 (2023), 20923-20934. https://doi.org/10.1016/j.ijhydene.2022.07.223

[6] PowerCell Group official website, Accessed: Mar. 06, 2025. [Online]. Available: https://powercellgroup.com/



Assessment of the performance of MEAs assembled with different polymers and catalysts for PEM Fuel Cells

Portarapillo M.*[a], Di Francia M. A. [a], Gagliardi G.G.[b], Borello D.[b] , Di Benedetto A. [a]

* corresponding author: Portarapillo Maria

[a] Department of Chemical, Materials and Production Engineering, University of Naples Federico II

[b] Department of Mechanical and Aerospace Engineering, University of Rome, La Sapienza

Keywords: Aquivion membranes, Polymer electrolyte membrane Fuel Cell, Platinum, Polarization curves

Abstract

Alternative membranes and low-Platinum catalysts are innovative approaches to enhancing PEMFC performance while reducing costs. Aquivion, a perfluorosulfonic acid ionomer with a shorter side chain than Nafion, is relatively new and less tested, keeping Nafion dominant. Reducing Platinum content without sacrificing performance can be achieved by doping catalysts with transition metals like Nickel or Molybdenum. This study investigates the effects of different membrane-catalyst combinations, comparing them to Nafion and pure Platinum. Aquivion enhances tensile strength, thermal stability, and proton conductivity, while optimized Pt-transition metal catalysts enable high mass activity with low Platinum loadings, potentially outperforming commercial membranes.

Introduction:

The use of a PEM has several advantages compared with a battery system: easy fuel recharge, better operation at low temperature and pressure, high efficiency, small system size and low weight [1]. However, several issues hinder the spreading of this technology. Firstly, it must be considered that the heart of a fuel cell is composed by a membrane, generally consisting of Nafion, a perfluorosulfonic polymer, highly studied under different operating conditions ensuring good lifespan of the device, and by two electrodes made of platinum, a noble metal able that facilitates the semi reactions occurring at the electrodes [2]. However, high cost and limited operating temperature range and humidity represent a strong limit to the commercialization of that technology. Research activities are focused on developing new Polymer Electrolyte Membrane (PEM) materials aiming at reducing costs while keeping the performance unchanged. Among several types of material, Aquivion has been considered an exceptional polymer that offers excellent results in terms of water uptake and proton conductivity, due to the presence of a higher number of functional groups. Several authors

[3-4] have reported that Aquivion contributes to lower ohmic resistance and the hydrogen cross-over while enhancing the electro-catalytic activity. Since Aquivion and Nafion have a similar chemical structure, Talukdar et al. [5] investigated the effect of the combinations of the two ionomers in the electrode as well as ionomers in the membrane. They demonstrated that using the short chain polymer, hydrogen crossover and ionomer degradation are reduced while having a lower peak power density. In this context, along with the membrane, catalysts play an important role in energy produced from a fuel cell. To address the high Platinum (Pt) demands, research is focusing on alternatives such as the use of catalysts with lower Pt loads, the utilization of non-critical metals or both. With this aim, the polyol method is a simple technique for the production of Platinum-transition metals (Pt-TMs) alloys which enables precise control over the structure, chemical nature and morphology of the particles [6]. Among different transition metals, Nickel and Molybdenum have attracted increasing interest due to their synergic electrochemical performance, which still remains not comparable to the commercial Pt [7-8]. In this prospective, optimizing the ratio of Pt and TMs can result in good electrocatalytic properties while preserving the cost of the catalyst. Indeed, alloying Pt with other metals can induce lattice strain, which can optimize the adsorption energy of oxygen intermediates and enhance catalytic performance [9].

The novelty of this study is to analyze and optimized the operating parameters of a PEM fuel cells using different MEAs assembled using a combination of two different perfluorosulfonic polymers and different catalysts multilayer membrane. Membranes were manufactured using the casting method. Platinum-transition metals alloys were prepared by the polyol method. The effect of cell temperature, flow rates and humidity, on the performance of these novel MEAs is investigated.

Material and methods:

Materials and precursor were obtained from several companies: Aquivion and Nafion dispersion and Pt/C from Fuel cell store. Nickel acetate tetrahydrate, Molybdenum dichloride dioxide, Polyvinyl pyrrolidone (PVP) MW 40 KDa and ethylene glycole were purchased from Sigma Aldrich. Different loadings were testes for anode and cathode electrodes in order to balance the metal content and the thickness of the catalyst layer. Carbon paper Sigracet 28 BC was the GDL. The process of casting a membrane consists of solvent evaporation [6]. Then, the polymer forms a film on the flat surface. For membranes preparation (both Nafion and Aquivion) the following procedure is adopted: dry it in the oven with annealing (100°C for 2 hours and 120°C for 1 hour). Afterwards, the membranes were treated at 80 °C by immersion in the following sequence lasted 1 hour: in water, in 3% wt. H_2 O_2, in water, in 0.5 M H_2SO_4 and in water. Then, the membranes were immersed in water overnight. A specific amount of Pt/C, Nickel and Molybdenum precursors were added to a solution of water and ethylene glycol (1:3 vol.) in a round neck bottom flask. Additionally, PVP was added with a PVP/metal atomic ratio equal to 0.1. PVP acts as surfactant and capping agent. A reflux column was

added to close the system, and the temperature was set to 160 °C for 2 hours. The solution was then filtered and the remaining PVP was converted into carbon by a pyrolysis step at 900 °C for 1 hour. The electrochemical performances (cell voltage and electrical current) of the fuel cell were measured by using the DL3031A potentiostat (Rigol). In this study, polarization curves were made varying temperature, anode and cathode flow rates to assess the optimal operating conditions to better exploit the above-mentioned membranes and catalysts.

Results:

Tests are currently ongoing. Preliminary results on Pt/C suggest the formation of a Pt-Ni alloy. Figure 1 propose the XRD of the prepared sample, showing the constrain of Pt lattice structure and therefore the doping of the metal.

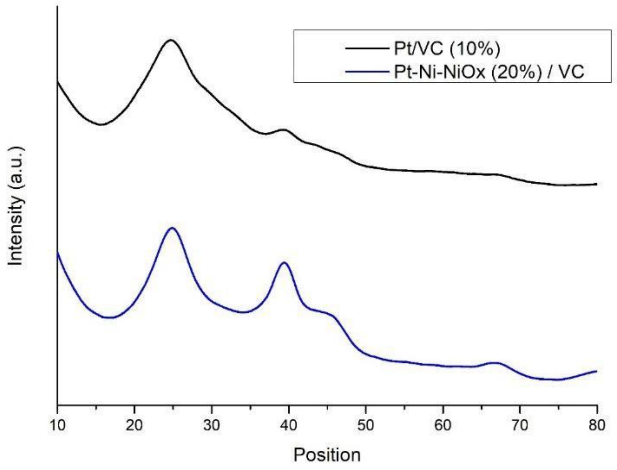


Figure 1 - XRD spectra of commercial Pt/C and Ni-doped Pt/C

Conclusions:

In this study, tests for assess the best operating conditions on a polymer electrolyte membrane fuel cell, using a combination of Aquivion as a membrane and as the Pt-TMs catalysts, were carried out. Preliminary tests demonstrated the effectiveness of using Aquivionin terms of stability and proton conductivity. This led to better performance than that obtained with the bare Nafion.

References

[1] https://doi.org/10.1016/j.adapen.2021.100011
[2] https://doi.org/10.1016/j.trd.2004.07.001
[3] https://doi.org/10.1021/acsomega.0c02110
[4] https://doi.org/10.1016/j.jpowsour.2010.12.084
[5] https://doi.org/10.1016/j.jpowsour.2019.227078
[6] https://doi.org/10.3390/cryst12030375
[7] https://doi.org/10.1016/j.electacta.2024.143912
[8] 10.1149/MA2019-01/30/149
[9] https://doi.org/10.1007/s11581-024-05767-z

European Fuel Cells and Hydrogen
PIERO LUNGHI CONFERENCE
September 17th–19th 2025
Capri / Italy

Integrated Modeling of a Fuel Cell Stack and Thermal Management System in a Fuel Cell Electric Bus Using Metaheuristic Optimization

Yebeen Kim[a], Jiwoong Kim [a], Seheun Kim [a], Sanggyu Kang [a], Kyoungdoug Min [*a]

* corresponding author: Kyoungdoug Min
[a] Seoul National University

Keywords: Fuel cell electric bus, Proton exchange membrane fuel cell, Thermal management system, Optimization

Abstract

Introduction: A proton exchange membrane fuel cell (PEMFC) serves as the primary power source in fuel cell electric buses (FCEBs), converting hydrogen into electricity while producing water and heat as by-products. To ensure stable operation, an efficient thermal management system (TMS) is essential for maintaining the fuel cell stack temperature within the optimal range of 60–80°C by effectively dissipating heat. The Balance of Plant (BOP) system, which comprises the air supply system, hydrogen supply system, and TMS, plays a crucial role in fuel cell performance by regulating reactant supply, managing heat dissipation, and enhancing overall system efficiency. However, current FCEBs heavily rely on carry-over components from passenger vehicles, resulting in suboptimal cooling strategies and inefficient thermal control. Addressing these challenges requires an integrated modeling approach to accurately analyze system behavior and optimize both design and control parameters.

Objectives: This study aims to enhance the TMS in a FCEB through metaheuristic optimization methods, including heat transfer search (HTS), particle swarm optimization (PSO), and the genetic algorithm (GA). The optimization targets key design parameters of TMS components, such as radiator fin spacing and heat exchanger size, to improve heat dissipation, maintain stable stack temperature, and enhance overall performance. To support this, we developed a simulation model that enables adjustments to geometric parameters and provides detailed analysis of their impact. This model offers accurate system predictions and serves as a valuable tool for evaluating design configurations, ensuring improved cooling efficiency in fuel cell electric buses.

Material and methods: A comprehensive dynamic model of the fuel cell stack and TMS was developed using MATLAB/Simulink, enabling precise simulation of electrochemical reactions, heat generation, and coolant flow dynamics. The model was validated against experimental

vehicle test data, achieving a relative error of less than 10%, confirming its reliability in predicting reactant consumption, thermal behavior, and system efficiency. To optimize key geometric parameters of TMS components, including the radiator and coolant pump, a multi-objective optimization framework was implemented in MATLAB using HTS, PSO, and GA to enhance heat dissipation, regulate stack temperature, and minimize power consumption. The optimization aimed to maximize heat exchanger effectiveness, reduce pressure losses, and improve thermal regulation. The developed model and optimization strategies provide a systematic approach for improving thermal management in FCEBs, ensuring stable operation and greater energy efficiency.

Results:

1. Development and Validation of the System Model

This study successfully developed a fully integrated TMS model, incorporating critical components such as the fuel cell stack, coolant pump, ion filter, radiator, heat exchanger, two valves, and interconnecting pipes. Each component was numerically modeled to accurately reflect real-world operational behavior. To validate the model, simulation results were compared with experimental data from real vehicle tests, demonstrating high accuracy with a correlation coefficient (R^2) exceeding 0.9 for both coolant flow rate and temperature predictions. This confirms that the developed model reliably represents the thermal behavior of the fuel cell system and serves as a solid foundation for optimization studies.

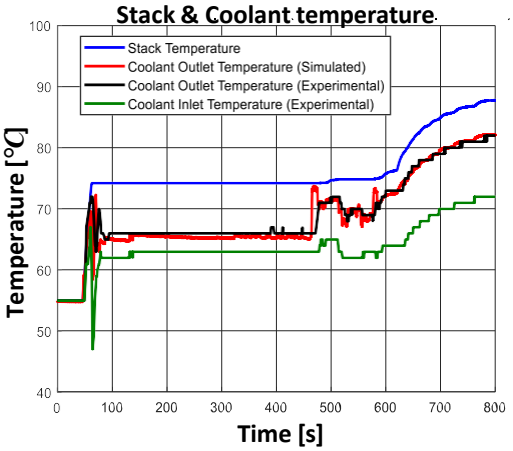


Fig.1 Stack temperature prediction and coolant temperature validation

2. Optimization of System Parameters

To enhance system performance, various optimization techniques were applied to refine the geometric parameters of key TMS components, such as the radiator and coolant pump. HTS,

PSO, and GA were utilized to identify optimal configurations that maximize heat dissipation, stabilize power output, and improve cooling system effectiveness.

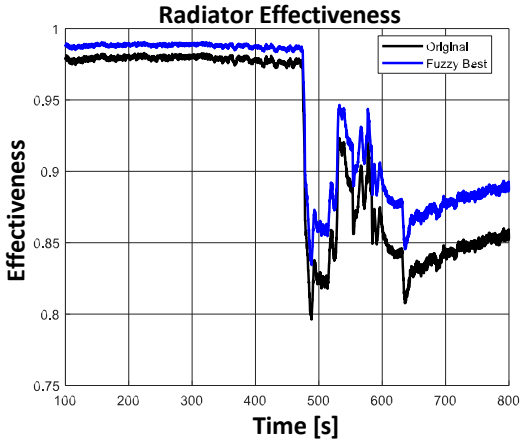


Fig.2 Simulated effectiveness for original and fuzzy-selected solutions

Conclusions: This study successfully developed and validated an integrated PEMFC-TMS model, providing a highly accurate thermal and electrochemical representation of a fuel cell electric bus system. By applying HTS, PSO, and GA, it demonstrated that optimizing key thermal management parameters enhances system efficiency, improves heat dissipation, and stabilizes power output. These findings contribute to the development of advanced cooling strategies, which are essential for the durability and efficiency of next-generation fuel cell vehicles.

References

[1] Choi, J. and Choi, J. (2020). Research status of hydrogen fuel cell system based on hydrogen electric vehicle. Energy Engineering, 29, 4, 26-34.

[2] Raja, B.D., Jhala, R.L., & Patel, V. (2017). Many-objective optimization of cross-flow plate-fin heat exchanger. International Journal of Thermal Sciences, 118, 320–339.

[3] Wang, C. C., Jang, J. Y., & Chiou, N. F. (1998). A heat transfer and friction correlation for wavy fin-and-tube heat exchangers. International Journal of Heat and Mass Transfer, 31, 808–813.

[4] Raja, B. D., Patel, V., & Jhala, R. L. (2017). Thermal design and optimization of fin-and-tube heat exchanger using heat transfer search algorithm. Thermal Science and Engineering Progress, 4, 45–57.

[5] Zhang, T., Chen, L., & Wang, J. (2023). Multi-objective optimization of elliptical tube fin heat exchangers based on neural networks and genetic algorithm. *Energy*, 269, 126729.

EFCH2 2025 European Fuel Cells and Hydrogen PIERO LUNGHI CONFERENCE
September 17th–19th 2025 Capri / Italy

Fast and reliable parameterization of PEMFC models – sequential optimization for efficient parameter estimation

Johanna Bartlechner*[a], Christoph Hametner[a], Stefan Jakubek[a]

* corresponding author: johanna.bartlechner@tuwien.ac.at
[a] TU Wien, Institute of Mechanics and Mechatronics, Getreidemarkt 9, 1060 Vienna, Austria

Keywords: fuel cell modeling, parameter optimization, PEM fuel cell, system identification

Abstract:
A fast and reliable methodology for parameterizing non-linear fuel cell models is presented and validated using real-life measurement data. The approach separates the dynamic fuel cell model into multiple submodels by using output measurements, enabling a sequential optimization strategy that estimates subsets of the parameter vector in consecutive steps. By splitting the high-dimensional optimization problem into smaller, more manageable subproblems, the proposed algorithm significantly reduces computational time while increasing model fit compared to traditional optimization methods.

Introduction: Low-temperature polymer electrolyte fuel cells (LT-PEMFCs) are a promising technology for alternative propulsion systems, particularly in heavy-duty applications. Their key advantages, including fast refuelling, long range, and high efficiency, make them well-suited for demanding transportation needs. To ensure optimal performance, safe operation and longevity, advanced fuel cell control strategies heavily rely on model-based approaches, which enable precise system analysis and predictive control. However, PEMFC behaviour varies across different systems for example due to sizing, material properties, manufacturing processes, or operating strategies. When deploying and transferring observer and control algorithms to new systems, reparameterization of the underlying models is essential to accurately capture the system dynamics. Traditional parameter estimation methods, however, can be time-consuming and computationally expensive. To address this challenge, fast and reliable algorithms for parameter estimations are needed. In this work, a novel sequential approach using output measurements is introduced. By splitting the multi-dimensional problem into smaller optimization problems, computational effort and model-plant mismatch can be reduced.

Objectives: To describe the complex behaviour of fuel cell systems, nonlinear physics-based models are used. These models must be reparametrized for different fuel cell configurations to ensure that the relevant system dynamics are captured. Traditional parameterization

methods are often computationally demanding and inefficient. The objective of this work is to develop an algorithm that estimates fuel cell model parameters efficiently and reliably.

Material and methods: The sequential optimization algorithm is tested by parameterizing a zero-dimensional non-linear performance model [1] designed for control applications to real-world measurement data [2]. The model in [1] is extended to include fuel cell temperature dynamics. The parameter vector comprises 19 parameters that characterize the thermodynamic, electrochemical, and thermal behaviour of the fuel cell system. Estimating all 19 parameters simultaneously presents a high-dimensional optimization challenge. To address this, the model is separated into three submodels: thermodynamic, electrochemical, and thermal. By incorporating output measurements, the coupling of the submodels can be reduced (see Figure 1) and the submodels can be parameterized sequentially, optimizing only the relevant subset of parameters at each stage.

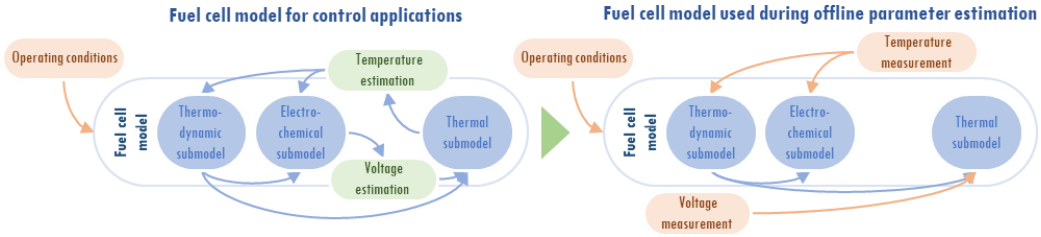


Figure 1: Schematics of model separation. By incorporating output measurements (red) in the offline parameterization, the submodels (blue) can be independently identified reducing the complexity of the high-order identification problem into multiple low-order optimization problems.

Results: The model is parameterized with the suggested methodology to measurement data from a PEM single cell excited with the fuel cell dynamic load cycle [3], whereby the first 20 minutes are used as training data and the next 20 minutes are used as validation data. The results of the suggested sequential optimization are compared to results obtained from a conventional parameter estimation where all 19 parameters are optimized simultaneously. For all parameterization steps, a gradient based algorithm (fmincon in MATLAB [4]) is used. With the suggested algorithm, the time for parameterization was reduced from around 3 hours to around 2 hours resulting in a reduction of around 30%. The coefficients of determination R^2 for voltage and temperature increased from 95.4% to 99.3% and from 5.7% to 66.5% respectively (see Figure 2). The low R^2 for temperature compared to voltage can be explained by the more dynamic voltage excitation compared to temperature (see also Figure 3). Measurement data and simulation for both parameterizations are compared in Figure 3. By splitting the parameterization problem into multiple subproblems, the fit for each output can be improved.

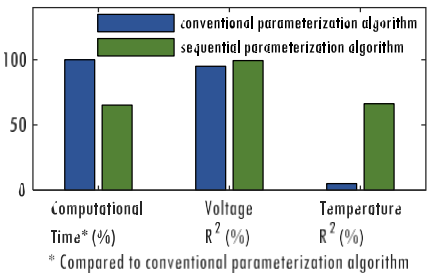


Figure 2: Results for conventional and sequential parameterization. With the suggested approach, computational time can be reduced while coefficient of determination (R^2) are increased.

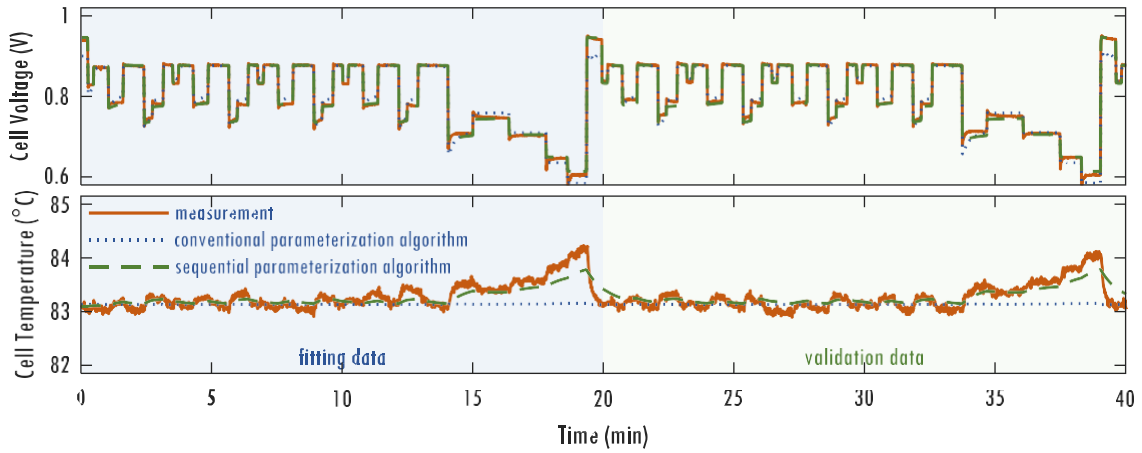


Figure 3: Results for model with parameters obtained from conventional and sequential parameterization compared to measurement data. The voltage (top) and temperature (bottom) response of the model are plotted and compared to the measurement data. In particular the temperature dynamics are tracked more accurately when optimizing the subset of the thermal model independently.

Conclusions:

A methodology for fast and reliable fuel cell identification was presented and tested on real-life measurements. By splitting the model into three submodels, the high-order optimization problem was split into multiple smaller problems. With the suggested methodology, the computational effort for parameterization was significantly reduced while also improving model fit. Methodologically, further investigations will focus on model-based experimental design, identifiability analysis using the Fisher Information Matrix, and increasing the robustness of the parameterization algorithm. The algorithm will further be tested on its applicability for efficient reparameterization for different PEMFCs realizations. Acknowledgment: This work was funded by the Austrian Research Promotion Agency (FFG) by the project AlpeDHues [grant number 884322]. The authors acknowledge the support of this work through the women's promotion program of the Faculty of Mechanical and Industrial Engineering (MWBF) at TU Wien.

References

[1] Bartlechner, J., Vrlić, M., Hametner, C., Jakubek, S. (2024). State-of-Health observer for PEM fuel cells – A novel approach for real-time online analysis. *Int. J. of Hydrogen Energy,* 95, 1112-1125. https://doi.org/10.1016/j.ijhydene.2024.03.061

[2] Zuo, J., Lv, H., Zhou, D., Xue, Q., Jin, L., Zhou, W., Yang, D., Zhang, C. (2021). Long-term dynamic durability test datasets for single proton exchange membrane fuel cell. *Data in Brief*, 35, 106775. https://doi.org/10.1016/j.dib.2021.106775

[3] Tsotridis, G., Pilenga, A., De Marco, G., and Malkow, T. (2015). EU harmonised test protocols for PEMFC MEA testing in single cell configuration for automotive applications. Publications Office, Luxembourg. OCLC: 954062997.

[4] MathWorks. (2024). Optimization Toolbox, version R2024a, The MathWorks Inc., Natick, Massachusetts.

EFCH2 2025 European Fuel Cells and Hydrogen PIERO LUNGHI CONFERENCE
September 17th–19th 2025 Capri / Italy

Gas Diffusion Electrode half cell: A Versatile Tool for Half-Cell PEMFC Characterization

Mitja Kostelec[a,b], Milena Šetka[c], Miha Hotko[a,b], Matija Gatalo[b,d], Nejc Hodnik[a,b]

* corresponding author: *Mitja.Kostelec@ki.si*

[a] University of Nova Gorica, Vipavska 13, SI-5000 Nova Gorica, Slovenia

[b] National Institute of Chemistry, Hajdrihova ulica 19, 1000 Ljubljana, Slovenia

[c] University of Chemistry and Technology, Technická 5, 160 00 Praha 6-Dejvice, Czech Republic

[d] ReCatalyst d.o.o., Hajdrihova ulica 19, 1001 Ljubljana, Slovenia

Keywords: Identical Location (IL) Analysis, Electrocatalyst, Gas Diffusion Electrode half-cell (GDE), Proton Exchange Membrane Fuel Cells (PEMFCs)

Abstract Introduction:

Understanding and improving electrocatalytic reactions is crucial for advancing electrochemical energy conversion technologies. Proton exchange membrane fuel cells (PEMFCs) have gained significant attention due to their high efficiency and potential for sustainable energy applications. The development of durable and efficient electrocatalysts requires precise characterization methods capable of capturing key electrochemical properties under realistic conditions.

Objectives:

This study aims to establish the gas diffusion electrode (GDE) half-cell as a standardized and versatile electrochemical measurement platform for characterizing electrocatalysts under conditions representative of real fuel cell operation. The approach seeks to bridge the gap between conventional thin-film rotating disk electrode (TF-RDE) techniques and full single-cell fuel cell tests.

Material and methods:

The GDE half-cell setup integrates a controlled gas diffusion environment with an electrochemical half-cell configuration. This method allows for the evaluation of catalyst active surface area, activity, and stability. Various sample types, including homemade catalysts integrated into GDEs and industrial catalyst-coated membranes (CCMs), were examined. Unique feature of the setup is also compatibility with identical location (IL) ex-situ characterization techniques, including IL-SEM, IL-EDS, IL-XRD, IL-XPS, IL-Raman, and IL-XRF.

Results:

The GDE half-cell provided electrochemical insights into catalyst performance under conditions that closely resemble real fuel cell operation. By enabling multi-scale analysis, this approach facilitated direct correlations between electrochemical behavior and structural, compositional, and morphological changes. The results demonstrated that GDE half-cell measurements offer improved stability and reliability compared to TF-RDE techniques, while maintaining compatibility with advanced characterization methods.

Conclusions:

The GDE half-cell represents a powerful tool for PEMFC research, enabling a more realistic evaluation of electrocatalysts and catalyst-layer architectures. Its ability to support both fundamental electrocatalyst studies and application-oriented investigations positions it as a key methodology for the development of next-generation fuel cell materials and electrode designs.

Acknowledgment

The authors would like to acknowledge the Slovenian research agency (ARRS) programs P2–0393 and I0–0003; the projects NC-0016, N2–0257 and J7–4637; EIC Transition project ENABLER (grant agreement ID: 101112991); European Research Council (ERC) Starting Grant 123STABLE (grant agreement ID: 852208); and K. M. acknowledges EKPO Fuel Cell Technologies GmbH for funding.

References

[1] Bals, J.; Epple, M. Deep Learning for Automated Size and Shape Analysis of Nanoparticles in Scanning Electron Microscopy. RSC Adv. 2023, 13 (5), 2795–2802. https://doi.org/10.1039/D2RA07812Kž.

[2] Ehelebe, K.; Schmitt, N.; Sievers, G.; Jensen, A. W.; Hrnjić, A.; Collantes Jiménez, P.; Kaiser, P.; Geuß, M.; Ku, Y.-P.; Jovanovič, P.; Mayrhofer, K. J. J.; Etzold, B.; Hodnik, N.; Escudero-Escribano, M.; Arenz, M.; Cherevko, S. Benchmarking Fuel Cell Electrocatalysts Using Gas Diffusion Electrodes: Inter-Lab Comparison and Best Practices. ACS Energy Lett. 2022, 7 (2), 816–826. https://doi.org/10.1021/acsenergylett.1c02659.

[3] Hodnik, N.; Cherevko, S. Spot the Difference at the Nanoscale: Identical Location Electron Microscopy in Electrocatalysis. Curr. Opin. Electrochem. 2019, 15, 73–82. https://doi.org/10.1016/j.coelec.2019.03.007.

[4] Kostelec, M.; Gatalo, M.; Hodnik, N. Fundamental and Practical Aspects of Break-In/Conditioning of Proton Exchange Membrane Fuel Cells. Chem. Rec. 2024, 24 (10). https://doi.org/10.1002/tcr.202400114.

European Fuel Cells and Hydrogen
PIERO LUNGHI CONFERENCE
September 17th–19th 2025
Capri / Italy

Analysis of aging effects based on electrochemical characterisations within a durability test

Eva Fensterle*[a], Jürgen Hunger [a], Frank Rabsahl [a], Florian Wilhelm [a], Christian Kolle Christensen [b], Adam Benson [c], Rami Al-Khamissi [d], Marine Tregaro [e], Sylvie Escribano [e], Joachim Scholta [a], Markus Hölzle [a]

* corresponding author: eva.fensterle@zsw-bw.de
[a] Zentrum für Sonnenenergie- und Wasserstoff-Forschung Baden-Württemberg (ZSW), 89081 Ulm, Germany
[b] IRD Fuel Cells A/S, 5220 Odense SØ, Denmark
[c] PowerCell Sweden AB, SE 418 34 Gothenburg, Sweden
[d] German Aerospace Center (DLR), Institute of Engineering Thermodynamics, 70569 Stuttgart, Germany
[e] Univ. Grenoble Alpes, CEA, LITEN, DEHT, 38000 Grenoble, France

Keywords: Aging effects, electrochemical characterisation, PEM fuel cell

Abstract

Introduction: The durability of proton exchange membrane fuel cell stacks (PEMFC) is a decisive factor for their long-term usability in heavy-duty applications. Studying the membrane electrode assembly (MEA) gives crucial insights for durability performance and efficiency of a fuel cell. The performance of the fuel cell deteriorates continuously as it ages. Already at the beginning of life (BoL), heterogeneities occur across the entire active surface area, which become more pronounced in the course of the aging process. These local differences in degradation have a significant impact on the overall performance of the fuel cell and represent a key challenge for its long-term stability.

Objectives: The aim of this work is to gain an in-depth understanding of the aging-related effects in a metallic fuel cell stack. To this end, a durability test is carried out in which the performance of the stack is analysed at regular intervals using electrochemical characterisation methods. The data obtained enables the quantification of parameters that contribute significantly to aging.

Material and methods: The durability tests are carried out employing the open-design metal stack, which was developed as part of the HyFaB[1] project and is employed in the RealHyFC[2]

[1] Funded by the State of Baden-Württemberg, Ministry for the Environment, Climate and Energy Industry under the funding reference L75 20112
[2] Funded by the Clean Hydrogen Partnership and its members Hydrogen Europe and Hydrogen Europe Research under the project ID 101111904

project [1]. The 10-cell short stack used is equipped with a current density measurement device between cells 5 and 6. The MEA defined in the RealHyFC project is used. A load cycle refined in the RealHyFC project based on the definition of the Pemtastic[3] project is used to simulate real operating conditions [2]. In order to analyse the aging-related effects, six different polarisation curves are recorded every 250 operating hours. In addition, further established electrochemical characterisation methods are carried out every 500 operating hours, including sensitivity tests, cyclic voltammetry (CV), linear sweep voltammetry (LSV) and electrochemical impedance spectroscopy (EIS). As part of a sensitivity study, the behaviour and performance of the fuel cell can be systematically investigated under varying operating conditions such as temperature, pressure, humidity and stoichiometry. The CV measurement facilitates determining key electrochemical properties such as the electrochemically active surface area (ECSA), the hydrogen crossover current and the double-layer capacity. EIS measurements provide detailed insights into membrane resistance and nanoscale processes such as diffusion, charge transfer and proton transport. With the current density distribution measurement board, the spatially resolved distribution of current density and temperature can be precisely analysed across the cell surface.

Results: First results from the current density data are listed below. Figure 1 shows the results of the current density distribution over the active area. The evaluation is carried out within the nominal polarisation curve defined in RealHyFC (T.Cl = 70 °C, T.Si.A/C = 75 °C, rh.A/C = 50%/35%, p.So.A/C = 2.6/2.5 bar_a, Stoic.A/C = 1.5/1.7) at BoL and as an example after 500 operating hours.

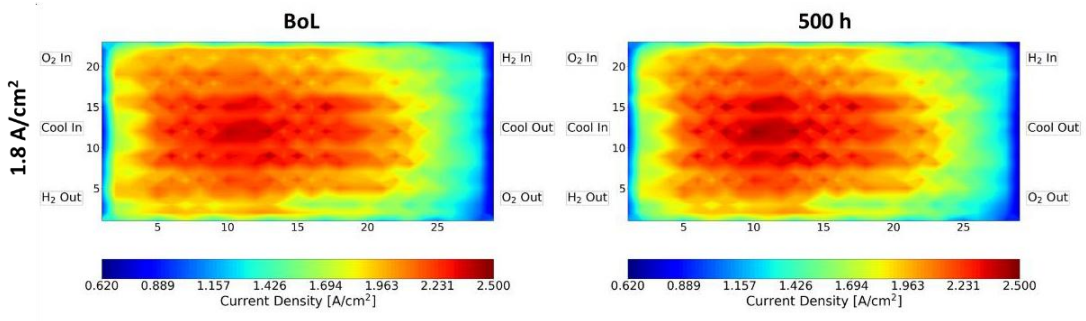


Figure 1: Current density distribution at 1.8 A/cm² under nominal RealHyFC conditions at BoL and after 500 h

Figure 1 shows that the current density distribution at BoL and after 500 operating hours is still very similar. However, some significant differences are already visible here. The current density gradient across the cell increases and the current density maximum shifts slightly towards the cathode inlet.

To quantitatively analyse the change in current density, the current density distribution is displayed using local polarisation curves. For this purpose, the active area is divided into three

[3] Funded by the Clean Hydrogen Partnership and its members Hydrogen Europe and Hydrogen Europe Research under the project ID 101101433

regions: inlet, middle and outlet. The measurement results of the respective current segments are averaged over the regions and displayed in comparison to the average polarisation curve of the stack (see Figure 2).

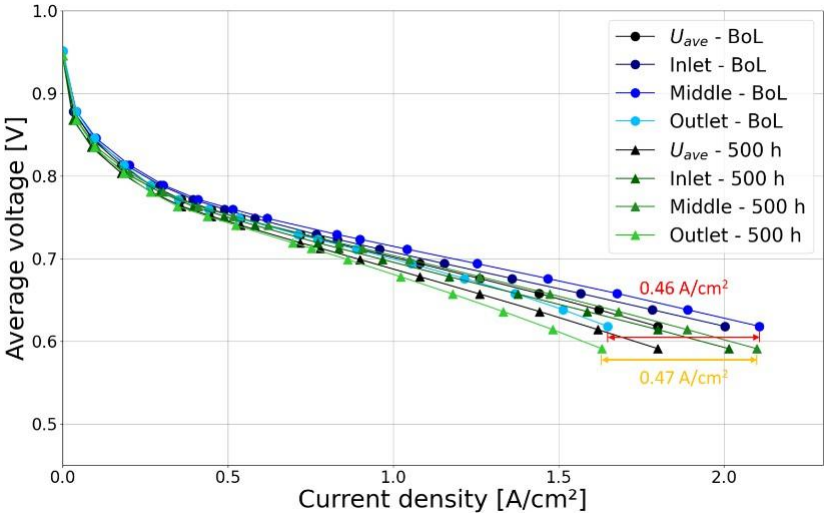


Figure 2: Global and local polarisation curves under nominal RealHyFC conditions at BoL and after 500 h

The overall polarisation curves clearly show that the load cycle induces an initial aging effect. In addition, the local measurements enable more detailed comparison of the performance on the local scale. An indication for the progressive degradation is the increasing spread of the current density between the middle and outlet regions. As can be seen in Figure 2 it has increased by 0.01 A/cm² after 500 hours. More detailed analysis covering further process of aging will be presented at the conference.

Conclusions: In this work, a recently developed load cycle and durability test program relevant for the heavy-duty application has been applied for the first time. Durability data has been recorded over a significant duration and comprehensive analysis methods have been applied to investigate global and locally resolved degradation effects in detail. First results already indicate significantly different local aging effects, thus focus will be placed on the heterogeneity of conditions and performance over the active area to reach the durability targets relevant for the heavy-duty application.

Acknowledgment

This work was performed within the framework of the RealHyFC project. The RealHyFC project is supported by the Clean Hydrogen Partnership and its members Hydrogen Europe and Hydrogen Europe Research under GA 101111904.

References

[1] Häußler, F. et al. (2024). The ZSW HyFaB Generic Stack (1.0). https://doi.org/10.5281/zenodo.14223364

[2] J. Sanchez-Monreal, J. Mitzel, C. Vacquier, P. Gazdzicki (2025). Application relevant load cycles for PEMFC component development and hybrid system optimization. (submitted manuscript)

EFCH2 2025
European Fuel Cells and Hydrogen
PIERO LUNGHI CONFERENCE
September 17th–19th 2025
Capri / Italy

Economic viability of sustainable railway propulsion systems: a decision-support framework

Gabriele Peyrani*[a], Marta Gandiglio [a], Paolo Marocco [a], Pierpaolo Cherchi [b], Massimo Santarelli [a]

* Corresponding author: gabriele.peyrani@polito.it
[a] Department of Energy, Politecnico di Torino, Corso Duca degli Abruzzi 24, 10129 Torino, Italy.
[b] Alstom Ferroviaria S.p.a., Via O. Moreno, 23, 12038 Savigliano (CN), Italy.

Keywords: Alternative propulsion systems, Decarbonization, Railway transport, Total Cost of Ownership

Abstract

Introduction: The railway sector is undergoing a significant transition towards more sustainable solutions, driven by ambitious decarbonisation targets. Non-electrified railway lines, which still rely heavily on diesel traction [1] through Diesel Multiple Units (DMU), represent a major challenge in this context, as can be noticed by Figure 1.

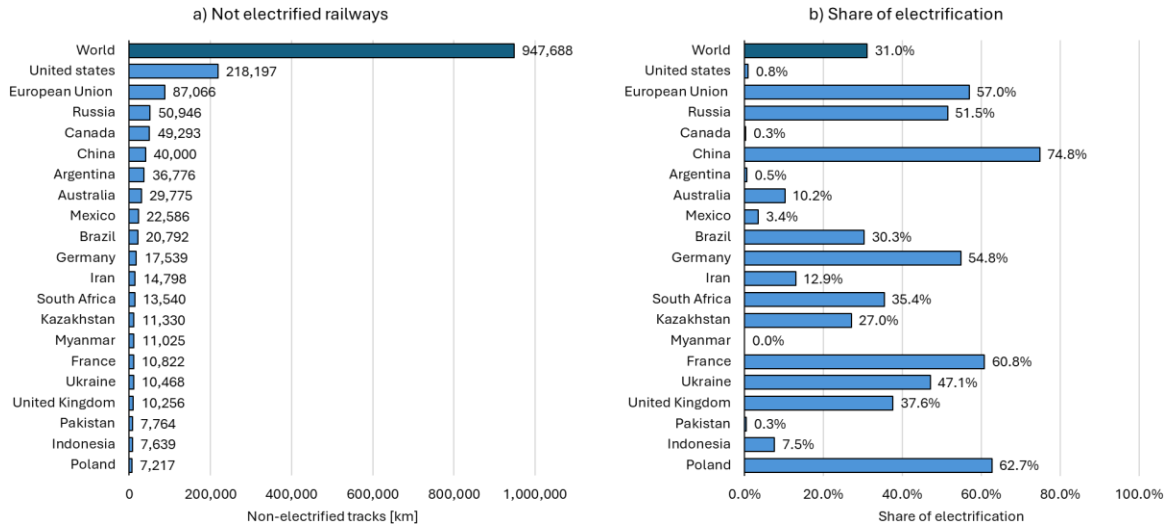


Figure 1: Current situation of worldwide railway system. a) Total length of non-electrified railway lines in the top 20 countries with the largest non-electrified networks; b) Electrification share of the railway network in each country [1][2].

Alternative propulsion systems, such as Battery Multiple Units (BMU), Hydrogen Multiple Units (HMU), and Electric Multiple Units (EMU), have emerged as promising options to reduce greenhouse gas emissions and improve energy efficiency. While EMU represent a well-established and mature solution, BMU and HMU are still emerging technologies with ongoing advancements in performance and infrastructure requirements. However, the economic feasibility of each solution heavily depends on operational and infrastructural characteristics

of the line. This study proposes a framework to assess the replicability of TCO (€/km) evaluations across railway networks, helping decarbonization decisions for non-electrified lines.

Objectives: The main objective of this study is to develop a decision-support tool capable of identifying the most economically viable propulsion solution for non-electrified railway lines based on a TCO assessment. Rather than determining a universally optimal solution, the model emphasizes a case-by-case approach, recognizing that each propulsion technology presents strengths and weaknesses depending on the specific context. The analysis explores the trade-offs between capital and operational costs for different technologies, considering the influence of traffic volumes, route characteristics, infrastructural constraints and many other decision parameters. The study aims to provide a flexible and scalable methodology that can be applied to regional and national railway networks to estimate their decarbonization path.

Material and methods: The analysis is based on multiple simulation results from detailed technical tools that model the different propulsion systems in order to better estimate the fuel consumption, which have been validated through industrial field data. Subsequently, pre-processed results are interpolated based on operational parameters, including train mass, speed profiles, number of stations, route gradients, and track length. The railway characteristics are sourced from an online database, enabling the analysis to be extended to any non-electrified route worldwide. Capital and operational cost data are then combined to calculate the TCO over the train's lifetime. This approach allows for the estimation of the economic viability of each propulsion method across various traffic volumes and infrastructural configurations, which may differ across countries and even regions, providing insights into the replicability of the methodology in different geographical contexts.

Results: The simulations permit the generalisation of the results in order to be interpolated and applied to different countries' railways. The results show how each propulsion system has an optimal operating condition where its TCO is the lowest among the available options:

- BMU: Low ranges, low traffic volumes;
- DMU: High ranges, high traffic volumes;
- EMU: Low and high ranges, high traffic volumes;
- HMU: High ranges, low traffic volume.

The HMU exhibits a cost pattern similar to the DMU. For this reason, the routes where electrification is not possible and high ranges exclude the usage of only-batteries, HMU is likely to emerge as the most promising option to replace inefficient diesel trains. In Figure 2, an example of the tool applied to the Lombardy region.

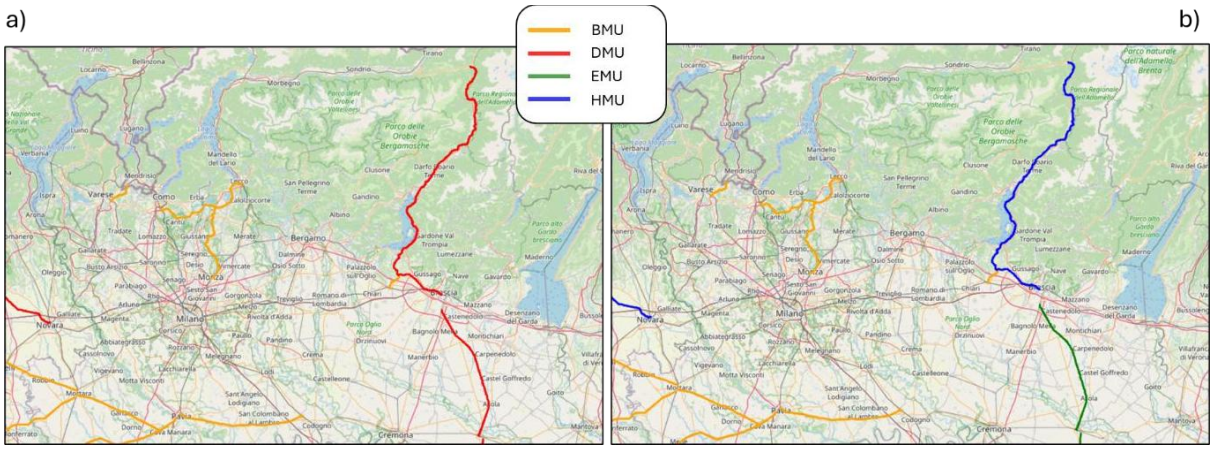


Figure 2: Example of the model applied to the Lombardy region. a) Current scenario (prices: diesel=1.23€/l, hydrogen=8€/kg); b) Substitution scenario (no diesel, hydrogen price=8€/kg)

Conclusions: The findings of this study highlight the importance of a case-by-case approach when evaluating alternative railway propulsion systems for non-electrified lines. The TCO analysis demonstrates that while EMUs remain the most cost-effective solution in heavily trafficked and electrifiable routes, BMUs and HMUs offer viable alternatives in specific operational contexts. BMUs perform well in short-range, low-frequency operations, whereas HMUs become competitive in long-distance scenarios where full electrification is not feasible. The results also underline the significant impact of fuel costs on the economic viability of hydrogen-powered trains, reinforcing the need for policy support and technological advancements to enhance their competitiveness. Ultimately, this framework provides a replicable methodology that can aid decision-makers in assessing the best decarbonization strategies for different railway networks.

Acknowledgment:

This research was funded by the European Union - Next Generation EU – Project ID: IPCEI-I1_0000003 CUP: B19J23000490004 coordinated by Alstom Ferroviaria S.p.A.

References:

[1] Eurostat, “Length of railway lines by number of tracks and electrification of lines.” Accessed: Dec. 09, 2024. [Online]. Available: https://ec.europa.eu/eurostat/databrowser/view/rail_if_line_na/default/table?lang=en

[2] “List of countries by rail transport network size - Wikipedia.” Accessed: Mar. 06, 2025. [Online]. Available: https://en.wikipedia.org/wiki/List_of_countries_by_rail_transport_network_size#cite_note-9

European Fuel Cells and Hydrogen
PIERO LUNGHI CONFERENCE
September 17th–19th 2025
Capri / Italy

Impact of bio-syngas contaminants on SOFC performance: experimental characterization and degradation model

Lucia Pera*[a], Marta Gandiglio[a], Paolo Marocco[a], Davide Pumiglia[b], Massimo Santarelli[a], Yuri De Pra[b], Alfredo Zingone[b]

* corresponding author: lucia.pera@polito.it

[a] Department of Energy, Politecnico di Torino, Corso Duca degli Abruzzi 24, Torino 10129, Italy
[b] ENEA - Italian National Agency for New Technologies, Energy and Sustainable Economic Development, Department of Energy Technologies and Renewable Sources (TERIN) Laboratory for Hydrogen and new Energy Vectors (H2V), Research Centre Casaccia, Roma, Italy

Keywords: Bio-syngas, Solid Oxide Fuel Cells fed by bio-syngas, Trace contaminants

Abstract Introduction:

Hydrogen technologies and fuel cells are gaining momentum for the achievement of decarbonization goal, with Solid Oxide Fuel Cell (SOFC) playing a key role due to their high efficiency and flexibility [1]. This research investigates SOFC degradation caused by contaminants species in unconventional gas mixtures. The study initially focuses on contaminants present in bio-syngas, identifying and characterizing trace contaminants to assess their impact on SOFCs, which are particularly sensitive to impurities. Experimental tests evaluate degradation effects of specific contaminants at concentrations typical of bio-syngas.

Objectives:

The aim of this work is to present an experimental campaign aimed at assessing the impact of specific contaminants on SOFCs, addressing a critical gap in the literature. While hydrogen sulfide (H_2S) has been widely studied, a comprehensive predictive model of its influence is lacking, and the effects of other contaminants remain largely unexplored. This research systematically examines SOFCs under controlled contamination conditions to identify key parameters affected by degradation mechanisms, considering several contaminants. A subsequent 0D modelling approach quantifies performance losses and provides insights into the degradation pathways.

Material and methods:

The experimental activity involves electrochemical characterization of button-type SOFCs. Diagram of test station is shown in Figure 1. Anode Supported Cells (ASC) with a Ni-YSZ anode, YSZ electrolyte, and LSCF cathode are used. Contaminants commonly found in biogas (e.g.,

DMS, COS, and D5) are added to the fuel gas mixtures (H_2, CO, CO_2, H_2O, N_2) at real-world concentrations [2]. Each contaminant is tested at two concentrations (low and high) to determine its impact and define tolerance levels. Experimental parameters such as temperature, fuel electrode flow rate, and gas composition remain constant. Each exposure lasts 120 hours, with the cell operating at nominal current density. Voltage-time trends monitor degradation effects, while Electrochemical Impedance Spectroscopy (EIS) is performed every 24 hours to track process evolution. EIS data is analyzed using Distribution of Relaxation Times (DRT), which separates and quantifies the effects of contaminants on different cell processes [3]. Equivalent circuit modeling, combined with this analysis, supports the development of a 0D degradation model predicting SOFC deterioration under steady operational conditions.

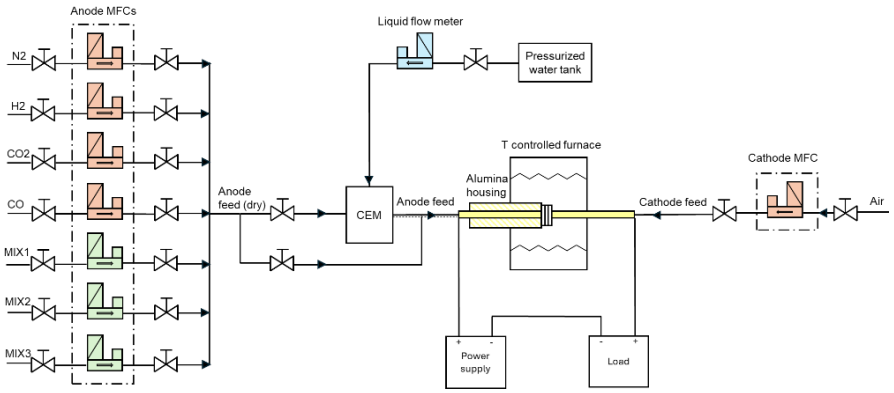


Figure 1. Diagram of the SOFC test station.

Results:

Significant performance degradation is observed for each tested contaminant. Experimental results from in-operando electrochemical characterization highlight SOFCs' sensitivity to these species, even at low concentrations. Voltage trends consistently show a decline over time due to progressive contaminant-induced degradation (see Figure 2 as an example). EIS spectra and DRT analysis provide valuable insights into relaxation processes contributing to increased impedance. Equivalent circuit modelling confirms that anode activation is primarily affected by degradation. The degradation model is refined by incorporating a time-dependent modification to the activation resistance. This adjustment is based on trends observed in the equivalent circuit model analysis, which quantifies the resistance variations induced by contaminant exposure. The evolving resistance behaviour is integrated into the exchange current density of the following equation:

$$V_{activation,\,fuel\ electrode} = \frac{R \cdot T_{op}}{F} \cdot sinh^{-1}\left(\frac{i_{op}}{2 \cdot i_{0,fuel\ electrode}}\right)$$

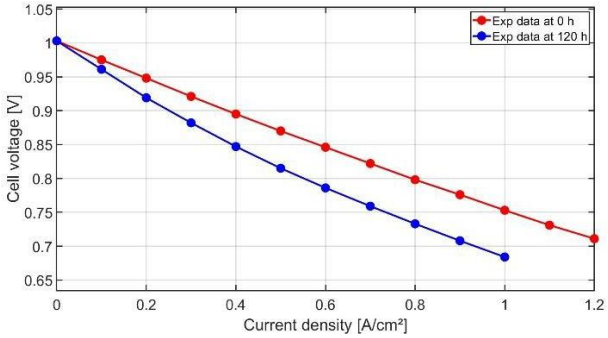


Figure 2. Experimental IV curve at 0 h (red curve) and 120 h (blue curve) with DMS at 1 ppm.

Conclusions:

This study examines the impact of biogas contaminants on SOFC performance, considering the variability in contaminant levels and their degradation effects. Experimental findings demonstrate that contaminants such as sulphur compounds and siloxanes cause measurable voltage declines and impact specific electrochemical processes, as revealed by EIS and DRT analysis. The validated 0D model successfully simulates these degradation mechanisms, offering a predictive tool for designing SOFC systems resistant to biogas contaminants. This work highlights the importance of precise contaminant management in the development of SOFCs for sustainable energy applications.

Acknowledgment

This research is funded by the European Union – NextGenerationEU from the Italian Ministry of Environment and Energy Security, POR H2 AdP MEES/ENEA with the involvement of the CNR and RSE, PNRR - Mission 2, Component 2, Investment 3.5 "Ricerca e sviluppo sull'idrogeno", CUP: I83C22001170006.

References

[1] M. Gandiglio, A. Lanzini, M. Santarelli, M. Acri, T. Hakala, and M. Rautanen, "Results from an industrial size biogas-fed SOFC plant (the DEMOSOFC project)," *Int J Hydrogen Energy*, vol. 45, no. 8, pp. 5449–5464, Feb. 2020, doi: 10.1016/j.ijhydene.2019.08.022.

[2] L. Pera, M. Gandiglio, P. Marocco, D. Pumiglia, and M. Santarelli, "Trace contaminants in biogas: Biomass sources, variability and implications for technology applications," Dec. 01, 2024, *Elsevier Ltd*. doi: 10.1016/j.jece.2024.114478.

[3] C. Boigues Muñoz *et al.*, "More accurate macro-models of solid oxide fuel cells through electrochemical and microstructural parameter estimation - Part I: Experimentation," *J Power Sources*, vol. 294, pp. 658–668, Jul. 2015, doi: 10.1016/j.jpowsour.2015.06.118.

EFCH2 2025 European Fuel Cells and Hydrogen
PIERO LUNGHI CONFERENCE
September 17th–19th 2025
Capri / Italy

Experimental analysis and control of a SOFC-Battery hybrid for use as powertrain on seagoing vessels

Daniele Fortunati*[a], Santiago Salas Ventura [a], Jan Hollmann[a], Marc P. Heddrich [a], S. Asif Ansar[a]

* corresponding author: Daniele.fortunati@dlr.de

[a] German Aerospace Center (DLR), Institute of Engineering Thermodynamics, Pfaffenwaldring 38-40, 70569 Stuttgart, Germany

Keywords: Control Strategies, Solid Oxide Fuel Cell, Transient Operation, Waterborne Transport

Abstract

Solid Oxide Fuel Cell (SOFC) systems offer promising potential for reducing CO_2 emissions in ship powertrains as they can provide electrical power at significantly higher conversion efficiency compared to conventional combustion engine gensets using the same fuel. However, the lack of commercially available SOFC-based gensets raises uncertainties regarding their scalability and operation. The NAUTILUS project addressed this gap by developing and testing a maritime SOFC-based hybrid genset. This study evaluates the SOFC system's ability to handle transient power demands within a hybrid system supported by a battery. Laboratory testing at the German Aerospace Centre (DLR) demonstrated successful load-following operation with a combined SOFC battery peak power output of ~28 kW. The findings highlight the feasibility of SOFC integration in modern ship powertrains, promoting sustainable maritime energy solutions.

Introduction:

Solid Oxide Fuel Cell (SOFC) systems have demonstrated electrical efficiencies exceeding 60% (LHV to AC) in stationary applications using natural gas [1]. This efficiency, along with significant reductions in CO_2 emissions and the near-elimination of NO_x, CO, PM, and methane slip, makes SOFC technology a promising alternative to conventional diesel- or LNG-fuelled gensets for maritime applications. However, SOFC gensets have yet to be demonstrated in relevant power classes for seagoing vessels. Key challenges, including system integration, transient response, optimal sizing, and real-world emissions reduction, remain unresolved. This study explores the feasibility of SOFC adoption in maritime power systems, assessing their performance and operational constraints.

Objectives:

The recently completed NAUTILUS project aims to bridge this research gap by developing and testing a maritime genset centred around an LNG-fuelled SOFC reactor [2]. The present study focuses on demonstrating the capabilities of an SOFC reactor operating within a hybrid system under ship-like conditions. Currently, SOFC systems do not have extensive testing results in transient operation, with the majority of experiments on this topic focuses on more steady-state approaches. In this study, the authors examine the system's response to dynamic power demands and evaluates whether an SOFC module, supported by a battery, can effectively handle transient load conditions. While the distribution of power demand between SOFC and battery is already analysed in [3] utilizing a higher-level energy management system (EMS), this study puts the focus on the control and operation of the SOFC under transient load conditions.

Materials and Methods:

At the Institute of Engineering Thermodynamics of the German Aerospace Centre (DLR-TT), a state-of-the-art test environment has been established for SOFC reactors [4]. This facility accommodates multiple fuel cell stacks with a combined maximum power output of 30 kW_{el}. Additionally, an in-house simulation framework has been developed and validated, enabling accurate predictions of reactor behaviour and facilitating the design of advanced operational strategies [5].Utilizing these tools, a Multi-Input-Multi-Output (MIMO) control strategy was developed to enable load-following operation of a large SOFC reactor. The strategy ensures that the reactor meets power demands dictated by a higher-level system controller, with lithium-ion battery support mitigating transient power fluctuations. Moreover, the control strategy maintains safe operating conditions by regulating voltage and temperature while optimizing fuel utilization. Once the Proof of Concept (PoC) was achieved, the hybrid system was further scaled into a demonstrator for high-power testing.

Results:

This study presents the PoC of a ship-based SOFC-battery hybrid system, including real-world laboratory results for power demand response and SOFC performance. Laboratory tests at PoC scale are compared with a higher-power demonstrator with a more complex fuel supply chain, due to anode off-gas recirculation, and with theoretical simulations results in order to analyse the achievable power ramp rates. The study demonstrate that the PoC can achieve a power ramp rate of 10% kWrated/min, compared to the 4%kWrated/min of the demonstrator, while comparing it with a theoretical maximum power ramp rate derived from a model-based investigation. Over an ~8-hour operational profile, the SOFC-battery hybrid successfully met ship-like power demands, generating a peak power of ~28 kW. The analysis details power demand coverage, SOFC voltage, and temperature behavior, demonstrating the system's capability to maintain stable and efficient operation under dynamic conditions.

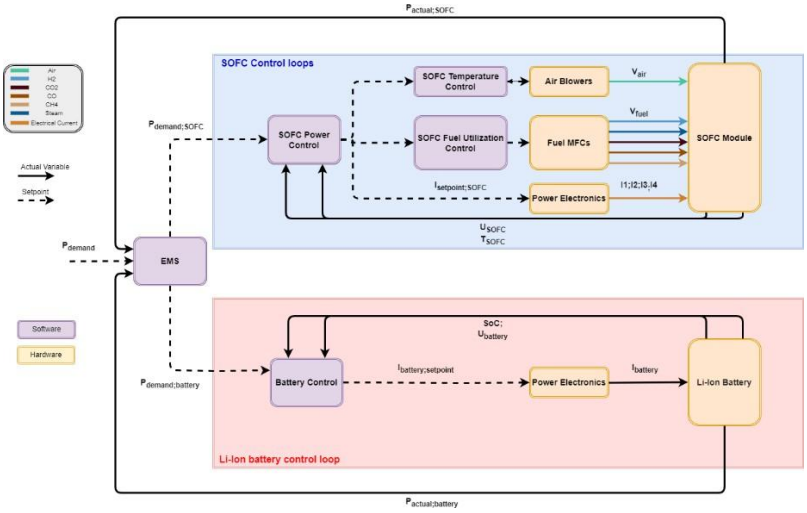


Figure 1: Overarching control loop for the SOFC-Battery Hybrid

Conclusions:

By providing these insights, this study underscores the feasibility of integrating SOFC technology into modern ship powertrains. The findings contribute to the broader goal of accelerating the industrial adoption of SOFC systems, paving the way for more sustainable and efficient maritime energy solutions

Acknowledgment:

This research was funded by the European Commission within the European Union's Horizon 2020 research and innovation program under the project NAUTILUS, grant number 861647.

References

[1] Åström, K.; Hakala, T.; and Fontell, E. (2020), Product development and experiences of a new Convion SOFC system, Proceedings of the 14 th European SOFC & SOE Forum, A0602, 124-130

[2] Salas Ventura S., Metten M., Fortunati D. et al, Electrochemical processes and energy systems towards step-wise emission reduction of maritime transport, Sustainable Shipping Days + Workshop on Ammonia FC Systems, 1-2 July 2024 Lucerne, Switzerland

[3] Ünlübayir, C., Youssfi, H., Khan, R. A., Ventura, S. S., Fortunati (2024). Comparative analysis and test bench validation of energy management methods for a hybrid marine propulsion system powered by batteries and solid oxide fuel cells.

[4] https://www.dlr.de/en/tt/research-transfer/research-infrastructure/test-facilities/galactica

[5] https://www.dlr.de/en/tt/research-transfer/research-infrastructure/modelling-tools/tempest

European Fuel Cells and Hydrogen
PIERO LUNGHI CONFERENCE
EFCH2 2025
September 17th–19th 2025
Capri / Italy

Tailoring exsolved NP in Fe-doped Lanthanum Strontium Chromite: implications on H_2/CH_4 utilization in SOFCs

D. Chinello *[a], B. Senoner [a], J. Cavazzani [a], A. Glisenti [a, b]

* Corresponding author: davide.chinello@phd.unipd.it

[a] Department of Chemical Sciences, Università degli Studi di Padova, Padova, Italy

[b] CNR-ICMATE INSTM, Padova, Italy

Keywords: SOFC, versatile anodes, perovskite, exsolution

Abstract:

Solid Oxide Fuel Cells (SOFCs) offer a promising route for efficient energy conversion, with methane gaining attention as a viable fuel due to its availability and existing infrastructure. This study explores La0.8Sr0.1Cr1-x-yFexMyO3 (M = Ni and/or Cu) perovskite materials as potential SOFC anodes, leveraging transition metal exsolution to enhance catalytic performance and stability. The controlled exsolution process, driven by A-site deficiency, led to the formation of metal nanoparticles, boosting both CH4 reforming and H_2 oxidation capabilities and thus highlighting the potential utilization of these materials as both traditional catalysts for Dry Reforming of Methane (DRM) and versatile SOFC anodes.

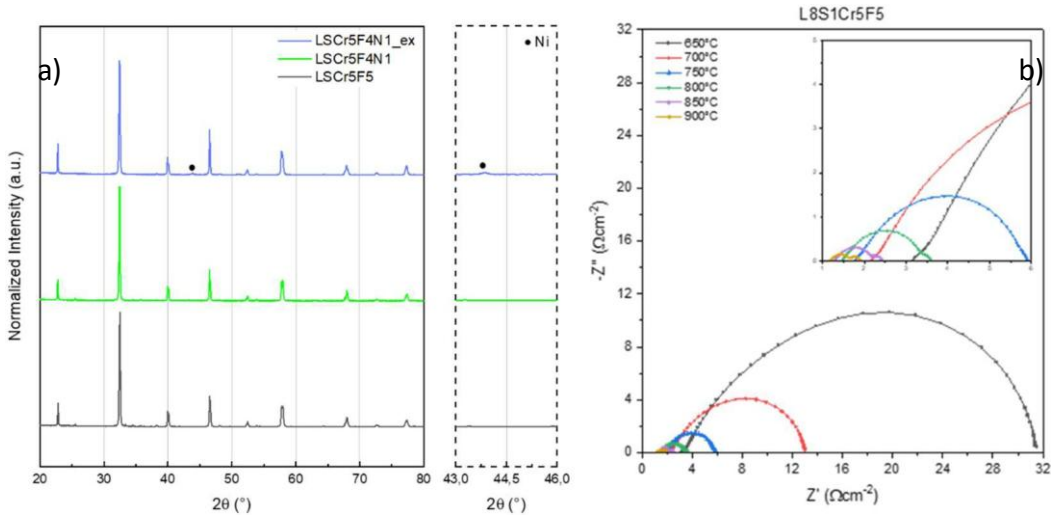
Introduction: While hydrogen remains the most conventional and studied SOFC fuel, methane is gaining significant attention as an alternative since it is readily available through natural gas extraction and biogas production, providing a well-established infrastructure for its distribution and storage. Moreover, hydrogen, which serves as a key fuel for SOFCs, is predominantly produced via methane reforming, making CH_4 a critical resource in the plethora of devices that convert chemical energy into electricity. $La_{0.8}Sr_{0.1}Cr_{1-X-Y}Fe_XM_YO_3$ perovskite (where M stands for Ni and/or Cu) materials show interesting catalytic activity towards both CH_4 reforming and H_2 oxidation, as well as high stability conferred by Cr presence in B-site, thus making their use as SOFC anode particularly promising. [1] Nanocomposition obtained by exsolution of the B-site transition metals, favoured by 10% deficiency in the A-site, can further enhance thermo- and electro- catalytic activity and improve electrical conductivity in SOFC devices. In particular, the simultaneous exsolution of Fe is reported to have a double impact on the overall properties, being Fe nanoparticles active towards methane dry reforming and having a stabilizing role on Ni nanoparticles, that otherwise are subjected to passivation due to coke deposition. [2-5] Cu nanoparticles, instead, acts as active site for CO_2 coordination and its subsequent reduction reaction, thus being fundamental in DRM applications. [6] A co-exsolution approach is therefore studied to

maximize the potential outcomes of these kind of materials, investigating in details the key roles of the different nanoparticles composition in DRM, CH_4 decomposition and anode utilization in SOFC devices.

Objectives: The main objective of this research is the rational design, characterization and catalytic performances evaluation of LSCrFM perovskite materials. The role of different metals exsolution on both morphological and catalytic activities will be investigated via the preparation of catalyst with different composition and loads in exsolvable metals, with particular attention to the formation of single metal nanoparticles or alloys.

Material and methods: LSCrFM materials, with 10% A-site deficiency in order to facilitate M-metal(s) exsolution, were synthesized following the citrate-nitrate route, with a ratio citric acid:cations equal to 2:1, followed by a calcination treatment at 1000°C for 6h and exsolution at temperatures up to 900°C in 5% H_2 atmosphere. Further considerations were carried out by means of XRD, H_2-TPR, XPS results and through SEM/EDX maps. The materials performances were eventually evaluated by GC analyses for CH_4 reforming/decomposition, while LSGM electrolyte-supported SOFC devices were characterized by EIS for electrochemical characterization and LP analyses for power density evaluation, employing different fuel mixtures.

Results: XRD pattern acquisitions have shown no appreciable presence of spurious phases, while H_2-TPR analyses up to 900°C have confirmed both the reducibility from M^{2+} to M^0 and the stability in reducing environment, thus indicating the overall eligibility of the materials as exsolvable matrixes.
The exsolution process, carried out at 900°C for 6h in a 5% H_2 atmosphere for all samples in order to minimize the temperature effect on the perovskite matrix and favoured by the intrinsic defectivity of the matrix given by the 10% A-site deficiency, led to the formation of metal nanoparticles (see Graph 1a) in the range 20-50 nm, as shown by SEM images, which nature (single metal or alloys) is under evaluation via EDX maps.
In-situ XAFS measurements in H_2-TPR analyses have confirmed the reduction of M-metal Catalytic tests showed a CH_4 conversion up to 20% in Ni-exsolved materials, coherently with literature data. [4] Interesting outcomes were obtained by testing the final electrolyte-supported SOFC device in 10% H_2 atmosphere, reaching a polarization resistance of 1.5 Ωcm^2 at 850°C (see Graph 1b). Further considerations derive by the results obtained from different feedings.



Graph 1: *XRD pattern of pristine perovskite matrix and exsolved one (a), EIS curves of LSCr5F5 anode in 10% H_2 atmosphere.*

Conclusions: The investigation of LSCrFeM perovskite materials demonstrates their strong potential as SOFC anodes, employing both hydrogen and methane gas mixtures. The exsolution of transition metal nanoparticles, facilitated by A-site deficiency, successfully enhances catalytic activity and stability in reducing environments. The co-exsolution approach, notably involving Fe and Ni, has proven effective in improving methane dry reforming and mitigating coke deposition, while Cu nanoparticles contribute to CO_2 activation. Catalytic testing confirmed promising CH_4 conversion rates, and electrochemical evaluations of SOFC devices yielded a polarization resistance of 1.5 Ωcm^2 at 850°C, reinforcing the material viability. These results highlight the significant role of LSCrFM perovskites as advanced and versatile SOFC anode technology.

Acknowledgment

This research was funded by the European Union's Knowskite-X project under grant agreement n°101091534.

References

[1] Tao, S; Irvine, J.T.S. Chem. Mater. 2004, 16, 4116-4121.
[2] Neagu, D. et al. Nat. Chem. 2013, 5, 916–923.
[3] Cavazzani, J. et al. Int. J. Hydrogen Energy. 2022, 47, 13921-13932.
[4] Zhang, J. et al. Int. J. Hydrogen Energy. 2024, 55, 572-580.
[5] Papargyriou, D. et al. Mater. Chem. A, 2019, 7, 15812.
[6] Yang, X. et al. J. Eur. Ceram. Soc., 2023, 43, 3414-3420.



Impact of Ammonia Decomposition on SOFC Performance: A DRT Study

Luigi Margutti*[a], Giovanni Cinti[a], Anna Donnadio[b]

* corresponding author: luigi.margutti@dottorandi.unipg.it

[a] University of Perugia, Department of Engineering, Perugia, Italy

[b] University of Perugia, Department of Pharmaceutical Sciences, Perugia, Italy

Keywords: Ammonia, DRT, EIS, SOFC

Abstract:

Ammonia is emerging as a promising carbon-free fuel to decarbonize the energy sector, particularly in power generation and maritime applications. Solid Oxide Fuel Cells (SOFCs) are considered one of the most efficient technologies for direct ammonia utilization due to their high efficiency and fuel flexibility. However, challenges remain regarding ammonia decomposition, electrochemical performance, and long-term durability. This study investigates the impact of ammonia cracking and nitrogen dilution on a SOFC operating with ammonia and hydrogen/nitrogen mixtures, employing electrochemical impedance spectroscopy (EIS) and Distribution of Relaxation Times (DRT) analysis.

Introduction: Ammonia has proved to be a promising alternative fuel for sustainable energy applications, offering a carbon-free energy cycle when produced from renewable sources. Among its various applications, its use in SOFCs has gained increasing attention, because at high operating temperatures, ammonia undergoes in situ decomposition into hydrogen and nitrogen, facilitating efficient electrochemical reactions within the SOFC anode. Nevertheless, ammonia utilization presents challenges, such as the competition between catalytic decomposition and charge transfer processes or gas diffusion [1]. EIS consent to identify the contribution of internal processes to polarization losses. DRT is a further elaboration that allows investigating separate contributions of different cell components [2].

Objectives: The test campaign aims to evaluate the effect of ammonia, when used as a fuel in SOFC, through EIS/DRT analysis. To achieve this goal the cell is fuelled with ammonia or hydrogen/nitrogen mixture. Firstly, the peaks in the DRT spectrum are paired with their corresponding electrochemical contributions, supported by literature regarding DRT on SOFC [2], [3]. Then the peak variations due to ammonia or nitrogen are investigated.

Material and methods: The tested anode-supported SOFC cell and the test rig were described in a previous article [1]. After start-up and validation, the cell was operated at two different gas conditions: pure ammonia and hydrogen-nitrogen mixture. The gas flow rate was designed to have in both conditions the same amount of hydrogen and nitrogen elements. EIS study is performed at Open Circuit Voltage (OCV) and 0,8 A, at three different temperatures, 600, 675, 750°C. DRT was obtained using free software DRTtools [4].

Results: DRT curves for tests conducted with pure ammonia at OCV are reported in Figure 1. The impact of temperature can be seen on the peak at low frequencies, in the range 10^{-1}:10^{1} Hz, and on the peaks in the 10^{2}:10^{4} Hz range. Considering current knowledge shared by the scientific literature, as discussed before, these frequency ranges correspond to the fuel electrode diffusion phenomenon and fuel electrode charge transfer, respectively. For the test at 600°C, a significant difference is highlighted. The peak at low frequencies is separated into two smaller peaks and these are distributed in a larger frequency range. This can be related to the ammonia cracking, which is slowed at lower temperatures. If ammonia is not completely decomposed, the remaining NH_3 is inert and causes diffusion losses or could complete the decomposition inside the cell.

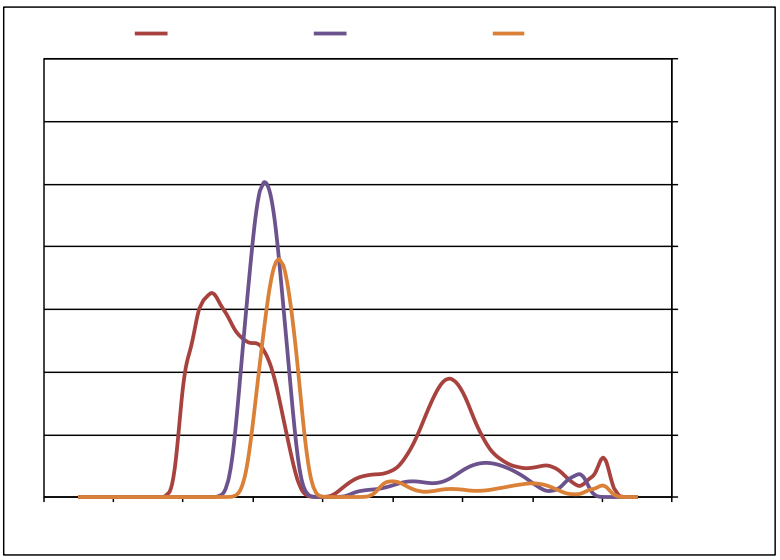


Figure 1: DRT of NH_3 mixture at 600°C, 675°C and 750°C.

Figure 2 compares DRT plots of ammonia and hydrogen and H_2/N_2 mixture test at 600°C and. At high frequencies these two plots are quite similar but differ in the 10^{-1}:10^{1} Hz and 10^{2}:10^{3} Hz ranges, related to fuel electrode diffusion and charge transfer, as previously described. The peak at low frequencies also shifts to lower ones for the ammonia case.

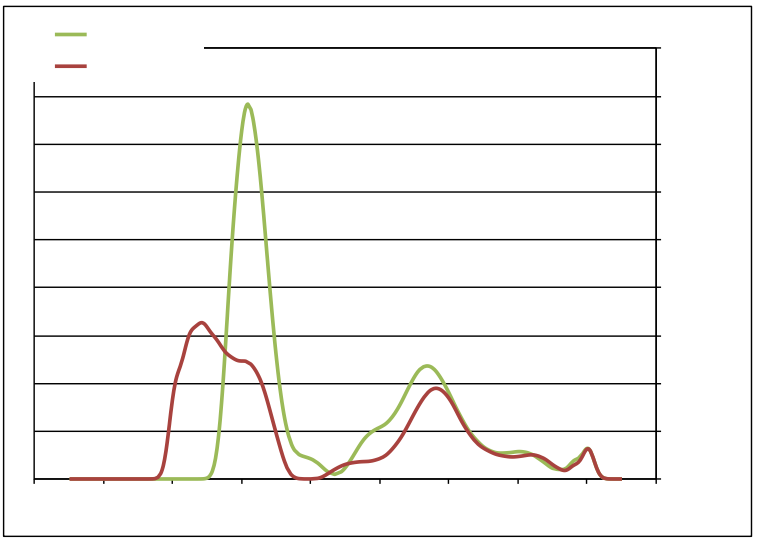


Figure 2: DRT of H_2N_2 and NH_3 mixture at 600°C.

Conclusions: A single SOFC is studied with DRT to better characterize the impact of ammonia as a fuel. Decrease in operational temperature highlights variations in peaks related to fuel electrode diffusion and charge transfer. At 600°C the lower frequency peak shows a separation into two smaller peaks on a larger frequency range. Furthermore, the DRT plots of a SOFC fuelled with direct ammonia also show that the peak at low frequency shifts to lower frequency values compared to decomposed ammonia fed SOFC.

Acknowledgment

This research was partially funded by the RASMUS project “ xcellence”, Grant Agreement number 101104447.

References

[1] G Cinti, A Baldinelli, G Bidini, and L Barelli, “ lectrochemical Impedance Spectroscopy study on ammonia-fed Solid Oxide Fuel Cells,” in *Journal of Physics: Conference Series*, 2022. doi: 10.1088/1742-6596/2385/1/012052.

[2] A. Leonide, V. Sonn, A. Weber, and E. Ivers-Tiffée, “ valuation and Modeling of the Cell Resistance in Anode-Supported Solid Oxide Fuel Cells,” *J Electrochem Soc*, vol. 155, no. 1, 2008, doi: 10.1149/1.2801372.

[3] A Baldinelli, A Staffolani, G Bidini, L Barelli, and F obili, “An extensive model for renewable energy electrochemical storage with Solid Oxide Cells based on a comprehensive analysis of impedance deconvolution,” *J Energy Storage*, vol. 33, 2021, doi: 10.1016/j.est.2020.102052.

[4] T Wan, M Saccoccio, C Chen, and F Ciucci, “Influence of the Discretization Methods on the Distribution of Relaxation Times Deconvolution: Implementing Radial Basis Functions with DRTtools,” *Electrochim Acta*, vol. 184, 2015, doi: 10.1016/j.electacta.2015.09.097.

European Fuel Cells and Hydrogen
PIERO LUNGHI CONFERENCE
EFCH2 2025
September 17th–19th 2025
Capri / Italy

Model-based Humidity Control of a Polymer Electrolyte Membrane Fuel Cell-based Electric Vehicle

Eva Neumair*[a,b], Maximilian K. Eisner[a], Fengmin Du[a], Volker Formanski[a], Hermann Rottengruber[b]

* corresponding author: Eva Neumair (Eva.Neumair@bmw.de)
[a] BMW Group, Knorrstraße 147, 80807 München, Germany.
[b] Otto-von-Guericke-Universität, Unversitätsplatz 2, 39106 Magdeburg, Germany.

Keywords: Fuel Cell Systems, Water Management, Membrane Humidifier, Model-based control

Introduction: Fuel Cell Electric Vehicles (FCEVs) are a promising complement to Battery Electric Vehicles (BEVs) in the automotive industry's efforts to decarbonise vehicle powertrains. Polymer electrolyte membrane (PEM) fuel cells are preferred for automotive applications due to their low operating temperature, fast and dynamic response.

Effective water management is essential to optimise the performance and longevity of PEM fuel cell systems [1, 2]. An excess of water can block the flow channels in the fuel cells, impeding the reactants from reaching the catalyst layer and hindering the electrochemical reaction. However, if the humidity in the membrane decreases, the proton conductance also decreases. Thus, the electric efficiency of the fuel cells is reduced. Furthermore, the dry operation can impact durability. Apart from the global aspects of water management, local differences in the membrane occur due to the continuous water production along the channel. As a result, the membrane dry-out may occur close to the inlet of the air flow. To mitigate this issue, external humidification is often employed to ensure adequate humidification of the inlet reactant streams. Due to low energy losses and no external water supply, membrane humidification is preferred for automotive solutions. Since water is produced as part of the reaction, the membrane humidifier uses the wet exhaust stream of the stack. It is passed over a membrane, where water is selectively transferred to the dry air inlet stream [3].

Objectives: This study aims to develop a model-based humidity controller, which regulates the relative humidity at the cathode stack inlet within a fuel cell electric vehicle. The controller operates by manipulating the position of the bypass valve and must support real-time

functionality, as it will be incorporated into the vehicle's software system. To implement the humidity controller, a real-time capable humidity model is required to predict the stack inlet humidity as a function of the bypass position. Thus, a humidifier model and a fuel cell stack humidity model are needed as a coupled relationship exists between these two systems. Figure 1 illustrates a schematic representation of the controlled system.

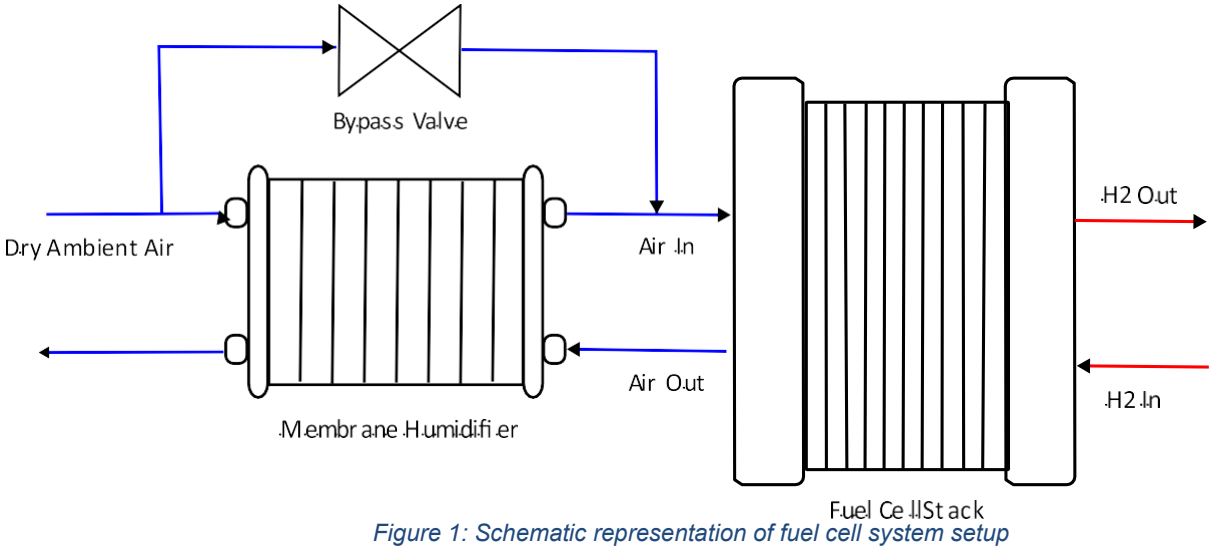


Figure 1: Schematic representation of fuel cell system setup that considers the fuel cell stack and the membrane humidifier.

Materials and methods: To ensure real-time capability, a lumped-parameter model approach was used for the fuel cell stack, considering both gas channels, the catalyst layer and the membrane separately. Moreover, the humidifier model of Schoenfeld et al. [3] was used, which employs an adapted analytical modelling approach for the humidifier model. This model effectively captures the key transport phenomena, including convective and diffusive mass transfer and sorption behaviour at the membrane-gas interfaces. Both models were implemented in Matlab-Simulink and validated against measurement data of a full-scale fuel cell system test bench.

In the next step, the coupled humidifier and stack models were employed to design an optimization-based control design. The controller manipulates the stack inlet humidity by adjusting the bypass valve; thus, changing the mix between dry and humidified gas. Furthermore, a state observer is utilized to estimate unmeasurable variables due to the absence of sensors.

Results: The simulations show that the model-based humidity controller effectively stabilises the relative humidity at the cathode stack inlet, preventing the risk of membrane damage. Compared to a fuel cell system without a humidity controller, the control system effectively

enhances the humidity distribution along the channels due to constant inlet humidity. Thus, flooding can be alleviated, and the humidifier can be utilised to its full capacity during dry operating conditions. By using the stack inlet humidity as the control variable, the system can proactively mitigate drying areas even before they become evident in impedance measurements of the membrane or the voltage output of the system. Impedance measurements are frequently used to monitor the humidity of the membrane.

Conclusions: This study presents a model-based humidity control strategy for a PEM fuel cell system that effectively regulates the relative humidity at the stack inlet. The developed models for the fuel cell stack and the membrane humidifier capture the key water transport phenomena and were validated against experimental data, ensuring real-time capability for integration into a vehicle's control system. The results indicate that a model-based humidity control loop with a membrane humidifier provides a stable and precise method for managing humidity. This approach reduces the risk of membrane damage and enhances the performance of the fuel cell systems.

While multiple humidity control algorithms exist, they either rely on variants of Proportional-Integral-Derivative (PID) controllers [5], or are only focused on regulating the membrane humidity itself by monitoring the voltage output or impedance measurements, neglecting the dynamic behaviour of membrane humidity devices [4] . Thus, our study provides a robust and effective humidity control strategy crucial for ensuring the efficient operation of PEM fuel cell systems within automotive applications. The proposed control strategy is effective in simulations and suitable for practical implementation in actual vehicles.

References

[1] Jeon, D. H., Kim, K. N., Baek, S. M., & Nam, J. H. (2011). The effect of relative humidity of the cathode on the performance and the uniformity of PEM fuel cells. *International Journal of Hydrogen Energy*, *36*(19), 12499-12511.

[2] Jiao, K., & Li, X. (2011). Water transport in polymer electrolyte membrane fuel cells. *Progress in energy and combustion Science*, *37*(3), 221-291.

[3] Schoenfeld, L., Kreitmeir, M., Wolfenstetter, F., Neumann, M., Klein, H., & Rehfeldt, S. (2024). Modeling mass and heat transfer in membrane humidifiers for polymer electrolyte membrane fuel cells. *International Journal of Heat and Mass Transfer*, *223*, 125260.

[4] Zhang, L., Pan, M., & Quan, S. (2008). Model predictive control of water management in PEMFC. *Journal of Power Sources*, *180*(1), 322-329.

[5] Liu, Z., Chen, J., Chen, S., Huang, L., & Shao, Z. (2017). Modeling and control of cathode air humidity for pem fuel cell systems. *IFAC-PapersOnLine*, *50*(1), 4751-4756.

EFCH2 2025
European Fuel Cells and Hydrogen
PIERO LUNGHI CONFERENCE
September 17th–19th 2025
Capri / Italy

Spatially and Temporally Resolved Stainless Steel Bipolar Plate Degradation Model for PEMFCs

Andraž Kravos*[a], Miha Gričar [a], Mitja Drab [a], Matej Prijatelj [a], Tomaž Katrašnik [a],

* corresponding author: andraz.kravos@fs.uni-lj.si
[a] Faculty of Mechanical Engineering, University of Ljubljana, Aškerčeva 6, Ljubljana, SI

Keywords: PEM fuel cell, Spatially and temporarily resolved degradation, Stainless Steel Bipolar Plate, Multi-scale multi-domain modelling

Abstract

Introduction: Proton exchange membrane fuel cells (PEMFCs) are a promising energy conversion technology for automotive and stationary applications. Despite significant advancements in performance and efficiency, achieving the projected operational lifetime for heavy-duty applications remains a challenge. Addressing this issue requires accurate models capable of monitoring and predicting degradation processes to ensure long-term durability. For the latter, degradation of stainless-steel bipolar plates (BPPs), which exhibit high electrical and thermal conductivity, good gas impermeability, superior mechanical properties and formability [1], plays an important role. In PEMFCs, it primarily arises from electrochemical and chemical processes, which dominate under normal operating conditions. Corrosion occurs when the applied potential exceeds the standard potential of the metal, particularly in humid environments, leading to the formation of a nonhomogeneous oxide passivation layer. The outermost layer of the passivation layer consists predominantly of iron and molybdenum oxides, with traces of nickel oxide, forming under high oxidation potentials during FC operation. Underneath this layer, a chromium(III) oxide and hydroxide-enriched layer provides primary corrosion resistance by limiting ion transport [2]. Closer to the metal substrate, a modified alloy layer forms, reflecting compositional gradients of Cr, Fe, and Mo, as well as localized element depletion or enrichment due to electrochemical gradients [2, 3]. While prevailing degradation mechanisms have been established [3], existing models in the literature are largely lumped or semiempirical [4]. To address this gap, this work presents a physics-based, spatially and temporally resolved model for stainless steel BPP degradation in PEMFCs. This model, for the first time, enables a physically accurate description of multi-layer oxide growth with heterogeneous composition and its breakdown. Building upon an extended PEMFC performance model [5] and point defect models (PDM) [6,7], it incorporates a back-coupling mechanism between electrochemical potential and the multilayer passive film structure. This ensures that local potential variations that are driven by changes in current

density, electrolyte chemistry, or temperature and are directly reflected in defect chemistry and ion fluxes across each layer. Consequently, the model captures interface evolution, including the dissolution of outer layers and the dynamic growth or thinning of the chromium-enriched region. These moving interfaces are critical for understanding long-term corrosion kinetics, as the protective layer continuously reconfigures in response to the electrochemical environment within the fuel cell. Through this integrated approach, the model provides a physically grounded and computationally efficient framework for predicting stainless steel BPP corrosion and its impact on PEMFC performance and lifetime.

Objectives: The objective of this work was to develop a physics-based model for the spatial and temporal evolution of oxide layers on stainless steel BPPs. The model aims to analyse the competitive growth of Cr and Fe oxides and their impact on corrosion resistance while investigating the role of metal vacancy formation, oxide transport, and electrochemical potential in degradation. A key focus is to predict critical conditions leading to oxide breakdown and localized pitting and to quantify Fe^{2+} and Fe^{3+} fluxes to evaluate their effects on the Fenton reaction and membrane degradation. By providing a framework for optimizing BPP material selection and operational strategies, this model serves as a tool to improve the durability and performance of PEMFCs.

Material and methods: The model is developed using fundamental electrochemical and transport principles, leveraging the extended PDM framework to describe growth and breakdown of multi-layer oxide with heterogeneous composition and degradation processes related to them in computationally efficient way. Governing equations are formulated based on reaction-diffusion models for vacancy transport, coupled with Butler-Volmer-type expressions for charge transfer reactions at oxide interfaces. The oxide growth mechanism is described using flux-based formulations that account for the formation and competitive interactions of Cr and Fe oxides. The transport of defects and electrons within the oxide layers is described by the Nernst–Planck equation in 1D that accounts for diffusion, migration due to electric fields, and potential gradients within the oxide layer. Additionally, the distribution of the potential over the oxide is described by the Poisson equation in 1D, which links the local charge distribution to the electrostatic potential profile, thereby governing the electric field effects within the oxide layer. Furthermore, the model incorporates failure criteria based on metal vacancy accumulation and oxide stability thresholds to predict breakdown and pitting initiation. Additionally, Fe^{2+} and Fe^{3+} fluxes are calculated to assess their roles in hydroxyl radical formation and fluoride emission based on previously developed model [8]. Numerical simulations are implemented using finite-difference methods to resolve transient layer evolution, and model validation is performed by comparing predictions with experimental degradation data [2] and literature-reported corrosion rates of stainless steel in PEMFC environments [3].

Results: The simulation results provide an insight into interplay between Cr and Fe oxide formation and their effect on the potential. The latter is studied through sensitivity analysis, which indicates that an increase in electrochemical potential enhances metal vacancy migration, further accelerating corrosion. Similarly, but through different mechanism lower pH values promote oxide thinning and localized film breakdown, leading to increased corrosion rates. Model validation was conducted using ToF-SIMS depth profiles of CrO_2 and FeO_2 [2], which provide sputtering times that serve as a benchmark for oxide layer thickness and composition analysis. Model predictions align well with experimental measurements of oxide thickness, and corrosion and oxide growth rates for stainless steel BPPs, confirming the validity of the approach.

Conclusions: The results of developed modelling framework show a high degree of agreement with experimental data capturing the spatial and temporal evolution of oxide layers under realistic operating conditions. The results provide for the first time insights into the fundamental mechanisms governing multi-layer oxide growth with heterogeneous composition and their breakdown, facilitating the design of improved materials and operational strategies. Furthermore, the model's ability to predict cation fluxes from passivation layer, provides critical insights into cation roles in aggravating the Fenton reaction, offering a pathway to enhanced membrane durability. Owing to its mechanistic basis the developed modelling framework can thus be utilised in both the system design phase, where it can be used to enhance membrane and BPP durability by optimised material selection, and as a model-based virtual sensor for advanced monitoring and control of the PEMFC system, not only improving performance but also mitigating degradation and reducing the degradation rate of PEMFC.

Acknowledgment

The research is partially funded by the Slovenian Research Agency (research core funding No. P2-0401). The authors also acknowledge financial support from the European Union's Clean Hydrogen Partnership and its members Hydrogen Europe, Hydrogen Europe Research, Horizon Europe Climate, Energy and Mobility under Grant Agreements RealHyFC No.: 101111904, MeasureD No.: 101101420, and NAHV No.: 101111927.

References

[1] Leng et al. (2020). Journal of Power Sources. 451. 227783.
[2] Wang et al. (2019). Corrosion Science. 165. 108395. 10.1016/j.corsci.2019.108395.
[3] Su et al. (2024). Corrosion Science. 236. 112277. 10.1016/j.corsci.2024.112277.
[4] Elferjani et al. (2021). International Journal of Hydrogen Energy. 46.
[5] Kravos et al. (2022). Journal of Power Sources. 541. 231598.
[6] Chao et al. (1981). J. Electrochem. Soc. 128. 1187. 10.1149/1.2127591
[7] Lin et al. (1981). J. Electrochem. Soc. 128. 1194. 10.1149/1.2127592
[8] Frühwirt et al. (2020). Physical Chemistry Chemical Physics. 22. 10.1039/C9CP04986J.

EFCH2 2025
European Fuel Cells and Hydrogen
PIERO LUNGHI CONFERENCE
September 17th–19th 2025
Capri / Italy

Improved Local Description of the Capillary Pressure - Saturation Relation to Enhance Reliability of CFD Results

Lukas König*[a], Sabina Schneider [a], Eva Fensterle [a], Florian Wilhelm [a], Joachim Scholta [a], Markus Hölzle [a]

* corresponding author: lukas.koenig@zsw-bw.de

[a] Zentrum für Sonnenenergie- und Wasserstoff-Forschung Baden-Württemberg (ZSW)

Keywords: CFD, GeoDict, Gas Diffusion Layer(GDL), Water managment

Abstract Introduction:

Proton exchange membrane fuel cells (PEMFCs) have experienced significant performance enhancements in recent decades, achieving current densities up to 3 A/cm² alongside improvements in efficiency and durability. Maintaining optimal water management and reactant transport within the catalyst layer necessitates the development and refinement of substrates and microporous layers (MPLs). These advancements introduce novel challenges to PEMFC simulation, requiring the development of updated models that accurately represent the evolving material characteristics.

Objectives:

This study aims to enhance the accuracy of computational fluid dynamic (CFD) simulations of proton exchange membrane fuel cells (PEMFCs). Although foundational research on modeling gas diffusion layer (GDL) permeability and wetting behavior in PEMFCs was conducted two decades ago [1, 2, 3], these early models exhibit limitations when applied to present state-of-the-art, high-performance GDLs. Therefore, the primary objective of this work is to develop an improved functional to describe the water inventory within the GDL substrate and MPL. Conventionally, the water inventory within these regions is described employing a specific representation of the relation between capillary pressure and water saturation called the Leverett J-function. While the standard J-function parameters, as presented in [6], derived from studies on porous rocks [5], provide reasonable first approximations, their applicability to state-of-the-art GDLs is suboptimal. This is supported by recent work [4], which demonstrates the potential of alternative functionals for improved representation of water distribution.

Material and methods:

To provide digitalized base structures, industrial GDLs are analyzed using micro-computed tomography (micro-CT) and focused ion beam-scanning electron microscopy (FIB-SEM). Thus, high-resolution three-dimensional (3D) images of both the substrate and MPL are aquired. Digital twins are generated from these scans using the GeoDict simulation software to model relevant material parameters, including diffusion and permeability. Furthermore, the GDL substrate is subjected to compression under a realistic channel-rib structure to obtain

representative mechanical data. Saturation-pressure curves for the materials are subsequently simulated using GeoDict, providing the basis for modifications within the CFD code. These newly derived parameters are then implemented in the Ansys Fluent PEMFC model, utilizing an automotive single-channel design based on the ZSW Generic HyFab design [7]. For validation purposes, the single-channel simulation results, specifically current density, are compared to experimental data obtained from short-stack experiments employing a current density scan shunt.

Results:

The simulated capillary pressure curves for the GDL substrate exhibit a significant deviation from the default parameters implemented in the CFD code, as illustrated in figure 1. Three different polynomial fits are applied to the data. Although a third-degree polynomial fit provides a reasonable approximation, a seventh-degree polynomial fit is selected to more accurately capture the sharp increase in capillary pressure from zero saturation, enhancing numerical stability in the CFD simulations (figure 2).

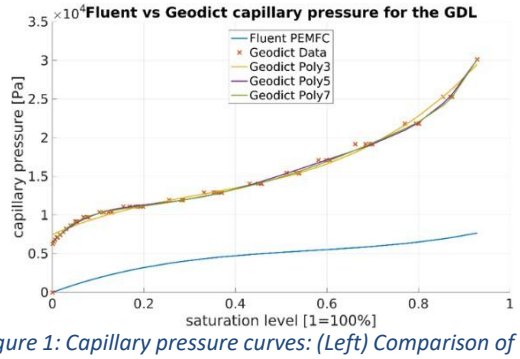


Figure 1: Capillary pressure curves: (Left) Comparison of the original Fluent implementation (blue) and the GeoDict simulation (red), along with their respective polynomial fits

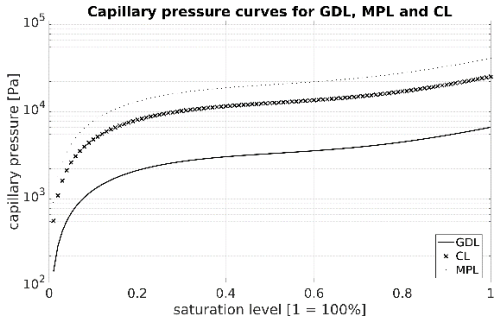


Figure 2: Implementation of the seventh-degree polynomial fit for the substrate, MPL, and catalyst layer (CL) with zero crossing for numerical stability

Implementation of these modified capillary pressure curves in the Fluent PEMFC model yields substantial changes in the predicted current density, as shown in figure 3. Overall, there is a quite good agreement of experimental results and the simulated current density distribution (figure 4). While the first two-thirds of the curve agree very well, the last part still requires some improvement.

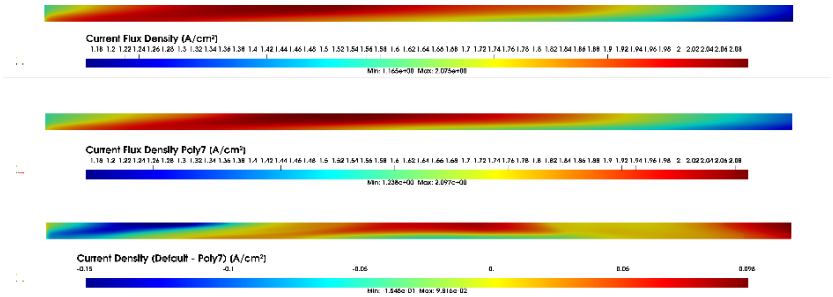


Figure 3: Current density from a single channel simulation for the default case, modified 7th degree polynomial fit and last the difference of both of them

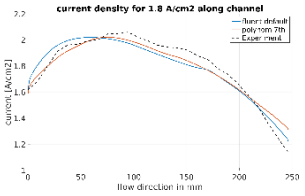


Figure 4: Current density average along the channel

Adjusting the parameters for all porous components (substrate, MPL, and CL) - as in Figure 2 above - results in the probably most accurate current density profile. Compared to the default case, the current density gradients between the rib and channel regions are more pronounced, due to higher liquid saturation and lower diffusion of oxygen under the ribs, while the overall current density distribution along the channel is more uniform. These initial results demonstrate the significant influence of the J-function on the predicted current density distribution within the PEMFC.

Conclusions:

The results presented above clearly demonstrate that while GeoDict simulations provide very valuable capabilities for characterizing GDL water inventory properties, implementing these enhanced parameters within a PEMFC CFD code still presents non-trivial challenges. The J-function significantly influences the predicted liquid water inventory within the fuel cell. Consequently, all water-related parameters require careful adjustment to correctly reflect the properties of recent, state-of-the-art material, to finally obtain realistic simulation results.

Acknowledgment

This work has received financial support by the German Federal Ministry for Digital and Transport within the framework of the GALLIA project (NIP II, 03B10114D).

References

[1] Gostick, Jeffrey T., et al. "Capillary pressure and hydrophilic porosity in gas diffusion layers for polymer electrolyte fuel cells." *Journal of power sources* 156.2 (2006): 375-387.

[2] Kumbur, E. C., K. V. Sharp, and M. M. Mench. "On the effectiveness of Leverett approach for describing the water transport in fuel cell diffusion media." *Journal of Power Sources* 168.2 (2007): 356-368.

[3] Kumbur EC, Sharp KV, Mench MM. Validated Leverett approach for multiphase flow in PEFC diffusion media. J Electrochem Soc 2007;154..

[4] Sarkezi-Selsky, Patrick, et al. "Lattice Boltzmann simulation of liquid water transport in gas diffusion layers of proton exchange membrane fuel cells: Parametric studies on capillary hysteresis." Journal of Power Sources 535 (2022): 231381.

[5] Leverett, MoC. "Capillary behavior in porous solids." Transactions of the AIME 142.01 (1941): 152-169.

[6] Ansys® Fluent PEMFC module, Release 24.2, Theory Guide, 20.1.4. Water Transport and Mass Transfer in PEMFC, ANSYS, Inc

[7] Häußler, F. et al. (2024). The ZSW HyFaB Generic Stack (1.0). https://doi.org/10.5281/zenodo.14223364

EFCH2 2025 European Fuel Cells and Hydrogen
PIERO LUNGHI CONFERENCE
September 17th–19th 2025
Capri / Italy

A simplified control strategy for optimal low-pressure operation of pemfc systems for aviation application

Dominik Murschenhofer*[a], Jonas Settele [a], Cornelie Bänsch[a]

* corresponding author: dominik.murschenhofer@dlr.de
[a] German Aerospace Center (DLR), Institute of Engineering Thermodynamics, Pfaffenwaldring 38-40, 70569 Stuttgart, Germany

Keywords: control strategy, design of experiment, low-pressure operation, PEMFC performance optimization

Introduction:

The use of PEM fuel cells as power source is a promising approach to contribute to the decarbonization of the aviation sector. The harsh environmental conditions, i.e. low temperature and low pressure, to which fuel cells are exposed in aviation applications strongly affect the fuel cell's performance [1]. In order to minimize the resulting power losses, an adaption of the control parameters is required. In previous studies, fuel cells were primarily characterized under low-pressure conditions [2], [3], [4] and some indications how to overcome the associated power losses at specific pressure levels were given [5], [6], [7].

Objectives:

The present study aims at deriving a full pressure dependent control strategy for low-pressure operation of a PEMFC system, i.e. optimal control parameters as functions of the pressure and the current density. Furthermore, the proposed optimization procedure shall be transferable to various other PEMFC systems for future aviation applications.

Experimental setup and methods:

A PEMFC system is operated inside a low-pressure chamber, where pressure and temperature can be controlled to simulate altitude conditions. The fuel cell system is composed of a self-humidifying 120 cells Hydrogenics HyPM HD 10-120 PEMFC stack with an active cell area of 195 cm² and 12 kW nominal power output, an anode recirculation pump and a cooling unit. A blower supplies the cathode inlet with air from the low-pressure atmosphere.
To identify the optimal operating conditions for low-pressure operation of the PEMFC system, a parameter study with 480 measuring points is performed based on statistical design of

experiment methods, i.e. using a D-optimal design approach. Therefore, the stack temperature T and the cathode stoichiometry λ are varied at different current density i and chamber pressure p levels. The experimental results allow to derive model equations for the system net power $P_{net}(t, p, i, T, \lambda)$ and the relative humidity $rH(p, i, T, \lambda)$. For P_{net}, a constant degradation is considered by incorporating the runtime t.

Results:

Initially conducted polarization curve measurements under low-pressure conditions by using the manufacturer's default parameters for T and λ control show significant net power losses of up to 59% at 491 hPa with respect to 980 hPa, see the black dashed line in Figure 1a. The power losses primarily result due to stack drying. From the results of the parameter study, the optimal values for T and λ control under low-pressure conditions are determined by optimizing the net power model equation such that $P_{net}(t, p, i, T_{opt}, \lambda_{opt}) = \max\{P_{net}(t, p, i)\}$. The optimal stoichiometry λ_{opt} exhibits a strong nonlinear dependence on p and i. However, the optimal stack temperature follows, in a first approximation, the linear relation $T_{opt}(p) = (26.48 + 0.037\ p)$ [°C], with p in hPa. Applying the optimized parameters yields a significantly higher net power at low-pressure operation compared to the use of the default parameters, see the black solid line in Figure 1a. At 497 hPa, the net power increase is as high as 29%, see the red line with the corresponding axis on the right in Figure 1a.

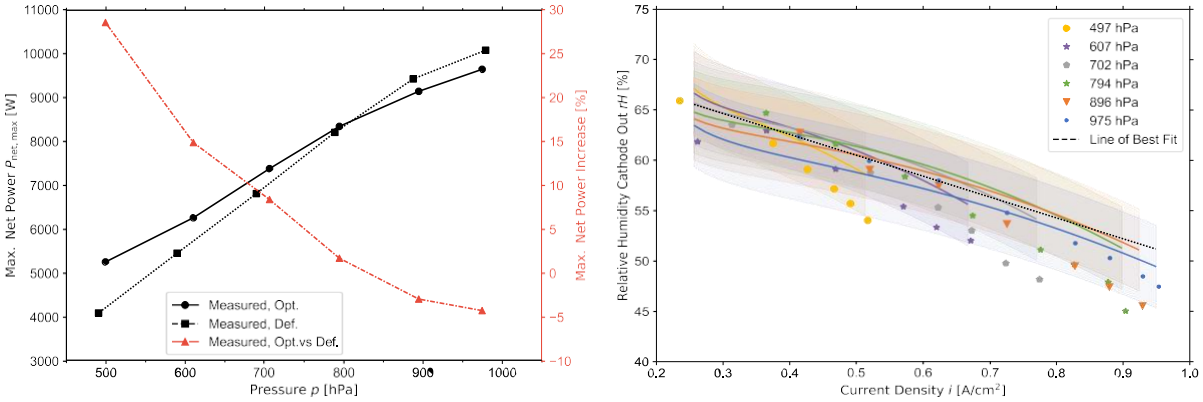


Figure 1: (a) Maximum net power obtained by using optimized and default parameters, the black lines correspond to the left axis. Increase of the maximum net power by applying optimal parameters, the red line corresponds to the right axis. (b) The solid lines show the model prediction of the optimal relative humidity $rH(p, i, T_{opt}, \lambda_{opt})$ for the different pressure levels. The model prediction intervals are indicated by the area shaded in the corresponding color. The black dashed line of best fit approximates the trend of all shown model prediction curves. The markers represent experimental data obtained with optimized control parameters.

It is well known that the maintenance of optimal fuel cell humidification conditions is crucial for high performance as well as durability. In Figure 1b the optimal relative humidity predicted by the regression model $rH(p, i, T_{opt}, \lambda_{opt})$ is shown for the investigated pressure levels. Remarkably, the prediction curves lie almost on top of each other. Moreover, they lie within each other's prediction intervals indicated by the shaded areas shown in the same color as the corresponding model prediction curves. This indicates that the optimal relative humidity at the cathode outlet is pressure independent and follows, in a first approximation, the black dashed line of best fit $rH_{opt}(i) = (70.9 - 20.7\ i)$ [%], with i in A/cm². For comparison, the

measured relative humidity during experiments with optimized control parameters, are shown as colored markers in Figure 1b.

Conclusions:

A simplified control strategy yielding high system net power at low-pressure operation can be implemented by controlling the pressure dependent stack temperature according to $T_{opt}(p)$ = (26.48 + 0.037 p) [°C]. On the other hand, the cathode stoichiometry can be used to maintain the relative humidity at the cathode outlet in its current density dependent optimal state according to $rH_{opt}(i)$ = (70.9 – 20.7 i) [%] with an accuracy of about ±5%. However, to achieve the highest possible net power, the stack temperature and the cathode stoichiometry have to be set according to the identified pressure and current density dependent optimal parameters $T_{opt}(p, i)$ *and* $\lambda_{opt}(p, i)$.

Acknowledgment

Funding of the project EnaBle (20M1905) by the German Federal Ministry for Economic Affairs and Climate Action is gratefully acknowledged.

References

[1] W. J. Song, H. Chen, H. Guo, F. Ye, and J. R. Li, "Research progress of proton exchange membrane fuel cells utilizing in high altitude environments," *International Journal of Hydrogen Energy*, vol. 47, no. 59, pp. 24945–24962, 2022, doi: 10.1016/j.ijhydene.2022.05.238.

[2] V. Chang and J. Gallman, "Altitude Testing of Fuel Cell Systems for Aircraft Applications," in *SAE Transactions*, SAE International, 2004, pp. 1943–1957. Available: https://www.jstor.org/stable/44738079

[3] R. J. Spiegel, T. Gilchrist, and D. E. House, "Fuel cell bus operation at high altitude," *Proceedings of the Institution of Mechanical Engineers, Part A: Journal of Power and Energy*, vol. 213, no. 1, pp. 57–68, 1999, doi: 10.1243/0957650991537437.

[4] T. Graf, R. Fonk, S. Paessler, C. Bauer, J. Kallo, and C. Willich, "Low pressure influence on a direct fuel cell battery hybrid system for aviation," *International Journal of Hydrogen Energy*, vol. 50, pp. 672–681, 2024, doi: 10.1016/j.ijhydene.2023.09.003.

[5] T. Hordé, P. Achard, and R. Metkemeijer, "PEMFC application for aviation: Experimental and numerical study of sensitivity to altitude," *International Journal of Hydrogen Energy*, vol. 37, no. 14, pp. 10818–10829, 2012, doi: 10.1016/j.ijhydene.2012.04.085.

[6] C. Werner, F. Gores, L. Busemeyer, J. Kallo, S. Heitmann, and M. Griebenow, "Characteristics of PEMFC operation in ambient- and low-pressure environment considering the fuel cell humidification," *CEAS Aeronaut J*, vol. 6, no. 2, pp. 229–243, 2015, doi: 10.1007/s13272-014-0142-z.

[7] C. Werner, G. Preiß, F. Gores, M. Griebenow, and S. Heitmann, "A comparison of low-pressure and supercharged operation of polymer electrolyte membrane fuel cell systems for aircraft applications," *Progress in Aerospace Sciences*, vol. 85, pp. 51–64, 2016, doi: 10.1016/j.paerosci.2016.07.005.

European Fuel Cells and Hydrogen
PIERO LUNGHI CONFERENCE
September 17th–19th 2025
Capri / Italy

Degradation-Aware Design and Control of Fuel Cells for Hybrid Aeronautical Power Systems

Paolo Aliberti*[a], Marco Minneci [a], Marco Sorrentino, Fabrizio Cuomo [b], Carmine Musto [b]
* corresponding author: Paolo Aliberti
[a] Department of Industrial Engineering, University of Salerno, via Giovanni Paolo II 132, Fisciano (SA), 84084, Italy.
[b] Leonardo Aircraft, Aircraft Systems, Viale dell'Aeronautica, Pomigliano d'Arco (NA), 80038, Italy

Keywords: Degradation-aware sizing and control, hybrid aircraft, multi-level control, proton exchange membrane fuel cells.

Abstract

Introduction: The integration of proton exchange membrane fuel cells (PEMFCs) with battery storage systems constitutes a highly promising approach for greening the aviation sector, where the optimization of energy efficiency, minimization of weight, and enhancement of reliability are fundamental requirements. Compared to other technologies, PEMFCs exhibit advantages in terms of dynamics response to load fluctuations, while featuring a power-to-weight ratio approaching the 2 kW/kg target at system level for aviation applications [1]. These characteristics have prompted the initiation of numerous research projects aimed at exploring their potential application on board aircraft [2]. Against this background, it is worth noting that system durability also represents a major bottleneck hindering the deep utilization of PEMFCs for aeronautical applications and, despite the recent advances achieved in terms of innovative materials and the construction techniques of such devices, suitable control policies are needed to extend their lifetime. In the current literature, PEMFCs degradation is typically addressed by relying on the empirical model [3], which recognizes idling, start-stop, high-power and rapid transients as the main sources of degradation. Therefore, coefficients are employed to quantify the PEMFC aging during a datum mission profile, which is then converted into equivalent hydrogen consumption or operating cost [4].

Objectives: The bottleneck of the degradation-oriented strategies listed above is that they quantify degradation based on a single mission profile, thus complicating the sizing of the PEMFC system (PEMFCS) according to the last flight. This paper considers a battery-supported PEMFCS hybrid unit for aviation applications and presents its degradation-aware design and control. Particularly, the control task is here executed via a multi-level approach. In the first layer, the power split between hybridizing components is determined through a specification independent blended rule-based controller (BRBC) that suitably manages high-power, low-power, and transient phases. Then, low-level corrective actions are introduced. Indeed, by considering the maximum allowable end-of-life voltage drop, a further feedback-based controller is developed to ensure the BRBC strategy is respected in the beginning-of-life (BoL) and end-of-life (EoL) scenarios. This approach advances existing literature by shifting the focus from stack-level degradation to a comprehensive system-level analysis.

Material and methods: Starting from the BoL design assumptions described in a previous work [5], EoL sizing and control of the PEMFCS included within the aircraft's hybrid electric unit is carried out. Particularly, in [5] an efficiency-driven model is proposed to determine stack's electrical variables as a function of the normalized efficiency curves at both system and stack level. The approach is further refined here through the calculation of the PEMFCS degradation occurring after a specified number of operating hours, leveraging the experimental data provided in [6]. As a result, the maximum EoL power deliverable at system level is determined under the hypothesis of non degrading balance of plant's ancillaries. This outcome is then embedded into an optimization framework in order to identify the PEMFCS optimal degree of oversizing such that the power split strategy found in BoL condition is respected at EoL. Once the BoL oversizing task is successfully executed, a low level controller is introduced, making possible the interaction between the BoL and EoL subsystems, as shown in Figure 1.

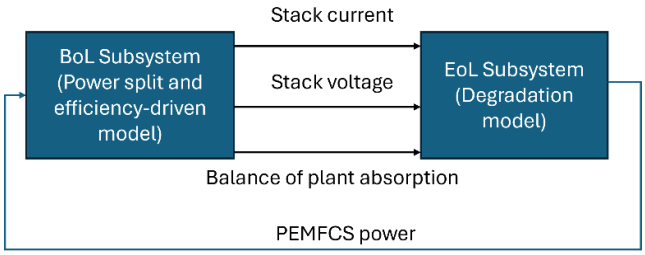
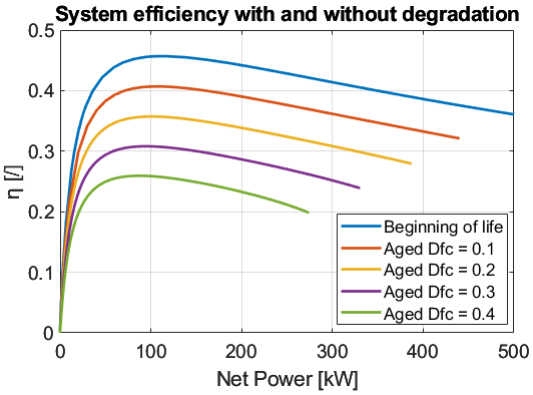


Figure 1. Interaction between the EoL and EoL subsystems.

In the first subsystem, the BRBC and efficiency-driven model are implemented to calculate BoL power supply, stack's voltage and current. In the second subsystem, the degradation is considered. A closed loop controller is thus realized by providing the resulting PEMFCS ouput power as a further input to the BoL block to adapt the BoL PEMFCS power supply to EoL specifications.

Results: The efficiency curves at different levels of degradation (Dfc), obtained via the approach described above, are shown in Figure 2. Particularly, the drop in net power between EoL and PEMFCS aged scenarios is attributable to the increased ancillaries' absorption. The required degree oversizing, which enables to respect the BRBC strategy at EoL is estimated to be approximately 45%, which would lead to an hydrogen consumption increase of about 50%.

Conclusions: The increasing push towards the greening of the aviation sector imposes to explore hydrogen-based fuel cell systems, which must be accurately sized and controlled according to end-of-life criteria. This paper tackles these issues by proposing a system-level framework for degradation analysis that enables the evaluation of performance under both healthy and degraded operating conditions.



(a)

Figure 2. Efficiency as a function of the PEMFCS net power with variable degradation coefficient

Acknowledgment

The authors gratefully acknowledge the European Defence Fund (EDF) for the financial support through the NEUMANN (Grant Agreement Number 101103504) project. Funded by the European Union. Views and opinions expressed are however those of the author(s) only and do not necessarily reflect those of the European Union. Neither the European Union nor the granting authority can be held responsible for them.

Co-funded by the European Union

References

[1] Clean Hydrogen Partnership. Strategic Research and Innovation Agenda (SRIA). https://www.clean-hydrogen. europa.eu/about-us/key-documents/strategic-research-and-innovation-agenda_en (accessed on March 2025).

[2] Clean Aviation, Clean Aviation's daring new projects online: https://clean aviation.eu/sites/default/files/2022-09/CleanAviation-daring new-projects-List_en.pd (accessed on March 2025).

[3] Pei, P., et al. (2008). A quick evaluating method for automotive fuel cell lifetime. *International Journal of Hydrogen Energy*, *33*(14), 3829-3836.

[4] Cheng, J., et al. (2024). Multi-objective adaptive energy management strategy for fuel cell hybrid electric vehicles considering fuel cell health state. *Applied Thermal Engineering*, *257*, 124270.

[5] Aliberti, P., et al. (2025). Efficiency-Based Modeling of Aeronautical Proton Exchange Membrane Fuel Cell Systems for Integrated Simulation Framework Applications. *Energies*, *18*(4), 999.

[6] Gemmen, R. S., et al. (2006). Evaluation of fuel cell system efficiency and degradation at development and during commercialization. *Journal of Power Sources*, *159*(1), 646-655.

EFCH2 2025 European Fuel Cells and Hydrogen
PIERO LUNGHI CONFERENCE
September 17th–19th 2025 Capri / Italy

Experimental validation of a PEMFC lumped dynamic model for on- board, diagnostic, prognostic and control applications

Massimo Sicilia [a], Davide Cervone [a], Pierpaolo Polverino *[a], Cesare Pianese [a]

* corresponding author: ppolverino@unisa.it

[a] *Department of Industrial Engineering, University of Salerno, via Giovanni Paolo II 132, 84084, Fisciano (SA), ITALY.*

Keywords: PEMFC; water management; diagnosis; modelling.

Abstract

Introduction: In the field of energy sustainable production, Proton Exchange Membrane Fuel Cells (PEMFCs) are a promising solution to produce electrical energy without significant pollutant emissions, reducing the environmental impact. Their working principle relies on the electrochemical reduction-oxidation reaction involving hydrogen and oxygen: with only water as sub-product, PEMFCs are able to produce electrical energy as direct current, with good efficiency, scaling-up versatility, and low operational temperature. PEMFCs are composed by three key components: two electrodes (i.e., anode and cathode) made of carbon porous material, and a Polymeric Electrolyte Membrane (PEM); to scale up electrical power, single cells can be electrically stacked in series arrangement [1]. To ensure best performance and low degradation, water management is fundamental: the PEM needs to be constantly humidified to allow protonic transport from anode to cathode; however, water can flood the electrodes impeding the gases diffusion down to the reaction sites, worsening the performance [2]. The water content needs to be constantly monitored, since PEMFC performance is strictly related to it; it is difficult to experimentally quantify the water content on-board, so a computational model can support the diagnosis to take control actions [3].

Objectives: The objective of this work is the development of a fast water management lumped mathematical dynamic model of PEMFCs stack in static and dynamic conditions, validated on experimental data of a commercial open-cathode, self-humidified, 100 W PEMFC stack acquired on a test bench.

Material and methods: The mathematical model [4] is based on the following physical assumptions: (i) mean-value modelling approach; (ii) mono-dimensional flows; (iii) equivalent single cell approach; (iv) uniform temperature distribution; (v) ideal heat transfer. The equivalent single cell is divided into three main control volumes: anode; membrane; cathode.

The two electrodes are subsequently divided in three sub-volumes: Gas Flow Channel (GFC); Gas Diffusion Layer (GDL); Catalyst Layer (CL). Every electrode is served by supply manifolds at constant pressure, together with discharge manifolds for outlet flows. For anode, hydrogen and water are the chemical species to be computed; cathode sub-volumes account for oxygen, nitrogen, and water; furthermore, water can be present in both vapor and liquid states, calculating evaporation and condensation rates. For every chemical species and for every sub-volume, filling-emptying equations are used to compute gases mass over time; the considered gas transport mechanisms are diffusion and convection, while convection and capillarity transport are addressed for liquid water. The membrane is modelled with a dedicated dynamic model [5]: the membrane water content is computed with first-order dynamics state equation, in which the steady-state solution is calculated with an analytical formulation accounting for electro-osmotic drag, diffusion, and convection water transport mechanisms across the membrane; the characteristic time is function of current density, temperature, and pressure gradient derived from a simplified Partial Differential Equation (PDE) of membrane water balance. The models described above are the main elements required for the calculation of cell performance, with the polarization curve accounting for activation, Ohmic, and concentration losses. The first principle thermal balance is computed to determine cell temperature over time. The physical parameters of the selected stack to be simulated are obtained from [6].

The tested cell is the H100 stack, by Horizon Technologies: it is a low power, open-cathode, self-humidified stack for research and teaching purposes, with a main fan for cooling and oxygen feeding purposes, a short-circuit unit for humidification, and a proprietary control unit to automatically manage purging and short-circuit operations, together with fan speed. The experimental procedure involves stack testing without its control unit, leaving user-controlled operations; the short-circuit unit is not used, while the purging valve is always kept closed; the fan is powered with 7 V, providing 250 lpm air on average. The current is set from 0 to 5 A with step variations every 10 minutes, to analyze both steady-state conditions and transient operations; a mass flow controller is also used to correctly fuel the stack with sufficient hydrogen, with set-point hydrogen mass flow as function of current summed with a constant value for possible leakages. The stack temperature is measured with a thermocouple inside the stack; the air blown by the fan is measured with a flow sensor positioned in a convenient straight tube mounted on fan for flow stabilization, to avoid measuring uncertainty.

Results: In Figure 1, the model validation on experimental data is reported: the top and bottom graphs show the stack voltage and temperature over time, respectively; in black solid lines experimental data are reported, while the red solid lines refer to model data. At steady-state, the RMSE shown by the model is 0.1075 V, with correlation coefficient R^2 equal to

0.99866. The computational speed (defined as computed seconds over real seconds) is equal to roughly 150 on a 11th gen Intel Core i7-1165G7 @2.8 GHz machine.

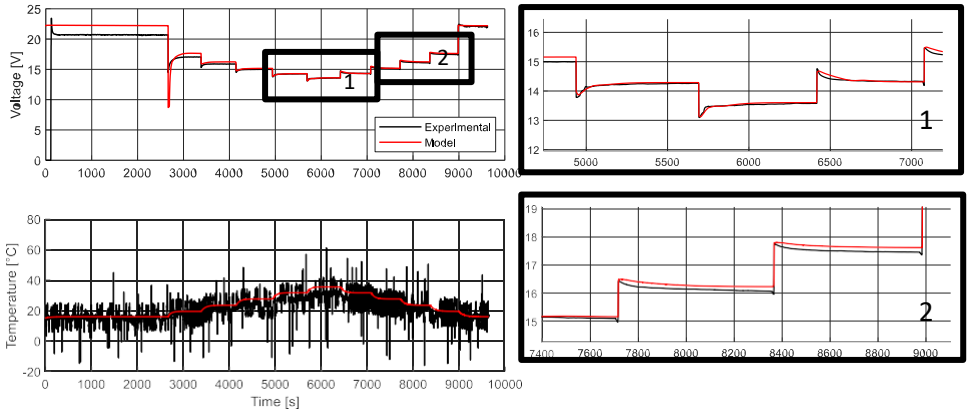


Figure 1. Model validation, with stack voltage (up) and temperature (down).

Conclusions: The proposed model is able to correctly reproduce stack performances in both steady-state and dynamic conditions. The steady-state performances are well represented with high correlation and low RMSE, while the combination of thermal and membrane dynamics ensures the physicality of voltage dynamics that are fundamental for control strategies design.

Acknowledgment

This project is partially funded by University of Salerno FARB 2024 project dealing with PEMFC model for diagnostics and control and by the Italian NRRP (National Recovery and Resilience Plan) as part of the Next Generation EU (NGEU) program. The Authors thank the National Centre for Sustainable Mobility - Spoke 2 “Cars & Tires.” MOST SPOKE II.

References

[1] LARMINIE, James; DICKS, Andrew; MCDONALD, Maurice S. *Fuel cell systems explained*. Chichester, UK: J. Wiley, 2003. DOI: 10.1002/9781118706992.

[2] JI, Mengbo; WEI, Zidong. A review of water management in polymer electrolyte membrane fuel cells. *Energies*, 2009, 2.4: 1057-1106. DOI: 10.3390/en20401057.

[3] WANG, X. R., et al. Review on water management methods for proton exchange membrane fuel cells. *International Journal of Hydrogen Energy*, 2021, 46.22: 12206-12229. DOI: 10.1016/j.ijhydene.2020.06.211.

[4] SICILIA, Massimo, et al. *Model-Based Algorithm for Water Management Diagnosis and Control of PEMFC Systems for Motive Applications*. SAE Technical Paper, 2024. DOI: 10.4271/2024-37-0004.

[5] SICILIA, Massimo, et al. Advancements on Lumped Modelling of Membrane Water Content for Real-Time Prognostics and Control of PEMFC. *Energies*, 2024, 17.19: 4841. DOI: 10.3390/en17194841.

[6] STRAHL, Stephan, et al. Performance improvement by temperature control of an open-cathode PEM fuel cell system. *Fuel Cells*, 2014, 14.3: 466-478. DOI: 10.1002/fuce.201300211.

European Fuel Cells and Hydrogen
PIERO LUNGHI CONFERENCE
September 17th–19th 2025
Capri / Italy

Mathematical and numerical modelling of High-Temperature Solid Oxide Fuel Cells

P. Gislon[a], D. Pumiglia[a], F. Arpino[b], G. Cortellessa[b], G. Ficco[b], G. Grossi*[b]

* corresponding author: giorgio.grossi@unicas.it

[a] ENEA Department of Energy Technologies and Renewable Sources, Laboratory for Hydrogen and new Energy Vectors (H2V), Casaccia Research Centre, Rome, Italy

[b] Department of Civil and Mechanical Engineering, University of Cassino and Southern Lazio, Cassino, FR, Italy

Keywords: Computational Fluid Dynamics (CFD), Fuel Cells, Heat Transfer, Validation

Abstract

This study conducts 3D numerical simulations to examine the complex multi-physics phenomena in an anode-supported planar solid oxide fuel cell (SOFC). The numerical model, validated against data from the scientific literature, is employed to evaluate the temperature gradient within the solid regions of the cell under co-flow and counter-flow configurations. Results show that the flow configuration significantly affects the temperature gradient distribution, with the maximum value predicted at the cathode inlet in both simulated configurations. This work represents the first stage of a broader research project aimed at investigating, both numerically and experimentally, the effects of various factors on the performance of anode-supported SOFCs, including the presence of contaminants and their impact on material aging.

Introduction

Green hydrogen plays a crucial role in the transition to renewable energy sources due to its versatility and compatibility with clean energy technologies such as fuel cells and electrolysers. These devices are promising replacements for traditional fossil fuel-based technologies but require detailed investigation of mass and energy transport phenomena and electrochemical processes for optimization. Numerical simulations, particularly using Computational Fluid Dynamics (CFD), provide a detailed description of these phenomena, which are challenging and costly to study experimentally. SOFCs are particularly attractive due to their high operating temperatures, which allow the use of less expensive catalysts, enable the processing of various fuels, and offer cogeneration possibilities, making them suitable for stationary applications. Despite advancements, SOFCs still face reliability issues and high production and operating costs. Building on previous research activities [1,2], this study uses CFD simulations to investigate a single-unit model of an anode-supported planar SOFC. The numerical model is validated with existing data and then used to evaluate the temperature gradient within the cell under different operating conditions. In fact, being it strictly related to thermal stresses, temperature gradient can significantly affect cell performance in terms of stability and lifetime.

Materials and methods

Numerical simulations are conducted in *Ansys Fluent*, using the *Fuel Cell and Electrolysis* addon module for the resolution of electrochemical phenomena. Mass, momentum, energy and species conservation equations are solved for anode and cathode parts, including a source term for heat generation from electrochemical reactions. The model assumptions include steady-state conditions, incompressible flow, negligible buoyancy forces, homogeneous properties for porous electrodes, and laminar flow (based on the typical values of Reynolds number for SOFCs). For the electric regions, ions transport across the electrolyte and electron conduction

through electrodes and interconnects follow a Poisson-type relationship. Activation overpotential is calculated using the Butler-Volmer equation. The study examines a planar anode-supported SOFC in both co-flow and counter-flow configurations, whose schematic is available in Figure 1. Boundary conditions include specified mole species fractions, velocities, and fixed temperatures at the anodic and cathodic inlets, with pressure specified at the outlets. The fuel is a mixture of hydrogen and water (95% H_2 and 5% H_2O by mole), while the oxidant is air. The inlet velocity of air is set to 1.153 m/s, while the fuel inlet velocity is equal to 0.461 m/s. The computational grid, shown in Figure 2, consists of 465,600 hexahedral cells.

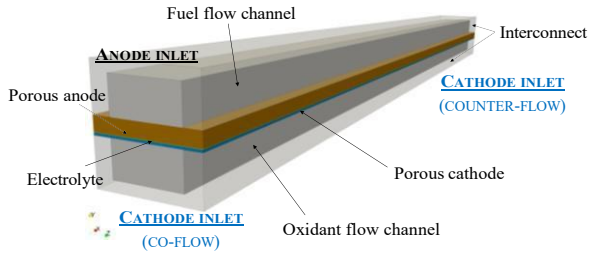


Figure 1. Geometry model of the anode-supported SOFC under study.

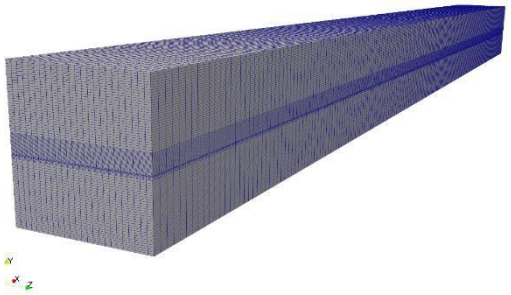


Figure 2. Computational grid employed for numerical simulations, composed of 465,600 cells.

The numerical model is validated by reproducing the polarization curve provided by Zhang et al. [3], for a cell temperature of 1073 K under co-flow configuration. The validated model is then applied to simulate heat transfer with the environment at a temperature of 973 K, assuming a convection heat transfer coefficient of 10 W/(m² K) and the flow streams entering the cell at the same temperature as the surrounding environment. For these specific analyses, the mean cell current density is fixed at 0.8 A/cm² and co-flow and counter-flow configurations are compared. The primary properties of the cell components used for validation can be found in the work of Zhang et al. [3].

Results

The validation of the numerical model shows a close agreement with the polarization curve provided by Zhang et al. [3], as shown in Figure 3, with an average error of 3.56%.

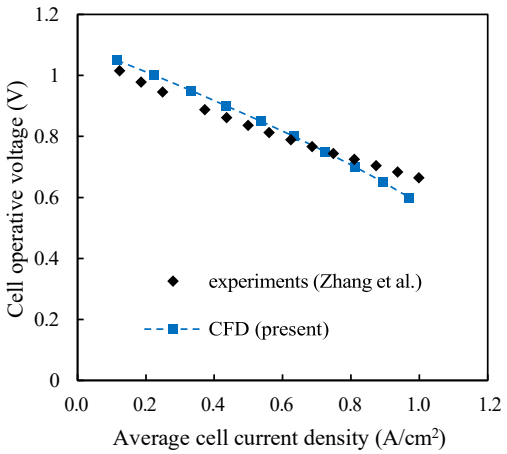


Figure 3. Operative cell voltage as a function of the average current density, compared with Zhang et al. [3].

The study then predicts temperature fields within the cell for co-flow and counter-flow configurations. Numerical results are presented in Figure 4 in terms of temperature contours on the x-y plane crossing the computational domain at its midpoint (z=0). In the case of co-flow streams, the temperature increases along the flow direction due to the heat source produced by electrochemical reactions. Since on the cathode side the flow

rate is much higher than on the anode side, at the same position (i.e., x-coordinate) along the cell, the air exhibits a lower temperature compared to the fuel. In the counter-flow arrangement, the temperature is initially lower at the inlet of the flow channels and gradually increases until reaching a peak, before decreasing at the outlet sections, again as a consequence of the electrochemical reactions. The flow configurations also significantly affect the temperature gradients in the solid regions of the cell. In the co-flow configuration, the maximum gradient (equal to 1514.73 K/m) is predicted at the cathode inlet. In the counter-flow configuration, two temperature gradient peaks are present, located at the inlets of the fuel and the oxidant. The maximum thermal gradient (equal to 1709.24 K/m, always found at the air inlet) is higher in the counter-flow configuration, suggesting an increase in thermal stresses and potential issues for cell stability.

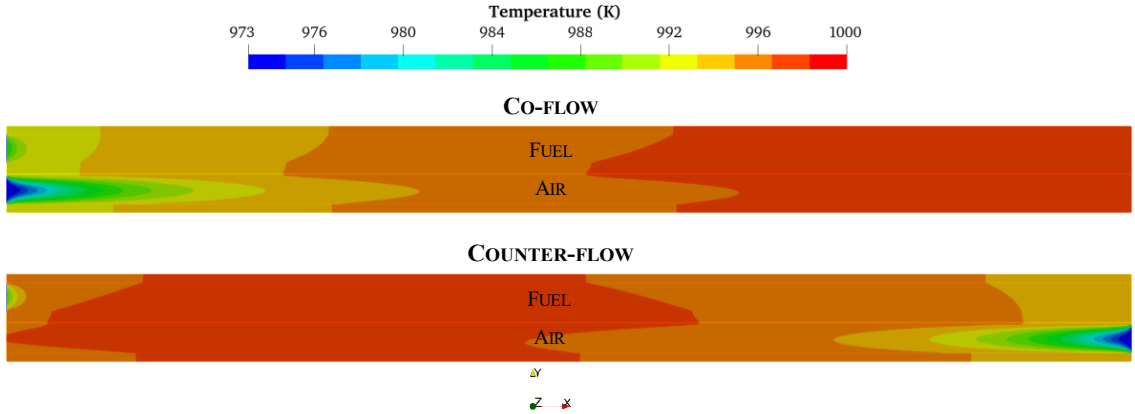


Figure 4. Predicted temperature contours on the x-y plane crossing the computational domain at its midpoint, for an operating temperature of 973 K, under co-flow and counter-flow configurations.

Conclusions

CFD simulations allowed for the numerical analysis of the thermal behaviour of a single-unit model of an anode-supported planar SOFC. The numerical model, validated by comparing the polarization curve with data available in the scientific literature, was used to predict temperature gradients in the solid regions of the cell, considering both co-flow and counter-flow configurations. The results showed that the flow configuration significantly affects the temperature gradient distribution, with the maximum value predicted at the cathode inlet in both simulated configurations. Future research will focus on an in-depth analysis of the effects of operating conditions on thermal stresses and the extension of the model to explore the use of alternative fuels to hydrogen. Another area of study will be the presence of contaminants (e.g., solid carbon deposition in the anode pores when feeding with hydrocarbons) and their impact on material aging.

Acknowledgment

This research was funded by the European Union - NextGenerationEU from the Italian Ministry of Environment and Energy Security, POR H2 AdP MEES/ENEA with involvement of CNR and RSE, PNRR - Mission 2, Component 2, Investment 3.5 "Ricerca e sviluppo sull'idrogeno", CUP: I83C22001170006.

References

[1] F. Arpino, N. Massarotti, Numerical simulation of mass and energy transport phenomena in solid oxide fuel cells, Energy 34 (2009) 2033–2041. https://doi.org/10.1016/j.energy.2008.08.025.

[2] A. Mauro, F. Arpino, N. Massarotti, Three-dimensional simulation of heat and mass transport phenomena in planar SOFCs, International Journal of Hydrogen Energy 36 (2011) 10288–10301. https://doi.org/10.1016/j.ijhydene.2010.10.023.

[3] Z. Zhang, D. Yue, G. Yang, J. Chen, Y. Zheng, H. Miao, W. Wang, J. Yuan, N. Huang, Three-dimensional CFD modeling of transport phenomena in multi-channel anode-supported planar SOFCs, International Journal of Heat and Mass Transfer 84 (2015) 942–954. https://doi.org/10.1016/j.ijheatmasstransfer.2015.01.097.

European Fuel Cells and Hydrogen
PIERO LUNGHI CONFERENCE
September 17th–19th 2025
Capri / Italy

3D Modelling of electrolyzer and fuel cells with NEOPARD-X framework: dimensionality effects

Andrey Koksharov*[a], Thomas Jahnke [a]

* corresponding author: andrey.koksharov@dlr.de
[a] German Aerospace Center (DLR)

Keywords: Modelling framework, Electrolyser, Fuel cell, Multidimensional

Abstract

Introduction: Despite significant differences in the used materials, operating conditions and detailed electrochemistry, from the modelling point of view modern promising technologies such as proton exchange membrane (PEM), protonic ceramic cells (PCC) or solid oxide cells (SOC) can be described by common governing equations for mass, charge and energy transport coupled with electrochemical reactions. The generalization of governing equations into conservation form and modular combination of the processes occurring in different phases, and different cell layers, permits a rapid model implementation within the newly developed NEOPARD-X framework.

Objectives: Traditionally, 1D models have been widely used to spatially resolve the processes within fuel cells and electrolyzers through the thickness of the layers. These 1D models have the advantage of reduced computational cost, but neglect heterogeneities occurring in the other dimensions such as along the channel and between channel and land. To overcome this limitation, recently an increasing number of 3D cell models has been presented in the literature (see [1] for a comprehensive review) but in most cases they feature either simplified electrochemical kinetic expression and transport models or are based on “black-box” commercial solvers. Usually the high computational cost also limits to steady state simulations. The presented novel modeling framework features a new approach to the separation of the numerical discretization and the mathematical model. This permits a simple change of the model dimensions and geometry, as well as effective performance scalability on modern CPU.

Material and methods: In this work the accent is made on the dimensionality of cell models. Using as basis a validated PEM cell model, consisting of 9 physical layers, a difference in results

for 1D, 2D and 3D geometries is discussed (see Fig. 1). Fig. 1 is simplified: both anode and cathode contain 4 layers with different properties and mathematical description.

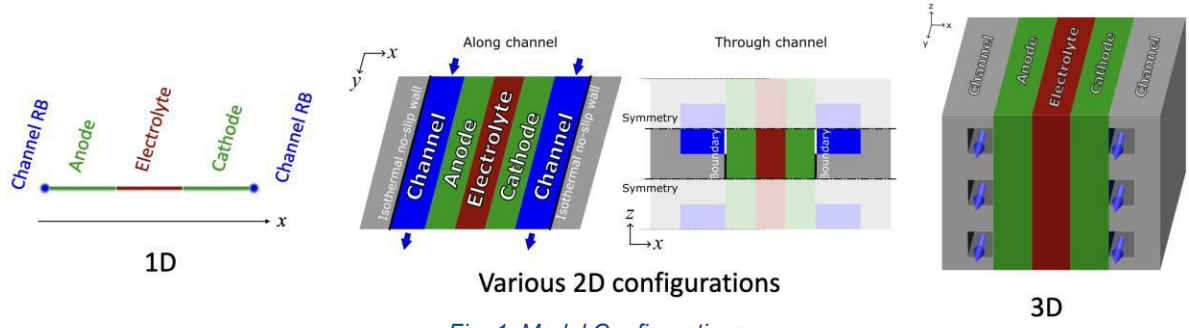


Fig. 1: Model Configurations

Results: For the current discussion a flow rate of 10.9 Nl/h (cathode) and 3.4 Nl/h (anode) is chosen, which ensures the O_2 consumption of 50% at 3 A/cm². Cell temperature is 80 ˚C, pressure is 2 bar and relative humidity is 80% at both cell sides. At low current densities model results are practically identical (compare Fig. 2, left, and Fig. 3, left) but when approaching the limiting current, results from different model configurations start to deviate significantly (compare Fig. 2, left, and Fig. 3, right). The main reasons for this discrepancy are the oxygen consumption along the channel and transport limitations under the land regions. Fig. 2 (right) shows the concentration of hydrogen (left half-cell) and oxygen (right half-cell). The concentration of hydrogen was scaled by factor 0.2 to make it comparable. Cell layers are displaced in the figure by 0.5 mm in order to improve the visibility. Fig. 2 (right) shows a significant gradient in the channel direction, as well as under the land, tangential to the channel. Additionally, the water production by the oxygen reduction reaction along the channel increases the cell humidity in channel direction, which in turn increases the protonic transport through the cell.

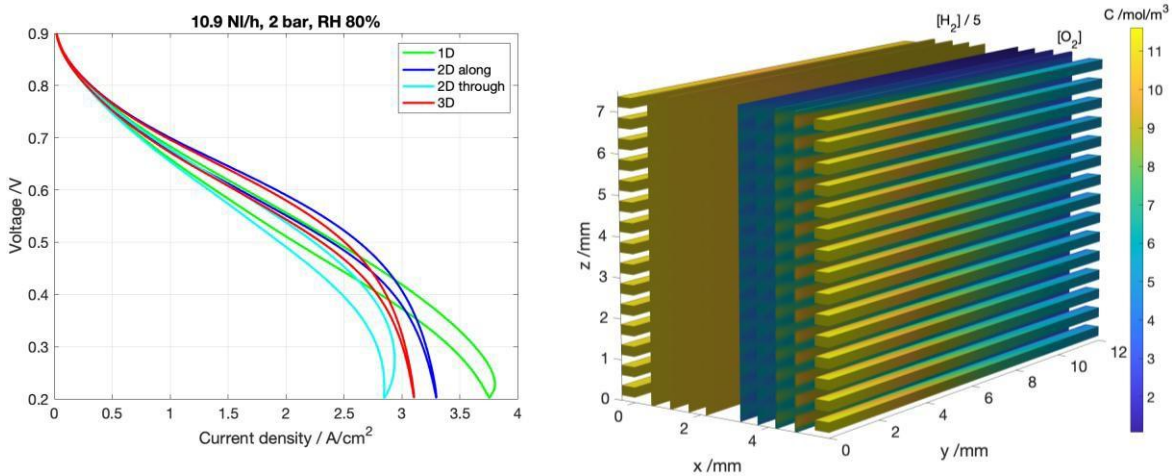


Fig. 2: Polarization curve dependency for different geometries (left), 3D plot at 3 A/cm² of hydrogen and oxygen concentration for anode and cathode side respectively (right)

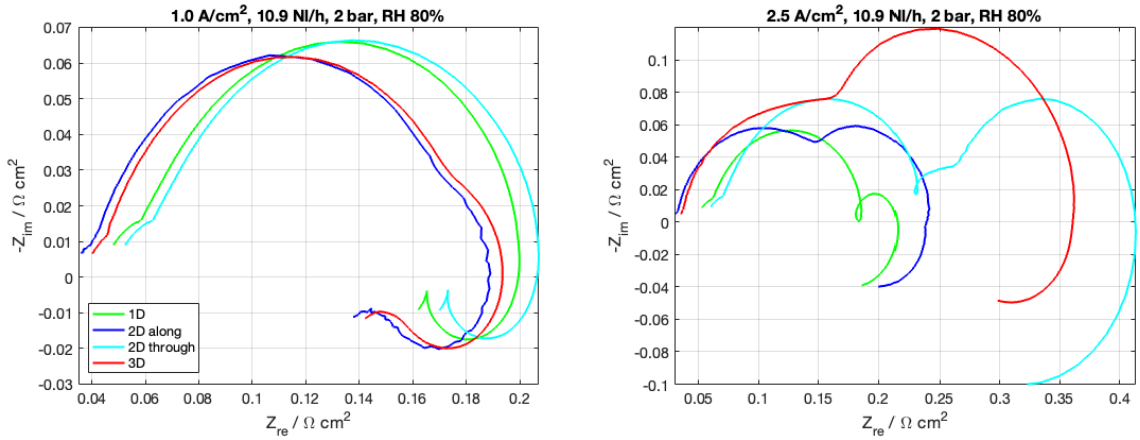


Fig. 3: Impedance simulation for different geometries

Conclusions: The framework feature for changing geometry from 1D to 3D, keeping the cell model unchanged, allows to investigate the applicability region of different geometries. The computational time of several seconds positions the 1D geometry as a possible digital twin for real-time applications but it neglects channel and land effects. 2D through and 2D along the channel provide more information either about transport under the land or about gas conversion effects along the channel. The detailed 3D geometry with a computational time of about 2 hours for the simulation of a transient polarization curve provides a reference case, accurately describing all dimensions. Thus, depending on the cell design and operating conditions, accurate simulation results require the use of the appropriate model geometry. The dimensionality effects are illustrated with impedances and polarization curves.

Acknowledgment

The project FURTHER-FC [2] has received funding from the Fuel Cells and Hydrogen 2 Joint Undertaking (now Clean Hydrogen Partnership) under Grant Agreement No 875025. This Joint Undertaking receives support from the European Union's Horizon 2020 Research and Innovation program, Hydrogen Europe and Hydrogen Europe Research.
The research leading to these results was also supported by the project PEMTASTIC (Grant Agreement No.101101433), funded by the Clean Hydrogen Partnership and its members Hydrogen Europe and Hydrogen Europe Research.

References

[1] Koksharov, Andrey, Arnulf Latz, and Thomas Jahnke. "NEOPARD-X: Multidimensional highly efficient and scalable modular framework for modelling of electrolysers and fuel cells." Electrochimica Acta 495 (2024): 144482

[2] https://further-fc.eu/

European Fuel Cells and Hydrogen
PIERO LUNGHI CONFERENCE
September 17th–19th 2025
Capri / Italy

Investigation of an Auxiliary High-Temperature Refrigeration System to Increase Cooling Capacity in Fuel Cell Vehicles

Steffen Heinke[a,*], Jakob Trägner[a], Nicholas Lemke[a,b], Wilhelm Tegethoff[a,b], Jürgen Köhler[a]

* corresponding author: s.heinke@tu-braunschweig.de

[a] Technische Universität Braunschweig, Institut für Thermodynamik,
Hans-Sommer-Str. 5, 38106 Braunschweig Germany

[b] TLK-Thermo GmbH, Rebenring 31, 38106 Braunschweig

Keywords: Cooling Capacity, Fuel Cell Vehicle, Refrigeration System, Thermal Management

Abstract

Introduction: Low-temperature (LT) PEM fuel cell (FC) systems are being discussed as an alternative drive concept for different vehicles due to their relatively high efficiency, short refuelling time and local emission-free operation. However, the cooling of such FC systems in vehicles is a challenge. Due to their low operating temperature (approx. 70 – 85 °C) and therefore low exhaust gas energy, most of the waste heat has to be rejected by a cooling system at low temperature differences to the ambient. The amount of waste heat to be removed by the cooling system per unit of temperature difference to the ambient (watts per kelvin) can be many times greater than for internal combustion engines at equivalent power output [1,2]. This is not always feasible with conventional liquid cooling systems. It may therefore be necessary to limit the power output of the FC system and, consequently, the driving speed [2]. The available cooling capacity is limited by the available cooling air mass flow rate, or more precisely, its heat capacity rate. For many applications, however, a significant increase in the cooling air heat capacity rate is not easily achievable due to design and installation space constraints [1].

Objectives: The objective of this work is to analyse and evaluate a high-temperature refrigeration system (HTRS) used to increase the available cooling capacity in an FC vehicle. The HTRS raises the temperature level of the waste heat without increasing the operating temperature of the FC. This allows more waste heat to be transferred to the same amount of cooling air and thus, better utilise the limited heat capacity rate. As shown in Figure 1 (left), the HTRS does not replace the liquid cooling system, but provides additional cooling capacity for critical driving conditions. Such a concept is referred to in this work as a hybrid cooling system. The investigations are carried out using an FC passenger car as an example. However, the basic findings are relevant to other vehicle types with analogous challenges, such as FC trucks.

Material, methods and results: A simulation model of a typical FC passenger car with a conventional liquid cooling system is developed in Modelica/Dymola using the TIL Suite [3–5]. Using this model, the conventional liquid cooling system is analysed for its maximum cooling capacity for a demanding uphill and high-speed driving scenario. By this, the requirements for the HTRS in terms of the necessary increase in cooling capacity and the boundary conditions for its operation in the vehicle are determined. Based on these results, an HTRS is constructed in the laboratory using off-the-shelf components of automotive air conditioning systems. The natural refrigerant R-600 (n-Butane) is used for the laboratory HTRS, which is also used for stationary high-temperature heat pumps [6]. The experimental results of the HTRS show coefficients of performance from 13.7 to 4 at cooling capacities from 7.6 kW to 24.1 kW under boundary conditions similar to the intended vehicle application. A simulation model of the laboratory HTRS is developed and validated with the experimental results. It is integrated into the model of the FC passenger car, resulting in a model of the hybrid cooling system (see Figure 1 left). In order to avoid an increase in the installation space required in the radiator pack in the front-end of the vehicle, the depth of the HT radiator is reduced by the depth of the HT condenser. As the power for the HTRS compressor must be supplied by the FC system, the waste heat from the FC system increases when the HTRS is running. The interdependence of the additional cooling capacity provided by the HTRS and the additional waste heat from the FC system is analysed, resulting in the definition of an effective cooling capacity of the hybrid cooling system:

$$Q_{\text{Cooling,eff}} = Q_{\text{HT Radiator}} + Q_{\text{Evaporator}} - \Delta Q_{\text{FC System,HTRS}} \,.$$

Here, $Q_{\text{HT Radiator}}$ is the cooling capacity of the HT radiator of the liquid cooling system, $Q_{\text{Evaporator}}$ is the gross additional cooling capacity of the HTRS and $\Delta Q_{\text{FC System,HTRS}}$ is the additional waste heat of the FC system due to the additional power demand of the HTRS compressor. It is shown, that the effective cooling capacity is subject to a maximum before the maximum compressor capacity is reached. Therefore, it is not sensible to operate the HTRS to its limit. Finally, the hybrid cooling system is compared with the conventional liquid cooling system. Figure 1 (right) shows the cooling capacity required for a demanding uphill and high-speed driving scenario compared to the maximum cooling capacity of the conventional liquid cooling system and the maximum effective cooling capacity of the hybrid cooling system. As can be seen, the hybrid cooling system can meet the cooling demand, unlike to the conventional liquid cooling system. However, the power requirement of the HTRS is up to 5.5 kW, i.e., up to almost 10 % of the vehicle's driving power. In addition, the hybrid cooling system based on the laboratory HTRS still requires an additional installation space of 8 L. However, the combined optimisation of the size of the HT radiator and the components of the HTRS promises a significant reduction in installation space.

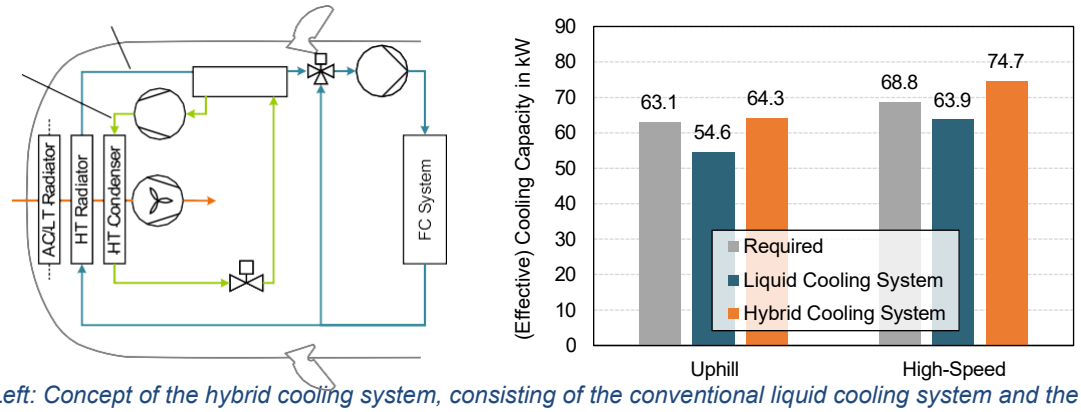


Figure 1: Left: Concept of the hybrid cooling system, consisting of the conventional liquid cooling system and the additional high-temperature refrigeration system. Right: Comparison of the required cooling capacity for a demanding uphill (100 km/h, 35 °C, 6 % slope) and high-speed (160 km/h, 40 °C, 0 % slope) driving scenario with the maximum available (effective) cooling capacity of the conventional liquid cooling system and the hybrid cooling system based on the laboratory high-temperature refrigeration system.

Conclusions: The results of this work show, that a hybrid cooling system can increase the available cooling capacity in an FC vehicle compared to a conventional liquid cooling system. In the exemplary FC passenger car, such a system can meet the cooling demand, unlike the conventional liquid cooling system. A hybrid cooling system can therefore be an alternative to a pure liquid cooling system, especially in warm climatic regions. However, the HTRS has a significant power demand and still requires some additional installation space. Further optimisation of the components and the layout of the hybrid cooling system is feasible in order to improve the effectiveness and efficiency of the hybrid cooling system.

References

[1] S. Rogg, M. Höglinger, E. Zwittig, C. Pfender, W. Kaiser, T. Heckenberger, Cooling Modules for Vehicles with a Fuel Cell Drive, Fuel Cells 3 (2003) 153–158. https://doi.org/10.1002/fuce.200332108.

[2] M. Wagenblast, M. Pollak, J. Trägner, S. Heinke, W. Tegethoff, J. Köhler, J. Swoboda, Design and Analysis of a Spray Cooling System for a Heavy-Duty Fuel Cell Truck, SAE Technical Paper 2022-01–5054 (2022). https://doi.org/10.4271/2022-01-5054.

[3] Modelica Association, Modelica - A Unified Object-Oriented Language for Systems Modeling: Language Specifications Version 3.6, (2023). https://specification.modelica.org/maint/3.6/MLS.pdf (accessed January 5, 2024).

[4] Dassault Systèmes, Dymola – Dynamic Modeling Laboratory, (2023). https://www.3ds.com/products/catia/dymola (accessed January 5, 2024).

[5] TLK-Thermo GmbH, TIL Suite 3.16.0, (2024). https://www.tlk-thermo.de/en/software/til-suite (accessed August 20, 2024).

[6] C. Arpagaus, F. Bless, M. Uhlmann, J. Schiffmann, S.S. Bertsch, High temperature heat pumps: Market overview, state of the art, research status, refrigerants, and application potentials, Energy 152 (2018) 985–1010. https://doi.org/10.1016/j.energy.2018.03.166.

EFCH2 2025
European Fuel Cells and Hydrogen
PIERO LUNGHI CONFERENCE
September 17th–19th 2025
Capri / Italy

CFD-Based Investigation of High Current Density Polarization Losses in PEM Fuel Cells

E. D'Alessio*[a], M. M. Abdelkader[a], G. Agati[b], F. Donato[c], D. Borello[b]

*emanuele.dalessio@uniroma1.it

[a] Dept. of Astronautical, Electrical and Energy Engineering, Sapienza University of Rome, Rome, Italy
[b] Dept. of Mechanical and Aerospace Engineering, Sapienza University of Rome, Rome, Italy
[c] Dept. for Energy Technologies, ENEA, Italian National Agency for New Technologies, Energy and Sustainable Economic Development, Rome, Italy

Keywords: PEM Fuel Cells, CFD, High Current Density, Mass Transport Losses, Pore Blockage, Water Removal Coefficient

Abstract

This study investigates high-current density polarization losses in Proton Exchange Membrane Fuel Cells (PEMFCs) using a three-dimensional multiphysics CFD model. The model is validated against experimental data from the Joint Research Centre (JRC) by applying it to a reduced computational domain of the tested cell (ZERO∇CELL). Preliminary results include the validation of the model via the numerical polarization curve, which shows good agreement with experimental data and a maximum relative error of 1.26%, confirming the model's accuracy in capturing flooding and polarization behaviour at high current densities.

Introduction

Computational Fluid Dynamics (CFD) modelling is a crucial tool for analysing the complex processes governing PEMFC operation. CFD studies have addressed various aspects of PEMFC performance [1]. Researchers have explored different flow channel configurations, such as parallel, serpentine and interdigitated geometries, to enhance reactant distribution [2,3]. Furthermore, studies have investigated the impact of microstructural properties on liquid water removal from the gas diffusion layer, aiming to optimize water management and mitigate flooding issues [4]. Despite the extensive application of CFD in PEMFC research, the majority of numerical models in the literature are validated primarily under low to moderate current density conditions [1]. Typically, these models focus on calibrating the activation and ohmic polarization regions. The lack of model validation in the high-current-density regime represents a critical research gap, as it limits the reliability of CFD simulations in predicting PEMFC performance under demanding operational conditions. This study aims to address this research gap by developing a high-fidelity 3D multiphysics CFD model capable of accurately predicting PEMFC performance at high current densities. The investigation will focus on identifying and quantifying the impact of pore blockage and water removal coefficients on mass transport losses through sensitivity analysis. Additionally, the study will analyze water saturation distribution within the GDL and flow channels, examining how these parameters influence reactant concentration variations and the interplay between water accumulation and reactant transport within the GDL under high-current-density operation.

Numerical model

A three-dimensional, steady-state, non-isothermal CFD model is implemented using ANSYS Fluent with User-Defined Functions to represent the governing physics of PEMFC operation. The model incorporates conservation equations for mass, momentum, energy, charge, and species transport. Electrochemical reactions are included as source terms, describing hydrogen oxidation at the anode and oxygen reduction at the cathode via Butler-Volmer kinetics. The Springer's empirical correlation is used to model the membrane with protonic conductivity dependent on both temperature and water content. The methodology described in [5] is used to calibrate the model parameters against experimental data in the activation and ohmic region of the polarization curve. The laminar governing equations are solved using the coupled pressure-based solver algorithm adopting a second-order upwind scheme. Numerical accuracy is ensured through grid independence analysis and residual monitoring, with convergence criteria based on current consistency between the anode and cathode side and reactants consumption [6].

Case description

The computational domain and operating conditions used in this study are based on the JRC ZERO∇CELL, a reference PEM fuel cell designed by the Europea JRC for developing a harmonized testing protocol [7]. The JRC ZERO∇CELL features a 10 cm^2 active area with straight parallel gas channels. The cell is designed to function at a steady-state current density of 4 A/cm^2 while maintaining laminar flow conditions (Re < 1000), a reactant pressure drop below 10 kPa, and a temperature variation of 1 °C across the active area. The uniformity of inlet conditions across all channels ensures a controlled environment suitable for high-fidelity CFD simulations. The membrane electrode assembly (MEA) includes an 18-micron membrane, 20-micron thick catalyst and microporous layers, and a 0.235 mm gas diffusion layer (Sigracet 25BC) on both electrodes. The bipolar plates have a thickness of 1 mm, with anode and cathode channel heights of 0.25 mm and 0.4 mm, respectively. Platinum loading is 0.1 mg/ cm^2 at the anode and 0.4 mg/ cm^2 at the cathode. Given the uniform conditions within the JRC ZERO∇CELL, a reduced computational domain was selected for the CFD model. Instead of simulating the entire cell, a subsection consisting of three anode channels and four cathode channels was chosen (Fig. 1a). The numerical simulations were carried out on a computational mesh composed of 770k hexahedral elements. The mesh quality was verified to ensure numerical stability and accuracy, with a maximum aspect ratio of 20 and a maximum skewness below 0.05. The simulations were performed under operating conditions matching the experimental setup: cell temperature of 80 °C, fuel and oxidant inlet temperatures of 85 °C, fully humidified reactants (100% RH), inlet pressures of 250 kPa (fuel) and 230 kPa (oxidant), and stoichiometric ratios of 8.0 (fuel) and 10.0 (oxidant).

Preliminary results

Model validation simulated the full polarization curve up to 3.2 A/cm^2 (onset of concentration losses), comparing numerical results against JRC experimental data (Fig. 1b). The CFD model demonstrates good agreement with the experimental curve in activation and ohmic regions and successfully captures the initial deviation due to mass transport limitations at high current densities. A maximum relative error of 1.26% was obtained by interpolating numerical data to experimental points using a hybrid log/linear approach. These results validate the model's ability to simulate PEMFC performance under high-demand conditions and provide a

solid foundation for the subsequent parametric analysis focused on flooding and reactant transport phenomena.

Conclusions

This study tackles a key limitation in PEMFC modelling by extending CFD validation into the high current density regime, where concentration losses prevail. A sensitivity analysis on the pore blockage and water removal coefficients was carried out to assess their influence on flooding and reactant distribution, improving understanding of the dominant mechanisms in this regime.

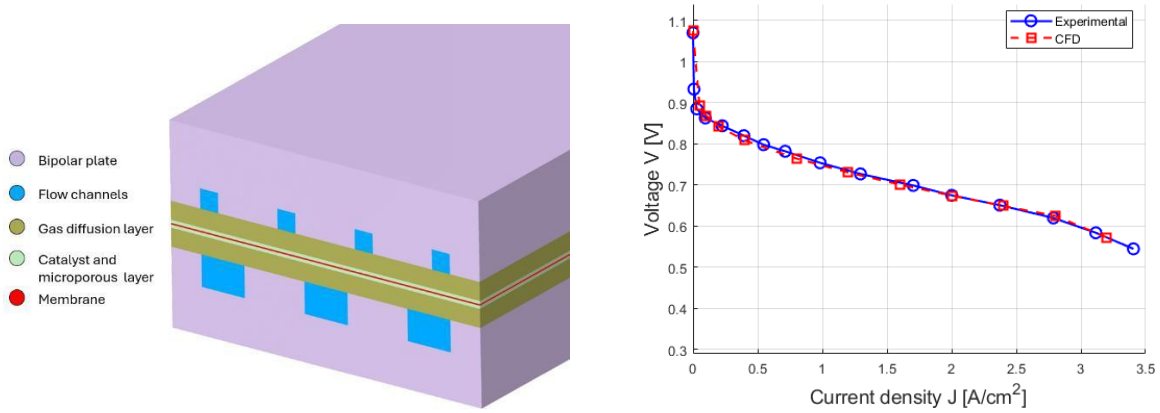


Fig 1 – a) Numerical domain; b) Numerical vs experimental polarization curve – validation up to 3.2 A/cm^2

References

[1] Edwards H, Pereira MP, Gharaie S, Omrani R, Shabani B. Computational fluid dynamics modelling of proton exchange membrane fuel cells: Accuracy and time efficiency. Int J Hydrogen Energy 2024;50. https://doi.org/10.1016/j.ijhydene.2023.09.004.

[2] Rostami L, Haghshenasfard M, Sadeghi M, Zhiani M. A 3D CFD model of novel flow channel designs based on the serpentine and the parallel design for performance enhancement of PEMFC. Energy 2022;258.

[3] Valentín-Reyes J, León MI, Pérez T, Romero-Castañón T, Beltrán J, Flores-Hernández JR, et al. Simulation of an interdigitated flow channel assembled in a proton exchange membrane Fuel Cell (PEMFC). Int J Heat Mass Transf 2022;194:123026. https://doi.org/https://doi.org/10.1016/j.ijheatmasstransfer.2022.123026.

[4] Dong Z, Liu Y, Qin Y. Coupled FEM and CFD Modeling of Structure Deformation and Performance of PEMFC Considering the Effects of Membrane Water Content. Energies (Basel) 2022;15.

[5] D'Alessio E, van Ginkel RM, Donato F, Agati G, Borello D. Accuracy estimation of a CFD multiphysics approach to study a mixed parallel and serpentine flow channels PEM fuel cell. J Phys Conf Ser, vol. 2893, Institute of Physics; 2024.

[6] Bednarek T, Tsotridis G. Issues associated with modelling of proton exchange membrane fuel cell by computational fluid dynamics. J Power Sources 2017;343.

[7] Commission E, Centre JR, Bednarek T, Tsotridis G. Development of reference hardware for a harmonised testing of PEM single cell fuel cells. Publications Office; 2021.

European Fuel Cells and Hydrogen
PIERO LUNGHI CONFERENCE
September 17th–19th 2025
Capri / Italy

Performance evaluation of a copper interdigitated over- humidification sensor

Maximilian Käfer*[a], Viktor Hacker [a], Merit Bodner [a]

* corresponding author: maximilian.kaefer@tugraz.at
[a] Institute of Chemical Engineering and Environmental Technology, University of Technology Graz, Austria

Keywords: Interdigitated sensor, Over-Humidification, PEFCs, Water management

Introduction:

Hydrogen fuel cells are a promising clean energy solution due to their high efficiency and zero-emission characteristics. However, water management remains a major challenge in polymer electrolyte fuel cells (PEFCs). Improper regulation leads to over-humidification, catalyst degradation, and performance loss. Accumulated water in the cathode and anode flow fields can block gas diffusion and accelerate carbon support corrosion [1]. While advanced imaging methods like X-ray tomography and neutron radiography offer insight into water distribution [2,3], they lack real-time monitoring capabilities and require specialized infrastructure.

Objectives:

This work aims to develop and evaluate a copper interdigitated electrode (IDE) sensor capable of detecting over-humidification and water condensation in fuel cells. The goal is to provide a low-cost, real-time diagnostic alternative to computational and imaging-based monitoring techniques.

Material and methods:

The sensor is fabricated on a flexible polyimide substrate using copper electrodes, and its working principle is based on measuring capacitance changes due to water accumulation. Data acquisition is performed using an Arduino system. The sensor was tested under controlled laboratory conditions, including droplet deposition and replicated fuel cell environments with varied humidity and water film thicknesses. Response time, recovery time, hysteresis, and sensitivity to condensation and liquid droplets were analyzed. Optical microscopy and scanning electron microscopy (SEM) were used to evaluate the copper traces before and after exposure to humidified hydrogen and air.

Results:

The sensor demonstrated fast response and recovery times (5 – 15 seconds), high sensitivity to moisture, and stability under cyclic wetting and drying conditions. Microscopic analysis revealed significant corrosion on the copper IDEs. However, the sensor maintained full functionality, demonstrating its robustness. It reliably detected water film formation and condensation events in real-time.

Conclusions:

The developed IDE sensor provides a cost-effective and reliable solution for real-time detection of over-humidification in PEFC systems. Despite visible corrosion, it maintained full functionality, highlighting its durability under harsh conditions. Its simple design and scalability make it a promising too for integration into fuel cell diagnostic systems, especially under dynamic operating conditions where rapid humid fluctuations occur.

Acknowledgment

This project is funded by the Climate and Energy Fond and is carried out within the framework of the programme “Zero Emission Mobility”.

References

[1] X.R. Wang, Y. Ma, J. Gao, T. Li, G.Z. Jiang, Z.Y. Sun, Review on water management methods for proton exchange membrane fuel cells, International Journal of Hydrogen Energy 46 (2021) 12206–12229. https://doi.org/10.1016/j.ijhydene.2020.06.211.

[2] N. Martinez, L. Porcar, S. Escribano, F. Micoud, S. Rosini, A. Tengattini, D. Atkins, G. Gebel, S. Lyonnard, A. Morin, Combined Operando High Resolution SANS and Neutron Imaging Reveals in-Situ Local Water Distribution in an Operating Fuel Cell, ACS Appl. Energy Mater. 2 (2019) 8425–8433. https://doi.org/10.1021/acsaem.9b01266.

[3] F.A. Aroge, B.S. Parimalam, J.A. MacDonald, F.P. Orfino, M. Dutta, E. Kjeang, Analysing operando 2D X-ray transmission images for liquid water distribution in polymer electrolyte fuel cells, Journal of Power Sources 564 (2023) 232820. https://doi.org/10.1016/j.jpowsour.2023.232820.

EFCH2 2025 European Fuel Cells and Hydrogen PIERO LUNGHI CONFERENCE
September 17th–19th 2025 Capri / Italy

Development of Advanced Conductive Bipolar Plates for Proton Exchange Membrane Fuel Cells: Synergistic Effects of Graphite Particle Size, Hybrid Systems, and Carbon-Based Additives.

Sahar Shojaei*[a,b], Ehsan Rostami-Tapeh-Esmaeil [a,b], Frej Mighri[a,b], Saïd Elkoun[a,c].

* corresponding author: Sahar Shojaei

[a] Research Center for High Performance Polymer and Composite Systems, CREPEC.

[b] Department of Chemical Engineering, Laval University, Quebec, Canada G1A 0A6.

[c] Department of Mechanical Engineering, Sherbrooke University, QC, Canada J1K 2R1.

Keywords: Proton Exchange Membrane Fuel Cell, Bipolar Plate, Nanocomposites, Carbon Based Fillers.

Abstract

Introduction: *Proton Exchange Membrane Fuel Cells (PEMFCs) are promising clean energy technologies due to their high efficiency, zero emissions, and suitability for portable, stationary, and automotive applications. One of the most critical components of PEMFCs is the bipolar plate (BPP), which accounts for nearly 80% of the fuel cell stack's weight and 40–60% of its total cost. Traditional BPPs made of graphite (GR) offer excellent corrosion resistance but suffer from brittleness and high manufacturing costs, while metal BPPs require protective coatings to prevent corrosion. Consequently, polymer composite BPPs have gained attention as a viable alternative to conventional materials. Although polymer-based materials typically exhibit lower electrical conductivity and mechanical strength, their properties can be enhanced with conductive carbon fillers, leading to improved mechanical strength, chemical stability, and more cost-effective processing.*

Objectives: The present project aims to develop and optimize conductive polymer composites for use in PEMFCs with a focus on enhancing the electrical, mechanical, and thermal properties of BPPs.

Material and methods: Polyvinylidene fluoride (PVDF; commercial grade Kynar® 720, density of 1.78 g/cm³, MFI of 7.0 g/10 min) was obtained from Arkema, USA. Polyethylene terephthalate (PET, commercial grade NEOPET 8, melting temperature of 248°C) was procured from NEOGROUP in Lithuania. Graphite (GR) fillers with three different sizes (G1: 17.8 µm, G2: 561 µm and G3: 561 µm) were supplied by Nouveau Monde Graphite (NMG), Québec, Canada, and reduced graphene oxide (rGO) was synthetized through improved hummer method. Carbon black (CB; Printex XE-2) was sourced from Degussa-Hüls, Germany, while carbon fiber (CF; density of 2 g/cm³, length of 2 mm, and diameter of ~7 µm) was purchased from Omnia Products, Oxford, USA. Multi-walled carbon nanotube (MWCNT; Graphit-strength C100) was purchased from Arkema, USA. Highly filled PVDF/PET composites with varying compositions of GR, CB, CF, rGO, and MWCNT were prepared via melt mixing (internal mixer) followed by compression molding. The morphological characteristics were analyzed using scanning electron microscopy (SEM). Thermal stability was evaluated using thermogravimetric analysis (TGA), while the flexural and compressive mechanical properties of the composites were assessed under bending and compressive forces. Electrical conductivity was measured in terms of through-plane and in-plane resistivity to assess the orientation effect of the solid conductive fillers in both vertical and horizontal directions, and water absorption was analyzed to evaluate the composite's suitability for fuel cell environments. Finally, injection-compression molding technique was used to manufacture the BPP prototypes.

Results: The results demonstrated that co-continuous PVDF/PET blends facilitated the selective localization of conductive fillers within the PET phase, enabling the formation of efficient conductive pathways. Among the nanocomposites containing a single type of graphite (GR), the composite with 60 wt.% medium-sized G2 exhibited the lowest through-plane resistivity (1.5 Ω·cm) and in-plane resistivity (0.84 Ω·cm), along with adequate flexural strength (29.8 MPa) and a high decomposition temperature (475°C). Synergistic effects were observed when combining different GR types. The G2/G3 mixture (45/15 wt.%) achieved a through-plane resistivity of 0.93 Ω·cm and an in-plane resistivity of 0.71 Ω·cm. Substituting 2 wt.% of G3 with reduced graphene oxide (rGO) further reduced the through-plane and in-plane resistivity to 0.89 Ω·cm and 0.62 Ω·cm, respectively. Water absorption tests showed that this hybrid system lowered water uptake from 0.78% to 0.05%. Based on these findings, the G2/G3 (45/15 wt.%) composite was selected for further enhancement by adding CB and CF. The incorporation of CB and CF decreased electrical resistivity, with the 5 wt.% CB–55 wt.% GR composite achieving the lowest through-plane and in-plane resistivity values of 0.19 Ω·cm and 0.15 Ω·cm, respectively. However, the composite containing 2.5 wt.% CF, 7.5 wt.% CB, and 50 wt.% GR demonstrated even lower resistivity, with through-plane and in-plane resistivity values of 0.18 Ω·cm and 0.09 Ω·cm, respectively. Flexural and compressive testing

indicated that adding CB and CF improved both flexural and compressive strength up to an optimal point, after which both properties declined. The highest flexural strength was achieved with 5 wt.% CB (48.6 MPa) and 7.5 wt.% CF (45.65 MPa). Similarly, the compressive strength peaked at 38.44 MPa for 5 wt.% CB and 16.63 MPa for 7.5 wt.% CF. Additionally, the 5 wt.% CB–55 wt.% GR composite exhibited the lowest water absorption (0.045%), confirming its suitability for BPPs applications in PEMFCs. To further enhance the conductivity and overall properties of the developed BPPs, MWCNTs were incorporated at concentrations ranging from 0.5 to 3 wt.%. The lowest resistivity was achieved with the addition of 3 wt.% MWCNT to the 2.5 wt.% CF, 7.5 wt.% CB, and 50 wt.% GR nanocomposites, reducing through-plane and in-plane resistivity to 0.08 Ω·cm and 0.04 Ω·cm, respectively. The nanocomposite with 3 wt.% MWCNT also exhibited the highest flexural strength (43.05 MPa) and modulus (36 GPa), while maintaining compressive strength above the DOE target (13 MPa). Moreover, the water absorption of the nanocomposite containing 1 wt.% MWCNT was only 0.02% after 168 hours, which is well below the DOE target.

Conclusions: The study highlights the synergistic effects of hybrid graphite particle sizes and the strategic incorporation of secondary carbon-based fillers to optimize the multifunctional properties of BPPs. The tailored distribution of GR within the co-continuous PVDF/PET matrix facilitated the enhancement of electrical conductivity without compromising mechanical integrity. Additionally, the inclusion of rGO and hybrid GR-GR systems proved effective in reducing resistivity while maintaining desirable mechanical and thermal properties. The developed materials present a cost-effective and scalable alternative to conventional graphite or metallic BPPs, addressing the key challenges of conductivity, durability, and manufacturability in PEMFC technology. These findings contribute to the advancement of fuel cell technologies by offering a sustainable and high-performance composite for next-generation BPPs, paving the way for improved efficiency and commercial viability of PEMFCs.

Acknowledgment

The authors are grateful to the Research Center for High Performance Polymer and Composite Systems (CREPEC).

References

[1] Shojaei, Sahar, Ehsan Rostami-Tapeh-Esmaeil, and Frej Mighri. "A review on key factors influencing the electrical conductivity of proton exchange membrane fuel cell composite bipolar plates." Polymers for Advanced Technologies 35.2 (2024): e6301.

[2] Shojaei, Sahar, et al. "Development of enhanced co-continuous PVDF/PET nanocomposites via synergistic effects of graphite particle size, hybrid systems, and reduced graphene oxide." International Polymer Processing 0 (2025).

EFCH2 2025 European Fuel Cells and Hydrogen PIERO LUNGHI CONFERENCE
September 17th–19th 2025 Capri / Italy

Effect of water vapor content in MSR reformate on in-plane performance distribution of an HT-PEMFC

Emilija Todorovski*[a], Filip Todorovski [a], Andrej Lotrič [a], Mitja Mori [a], Mihael Sekavčnik [a]

* corresponding author: emilija.todorovski@fs.uni-lj.si
[a] University of Ljubljana, Faculty of Mechanical Engineering, Slovenia

Keywords: fuel cell diagnostics, HT-PEMFC, in-plane distribution, methanol reformate

Abstract

Introduction: High-temperature polymer electrolyte membrane fuel cells (HT-PEMFCs) are a promising technology for energy generation due to their high tolerance to fuel impurities and simplified water management. Methanol, an attractive fuel for HT-PEMFCs, can be reformed on-site to produce a hydrogen-rich gas mixture via steam reforming (MSR) [1]. However, the composition of the reformate—including carbon monoxide, carbon dioxide, unconverted methanol, and residual water—can significantly impact the fuel cell's electrochemical performance [2]. In this study, reformate gas compositions were selected based on theoretical MSR outputs with steam-to-carbon (S/C) ratios of 1.3 to 1.5, which are commonly used in practice. The investigated syngas mixtures consisted of 75% H_2 with changing levels of CO and CO_2. For each case, four relative humidity (RH) levels were examined (1.0, 1.5, 2.0, and 2.5), corresponding to typical water vapor content in MSR-produced syngas under these operating conditions. Despite extensive studies on global metrics [3], [4], [5], spatial in-plane variations within the MEA remain underexplored. In reality, local fuel composition, membrane hydration, and reaction kinetics can lead to in-plane non-uniformities, affecting durability and reliability.

Objectives: This study aims to investigate the effect of water vapor content in methanol reformate on the spatial performance of an HT-PEMFC. The focus is on evaluating in-plane current density distribution changes under varying reformate compositions using segmented cell measurements and visualizing performance shifts relative to a dry baseline.

Material and methods: The fuel cell used in this study was equipped with a pre-doped phosphoric acid polybenzimidazole (PBI) membrane electrode assembly (MEA), featuring a carbon cloth gas diffusion layer and an active area of 45.2 cm^2 and bipolar plates with serpentine flow channels. All tests were conducted on a Greenlight G60 test station using simulated reformed gas mixtures, composed of H_2, CO_2 and CO with varying water vapor

content. The cell fixture used was an oil-heated Baltic qCf FC50/125 Fixture Unit. Spatial current density measurements were performed using an S++ segmented current collector plate, 12×12 segmented grid (144 points) for in-plane performance mapping. All measurements were conducted at a constant current density of 0.4 A/cm², temperature of 170°C and anode/cathode stoichiometry of 1.5/3. The reformate compositions were selected to reflect typical methanol steam reforming outputs at steam-to-carbon (S/C) ratios of 1.3 to 1.5, with CO concentrations of 1% and 2% and RH levels from 1.0 to 2.5. Each condition was compared to a dry baseline to evaluate the local effect of water vapor addition. Data analysis included current density classification per segment based on the change relative to the baseline. Cubic interpolation was used to generate smooth contour plots of spatial performance shifts.

Results: To quantify the localized impact of water vapor addition, each MEA segment was classified as "Better", "Same", or "Worse" based on the change in current density relative to the dry baseline. Table 1 summarizes the percentage of segments in each category across all tested CO and RH levels. The data shows a consistent trend of increasing "Better" segments and decreasing "Same" segments with rising RH, particularly for higher CO contents.

Table 1: Classification of MEA segments as Better, Same, or Worse (%) in comparison to the dry baseline, and relative voltage increase at 0.4 A/cm², for different RH levels in simulated MSR reformate (75% H_2 with varying CO and CO_2 content)

Reformed gas composition	RH	Segment category			Relative voltage Increase (%) at 0.4 A/cm²
		Better (%)	Same (%)	Worse (%)	
75%H_2, 24%CO_2, 1%CO	1%	18.1	63.2	18.8	1.0
	1.5%	22.9	60.4	16.7	2.2
	2%	31.2	49.3	19.4	3.4
	2.5%	36.8	34	29.2	4.5
75%H_2, 23%CO_2, 2%CO	1%	0	94.4	5.6	0.2
	1.5%	6.2	86.8	6.9	0.8
	2%	35.4	34.7	29.9	2.3
	2.5%	37.5	28.5	34	2.8

Figure 1 presents the current density distribution under 2% CO reformate conditions, along with the relative changes at 1.5% and 2.5% RH compared to the dry baseline. At 1.5% RH, performance remains largely unchanged across the MEA, with minimal current redistribution and localized suppression in regions of initially high current density. In contrast, 2.5% RH results in a pronounced current increase in the upper half of the MEA, particularly near the anode inlet (1,1), while the most notable performance decline appears in the lower half near the anode outlet (12,12). At 0.4 A/cm², the cell voltage increased from 0.475 V (dry) to 0.486 V at 2.5% RH in the 2% CO case, supporting the spatial performance improvements observed through S++ mapping.

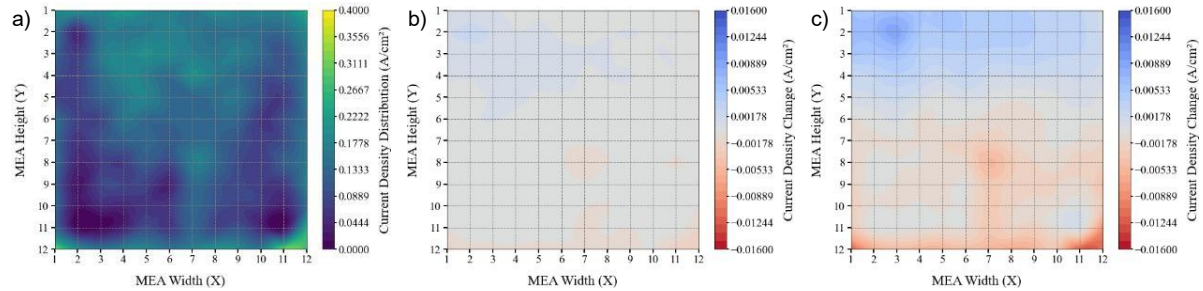


Figure 1: (a) - Current density distribution for 75% H_2, 23% CO_2, 2% CO reformate – dry conditions; Current density change distribution maps for 75% H_2, 23% CO_2, 2% CO reformate with increasing RH levels: (b) 1.5% RH, (c) 2.5% RH

Conclusions: The observed improvement in local performance with added RH can be attributed to both physicochemical and electrochemical effects. Water vapor facilitates CO desorption from the Pt surface, reducing catalytic site blocking, and may support the water–gas shift reaction to some extent. In parallel, increased hydration enhances proton conductivity in the membrane, particularly in the drier zones, contributing to more balanced current distribution. The most significant performance gains are observed in the upper half of the MEA, near the anode and cathode inlets, where reactants first enter the cell. In contrast, the lower half exhibits milder but spatially consistent improvements, indicating enhanced uniformity and reduced segment-level disparities with increasing RH. This spatial improvement is consistent with the overall performance trend, where cell voltage at 0.4 A/cm² increased by up to 4.5% with added RH in the 1% CO case, and 2.8% in the more CO-rich 2% CO case.

Acknowledgment

The authors acknowledge financial support from Slovenian Research and Innovation Agency (research core fundings No. P2-0401).

References

[1] N. Li *et al.*, “A review of reformed methanol-high temperature proton exchange membrane fuel cell systems,” *Renewable and Sustainable Energy Reviews*, vol. 182, p. 113395, Aug. 2023, doi: 10.1016/J.RSER.2023.113395.

[2] J. Xu, Y. Wu, S. Xiao, Y. Wang, and X. Xu, “Synergic effect investigation of carbon monoxide and other compositions on the high temperature proton exchange membrane fuel cell,” *Renew Energy*, vol. 211, pp. 669–680, Jul. 2023, doi: 10.1016/J.RENENE.2023.05.008.

[3] S. S. Araya, I. F. Grigoras, F. Zhou, S. J. Andreasen, and S. K. Kær, “Performance and endurance of a high temperature PEM fuel cell operated on methanol reformate,” *Int J Hydrogen Energy*, vol. 39, no. 32, pp. 18343–18350, Oct. 2014, doi: 10.1016/J.IJHYDENE.2014.09.007.

[4] S. Thomas, J. R. Vang, S. S. Araya, and S. K. Kær, “Experimental study to distinguish the effects of methanol slip and water vapour on a high temperature PEM fuel cell at different operating conditions,” *Appl Energy*, vol. 192, pp. 422–436, Apr. 2017, doi: 10.1016/J.APENERGY.2016.11.063.

[5] C. Huang, Z. Wu, and J. Zheng, “Effects of concentrated CO2 on the performance of a PBI/H3PO4 high temperature proton exchange membrane fuel cell,” *J Power Sources*, vol. 614, p. 235053, Sep. 2024, doi: 10.1016/J.JPOWSOUR.2024.235053.

EFCH2 2025
European Fuel Cells and Hydrogen
PIERO LUNGHI CONFERENCE
September 17th–19th 2025
Capri / Italy

Impedance Modeling Framework for Proton Exchange Membrane Fuel Cells

Francesco Mazzeo*[a], Massimiliana Carello [a]

* Corresponding Author: Francesco Mazzeo

[a] Politecnico di Torino

Keywords: Proton Exchange Membrane Fuel Cells (PEMFC), Electrochemical Impedance Spectroscopy (EIS), Impedance Modeling

Abstract

A comprehensive PEMFC cathode impedance model is developed by incorporating the charge and mass transport equations for both the catalyst layer (CL) and the gas diffusion layer (GDL), under the hypothesis of constant oxygen concentration (high oxygen stoichiometry) along the channel (CH) and it is solved numerically to obtain a generalized impedance response. The numerical solution is compared with a low-current analytical approximation, highlighting the operational conditions under which the analytical approach remains valid. An overview of the computational time is provided to give an idea of the duration required to solve the system of equations and to fit possible experimental impedance data.

Introduction

Electrochemical impedance spectroscopy (EIS) is a powerful diagnostic tool that offers deep insights into the electrochemical processes and transport phenomena within proton exchange membrane fuel cells (PEMFCs) [1]. Traditional equivalent circuit models (ECM) are often employed to fit EIS spectra; however, they rely on empirical parameters and may lack a direct connection to the underlying physical processes, leading to ambiguities in interpreting overlapping phenomena [2]. In contrast, a physics-based model explicitly incorporates the fundamental charge and mass transport equations, thereby providing a more robust and accurate representation of the system. This approach links model parameters directly to physical properties, such as diffusion coefficients, reaction kinetics, and capacitances, enhancing both the predictive capability and our understanding of the cell's performance [3]. Given that the oxygen reduction reaction (ORR) and oxygen diffusion represent the most critical limitations in PEMFCs, this work focuses on the cathode processes (in CL and GDL) under the hypothesis of high air stoichiometry.

Objectives

The objective of this work is to provide a framework for physics-based impedance modeling, offering a robust alternative to traditional resistance extraction methods, such as equivalent circuit models (ECMs), for fitting experimental impedance data obtained at high stoichiometry in PEMFCs. This approach enables the direct extraction of key physical parameters, including the oxygen diffusion coefficients in the GDL and the void pores of the CL, the proton conductivity in the catalyst layer, the double layer capacitance, and the Tafel slope.

Material and methods

To model the impedance of a PEMFC, one must consider the conservation equations for voltage, current, and oxygen concentration in the cathode catalyst layer. Assuming Tafel kinetics for the ORR, Fickian diffusion of oxygen, neglecting electron conduction and a small sinusoidal perturbation under steady-state conditions, the system can be linearized. This leads to two sets of spatial differential equations, one for the steady state and one for the perturbation, whose solution provides the impedance response.

Results:

Under the assumption of very low currents, the system of equations for both the steady state and perturbation conditions admits an analytical solution [3]. This solution was compared with the numerical one to ensure consistency and to identify when deviations begin to occur. The results are presented in Figure 1. A perfect agreement is observed at low currents; however, it can be seen that the diffusive contribution is underestimated by the analytical solution, which assumes constant concentrations in the CL, while it becomes more significant in the more realistic numerical solution.

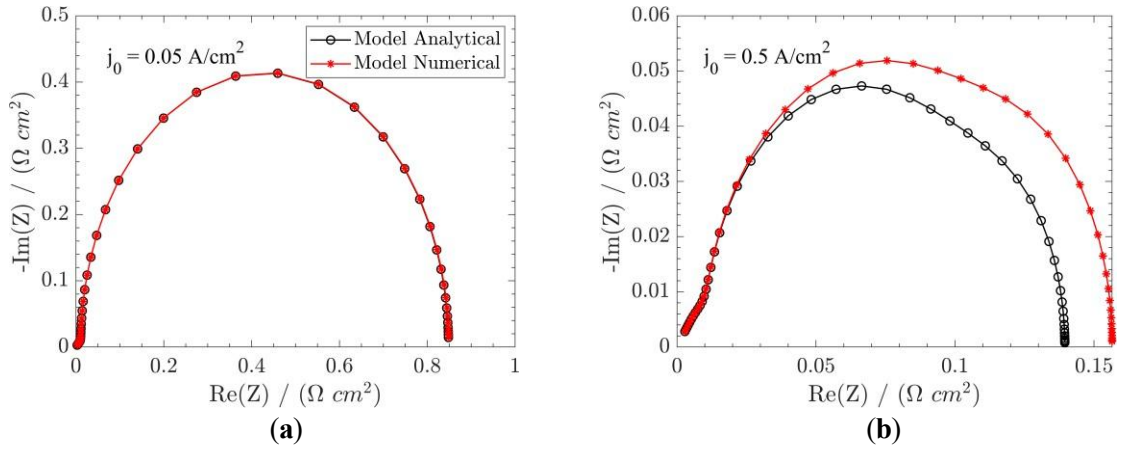


Figure 1. Comparison between Analytical solution and numerical solution for two different current densities: 0.05 A/cm^2 (a) and 0.5 A/cm^2 (b).

The time for obtaining impedance response is about 1s. For fitting of experimental data purposes, minimization algorithms are employed, which require numerous iterations to converge to an optimal solution. Usually, a satisfactory fit is achieved after roughly 150–200 iterations, corresponding to a computational time of approximately 150–200 seconds (i.e., about 2.5–3.5 minutes).

Conclusions

This work presents a framework for 1-D physics-based impedance modeling of a PEMFC operating under high oxygen stoichiometry hypothesis. The transient equations are linearized, transformed into the frequency domain, and solved numerically to obtain the impedance response. The numerical model is validated against the low-current analytical solution to ensure accuracy. An overview of the computational time required to fit possible experimental data is provided, showing that it typically falls within the range of a few minutes.

Acknowledgment

This work is part of the project PNRR-NGEU which has received funding from the MUR – DM 352/2022 and from Eaton for the Ph.D. scholarship.



References

[1] S. Wang, J. Zhang, O. Gharbi, V. Vivier, M. Gao, and M. E. Orazem, 'Electrochemical impedance spectroscopy', *Nat Rev Methods Primers*, vol. 1, no. 1, Art. no. 1, Jun. 2021, doi: 10.1038/s43586-021-00039-w.

[2] D. A. Harrington and P. van den Driessche, 'Mechanism and equivalent circuits in electrochemical impedance spectroscopy', *Electrochimica Acta*, vol. 56, no. 23, pp. 8005–8013, Sep. 2011, doi: 10.1016/j.electacta.2011.01.067.

[3] A. Kulikovsky, 'Analytical Impedance of Oxygen Transport in the Channel and Gas Diffusion Layer of a PEM Fuel Cell', *J. Electrochem. Soc.*, vol. 168, no. 11, p. 114520, Nov. 2021, doi: 10.1149/1945-7111/ac3a2d.

[4] T. Reshetenko and A. Kulikovsky, 'Impedance Spectroscopy Characterization of Oxygen Transport in Low– and High–Pt Loaded PEM Fuel Cells', *J. Electrochem. Soc.*, vol. 164, no. 14, p. F1633, Dec. 2017, doi: 10.1149/2.1131714jes.

[5] S. Cruz-Manzo and P. Greenwood, 'Analytical Warburg Impedance Model for EIS Analysis of the Gas Diffusion Layer with Oxygen Depletion in the Air Channel of a PEMFC', *J. Electrochem. Soc.*, vol. 168, no. 7, p. 074502, Jul. 2021, doi: 10.1149/1945-7111/ac1031.

EFCH2 2025 European Fuel Cells and Hydrogen PIERO LUNGHI CONFERENCE
September 17th–19th 2025 Capri / Italy

Evaluating the combined effect of humidification, backpressure, and cathode stoichiometry on HT-PEMFC performance using DRT analysis

Filip Todorovski*[a], Emilija Todorovski [a], Andrej Lotrič[a], Mitja Mori[a], Mihael Sekavčnik[a]

* corresponding author: filip.todorovski@fs.uni-lj.si
[a] University of Ljubljana, Faculty of Mechanical Engineering, Slovenia

Keywords: backpressure, DRT analysis, HT-PEMFC, reactant humidification

Abstract

Introduction: High-temperature proton exchange membrane fuel cells (HT-PEMFCs) are well-suited for integration with reformers and simplified water management systems due to their high operating temperature and possibility for dry gases operation [1], [2]. Although relatively independent from external humidification, small changes in inlet gas humidity, pressure, and stoichiometry can still affect performance by altering proton conductivity, reactant transport, and reaction kinetics. While these effects have been studied individually, their combined impact and interactions remain insufficiently explored. In particular, the potential benefit of mild humidification under varying backpressure and stoichiometry has not been systematically evaluated. To isolate cathode-side effects, pure hydrogen was used as the anode gas, eliminating fuel-side impurities.

Objectives: This study aims to investigate the combined influence of RH, reactant pressure, and cathode stoichiometry on the electrochemical behaviour of HT-PEMFC. Using DRT analysis, the focus is on quantifying changes in ohmic, charge transfer, and mass transport resistances, and identifying the interactions and trade-offs between humidification and pressurization that affect overall cell performance during operation with pure hydrogen.

Material and methods: p-PBI-based MEAs (25 cm², 981 µm), with catalyst coated on carbon cloth and the membranes produced under the BASF license, were tested on a GreenLight G60 fuel cell station. All measurements were performed at 160 °C at constant anode stoichiometry of 1.25, with 30 minutes of stabilization before each test. Polarization curves were recorded down to 0.3 V, and EIS was conducted at 0.2–0.8 A/cm² using a Gamry Reference 3000 (5 mV AC, 0.01 Hz-1 kHz). Three EIS measurements were averaged for each condition (average SD = 0.01%), with results at 0.4 A/cm² presented here. The test matrix includes varying cathode

stoichiometry (air: 1.8, 2.5, 4.0, 8.0; O_2: 1.8), reactant pressures (0.0–0.0, 1.5–1.3, 2.0–1.8 barg), and RH levels (0–0% RH and 5–5% RH).

Results: Fig. 1 shows the impact of oxidant stoichiometry and pressurization on the DRT spectra under dry-gas operation. Operation with oxygen eliminates the low frequency peak (P3) [3], typically associated with mass transport resistance at the GDL – catalyst layer interface, but introduces peaks in very low frequency range (P4), which is associated with convective transport resistance between the flow channels and the GDL (confirmed by testing at reduced cathode stoichiometry). The observed increase in charge transfer resistance associated with ORR (P2) during oxygen and pressurized operation may result from phosphoric acid redistribution [3]. Even though O_2 availability increases with pressure, proton transport might become rate-limiting, especially if acid distribution is uneven.

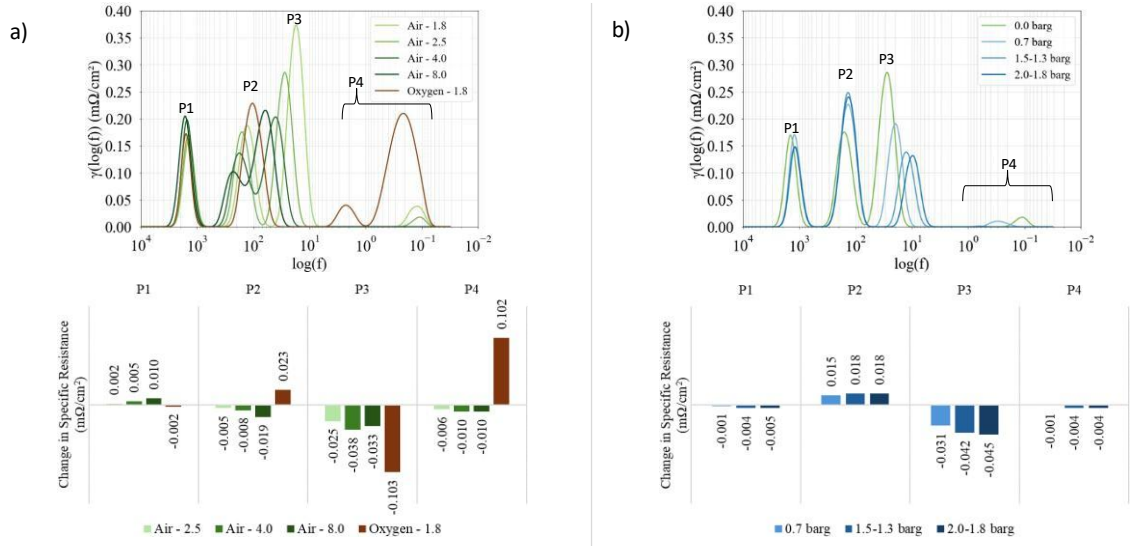
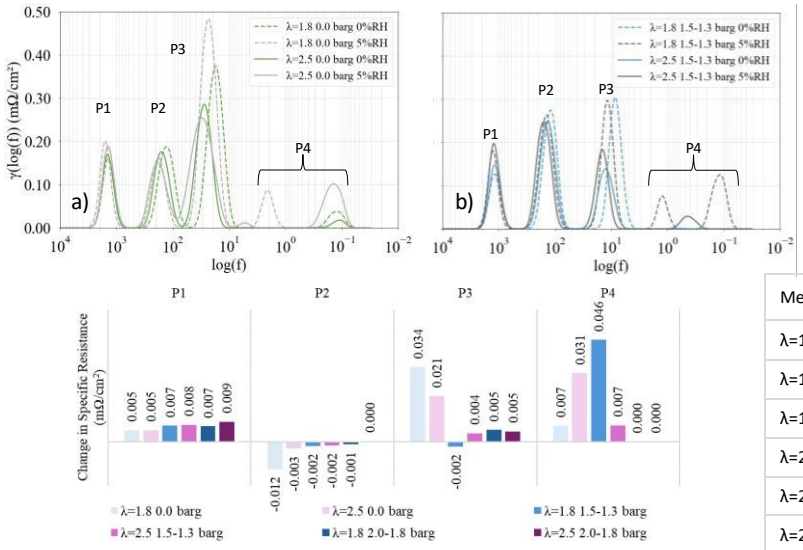


Fig. 1: Top diagrams show DRT spectra while bottom diagrams show change in specific resistance (calculated from peak area of DRT spectra analysis (a) Air – 1.8 as reference case, b) 0.0 barg as reference case)) under various operating conditions: (a) varying air stoichiometry and oxygen operation at atmospheric pressure, and (b) varying reactant pressure at 1.25-2.5 (anode-cathode) stoichiometry

Fig. 2 presents the influence of relative humidity (5-5% RH vs. 0-0% RH) – under various reactant pressures and cathode stoichiometry – on the DRT spectra, peak-specific resistance differences, and corresponding cell voltage changes at 0.4 A/cm². A slight increase in P1 is observed with rising RH, indicating increased ohmic resistance [4], [5], likely due to PA redistribution. The charge transfer resistance associated with ORR (P2) decreases notably at atmospheric pressure, but this improvement becomes progressively smaller with increasing pressure, dropping to the same value as at 0-0% RH. P3 increases with rising RH, indicating increased interfacial mass transport resistance; however, this effect diminishes at higher stoichiometry and pressure, where elevated pressure more strongly suppresses the peak. At the highest pressure (2.0 – 1.8 barg), P4 is fully suppressed regardless of RH, confirming the elimination of mass diffusion limitations under these conditions.



Measurement	Cell Voltage Change for 5% RH at 0.4 A/cm² (mV)
λ=1.8 0.0 barg	-51.12
λ=1.8 1.5-1.3 barg	-25.67
λ=1.8 2.0-1.8 barg	-33.22
λ=2.5 0.0 barg	-51.99
λ=2.5 1.5-1.3 barg	-22.68
λ=2.5 2.0-1.8 barg	-24.77

Fig. 2: Top: DRT spectra for 0-0% RH and 5-5% RH with cathode stoichiometry of 1.8 and 2.5 at varying anode-cathode reactant pressures of: a) 0.0-0.0 barg, b) 1.5-1.3 barg, c) 2.0-1.8 barg; Bottom left: Change in specific resistance (calculated from peak area of DRT spectra analysis (0-0% RH as reference case)) between 5-5% RH and 0-0% RH on anode and cathode feed; Bottom right: Cell voltage change between 5-5% RH and 0-0% RH

Conclusions: These results demonstrate that even minimal humidification can significantly reduce charge transfer losses under atmospheric pressure, but its benefits are diminished when pressure and stoichiometry are increased. Despite the reduction in P2, a simultaneous increase in mass transport resistances (P3 and P4) led to an overall performance decline. Although P4 disappeared at the highest pressure conditions (2.0–1.8 barg), the smallest cell voltage loss (−22.7 mV) occurred at 1.5–1.3 barg and λ=2.5, suggesting this operating point offers the best trade-off between humidification effects and pressure-driven transport improvements.

Acknowledgment:

The authors acknowledge financial support from Slovenian Research and Innovation Agency (research core fundings No. P2-0401)

References

[1] D. Yu, X. Li, S. S. Araya, S. L. Sahlin, and V. Liso, “Data-driven diagnosis of high temperature PEM fuel cells based on the electrochemical impedance spectroscopy: Robustness improvement and evaluation,” *Journal of Energy Chemistry*, vol. 96, pp. 544–558, Sep. 2024, doi: 10.1016/j.jechem.2024.05.014.

[2] J. Kim, M. Kim, B. G. Lee, and Y. J. Sohn, “Durability of high temperature PEM fuel cells in daily based start-stop operation mode using reformatted gas,” *Int J Hydrogen Energy*, vol. 40, no. 24, pp. 7769–7776, Jun. 2015, doi: 10.1016/j.ijhydene.2014.12.122.

[3] A. Weiß, S. Schindler, S. Galbiati, M. A. Danzer, and R. Zeis, “Distribution of Relaxation Times Analysis of High-Temperature PEM Fuel Cell Impedance Spectra,” *Electrochim Acta*, vol. 230, pp. 391–398, Mar. 2017, doi: 10.1016/j.electacta.2017.02.011.

[4] S. Schindler, A. Weiß, S. Galbiati, F. Mack, M. A. Danzer, and R. Zeis, “Identification of Polarization Losses in High-Temperature PEM Fuel Cells by Distribution of Relaxation Times Analysis,” *ECS Trans*, vol. 75, no. 14, pp. 45–53, Aug. 2016, doi: 10.1149/07514.0045ecst.

[5] N. Bevilacqua, M. A. Schmid, and R. Zeis, “Understanding the role of the anode on the polarization losses in high-temperature polymer electrolyte membrane fuel cells using the distribution of relaxation times analysis,” *J Power Sources*, vol. 471, Sep. 2020, doi: 10.1016/j.jpowsour.2020.228469.

EFCH2 2025 European Fuel Cells and Hydrogen
PIERO LUNGHI CONFERENCE
September 17th–19th 2025
Capri / Italy

Application of the differential impedance analysis for deeper insight into solid oxide cells degradation

D. Vladikova* [a,b], R. Spotorno[c], M. Krapchanska [a,b], B. Burdin[b], P. Piccardo[c]

* corresponding author: d.vladikova@iees.bas.bg

[a] Trakia University, Student Campus, 6000 Stara Zagora, Bulgaria

[b] Institute of Electrochemistry and Energy Systems – Bulgarian Academy of Sciences, 10 Acad. G. Bonchev str., 1113 Sofia, Bulgaria

[c] Department of Chemistry and Industrial Chemistry, University of Genoa, Via Dodecaneso 31, 16146 Genoa, Italy

Keywords: Differential Impedance Analysis, Solid Oxide Cells, Degradation, Artificial Aging

Abstract

Differential Impedance Analysis (DIA) is an advanced technique for impedance data analysis, which follows the approach of the structural identification. The method increases the objectivity and exactness of the model recognition, since it eliminates the necessity of an initial working hypothesis and performs the structural and parametric identification directly from the experimental data. The improved analytical power of the DIA is based on the combination of a scanning procedure with a local parametric analysis. This study applies DIA to investigate Solid Oxide Cell (SOC) degradation through redox cycling of the Ni/YSZ fuel electrode in button cells.

Introduction:

The Differential Impedance Analysis, developed by Zdravko Stoynov [1] marks a unique advantage in the impedance data analysis. It identifies both the structure $\hat{S}$ and the parameters $\hat{M}$ of the system and thus eliminates the necessity for initial working hypothesis, improving the information capability and objectivity of Electrochemical Impedance Spectroscopy.

The following steps describe the procedure of the structural and parametric identification:

- Scanning with a simple local operating model (LOM) - a mesh of resistance *R* and capacitance *C* in parallel, extended with additive term *Ad* connected in series, throughout the whole frequency range with a scanning window of a single frequency point.
- Parametric identification of the LOM at every working frequency for which the initial set of impedance data is extended with two additional terms – the derivatives of the real and imaginary components of the impedance with respect to the frequency. As a result, a new experimental D3 set of data is produced:

$$\boldsymbol{D}_3 \left[\lg\omega_i, \lg\hat{R}_{\mathrm{ad}_i}, \lg\hat{C}_i, \lg\hat{R}_i, \lg\hat{T}_i \right]. \qquad (1)$$

The frequency dependence of the parameters' estimates of impedance data (Fig. 1a) is presented in so called temporal plots, (Fig. 1b). If the LOM parameters' estimates are frequency independent in a given frequency region, the sub-model corresponding to this frequency segment follows the LOM

structure, i.e. it is described with a parallel combination of capacitance and resistance. Thus, the number of the plateaus gives the number of the time-constants in the model (Fig. 1b). The results may be presented in the more illustrative spectral form by the Spectral Transform procedure which converts the plateaus into spectral peaks by accumulating similar values of the respective parameters (Fig. 1c) [1]. Additional procedure - Secondary DIA [1], recognizes frequency-dependent elements (CPE, Warburg, Bounded Warburg etc.), as well as their presence in more complicated models.

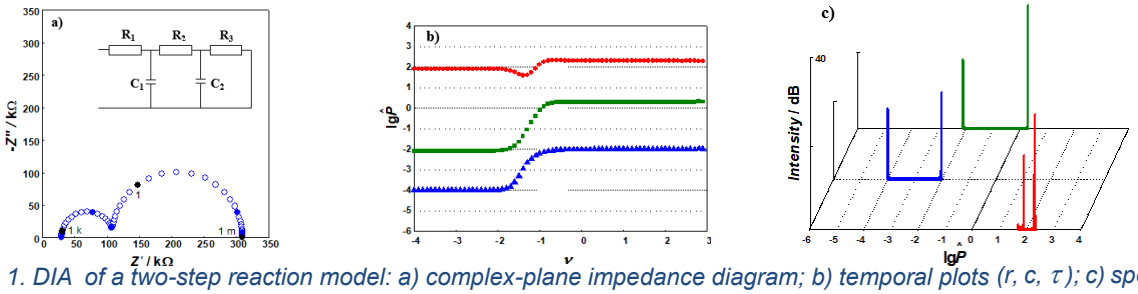


*Fig. 1. DIA of a two-step reaction model: a) complex-plane impedance diagram; b) temporal plots (r, c, τ); c) spectral plots (**r**, **c**, **τ**), ($\hat{\tau}_i = lg T_i$, $\hat{r}_i = lg R_i$, $\hat{c}_i = lg C_i$) and $\nu_i = lg(\omega_i^{-1})$.*

DIA opens new horizons for the impedance spectroscopy, increasing its objectivity, reliability and information capabilities. The method gradually entered in the impedance studies of electrochemical energy sources.

Objectives and Materials:

This study applies DIA to investigate Solid Oxide Cell (SOC) degradation through redox cycling of the Ni/YSZ fuel electrode in button cells with an 8 mol % Y_2O_3-stabilized zirconia electrolyte and LSCF oxygen electrode with a GDC barrier layer. Degradation is assessed via Accelerated Stress Tests (AST) using *ex-situ* redox cycling, enabling controlled degradation monitoring through impedance measurements [2]. Electrochemical testing combines *i-V* curves and Impedance spectroscopy with microstructural SEM characterization.

Previous long-term field tests on the same system were used for benchmark (Table 1). The AST was evaluated by the Acceleration Factor (AF), determined by the ratio between long-term and accelerated test durations yielding the same degradation level.

Results:

Comparison of voltage decrease (Aging Factor, AgF) over 20 redox cycles (~ 60 hours) and nominal operation (4000 hours) reveals a strong correlation, defining an AF of ~ 60 (Table 1).

Table 1. Voltage decrease at constant current density extracted from the *i-V* curves for accelerated aging via redox cycling and nominal aging.

Redox cycling				Nominal Aging		
	Initial	20 redox cycles		Initial	4000 h	
i, A/cm²	*U*, mV	*U*, mV	AgF_U, %	U, mV	U, mV	AgF_U, %
0.28	961	937	2.5	917	898	2.07

0.50	864	830	4.5	827	791	4.35

Impedance analysis of artificially aged cells (Fig. 2) shows increased ohmic and polarization resistance. Classical non-linear equivalent circuit fitting describes pristine and aged samples with three steps with CPE behaviour of the capacitance, while DIA reveals a four-step process with 3 kernels of time-constants and one step with frequency distributed behaviour (Fig. 2b).

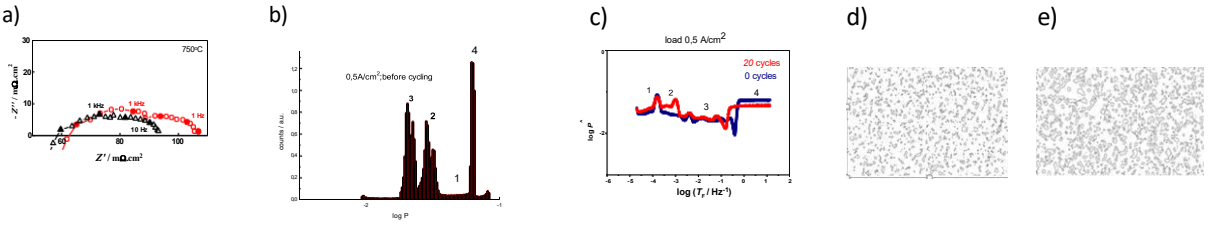


Fig. 2. DIA results of impedance measurements at 0.5 A/cm^2: a) impedance diagram before cycling (blue) and after 20 cycles (red); b) spectral plot before cycling; c) temporal plots before and after cycling; d) porosity of the fuel electrode before aging and e) after aging.

The temporal plots, which separate 4 steps (Fig. 2c) show that the increase of the resistance after 20 redox cycles is dominating in Step 2, while Step 4, which is the rate-limiting one before cycling, reduces its resistance. This is obviously linked to the increased porosity caused by the artificial aging (Fig. 2d,e).

Conclusions:

This result shows that even at linear *i-V* curve regions, transport limitations significantly impact performance. Those observations, as well as the comparison of the impedance behaviour for 0.28 and 0.5 A/cm^2 will be discussed in detail.

Acknowledgments

The authors (DV, MK, BB) acknowledge the support of: (i) the Bulgarian Ministry of Education and Science under the National Roadmap for Research Infrastructure 2020 -2027 “Energy storage and hydrogen energetics (ESHER)” under grant agreement No. DO1-349/13.12.2023, and under the Bulgarian National Recovery and Resilience Plan, Component "Innovative Bulgaria", Project № BG-RRP-2.004-0006-C02 "Development of research and innovation at Trakia University in service of health and sustainable well-being" and (ii) the European Union under Horizon Europe (project 101136692).

References

[1] A. Stoynov, D. Vladikova, in Encyclopedia of Electrochemical Power Sources, U. Garche (Ed.), Elsevier, 2009, p. 632

[2] D. Vladikova, M. Krapchanska, B. Burdin, A. Sheikh, Journal of Solid State Electrochemistry 28 (5) (2024) 1743-1759, https://doi.org/10.1007/s10008-024-05803-y

EFCH2 2025 European Fuel Cells and Hydrogen PIERO LUNGHI CONFERENCE
September 17th–19th 2025 Capri / Italy

PEM Fuel Cell Stack with Dead-Ended Anode for Electric Aviation: Efficient Operating with Low Degradation

Jakob Trägner*[a], Steffen Heinke[a], Wilhelm Tegethoff[a], Jürgen Köhler[a]

*corresponding author: j.traegner@tu-braunschweig.de

[a] Technische Universität Braunschweig, Institut für Thermodynamik, Hans-Sommer-Str. 5, 38106 Braunschweig

Keywords: Dead-Ended Anode, Degradation, Dynamic Simulation, PEM Fuel Cell Stacks

Abstract

Introduction: The use of polymer electrolyte membrane fuel cells (PEMFCs) in electric aircraft is a promising technology for reducing the climate impact of aviation. The current state-of-the-art method for supplying hydrogen in mobile systems is the active anode gas recirculation, in which hydrogen is supplied over-stoichiometrically and unused hydrogen is recirculated via a hydrogen recirculation blower (HRB) where it is mixed with fresh hydrogen from the tank. In the investigated dead-ended anode (DEA) concept, no anode gas recirculation is intended; the purge valve at the anode outlet remains predominantly closed while hydrogen is supplied stoichiometrically by controlling the pressure at the anode inlet. Nitrogen and liquid water may accumulate at the anode outlet, causing local hydrogen starvation, thereby reducing cell voltage and potentially causing degradation. To address this, the purge valve is periodically opened to supply the whole cell with fresh hydrogen (see Figure 1(a)). Fault tolerance and system weight/volume are crucial points for aviation, which might be improved with DEA on a system level due to the reduced number of components. However, the purge strategy – meaning the interval between the valve opening and the duration of the valve opening itself – is crucial for an efficient and low-degrading operation with DEA. Finding a suitable purge strategy is time- and resource-intensive, especially when taking degradation into account.

Objectives: In this study, the performance and degradation of a PEMFC with DEA are investigated. To increase power density and lifetime of the PEMFC, the purge strategy is optimized to increase efficiency and reduce degradation using simulation models.

Material and methods: An in-house-developed dynamic simulation model of a PEMFC stack with spatial discretization through the MEA and along-the-channel was used [1]. It was coupled with a degradation model for the cathode catalyst layer that describes platinum

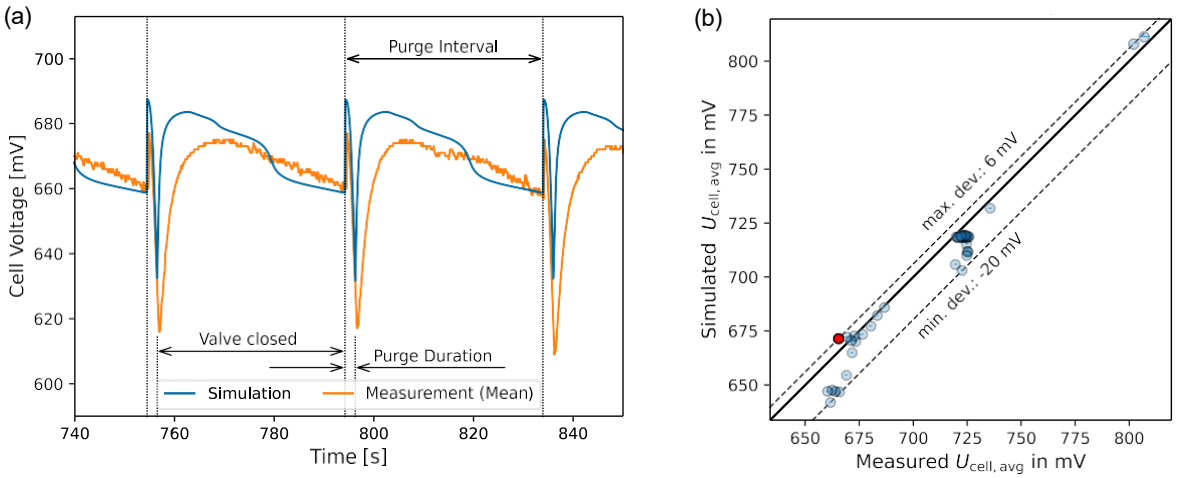


Figure 1: (a) Exemplary purge cycle with dead-ended anode operation. The purge valve is periodically opened for the purge duration. The purge interval is defined as the time span between the beginning of two purge events. The accumulation of nitrogen leads to reversible voltage losses. (b) Parity plot with simulated versus measured time-averaged unit cell voltage. Exemplary operating point shown in (a) is marked in red.

surface oxidation, platinum dissolution, platinum band formation, electrochemical Ostwald ripening and carbon corrosion [2,3]. The stack model was calibrated and validated using measurement data of a PEMFC stack operated with open-anode and DEA under varying operating conditions such as temperature, humidity, load, purge duration, and purge interval.

Results: Good agreement between simulation and measurement was found for both the time-averaged and dynamic cell voltage and hydrogen mass flow over a broad combination of operating conditions (see Figure 1). The locally resolved PEMFC model shows that under most operating conditions investigated, nitrogen accumulation at the anode outlet causes a decrease in cell voltage during DEA. The increase of interfacial electrode potential at the anode outlet and the opposite cathode electrode leads to accelerated degradation for higher purge intervals. The highest hydrogen utilization was found for high purge intervals and short purge durations, while the highest voltage was found for short purge intervals and moderate purge durations. The efficiency of the stack

$$\eta_{\mathrm{PEMFC}} = \frac{n_{\mathrm{cells}} U_{\mathrm{cell,avg}} I_{\mathrm{avg}}}{\dot{m}_{\mathrm{H_2,avg}} \, \mathrm{LHV}_{\mathrm{H_2}}},$$

was defined as the ratio of electric power produced by the PEMFC stack to the supplied energy with H_2 using its lower heating value $\mathrm{LHV}_{\mathrm{H_2}}$, the number of fuel cells in the stack n_{cells}, the time-averaged unit cell voltage $U_{\mathrm{cell,avg}}$, the time-averaged current I_{avg}, and the time-averaged hydrogen mass flow into the stack $\dot{m}_{\mathrm{H_2,avg}}$, respectively. For the investigated operating point, the efficiency is the highest for purge intervals below 30 s and purge durations of approximately 0.1 s (see Figure 2 (a)). Lower purge intervals were found to be less pronounced to catalyst degradation (see Figure 2(b)).

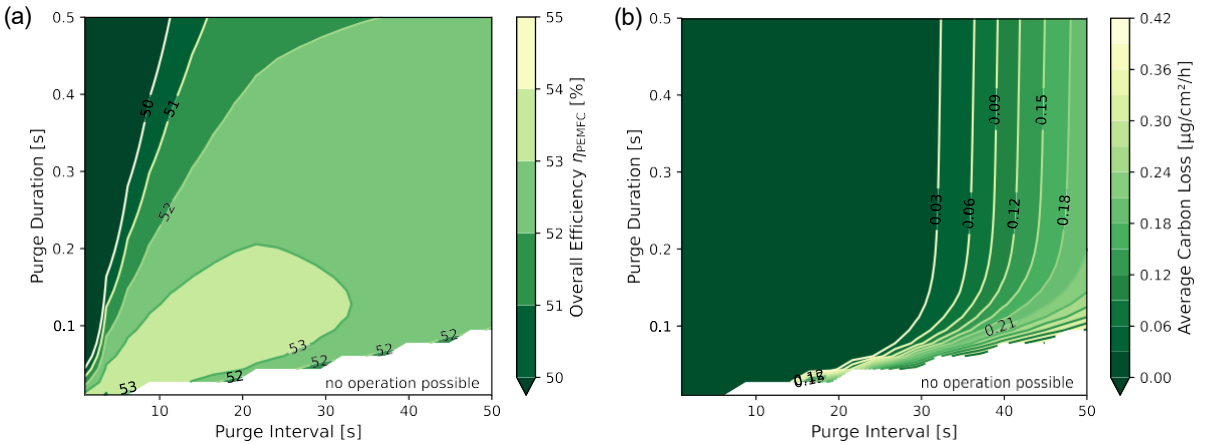


Figure 2: Simulation results with varying purge durations and intervals. The contour plot indicates: (a) Efficiency η_{PEMFC} that is equal to the ratio of the electric power produced by the PEMFC stack to the supplied energy with H_2 using the lower heating value of hydrogen. (b) Average carbon loss rate of the cathode catalyst layer.

Conclusions: The measurements of a PEMFC stack operated with DEA show the technical feasibility of this alternative anode gas supply concept. The PEMFC stack simulation model also demonstrated its predictive capability even at highly dynamic operating points. It was found that a PEMFC stack can be operated with high efficiency and low degradation when a suitable purge strategy with sufficiently low purge interval is applied.

Acknowledgment

We would like to acknowledge the funding by the *Bundesministerium für Wirtschaft und Klimaschutz* (BMWK, Federal Ministry for Economic Affairs and Climate Action) within the project SKAiB (Fkz. 20M2101I).

References

[1] Tang, Tian; Heinke, Steffen; Thüring, André; Tegethoff, Wilhelm; Köhler, Jürgen (2017): A spatially resolved fuel cell stack model with gas–liquid slip phenomena for cold start simulations. In: International Journal of Hydrogen Energy 42 (22), S. 15328–15346. DOI: 10.1016/j.ijhydene.2017.03.236.

[2] Trägner, Jakob; Heinke, Steffen; Tegethoff, Wilhelm; Köhler, Jürgen (2023): Numerically Efficient Degradation Model of Catalyst Layers in PEM Fuel Cells using Modelica. DOI: 10.3384/ecp204665. In: 15th International Modelica Conference, Aachen, Germany, October 9-11, 2023. Linköping Electronic Conference Proceedings, 204.

[3] Mittermeier, Thomas; Weiß, Alexandra; Hasché, Frédéric; Gasteiger, Hubert A. (2018): PEM Fuel Cell Start-Up/Shut-Down Losses vs Relative Humidity: The Impact of Water in the Electrode Layer on Carbon Corrosion. In: J. Electrochem. Soc. 165 (16), F1349-F1357. DOI: 10.1149/2.0931816jes.

European Fuel Cells and Hydrogen
PIERO LUNGHI CONFERENCE
September 17th–19th 2025
Capri / Italy

Development of composite sPEEK membranes containing zeolite imidazole frameworks as ionic cross-linkers for energy applications.

A. Carbone*[a], V. P. Kallupadi [a], R. D'Agostino [a], F. Librizzi [a], I. Gatto [a]

* corresponding author: Alessandra Carbone
[a] CNR - Istituto di Tecnologie Avanzate per l'Energia (ITAE)

[a]Task 31 Member, Advanced Fuel Cells Technology Collaboration Programme

Keywords: Proton exchange membrane, sulphonated PEEK, ZIF-8, proton conductivity, PEFC

Introduction:

Nowadays, electrochemical energy-conversion devices using green hydrogen, such as polymer electrolyte membrane fuel cells (PEMFCs) play a key role due to their high energy conversion efficiency. Perfluorinated-based polymer membranes are still considered as a benchmark but, recently, fluorine was inserted by EU in the Critical Raw Materials list, so significant efforts have been focused on alternative polymers. In this context, sulfonated polyetheretherketone (sPEEK) membranes can be considered as an alternative to conventional PFSA membranes due to high proton conductivity at high sulfonation degree, good mechanical properties and reduced hydrogen crossover and costs [1]. Properties of sPEEK membranes can be tailored controlling the sulfonation degree, even if at high sulfonation level the mechanical strength and membrane stability decrease due to the high swelling. In this work, the development of composite membranes with fillers able to interact with SO_3H groups of the polymer with reduced swelling, maintaining the proton conductivity and performance are studied.

Objectives

The objective of this work is to develop highly sulphonated composite membranes containing filler based on nitrogenous groups (ZIF-8) able to reduce swelling effect for application in PEFC and electrochemical H_2 purification. In particular, the effect of acid treatment on the physico-chemical properties of the membranes was investigated.

Material and methods:

Sulfonatedf PEEK with a degree of 65% was prepared following the method described elsewhere [2]. ZIOF-8 was selected as a filler for composite membranes development. Different ZIF-8 loadings ranging from 1 to 5 wt%, were investigated. Membranes were prepared by solubilizing the polymer in dimethylsulfoxide (DMSO) (10 wt%), adding the filler and casting with a Doctor-blade technique [2]. Post-casting acid treatments in HCl and H_2SO_4 were carried out. The membranes were characterized in terms of ion-exchange capacity (IEC), water uptake (Wup%), creep tests, XRD and proton conductivity.

Results:

The effect of ZIF-8 introduction on the properties of composite sPEEK membranes was evaluated in terms of loading and acid treatment. The physico-chemical data as a function of ZIF loading and different acid treatment are reported in table 1 and 2

Table 1 Physico-chemical properties after sulfuric acid treatment

MEMBRANE	Acid treatment	Loading ZIF8, wt %	IEC, meq/g	Wu 30°C	Wu 60°C	T_g, °C
sPEEK-recast	H_2SO_4	-	2.06	44	-	210
sPEEK -1%	H_2SO_4	1	2.13	38	58	211
sPEEK-3%	H_2SO_4	3	1.89	40	57	212
sPEEK-5%	H_2SO_4	5	2.1	33	57	204

The introduction of ZIF-8 in the polymer backbone produces a variation in the IEC and water uptake of composite membranes. In fact, there is a slight increase in the IEC respect the recast value, followed by a reduction, with the 3 wt % content, and again an increase up to the recast value. This behaviour corresponds to a reduction in water uptake, in particular at 60 °C, where the effect of the swelling is more pronounced. The recast membrane was solubilized at 60°C, due to the high sulfonation level of the polymer. This behaviour can be associated to the interaction of imidazolate group with sulfonic that stabilizes the polymer matrix. The glass transition was found to be very similar, and a slight reduction was detected for 5 wt % loading.

Table 2 Physico-chemical properties after hydrochloric acid treatment

MEMBRANE	Acid treatment	Loading ZIF8, wt %	IEC, meq/g	Wu 30°C	Wu 60°C	T_g, °C
sPEEK-recast	HCl	-	2.08	44	398	208
sPEEK-1%	HCl	1	2.16	40	56	214

sPEEK-3%	**HCl**	**3**	**1.99**	**37**	**55**	**210**
sPEEK-5%	**HCl**	**5**	**2.09**	**35**	**56**	**209**

Similar behaviour was found also for samples treated in HCl (table 2)meaning that the acid treatment does not strongly affect the physico-chemical properties of the membranes.
The proton conductivity was measured with fully humidified gas in the in-plane section of the membranes. In Figure 1 a and b are reported the comparison among the composite membranes with different acid treatments and pure recast sPEEK membrane.

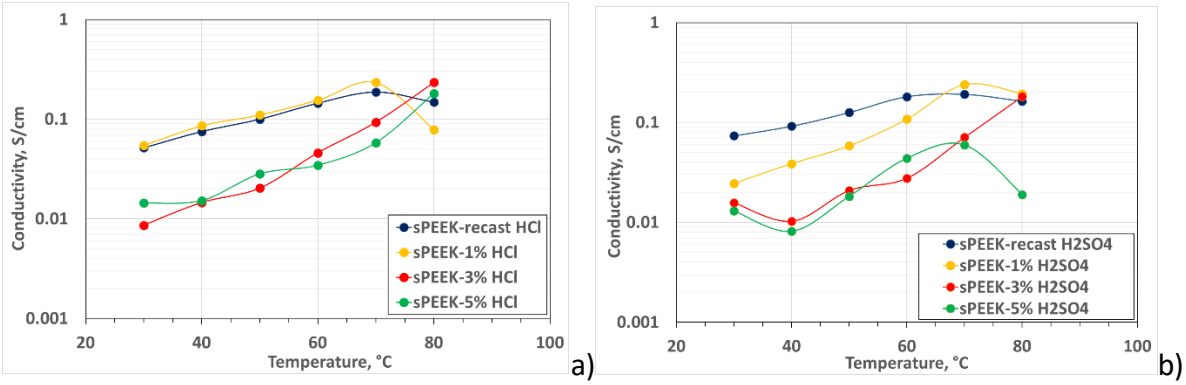


Figure 1 a) proton conductivity of HCl treated membranes; b) proton conductivity of H_2SO_4 treated membranes versus temperature.

The effect of acid treatment is more pronounced in proton conductivity measurements, in fact composite membranes treated with HCl show higher conductivity than membranes treated with H_2SO_4. A more stable behaviour is evident for HCl-based membranes with higher filler content.

Conclusions:

The introduction of imidazolate filler (ZIF-8) in sPEEK membranes produces a variation in the IEC and water uptake, in particular at high temperatures. This behaviour can be associated to the interaction of imidazolate groups with sulfonic that stabilizes the polymer matrix. The effect of acid treatment is more pronounced in proton conductivity measurements, where HCl-treated membranes show higher conductivity than membranes treated with H_2SO_4.

References

[1] R. Pedicini, M. Romagnoli, P. E. Santangelo, A Critical Review of Polymer Electrolyte Membrane Fuel Cell Systems for Automotive Applications: Components, Materials, and Comparative Assessment, Energies 2023, 16, 3111.
[2] A. Carbone, M. Castriciano, L. Monsù, I. Gatto, “Novel Polymeric Composite TPPS/s-PEEK Membranes for Low Relative Humidity PEFC”, Polymers, 12, 2020, 1431-1444

EFCH2 2025 European Fuel Cells and Hydrogen PIERO LUNGHI CONFERENCE
September 17th–19th 2025 Capri / Italy

Towards Zero-Emission Shipping: SOFC-ICE Hybrid Propulsion for Maritime Decarbonization

M. Gandiglio*[a], G. Peyrani[a], P. Marocco[a]

* corresponding author: marta.gandiglio@polito.it

[a] Department of Energy, Politecnico di Torino, C.so Duca degli Abruzzi 24, 10129 Torino, Italy

Keywords: Fuel Cells, Hybrid Systems, Maritime Decarbonization, SOFC-ICE Integration

Abstract

In the context of growing international maritime commerce and the associated increase in CO_2 emissions, the International Maritime Organisation (IMO) has set ambitious decarbonization targets for the sector: -20% GHG emissions by 2030, -70% by 2040, and net-zero by 2050. To support these goals, the present study investigates integrated hybrid propulsion systems that combine Solid Oxide Fuel Cells (SOFC) and Internal Combustion Engines (ICE), powered by Natural Gas (NG) or other low-carbon fuels (such as hydrogen and ammonia), as a potential solution for decarbonizing various vessel types. The work aims to demonstrate the feasibility of SOFC-ICE retrofitting, focusing on reducing fuel consumption and emissions during hoteling and manoeuvring operations.

Introduction:

The maritime sector currently accounts for 3% of global CO_2 emissions and is projected to increase in the coming decades due to growing international maritime commerce. This trend underscores the need for urgent decarbonization strategies in line with the IMO target of net-zero GHG emissions by 2050. When electrification with batteries is not feasible from an economic or technical perspective, decarbonization strategies involve the use of low-carbon fuels (such as ammonia, hydrogen, and methanol) and the implementation of more efficient propulsion systems, like fuel cells.

Previous studies have highlighted the potential fuel cells (both low- and high-temperature systems) to decarbonise the maritime sector while operating on various fuels [1]. Haseltalab *et al*. [2] specifically investigated the role of SOFCs for maritime applications, supported by batteries and gas engines, demonstrating the potential to reduce CO_2 emissions by up to 53%. An integrated SOFC and ICE layout was also explored in studies by Sapra *et al*. [3] and Chuahy *et al*. [4]. However, despite several modelling studies and conceptual designs, real-scale feasibility assessments tailored to specific vessel types are still limited. The PRIN PNRR SOFFHICE project (SOFC Hybridization with Internal Combustion Engine fuelled by Natural Gas for Maritime Applications) [5] addresses this gap by developing a comprehensive modelling

framework and assessing hybrid system performance aiming at generalising the results and provide guidelines for the application of the integrated SOFC-ICE concept in various scenarios.

Objectives:

This study evaluates the energy and environmental performance of three hybrid propulsion configurations applied to a reference short-distance ferry with natural gas as a reference fuel (views as transitioning fuel towards low-carbon ones). The objective is to optimize SOFC and ICE integration, leveraging SOFC efficiency for hotelling demands while enhancing ICE combustion with SOFC anode off-gases.

Material and methods:

A thermodynamic and electrochemical SOFC model was developed, integrating Balance of Plant components. ICE performance was modeled using operational data, focusing on efficiency-load relations. Three configurations were assessed (Figure 1):

1. ICE-only
2. Non-integrated SOFC-ICE system
3. Fully integrated SOFC-ICE with anode off-gas recirculation

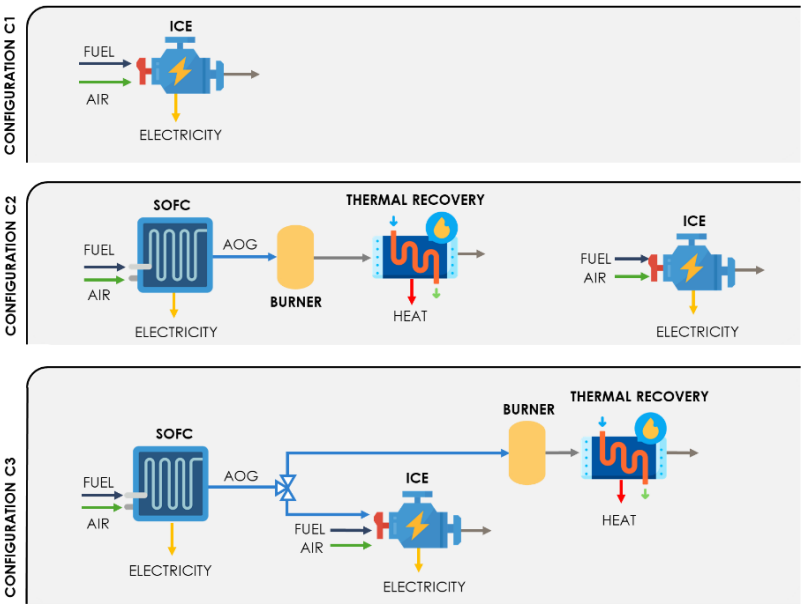


Figure 1. Configurations investigated in the study: C1 engine-only, C2 non-integrated SOFC-ICE layout, C3 integrated SOFC-ICE layout.

The hybrid system was tested under realistic daily load profiles, including port hoteling, cruising, and manoeuvring. The case study focused on a short ferry operating in Sardinia, connecting San Pietro Island. The power demand profile includes hoteling phases with a continuous load of 150 kW in port, peak propulsion demands up to 1,200 kW during navigation, and a reduced load of 75 kW during nighttime mooring. In the hybrid configuration, the SOFC covers the baseload, while the ICE manages additional power requirements during navigation and manoeuvring.

Results:

Hybridization with SOFC resulted in a 20% reduction in daily fuel consumption compared to the ICE-only baseline. This translates to a decrease in daily CO_2 emissions from approximately 880 kg (ICE-only) to 700 kg with the hybrid SOFC-ICE system.

During port operations, where hoteling loads dominate, the integrated SOFC-ICE system achieved emission reductions greater than 60%. Specifically, CO_2 emissions decreased from 90 kg/day (ICE-only) to 35 kg/day with the hybrid system; NO_x emissions dropped from 2.5 kg/day to 1.0 kg/day; and CO emissions were reduced from 1.8 kg/day to 0.6 kg/day. These results demonstrate the effectiveness of SOFC technology in reducing local pollutant emissions in coastal and harbour areas. Additionally, the integration of SOFC anode off-gases into the ICE improved engine efficiency by up to 7%, further enhancing the environmental benefits of the system.

Conclusions:

The SOFC-ICE hybrid system offers a viable solution for maritime decarbonization. It provides significant improvements in fuel efficiency and emission reductions, serving as a transitional step towards zero-emission shipping. The results of SOFFHICE support the feasibility of retrofitting existing vessels with hybrid systems and lay the groundwork for future low-carbon-fuelled applications. Further work will explore different vessel typologies, including ferries, offshore support vessels, and cruise ships, to assess the scalability and adaptability of the SOFC-ICE integration to diverse maritime applications.

Acknowledgment

This research is funded by the PRIN 2022 PNRR SOFFHICE project (CUP E53D23017220001), co-financed by the Italian Ministry of University and Research (MUR).

References

[1] L. van Biert *et al.*, A review of fuel cell systems for maritime applications, Journal of Power Sources, 2016, https://doi.org/10.1016/j.jpowsour.2016.07.007.

[2] A. Haseltalab *et al.*, Component sizing and energy management for SOFC-based ship power systems, Energy Conversion and Management, 2021, https://doi.org/10.1016/j.enconman.2021.114625.

[3] H. Sapra *et al.,* Purushothaman Vellayani, Hans Hopman, Integration of solid oxide fuel cell and internal combustion engine for maritime applications, Applied Energy, 2021 https://doi.org/10.1016/j.apenergy.2020.115854.

[4] F. D.F. Chuahy *et al.*, Solid oxide fuel cell and advanced combustion engine combined cycle: A pathway to 70% electrical efficiency, Applied Energy, 2019, https://doi.org/10.1016/j.apenergy.2018.10.132.

[5] SOFFHICE Project – SOFC Hybridization with Internal Combustion Engine fuelled by Natural Gas for Maritime Applications, PRIN PNRR 2022, CUP E53D23017220001.

EFCH2 2025 European Fuel Cells and Hydrogen PIERO LUNGHI CONFERENCE
September 17th–19th 2025 Capri / Italy

Comparison of different fuel mixture for direct ammonia fuel cell

Michele Rizzi*[a], Luca Pratticò [a], Oscar A. Bernabé [a], Dario Montinaro [b], Matteo Testi [a]

* Corresponding author: mirizzi@fbk.eu
[a] Hyres unit, Sustainable Energy centre, Bruno Kessler Foundation (FBK)
[b] SolydEra S.p.a.

Ammonia SOFC; SOFC; Ammonia fuel; Green Ammonia.

Introduction:

Nowadays, ammonia (NH_3) production accounts for approximately one-third of global hydrogen demand and is the primary market for hydrogen consumption. Additionally, it is also considered a promising carrier for green hydrogen [1]. As an energy carrier, ammonia could be utilized in high-temperature fuel cells, particularly solid oxide cells, for efficient power generation.

Objectives:

The objective of this testing activity is to analyze the performance of a Solid Oxide Fuel Cell (SOFC) when injected different fuels, such as hydrogen and ammonia, aiming for an overall efficiency of 70%. Ammonia can be exploited in two ways within the technological limits of an SOFC. The first approach involves cracking the ammonia before it enters the cells, a process that occurs spontaneously in environments with temperatures above 400°C. The second method consists of directly feeding the fuel cell with NH_3 [2].

Material and methods:

The Bruno Kessler Foundation (FBK) is leading a comprehensive test campaign aimed at mapping the performance of a six-cell short-stack Solid Oxide Fuel Cell, with each cell having an Electrochemical Surface Area (ECSA) of 80cm², the short stack is provided by SolydEra S.p.A. These activities are part of the CHE-JU AMON project, which focuses on designing and integrating components such as the fuel cell, ammonia burner, and heat exchanger to develop an engineered, ammonia-compliant Balance of Plant (BoP). The project aims to create an 8kW fuel cell system that will be tested for more than 3000 h in a relevant environment.
Zendrini et al. [3] compared the performance of cells provided by SolydEra under different fuel conditions: hydrogen, ammonia, and a stoichiometric blend of H_2 and N_2 in a 3:1 ratio, simulating complete ammonia cracking before the stack. The results showed that in the case of pure NH_3, performance exhibited a drop that limited the maximum power output to

approximately 0.29 W/cm² lower than the corresponding hydrogen flow, which reached 0.32 W/cm² at 760°C and a fuel utilization of 68%.

As part of the actual European project, several tests were performed on a similar SOFC short stack, also provided by SolydEra S.p.A. The performance of the short stack was analyzed under different operating temperatures, ranging from 690°C to 770°C, and with various input fuels. To assess stack degradation during power generation with ammonia as the inlet fuel, a medium-term test of 100 hours was conducted. Additionally, the test campaign included simulations of a potential future recycling of the outlet flow rate to increase the overall efficiency of the system by reusing unexploited fuel.

Results:

Since the Zendrini test campaign, an upgrade of the test rig has been performed. Thanks to this upgrade of the FBK test bench and the innovative technologies adopted by SolydEra on the short stack, it was possible to achieve better results. In particular, no significant differences between the utilization of ammonia and pure hydrogen have been observed, as depicted in Figure 2.

Moreover, even during the long-term durability test of 100 hours, when the short stack was directly fed with ammonia, no significant degradation was observed. However, from some recurrent benchmark tests performed at different stages of the test campaign, minor degradation was detected. This degradation could be attributed to the corrosive environment resulting from the persistent presence of pure ammonia, as well as the intrinsic degradation associated with prolonged SOFC operation. A significantly longer test duration would be required to confirm these trends. The degradation test results are shown in Figure 1.

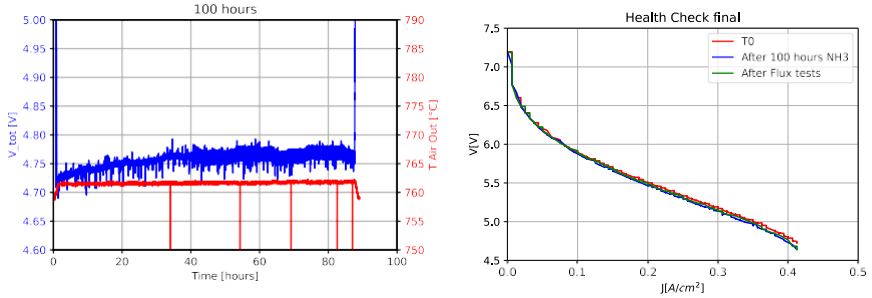


Figure 1: Degradation diagrams: a)100 hours long-term test, b) Benchmark curves alongside the test campaign.

Furthermore, the recirculation test allowed for an analysis of the short stack's performance under varying pressure conditions and different blend compositions. Initially, a blend of H_2-N_2 was injected, with a fuel utilization of 70% and a stoichiometric ratio of 3:1, to simulate complete ammonia cracking before the SOFC inlet. Then, to simulate recirculation, the N_2 flow rate was gradually increased up to a recirculation factor of 90% at a current of 32 A. As the recirculation rate increased, the short stack's performance decreased. However, the overall electrical efficiency of the system improved, rising from 30% to 67%. In an ideal case,

where external ammonia cracking does not consume any energy, the electrical efficiency could reach 76%. The results of the recirculation rate tests are depicted in Figure 2.

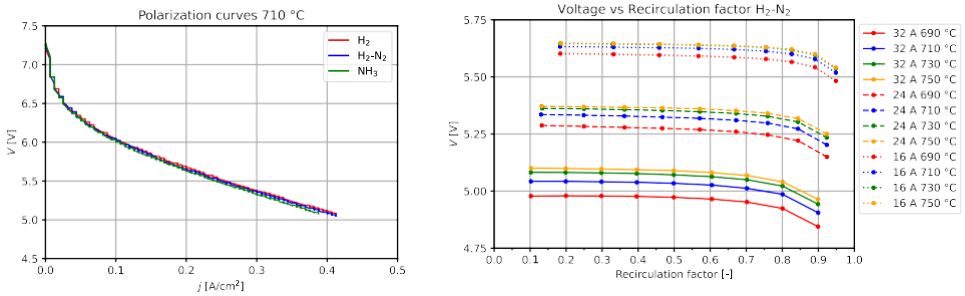


Figure 2: a) Polarization curve of the SOFC short stack performed at 710°C. b) Recirculation factor influences on the short stack performance.

Conclusions:

The results of the test campaign conducted at the Bruno Kessler Foundation are promising, demonstrating a low degradation rate of the short stack and strong overall system performance. In small-scale applications, the system successfully reaches and overtook the targeted 70% efficiency set by the AMON project when recirculation is active.

To better understand the feasibility of scaling up, a long-term 2000-hour test is planned, during which the stack will be fed with pure ammonia, along with additional tests.

Although the pilot demonstration will take place on a small scale, the AMON project aims to scale up the engineering to develop a system suitable for applications in ports, maritime environments, and autonomous power systems. AMON Project has an interdisciplinary consortium of 13 renowned partners coordinated by Fondazione Bruno Kessler, through the Center for Sustainable Energy.

Acknowledgment:

The project has received funding from the Clean Hydrogen Partnership under Grant Agreement n°101101521 — AMON. The Partnership receives support from the European Union's Horizon Europe research and innovation program, Hydrogen Europe, and Hydrogen Europe Research. Co-funded by the European Union. Views and opinions expressed are however those of the author(s) only and do not necessarily reflect those of the European Union or the Clean Hydrogen Partnership. Neither the European Union nor the granting authority can be held responsible for them.

References:

[1] IEA (2024), *Global Hydrogen Review 2024*, IEA, Paris https://www.iea.org/reports/global-hydrogen-review-2024, Licence: CC BY 4.0

[2] K. Trangwachirachai, K. Rouwenhorst, L. Lefferts, J. A. Faria Albanese, 'Recent progress on ammonia cracking technologies for scalable hydrogen production', Current Opinion in Green and Sustainable Chemistry, vol.49, 2024, 100945, ISSN 2452-2236, https://doi.org/10.1016/j.cogsc.2024.100945.

[3] M. Zendrini, M. Testi, M. Trini, P. Daniele, J. Van Herle, and L. Crema, 'Assessment of ammonia as energy carrier in the use with reversible solid oxide cells', International Journal of Hydrogen Energy, vol. 46, no. 58, pp. 30112–30123, Aug. 2021, doi: 10.1016/j.ijhydene.2021.06.139.

EFCH2 2025
European Fuel Cells and Hydrogen
PIERO LUNGHI CONFERENCE
September 17th–19th 2025
Capri / Italy

Enhancing Carbon Capture in the Steel Sector through MCFC and PEM Electrolyzer Integration

Riccardo Risso[a], Dario Bove*[,a], Barbara Bosio[a]

* corresponding author: dario.bove@unige.it

[a] Università degli studi di Genova – Dipartimento di ingegneria Civile, Chimica e Ambientale

Keywords: Carbon capture and storage (CCS), Molten carbonate fuel cells (MCFC), hydrogen, electrolysis

Abstract

The growing urgency of addressing climate change has intensified the search for efficient and sustainable carbon capture solutions. The integration of Carbon Capture and Storage (CCS) with renewable hydrogen technologies presents a promising avenue for this goal. This study investigates the synergistic coupling of a Proton Exchange Membrane (PEM) electrolyzer with a Molten Carbonate Fuel Cell (MCFC), exploring its potential for CO_2 capture and hydrogen utilization. Through modeling and simulation, energy balances, capture efficiency, and system scalability are assessed utilizing flue gases from a real industrial steel production plant. The findings highlight the benefits and technical challenges of this hybrid system, analyzing its practical feasibility for industrial decarbonization applications.

Introduction:

Carbon emissions are contributing to the growing concerns of climate change and are therefore undergoing strong scrutiny both from a legal but also from an ethical point of view. The steel and iron industry in particular are very impactful, as it accounts for around 11% of the global CO_2 emissions. Carbon Capture and Storage (CCS) technologies, combined with renewable hydrogen systems, present an innovative solution to counteract this issue. These technologies enable already existing plants, as will be demonstrated by the real case of a steel plants[1] analyzed in this work, to continue working without undergoing major changes or incurring in financial penalties.

Objectives:

This study aims to explore the synergetic integration of Carbon Capture and Storage (CCS) technologies with renewable hydrogen production by coupling a Proton Exchange Membrane (PEM) electrolyzer with a Molten Carbonate Fuel Cell (MCFC). The goal is to evaluate the above-mentioned system configuration by looking at a few important parameters being: carbon capture efficiency, that allows for evaluating how much the system is able to reduce

the greenhouse impact of the studied plant, energy consumption, to see the impact this system has on the overall plant balance, and industrial feasibility.

Material and methods:

The modeling approach involves a steady-state simulation of the coupled PEM-MCFC system using DWSIM.

The PEM cell has been simulated using data available in literature[2] in terms of consumption, whilst the MCFC cell has been simulated through the utilization of a 0D model[3]. The MCFC model includes charge and mass balances for the anode and cathode, thermal balances, and a detailed electrochemical evaluation[3].

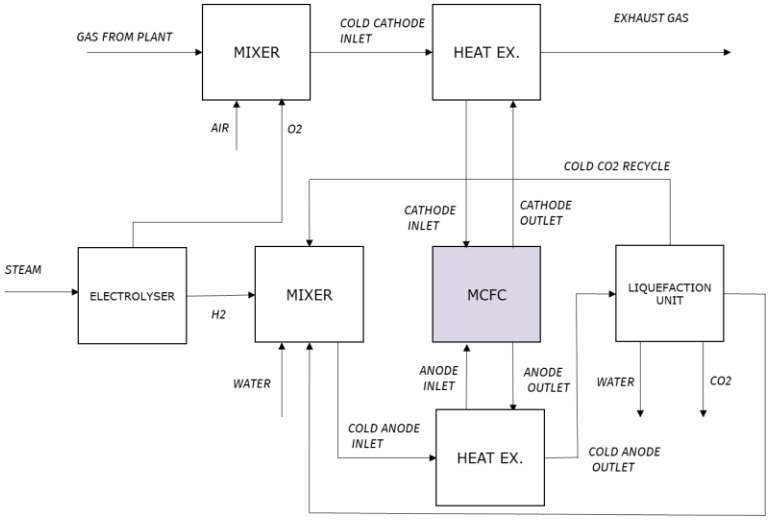


Figure 1 MCFC and PEM carbon capture system

The system has been designed as can be seen in Figure 1, where the flue gases are enriched with air and oxygen and then sent into the fuel cell after a preheating process with the exhaust gases. This is necessary as the flue gasses contain under 1% of oxygen, and the electrochemical reaction in the MCFC requires oxygen to take place. On the anodic side, the hydrogen from the electrolyzer is enriched with small percentages of CO_2 and H_2O to avoid carbon deposition and carbonate evaporation from occurring. Then the CO_2 is separated from the generated water of electrochemical reactions and the unreacted hydrogen in a cryogenic liquefaction unit.

Results:

The simulation provides several noteworthy findings that can show some of the weaknesses and advantages of the synergistic coupling. Firstly, the amount of hydrogen required for the capture requires a huge power for the electrolyzers (around 16 MW). Through an energy balance, it is possible to see that the MCFC is not able to sustain the consumption by itself, covering only 33% of the overall consumption, and the rest being required from alternate sources.

Furthermore, the oxygen that is being produced is insufficient to cover the need required to reach a 10% oxygen cathodic feed, that can be considered sufficient to guarantee a good cell performance. This means that a stream of air is required to increase the concentration of O_2 further. This also implies an increase in volumes, as there is a high percentage of inert nitrogen inside the air stream. The maximum achievable capture rate is approximately 85%, with an energy to capture rate of 1.7 $MWh_{required}/t_{CO2captured}$ (which is in line with literature data for CCS processes[4]) and a cell dimension to capture rate of 1.07 $MWh_{produced}/t_{CO2captured}$.

In terms of system integration, the CCS module does not require any fossil fuel and is able to partially cover its own water requirements needed for the electrolyzer. Considering this, it only requires 235 kg/h of water to be fed to the system. The output on the other hand is around 6131 kg/h of liquefied CO_2, with a purity of around 97%, and the combustion gases with a CO_2 content of 0.9%.

The heat balance of the system, on the other hand, indicates the availability of a heat flux of around 4200 kW (373 °C to 30°C) from the CCS module towards the rest of the plant. This thermal flux originates from the condensation of the steam in the anodic output gases.

Conclusions:

The primary challenge of the proposed system lies in the relatively low energy efficiency currently achievable with PEM electrolyzers. Significant advancements in this technology are essential to enhance the overall performance and viability of the integrated system. Closely related to this limitation is the considerable space requirement of the setup, which may pose constraints for deployment in space-limited industrial environments.

Despite these challenges, the system demonstrates strong potential for carbon capture applications. Its reliance on renewable hydrogen, rather than fossil fuels, and its energy-to-capture ratio—comparable to conventional amine-based systems—highlight its feasibility. Ongoing improvements in electrolyzer technology are expected to further increase the system's efficiency, making it a competitive solution for industrial decarbonization future.

References

1. Hasanbeigi A. Steel Climate Impact. 2022;(April). https://www.globalefficiencyintel.com
2. nel. PSM series electrolyser. Accessed March 31, 2025. https://nelhydrogen.com/product/psm-series-electrolyser/
3. Audasso E, Bosio B, Bove D, et al. New, Dual-Anion Mechanism for Molten Carbonate Fuel Cells Working as Carbon Capture Devices. *J Electrochem Soc*. 2020;167(8):084504. doi:10.1149/1945-7111/ab8979
4. Yuan B, Zhan G, Chen Z, et al. Intrinsic insight of energy-efficiency optimization for CO2 capture by amine-based solvent: effect of mass transfer and solvent regeneration. *Int J Greenh Gas Control*. 2022;118(January):103673. doi:10.1016/j.ijggc.2022.103673

EFCH2 2025
European Fuel Cells and Hydrogen
PIERO LUNGHI CONFERENCE
September 17th–19th 2025
Capri / Italy

Innovative approaches to MCFC component development for industrial-scale implementation

Dario Bove[a,*], Riccardo Risso[a], Lucia Cardona[a], Kosar Hasanpour[a], Martino Prati[a], Fiammetta Bianchi[a], Barbara Bosio[a]

* corresponding author: dario.bove@unige.it

[a] Università degli studi di Genova – Dipartimento di ingegneria Civile, Chimica e Ambientale

Keywords: Carbon capture and storage (CCS), Molten carbonate fuel cells (MCFC), hydrogen, scalability

Abstract

Molten Carbonate Fuel Cells (MCFCs) are a promising technology for carbon capture systems, particularly in retrofit applications. However, the industrial deployment of MCFCs faces challenges related to component durability, performance optimization, and cost-effectiveness. This work explores innovative strategies for enhancing MCFC components to enable scalable and reliable operation. Advances in material selection for electrodes and matrix are discussed, with a focus on improving microstructure and electrochemical performance. Additionally, manufacturing techniques and system integration approaches are preliminarily evaluated to facilitate industrial-scale adoption. By addressing these critical factors, this work study contributes to the broader implementation of MCFC technology in sustainable energy systems.

Introduction

The global energy transition is accelerating, driven by the urgent need to reduce greenhouse gas emissions and achieve carbon neutrality. International policies, such as the European Green Deal [1] are promoting large-scale adoption of low-carbon technologies, while countries worldwide are investing in carbon capture, utilization, and storage (CCUS) solutions [2]. Among these, Molten Carbonate Fuel Cells (MCFCs) have emerged as a promising technology due to their high efficiency and fuel flexibility, making them particularly attractive for industrial applications and large-scale power generation [3].

Currently, MCFCs are primarily optimized for power production, with applications in distributed energy systems and combined heat and power (CHP) solutions [4]. However, their intrinsic capability to capture CO_2 during operation has sparked growing interest in their potential role within CCUS strategies. Unlike conventional carbon capture systems, which require additional energy inputs, MCFCs can integrate CO_2 separation directly into their electrochemical process, theoretically enhancing overall system efficiency [5]. Despite this advantage, the industrial implementation of MCFCs for carbon capture remains limited due to challenges in component durability, process optimization, and large-scale feasibility.

Objectives

This study explores innovative approaches to optimize MCFC components for scalable carbon capture applications, addressing the material and design modifications required to shift their primary function from power generation to efficient CO_2 separation. Advances in electrode and matrix materials, microstructure engineering, and manufacturing techniques will be discussed, providing a pathway toward the industrial deployment of MCFCs as a viable CCUS technology.

Material and methods:

The state of the art primarily involves the use of ceramic matrices in γ-LiAlO2 or α-LiAlO2, obtained through tape-casting, which are employed to provide effective support for the electrolyte and ensure safe separation of the electrode gases. However, these matrices are somewhat fragile, increasing the risk of gas cross-over phenomena. This study aims to enhance the mechanical strength of the matrices by optimizing the distribution and size of the pores, which must still ensure a high capillary force to effectively retain the liquid electrolyte. To achieve this, the diameter of the LiAlO2 particles, the choice of organic binders, and the burn-out procedure are optimized.

From the electrode perspective, the study focused on optimizing the performance of the electrodes by improving their microstructural properties to facilitate gas diffusion and reaction. Various sintering times and atmospheres were investigated to identify the best conditions. Furthermore, to optimize large-scale production, alternative electrode manufacturing processes, such as electrochemical deposition and spray methods, were preliminarily studied.

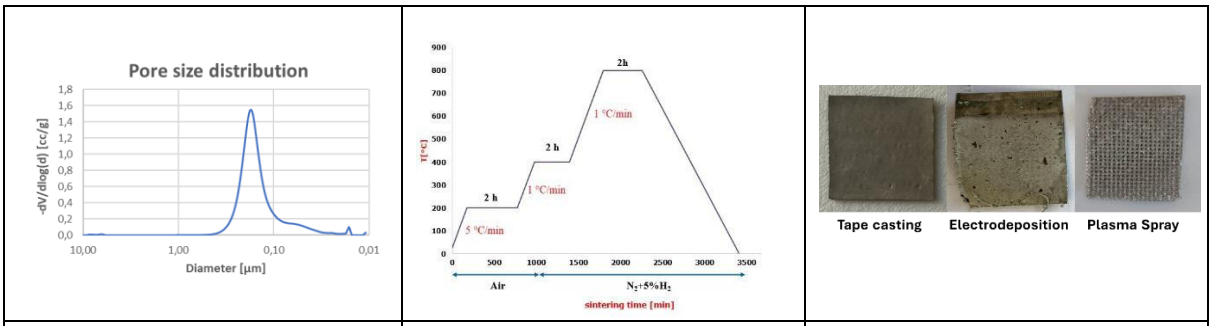
Results:

For the matrix, the mixing times and component quantities were optimized (as shown in Table 1) to achieve a homogeneous pore distribution in accordance with the optimal characteristics found in the literature [6], as shown in Figure 1a.

Component	Mass Percentages
Raw powder	36%
Solvent	47%
Binder	9%
Defoamer	0,6%
Dispersant	1,4%
Plasticizer	6%

Table 1. Mass percentages of the matrix components

For the electrodes, the various sintering stages were optimized by adjusting the times and determining the correct gas composition for sintering, as shown in Figure 1b. Additionally, preliminary analyses were conducted to compare different scalable electrode production technologies at an industrial level with the traditional tape-casting method, as illustrated in Figure 1c.



(a)	(b)	(c)

Figure 1. a) Pore size distribution of the matrix; b) Sintering procedure for electrodes; c) electrode production technologies

Conclusions:

In conclusion, this work has preliminarily explored strategies for optimizing Molten Carbonate Fuel Cells (MCFCs), focusing on enhancing component durability and electrochemical performance. The approaches developed for material selection, electrode and matrix optimization, and manufacturing techniques offer promising steps toward improving the scalability of MCFC technology, potentially supporting its future industrial adoption.

References

[1] European Commission, The European green deal, https://commission.europa.eu/strategy-and-policy/priorities-2019-2024/european-green-deal_en, 2020 (accessed 02 March 2025)
[2] International Energy Agency, Net Zero by 2050: A roadmap for the global energy sector, https://www.iea.org/reports/net-zero-by-2050, 2021 (accessed 02 March 2025)
[3] L. Caprile, B. Passalacqua, A. Torazza, Carbon capture: Energy wasting technologies or the MCFCs challenge?, International Journal of Hydrogen Energy 36 (2011) 10269-10277 https://doi.org/10.1016/j.ijhydene.2010.10.028
[4] R. Rashidi, P. Berg, I. Dincer, Performance investigation of a combined MCFC system, International Journal of Hydrogen Energy 34 (2009) 4395-4405 https://doi.org/10.1016/j.ijhydene.2009.03.038
[5] D. Bove, E. Audasso, T. Barckholtz, G. Kiss, J. Rosen, B. Bosio, Process analysis of molten carbonate fuel cells in carbon capture applications, International Journal of Hydrogen Energy 46 (2021) 15032–15045. https://doi.org/10.1016/j.ijhydene.2020.08.020
[6] A. A. Sheikh, F. R. Bianchi, D. Bove, B. Bosio, A review on MCFC matrix: State-of-the-art, degradation mechanisms and technological improvements, Heliyon 10 (2024) e25847. https://doi.org/10.1016/j.heliyon.2024.e25847

EFCH2 2025
European Fuel Cells and Hydrogen
PIERO LUNGHI CONFERENCE
September 17th–19th 2025
Capri / Italy

Performance analysis of solid oxide fuel cell fed with simulated gas produced by biomass gasification process

M. J. Escudero*, E. Ruiz, E. Millán
Department of Energy
CIEMAT, Av. Complutense 40, 28040 Madrid, Spain;

Keywords: Biomass, degradation, electrochemical characterization, solid oxide fuel cell

Abstract

In this study, a Ni/YSZ anode supported solid oxide fuel cell (SOFC) has been operated at 750 °C in H_2 and in a syngas composition (CH_4/CO/CO_2/H_2=10/15/15/60) representative of a biomass steam gasification process. The electrochemical behaviour of the cell was studied under three load demands (200, 500 and 600 mA/cm^2) during 2 h each of them, by means of load demand, IV curves, impedance spectroscopy (IS) and Distribution Relaxation Time (DRT). Then, a long-term test was conducted in syngas under 500 mA/cm^2 during 1050 h. A performance loss was detected with a degradation rate of ~ 0.049 mV/h caused by an increase in polarization resistance, mainly associated to the process of gas diffusion in the anode.

Introduction: Biomass can be a renewable energy source if used sustainably. It has great energy potential because it is found around the world. When biomass is produced and used at the same rate, it does not add to CO_2 emissions in the atmosphere. On the other hand, solid oxide fuel cell (SOFC) is a promising technology for generating energy from biomass, since it shows advantages such as fuel flexibility, quiet operation, low or zero emission and high efficiency. The integration of biomass gasification process with SOFC could be a potential way to use carbonaceous wastes and/or bioproducts as feedstock [1]. The produced syngas, mainly H_2, CH_4, CO, and CO_2, can be used as fuel for SOFCs, enhancing the energy value of biomass. However, nickel/yttrium-stabilized zirconia (Ni/YSZ) cermet is the most commonly used SOFC anode material due to its catalytic effect on the electrochemical oxidation of fuel, but Ni is also an excellent catalyst for carbon deposition reactions. The deposited carbon can cause deactivation of Ni catalyst leading to a degradation in the cell performance. Therefore, it is important to understand the electrochemical behaviour of the cell under simulated syngas in order to the implementation of the gasification-SOFC system.

Objectives: In this present work, we have investigated the durability of a Ni-YSZ anode supported cell fed with a syngas simulating that from a biomass steam gasification process at 750 °C.

Experimental: Experiments were conducted using an anode-supported cell (Kceracell Co) that consists of NiO-YSZ cermet as anode, YSZ as electrolyte, Gd-doped ceria as barrier layer and LSCF ($(La_{0.6}Sr_{0.4})_{0.97}Co_{0.2}Fe_{0.8}O_{3-\delta}$) as cathode with an effective area about 0.5 cm^2. First, the button cell was tested in H_2 (50 ml/min) as fuel and in static air as oxidant. Then, the anode fuel was replaced by a simulated gas mixture ($CH_4/CO/CO_2/H_2$ =10/15/15/60) resembling the typical composition of syngas from biomass steam gasification [2]. The electrochemical performance of the cell was evaluated in H_2 and syngas under open circuit voltage (OCV) and under load demand of 200, 500 and 600 mA/cm^2 for 2 h each. IV curves and impedance spectra were recorded before and after load demands. After that, stability test was carried out under 500 mA/cm^2 for 1050 h. The IV curves and impedance spectra were measured intermittently. The IV curves were obtained using linear sweep voltammetry at a scan rate of 10 mV/s and the impedance spectra were recorded under OCV in a frequency range from 50 kHz to 50 mHz with an AC= 5 mA. The impedance data were analysed by DRT using the DRtools program developed by Ciucci's group [3].

Results: In the electrochemical performance tests in H_2, the cell reached a value of OCV of 1.08 V that is very close to the theoretical value estimated by the Nernst equation, indicating no gas leakage. Under load demand, the cell behaviour was stable achieving values of power density of 194, 437 and 507 mW/cm^2 at 200, 500 and 600 mA/cm^2, respectively. When the cell was fed with syngas, the OCV value decreases to 1.02 V, and the power densities values decreased up to 160, 305 and 336 mW/cm^2. Similar IV curves and impedance spectra were recorded before and after load demand for both gas compositions. The maximum power density measured were 647 and 385 mW/cm^2 in H_2 and syngas respectively. Impedance spectra revealed that the ohmic resistance (R_Ω) remained practically constant around 0.15 Ωcm^2, while the value of polarization resistance (R_p) increased from 0.79 Ωcm^2 in H_2 to 1.03 Ωcm^2 in syngas. Then, the decrease in cell power density under syngas is associated to the increase in R_p. In order to understand the electrode reaction processes, the impedance data have been analysed by the DRT method. Five peaks, denoted as P1 to P5, can be distinguished from high to low frequencies. Each peak in the DRT curves represents at least a process and the area enclosed by each peak corresponds to its contribution to polarization resistance. Based on bibliography [4,5] and on previous results [6], the corresponding relationship between characteristic peaks and electrode processes can be summarised as follows: P1 to charge transfer and ionic conduction processes at the anode, P2 to oxygen surface exchange and oxide ion diffusion in the bulk of the cathode, P3 to gas diffusion process in the anode substrate for anode-supported cells, P4 to gas phase diffusion process in the cathode and P5 to gas conversion process at the anode side. In H_2, the processes associated to the P2 are dominant in R_p. In syngas, all peaks showed higher areas and a shift towards high frequency, except P5. To note that the P3 area suffered the higher increase, being the main responsible

in the increase of R_p. So, the process of gas diffusion in the anode is hindered in syngas reducing the cell performance.

Then, the long-term stability of the cell was studied in syngas under 500 mA/cm^2 during 1055 h at 750 °C. Initially, the cell reached a power density around 305 mW/cm^2, which kept stable during 250 h. After that, the cell performance started to decrease up to 282 mW/cm^2 (~7.5 %) with a degradation rate of ~ 0.049 mV/h. The IV curves revealed the highest values of maximum power density (384-381 mW/cm^2) during the first 250 h of operation, after that the values decreased being the lowest one of 320 mW/cm^2 obtained at the end of testing. The impedance spectra analysis showed an increase in R_p (~18.8 %) and no significant variations were detected in R_Ω. DRT analysis showed higher area of the P3 peak, indicating that it is the main responsible in the increase of R_p and, so, to the performance degradation, probably caused by the carbon deposition.

Conclusions: The electrochemical behaviour of the of a Ni/YSZ anode supported cell was evaluated under three load demands of 200, 500 and 600 mA/cm^2 during 2 h each, in H_2 and syngas (10 % CH_4, 15% CO, 15% CO_2 and 60 %) at 750 °C. The cell performance increased with the load demand reaching the highest values of maximum power density of 507 and 336 mW/cm^2 in H_2 and syngas, respectively. Impedance data revealed an increase in polarization resistance in syngas due to the processes of gas diffusion in the anode are hindered, which led to a reduction of the cell performance. A long-term test was carried out under 500 mA/cm^2 during 1050 h in syngas at 750 °C and revealed a cell performance stable during the first 250 h, after that a performance loss was detected with a degradation rate of 0.049mV/h caused by a higher resistance to gas diffusion in the anode

Acknowledgment:

Funding by the Ministry of Science, Innovation and Universities of Spain (ECO-H2 project: PID2023-149998NB-I00), and by the Ministry of Ecological Transition and Demographic Challenge with NextGeneration EU funds (Val2H2 project; Ref: R-H2CVAL4-C1- 2022-0096) is acknowledged.

References

[1] Z.U. Din, Z.A. Zainal, Renewable Sustainable Energy Rev. 53 (2016) 1356-1376.
[2] M. Faizan, H.Song, J. Cleaner Prod 408 (2023) 137224.
[3] T.H. Wan, M. Saccoccio, C. Chen, F. Ciucci, Electrochim. Acta 184 (2015) 483-499.
[4] H. Sumi, H. Shimada, Y. Yamaguchi et. al., Electrochim. Acta, 339 (2020) 35913.
[5] P. Caliandro, A. Nakajo, S. Diethelma, J. Van herle, J. Power Sources, 436 (2019) 226838.
[6] M.J. Escudero, C.A. Maffiotte, J.L. Serrano, Electrochim. Acta 427 (2023) 140852.

European Fuel Cells and Hydrogen
PIERO LUNGHI CONFERENCE
September 17th–19th 2025
Capri / Italy

Sub-Optimal Control Strategy for Hydrogen Fuel Cell Heavy-Duty Trucks: A Fuzzy Logic Approach

Isa Banagar *[a], Edoardo Cennamo [b], Lorenzo Bartolucci [b], Meisam Babaei [c], Amin Andwari [a], Juho Könnö [a]

* Corresponding author: Isa Banagar

[a] Machine and Vehicle Design (MVD), Materials and Mechanical Engineering, Faculty of Technology, University of Oulu, 90014 Oulu, Finland.
[b] Tor Vergata University of Rome, Department of Industrial Engineering, Via Del Politecnico 1, 00133, Rome, Italy.
[c] School of Mechanical Engineering, University of Leeds, Leeds LS2 9JT, UK.

Keywords: Heavy-duty vehicle electrification, Fuel cell, Optimized energy management strategy, Fuzzy logic control

Abstract:

Fuel cells offer an efficient solution for heavy-duty powertrain electrification, but optimized energy management is crucial to improve overall efficiency. System behaviour varies across driving conditions, requiring an optimization framework to enhance efficiency. This study models a fuel cell hybrid electric truck to evaluate energy utilization and drivability. Introduction: Fuel Cell (FC) powertrains demonstrated significant potential to reduce carbon emissions in the automotive sector (Bartolucci et al., 2023). Fuel cell Hybrid Electric Vehicles (FCHEVs) combine fuel cells and batteries, leveraging their complementary roles to allow the fuel cell to run in its high-efficiency region while the battery handles transient power demands and captures regenerative energy, thereby improving overall system efficiency (Ragab et al, 2023). A critical aspect to exploit these synergies is the Energy Management Strategy (EMS), which is crucial for optimizing energy flows, minimizing hydrogen consumption, and maximizing the lifespan of components (Bartolucci et al., 2024).

Objectives: The objective of the present work is the analysis of the performance of a heavy-duty truck, with the main aim feasibility study of a fuel cell hybrid electric truck. For the analysis, a sub-optimal control strategy is proposed, aiming at minimizing hydrogen consumption while ensuring safe components operation. By exploiting the global optimal results with a Dynamic Programming (DP) algorithm on a standard driving cycle in different environmental situations, a Fuzzy Logic controller is trained to enable the real-time applicability of the strategy.

Material and methods: The vehicle module of Cruise M has been used for vehicle longitudinal dynamics calculations to analyze dynamic forces, including road inclination, rolling resistance, acceleration, deceleration, aerodynamic forces, drivetrain loss, and dynamic wheel loads. In this study, the research truck of the Machine and Vehicle Design (MVD) research group (Banagar et al., 2024) has been considered. To achieve better accuracy, resistance forces are simulated for multiple scenarios with the same deriving cycle, emulating harsh environmental conditions. The powertrain architecture consists of a high-voltage bus supplying energy from three fuel cell stacks and two battery packs to an electric motor (E-Motor) (Figure 1). The

overall driveline efficiency has been set at 83% in line with literature-reported values for the baseline vehicle (Banagar et al., 2024)(Salek et al., 2023). This comprehensive modeling approach enables a detailed analysis of energy efficiency, driving resistance forces, and overall vehicle performance in hydrogen-electric truck applications.

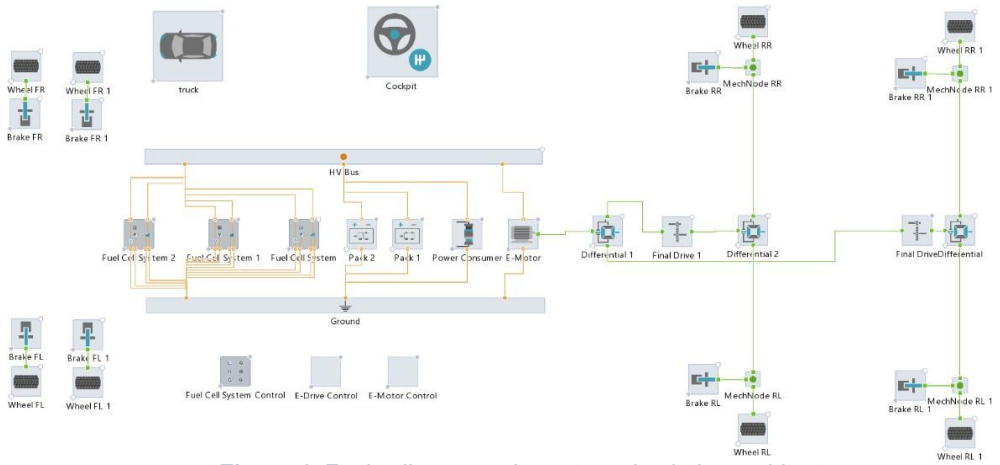


Figure 1. *Fuel cell powertrain system simulation architecture*

Concerning the EMS, which is in charge of distributing the power between the energy sources, a rule-based optimized approach has been implemented. Starting from a simplified model of the powertrain, a global optimization algorithm (namely, DP) has been used for determining the optimal FC power profile and the resulting battery State Of Charge (SOC). The input of the DP algorithm has been the motor request profile, obtained through a simulation on a typical truck driving cycle, and the target is the minimization of the hydrogen consumption over the whole mission. Moreover, the constraint of $SOC_{in} = SOC_{end}$ (70%) has been imposed on the algorithm to achieve a charge-sustaining operation mode for the battery. Subsequently, a simpler Fuzzy Logic controller has been trained through a Genetic Algorithm to emulate the optimal results on the same driving cycle. This phase aims to obtain a real-time controller, thus overcoming the offline characteristic nature of the DP. Further details on the methodology can be obtained in (Bartolucci et al., 2024).

Results: Figure 2 illustrates the effect of control of SOC as the target value. The simplified DP is designed to sustain the battery SOC under two load conditions, simulating differences in the vehicle's gross weight. The SOC profile can be divided into two stretches: in the first part, a recharge phase occurs. The extra energy is subsequently used in the second stretch of the mission, where the truck load increases significantly. This enables achieving a final SOC similar to the initial one (70 %), while operating the FC system in a safe manner. Moreover, it is worth noting that the trained Fuzzy Logic controller can accurately replicate the optimal DP results. However, implementing the trained Fuzzy Logic controller in the forward kinematic simulation, including the dynamic response of other vehicle control parts, a deviation of 7% SOC at the end of the high load and 0.5% in low load mission will occur. The implementation

of the rule-based optimized controller enables operating the powertrain in a sub-optimal manner, while granting real-time applicability. The solution can be improved further by including more data in the fuzzy training phase, such as the remaining distance to the destination.

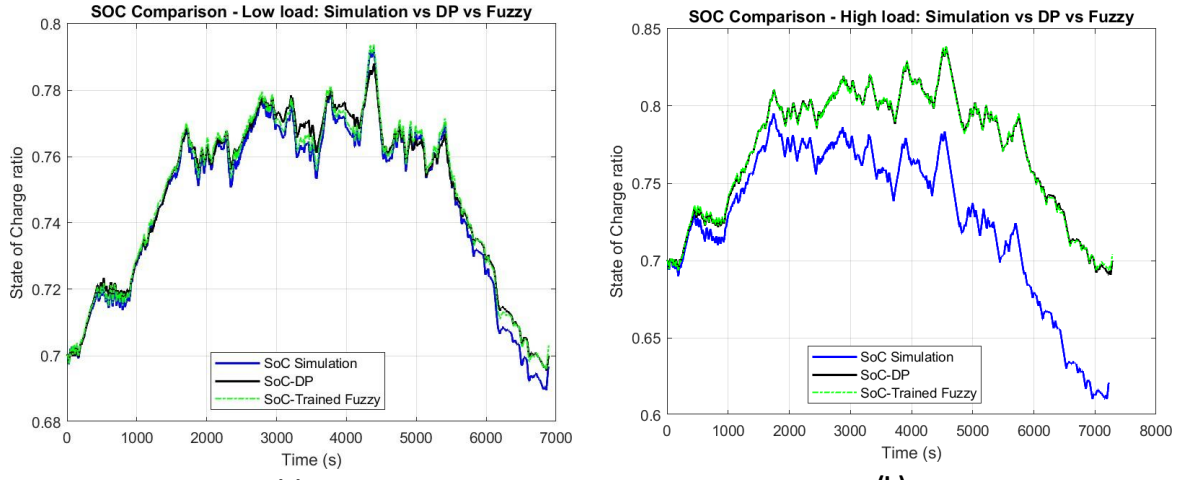


Figure 2. *DP, trained Fuzzy Logic and simulation SoC comparison. (a) High load; (b) Low load*

Conclusions: A reliable and accurate model of a fuel cell hybrid electric truck has been developed and used as a simulation platform for energy management strategies testing. The DP approach has demonstrated strong potential in operating the powertrain in a sub-optimal manner, properly exploiting the coexistence of two energy sources to fulfil the entire mission. Moreover, the real-time applicability of the trained controller enables overcoming the computational issues of the optimization algorithm, thus paving the way for the decarbonization of the heavy-duty transport sector. Furthermore, a more detailed powertrain model will be implemented into the DP algorithm, thus granting a more reactive controller to the varying operating condition, such as the driving cycle and the truck payload.

References

Banagar, I., Huhtala, T., Könnö, J., & Andwari, A. M. (2024, May 17). *Configurable Design Approach for Heavy-duty Vehicle Powertrain Design*. https://doi.org/10.3217/xh0h5-xg862

Bartolucci, L., Cennamo, E., Cordiner, S., Donnini, M., Grattarola, F., & Mulone, V. (2024, April 9). Fuel Cell Hybrid Electric Vehicle: An Integrated Approach for Sub-Optimal Controller in Real-Time Application. *SAE Technical Papers*. https://doi.org/10.4271/2024-01-2187

Bartolucci, L., Cennamo, E., Cordiner, S., Mulone, V., Pasqualini, F., & Boot, M. A. (2023). Digital twin of a hydrogen Fuel Cell Hybrid Electric Vehicle: Effect of the control strategy on energy efficiency. *International Journal of Hydrogen Energy*, *48*(54), 20971–20985. https://doi.org/10.1016/j.ijhydene.2022.11.283

Ragab, A., Marei, M. I., & Mokhtar, M. (2023). Comprehensive Study of Fuel Cell Hybrid Electric Vehicles: Classification, Topologies, and Control System Comparisons. *Applied Sciences*, *13*(24), 13057. https://doi.org/10.3390/app13241305

Salek, F., Abouelkhair, E., Babaie, M., Cunliffe, F., & Nock, W. (2023, April 11). Multi-Objective Optimization of the Fuel Cell Hybrid Electric Powertrain for a Class 8 Heavy-Duty Truck. *SAE Technical Papers*. https://doi.org/10.4271/2023-01-0473

European Fuel Cells and Hydrogen
PIERO LUNGHI CONFERENCE
September 17th–19th 2025
Capri / Italy

Development and Optimization of a Solid Oxide Fuel Cell System for Combined Heat and Power: The SO-FREE Project

Giacomo Tamburrano*[1], Juan Diego Palacios Aparicio[1], Enrico Bocci[1], Juan Francesco Marino[2], Andrea Monforti[3], Davide Pumiglia[3], Massimiliano Della Pietra[3], Viviana Cigolotti[3], Francesca Santoni[3], Michal Wierzbicki[4], Piotr Ostrowski[4], Usman Mushtaq[5], Saeed Rehman[5], Valtteri Vedensola[5], Ali Shahanaghi[5], Stefan Megel[6], Jens Schnetter[6], Carlo Tregambe[7], Stephen Mcphail[8]

* corresponding author: Giacomo Tamburrano

[1]Università degli Studi Gugliemo Marconi, Italy
[2]Università degli Studi di Napoli Parthenope, Italy
[3]ENEA Italian National Agency for New Technologies, Energy and Sustainable Economic Development, Casaccia Research Centre, Italy
[4]IEN Institute of Power Engineering, Poland
[5]Elcogen, Estonia
[6]Fraunhofer-Institut für Keramische Technologien und Systeme IKTS, Germany
[7]ICI Powering Evolution, Italy
[8]KIWA, Netherlands

Solid Oxide Fuel Cell, Combined Heat and Power, Energy Efficiency, Fuel Flexibility

Objectives:

Within the framework of the SOCIETAL CHALLENGES - Secure, Clean, and Efficient Energy objective under the European Horizon 2020 research and innovation funding program, the SO-FREE project has developed a fully future-ready Solid Oxide Fuel Cell (SOFC) system layout for high-efficiency Combined Heat and Power (CHP) generation. The system is designed to combine low emissions, fuel flexibility, modular power production and integrated heat recovery, while maintaining a simple and cost-effective architecture. A distinctive feature of the system is the interchangeability of two SOFC stack technologies operating at different temperatures, which enhances adaptability and improves overall system integration.

Material and methods

The development process began with a comparative performance analysis of two short SOFC stacks, tested under identical configurations by IEN and ENEA using three fuel compositions: 100% H_2, 100% CH_4, and a 67% H_2–33% CH_4 mixture. The results showed less than 2% variation between test benches, validating the experimental approach. Performance maps derived from these tests were used by USGM to build the Aspen Plus model of the whole system. The final simulated layout, whose flowsheet is shown in Figure 1, included an autothermal reformer (ATR), a high temperature blower, a SOFC stack, a burner, four heat exchangers, low-temperature compressors and various splitters/mixers. Simulations were conducted for six operating scenarios, combining two anodic inlet temperatures (600 °C and 700 °C) with three fuel compositions. The resulting simulation data—temperature profiles, flow rates, and heat distribution—were used by ICI Caldaie to design the Piping and Instrumentation Diagram (P&ID) for the real prototype. The definition of the final layout followed a cyclical workflow, alternating between design refinements, supplier consultations, and Aspen-based validations. This iterative process aimed to reduce high-temperature components, simplify control, and ensure that the selected technologies were not only efficient and compatible, but also realistically implementable with reliable and commercially available components.

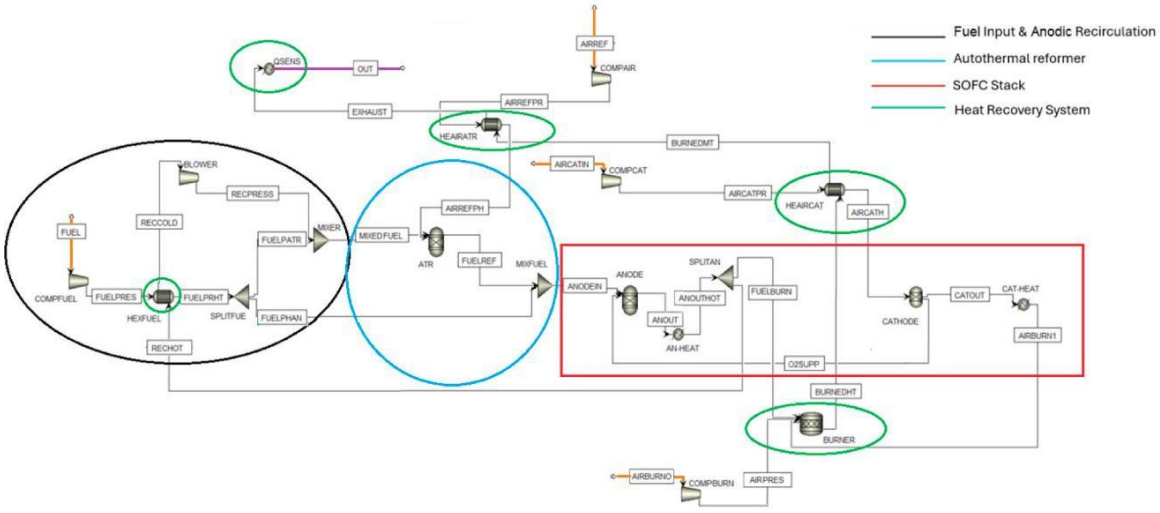


Figure 1 The flowsheet of the Aspen simulation of the SO-FREE system.

Results

The simulations revealed an electrical efficiency for the stack SOFC between 60% and 77%, a system utilization factor above 90%, and heat recovery rates exceeding 60%. The Aspen SOFC model was validated against experimental data, showing compositional deviations below 2.5% by volume and thermal distributions consistent with experimental data. The optimized

model configuration demonstrated stable power generation (~5 kW) across all fuel scenarios, with operative conditions such as temperature, flow rates and composition for all components maintained within the expected ranges. The heat recovery system achieved good performance, recovering 55–65% of the thermal energy from the burner for preheating the inlet air to the cathode and the ATR, while 30–35% remained available for cogeneration purposes. The chemical energy balance indicated that nearly all input power was converted into useful energy, with only 5–14% dedicated to maintaining the system's thermal regime. The final P&ID layout enabled a reduction in the number of high-temperature components, resulting in a compact and cost-efficient system built with reliable commercial components, while offering fine control for effective operation and integration.

Conclusions:

The proposed SOFC system introduces several technical innovations that enhance its practical applicability. The dual-stack compatibility and fuel flexibility allow for dynamic adaptation to different operating conditions without requiring auxiliary subsystems or hardware changes. One of the main advancements is the fuel preheating strategy, which recovers heat from the SOFC exhaust to reduce thermal stress and boost energy efficiency. Additionally, a fuel-splitting mechanism enables precise distribution between the ATR and the stack anode, ensuring stable operation with various fuels. The system layout minimizes component count, and its reliance on off-the-shelf technologies supports its potential as a viable solution for decentralized, high-efficiency, low-emission power generation. Future work will focus on building the physical prototype and assessing long-term operational stability under real-world conditions.

Acknowledgment

This research was funded by the European Commission, grant number 101006667, within the framework of the SOFREE project under the Horizon 2020 research and innovation programme (Societal Challenges – Secure, Clean and Efficient Energy).

Data supporting reported results can be found in SO-FREE project web site (https://cordis.europa.eu/project/id/101006667/results) and in the related open source repository (Zenodo).

The authors would like to acknowledge all the SO-FREE project partners, especially Elcogen and IKTS for providing the SOFC stacks used in the experiments.

EFCH2 2025
European Fuel Cells and Hydrogen
PIERO LUNGHI CONFERENCE
September 17th–19th 2025
Capri / Italy

Quantifying the impact of nickel “shocking” in microbial fuel cells fed with synthetic fermentation broths

Ioannis Ieropoulos*[a], Jack Morton [a]

* corresponding author: i.ieropoulos@soton.ac.uk

[a] Water and Environmental Engineering Group, University of Southampton, Southampton, United Kingdom

Keywords: Biofilm, Microbial Fuel Cell, Nickel, Wastewater Treatment

Abstract Introduction:

Microbial fuel cells (MFCs) have been shown to be resilient and adaptable systems in the field of wastewater treatment, with efficacies shown in many diverse applications. Fermentation broths contain highly biodegradable volatile fatty acids, which cement their position as an effective feedstock in MFCs, whilst also providing the opportunity for wastewater treatment and the provision of electrical energy. Fermentation broths do not consist of a fixed solution, varying in concentration, pH, chemical composition, depending on the fermentation parameters employed and the type of wastewater or other feedstock utilised. Contaminants within the feedstocks can have major impacts on the electrical performance of the cell, largely through the impacts on the established microbial community. Whilst we can establish the optimal feedstocks for a wastewater, and the impact of different chemical species on performance, the impacts of chemical "shocks" on performance are less explored. "Shocks" are here defined as a short-term exposure of the microbial community to a chemical species through addition to the feedstock, followed by a return to the baseline in the subsequent feed. The impact of the “shock” can be quantified through measuring the electrical performance shift when the perturbation is applied when compared to the baseline feedstock.

Objectives:

This study aimed to elucidate the impacts of chemical “shocking” on the performance of a microbial fuel cell and the mechanism by which the performance changed. The time frame over which the impacts were felt was a key parameter in assessing the “shock” impact.

Material and methods:

Two triplicates were inoculated with return activated sludge and brought to maturity with nutrient broth no. 3 (NutriSelect® Plus). The cells were then stabilised on a synthetic fermentation broth, consisting of a mixture of volatile fatty acids and salts to model a municipal sewage sludge fermentation broth. The MFC chassis were 3D printed, and consisted of two chambers, each with a 25 mL working volume. Folded carbon veil electrodes with an area of 270 cm2 were used for the anode and cathode; 8.75 cm^2 stainless steel mesh acted as a current collector in the cathode. The cells were maintained with the anolyte in looped continuous flow and batch-fed 0.1 M potassium hexacyanoferrate as catholyte.

Continuous voltage measurement was performed using an ADC-24 Channel Pico Data Logger. One triplicate acted as a control, whilst perturbations were applied to the other in the form of a predetermined "shock" cycle. Nickel, in the form nickel (II)chloride hexahydrate, was added in increasing concentrations, with the baseline feedstock fed between each nickel addition (0 ppm, 0.1 ppm, 0 ppm, 1 ppm, 0 ppm, 10 ppm, 0 ppm, 50 ppm, 0 ppm, 100 ppm). Daily polarisations were performed in one MFC from each triplicate with 1 minute time intervals, from 30 kΩ to 1 Ω, giving an indication of the open circuit voltage and the maximum power generated from each cell.

Results:

The nickel fed microbial fuel cells showed an average voltage of 169 mV after feeding in the baseline prior to the first nickel addition. Significant average voltage performance was first detected whilst the nickel feedstock containing 10 ppm was being fed, with an average of 290 mV.

Polarisation data showed an increase in maximum power measured from 47 mV in the baseline experiment prior to the addition of 0.1 ppm nickel to 923 mV for the baseline after the addition of 100 ppm nickel.

Conclusions:

MFCs fed anolytes containing nickel showed a pattern of sustained significantly increased electrical performance compared to the control cells, reaching a maximum power of 989 microwatts. High power output was sustained for several weeks, whilst regular feeding with solely baseline feedstock was continued.

References

[1] Malik, S., Kishore, S., Dhasmana, A., Kumari, P., Mitra, T., Chaudhary, V., Kumari, R., Bora, J., Ranjan, A., Minkina, T., & Rajput, V. D. (2023). A Perspective Review on Microbial Fuel Cells in Treatment and Product Recovery from Wastewater. Water, 15(2), 316. https://doi.org/10.3390/w15020316

[2] Hamedani, E. A., Abasalt, A., Talebi, S. (2024). Application of microbial fuel cells in wastewater treatment and green energy production: A comprehensive review of technology fundamentals and challenges. Fuel, 370. https://doi.org/10.1016/j.fuel.2024.131855.

EFCH2 2025 European Fuel Cells and Hydrogen PIERO LUNGHI CONFERENCE
September 17th–19th 2025 Capri / Italy

Study on experimental parameters of PEMFC stack under CO contamination with Machine Learning Technique

Luca Pratticò*[a], Gregorio Casagrande*[a], Andrea Gobbi*[b], Johannes Lehmuskoski [c], Lius Daniel [c], Jari Ihonen [c], Matteo Testi [a]

* Corresponding authors: prattico@fbk.eu, casagrande@fbk.eu

[a] HyRES unit, Sustainable Energy centre, Bruno Kessler Foundation, Via Sommarive 18 Trento, Italy.
[b] DSIP unit, Digital Industry centre, Bruno Kessler Foundation, Via Sommarive 18 Trento, Italy.
[c] Hydrogen Applications, VTT Technical Research Centre of Finland Ltd., Tietotie 4C Espoo, Finland.

Keywords: PEMFC, industrial grade hydrogen, degradation, Machine learning

Abstract

It's well-known that Proton-exchange membrane fuel cells (PEMFCs) require high purity level of hydrogen. To encourage the adoption of this technology and reduce its cost, they should be able to accept industrial-grade hydrogen without additional purification steps [1]. Carbon monoxide (CO) is a common PEMFC impurity, appearing whenever methane is converted into hydrogen through reforming, or in the presence of other impurities at the anode side. Additionally, PEMFCs merge chemical and physical processes, and their materials can degrade under demanding conditions. Enhancing modelling techniques to capture their evolving operational characteristics more effectively has also become of great interest [2]. Data-driven models offer a powerful approach to model CO contamination in PEMFCs by leveraging the dynamic equilibrium between CO adsorption and oxidation on the anode catalyst [3]. By training with input-output relationships and capturing nonlinear dependencies among key variables, data-driven models are a powerful tool to predict performance degradation and optimize operating conditions.

This study examines how experimental parameters affect the performance of a 10-cell proton exchange membrane fuel cell stack, using hydrogen contaminated with carbon monoxide and operating in recirculation mode. The aim is to assess the impact of these parameters on the generalizability of machine learning models trained to predict the average cells potential based on a fixed set of sensor data. This approach enables more targeted experiments that produce comprehensive datasets, supporting the Horizon Europe "CLEANER" project in developing a fuel cell system capable of operating on industrial-quality hydrogen.

Twelve experiments were conducted with the same 10-cell stack, each combining one of three purge intervals (5s, 60s, 400s), two recirculation rates (10% and 30% of the nominal recirculation pump power) and two values of cathode relative humidities (60%, 80%). A constant 0.8 ppm CO concentration contaminated the hydrogen supply for all tests, where the stack is conducted at constant duty by galvanometric control [4]. After a stabilization period, where no CO is injected, the CO mass flow controller is activated, and the poisoning test starts. Measurements include voltage, current, temperature, pressure, flow rates and other physical parameters. In the following picture three of the twelve voltage curves are represented:

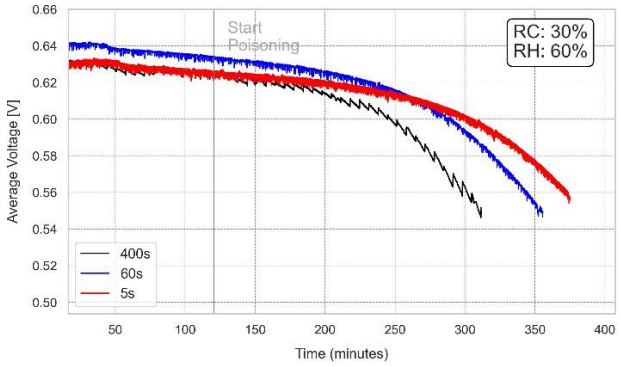


Figure 1- Output average voltage curves of the stead load cycle experiments conducted at a constant value of recirculation rate and relative humidity of respectively 30% and 60%, at three different purge intervals: 5s in red, 60s in blue and 400s in black.

The twelve individual datasets were grouped by keys, where each key fixed one of the three experimental variables (e.g., a 5s purge interval) and allowed the other variables to vary. A key represents a group of datasets linked by a common experimental variable. These keys were used to train and test a CatBoost-based ML model [5], resulting in a 7×7 grid of train–test combinations. Each cell in this grid corresponds to a model trained on one key and tested on another. The resulting score inside each cell represents the predictive quality (a combination of the R^2 score and the normalized reconstruction error) of the model produced by the corresponding keys combination, the higher the better. The scores of these combinations are reported in Figure 2 and represented as a heat map.

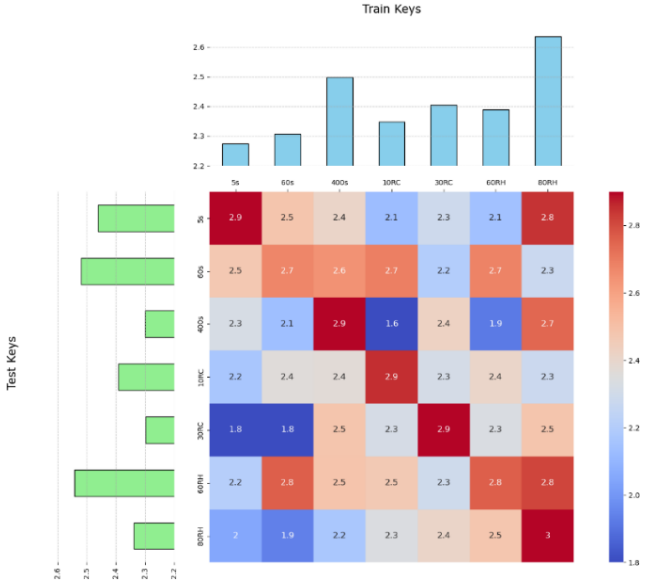


Figure 2- Heatmap representing the model score for each train-test key combination.

It is possible to notice that the diagonal entries indeed have the highest scores, indicating that models trained and tested on closely related datasets achieve better accuracy than when the datasets differ more substantially. The bar plots at the top and left of the heatmap reveal average scores per column and row, where the green bar indicates easily a key can be

predicted and the blue bar plot shows how well that key predicts other keys. Notably, these plots tend to shift in opposite directions: a strong testing score often pairs with a lower training score, reflecting that a highly predictive key can be harder for other datasets to predict.

These results highlight, as expected, that certain experimental parameters present greater challenges in extrapolation than interpolation. This is particularly evident when combining keys such as using 400s and 5s to interpolate the 60s key, while extrapolating 400s from the combination of 5s and 60s results in more inaccurate models. Moreover, relative humidity appears to have less impact on machine learning models performances, while purge intervals showed a higher influence. These findings can be used to establish an efficient test schedule, where different, and more varied, values of recirculation rates, relative humidities and recirculation rates are explored to produce valuable data for machine learning models. Future improvements could involve expanding beyond traditional machine learning frameworks and exploring deep learning architectures.

Acknowledgment

The development of the degradation model was supported by CLEANER project. The CLEANER project is supported by the Clean Hydrogen Partnership and its members. The project is co-funded by the Research Council of Norway and the UK Research and Innovation (UKRI) under the UK government's Horizon Europe funding guarantee. Co-funded by the European Union. Views and opinions expressed are however those of the author(s) only and do not necessarily reflect those of the European Union or Clean Hydrogen JU. Neither the European Union nor the granting authority can be held responsible for them.

The datasets were acquired during MetroHyVe 2 project. This project "Metrology for Hydrogen Vehicles 2" (MetroHyVe 2) has received funding from the EMPIR programme co-financed by the Participating States and from the European Union's Horizon 2020 research and innovation programme under Grant agreement No [19ENG04]

References

[1] «Global Hydrogen Review 2023 – Analysis», IEA. Consultato: 12 marzo 2025. [Online]. Disponibile su: https://www.iea.org/reports/global-hydrogen-review-2023

[2] T. Jahnke *et al.*, «Performance and degradation of Proton Exchange Membrane Fuel Cells: State of the art in modeling from atomistic to system scale», *J. Power Sources*, vol. 304, pp. 207–233, feb. 2016, doi: 10.1016/j.jpowsour.2015.11.041.

[3] H. Becker *et al.*, «Operando characterisation of the impact of carbon monoxide on PEMFC performance using isotopic labelling and gas analysis», *J. Power Sources Adv.*, vol. 6, p. 100036, dic. 2020, doi: 10.1016/j.powera.2020.100036.

[4] «metrohyve-2---deliverable-8---report-on-standard-test-protocols-concerning-fc-stack-measurements_rev0.pdf». Consultato: 19 marzo 2025. [Online]. Disponibile su: https://www.sintef.no/globalassets/projectweb/metrohyve-2/metrohyve-2---deliverable-8---report-on-standard-test-protocols-concerning-fc-stack-measurements_rev0.pdf

[5] «CatBoost - state-of-the-art open-source gradient boosting library with categorical features support». Consultato: 14 marzo 2025. [Online]. Disponibile su: https://catboost.ai

EFCH2 2025 European Fuel Cells and Hydrogen PIERO LUNGHI CONFERENCE
September 17th–19th 2025 Capri / Italy

Electrospun polybenzimidazole: optimization of a novel proton exchange membrane for high temperature fuel cells

Davide Principe [a, f], Miryam Gulino [a], Ottavio Longo [b, f], Emmanuel De Gregorio [c], Teo Martin [d], Andrea Pucci [e], Maria Assunta Navarra *[a], Valentina Naticchioni *[d, f]

* corresponding authors: mariassunta.navarra@uniroma1.it, valentina.naticchioni@enea.it

[a] Department of Chemistry, University of Rome La Sapienza, Rome, Italy
[b] Department of Mechanical, Energy and Management Engineering (DIMEG), University of Calabria, Rende (CS), Italy
[c]Department of Engineering, University of Naples 'Parthenope', Centro Direzionale, Isola C4, 80143 Napoli, Italy
[d] ENEA, Italian Agency for New Technologies, Energy and the Environment Department of Renewable Energies, Via Anguillarese, 301-00123 Rome, Italy
[e] Dipartimento di Chimica e Chimica Industriale, Università di Pisa, Via Risorgimento 35, 56126 Pisa, Italy
[f] Task 31 Member, Advanced Fuel Cells Technology Collaboration Programme

Keywords: ELECTROSPINNING, HIGH TEMPERATURE FUEL CELLS, PEM, PBI.

Abstract

Polybenzimidazole based membranes are promising materials currently investigated for their application in high temperature proton exchange membrane fuel cells, due to their great thermal and chemical stability. In this study we investigated the possibility to enhance its conductivity by manufacturing an electrospun mat of polybenzimidazole nanofibers, starting from a synthetic material instead of a more conventional commercial one. Optimized membranes have then been produced through electrospinning technique and characterized in their morphological, mechanical and electrochemical properties. The obtained mats are made of fibers with diameters around 200 nm and show an increased conductivity compared to solvent casted ones.

Introduction: *Recently, polybenzimidazole (PBI) based membranes have gained attention as promising materials for ion-exchange applications, both cationic and anionic, due to their good mechanical and conductive properties. In particular, phosphoric acid (PA) doped PBI has already been employed in high temperature proton exchange fuel cells (HT-PEMFC), since it*

retains its excellent properties even in the harsh conditions of 140-160 °C and 0% relative humidity needed in such devices [1].

Objectives:

Starting from the polymer synthesis, the aim of this work is to enhance even further the material's great properties of mechanical strength and conductivity by manufacturing an electrospun mat of PBI nanofibers. In this way, the greater surface to volume ratio combined with a good pore interconnectivity should make the following PA doping and the consequent proton conduction mechanism even more efficient.

Material and methods: PBI has been synthetised by the polycondensation of isophthalic acid and 3,3'-diaminobenzidine with polyphosphoric acid (PPA) as catalyst [2]. Since molecular weight and its distribution are fundamental parameters for both processability and membrane performances, the synthetised polymer has been then characterized through gel permeation cromathography. To evaluate physical-chemical properties the synthetised material was also characterized by thermal-gravimetric analysis (TGA) and differential scanning calorimetry (DSC). Starting from a synthetic PBI, several spinning conditions, pre-treatments of the sample and polymer/dimethylacetamide concentrations have been investigated, together with characterization of the microscopic morphology and the fibers diameters of the electrospun materials through optical and scanning electron microscopy. Finally, the optimized membranes have been mechanically and electrochemically characterized through stress strain, specific resistance and conductivity measurements.

Results: An optimized synthesis procedure, with good reproducibility, was established at 200 °C, from which a molecular weight of around 30 kDa was obtained. The establishment of a consistent design of experiments led to the achievement of reproducible PBI electrospun mats made of nanofibers with a diameter of around 200 nm, obtained from a 16 wt % polymer solution and 1 wt % of LiCl in dimethylacetamide. The optimized membranes have shown values of conductivity at 140-160 °C and 0 % RH higher than 100 mS/cm.

Conclusions: Lowering synthesis temperature down to 200 °C has limited the polycondensation reaction and reduced polymer's molecular weight, allowing to process it with the electrospinning technique. In this way, the already good mechanical and electrochemical properties of PBI have been improved even further. In particular, the high surface to volume ratio given by the nanometric fibers has enhanced the PA doping, leading

to interesting values of conductivity in the HT-PEMFC working conditions. According to the presented results, electrospun PBI surely is a promising candidate for proton exchange membranes in high temperature fuel cells, even though new solutions to strengthen its mechanical properties could be implemented, for example by introducing inorganic fillers.

Acknowledgment

POR H2 - W.P. 3.1 - Ricerca e sviluppo di tecnologie di stack, componenti e processi, per migliorarne le prestazioni e ridurne i costi. LA 3.1.1 Sviluppo di processi per la produzione di membrane a conduzione protonica ad alta temperature.

References

[1] Jahangiri S, Aravi İ, Işıkel Şanlı L, Menceloğlu YZ, Özden-Yenigün E. Fabrication and optimization of proton conductive polybenzimidazole electrospun nanofiber membranes. Polym Adv Technol. 2018; 29: 594–602. https://doi.org/10.1002/pat.4169

[2] Yoda, N. and Kurihara, M. (1971), New polymers of aromatic heterocycles by polyphosphoric acid solution methods. J. Polym. Sci. Macromol. Rev., 5: 109-193. https://doi.org/10.1002/pol.1971.230050102

EFCH2 2025 European Fuel Cells and Hydrogen
PIERO LUNGHI CONFERENCE
September 17th–19th 2025
Capri / Italy

Numerical Performance Comparison of Battery and PEM Fuel Cell Models for Lightweight Aircraft Applications

Abolfazl Movahedian*[a], Gianluca Marinaro[b], Emma Frosina [a]

* corresponding author: a.movahedian@studenti.unisannio.it
[a] University of Sannio, piazza Roma, 21, Benevento (Italy)
[b] CIRA, via Maiorise SNC, Capua (Italy)

Keywords: Battery, Lightweight aircraft, PEMFC, Propulsion systems

Abstract

This paper compares the dynamic performance of two propulsion systems—proton exchange membrane fuel cell (PEMFC)-only and battery-only—integrated into a lightweight aircraft. The mission profile comprises four distinct flight phases: takeoff, climb, cruise, and descent. A numerical study was conducted in the Simulink environment to investigate key parameters such as voltage, current, required aircraft power, and energy consumption. The results indicate that both systems successfully completed the flight mission. However, the PEMFC system exhibited transient spikes at the beginning of each flight phase, whereas the battery system displayed only minor fluctuations.

Introduction:

Fossil fuels have long been recognized as major contributors to environmental degradation, primarily due to the emission of harmful pollutants such as CO_2 into the atmosphere [1]. In 2013, the aviation industry emitted approximately 700 million tons of CO_2. A figure projected to triple by 2050 if no mitigating actions are taken [2, 3]. To address these challenges, electrified propulsion systems have emerged as viable alternatives to conventional internal combustion engines (ICEs), as they rely on emission-free energy sources throughout the entire flight mission.

In recent years, electrified aircraft have attracted significant attention from researchers aiming to achieve zero-emission aviation. These propulsion systems can utilize various electrochemical energy sources, among which PEMFCs and lithium-ion batteries have demonstrated strong potential for reducing environmental impact. This paper presents a comparative analysis of these two configurations, PEMFC-only and Battery-only, under a representative flight mission profile.

Objectives:

1- Develop two numerical models, PEMFC-only and battery-only systems in lightweight electric aircraft during various flight phases.

2- Perform a comparative study to evaluate various parameters, including State of Charge (SoC), hydrogen consumption, current and voltage.
3- Determine the pros and cons of each system and suggestions for improving performance.

Material and methods:

As shown in Figure 1, both architectures examined in this study follow the same mission profile, with identical aircraft power demands for both systems. The altitude varies between 0 and 3000 meters, and the total simulation time is 4000 seconds. The aircraft velocity remains constant throughout all main mission phases.

A dynamic PEM fuel cell model is developed for the propulsion system to represent the aircraft's power source, providing current and voltage responses based on load variations. The transient behavior of the PEMFC includes activation, ohmic, and concentration losses [4]; the air supply system is modeled in detail and includes compressor dynamics, cooling and humidification subsystems. In particular, the fuel cell stack has 381 cells in series. For the second model, a Battery Equivalent Circuit (BEC) is used to model the dynamic behavior of the battery, which serves as the sole electrochemical energy source. In particular, battery pack has an energy capacity of 25 kWh, achieved with an architecture of 18P93S 4000mAh Li-ion cylindrical cell. The weight of the two propulsive architectures is comparable, the fuel cell-based system has a weight of 190 kg, while the battery pack, including auxiliary systems, weighs 189 kg.

Both configurations share the same DC/DC converter, inverter and permanent magnet synchronous motor, propeller and aircraft models. The modeling of these subsystems is not presented here due to scope limitations.

Results:

1. Consumed Hydrogen and SOC

Figure 2 presents a comparison of energy consumption for both architectures during the flight mission. As shown, the fuel cell system consumes approximately 0.9 kg of hydrogen to complete the entire mission, while the battery-based system retains a residual State of Charge (SOC) of around 20% at the end of the mission.

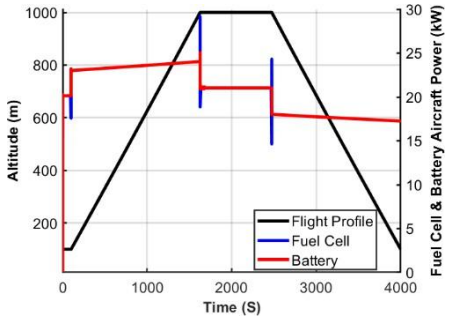


Figure 1. Mission Profile and Fuel Cell & Battery Aircraft Power

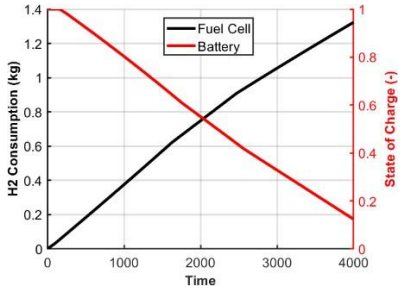


Figure 2. Hydrogen Consumption and State of Charge

Current and Voltage

Figure 3 compares the current demand for the battery and fuel cell over time. The average current values are approximately 83 A for the fuel cell and 52 A for the battery. This difference is attributed to the higher operating voltage of the battery system, as visible in Figure 4.

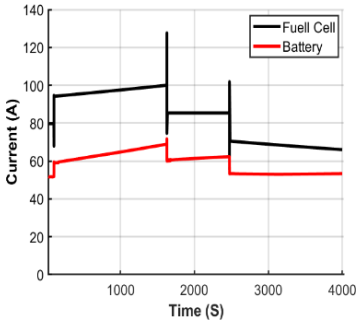


Figure 3. Fuel Cell and Battery Current

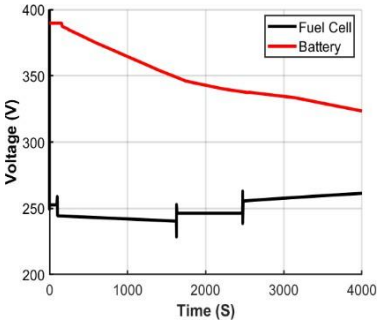


Figure 4. Fuel Cell and Battery Voltage

2. Power Demand

The power required by the aircraft, derived from flight dynamics, is shown in Figure 1 for both the fuel cell and battery systems. During transient phases, the fuel cell exhibits power spikes, while the battery system responds more rapidly and displays only minor fluctuations.

Conclusions:

In this study, two aircraft models—one powered by a proton exchange membrane fuel cell (PEMFC) and the other by a battery—were developed and analyzed under a mission profile with comparable power demand. In the battery system, the voltage decreases significantly due to the declining state of charge (SOC), whereas the fuel cell voltage gradually increases over time. The power response of the fuel cell during transient phases demonstrates slower dynamic behavior compared to the battery.

As a result, the implementation of a hybrid propulsion system that combines both fuel cell and battery technologies is recommended to compensate for the limitations of each system during different phases of the mission profile.

References

1. González-Espasandín, Ó., T.J. Leo, and E. Navarro-Arévalo, *Fuel cells: A real* option for unmanned aerial vehicles propulsion. The Scientific World Journal, 2014.
2. Available online: https://news.nationalgeographic.com/energy/2015/04/150409-epa-aviation-emissionsrules-for-airplanes/ (accessed on 29 June 2018).
3. Frosina, E., et al., Development of a lumped parameter model for an aeronautic hybrid electric propulsion system. Aerospace, 2018. 5(4): p. 105.
4. Cultura, A.B. and Z.M. Salameh, Dynamic analysis of a stand alone operation of PEM fuel cell system. Journal of Power and Energy Engineering, 2014. 2(1): p. 1-8.

European Fuel Cells and Hydrogen
PIERO LUNGHI CONFERENCE
September 17th–19th 2025
Capri / Italy

Performance evaluation and durability analysis of pem fuel cells for sustainable energy applications

Ottavio Longo*[a,d], Matteo Genovese[a], Petronilla Fragiacomo*[a], Davide Principe[b], Miryam Gulino[b], Nicola Sanzò[c], Livia Della Seta[c], Valentina Naticchioni*[c,d]

* lngttv98r11c352n@studenti.unical.it

* Corresponding authors: petronilla.fragiacomo@unical.it, valentina.naticchioni@enea.it

[a] Department of Mechanical, Energy and Management Engineering (DIMEG), University of Calabria, Rende (CS), Italy
[b] Department of Chemistry, University of Rome La Sapienza, Rome, Italy
[c] ENEA, Italian Agency for New Technologies, Energy and the Environment Department of Renewable Energies, Lungotevere T. Di Revel, 76-00196 Rome, Italy
[d] Task 31 Member, Advanced Fuel Cells Technology Collaboration Programme

Keywords: DURABILITY, PEM, PERFORMANCE, POLARIZATION CURVE.

Abstract

This study highlights the pivotal role of green hydrogen as a sustainable energy vector and fuel for Proton Exchange Membrane Fuel Cells. The main goal is to evaluate performance and durability of different MEAs by comparing homemade assemblies to commercial ones, with results expressed in terms of key performance indicators (KPIs). Performance tests, including the evaluation of polarization and power curves, are conducted by varying electrodes, membranes, and temperature, while impedance spectra and long-term durability assessments further support the analysis.
A morphological analysis using SEM provides valuable insights into structural degradation, enabling the optimization, advancement, and deployment of this technology in commercial applications to drive the energy transition.

Introduction: *In a world working hard for cleaner energy solutions, where every technological advancement is crucial to the future energy transition, hydrogen stands out for its unique properties and potential. Fuel cells, especially polymer electrolyte membrane fuel cells (PEMFCs), are emerging as one of the best options as end-use of hydrogen for sustainable energy, offering high efficiency and zero harmful emissions. This technology plays a fundamental role by utilizing green hydrogen, produced by renewable sources as an energy vector, converting its chemical energy into electricity when needed.*

Objectives: This experimental work focuses on efficiency and long-term stability, aiming to better understand the conditions and variables that can affect these crucial parameters. The main goal is to compare results, expressed in terms of key performance indicators (KPIs), obtained from different 5cm^2 membrane electrode assemblies (MEAs) by varying electrodes, membranes and temperature. The study highlights that operational efficiency and durability are two critical aspects for advancing, understanding, and improving PEMFC technology**.**

Material and methods: Two different types of 5-layers MEAs were tested and evaluated in this study: homemade MEAs and commercial ones.

The homemade MEAs were produced using Nafion membranes with different thicknesses (N-115, N-117, and the thinner N-212), two specific platinum-based electrodes (EFE3T with a platinum loading of 0.56 mg/cm² and EFE3D with a platinum loading of 0.44 mg/cm²), and carbon paper as the GDL, assembled by hot-pressing (130°C @ 50 kg/cm²).

The commercial MEA used was a 5-layers Membrane Electrode Assembly with integrated Gas Diffusion Layers (GDL) for use in Hydrogen/O_2 Fuel Cells, featuring a platinum loading of 0.5 mg/cm², a 0.002" Nafion membrane, and a 410-micron thick woven carbon cloth as the GDL.

Performance testing was conducted by recording both polarization and power curves at different temperatures (50, 60, 70, and 80°C) to investigate current density behaviour and voltage losses. Polarization curves were obtained under reverse mode operation.

Impedance analysis was carried out through high-frequency resistance (HFR) measurements and electrochemical impedance spectroscopy (EIS). The results were modelled using Nyquist and Bode diagrams derived from an equivalent electrical circuit.

Durability was assessed through long-term tests based on recording polarization and power curves at regular intervals (every 50 to 100 hours), as well as performing constant current tests with the cell operating under a simulated load.

Experimental tests enabled a quantitative assessment of performance degradation over time, providing valuable insights into the practical usability of the MEAs not only in laboratory settings but also in the energy industry.

Morphological analysis, obtained by scanning electron microscopy (SEM), and chemical composition, evaluated by energy-dispersive X-ray (EDS) analysis, were used to investigate component degradation.

Results: The experimental campaign demonstrated that superior efficiency and overall performance were achieved when using the thinnest membrane, type N-212, in combination with EFE3T electrodes, compared to other configurations employing N-115 or N-117 membranes. Based on these results, the most promising MEA configuration was selected by combining the thinnest membrane with the best-performing electrode. A 150-hour durability test was then carried out, revealing a significant performance drop of the cell, which decreased from over 2 A/cm² to less than 1 A/cm².

In contrast, the durability test performed on the commercial MEA showed a much lower degradation, with performance decreasing by only 10–20% after 150 hours, compared to a drop of over 50% observed in the non-commercial MEA (Fig. 1).

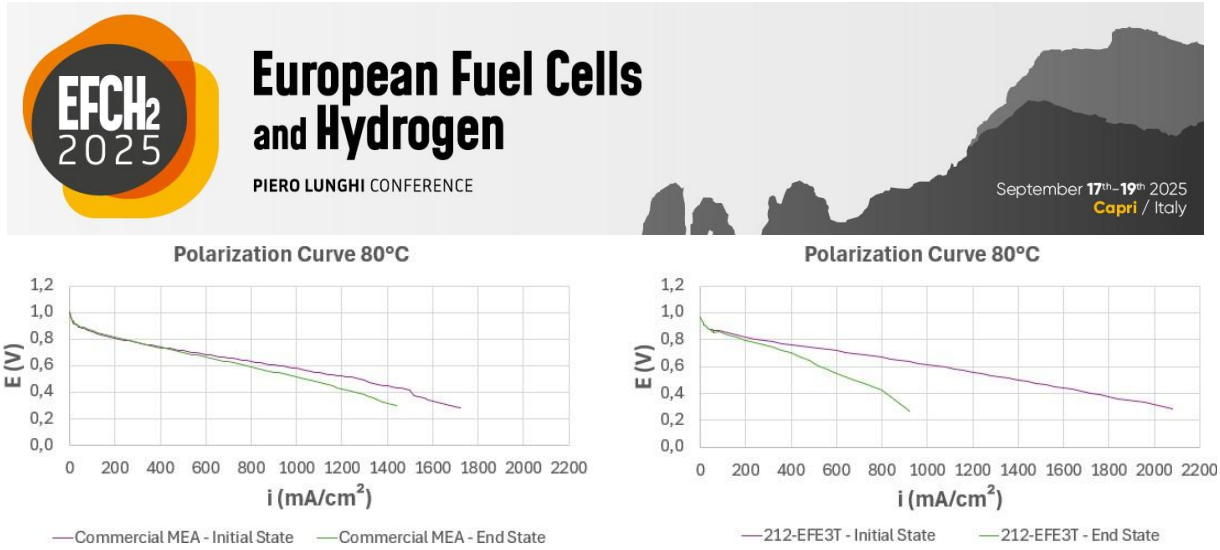


Figure 1: Perfomance drop comparison between Initian and End State

To better understand experimental results, SEM and EDS analyses were performed. SEM images revealed surface cracks in the catalyst layer, which appeared larger and deeper in the best-performing electrode (EFE3T), maybe contributing to an increased contact area and, consequently, improved performance (Fig. 2).

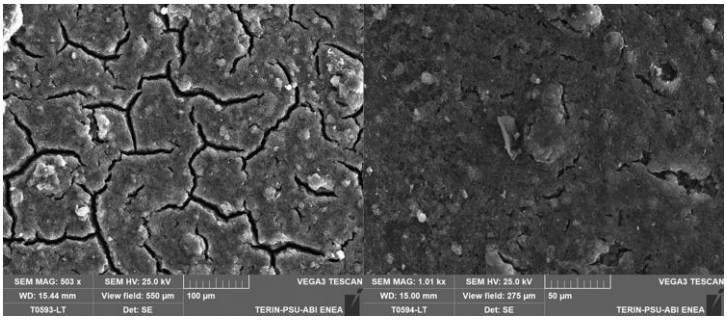


Figure 2: Surface morphology comparison between EFE3T (left) and EFE3D (right)

Another relevant phenomenon, highlighted by SEM and EDS analyses, is the occurrence of platinum aggregation and the presence of cracks in the gas diffusion layer, which are likely responsible for the increase in charge transfer resistance and mass transport limitations observed in the impedance measurements.

Conclusions: This work aims to further advance the understanding of this important technology in the context of the upcoming energy transition. It focuses on key areas for development and improvement, highlighting some of the most significant limitations as well as numerous advantages. The study is intended to support ongoing research efforts with the goal of contributing to the advancements needed to bring fuel cells into widespread industrial use and establish them as a major reliable technology, including the development of more robust catalyst anchoring strategies to prevent detachment, as well as manufacturing processes, such as the use of carbon clot, to minimize GDL cracking.

Acknowledgment

W.P. 3.1 - Ricerca e sviluppo di tecnologie di stack, componenti e processi, per migliorarne le prestazioni e ridurne i costi LA 3.1.1 Sviluppo di processi per la produzione di membrane a conduzione protonica ad alta temperature

EFCH2 2025 European Fuel Cells and Hydrogen
PIERO LUNGHI CONFERENCE
September 17th–19th 2025 Capri / Italy

Techno-economic analysis of 10 MW SOFC powertrain system fed by hydrogen carriers in shipping

M. Minutillo[a], S. Di Micco *[b], A. Cappiello [b]

* corresponding author: simona.dimicco@uniparthenope.it

[a] Department of Industrial Engineering, University of Salerno, Fisciano, Italy

[b] Department of Engineering, University of Naples "Parthenope", Naples, Italy

Keywords: shipping decarbonization, methanol, ammonia, SOFC maritime propulsion system.

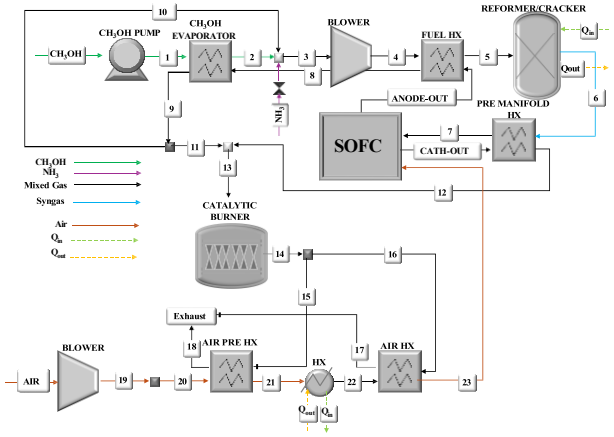
Abstract:

This study is devoted at analysing from techno-economic perspective the applicability on board an oceanic going vessel of a SOFC-based propulsion system supplied by hydrogen carriers as methanol and ammonia.

Introduction: *Hydrogen carriers as methanol and ammonia can be considered promising fuels for shipping due to their simplicity in storage and handling.*

Objectives: In this paper, methanol and ammonia based-SOFC systems designed to be installed on board an oceanic going vessel are analysed from techno-economic perspective. First, the systems are modelled by means of a thermodynamic approach and then the economic performances are estimated by introducing and calculating useful Key Performance Indicators (KPIs).

Material and methods: 10 MW SOFC power system fed with ammonia or methanol is considered as propulsion system for a container ship. In order to calculate the fuel consumption of the system in different operating conditions according to the selected ship mission profile [1], a thermodynamic model in Aspen Plus Environment is developed. Fig.1 depicts the model flowsheet of the system for different feeding fuels (ammonia or methanol). It can be noticed that in the case of methanol feeding, two additional components have to be considered for assuring its vaporization and compression (pump and evaporator). On the other hand, in the case of ammonia, it is sufficient to install a throttling valve for ensuring its vaporization. For both feeding fuels, the mixing with the anode off-gas (10) is realized before entering the recirculation blower. Thus, the mixture fuel and anode-off gas (4) is heated and then processed in a reforming unit or cracking unit if methanol or ammonia is used, respectively.



The synthesis gas (6) is furtherly heated for reaching the operating temperature of the SOFC system. The air needed for feeding the cathodic side is heated in more Heat Exchangers by exploiting the hot gases from the catalytic burner in which anodic and cathodic exhaust are sent.

Fig.1. Methanol/ammonia based SOFC system schematic layout

Results of the thermodynamic analysis are used for assessing the economic feasibility of the proposed system. To this aim, three economic KPIs are defined: i) the Specific Fixed Capital Cost (SFC); ii) the Specific Operating Cost (SOC) and iii) the Specific Net Present Cost (SNPC). These costs are defined with respect the installed power (*P*). These KPIs allow to evaluate the competitiveness of the proposed systems over their entire lifetime (N), assumed equal to 10 years (the number of trips per year is assumed equal to 25). The analysis is performed considering 2 time scenarios: i) Scenario1, referred to 2030 and ii) Scenario2 referred to 2050.

$$KPI_1 = S_{FC} = \frac{C_{FC}}{P} = \frac{CAPEX \cdot C_{sys\ inst}}{P} = \frac{(C_{stack} + C_{BoP}) \cdot C_{sys\ inst}}{P} \left[\frac{€}{kW}\right] \quad (1)$$

Where C_{FC} is the total fixed costs that is the investment cost (CAPEX) of the systems (stack and BoP) increased of a coefficient C_{sys_inst} that takes into account some cost factors (f) related to the installation of the system like: piping (f_p),materials (f_m), instrumentation and control n(f_i), equipment erection (f_{er}), offsites (OS), Design and engineering ($D\&E$), contingency (X).

This coefficient is calculated applying the following equation [2]:

$$C_{sys_inst} = [(1 + f_p) \cdot f_m + (f_{er} + f_i)] \cdot (1 + OS) \cdot (1 + D\&E + X)$$

The other KPIs are defined as:

$$KPI_2 = S_{OP} = \frac{\sum_{n=0}^{N-1}(C_{O,n})}{P} \left[\frac{€}{kW}\right] \quad (2)$$

$$KPI_3 = S_{NPC} = \frac{NPC}{P} = \frac{C_{FC} + \sum_{n=0}^{N-1}(C_{O,n} + C_{M,n} - R_{CO_2,n})}{P} \left[\frac{€}{kW}\right] \quad (3)$$

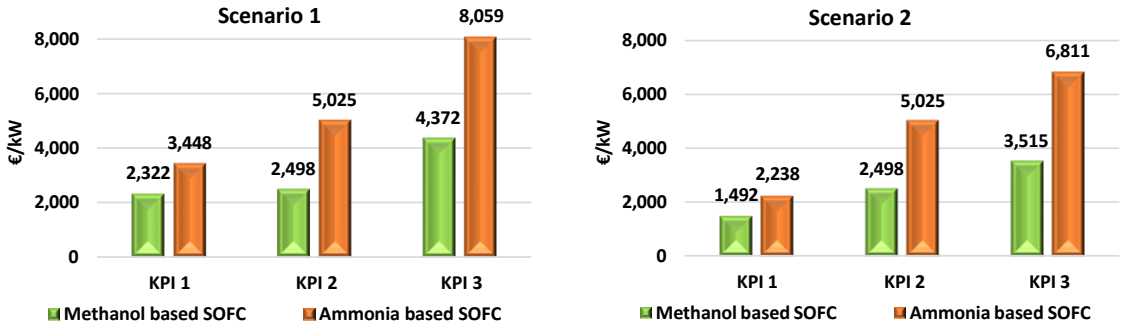
where $C_{O,n}$ is the operating costs, $C_{M,n}$ is the maintenance cost and $R_{CO_2,n}$ is the revenue (or the saving cost) due to avoided CO_2 (according to the Emission trading System).

Results: The main results of the thermodynamic models in terms of components' size, fuel consumption and CO_2 emissions are listed in Table 1. These results have allowed to estimate the investment and operating costs (table 1) and to calculate the KPIs. The maintenance cost

for each component is calculated as 2% of its investment cost. Figs.2a and 2b illustrate the comparison among the obtained KPIs for both scenarios.

Table 1. Desing and cost data for the NH3/CH3OH based SOFC system

	Design data	Ammonia	Methanol	Costs	Ammonia	Methanol
SOFC System	Power (MW)	10	10	Inv. Cost (k€)	1,412.0	1,412.0
Cracker/Reformer	*Heat Duty (MW)*	2.31	1.53	Inv. Cost (k€)	140.0	93.0
Rec. Blower	*Power (kW)*	103	38.3	Inv. Cost (k€)	3.3	1.2
Fuel Evaporator	*Heat Duty (MW)*	-	1.06	Inv. Cost (k€)	-	259.0
Fuel HX	*Heat Duty (MW)*	1.76	1.70	Inv. Cost (k€)	427.0	412.0
Pre-manifold HX	*Heat Duty (MW)*	1.06	0.87	Inv. Cost (k€)	257.0	211.0
Catalytic Burner	*Out. Temp. (°C)*	779	691	Inv. Cost (k€)	31.0	29.0
Air Blower	*Power (kW)*	282.0	281.7	Inv. Cost (k€)	9.0	8.4
Air HX	*Heat Duty (MW)*	0.50	0.71	Inv. Cost (k€)	122.0	172.0
Air PreHX	*Heat Duty (MW)*	15.32	6.41	Inv. Cost (k€)	3,724.0	1,560.0
Fuel Consumption	*(tons/trip)*	212.92	162.34	Op. Costs (k€)	4,042.0	2,010.0
CO_2 emission	*(tons/trip)*	-	-	Revenues (k€)	330.0	330.0



(a) (b)

Fig.2. KPIs comparison in (a) Scenario 1 and (b) Scenario 2

Conclusions: The methanol-based SOFC system is the best solution from the economic perspective, as demonstrated by the lower value reached for each KPI in both scenarios.

Acknowledgment

Research funded by the European Union – NextGeneration EU from the Italian Ministry of Environment and Energy Security POR H2 AdP MMES/ENEA with involvement of CNR and RSE, PNRR - Mission 2, Component 2, Investment 3.5 "Ricerca e sviluppo sull'idrogeno", CUP: I83C22001170006.

References

[1] S. Di Micco, V. Cigolotti, L. Mastropasqua, J. Brouwer, M. Minutillo, En Conv and Man: X, 2024, 100539
[2] G. P. Towler and R. K. . Sinnott, Chemical engineering design : principles, practice and economics of plant and process design. Butterworth-Heinemann is an imprint of Elsevier, 2022.

EFCH2 2025 European Fuel Cells and Hydrogen PIERO LUNGHI CONFERENCE
September 17th–19th 2025 Capri / Italy

Microbial Fuel Cells Fed with Microbial Electrolysis Cell Effluent for Sustainable Energy Applications

Pietrelli A. * [a], Khorvash S.[b], Gagliardi G.[b], Lovecchio N.[a], Zeppilli M. [b], Marchetti A.[b], Allard B.[d], Mieyeville F. [d] and Borello. D. [c]

* corresponding author: andrea.pietrelli@uniroma1.it

[a] Department of Information Engineering Electronics and Telecommunications, Sapienza University of Rome, Rome, Italy

[b] Dept. of mechanical and aerospace engineering, Sapienza University of Rome, Rome Italy

[c] Department of Chemistry, Sapienza University of Rome, Rome, Italy

[d] Université de Lyon, INSA Lyon, UCBL 1, ECL, CNRS, Ampère, UMR5005, Villeurbanne, France

Keywords: Microbial fuel cell, Microbial Electrolysis cell, Energy Harvesting, Low power electronics

Abstract

This paper investigates the performance of wastewater microbial fuel cells (WWMFCs) when fed with effluent derived from a microbial electrolysis cell (MEC) designed for hydrogen production. Using a custom low-cost measurement system, three lab-scale WWMFC prototypes were monitored over a three-week period. The results demonstrate the viability of integrating MFC and MEC systems for dual-purpose energy generation and wastewater treatment. The maximum power output recorded was 410 µW under a 200 Ω load for a sampling time of 3 seconds. Variations in performance among the three cells underscore the influence of substrate composition and microbial community development over time.

Introduction: Microbial fuel cells (MFCs) represent a promising technology for sustainable energy generation, capable of converting organic waste into electricity through the metabolic activity of electrogenic bacteria [1]. Wastewater-based MFCs, in particular, offer dual benefits of energy recovery and wastewater treatment.

Objectives: The present work explores the integration of WWMFCs with microbial electrolysis cells (MECs) able to produce hydrogen, using the MEC effluent as the sole substrate for the MFCs. Such a coupling aims to enhance resource utilization and system efficiency.

Material and methods:

MFC Prototypes: Three identical single-chamber, air-cathode WWMFCs were constructed using PVC drainage tubes with a total internal volume of 0.7 L (Fig. 1). The anodes consisted of carbon fiber brushes (projected area: 100 cm²), while the cathodes were fabricated manually using carbon cloth (Teflon-treated, 30%) layered with 1.56 mg/cm² of carbon black and 0.5 mg/cm² of platinum.

MEC Effluent and Feeding Regimen: Each MFC was fed with freshly collected MEC effluent, which contained sodium acetate (0.088 g/L), glucose (0.34 g/L), yeast extract (0.075 g/L), peptone (0.088 g/L), and a COD of 255 mg/L. The pH was at 5.95. The acetate concentration

was adjusted to 1 g/L to standardize input conditions, the system was analyses before and after the addiction of sodium acetate.

Measurement System: A custom electronic system dedicated to MFCs [2] was employed to collect electrical data, including voltage and power output, across varying external resistances (100–400 Ω). The system enabled long-term monitoring and high-precision measurements, employing variable stop times up to 360 seconds to stabilize readings.

Results:

Measurements were taken across external resistances ranging from 100 to 400 Ω, with stop times up to 360 seconds used to ensure more stable and reliable readings. The resuilts are shown in Fig. 2 for three different reactors measured with different channel of the measurement system. In order to simulate the use of mfc to supply low power system as a node of a wireless sensor network, measurements with stop time of 3 second was done resulting in a peak power of 410uW at 200 Ω or even 460uW at 110 Ω as in Fig. 3 for the reactor number two..



Fig. 1. Photo of a water Microbial fuel cell lab scale prototype used in the experiments

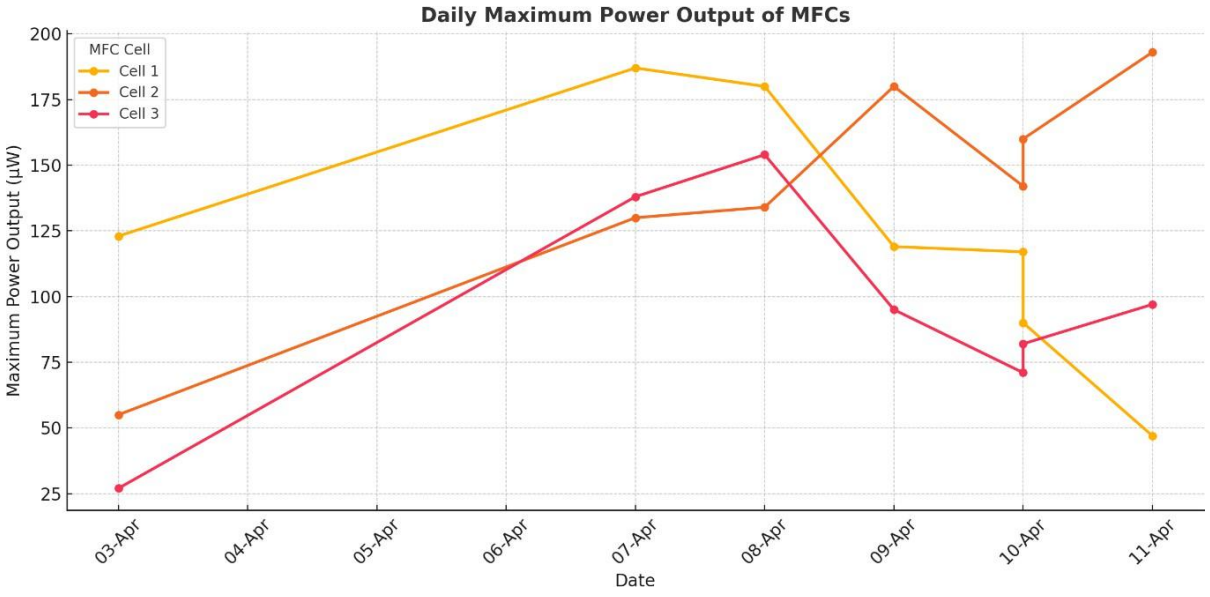


Fig.3 Maximum Power Output Over Time at a sample time of 360 s

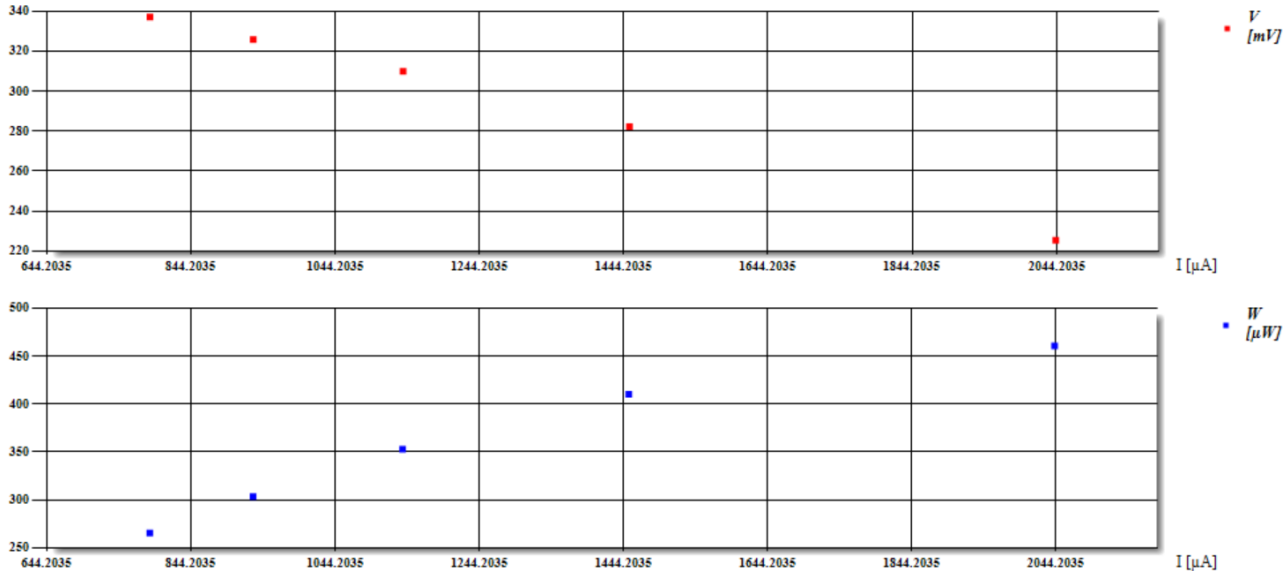


Fig.3 Maximum Power Output Over Time at a sample time of 3 s

Conclusions:

The results highlight significant heterogeneity in MFC behaviour even under nominally identical conditions but in a limited range. The maximum power point was found with external resistance of 200 Ω for a sampling time of 360s. This sampling time of 360 s simulate a long term use of the reactors because the current delivered is stabilized over time.

The use of MEC effluent as a substrate demonstrated feasibility, aligning with the broader goal of integrated bioelectrochemical systems. The Coulombic efficiency and energy efficiency of the MEC (around 109%) likely contributed to the high-quality effluent, supporting subsequent electricity generation in MFCs.

These findings support the viability of WWMFC-MEC coupling as a sustainable solution for decentralized energy systems, particularly in resource-limited or off-grid scenarios.

Indeed, this study confirms the practicality of using MEC effluent to sustain WWMFCs for electrical energy generation. Variations in cell performance reflect the complex interplay of microbial dynamics and electrochemical conditions. Continued optimization, including adaptive impedance control and microbial community engineering, may further enhance output consistency and power density. Such systems hold promise for future integration into smart environmental monitoring networks and standalone renewable energy platforms.

References

[1] Ancona, V., Caracciolo, A. B., Borello, D., Ferrara, V., Grenni, P., & Pietrelli, A. (2020). Microbial fuel cell: an energy harvesting technique for environmental remediation. *International Journal of Environmental Impacts*, *3*(2), 168-179

[2] Lovecchio N, Di Meo V, Pietrelli A. Customized Multichannel Measurement System for Microbial Fuel Cell Characterization. Bioengineering. 2023; 10(5):624. https://doi.org/10.3390/bioengineering10050624

EFCH2 2025 European Fuel Cells and Hydrogen
PIERO LUNGHI CONFERENCE
September 17th–19th 2025
Capri / Italy

Application of a Multiphysics Equivalent Stiffness Model of a PEMFC integrating the nonlinear mechanical behaviour of MEA components

Luca Marcelli*[,a,b,c,d], Dominique Chamoret [c], Xavier François[b], Yann Meyer[d], Denis Candusso[a,b]

* corresponding author: luca.marcelli@universite-paris-saclay.fr

[a] SATIE (UMR CNRS 8029), Université Paris Saclay, ENS Paris Saclay, Université Gustave Eiffel, 25 Allée des Marronniers, 78000, Versailles Satory, France

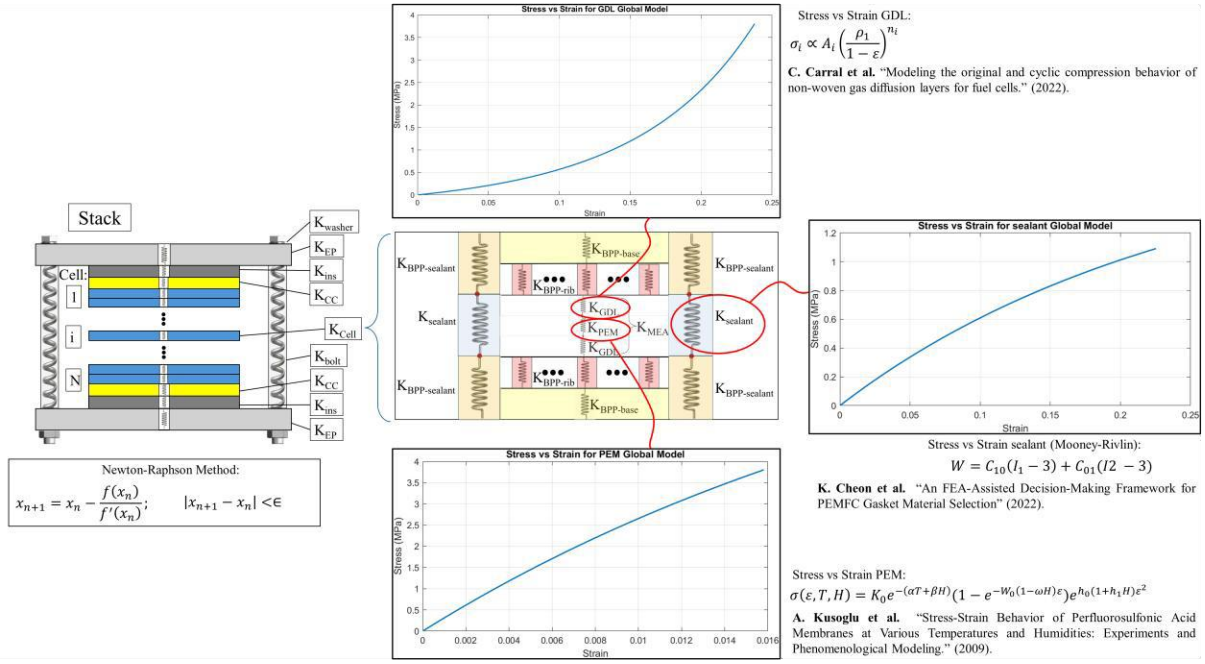
[b] FCLAB, Plateforme Hydrogène Energie, UTBM, Rue Thierry Mieg, 90010, Belfort Cedex, France

[c] Université Marie et Louis Pasteur, UTBM, CNRS, Laboratoire Interdisciplinaire Carnot de Bourgogne ICB UMR 6303, 90010 Belfort, France

[d] Univ. Savoie Mont Blanc, SYMME, 74000, Annecy, France

Keywords: PEMFC, Equivalent Stiffness Model, Mechanical behaviour, Stack

Graphical abstract



Abstract

Introduction: Proton Exchange Membrane Fuel Cells (PEMFCs) have gained considerable attention due to their high efficiency, relatively low operating temperature, and suitability for both stationary and mobile applications [1]. Mechanical compression and pressure distribution in PEMFC stacks play a crucial role in optimising the contact between components, mitigating gas leakage, and reducing interfacial resistances [2]. The complexity of these phenomena is amplified by the large number of cells required within a fuel cell stack to meet specific power demands. The interactions among multiple components and dynamic operational conditions necessitate simulation tools capable of capturing multi-scale and

multi-physical phenomena. Typically, such detailed models require substantial computational resources, posing practical limitations for extensive parametric studies or optimisation processes. In this context, more recent studies advocate for innovative modelling approaches capable of integrating mechanical, thermal, and electrochemical phenomena to expedite design iterations [3]. Among them, several Equivalent Stiffness Models (ESMs) have been proposed in recent literature [3, 4].

Objectives: An ESM represents the mechanical behaviour of complex systems through simplified yet accurate stiffness formulations, significantly reducing computational costs but generally neglecting the nonlinear mechanical behaviour of the components. The nonlinearities are considered only in Fly et al.'s model [5], but with some limitations concerning the possibility of integrating more nonlinearities in series.

Material and methods: In this work, we reported the evaluation of the results obtained exploiting an ESM that originally integrates the nonlinear mechanical behaviours of the MEA components through selected constitutive models in the literature. Integrating the Newton-Raphson method makes it possible to update the equivalent stiffness of the Proton Exchange Membrane (PEM), Gas Diffusion Layers (GDLs) and sealants iteratively. Additionally, our approach permits the selection of various materials, components and operating conditions in each simulation, thereby correlating the influence of component-scale properties with the overall mechanical behaviour of the stack. The GDL constitutive model allows the inclusion of five different GDLs in the global framework: the 36AA, 36BB, H060, H23C7, and 22BB from the Carral et al.'s publications [5, 6]. The coefficients of the Mooney-Rivlin hyper-elastic model of five different materials (EPDM, ACM, NBR, FKM, and VMQ) for the sealants are collected from Cheon et al. [7]. Furthermore, the constitutive model used for the PEM concerns only the non-reinforced membrane Nafion112 but includes the influence of temperature and humidity on mechanical behaviour [8]. Finally, several materials for the other components are included in the model. In this way, the model allows for the evaluation of a wide range of combinations, enabling the design of several stack configurations (see Table 1).

Inputs	***Outputs***
Thermal conditions (6 cases)	*Variation of the stiffnesses*
GDL type (5 types)	*Stress vs strain of MEA components*
Sealant material (5 materials)	*Force vs Displacement*
PEM humidity (50%-90%)	*Pressures*
EPs material (3 materials)	*Contact resistance between BPP and GDL*
CCs material (3 materials)	*GDL porosity*
Insulator plates material (3 materials)	*Ideal tightening torque*
BPPs material (4 materials)	*Safety criteria for the tightening torque*
Number of cells	*Polarisation curves*

Table 1 - Inputs and outputs of the ESM.

Results: The model computes the deformation of individual components as well as that of the entire system, including thermal deformations and determines the ideal tightening torque. Furthermore, polarisation curves are generated to illustrate the performance under coupled mechanical, thermal and electrochemical influences.

Conclusions: This study highlights that this multiphysics ESM offers a versatile and efficient tool for the preliminary design of PEMFC stacks.

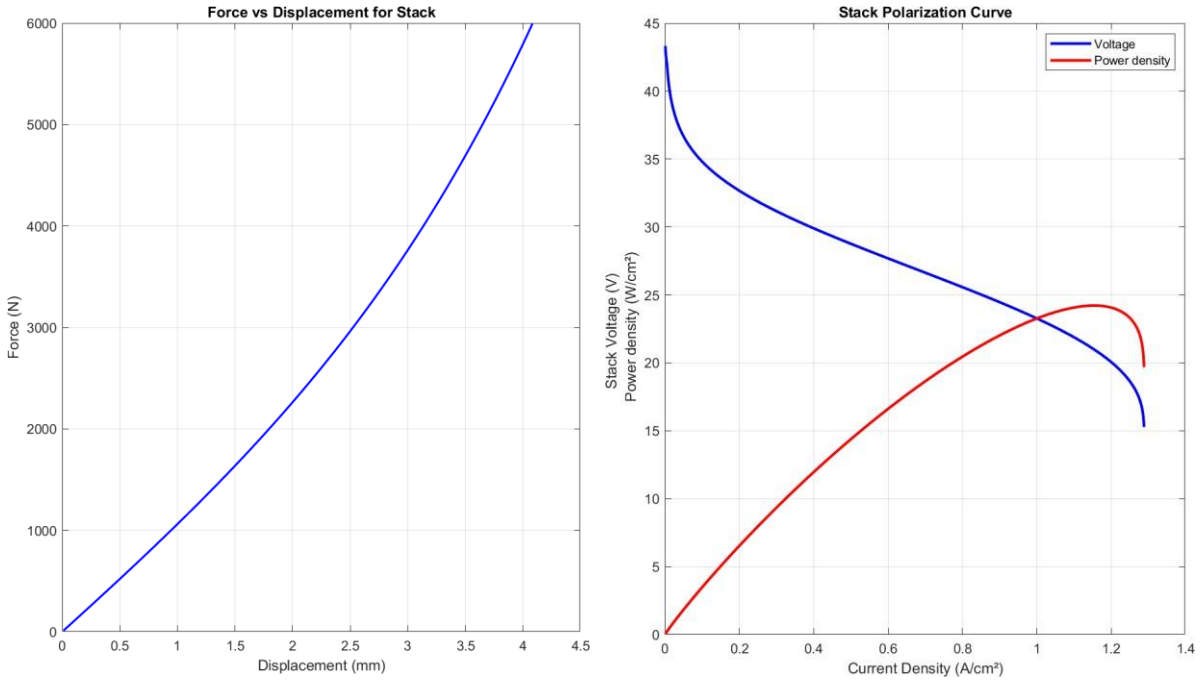


Figure 1 – Example of results for the following stack configuration: T_{amb}*=20°C;* $T_{active\ area}$*=80°C;* ***GDL:*** *H23C7;* ***Sealant material:*** *EPDM;* ***PEM humidity:*** *90%;* ***EP material:*** *Aluminium;* ***Insulator plates material:*** *Polymeric;* ***CCs material:*** *Copper;* ***BPPs material:*** *Graphite;* ***Number of cells:*** *50.*

References

[1] E. B. Agyekum et al., 2022, doi: 10.3390/membranes12111103.
[2] El Mahdi Khetabi et al., 2019, doi: 10.1016/j.jpowsour.2019.03.071.
[3] L. Marcelli et al., 2025, doi: 10.1016/j.ijhydene.2025.03.004.
[4] P. Lin et al., 2009, doi: 10.1016/j.jpowsour.2009.04.068.
[5] A. Fly et al., 2018, doi: 10.1115/1.4039141.
[6] C. Carral et al., 2022, doi: 10.1016/j.ijhydene.2022.05.121.
[7] M. Ouerghemmi et al., 2024, doi: 10.1016/j.ijhydene.2024.04.200.
[8] K.-M. Cheon et al., 2022, doi: 10.3390/en15072580.
[9] A. Kusoglu et al., 2009, doi: 10.1115/1.2971069.

European Fuel Cells and Hydrogen
PIERO LUNGHI CONFERENCE
September 17th–19th 2025
Capri / Italy

An oriented green approach to the Matrix Fabrication for Molten Carbonate Cells (MCCs)

Irfan*[a], Davide Astiaso Garcia[a], Massimiliano Della Pietra[b], Stefano Frangini[b]

* corresponding author: Irfan

[a] Department of Astronautical Electrical and Energy Engineering, Sapienza

University of Rome

Email: irfan.chemicalengg@gmail.com

Email: davide.astiasogarcia@uniroma1.it

[b] Department of Energy Technologies and Renewable Sources, Laboratory for Hydrogen and new Energy Vectors (TERIN-DEC-H2V), ENEA Italian National Agency for Energy, NewTechnologies and Sustainable Economic Development, C.R. Casaccia, Rome, Italy.

Email: massimiliano.dellapietra@enea.it

Email: stefano.frangini@enea.it

Keywords: Ceramic powder,Matrix,Porosity,Tape casting

Introduction:

The matrix acts as a basic component in molten carbonate cells (MCCs) [1]supporting the electrolyte and providing a separation medium between anode and cathode. The matrix must have certain types of properties (1) efficient mechanical strength (2) good capillary action to retain electrolyte (3) gas sealing properties (4) pore size <1µm with total porosity between 40-70%[2].

Matrixes for Molten Carbonate fuel Cells (MCFCs) are usually fabricated by the tape casting technique. The most important step in matrix tape casting is slurry preparation. Gamma lithium aluminate powder is typically the ceramic material used in the slurry formulation along with different types of reagents like plasticizer, binder, dispersant, solvent and defoamer for uniform preparation of slurry. The correct selection of the reagents, their amount and their mode of mixing in the slurry is crucial because it affects the final quality of the matrix tapes. Recent research efforts basically focus on the optimization of the matrix

structure and its functional performance, through improvements in slurry compositions and addition of mechanical reinforcement agents but little attention has been devoted to improve the sustainability of the slurry chemistry using less hazardous chemicals. Therefore in this study we mainly focus on oriented green approach for fabricating an efficient matrix with good flexibility, plastic behavior, and optimum porosity using all green chemicals that have no adverse effects on the environment. With the current tape casting technology matrix thickness is limited to about 250-300 µm in thickness, which means that several matrix layers (2-3layers) must be put together in real MCC systems to fabricate an effective separator component. However, a layered matrix structure is believed to be deleterious for high performance since additional contact resistance will be created in the layer discontinuities. Thus, a second purpose of our work is also fabricating a robust, thick matrix of 600-700µm in order to produce a single layer separator with higher performance. The surface morphology was examined using SEM, and phase structure was checked by using XRD analysis, Particle size analyzer was used to check the particle size of commercial gamma lithium aluminate powder. Viscosity of the slurry was analyzed to control the rheological properties of the slurries. With our green and advanced slurry formulations, various tapes with thicknesses ranging from 300 to 700µm were fabricated with good flexibility, plastic behavior, and optimum porosity.

Objectives:

The main objectives of this research are listed below:

- An oriented green approach for fabrication of various types of matrix tapes with various thicknesses ranging from 300 to 700 µm.
- Scanning Electron Microscope (SEM) technique was used to study the surface morphology of the fabricated tapes.
- X-ray Power diffraction technique (XRD) was used to compare the peaks of the commercial gamma aluminate powder and sintered powder.
- Viscosity of the slurries was checked in order to examine the rheological properties of the slurries.

Materials and methods:

Commercial, high surface area ceramic powder (gamma lithium aluminate) was used as the primary matrix material. The powder was carefully sieved to remove any lumps and agglomerates before use. A binder material (e.g., polyvinyl butyral (PVB), was used to hold the particles together during the casting and drying process. The binder provides green strength to the tape before sintering. A plasticizer, such as Polyethylene glycol (PEG-200) and Polyethylene glycol (PEG-400), were used to increase the flexibility of the

green tape during the fabrication process. Eco-friendly and cheap solvent as commercial ethanol was used to dissolve the binder and plasticizer, forming a slurry. To ensure uniform dispersion of powder particles and prevent agglomeration, dispersants such as commercial DisperByk was used. A PFAS- free commercial Agitan defoamer was added for air degassing. A planetary mixer was used instead of the most commonly used ball miller mixers to enhance process sustainability by minimizing materials and electric power wastes. Finally the slurry was then manually deposited on a simple table top laboratory mini-tape caster equipped with a single doctor blade moving tool. Post-processing warm rolling was usually applied for improved tape surface flateness.

Results:

- Various matrixes with good flexibility, efficient plastic behavior and optimum porosity were obtained. Viscosity of the slurries was checked and it was examined that the slurries behaves as pseudo plastic behavior. XRD Characterization technique was performed for the commercial and sintered gamma aluminate powder and observed the consistency in the peaks. Scanning Electron Microscope (SEM) was used to check the surface morphology of the fabricated matrix. Particle size of the gamma aluminate powder was checked with the particle size analyzer and found that there was consistency in the particle size.

Conclusions:

In conclusion, the tape casting fabrication of MCC electrolyte matrix using an improved and green oriented approach for the slurry formulation has demonstrated promising results in terms of material characteristics and processing. The X-ray diffraction (XRD) analysis revealed absence of hydrolysis reaction of gamma lithium aluminate powder with water contained in the commercial ethanol during the slurry preparation. The Scanning Electron Microscopy (SEM) images provided valuable insights into the microstructure, showing uniform distribution and consistent morphology of the particles within the matrix.

Acknowledgment:

One of the authors (Irfan) expresses his gratitude to both Sapienza University and ENEA for the financial support of his PhD studies and for the continued technical/scientific assistance providing during his work. Special thanks also to Livia Della Seta in performing SEM/EDX analysis, Beatrice Celata for XRD analysis and to Silvia Lo Conte for her kind guidance in the initial matrix testing experiments.

References

[1] J. J. Lee, H. J. Choi, S. H. Hyun, and H. C. Im, “Characteristics of aluminum-reinforced γ-LiAlO2 matrices for molten carbonate fuel cells,” *J. Power Sources*, vol. 179, no. 2, pp. 504–510, 2008.

[2] H. LIN, B. lian YI, L. ZHOU, C. HE, L. ying KONG, and E. jun ZHANG, “A Study on the Performance of Matrix Prepared by Tape Cast and Its Molten Carbonate Fuel Cells (MCFCS),” *J. Electrochem.*, vol. 7, no. 1, 2001.



Membrane-Electrode Interactions in PEM Fuel Cells: The Role of Ionomers in Hydrocarbon-Based Membranes

Carlo De Luca*[a,c], Emmanuel De Gregorio[b,c], Giuseppina Roviello[b], Claudio Ferone[b], Elio Jannelli[b], Valentina Naticchioni[c], Viviana Cigolotti[c], Martina Butori[d], Björn Eriksson[d], Rakel W. Lindström[d], Oreste Tarallo[a]

* corresponding author: carlo.deluca2@unina.it

[a] University of Naples Federico II, Department of Chemical Sciences, Complesso Universitario di Monte Sant'Angelo, 80126 Naples (Italy)

[b] University of Naples Parthenope, Department of Engineering, Centro Direzionale Isola C4, 80133 Naples (Italy)

[c] ENEA - Italian National Agency for New Technologies, Energy and Sustainable Economic Development, Via Anguillarese 301, 00123 Rome (Italy)

[d] KTH Royal Institute of Technology, Department of Chemical Engineering/Applied Electrochemistry, SE-100 44 Stockholm (Sweden)

Keywords: Fluorine-free polymers, Hydrocarbon-based membranes, Poly(phenylene oxide), Single Cell testing

Introduction:

In recent years, hydrocarbon-based membranes have emerged as a promising alternative to perfluorosulfonic acid (PFSA) membranes such as Nafion® for use in proton exchange membrane fuel cell (PEMFCs). These materials offer a molecular architecture that can be tailored to fine-tune properties like ion-exchange capacity, water uptake, and mechanical strength [1]. They also present cost advantages and improved thermal and oxidative stability, both critical for long-term performance and next-generation fuel cell demands. Unlike PFSAs, hydrocarbon membranes maintain high performance over a wider range of humidity and temperature, making them attractive for cars and portable devices [2]. One example is Pemion®, a fluorine-free, fully hydrocarbon polymer pairing high proton conductivity with strong chemical durability [3]. Within this class of materials, poly(phenylene oxide) (PPO) is especially promising: its aromatic backbone gives it excellent thermal and mechanical stability, and simple sulfonation procedures allow its functionalization with proton-conducting groups without compromising the polymer's structural integrity.

Objectives:

This study aims to investigate how the compatibility between ionomers and hydrocarbon-based membranes based on sulfonated poly(phenylene oxide) (sPPO) influences membrane-electrode interactions and overall fuel cell performance. Specifically, it seeks to (i) evaluate the electrochemical behavior of sPPO membranes in MEAs, (ii) compare the impact of Nafion®, Pemion®, and sPPO ionomers on proton transport and resistance, and (iii) identify strategies to enhance the efficiency of fully hydrocarbon-based PEMFC systems.

Material and methods:

sPPO membranes with an average IEC of 2 meq/g (80 um thickness) were prepared from commercial PPO powders via solution casting and a subsequent solid state sulfonation procedure. The membranes were then coated with a Pt based catalyst (40% wt. Pt on C, Tanaka) using an automated system (Sonotek) to create catalyst-coated membranes (CCMs). Membrane-electrode assemblies (MEAs) with Nafion® (sPPO/Nafion), Pemion® (sPPO/Pemion), and sPPO (sPPO/sPPO) ionomers were prepared with an I/C ratio of 0.3, 0.2, and 0.2, respectively. The MEAs were tested in single-cell PEM fuel cells (0.95 cm^2 of active area, Fuel Cell Technology Inc.) using a Gamry 5000E potentiostat. EIS and polarization curves were collected under various humidity and temperature conditions to evaluate proton conductivity, stability, and overall performance.

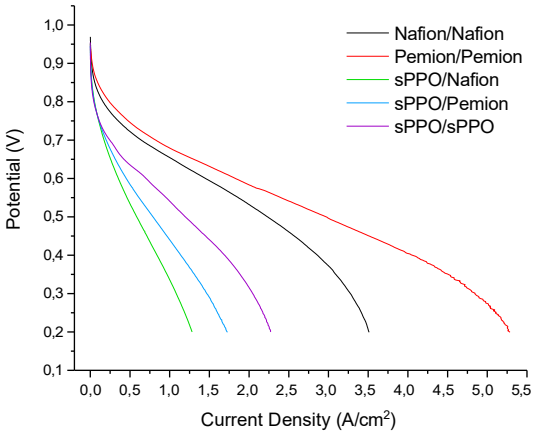
Results:

Fig. 1 shows polarization curves for the different MEAs obtained. Overall, sPPO based MEAs show lower performance in respect the Nafion/Nafion and Pemion/Pemion benchmarks, yet the all-sPPO MEA clearly outperforms the mixed pairs (sPPO/Nafion and sPPO/Pemion), especially above 1 A cm^{-2}, highlighting that matching the membrane and ionomer chemistry is crucial, especially under demanding operating conditions. EIS and conductivity data (Fig. 2 and 3) highlight the promising potential of sPPO-based membranes for high-performance applications: the sPPO/sPPO MEA shows the lowest high-frequency resistance (0.108 Ω cm^2) and a highest proton conductivity (74 mS cm^{-1}) that is even higher than that recorded for the Nafion/Nafion control. In contrast, the sPPO/Nafion MEA had the worst high-frequency resistance and the lowest conductivity (22 mS cm^{-1}).

Conclusions:

sPPO membranes were developed as PFAS-free alternatives for PEMFCs. Three series of membrane–electrode assemblies were prepared, each incorporating an identical sPPO membrane but employing Nafion®, Pemion®, or sPPO as the ionomer in the catalyst layers. All configurations exhibited satisfactory proton conductivity across a broad range of temperature and humidity; however, the sPPO/sPPO MEA delivered the highest overall

performance. These better results were attributed to the chemical homogeneity between membrane and ionomer, which promotes a more efficient membrane–catalyst interface. The findings underscore the critical role of membrane–ionomer compatibility and confirm the promise of fully hydrocarbon, PFAS-free systems for next-generation PEMFC applications.



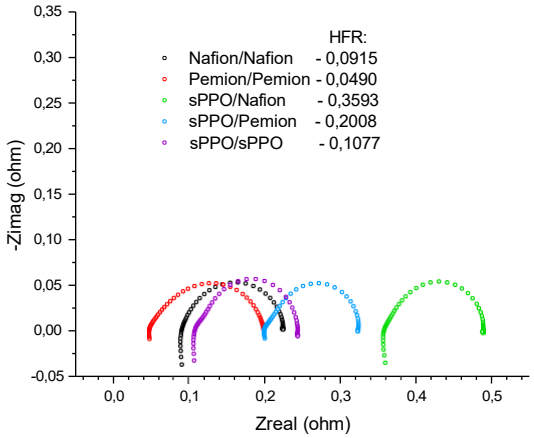


Fig.1 - Polarization curves (80°C, 70% R.H.). *Fig.2 - GEIS recorded at 0.5 A/cm² from 1MHz to 1 Hz (80°C, 70% R.H.)*

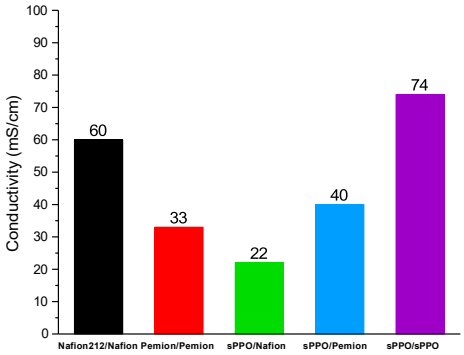


Fig.3 - Proton conductivity of MEAs (70% R.H.) obtained by GEIS collected at 1 A/cm².

References

[1] Mauritz et al., **2004**, Chemical Reviews, 104, 4535–4585.
[2] Zhang et al., **2012**, Chemical Reviews, 112, 2780–2832.
[3] Holdcroft et al., **2021**, Sustainable Energy & Fuels, 5, 2580–2588.

European Fuel Cells and Hydrogen
PIERO LUNGHI CONFERENCE
September 17th–19th 2025
Capri / Italy

Numerical analysis of an optimised serpentine HTPEM Fuel Cell with BP-integrated cooling channels

V. K. Krastev*[a], M. Baldelli [b], L. Bartolucci[b], F. Donato[c], M. Kheir Rouz[b] and V. Mulone[b]

*Corresponding author: krastev@dii.uniroma2.it
[a] Enterprise Engineering Department, University of Rome "Tor Vergata", 00133 Rome, Italy
[b] Industrial Engineering Department, University of Rome "Tor Vergata", 00133 Rome, Italy
[c] Energy Technologies Department, ENEA, 00123, Rome, Italy

Keywords: HTPEM, Fuel Cell, Cooling Channels, CFD

Abstract

Introduction: In HTPEM Fuel Cells, management and control of thermal fluxes is crucial, both during cold start-ups and at rated power operation [1–3]. While low-power applications can be usually managed with different forms of air cooling solutions, for stack applications above 2 kW_e thermal control through liquid cooling is preferable [4]. Serpentine-type channels allow for a more uniform coolant distribution, but they tend to produce excessive backpressure levels even at moderate flow rates. Therefore, in high-power stacks straight channels or mixed serpentine-straight channels are needed, which may be included in separate cooling plates or directly integrated within the stack Bipolar Plates (BP) [4].

Objectives: The present work applies CFD modelling to evaluate the performances of a liquid-cooled single HTPEM Fuel Cell, with BP-integrated coolant channels and a 45 cm^2 MEA. The cell flow-fields have been previously optimised to reduce differential pressure acting on the MEA and to improve the reactant distribution uniformity [5]. The final goal of this research activity is to develop a combined numerical-experimental framework for the optimisation of liquid-cooled HTPEM stacks, within the POR-H2 project.

Material and methods: The analysis has been made on a three-dimensional single cell model configuration. The computational domain includes the membrane, Catalyst Layers (CLs), Microporous Layers (MPLs), Gas Diffusion Layers (GDLs), BPs and cooling channels. Figure 1 shows details on the coolant and gas channels arrangement. The domain is discretized using a hybrid unstructured grid with a total of 10M elements. The fluid flow, energy and electrochemistry equations are solved numerically through the PEMFC module of the Ansys® Fluent commercial CFD code [6].

Results: a preliminary set of runs has been made to evaluate the pressure drop trend in coolant channels. The chosen coolant fluid is a paraffinic oil for high temperature applications. Figure 2a shows the pressure drop trends at the anode and cathode side, for flow rates ranging from 0.25 to 1.5 l/min.

When the flow rate goes above 1 l/min, the backpressure exceeds the capacity of the coolant circulation pump which has been selected for the HTPEM stack experimental activity. As such, the maximum allowable coolant flow rate has been set at 1 l/min.

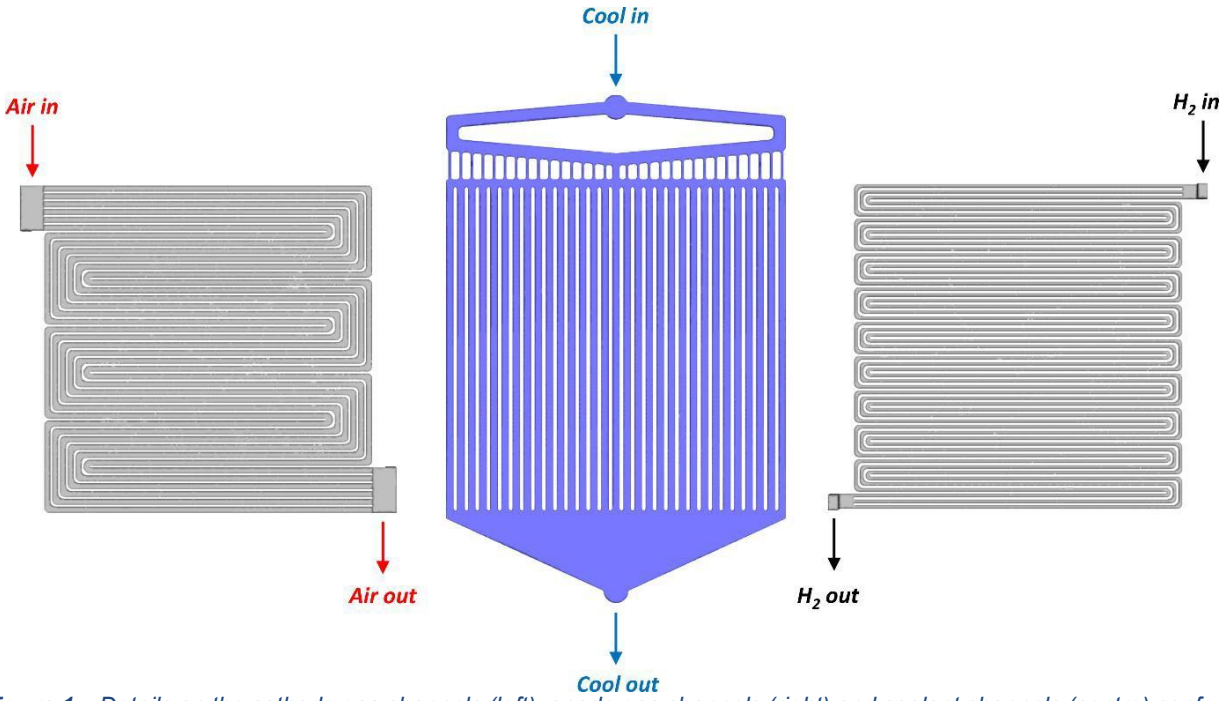
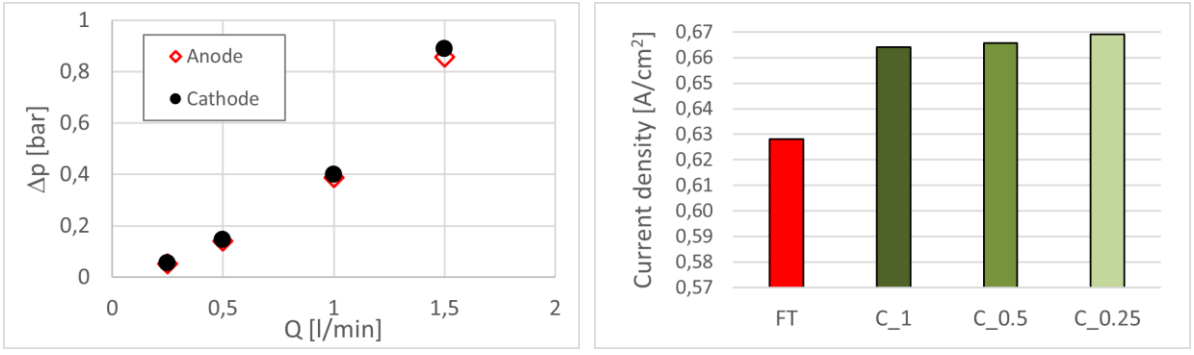


Figure 1 – *Details on the cathode gas channels (left), anode gas channels (right) and coolant channels (centre) confgurations. The coolant channels geometry is the same for the cathode and anode side.*



(a) (b)

Figure 2 – a) *pressure drop trend in the coolant channels;* ***b)*** *MEA-averaged current density comparison between the Fixed Temperature and coolant channel cases at different coolant flow rates.*

Figure 2b compares different coolinng strategies and coolant flow rates, in terms of the MEA-averaged current density. Simulations have been carried out at a cell voltage of 0.5 V, with reactant gases entering their respective channels at 120 °C and 1 atm. Gas flow rates are calculated based on their respective stoichiometries (1.2 for the anode, 2 for the cathode) and on a reference current density of 1 A/cm^2. The coolant channel strategy is compared against a simple fixed temperature (FT) boundary condition imposed at the cell terminals. The latter assumes a uniform temperature

distribution equal to the cell nominal operating temperature (T_n = 160 °C). The coolant itself enters the doman at $T=T_n$. Results show that the coolant channels strategy allows for higher current densities, which is linked to a higher average MEA effective temperature. Additionally, lower coolant flow rates produce slightly higher current densities, which might be taken into account to balance pressure drop requirements with the MEA long-term response to higher thermal stresses.

Conclusions: The proposed single-cell analysis showed that a BP-integrated cooling channel design is effective in controlling and maintaining optimal MEA temperature conditions in HTPEM Fuel Cell applications. The coolant flow rate must be kept as low as possible to avoid excessive backpressures, but additional care is required at higher current density operating conditions to limit the temperature rise within the MEA assembly. Further research activity is ongoing to explore different gas vs. coolant flow arrangements (see Fig. 1) and operating points. A full 5-cell liquid-cooled stack model is also under development.

Acknowledgments

This research has been funded by the European Union – NextGeneration EU and by the Italian Ministry of Environment and Energy Security, POR H2 AdP MEES/ENEA with involvement of CNR and RSE, PNRR - Mission 2, Component 2, Investment 3.5 "Ricerca e sviluppo sull'idrogeno" WP 3.1 LA 3.1.4 "Gestione e validazione dell'ingegneria di stack di celle a combustibile a membrana polimerica".

References

[1] E.H. Reddy, S. Jayanti, D.S. Monder, Thermal management of high temperature polymer electrolyte membrane fuel cell stacks in the power range of 1-10 kWe, Int J Hydrogen Energy 39 (2014) 20127–20138. https://doi.org/10.1016/j.ijhydene.2014.09.132.

[2] H. Huang, Y. Zhou, H. Deng, X. Xie, Q. Du, Y. Yin, K. Jiao, Modeling of high temperature proton exchange membrane fuel cell start-up processes, Int J Hydrogen Energy 41 (2016) 3113–3127. https://doi.org/10.1016/j.ijhydene.2015.12.134.

[3] G. Varghese, V. Babu K.P., T.V. Joseph, P. Chippar, A Numerical Investigation on Thermal Gradients and Stresses in High Temperature PEM Fuel Cell During Start-up, Int J Heat Mass Transf 175 (2021). https://doi.org/10.1016/j.ijheatmasstransfer.2021.121365.

[4] M.H.S. Bargal, M.A.A. Abdelkareem, Q. Tao, J. Li, J. Shi, Y. Wang, Liquid cooling techniques in proton exchange membrane fuel cell stacks: A detailed survey, Alexandria Engineering Journal 59 (2020) 635–655. https://doi.org/10.1016/j.aej.2020.02.005.

[5] V.K. Krastev, M. Baldelli, L. Bartolucci, F. Donato, M. Kheir Rouz, V. Mulone, Optimal cathode design of a single HTPEM Fuel Cell: a computational study, Accepted for Publication in the International Journal of Hydrogen Energy (2025).

[6] Ansys Inc., ANSYS® Academic Research CFD, Release 2024 R1, Fluent User's Guide, 2024. http://www.ansys.com.

EFCH2 2025 European Fuel Cells and Hydrogen PIERO LUNGHI CONFERENCE
September 17th–19th 2025 Capri / Italy

Dynamic modelling of sofc systems for hybrid maritime solutions

Massimo Rivarolo*,[a], Ahmed G. Elkafas [a], Stefano Barberis [a], Luca Mantelli [a]
* corresponding author: massimo.rivarolo@unige.it
[a] Thermochemical Power Group (TPG)-DIME, via Montallegro 1, University of Genoa (IT)

Keywords: Solid Oxide Fuel Cells, Maritime Hybridization, dynamic analysis, control systems.

Abstract

This paper investigates an innovative hybrid system integrating pressurized Solid Oxide Fuel Cells (SOFC) and Internal Combustion Engines (ICE), both fuelled by natural gas onboard passenger ships. The ICE is employed during for main propulsion, while the SOFC operates to satisfy hotel loads both in cruise and in port. A dynamic model was developed and the results are presented for a short-sea vessel operating in Sardinia (Italy), investigating the behaviour of the system when the vessel enters port, the ICE is shut-down and during SOFC transients.

Introduction: The importance reducing emissions from the maritime transportation sector is widely recognized, both for CO_2 and pollutants as NO_x and SO_x [1]. This aspect underlines the opportunity for innovative technologies, such as fuel cells. Solid Oxide Fuel Cells (SOFC) have a very high efficiency (50-55%), low noise and zero SO_x, NO_x emissions. Moreover, thanks to their high operating temperature, they present interesting opportunities also for waste heat recovery and thermal integration with other components, such as internal combustion engines (ICE) [2]. However, they cannot be employed as main generator of propulsive power as they are limited by many factors, such as high thermal capacity and consequential slow transients. Thus, their application for maritime is to provide auxiliary power and hotel load demand, which is quite constant. In this research, an integrated SOFC-ICE system, where the off-gases from the SOFC are employed in the main ICE, is investigated.

Objectives: The analysis is carried out considering a real case study, the short sea passenger vessel *Anna Mur* operating in Sardinia (Italy), already investigated by the Authors in previous studies [3][4]. The installed power is 1.2 MW, with 960 kW from ICE and 240 kW from four pressurised SOFC modules (60 kW each). The vessel operates between Porto Vesme (Sardinia) and San Pietro island: the estimation for energy demands in port and in cruise are reported in Figure 1. The aim of this research is to simulate the behaviour of the system, with particular focus on the SOFC, when the ship is entering port, the ICE is not operating and the SOFC modules are operating in transient conditions.



Figure 1. Estimated power demands in port and cruise conditions.

Material and methods: The study is carried out by using the in-house TRANSEO simulation tool, developed by the Thermochemical Power Group (TPG) for the transient and dynamic simulation of energy systems [4], to model the different components and simulate the turbocharged SOFC system. The current research focuses on the definition and implementation of components and logics for the transition between the operation of the SOFC system between navigation and port, and to manage SOFC power load variations when the ship is docked in the port. SOFC power transients during navigation are not investigated because the SOFC is always supposed to work at nominal load, with any variation in power demand covered by the ICE. The plant layout is reported in Figure 2. According to the different energy demands and navigation modes (port, cruise), the Anode Off-Gases (AOG) from SOFC can be used in the ICE (cruise operation) or recirculated to the SOFC (only the SOFC is operating in port to limit emissions) throughout the three-way Butterfly Valves (BV).

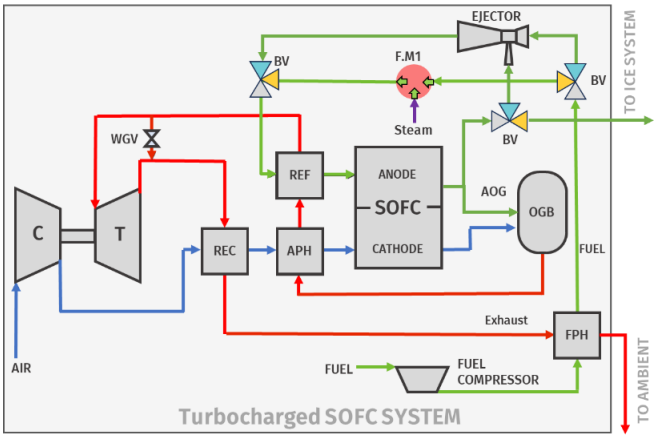


Figure 2. Plant layout for integration of turbocharged SOFC and ICE systems.

To operate the valves and manage the transition, a signal named *PortNav* was defined, as follows:

- When the ship is in navigation: *PortNav* = 0, the BV valves exclude the ejector from the anode loop (FO = 0), leading the AOG from the SOFC to the ICE through the yellow ports in Figure 2.
- When the ship in port: *PortNav* = 1, the valves connect the ejector to the anode loop through the teal ports in Figure 2, and cut off the SOFC anode outlet flow from the ICE.
- During transitions, *PortNav* varies in the [0-1] range.

Depending on the SOFC power load and the value of *PortNav*, the steam flow is adjusted to guarantee desired conditions in the reformer, i.e., steam-to-carbon ratio over 2.25. The controller system regulating the SOFC temperature is not implemented yet, and its design will be based on the outcomes of the present study. The model has been tested to verify its capability to properly manage the transition between navigation and port modes, as well as to perform power load changes inside the port. It is important to highlight that all the components of the SOFC system have been developed and validated in previous research by the Authors' research group [6].

Results: The simulation from navigation to port was performed at maximum load for SOFC, corresponding to a nominal current density of 0.239 A/cm^2. After 10 s, the transition started, changing the value of *PortNav* from 0 to 1 over 60s. Then, the response of the system was observed for 230s, reaching a total simulation time of 300s. Figure 3 (left) shows how the SOFC performance changes when the system shifts from navigation to port mode. The mass flow and pressure ratio of the

compressor are affected by the energy content of the flow entering the turbine, which changes between the two modes. This effect determines the variations of power generated by the fuel cell, which will be more limited after the implementation of a temperature control system on the SOFC.

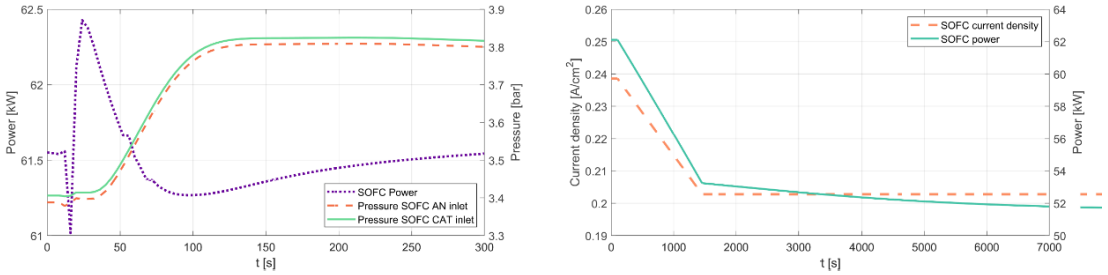


Figure 3. Variations of SOFC inlet pressures and total power during the transition from navigation to port mode (left) and Variations of SOFC current density and total power during load reduction (right).

The model was then tested to verify its capability to simulate the SOFC system during power load transients in port mode, as well as to observe its response in terms of mass flows, temperatures, pressures, etc., considering a current density ramp from 100% to 85% of the nominal value over 1350 s. As shown in Figure 3 (right), even if the reduction of generated power follows closely the trend of current, it takes a long time to reach a steady value after the end of the ramp. This behaviour was expected, being consistent with the high thermal capacity of the SOFC stack and will be less pronounced when thermal management logics are implemented on the system.

Conclusions: This study demonstrated the capabilities of the dynamic model developed by TPG to simulate the SOFC module of a SOFC-ICE hybrid system for marine applications. The transition between navigation and port mode was successfully managed acting on a set of 3-way valves and controlling the external steam flow. A power transient was also simulated, highlighting the slow thermal dynamics of the SOFC and how they affect the transient performance of the whole system. The outcomes of this analysis will be used to design an effective temperature control system capable of improving the responsiveness of the SOFC.

Acknowledgments: The Authors acknowledge the SOFFHICE (SOFC Hybridization with Internal Combustion Engine fuelled by Natural gas for maritime applications), Prot. P2022K3TMP, funded by the European Union – NextGenerationEU, under the National Recovery and Resilience Plan (PNRR), Mission 4 Component 2 Investment 1.1 – National Program of Research (PNR) and Research Projects of Relevant National Interest (PRIN), Call for tender n. 1409 of 14-9-2022 of University and Research Ministry (MUR).

References

[1] International Maritime Organization official website, accessed 19/05/2025, https://www.imo.org/
[2] Güler E, Ergin S, Investigation of a solid oxide fuel cell integrated into an internal combustion engine with carbon capture for maritime applications, En Conv and Management, 314 (2024), 118660.
[3] Elkafas AG, Mantelli L, Barberis S, Rivarolo M, Design performance analysis of a turbocharged solid oxide fuel cell integrated with internal combustion engine for maritime applications, Applied Thermal Eng, 272 (2025), 126335.
[4] Delcomar company official website, accessed 19/05/2025, https://delcomar.it/en/anna-mur-ferry/
[5] Thermochemical Power Group official website, accessed 19/05/2025, https://tpg.unige.eu/transeo/
[6] Mantelli L, Ferrari ML, Magistri L, Off-design performance analysis of a turbocharged solid oxide fuel cell system, Appl Thermal Eng 183 (2021) 116134.

European Fuel Cells and Hydrogen
PIERO LUNGHI CONFERENCE
September 17th–19th 2025
Capri / Italy

A multi-criteria approach to evaluate the use of solid oxide fuel cells (sofc) onboard vessels

Simone Piccardo *,[a], Ahmed G. Elkafas [a], Ahmed M. A. Saadeldin [a], Stefano Barberis [a], Massimo Rivarolo [a]

* corresponding author: simone.piccardo@edu.unige.it

[a] Thermochemical Power Group (TPG)-DIME, via Montallegro 1, University of Genoa (IT)

Keywords: Solid Oxide Fuel Cells, Maritime Hybridization, multi-criteria analysis, emissions' reduction.

Abstract

This study explores the potential of a hybrid system integrating pressurized Solid Oxide Fuel Cells (SOFC) and Internal Combustion Engines (ICE), both fuelled by natural gas onboard passenger vessels. The SOFC is employed as Auxiliary Power Unit (APU) to satisfy the hotel load both during cruise and in harbour, while the ICE operates to guarantee propulsion in navigation. A multi-criteria analysis is performed to evaluate the technical, environmental and economic performance for a passenger vessel, also comparing the proposed solution with the state-of-the-art ones.

Introduction: In 2023 the International Maritime Organization (IMO) has published its strategy to cut GHG emissions in the maritime sector and in 2024 [1] the Emission Trading System to regulate GHG has been extended to large ships, over 5,000 GT (gross tonnage) [2]. This suggests the opportunity for new technologies with alternative low-carbon fuels, i.e. fuel cells. In this research, the possibility of installing SOFC and ICE, both fed by CH_4 or bio-CH_4, is evaluated, considering a multi-criteria comparison with the state-of-the-art solution, represented by ICE fed by Marine Gas Oil (MGO).

Objectives: The in-house software tool HELM (Helper for Energy Layouts in Maritime applications), developed by Thermochemical Power Group [3], allows for performing a multi-criteria analysis to compare different solutions for energy storage and generation onboard different passenger vessels, to demonstrate the performance and emission reduction benefits of SOFC and ICE fed by natural gas in real case study. Although the use of ICE-LNG is already well known to reduce emissions compared to ICE-MGO, SOFC can represent an interesting technology due to high efficiency, low noise and zero pollutant emissions (NOx, SOx, PM). The study aims to analyse their possible application to satisfy the hotel loads for different passenger vessels, as the electrical energy consumption for auxiliaries on this ship type is significant, in particular for the larger ones (5,000 GT). In a detailed study recently conducted by the Authors on a short-sea passenger vessel, operating in Sardinia island, the importance of choosing a case study with a high number of operational hours, also avoiding as much as possible SOFC shutdowns that would negatively affect their lifetime, was highlighted [4].

Material and methods: In maritime applications, the identification of the most promising technologies must take into account various key parameters on which the multicriteria assessment should be based (e.g. costs, GHG and NOx emissions, volumes, weights, and fuel environmental hazards). The main inputs are represented by the vessel's energy requirements—including installed power, operational power, and operating hours. These variables enable the determination of absolute values for key parameters of each technology, based on correlations derived from an extensive

database of commercially available solutions. Additional inputs—such as vessel type and dimensions, navigation characteristics, fuel prices—are also considered. Together, these factors contribute to assigning a score to each technology for each key parameter. The overall score for each technology is then determined by summing the individual parameter scores, thereby completing the comparative evaluation process. The technology solutions assessed consist of a combination of storage systems, power units, batteries (where applicable), and exhaust after-treatment systems. HELM takes into account a wide range of technologies, each thoroughly characterized through editable parameters such as power unit efficiency, hydrogen storage pressure (for CH2), substitution rate (for dual-fuel ICE), and battery support in terms of energy demand, if required. Besides its large and up-to-date database, one of HELM greatest advantages is represented by the modular structure, which allows including both new technologies and updating performance maps easily, without modifying the core of the software.

Results: A real case study was simulated, based on a ferry with an approximate gross tonnage of 27,500 GT. The vessel has a capacity of 936 passengers and 170 cars, and is equipped with an installed propulsion power of 21,600 kW. This is provided by two four-stroke main engines, which are directly coupled to the propellers via gearboxes. For the purposes of this study, the auxiliary power requirement was estimated at approximately 1,270 kW, with an operational range of 48 hours. The main results in terms of performance scores are presented in Figure 1. As highlighted in Figure 2, when focusing on volume, the power unit accounts for the largest share of total volume in the case of SOFCs. However, PEMFCs exhibit the highest overall volume requirements due to the substantial space needed for H_2 storages, which negatively impact their volume score. When ICEs are included in the comparison, their low power unit volume utilization provides a significant advantage. From a cost perspective, SOFCs can compete with ICEs due to high efficiency, resulting to significant fuel savings. In contrast, the high cost of H_2 negatively impacts the economic viability of PEMFCs. Furthermore, in this context, SOFCs enable an annual reduction of approximately 87.4 tons of NOx emissions compared to conventional ICEs powered by MDO.



Figure 1: Total scores from the HELM's output interface

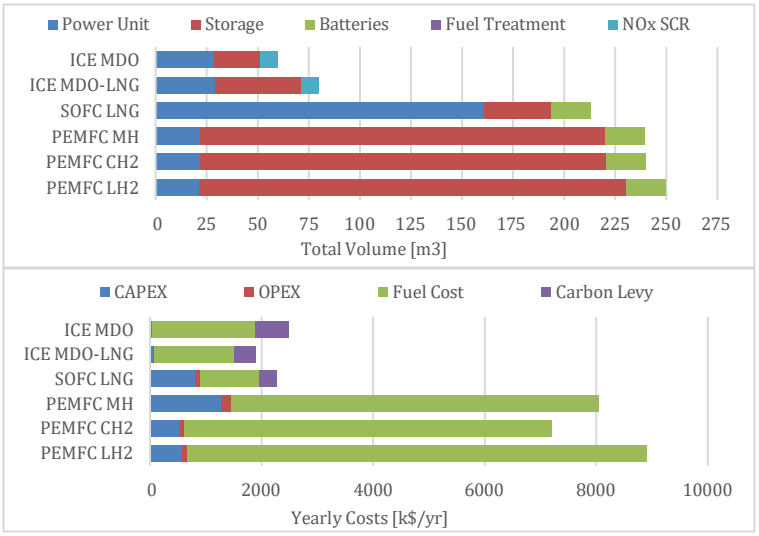


Figure 2: Absolute volume and cost values for the focused technologies

The high efficiency of SOFCs allows for fuel savings and, consequently, reduced storage requirements—specifically when a long operational range is needed. For this reason, as shown in Figure 3, a sensitivity analysis was performed by simulating different operational ranges. As illustrated, SOFCs become the most promising fuel cell technology when the required operational range exceeds approximately 40 hours, due to their lower fuel consumption. However, ICEs remain the most promising overall solution although the performance gap between ICEs and fuel cells decreases as the operational range increases.

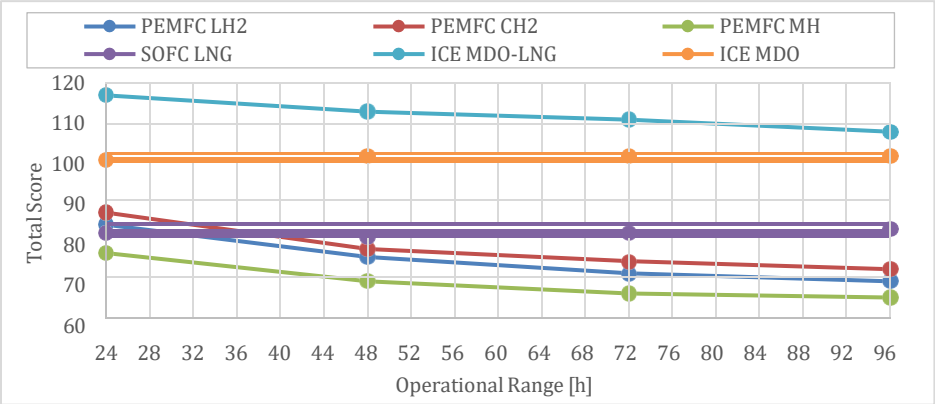


Figure 3. Effect of range modification on total score

Conclusions: The study demonstrates the feasibility of installing an SOFC system to manage the hotel loads of medium-sized ferries. In comparison with PEMFCs, SOFCs offer advantages in both cost and volume. However, ICEs still maintain a significant edge from these perspectives. Nonetheless, SOFCs enable a substantial reduction in NOx emissions, making them more suitable for operation in sensitive areas such as Emission Control Areas (ECAs). Furthermore, if high carbon levies are implemented, the lower GHGs of SOFCs could lead to additional cost savings. When longer operational ranges are considered, the high efficiency of SOFCs enables greater fuel savings, further narrowing the performance and economic gap with ICEs.

Acknowledgments: The Authors acknowledge the SOFFHICE (SOFC Hybridization with Internal Combustion Engine fuelled by Natural gas for maritime applications), Prot. P2022K3TMP, funded by the European Union – NextGenerationEU, under the National Recovery and Resilience Plan (PNRR), Mission 4 Component 2 Investment 1.1 – National Program of Research (PNR) and Research Projects of Relevant National Interest (PRIN), Call for tender n. 1409 of 14-9-2022 of University and Research Ministry (MUR).

References

[1] International Maritime Organization official website, accessed 06/05/2025, https://www.imo.org/

[2] European Commission official website, accessed 06/05/2025, https://climate.ec.europa.eu/eu-action/transport/reducing-emissions-shipping-sector_en

[3] Thermochemical Power Group official website, accessed 06/05/2025, www.tpg.unige.eu/helm/

[4] Elkafas AG, Rivarolo M, Barberis S, Massardo AF. TECHNO-ECONOMIC ASSESSMENT OF AN ADVANCED INTEGRATION BETWEEN SOFC AND ICE ONBOARD A SHORT-DISTANCE FERRY, Proceedings of ECOS 2024, 204-215.

[5] Rivarolo M, Piccardo S, Montagna GN, Bellotti D. A multi-criteria approach for comparing alternative fuels and energy systems onboard ships. Energy Conversion and Management: X 2023;20:100460. https://doi.org/10.1016/j.ecmx.2023.100460.

European Fuel Cells and Hydrogen
PIERO LUNGHI CONFERENCE
September 17th–19th 2025
Capri / Italy

Exploring the possibility of using hydrogen in po river inland waterways

Stefano Barberis *[,a], Massimo Rivarolo[a] ,Loredana Magistri [a],
* corresponding author: Stefano.barberis@unige.it
[a] Thermochemical Power Group (TPG)-DIME, via Montallegro 1, University of Genoa (IT)

Keywords: PEM Fuel Cell, Inland Waterways, Barges, Po River

Abstract

This study explores the possibility of using hydrogen in Po River inland waterways via a three fold approach. First of all the navigability of the Po River is assessed along its full length, assessing river depth and also the potential barges class that could navigate in such type of basins. Afterwards, a sensitivity analysis is performed to identify the potential FC power and hydrogen storage needs of a class IV barge targeting to navigate on the Po River. In the end, having identified the most suitable layout for a H_2 fuelled barge active on the river, the potential full hydrogen transition of the current Po River freight barges is analysed looking at the overall annual hydrogen demand and the potential investment needs in the River Basin area in terms of number of barges for a "H_2 ready fleet".

Introduction: Inland waterway transport (IWT) is recognized by its social, environmental, and economic advantages if compared with other transportation means [1]. Thanks to low navigation speed, limited water resistance and short navigations journey (particularly in EU Rivers) , power needs and fuel storage capacity of this type of vessels is not so significant [2], thus using hydrogen and FC in barges for freight active in IWT has been widely investigated [3] also via specific EU funded projects (like FLAGSHIPS [4]. The focus of this work (realized in the framework of RH2IWER project [5]) is on the Po River to analyse the possibility to use hydrogen to decarbonize the main Italian IWT segment.

Objectives: Starting from the navigability analysis of the Po River and having assessed the potential propulsion and hydrogen storage needs of a type IV barge for IWT, this study performed a preliminary sensitivity analysis to explore the possibility to transition to hydrogen of the whole freight operating in the Po River.

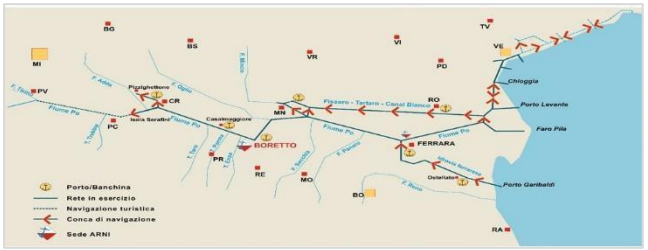


Figure 1. Schematic representation of the navigability of the Po River [6]

Material and methods: The Po River (Fig.1) can be navigated a systemic inland waterway (also considering its affluents) along 812 km , whereof 564 km can be navigated by IWT freight barges. The main IWT route is 280 km long (Cremona - faro Pila in Adriatic Sea) while other routes are significant for freight too like Idrovia Ferrarese(70 km) , Idrovia Fissero –Tartaro-Canale bianco (117km). Limitation in the navigation All in all around 1 Mt of goods are transported on Po river, mostly related to industrial and agricultural products of the area (like metals, chemicals, grain, crops…) and fuels. It

was acknowledged that Type IV and Type Va barges are the most suitable type of vessels that can operate thereby. The power need of the barges (and its dependency from navigation speed) are assessed via state of the art equations in order to evaluate the FC and the hydrogen storage preliminary features (from commercially available assets) and the impact on the payload of retrofitting/re-disegning one of this type of barges towards a Fuel Cell propulsion. Having identified, via a sensitivity analysis, the most strategic preliminary setup of the barge in terms of FC and H_2 storage capacity, the annual H_2 needs and the overall annual emission savings of transitioning to hydrogen the whole River Po freight sector is investigated. The IWT that goes from Isola Serafini/Cremona up to the Adriatic sea is considered (280 km) as well as the potential extension of this IWT (currently under realization) up to Mantova/Ticino (further 97 km)

Results: Due to limited width and depth of the river basin and the presence of bridges and piers, Type IV and Type Va barges [7] are the most suitable type of barges for Po River IWT navigation. Type IV barges will be analysed in this study, as the ones that can operated without any limitations in the whole Po IWT basins (including some affluents). This type of vessel has a DWT up to 1500 t, a maximum speed up to 16 km/h and typical engine speed that could span between 515 and 750 kW.

To calculate the power capacity of a barge engine the current literature equation can be considered

$$P_{engine} = \frac{k * \beta * T^{\frac{2}{3}} * V_{barge}{}^{3}}{\eta} \quad \text{(Eq.1) where:}$$

Where:

- k is a drag coefficient depending on the design of the barge and the type of cargo (typical value 0.005−0.01 for river barge) and influenced by the hull shape, hull surface roughness, and the overall hydrodynamic efficiency of the design. As for class IV, hydrodynamic optimization is not always a priority, and an average value of k=0.007 is a good initial estimation
- β expresses the relationship between the tonnage and barge's wetted area and it varies as a function of the hull geometry and the design of the barge. It is used to estimate the increase in hydrodynamic resistance as the load carried varies. For class IV β is typically around 5 and 10 t/m^2
- η is the overall efficiency of the propulsion system from engine to propeller (here assumed 0,9).

Eq.1 has been used to perform a sensitivity analysis (on speed [V - km/h] and DWT (T – t], in order to size the FC and the hydrogen storage for a journey along the 280 km of the IWT and assess the impact on the payload of the FC and hydrogen storage installation on board of the vessel, considering that both of them have to be installed on dry dock for safety reasons (as already done in other barges – Fig.2 [4]), thus limiting/reducing both payload and charging available surface of the barge.



Figure 2. Example of FC and hydrogen storage installation on board of a barge [4]

The goal of the sensitivity analysis has been to identify the specs of a barge that could be used as "Sample" towards the transition to hydrogen of the whole Po River IWT, thus targeting the setup of a potential "hydrogen fleet" able to transport 1 Mt/yr of goods with the minimum number of barges

(navigating back and forth along the year) and fleet consumption along the year [t/yr]. Such sensitivity analysis brought to "theoretical" values of FC Power capacity that were always scaled up/down to closer value of actual power capacity to be potentially installed on board via a modular approach calibrated (also to calculate H_2 consumption) on the performance values coming from the datasheet of commercial MARINE System 200 by PowerCell Group [8]. State of the art compressed hydrogen storage at 350 bar bundles (sizes, volume, weight) have been considered. The best case scenario identified a barge with the features reported in table below, with a reduced surface for goods transportation on the dry dock between 55 and 80 m^2 (~ 10% of the available surface)

Overall DWT[t]	Theoretical/Actual FC Power [kW]	Goods Payload [t]	Fleet barges	H2 consumption along the year [t]
1500	539,4/600	1484	5	407,5

Two further sensitivity analysis were performed also foreseeing: a) the possibility to increase the navigation journey to Mantova (377 km), b) the possibility of installing a HRS along the IWT and reduce the hydrogen storage capacity on board (but increasing the duration of the journey due to refuelling period), with no major impact on the identification of the above reported best sizing (except for H2 consumption for case a) the reduction of the number of barges in case b) thanks to higher payload, but considering slightly longer navigation journeys (~ 2hrs long refuelling period are considered).

Conclusions: At the end of this preliminary study, the following conclusions can be wrapped up. - Class IV barges can be easily integrated with FCH solutions: the payload does not significantly reduce with speed and tonnage (max 2÷5% variation) and drydock installations facilitate barges' setup also in terms of limited investments. Furthermore considering the current limited freight on Po river, fleets could be limited in terms of number of H_2 barges. Even the annual amount of H_2 needed does not seem to be particularly significant (400÷500 t/yr ➔ 25 MW electrolyser operating 8000 hr/yr), therefore potentially producible by a local electrolyser that could also operate in synergy with different Hard-to-Abate industries (as further off-takers) present in the area.

Co-funded by the European Clean Hydrogen Partnership

Acknowledgments: The Authors acknowledge financial support under the RH2IWER project which is supported by the Clean Hydrogen Join Undertaking (CHJU) and its members Hydrogen Europe and Hydrogen Europe Research. Views and opinions expressed are however those of the author(s) only and do not necessarily reflect those of the EU or CHJU. Neither the EU nor the granting authority can be held responsible for them.

References

[1] N. Calderón-Rivera et al., "Barriers and solutions for sustainable development of inland waterway transport: A literature review", Transport Economics and Management, 2024, https://doi.org/10.1016/j.team.2024.01.001

[2] H. Fan et al, "Two decades of hydrogen-powered ships (2000–2024): Evolution, challenges, and future perspectives", Renewable and Sustainable Energy Reviews, Volume 219, 2025, https://doi.org/10.1016/j.rser.2025.115878.

[3] Y. Wang et al., "Modelling environmental life cycle performance of alternative marine power configurations with an integrated experimental assessment approach: A case study of an inland passenger barge", Science of The Total Environment, Volume 947, 2024, https://doi.org/10.1016/j.scitotenv.2024.173661

[4] HORIZON 2020 FLAGSHIPS Project Official Website, Accessed: May. 01, 2025 [Online], Available: https://flagships.eu/

[5] HEU RH2iWER Project Official Website, Accessed: May. 01, 2025 [Online], Available: https://rh2iwer.eu/

[6] I. Galvani, AIPO, Navigazione e Bilancio Idrico,

[7] Istituto Italiano di Navigazione, 2011, LE UNITA' NAVALI PER IL SISTEMA IDROVIARIO ITALIANO

[8] PowerCell Group official website, Accessed: May. 01, 2025. [Online]. Available: https://powercellgroup.com/

European Fuel Cells and Hydrogen
PIERO LUNGHI CONFERENCE
September 17th–19th 2025
Capri / Italy

Manufacturing Approaches for Proton-Conducting SOCs

Angela Gondolini*[a], Elisa Mercadelli [a], Andrea Bartoletti [a], Massimiliano Lo Faro[b], Fabiana Matos de Oliveira[c], Sara Massardo[d], Sabrina Presto[d], Massimo Viviani[d], Martina Marasi[e], Alessandro Donazzi[e], Alessandra Sanson[a]

* corresponding author: angela.gondolini@issmc.cnr.it

[a] Institute of Science, Technology and Sustainability for Ceramics (ISSMC) of the National Research Council (CNR), Via Granarolo 64, I-48018 Faenza (RA), Italy;
[b] Institute for Advanced Energy Technologies "Nicola Giordano" (ITAE) of the National Research Council (CNR), Via Salita S. Lucia sopra Contesse 5, 98126 Messina, Italy;
[c] Instituto de Quimica de São Carlos - USP, Av. Trab. São-carlense, 400, Brazil;
[d] Institute of Condensed Matter Chemistry and Technologies for Energy (ICMATE), National Research Council (CNR), c/o DICCA-UniGe, Via all'Opera Pia 15, 16145 Genoa, GE, Italy;
[e] Department of Energy, Politecnico di Milano, Via Lambruschini, 4, 20156 Milano/Italy.

Keywords: Manufacturing, Proton conducting Cells, Tape Casting, Freeze Casting.

Abstract

This work addresses key challenges associated with the fabrication of Proton-Conducting Cells (PCCs) based on barium cerate-zirconate (BCZY) using different methods namely conventional tape casting and a combination of screen printing/freeze casting. The study investigates critical parameters required for the development of porous- dense-porous microstructures for PCCs. For the tape casting technique, the effects of the composition and sintering conditions (T and atmosphere) on the microstructural properties of the cell were analyzed. In the combined screen printing/freeze casting route, the tailored freeze cast formulation of water-based BCZY suspensions, along with the optimization of screen-printable inks, enabled the production of robust BCZY structures with a gas-tight dense electrolyte layer supported on a highly porous backbone with unidirectional porosity. Preliminary tests in electrolysis and fuel cell modes allows the correlation between cell processing and performance.

Introduction: *High-temperature proton-conducting ceramics (PCEs) are key materials for protonic ceramic fuel cells (PCFCs), electrolysis cells (PCECs), and membrane reactors, enabling efficient operation at intermediate temperatures (500–650 °C). Among PCEs, Y-doped $BaCeO_3$–$BaZrO_3$ solid solutions (BCZY) show the best balance of conductivity and chemical stability. Despite recent progress, the scalable fabrication of PCCs remains challenging and cell architectures with engineered electrodes and enhanced performance are still under development. In particular, aligned-porous electrodes have been considered effective in reducing tortuosity and polarization resistance in these systems.*

Objectives: *The main challenges related to the fabrication of BCZY-based electrode-supported cells are addressed by exploring different approaches: conventional tape casting and a hybrid screen printing and freeze casting process. The study focuses on the processing parameters required to achieve optimized porous/dense/porous structures for enhanced electrochemical performance.*

Material and methods: *The production of $BaCe_{0.65}Zr_{0.2}Y_{0.15}O_{3-d}$ (BCZY, Cerpotech) based electrode-supported cells was examined. A conventional tape casting route was considered to produce NiO-BCZY/BCZY/LSCF-BCZY cells. The process involves the formulation of suitable slurries for supporting and functional electrode, as well as for the electrolyte. Each tape is cut, stacked, laminated and thermal treatments were optimized to obtain perfectly planar BCZY-NiO/BCZY half cells to be deposited with LSCF-BCZY electrode on top. An innovative freeze casting process coupled with screen printing was optimized to obtain a BCZY porous/dense backbone (Figure 1). Ad-hoc BCZY-based water suspension using ZnO as sintering aid was prepared [1]. The as-obtained freeze cast support was then screen printed with a BCZY ink. The obtained bilayer was then sintered at 1400°C [2]. The backbone was then screen printed with a BCZY-LSCF ink (air electrode) and infiltrated by drop casting with a Ni-based precursor solution on the porous side.*

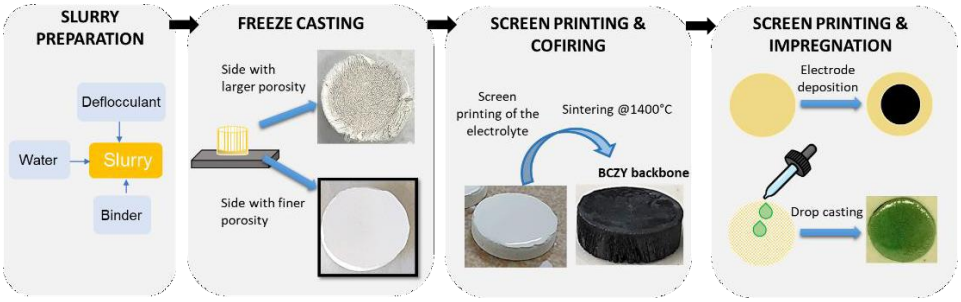


Figure 1 *Scheme of freeze casting/screen printing process to obtain BCZY-based cell.*

Results: *The fabrication of BCZY-based PCCs faces several challenges, the most critical is the barium volatilization during the sintering process. Sintering Ba-containing perovskites such as BCZY is, in fact, particularly demanding, as high T required for full densification often lead to significant Ba loss. This loss negatively affects both electrolyte phase stability and level of density. Sintering PCCs in the 1350–1500 °C range without atmospheric control consistently resulted in porous electrolytes and the undesirable formation of a fluorite secondary phase at the expense of the perovskitic structure. A controlled atmosphere during the cofiring process [2] enables the retention of the BCZY perovskite phase and produces dense, gas-tight electrolytes across a broad sintering temperature window.*

The development of porous/dense BCZY backbones via freeze casting required a stable, pseudoplastic water suspension suitable for casting. To stabilize the negative charged BCZY

surface in water, ammonium polyacrylate was added. Polyvinyl alcohol acted as a binder to ensure proper rheology without altering pore structure, while a surfactant (Surfynol) was included to prevent bubble formation. Rheological tests confirmed pseudoplastic behavior in the 1–100 s^{-1} range, ideal for casting. Samples were frozen at –40 °C and water was removed under vacuum. A BCZY-ZnO ink was screen printed on one side to form a dense layer. After sintering at 1400 °C for 4 h, asymmetric structures were obtained, consisting of a highly porous support and a thin, gas-tight electrolyte. SEM images revealed vertically aligned pores (~33 ± 10 µm), 40.6 ± 2.0% porosity, and a permeability of 2.64 × 10^{-12} ± 2.03 × 10^{-13} m^3. The dense layer measured 32.7 ± 3.0 µm with polygonal grains (5.1 ± 1.9 µm) of the desired phase.

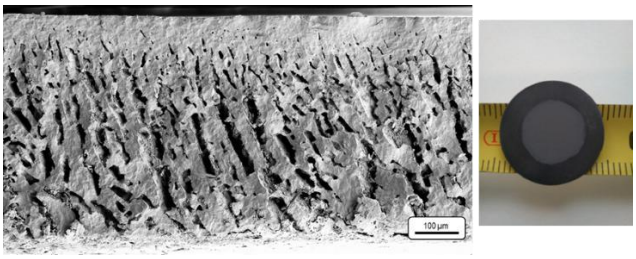


Figure 2 *Freeze cast/screen printed BCZY porous-dense backbone (on the left), final complete cell with ice-templated microstructure (on the right)*

Conclusions: *This work explored fabrication methods for BCZY-based proton-conducting half-cells, focusing on the development of optimized porous/dense/porous structures and minimizing barium loss during sintering. Freeze casting/screen printing coupling is particularly effective, enabling the formation of asymmetric structures with aligned porosity and dense, gas-tight electrolytes. The individuation and optimization of critical parameters played a key role in preserving the perovskite phase and ensuring the obtaining of suitable microstructure, for PCCs. The link between process parameters and cell performance was investigated as well.*

Acknowledgment

This research was funded by the European Union – NextGeneration EU from the Italian Ministry of Environment and Energy Security POR H_2 AdP MMES/ENEA with involvement of CNR and RSE, PNRR - Mission 2, Component 2, Investment 3.5 "Ricerca e sviluppo sull'idrogeno" and "Nanocomposite multi-ionic Ceria Carbonate Electrodes for New reversible Electrolysis – NICENESS", PRIN 2022, Prot. 2022S999EK, financed by Next GenerationEU and Ministero dell'Università e della Ricerca.

References

[1] A. Gondolini, A. Bartoletti, E. Mercadelli, et al. J. Membr. Sci. 684, (2023), 121865.

[2] D. Montaleone, E. Mercadelli, A. Gondolini, et al. J. Eur. Ceram. Soc.39 (2019) 21–29.

European Fuel Cells and Hydrogen
PIERO LUNGHI CONFERENCE
September 17th–19th 2025
Capri / Italy

Electrochemical Modelling of Dual-ion Effect in Molten Carbonate Fuel Cells

Juan Pedro Pérez Trujillo*[a], Riccardo Risso [b], Barbara Bosio[b], Göran Lindbergh[a], Carina Lagergren[a]

* corresponding author: jppt@kth.se, jp.pereztrujillo@hotmail.com
[a] Applied Electrochemistry, Department of Chemical Engineering, KTH Royal Institute of Technology, SE-100 44, Stockholm, Sweden
[b] PERT, DICCA, University of Genoa, 16145, Genoa, Italy

Keywords: Carbon Capture; Dual-ion mechanism; carbonate and hydroxide effect; Molten Carbonate Fuel Cell.

Abstract

Introduction: *Molten Carbonate Fuel Cells (MCFCs) are a type of high-temperature fuel cell that operate at approximately 650°C. Although MCFC technology has been studied for several decades, it is now receiving renewed attention due to its unique capability to facilitate carbon capture and storage (CCS) while simultaneously generating power [1]. MCFCs can capture carbon dioxide directly from both fuel and oxidant streams, offering the dual benefit of power production and emissions reduction. Furthermore, their high energy conversion efficiency positions them as a promising candidate for integration into future hydrogen-based and low-carbon energy systems [2]. Traditionally, a mechanism based on carbonate ion migration through the electrolyte has been considered to be governing the cell behaviour [3]. However, recent studies have demonstrated that this single-ion model is insufficient to accurately represent cell behaviour under all operating conditions [4]. The formation and participation of hydroxide ions have been shown to enhance electrochemical performance while also accounting for decreased CO_2 utilization. In this work this dual-ion phenomenon is studied experimentally and an improvement towards the previous iteration of kinetic models describing this behaviour has been proposed.*

Objectives: The aim of the work is to show and quantify the effect of water content in the nickel oxide electrode under the operation of a molten carbonate fuel cell which promotes the formation of hydroxides causing, together with the carbonates, a double ion mechanism.

Experimental conditions: The double-ion mechanism present in molten carbonate fuel cells under the presence of water in the oxygen electrode is studied experimentally using a button cell of ~3 cm^2. The cell consists of a porous Ni-Cr electrode as the fuel electrode, whereas the oxygen electrode is a porous NiO electrode that is oxidized and lithiated in situ. The current

collectors are made of Ni and SS-316 at the fuel and oxygen electrode, respectively. A porous matrix of $\gamma - LiAlO_2$ separates the electrodes and supports the electrolyte, which is a eutectic mixture of 62/38 mol% of Li_2CO_2/K_2CO_3 [5].

Three different temperatures were tested 600°C, 625°C and 650°C. The inlet flow rate of the gases was 150 mL·min^{-1} for both electrodes. The gas mixture on the fuel electrode was kept constant, consisting of 64% H_2, 16% CO_2, and 20% H_2O. The gas composition was varied to study the effect of the OH^- ion and the combined effect of the two ions in Table 1, and Table 2, respectively.

Table 1. Gas composition tested to study the effect of the hydroxide ion.

Gas group No.	O_2, %	CO_2, %	H_2O, %
1	15	0	5-20
2	30	0	5-200

Table 2. Gas composition tested to study the effect of the double ion, carbonate and hydroxide.

Gas group No.	O_2, %	CO_2, %	H_2O, %
1	15	30	5-20
2	15	5	5-20
3	30	15	5-20

Results: The presence of water at the oxygen electrode indicates an additional mechanism involving the OH^- ions when operating in fuel cell mode. When the inlet gas stream contains CO_2, O_2 and H_2O, a dual mechanism involving both CO_3^{2-} and OH^-ions is present. It is assumed that the OH^- based mechanism becomes dominant at low CO_2 concentrations. Thus, the contribution of the CO_3^{2-} mechanism can be quantified as the difference in current density between a gas mixture containing CO_2, O_2 and H_2O, and a mixture containing only O_2 and H_2O. This comparison is reflected in the difference between the results obtained from experimentation of conditions of Table 2 and Table 1.

Figure 1 shows the transfer number of CO_3^{2-}, indicating that its contribution remains below 50% at the lowest CO_2 concentration (5%). However, at higher CO_2 concentrations and high current densities, this balance shifts, and the CO_3^{2-} mechanism becomes more dominant, contributing up to approximately 60% of the total current.

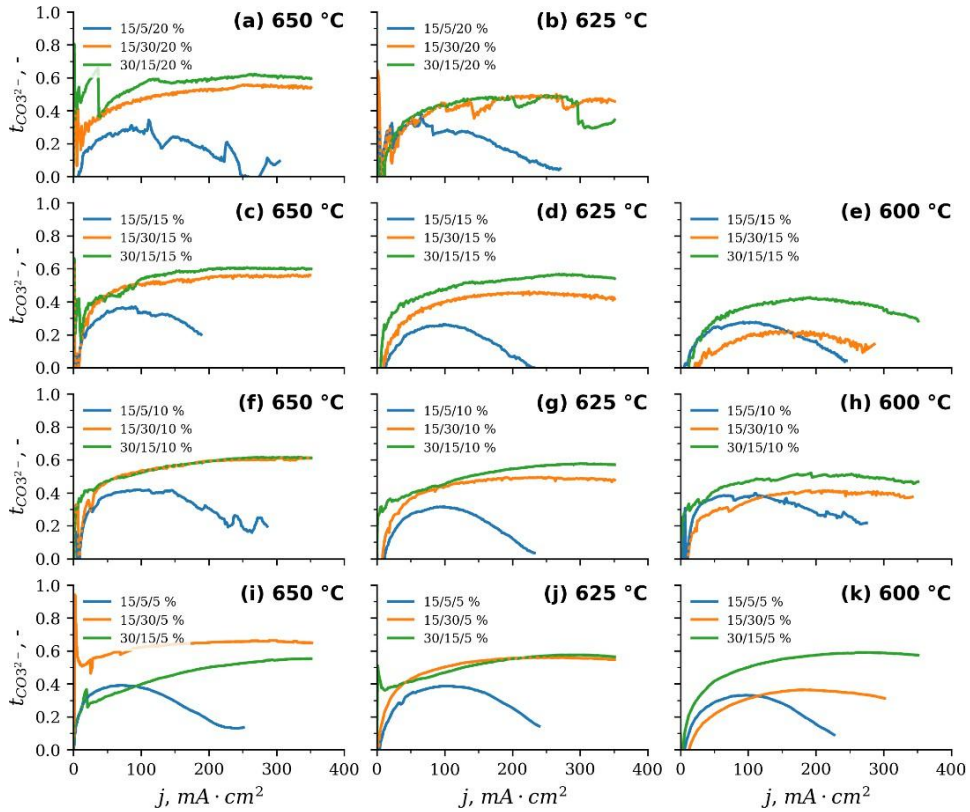


Figure 1. Transfer number of the carbonate ions with respect to the operating conditions of Table 2.

Conclusions: The dual-ion transport mechanism, involving both carbonate and hydroxide ions, has been investigated through experimental and numerical methods. Results demonstrate that the hydroxide ion predominates at low CO_2 concentrations, conditions relevant to carbon capture applications, while carbonate becomes the dominant ion at higher CO_2 levels, contributing up to approximately 60% of the total current. The electrochemical behaviour of the system was modelled using the Butler-Volmer equation to account the activation overpotentials. The model showed good agreement with experimental data, achieving coefficients of determination of 87.88% and 97.01%, for the datasets presented in Table 1 and Table 2, respectively.

References

[1] L. Mastropasqua, et al. Molten Carbonate Fuel Cells retrofits for CO2 capture and enhanced energy production in the steel industry. Int. J. GreenHouse Gas control, 88 (2018).
[2] M. Cassir, et al., 3 – Molten Carbonate Fuel Cells. Compendium of Hydrogen energy. 2016 (3)
[3] D. W. Green, R. H. Perry. Perry's Chemical Engineers' Handbook. Eight Edition. McGrawHill.
[4] D. Bove, et al. Process analysis of molten carbonate fuel cells in carbon capture applications. Int. J. Hydrogen Energy. 46 (2021)
[5] L. Hu. Molten Carbonate Fuel Cells for Electrolysis. Ph.D. thesis. KTH Royal Institute of Technology, Stockholm, Sweden (2016).

EFCH2 2025
European Fuel Cells and Hydrogen
PIERO LUNGHI CONFERENCE
September 17th–19th 2025
Capri / Italy

A Virtual H_2 Sensor for improved Fuel Cell Control

Diana Maria Otalvaro Gutierrez*[a], Markus Kretschmer, Sebastian Zaiser

* corresponding author: Robert Bosch GmbH

Keywords: virtual sensor, hybrid modelling, Fuel Cell system control

Introduction:

Fuel cell-powered vehicles (FCEVs) are a sustainable pathway to achieving zero-emission transportation. The dominant technology in FCEV is the proton exchange membrane fuel cell (PEMFC). The PEMFC has proven to be viable in on-the-road vehicles and remains the state-of-the-art fuel cell variant for mobile applications, giving an edge in their low temperature operation, high power density, short start-up times, rapid response to dynamic loads and their efficiency. As the FCEVs gain popularity and market share, the focus will be shifted towards increasing efficiency and driving range. With our work we show a way to increase both by a physical model that provides critical insight on the fuel cell anode operating conditions in real time.

In modern fuel cell architectures, the unreacted hydrogen in the anode is recirculated, with the goal of reducing overall fuel consumption. Nevertheless one, as yet, unavoidable feature of the PEMFC membrane is its permeability to N_2 diffusion from the cathode to the anode, which has the detrimental effect of diluting the H_2 concentration in the fuel cell anode. This H_2 depletion, when excessive, can have catastrophic consequences for the fuel cell membrane when the gas mixture is recirculated as, in the absence of sufficient hydrogen, the membrane is oxidized and pinholes are created. To avoid this grim scenario, a purge valve is installed downstream of the fuel cell stack to evacuate N_2. In the process, however, H_2 is also expelled together with the N_2 and other trace gases. While some loss of H_2 is unavoidable, this loss represents a fuel efficiency penalty and thus there is a monetary advantage in minimizing it.

Objectives:

This situation can be remedied to some extent by controlling the purge valve operation, such that it is only opened when the H_2 concentration in the anode falls below some threshold and closed once a second, higher, threshold is exceeded. Nevertheless, deriving the hydrogen concentration in the anode is no easy task, as the full complexity of the fuel cell comes to

bear in the hydrogen concentration. In this work, we prove and verify methods to arrive at the H_2 concentration in the anode accurately and reliably.

Material and methods:

For this purpose, we use methods that combine fundamental underlying physics of the fuel cell in operation and are reinforced with AI. In our methods, we use the hydrogen exhaust safety sensor as a key input to our model. This safety sensor is widely present in fuel cell systems of many manufacturers and can be used to detect component ageing thus justifying its inclusion in modern FCEVs. We use a select group of fuel cell signals in state-of-the-art (embedded) AI, complex solvers, fluid dynamics modelling and embedded programming. Our algorithms can be deployed in fuel cell control units to calculate the H_2 concentration and this information can be further used in control of the fuel cell system.

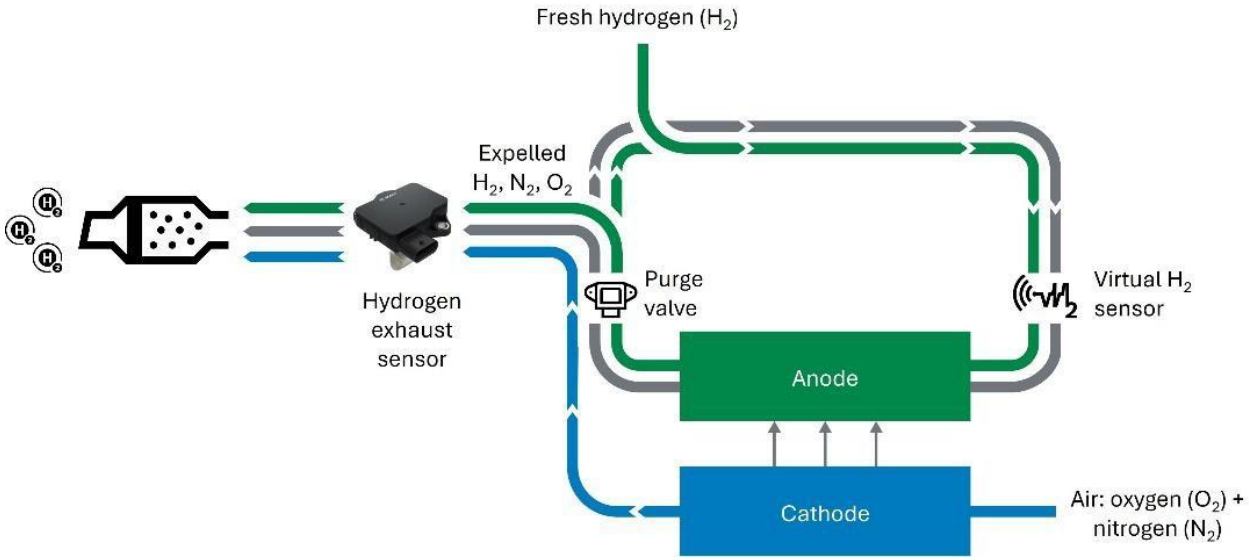


Figure 1: schematic depiction of a fuel cell with emphasis on the anode recirculation loop.

Results:

With the exhaust hydrogen safety sensor, thermodynamics, and fluid dynamics knowledge we derive the H_2 concentration within 5% of the measured value. We capture the dynamics of the H_2 concentration (increase when the purge valve is open, decrease when it is closed) as well as the bias (H_2 concentration value) with an accuracy above 95%.

Furthermore, we show that there are several successful ways to model the H_2 concentration. In one approach we use a LSTM cell which we trained in data sets with high dynamics (i.e. fuel cell current variations) and show that with a very small set of input variables and optimized choices of look-back length and cell memory size, we can extrapolate the model to different purge and load operating strategies, while remaining within a 5% error envelope of the measured values.

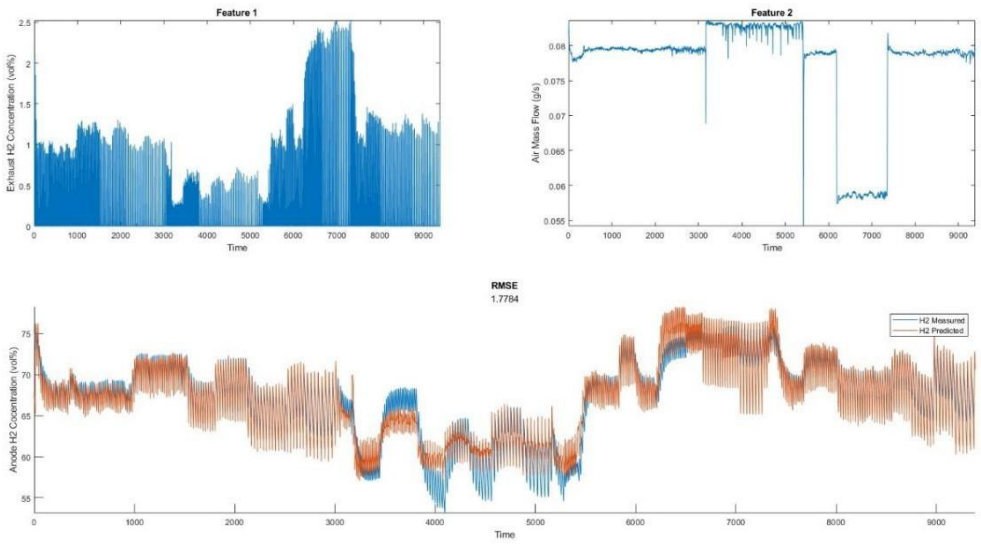


Figure 2: Training results of a LSTM model based on two signals.

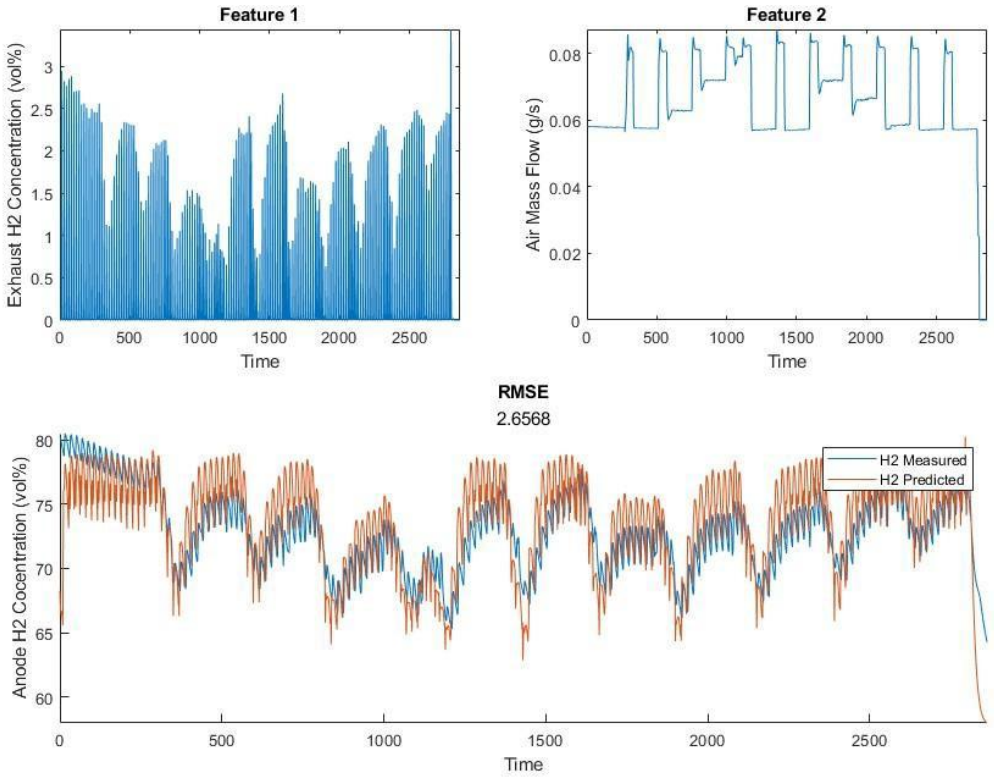


Figure 3: Test results of the 2 signal LSTM model

Alternatively, a simple empirical approach to the bias and dynamics of the H_2 concentration delivers similar accuracies while retaining its simplicity. This model uses the exhaust H_2

sensor and the stack current to derive the H_2 concentration finding correlations between these quantities.

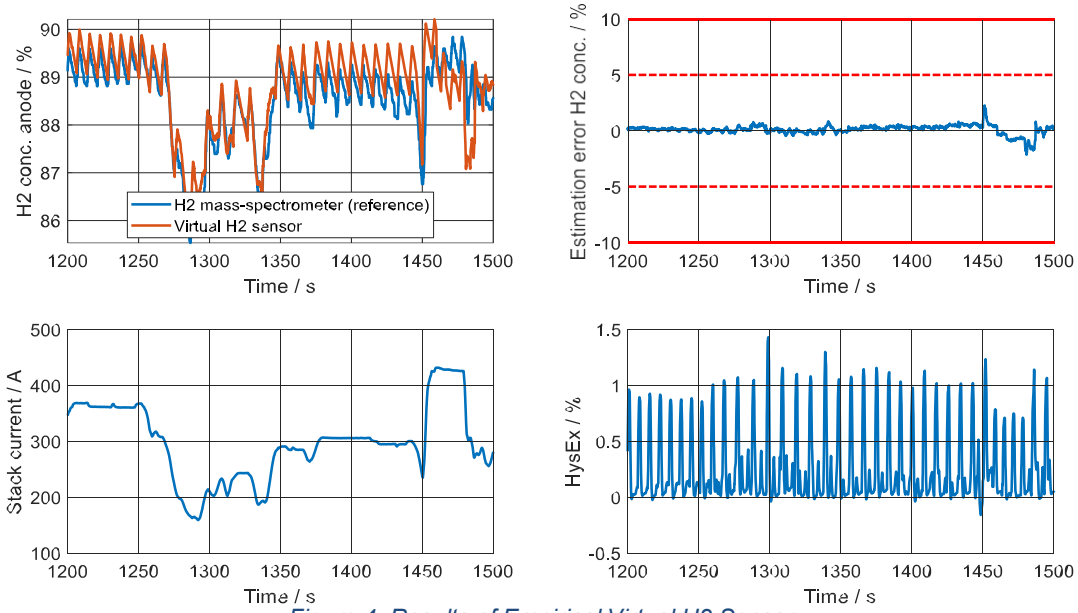


Figure 4: Results of Empirical Virtual H2 Sensor

Lastly, we have developed an analytical model, where we use the throttle equation for ideal gases and physical laws to arrive at the H_2 concentration during a purge event, as well as its dynamics. It accurately describes the effect of N_2 diffusion as well as the effect of purge valve operation.

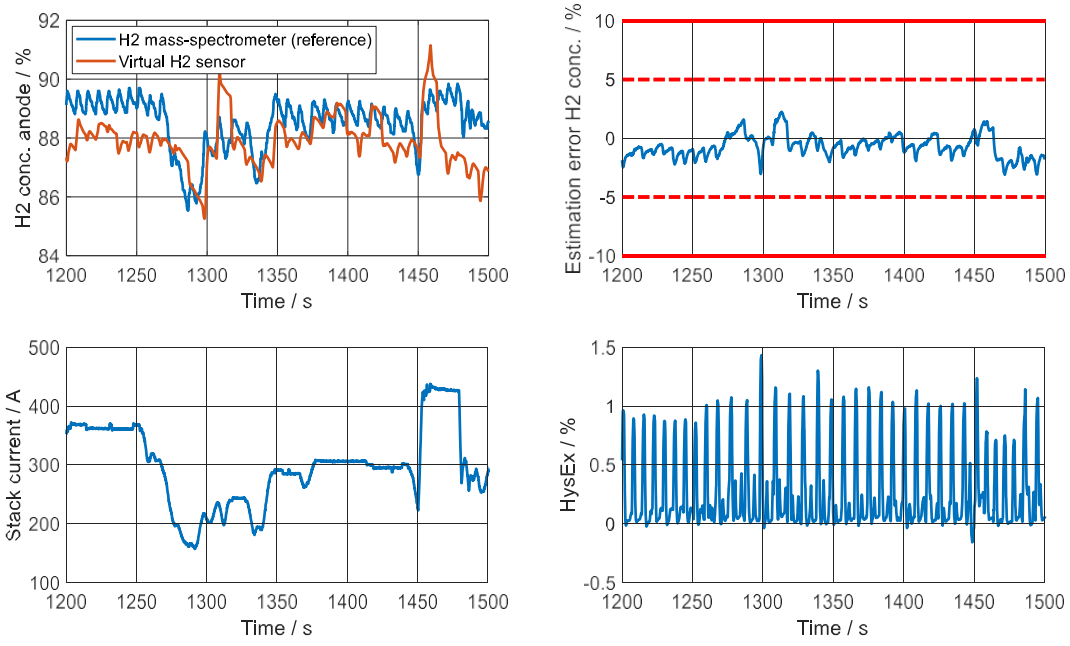


Figure 5: Results of Analytical Virtual H2 Sensor

Conclusions:

We have tested our models in fuel cells systems that have already been deployed on the road and show that our models are reliable, accurate and can be leveraged to optimize fuel efficiency and thereby increase driving range.

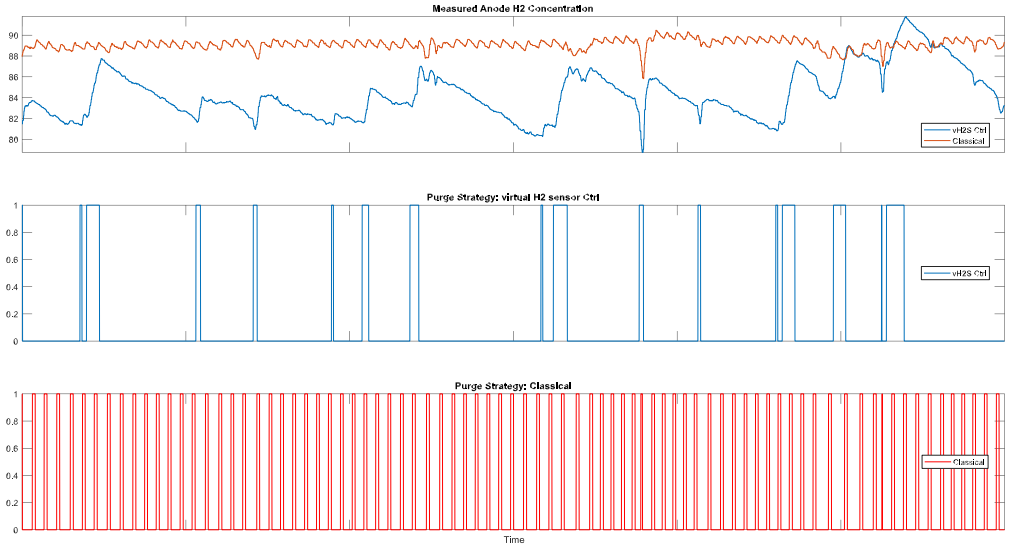


Figure 6: Classic (red) and hydrogen concentration based purge valve operation (blue)

Acknowledgment

We would like to acknowledge Robert Bosch GmbH corporate research for valuable discussions and measurement data.

References

[1] Development of Virtual Sensors for Gas Composition in the Anode Subsystem of a PEM Fuel Cell System, Manlin Zhan, Master Thesis, Technical University of Berlin, 2022

EFCH2 2025 European Fuel Cells and Hydrogen PIERO LUNGHI CONFERENCE
September 17th–19th 2025 Capri / Italy

Techno-Economic Optimization of a SOFC-Based Biogas Power Plant Integrated with Green Hydrogen in a Local Energy System

Dario Colombari *[a], Vittorio Urciuoli [a], Andrea Rossetti [a]

* corresponding author: dario.colombari@rse-web.it

[a] RSE – Ricerca sul Sistema Energetico S.p.A.

Keywords: Biogas, Energy System Integration, Solid-Oxide Fuel Cell, Techno-Economic Optimization.

Abstract

Solid-oxide fuel cells (SOFC) can be an efficient and cost-effective exploitation pathway for agricultural biogas. SOFC's fuel flexibility gives the opportunity to easily integrate hydrogen enabling energy storage from additional renewable energy sources (PV) available on-site. An innovative plant layout has been developed, and its techno-economic optimization is presented. The proposed configuration is bound to have high operational flexibility as it includes both electrical self-consumption of a local energy system and hourly scheduling of electricity market strategy. Results show that optimal design is the one the maximizes energy self-consumption and the optimized configuration appears to be economically competitive against reference solutions. Nevertheless, optimization deters the production of hydrogen in favour of a prioritized direct usage of photovoltaic power. Flexibility can still be achieved through biogas storage that has lower losses and higher energy density.

Introduction:

Efficient and cost-effective biomass exploitation may be a key for the decarbonization of energy sector. Nevertheless, European and Italian biogas sectors are currently stagnating due to limited profitability and technological limitations: biogas is currently employed in internal combustion engines with limited electrical efficiency while upgrading to biomethane is struggling due to lacking infrastructure and high costs. Solid-oxide fuel cells operate with very high efficiency, and they have the potential to improve economic and environmental sustainability of biogas power plants. Operational flexibility is a key advantage of biomass: the synergy between biogas and other RES is likely to provide an effective solution to increase the overall availability. Additional flexibility might arise from the use of hydrogen as energy storage vector which can be easily integrated in plant layout thanks to SOFC's fuel flexibility. From these considerations, the integrated multi-energy system in Figure 1 is considered.

Objectives:

The goal is to assess the overall economical profitability of the proposed solution by identifying optimal design and scheduling.

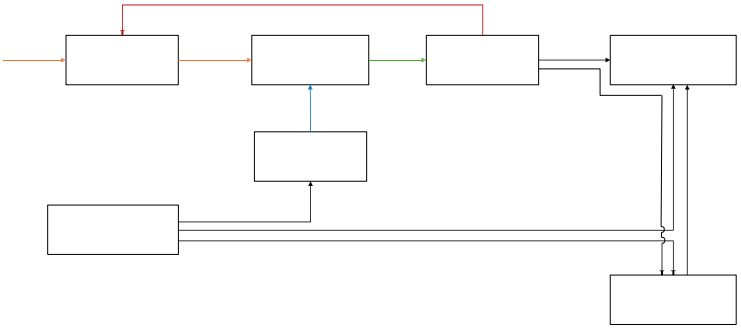


Figure 1 - Plant layout of the integrated multi-energy system.

Material and methods:

The techno-economic optimization has been performed by implementing a MATLAB model that solves mass and energy balances on each plant component. Operational scheduling is defined on hourly basis basing on instantaneous values of electricity price (using an optimized selling price threshold), endogenous electrical demand, storage level, biogas and PV production. A biogas plant located in the province of Novara (1 MW internal combustion engine) has been considered as descriptive case study. The developed system model includes dedicated sub-models for all components:

- Anaerobic digester. Biogas production is an input boundary condition [1]. Digester thermal demand is estimated from literature as well as its thermal inertia [2].
- PV. Hourly production curve is location dependent as well as on-site PV free area.
- SOFC and Electrolyser. Performances are given by electrical/thermal efficiency curves [3].
- Gas storage. A custom model based on molar balance is solved at each timestep. The model tracks gas mixture composition as well as filling level.

The goal function is the minimum specific cost of electricity for the supply of the local energy system considering grid exchange as additional costs and revenues.

Optimization results have been put in comparison with two refence configurations:

- Grid-Only. Local energy system is supplied by electricity grid only.
- Biogas ICE. Biogas is used in an internal combustion engine running at nominal power.

Results:

A summary of optimization results, as function of load size, is proposed in the following table.

Load	kW	240	480	710	950	1190	1430	1660	1900	2140	2380	2620	2850
Storage	Nm^3	4783	2391	2391	2391	2391	2391	2391	2391	2391	2391	0	0
SOFC	kW	1667	1427	1427	1427	1427	1667	1667	1667	1667	1667	1667	1667
Electrolyser	kW	0	0	0	0	0	0	0	0	0	0	0	0
PV	kW	950	950	475	950	950	950	950	950	950	950	950	950
Price Coefficient	-	0.5	0.5	0.5	1.0	1.0	1.5	1.5	1.5	1.5	1.5	1.5	1.5

Independently from load size, the optimization procedure never predicts the installation of an electrolyser. To achieve operational flexibility, the optimization deters the production of hydrogen: direct usage of photovoltaic power is always prioritized over hydrogen production as SOFC can be partialized without energy losses and biogas can be easily stored.

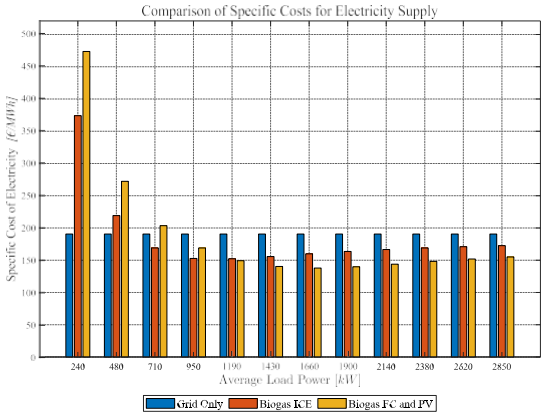


Figure 1 - Specific cost of electricity supply for local energy system.

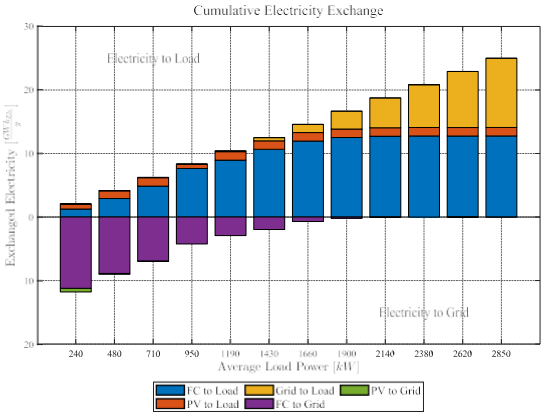


Figure 2 - Electricity exchange in optimized configurations.

Figure 1 shows the objective function of the proposed solution in comparison with reference ones. The analysed layout appears to be economically competitive against reference solutions and the minimum electricity cost is achieved with an average load size of 1660 kW. The proposed configuration has much higher capital cost, but they are compensating by higher efficiency and flexibility. Figure 2 shows cumulative energy exchange during one year of operations. The optimal design matches the highest level of energy self-consumption.

Conclusions and Future Works:

The implemented model successfully optimized design and scheduling of the proposed energy system. The solution appears to be economically competitive, and the optimal solution is oriented to self-consumption. Biogas storage shall be preferred instead of hydrogen production underling the potential synergy between biogas and hard-to-dispatch RES. Several aspects require further investigation: the technical feasibility of the solution must be proven and SOFC performances with variable fuel gas mix must be validated.

Acknowledgment

This research was funded by the European Union - NextGenerationEU from the Italian Ministry of Environment and Energy Security, POR H2 AdP MEES/ENEA with involvement of CNR and RSE, PNRR - Mission 2, Component 2, Investment 3.5 "Ricerca e sviluppo sull'idrogeno", CUP: J49I21000200001.

Funded by the European Union
NextGenerationEU

References

[1] J. Piekutin, M. Puchlik, M. Haczykowski and K. Dyczewska, "The Efficiency of the Biogas Plant Operation Depending on the Substrate Used," *Energies,* vol. 14, no. 11, p. 3157.

[2] T.-B. L. A. A. Avila-Lopez M. Robles Rodriguez C.E., "Toward thermal autarky for large-scale biogas plants: dynamic energy modeling for energy efficiency in anaerobic digesters with enhanced multimembrane gasholders," *Fuel,* vol. 339, 2022.

[3] Curletti F., Gandiglio M., Lanzini A., Santarelli M., Marechal F., "Large size biogas-fed Solid Oxide Fuel Cell power plants with carbon dioxide management: technical and economic optimization," *Journal of Power Sources,* vol. 294, pp. 669-690, 2015.

EFCH2 2025 European Fuel Cells and Hydrogen
PIERO LUNGHI CONFERENCE
September 17th–19th 2025
Capri / Italy

Multi-modal porous microstructure for high temperature fuel cell application

T. Wejrzanowski[a], S. Haj Ibrahim[a], K. Cwieka[a], M. Loeffler[b], J. Milewski*[c], E. Zschech[d], C.-G. Lee[e]

* corresponding author: jaroslaw.milewski@pw.edu.pl

[a] Warsaw University of Technology, Faculty of Materials Science and Engineering Woloska 141, 02507 Warsaw, Poland
[b] TU-Dresden, Germany
[c] Warsaw University of Technology, Faculty of Power and Aeronautical Engineering, Institute of Heat Engineering, Nowowiejska 21/25, 00665 Warsaw, Poland
[d] Fraunhofer Institute for Ceramic Technologies and Systems, Dresden, Germany
[e] Deptartment of Chemical Engineering, Hanbat National University, San 16-1, Dukmyung-dong, Yuseong-gu, Daejeon, Korea 305-719

Keywords: Molten Carbonate Fuel Cell (MCFC), Porous Microstructure, Cathode Performance, Electrode Fabrication

Abstract

This study investigates the effect of a multimodal porous microstructure on the performance of high-temperature fuel cell cathodes, specifically within molten carbonate fuel cells (MCFCs). Cathode materials were fabricated using a tape casting method, with porosity variations introduced through different porogens. The structural properties were extensively analyzed using X-ray tomography, scanning electron microscopy (SEM), mercury porosimetry, and BET methods. Additionally, single-cell performance tests under MCFC operational conditions assessed the impact of microstructure modifications. Results indicate that multimodal pore distribution significantly enhances power density compared to conventional structures. A model based on 3D tomography image transformation is proposed to further understand these microstructure effects.

Introduction

High-temperature fuel cells, particularly molten carbonate fuel cells (MCFCs), are a promising energy technology for stationary power generation. Their advantages include high efficiency, fuel flexibility, and low environmental impact. However, their performance and longevity are highly dependent on the materials used in their electrodes. The MCFC cathode, responsible for oxygen reduction and carbonate ion formation, plays a critical role in determining overall

efficiency and stability. This study focuses on optimizing the microstructure of the cathode to improve electrochemical performance and durability under operational conditions.

Objectives

- To investigate the impact of multimodal porous structures on MCFC cathode performance.
- To fabricate and characterize nickel-based cathodes with varying porosity using different porogens.
- To analyze structural and electrochemical properties using advanced imaging and characterization techniques.
- To propose a computational model for microstructure-performance correlation.

Materials and Methods

Cathode samples were manufactured using a tape casting technique. Nickel powder was mixed with polymeric binders and solvents, with porosity controlled by introducing starch (P1) and polyvinyl butyral (P2) as porogens. The fabricated materials underwent thermal processing in a controlled atmosphere. Characterization techniques included SEM, X-ray tomography, mercury porosimetry, and BET analysis. Single-cell performance was tested under MCFC operating conditions at 650°C using a test rig that measured voltage, current density, and power output.

Results

Microstructural analysis revealed that cathodes with multimodal porosity exhibited increased open porosity and larger effective surface areas, facilitating enhanced mass transport and electrolyte infiltration. Single-cell performance tests showed that cathodes with a combination of small and large porogens doubled the power density compared to reference structures. SEM imaging confirmed in situ oxidation of Ni to NiO, with optimal electrolyte penetration observed in multimodal structures. Computational modeling supported these findings, demonstrating that multimodal porosity reduces mass transport limitations and enhances electrochemical reaction sites.

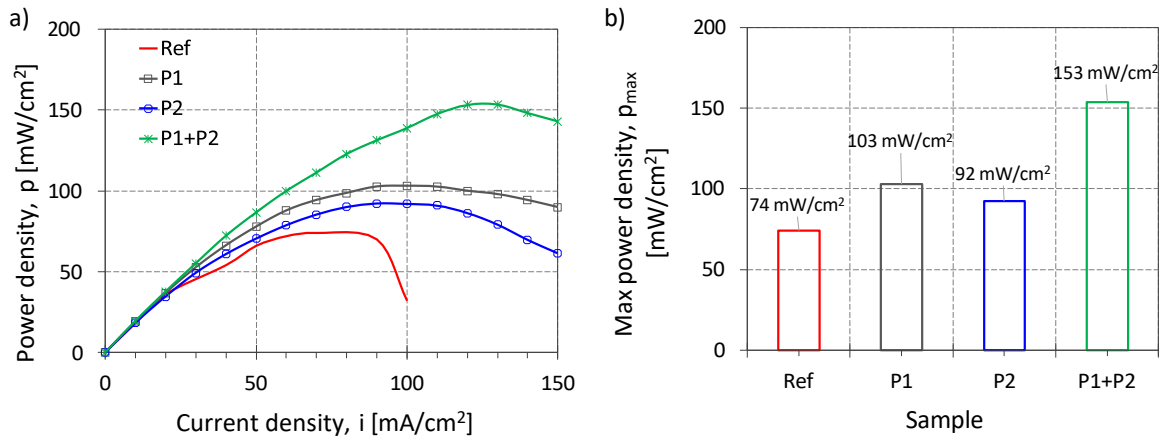


Figure 1: Performance of the single-cell with the cathodes studied herewith: a) power density vs current density and b) maximum power density

Conclusions

The introduction of multimodal porosity in MCFC cathodes significantly improves their electrochemical performance. Enhanced gas and ion transport, along with increased triple-phase boundary area, contribute to higher power density. The findings suggest that tailoring pore architecture is a viable strategy for improving MCFC cathode efficiency and longevity. Future work will focus on refining the computational model and exploring alternative materials for further performance enhancements.

Acknowledgment

The research was funded by the Warsaw University of Technology within the framework of the Initiative for Excellence - Research University (IDUB) Program.

European Fuel Cells and Hydrogen
PIERO LUNGHI CONFERENCE
September 17th–19th 2025
Capri / Italy

A mechanistic interrogation of pgm-free oer catalyst for pem water electrolysis

Di-Jia Liu[a,b,c]

* corresponding author: djliu@anl.gov

[a] Chemical Sciences & Engineering Division, Argonne National Laboratory, Lemont, ILL 60439, USA

[b] Pritzker School of Molecular Engineering, University of Chicago, Chicago, IL 60637, USA

[c] Task 31 Member, Advanced Fuel Cells Technology Collaboration Programme

Keywords: PGM-free, OER, PEMWE, hydrogen

Abstract:

This presentation discusses the investigation of La/Mn doped cobalt spinel as potential replacement of Ir as the catalyst to promote oxygen evolution reaction in proton exchange membrane water electrolyzer. Very promising activity and durability were demonstrated for the first time in the operating electrolyzer. High level structural characterization, combined with computational modelling revealed origins of catalyst's improved activity and durability under the acidic and oxidative conditions.

Introduction: Low temperature proton exchange membrane water electrolyzer (PEMWE) represents a critical technology for hydrogen production. It offers the advantages of significantly higher current density and higher H_2 purity, rendering it a preferred technology when high energy efficiency and low footprint are essential. Working in the oxidative and acidic environment under high polarization voltage, however, adds substantial demand to the electrode catalyst and the support. This is particularly the case in the anode where the oxygen evolution reaction (OER) takes place. At present, the platinum group metal (PGM) materials such as Ir black or Ir oxide are catalysts of choice. Their high cost and limited reserve add a significant cost barrier to PEM electrolyzer, which contributes to the overall expense of hydrogen production next only to the cost of electricity. Replacing Ir with earth-abundant transition metal oxides could help to reduce the electrolyzer system cost.

Objectives: The objective of this research is to develop platinum-group-metal-free, or PGM-free catalyst using inexpensive materials such as transition metal oxide. The study aims at a) demonstrating the feasibility and b) understanding the fundamental mechanism behind OER catalysis using these low-cost materials.

Material and methods: For PEMWE application, a PGM-free anodic catalyst must be highly active to match the performance of Ir. Furthermore, it must be stable against oxidative acid corrosion. At Argonne National Laboratory, we recently developed a new PGM-free OER of a nanofibrous cobalt spinel catalyst co-doped with lanthanum and manganese (LMCF). [1] The catalyst was synthesized from the precursor of cobalt zeolitic methyl-imidazolate framework (Co-ZIF) doped with manganese and lanthanum. The Co-ZIF was mixed with a polymer solution and electrospun into nanofiber before being converted to fibrous cobalt spinel under low temperature oxidation to remove all the organics and carbon. (**Fig. 1**)

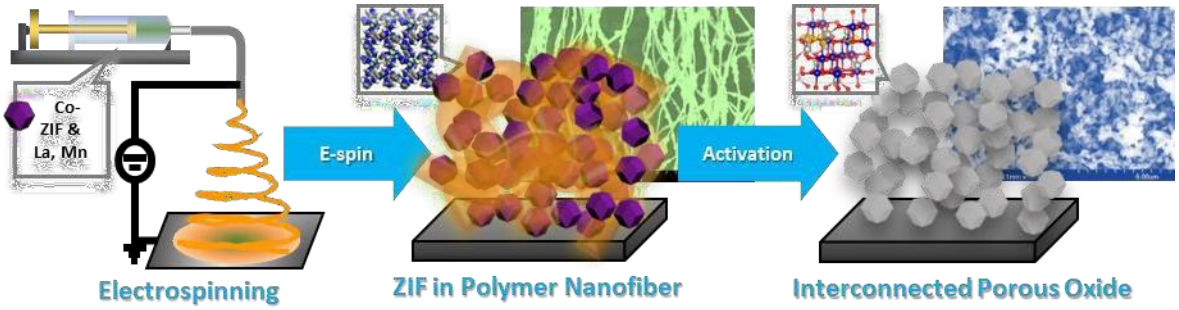
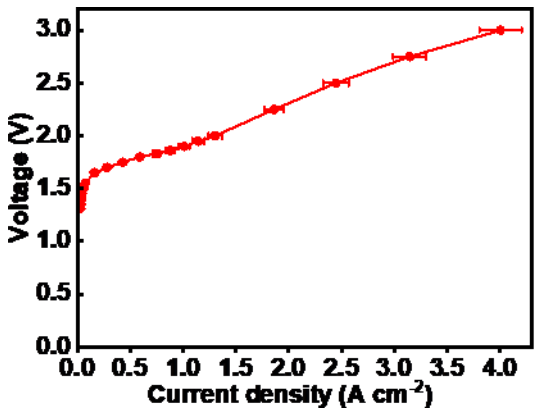


Figure 1. Scheme of preparing La/Mn-doped porous Co3O4 using electrospin followed low-temperature oxidation

Results: When tested by rotating disk electrode (RDE), the La/Mn-Co_3O_4 catalyst demonstrated a low overpotential of 353 mV (RHE) at 10 mA/cm^2 and a low OER degradation over 360 hours in acidic electrolyte. A PEMWE containing this catalyst at its anode at ~2.0 mg/cm^2 demonstrated a current density of 2000 mA/cm^2 at 2.47 volts (Nafion® 115 membrane) or 4000 mA/cm^2 at 3.00 volt (Nafion® 212 membrane). The membrane electrode was also subjected to accelerated-stress-test (AST) in both voltage cycling and galvanostatic run at different current densities. Low degradation rates under both ASTs were observed.

Figure 2. The current-voltage polarization of a PEMWE containing ANL's PGM-free OER catalyst at anode. Anode = ANL- PGM-free, 1 mg/cm^2, Cathode = Pt/C, 0.5 mg/cm^2, Membrane = N211, 5 cm^2 cell, CCM, 60 ˚C, 10 psi DI



In addition to catalyst design and synthesis, we also conducted extensive structural characterizations, stability measurement, as well as computational modeling. Our in situ study found that the OER process involves significant lattice oxygen movement, leading to lowering instead of raising the cobalt oxidation state during the electrolysis. The measurement of the stability number, combined with computational Pourbaix diagram, elucidated the importance of the operating potential in reducing catalyst dissolution. These findings offer in-depth understanding and direction of future development for PGM-free OER catalyst in PEM water electrolyzer.

Conclusions: Argonne's Co-ZIF derived PGM-free OER catalyst showed very good activity and durability in acidic electrolytes compared to Ir benchmarks, delivering a current density of 2000 mA/cm^2 at 2.2 V, representing the first demonstration of PGM-free OER catalyst with commercially relevant current density. The PGM-free catalyst performance still requires significant improvement as viable alternative to precious metals. The durability of PGM-free catalyst also needs improvement before serving as a viable replacement for iridium

Acknowledgment

This work is supported by the U.S. Department of Energy, Office of Energy Efficiency and Renewal Energy, Hydrogen and Fuel Cell Technologies Office, and by Laboratory Directed Research and Development funding of Argonne National Laboratory, provided by the Director, Office of Science, of the U.S. Department of Energy under Contract No. DEAC02-06CH11357. Work performed at the Center for Nanoscale Materials and Advanced Photon Source, both U.S. Department of Energy Office of Science User Facilities, was supported by the U.S. DOE, Office of Basic Energy Sciences, under Contract No. DE-AC02-06CH11357.

References

[1] "La- and Mn-doped cobalt spinel oxygen evolution catalyst for proton exchange membrane electrolysis" Lina Chong, Guoping Gao, Jianguo Wen, Haixia Li, Haiping Xu, Zach Green, Joshua D. Sugar, A. Jeremy Kropf, Wenqian Xu, Xiao-Min Lin, Hui Xu, Lin-Wang Wang, Di-Jia Liu, *Science* 380, 609–616 (**2023**)

EFCH2 2025
European Fuel Cells and Hydrogen
PIERO LUNGHI CONFERENCE
September 17th–19th 2025
Capri / Italy

Engineering Laboratory-Scale Multi-Stack Fuel Cell Systems

Jannik Holtorf*[a], Markus Schorr [a], Florian Pillath[a], Christoph Gentner[a]

* corresponding author: Jannik Holtorf
[a] German Aerospace Center (DLR), Institute of Engineering Thermodynamics, Hein-Saß-Weg 22, 21129 Hamburg, Germany

Keywords: PEMFC system, multi-stack fuel cell system, electric propulsion, dynamic control

Abstract

Introduction: (Hybrid) electric flight represents a transformative approach to reducing the environmental impact of aviation. Among the various technological pathways under investigation, hydrogen-powered polymer electrolyte membrane (PEM) fuel cells offer a promising low-emission source of electrical energy [1]. While PEM fuel cells are already deployed in select mobile applications, including the automotive and heavy goods transport industries, significant technological challenges remain for their application in aerospace contexts [2]. The unique demands of aviation necessitate addressing critical factors such as reducing system mass, enhancing overall efficiency and reliability under dynamic environmental and load conditions. Furthermore, the scalability of fuel cell systems into the megawatt range remains an area of primarily theoretical exploration. [3]
Although research on the control and regulation of fuel cell systems for ground-based applications is well-documented, there is limited literature focusing on aviation-specific requirements [4]. In particular, there is a lack of experimental studies that validate multi-stack fuel cell systems (MFCS) and investigate their scalability for high-power aviation applications [5, 6]. This work aims to address these gaps by examining critical design decisions in engineering a multi-stack fuel cell system.

Objectives: The primary objective of this study is to examine key design decisions in the development of a multi-stack fuel cell system for aerospace applications, focusing on identifying critical factors at the subsystem level that influence successful operation. Additionally, indicative design calculations for major balance of plant components will be provided to support future system designs. By addressing these objectives, the study aims to contribute to the broader understanding of how to implement fuel cell systems in aviation propulsion applications, particularly regarding system architecture, operational control, and scalability.

Material and methods: The engineering and theoretical concepts are applied to a laboratory-scale multi-stack fuel cell system (MFCS) consisting of two 6 kW PEM fuel cell short stacks, resulting in a total output power of 12 kW. This system is the direct outcome of hands-on engineering work, integrating theoretical analysis, detailed calculations, and practical trade-offs. The design process was guided not only by theoretical and analytical frameworks but also by the availability and performance limitations of off-the-shelf components.

The experimental setup replicates realistic operating conditions while enabling precise control and continuous monitoring of critical performance parameters. This allows for the evaluation of system behavior under varying dynamic loads and environmental factors, facilitating the identification of operational bottlenecks and areas requiring optimization.

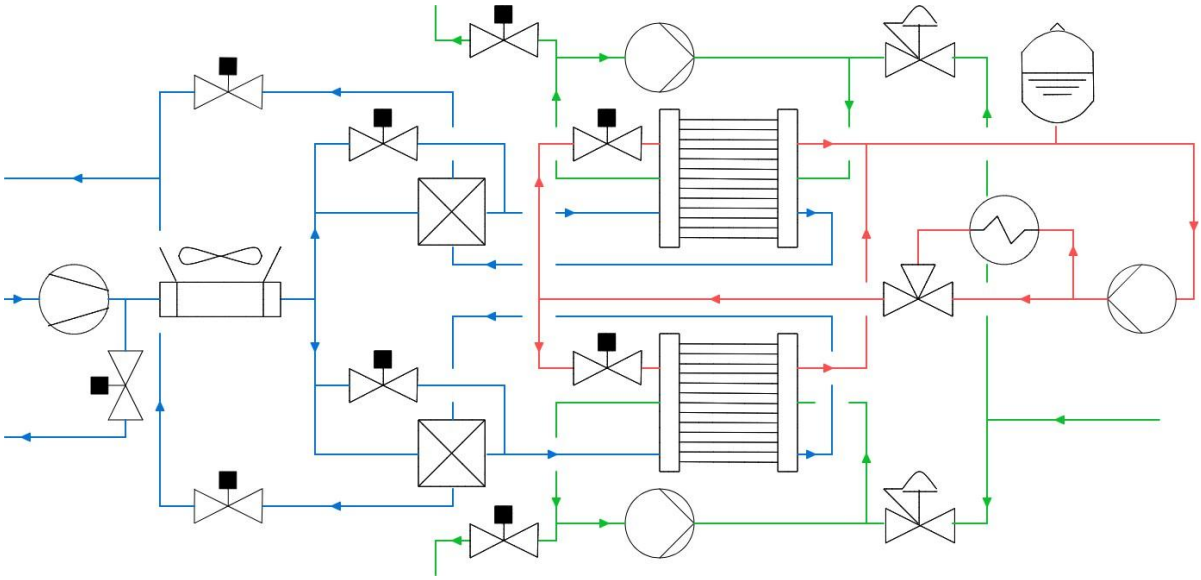


Figure 1 Architecture variant of a MFCS

Results: The experimental study led to the successful development of a laboratory-scale multi-stack fuel cell system with a total power output of 12 kW. This test-rig provides a foundation for evaluating the feasibility of the design choices and corresponding control approaches. Each design decision underwent practical implementation and testing, culminating in the construction of a fully operational test-rig. Basic control loops are included to regulate reactant flow, maintain thermal balance, and manage electrical loads, ensuring stable operation. Key design choices regarding subsystem integration and control methodologies were validated to ensure stable operation for up-coming experimental campaigns. The proposed engineering solutions serve as a reference point for refining control strategies and addressing the dynamic behavior of fuel cell systems in aerospace applications.

Conclusions: This work presents a practical approach to designing a multi-stack fuel cell system for aerospace applications, offering insights into key design trade-offs and their impact on system performance. The laboratory-scale test-rig represents an initial step toward understanding the complexities of multi-stack fuel cell systems. Future investigations will focus on investigating the dynamic behavior of MFCS under varying operational conditions to develop optimized control strategies and automation procedures. Additionally, further studies are required to explore the scalability of the proposed architecture to multiple full stack setups.

Acknowledgment

The author would like to thank the Federal Ministry for Economic Affairs and Climate Action of Germany for the financial support for this work (research project number *20M2101E*).

References

[1] McKinsey & Company, Hrsg., Hydrogen-powered aviation: a fact based study of hydrogen technology, economics, and climate impact by 2050, Publications Office of the European Union, 2020.

[2] Wu, H.-W. (2016). "A review of recent development: Transport and performance modeling of PEM fuel cells." Applied Energy 165: 81-106

[3] Hinz, Arne: Electrical propulsion systems for civil transportation aircraft. RWTH Aachen University, Aachen, 2022. DOI: 10.18154/RWTH-2022-06933

[4] Pukrushpan, J. T., A. G. Stefanopoulou and H. Peng (2004). Fuel Cell System Model: Fuel Cell Stack. Control of Fuel Cell Power Systems: Principles, Modeling, Analysis and Feedback Design. J. T. Pukrushpan, A. G. Stefanopoulou and H. Peng. London, Springer London: 31-56.

[5] Qiu, Y., Zeng, T., Zhang, C., Wang, G., Wang, Y., Hu, Z., Yan, N. M., & Wei, Z. (2023). Progress and challenges in multi-stack fuel cell system for high power applications: Architecture and energy management. Green Energy and Intelligent Transportation, 2(2), 100068. https://doi.org/10.1016/j.geits.2023.100068

[6] Zhou, S., Fan, L., Zhang, G., Gao, J., Lu, Y., Zhao, P., Wen, C., Shi, L., & Hu, Z. (2022). A review on proton exchange membrane multi-stack fuel cell systems: architecture, performance, and power management. Applied Energy, 310, 118555. https://doi.org/10.1016/j.apenergy.2022.118555

EFCH2 2025
European Fuel Cells and Hydrogen
PIERO LUNGHI CONFERENCE
September 17th–19th 2025
Capri / Italy

Experimental Investigation of High-Frequency,high-Amplitude Current Ripples on PEMFC Stack Degradation

Manish Kumar*[a], Florian Becker [a], Christoph Gentner[a]

* corresponding author: manish.kumar@dlr.de
[a] German Aerospace Center (DLR)

Keywords: EIS, HFCR, high-amplitude ripple, PEMFC degradation

Abstract

Introduction: Proton exchange membrane fuel cells (PEMFCs) are increasingly adopted in aerospace for their high-power density and environmental benefits. However, their integration with power electronics (Buck/Boost converters and inverters)—essential for energy conversion—introduces high-frequency (kHz) current ripples. Existing studies focus on low-amplitude ripples (<50 A peak to peak) typical of automotive systems, but aerospace applications operate at vastly higher power levels, where converters generate ripples exceeding 300 A peak-to-peak that may accelerate stack degradation.

Objectives: While numerous studies have investigated the effects of low-amplitude ripple currents on PEMFC performance [1 - 4], there remains a lack of empirical data on the impact of extreme ripple conditions—characterized by frequencies exceeding 8 kHz and amplitudes up to 300 A peak-to-peak—commonly encountered in high-power applications. This study aims to address this gap by evaluating the degradation mechanisms in a 6 kW PEMFC stack subjected to ripple currents ranging from 8 kHz to 16 kHz, with amplitudes reaching 300 A peak-to-peak. The experimental conditions are designed to replicate the electrical stress imposed by power electronics, providing critical insights into the durability of PEMFCs under such operating conditions.

Experimental Setup: This study was conducted using a 6 kW proton exchange membrane fuel cell (PEMFC) stack comprising 20 cells, each with an electrochemically active surface area of 300 cm^2 and metallic bipolar plates. Baseline characterization was performed through polarization (V-I) curves and electrochemical impedance spectroscopy (EIS) measurements under controlled operating conditions: a temperature of 68°C, 95% relative humidity, and a cathode stoichiometry of 2.

EIS measurements were conducted using a Zahner IM6 electrochemical workstation in conjunction with an EL1000 electronic load. A 6.4 kW H&H electronic load was employed to set the operating point, while a second load was modulated via an analog signal from a function generator to introduce sinusoidal current ripples, as illustrated in Fig. 1. Ripple amplitudes were systematically increased from 50 A to 300 A peak-to-peak at frequencies of 8 kHz and 16 kHz. Each 1.5-hour continuous current ripple test was preceded and followed by polarization curve and EIS measurements to assess degradation effects.

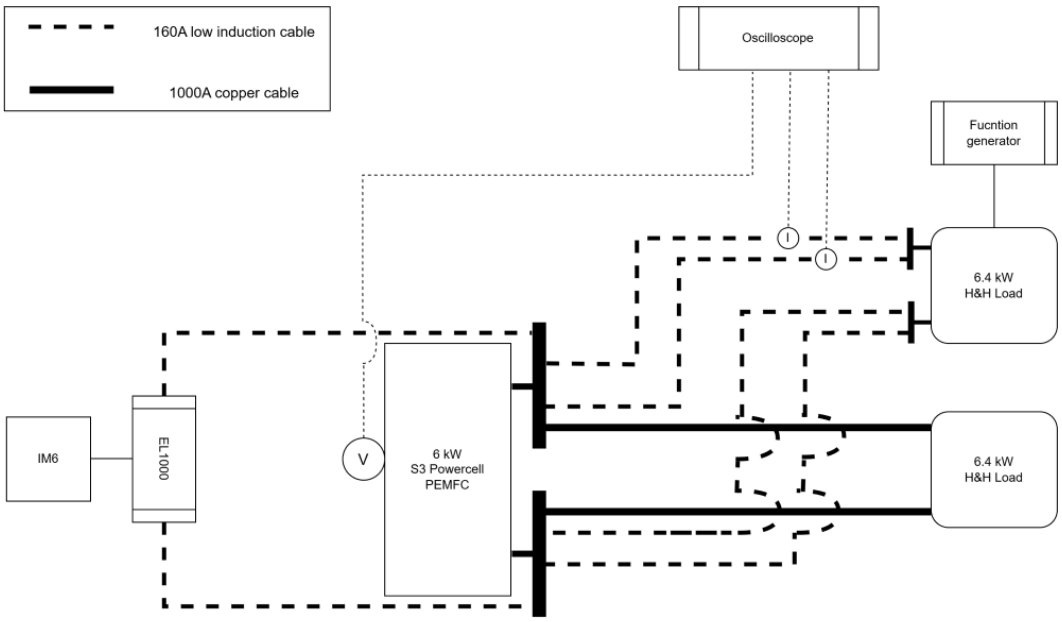


Fig 1. Experimental setup for performing Baseline characterization and conducting high frequency current ripple tests.

Results: As shown in Fig. 2, the degradation induced by current ripples is reversible, as evidenced by voltage recovery after a break. The double-layer capacitance at both the anode and cathode effectively filters high-frequency components [2], preventing measurable performance degradation even at ripple amplitudes of up to 300 A peak-to-peak. The PEMFC stack exhibited resilience to high-frequency disturbances, maintaining stable polarization curves and impedance spectra throughout the testing period. These findings indicate that the stack's electrochemical performance remains largely unaffected by extreme ripple conditions, reinforcing its suitability for high-power applications.

Conclusions: This study demonstrates that PEMFC stacks exhibit a high degree of tolerance to high-frequency, high-amplitude current ripples, addressing a key uncertainty in the design of aerospace power systems. The findings suggest that aggressive ripple suppression may not

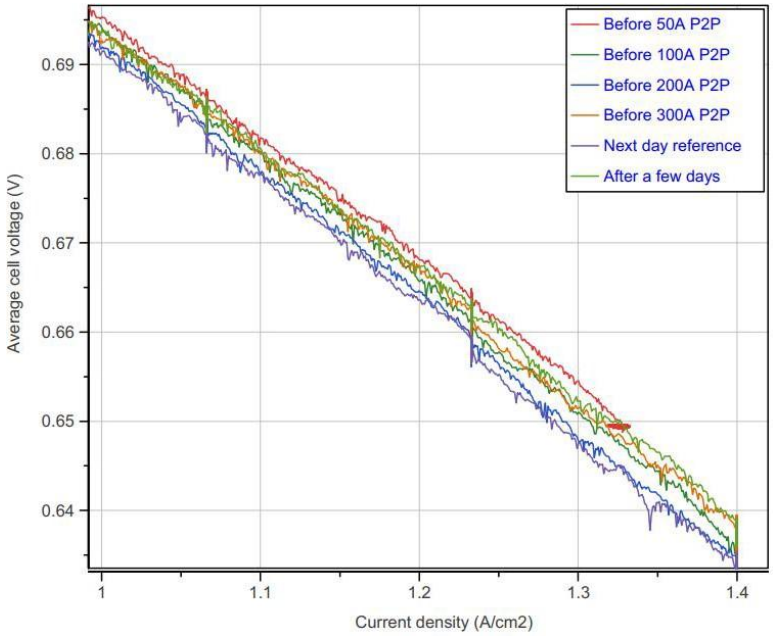


Fig 2. Polarization curve plotted before each ripple test.

be necessary, enabling the development of lighter, more cost-effective, and energy-efficient PEMFC-based architectures for short-duration flight applications. Future work will focus on extending the testing to multiple 1.5-hour cycles to assess the long-term effects of ripple exposure on PEMFC durability in short-duration flight scenarios. Additionally, similar investigations can be conducted for long-duration flights and higher current ripple amplitudes to further refine design considerations for aerospace applications.

Acknowledgment

The author would like to thank the Federal Ministry for Economic Affairs and Climate Action of Germany for the financial support for this work (research project number 20M2102B).

References

[1] Wahdame, Bouchra, et al. "Impact of power converter current ripple on the durability of a fuel cell stack." 2008 IEEE international symposium on industrial electronics. IEEE, 2008.
[2] Fontes, Guillaume, et al. "Interactions between fuel cells and power converters: Influence of current harmonics on a fuel cell stack." IEEE Transactions on Power Electronics 22.2 (2007): 670-678.
[3] Kim, Jong-Hoon, et al. "An experimental analysis of the ripple current applied variable frequency characteristic in a polymer electrolyte membrane fuel cell." Journal of Power Electronics 11.1 (2011): 82-89.
[4] Gerard, Mathias, et al. "Ripple current effects on PEMFC aging test by experimental and modeling." (2011): 021004.

EFCH2 2025
European Fuel Cells and Hydrogen
PIERO LUNGHI CONFERENCE
September 17th–19th 2025
Capri / Italy

Anomalous Diffusion of Water and Oxygen in Nafion Membrane

Makihito Nakamura*[ab], Gianpietro Moras[a], Michael Moseler[ab], Konstantinos Gkagkas[c], Kerstin Falk [a]

* corresponding author: Makihito Nakamura, makihito.nakamura@iwm.fraunhofer.de
[a] Fraunhofer Institute for Mechanics of Materials, Wöhlerstr. 11,
79108 Freiburg, Germany
[b]Institute of Physics, University of Freiburg, Stefan-Meier-Straße 21, 79104 Freiburg, Germany
[c]Toyota Motor Europe NV/SA, Technical Center, Hoge Wei 33B,
B-1930 Zaventem, Belgium

Keywords: Nafion, Molecular Dynamics, Anomalous Diffusion, Continuous Time Random Walk

Abstract

The diffusion of oxygen and water molecules in hydrated Nafion membranes was examined with molecular dynamics simulations for different hydration levels. This study shows that both oxygen and hydrogen exhibit sub-diffusive behavior where the mean squared displacement does not grow linearly in time but rather at slower rates characterized by a power law scaling t^{α} with $0.6 \lesssim \alpha < 1$. The mobility of water molecules is greatly affected by electrostatic attraction from Nafion and depends strongly on the hydration level. In contrast, oxygen diffusion is much less prone to changes in water content. The anomalous diffusion dynamics of oxygen molecules can be explained by their intermittent hops between nanopores in the membrane within the framework of the continuous-time random walk theory.

Introduction

Nafion is a perfluorinated polymer with electrochemical functionalities best known for its common use in proton exchange membrane fuel cells (PEMFC). When utilized as a binder in the cathode catalyst layer (CL) of PEMFC, the Nafion membrane serves as a pathway not only for protons but also for oxygen gas and for water, particularly in the vicinity of catalyst nanoparticles. The transport of each species in the CL directly relates to the rate of catalytic reaction and hence affects the overall performance of PEMFC [1] [2] [3] [4] [5].

Although numerous efforts have been made on studying fluid transport in PEMFC [6] [7], microscopic details of the transport mechanism are not yet understood. In this study, we explore nanoscale diffusion dynamics of oxygen and water in Nafion membranes by means of all-atom molecular dynamics (MD) simulations.

Objectives

In this MD study, we aim to investigate and understand the transport dynamics of oxygen and water molecules in Nafion membranes. In particular, we explore how the transport is affected by varying degrees of hydration of the membrane. In that regard, we seek to identify connections between the diffusive transport and microscopic structural properties of the membrane.

Material and methods

We modelled a Nafion chain with 10 repeated monomeric units, each consisting of seven fluorocarbon backbone monomers and a sidechain terminated with a sulfonic acid group, corresponding to the equivalent

weight of 1100 g/mol. Eight such polymer molecules, ionized in a way that each of the hydrogen atoms in the sulfonic acid groups dissociates into a hydronium ion, are positioned in a cubic box with the periodic boundary condition applied in all dimensions. The hydration degree is characterized by the ratio λ of number of water molecules to number of sulfonic acid groups and five different values of $\lambda = 2, 4, 6, 8, 10$ are tested. Furthermore, 20 oxygen molecules are added and their trajectories are kept track of up to 100 nanoseconds as well as those of water.

The intra- and inter-molecular interactions of Nafion, hydronium ions, and oxygen are described by the General Amber Force Field with parameters taken from Venkatnathan et al. [8] [9], while water molecules are represented by the TIP4P-Ew model [10].

All production runs were carried out at constant temperature of 300K using a constant volume Nose- Hoover thermostat implemented in LAMMPS software [11] [12].

Results

The mean squared displacement (MSD) measurements reveal that neither water nor oxygen follow Fickian dynamics, i.e. MSD growing linearly in time. Instead, they both show a power law relationship MSD$\sim t^{\alpha}$ with exponents α less than one, which is a characteristic of sub-diffusion.

In case of water, α is lower than 0.6 at the lowest studied hydration degree of $\lambda = 2$ but increases as λ gets higher. At the highest studied hydration level $\lambda = 10$, a rather high value of $\alpha = 0.93$ is observed, suggesting a possible transition into Fickian dynamics. This transition is attributed to the change in electrostatic interaction between water and the sulfonic groups of Nafion: at low hydration levels, water molecules are strongly attracted to the sulfonic groups so that they can hardly travel a long distance away. With higher water contents, however, water molecules self-aggregate and form wide channels in the membrane, which enables them to move freely as in bulk without being influenced by the electrostatic interaction. Results from a hydrogen bond analysis also indicate that water stays around the sulfonic groups for shorter times when λ is increased.

As for oxygen, the exponent stays almost constant at all hydration levels, namely $\alpha \sim 0.8$. By analyzing individual molecular trajectories, it turns out that each oxygen molecule tends to reside in a small area corresponding to a membrane pore space for some time before it moves on to another, indicating that the sub-diffusive character observed here is a confinement effect from the highly nanoporous structure of the membrane. Furthermore, we show that the dynamics of oxygen transport can be modelled in the framework of the continuous time random walk theory which yields theoretical predictions for the power law exponent α and the generalized diffusion coefficient consistent with results obtained from curve fitting of ensemble-averaged MSDs.

Conclusions

This study provides insight into the anomalous character of fluid transport in Nafion membranes. The diffusive transport of oxygen and water molecules in Nafion membranes was studied by means of equilibrium MD simulation. It was found that both oxygen and water undergo sub-diffusion, albeit for different reasons: while water dynamics is slowed down due to electrostatic attraction from the sulfonic groups of Nafion, oxygen sub-diffusion is attributed to the confined pore space geometry of the membrane. These results clearly demonstrate the onset of anomalous diffusion dynamics of oxygen and water in nanoporous ionomer membranes and hence highlight the importance of evaluating the nanoscopic structure of the membrane material in fuel cell modelling where the fluid transport plays a pivotal role in its overall operation.

Acknowledgment

We acknowledge funding from the European Union's Horizon Europe research and innovation program under the Marie Sklodowska-Curie project BLESSED grant agreement No - 101072578.

References

[1] K. J. Lange, P. Sui and N. Djilali, "Pore Scale Simulation of Transport and Electrochemical Reactions in Reconstructed PEMFC Catalyst Layers," *J. Electrochem. Soc.,* vol. 157, no. 10, pp. 1434-1442, 2010.

[2] Z. Huang, L. Xing and Z. Tu, "Load changing characteristics of the hydrogen-air and hydrogen-oxygen proton exchange membrane fuel cells," *Int J Energy Res.,* vol. 46, no. 2, pp. 1909-1921, 2022.

[3] K. Kim, K. Lee, S. Lee, E. Cho, T. Lim, H. Kim, S. Yoon, S. Kim, T. Lim and J. Jang, "The effects of relative humidity on the performances of PEMFC MEAs with various Nafion ionomer contents," *Int. J. Hydrog. Energy,* vol. 35, no. 23, pp. 13104-13110, 2010.

[4] D. Morris and X. Sun, "Water-sorption and transport properties of Nafion 117 H," *J. Appl. Polym. Sci.,* vol. 50, no. 8, pp. 1445-1452, 1993.

[5] R. Zhang, T. Min, L. Chen, H. Li, J. Yan and W. Tao, "Pore-scale study of effects of relative humidity on reactive transport processes in catalyst layers in PEMFC," *Appl. Energy,* vol. 323, p. 119553, 2022.

[6] O. S. Ijaodola, Z. El-Hassan, E. Ogungbemi, F. N. Khatib, T. Wilberforce, J. Thompson and A. G. Olabi, "Energy efficiency improvements by investigating the water flooding management on proton exchange membrane fuel cell (PEMFC)," *Energy,* vol. 179, pp. 246-267, 2019.

[7] P. C. Sui, X. Zhu and N. Djilali, "Modeling of PEM Fuel Cell Catalyst Layers: Status and Outlook," *Electrochem. Energ. Rev.,* vol. 2, no. 3, pp. 428-466, 2019.

[8] Wang, J.; Wolf, R. M.; Caldwell, J. W.; Kollman, P. A.; Case, D. A., "Development and testing of a general amber force field," *J Comput Chem.,* vol. 25, no. 9, pp. 1157-1174, 2004.

[9] A. Venkatnathan, R. Devanathan and M. Dupuis, "Atomistic Simulations of Hydrated Nafion and Temperature Effects on Hydronium Ion Mobility," *J. Phys. Chem. B,* vol. 111, no. 25, pp. 7234-7244, 2007.

[10] H. W. Horn, W. C. Swope, J. W. Pitera, J. D. Madura, T. J. Dick, G. L. Hura and T. Head-Gordon, "Development of an improved four-site water model for biomolecular simulations: TIP4P-Ew," *J. Chem. Phys.,* vol. 120, no. 20, pp. 9665-9678, 2004.

[11] W. Shinoda, M. Shiga and M. Mikami, "Rapid estimation of elastic constants by molecular dynamics simulation under constant stress," *Phys. Rev. B.,* vol. 69, no. 13, p. 134103, 2004.

[12] A. P. Thompson, H. M. Aktulga, R. Berger, D. S. Bolintineanu, W. M. Brown, P. S. Crozier, P. J. in 't Veld, A. Kohlmeyer, S. G. Moore, T. D. Nguyen, R. Shan, M. J. Stevens, J. Tranchida, C. Trott and S. J. Plimpton, "LAMMPS - a flexible simulation tool for particle-based materials modeling at the atomic, meso, and continuum scales," *Comput. Phys. Commun.,* vol. 271, p. 108171, 2022.

EFCH2 2025 European Fuel Cells and Hydrogen PIERO LUNGHI CONFERENCE
September 17th–19th 2025 Capri / Italy

Enhanced Electrochemical Performance of PBA@CNF-rGO Cathodes for Sodium-Ion Batteries

Catia Algieri*[a], Saurav Bhattacharyya[a,b], Veronica Cozzolino[a,c], Enrica Fontananova[a], P. Zito[a], Adolfo Iulianelli[a]

*Corresponding author: Dr. Catia Algieri, c.algieri@itm.cnr.it

[a] National Research Council – Institute on Membrane Technology (CNR-ITM), via P. Bucci 17C, Rende (CS) – 87036, Italy

[b]Department of DIBEST, University of Calabria, Via Pietro Bucci, Rende 87036, Italy

[c]Department of DIMES, University of Calabria, Via Pietro Bucci, Cubo 42A, Rende 87036, Italy

Keywords: Sodium-Ion Batteries, Prussian blue analogues, Carbon nanofibers,

Abstract

The increasing demand for cost-effective and efficient energy storage solutions has driven research into sodium-ion (Na-ion) batteries as a viable alternative to lithium-ion (Li-ion) systems. Prussian blue analogues (PBAs) are promising cathode materials due to their open-framework structure. However, these chemical species exhibit low electrical conductivity. The dispersion of PBAs on CNFs ensures interesting electron transport during the charge and discharge cycles.

In this study, PBA dispersed/anchored on carbon nanofibers (PBA@CNFs) were synthetised. In addition, some of the prepared samples were doped with reduced graphene oxide. Physical structure, size, and arrangement of the PBA on the CNFs were evaluated. The electrical properties (e.g. specific capacity) were also analysed.

Introduction

The growing reliance on renewable energy sources like solar and wind necessitates efficient, cost-effective energy storage solutions for grid stability [1,2]. While various storage technologies exist, room-temperature rechargeable batteries stand out for their scalability and efficiency. However, achieving an economically viable energy storage system below $100/kWh remains a challenge, particularly for lithium-ion (Li-ion) batteries [3].

Sodium-ion batteries (SIBs) offer a promising alternative due to their lower cost and similar charge-storage mechanisms to Li-ion batteries [4]. However, conventional cathode materials, including layered oxides and polyanion-based frameworks, face limitations in capacity and energy-intensive synthesis, making large-scale application difficult.

Prussian blue analogues (PBAs) represent an attractive alternative due to their open-framework structure, which enables Na+ ions to pass through rapidly [5]. Furthermore, PBAs exhibit high specific capacities and good cycling stabilities. Additionally, their low-temperature synthesis reduces production costs. However, the low electrical conductivity and poor cycling performance of the PB cathode require improvement, further limiting its application to SIBs. Recently, research groups found that the addition of conductive reduced graphene oxide (rGO) or their dispersion on CNFs can greatly improve both the electrode's ability to store and release charges and also its stability.

This study was focused on the development highly crystalline Prussian blue anchored on electrospun carbon nanofbers (PBA@CNFs) for Na-ion-battery. The aim of the work is to obtain structurally stable and protective electrodes with good electrical conductivity for an improvement of the battery capacity and cyclability. In addition, some samples were prepared embedding PBA materials in conductive reduced graphene oxide (rGO) for obtaining a further improvement of the electronic conductivity and flexibility. The synthesized materials were subjected to chemical-physical investigations and electrochemical measurements.

Objectives

- **(i) Synthesis of PBa@CNFs for sodium ion battery.**
- **(ii) Synthesis of r-GO@PB@CNFs for sodium ion battery**
- **(iii) Improvement of Structural Stability**
- **(iv) Electrochemical Advancements** (Achievement of superior stability, high-rate capability, and prolonged cycle life for Na-ion-batteries)
- **(v)** Cost-Effective Energy Storage

Material and methods

PBA was synthesized using the co-precipitation method. Subsequently, CNFs were prepared by a traditional electrospinning and further carbonization process. In addition, reduce graphene oxide (rGO), was synthesized via Hummer's method. Subsequently, an uniform slurry was obtained dispersing the presynthesized PBA in an opportune solvent, then mix with CNFs to form a uniform slurry. Finally, after 24 hours, the obtained material was washed with distilled water and ethanol. The same procedure was performed adding in the slurry PBA-CNFs the synthesized r-GO. The prepared materials were dried overnight in a vacuum oven at 110 C before used as electrode materials.

The morphology of the synthesized hybrid nanocomposite was analysed using scanning electron microscopy (SEM), while energy-dispersive X-ray spectroscopy (EDX) was also performed for evaluating the elementalcomposition of the prepared PBA@CNF materials. Electrochemical measurements were performed to evaluate the specific capacity and overall performance of the synthetised material.

Results

Particle size and surface characteristics of the PBA@CNFs with and without r-GO were evaluated by SEM analyses. In addition, EDX characterization was performed to identify the chemical species present in the PBA-CNF composite cathode. In addition, the specific capacity was measured to know how much energy the cathode can provide during the charge and discharge cycles.

Conclusions:

In this study, PBA@CNF electrode was fabricated using electrospun carbon nanofibers as electron-donating agents and carbon skeletons. The prepared materials were doped with rGO for improving their electronic conductivity and flexibility. The morphological and electrical properties of the cathode material were also evaluated/studied.

Acknowledgment

This work received funds by the “ORgANics for Green Electrochemical Energy Storage (ORANGEES)” project in the framework of the “Research Projects of the Energetic System – Theme 1.2: Storage systems, including electrochemical and power to gas, and related interfaces with networks for the: Study and development of materials for storage systems” – RdS_MASE - CUP: B93C22001330007.

References

[1] T. Wang, P. Shi, J. Chen, S. Cheng and H. Xiang, J. Nanopart. Res., 2016, 18, 1-9.
[2] M. Chen, X. Liang, F. Wang, D. Xie, G. Pan and X. Xia, J. Mater. Chem. A, 2019, 7, 6644.
[3] L. Sun, M. Li, Y. Jiang, W. Kong, K. Jiang, J. Wang and S. Fan, Nano Lett., 2014, 14, 4044-4049.
[4] H. J. Peng, J. Q. Huang and Q. Zhang, Chem. Soc. Rev., 2017, 46, 5237-5288.
[5] Z. Gong, Q. Wu, F. Wang, X. Li, X. Fan, H. Yang and Z. Luo, RSC Adv., 2016, 6, 37443-37451.

European Fuel Cells and Hydrogen
PIERO LUNGHI CONFERENCE
September 17th–19th 2025
Capri / Italy

Anode Purge Strategy Simulation for a Multi-Stack Fuel Cell System

Manuel Kutz*[a], Xenia Strocka[a], Magnus Lenger[a,c], Jannik Holtorf [b], Markus Schorr[b], Wilhelm Tegethoff [a,c]

* corresponding author: m.kutz@tlk-thermo.com
[a] TLK-Thermo GmbH, Rebenring 31, 38106 Braunschweig
[b] German Aerospace Center (DLR), Institute of Engineering Thermodynamics, Hein-Saß-Weg 22, 21129 Hamburg, Germany
[c] Technische Universität Braunschweig, Institut für Thermodynamik, Hans-Sommer-Str. 5, 38106 Braunschweig Germany

Keywords: Multi-stack fuel cell system, PEMFC system, Purge strategy, Recirculation anode, Transport application

Abstract

Introduction: Among the different types of fuel cells, proton exchange membrane fuel cells (PEMFCs) are particularly well suited to transport applications because they are pollution-free and offer a high power density [1]. PEMFC systems consist of various subsystems, the air supply system, the thermal management system and the hydrogen supply system. In this work, we focus on the hydrogen supply system with recirculation as a component of a multi-stack fuel cell system (MFCS). The anode recirculation yields an improved water management [2]. During recirculation, nitrogen accumulates in the hydrogen supply system. This makes purging necessary to prevent degradation and efficiency losses. Simultaneously, minimizing hydrogen loss is essential. To optimize the overall system efficiency, different purge strategies are implemented and analyzed by simulation of the MFCS. In addition to hydrogen utilization, stack and system efficiencies as well as stable operating conditions are used as criteria for evaluating purging strategies. In this work, a new purge strategy similar to the electric current integration method [3] is introduced and evaluated using the presented simulation model.

Objectives: The objective of this work is to show that the dynamic simulation model developed in this study can be used to evaluate different purge strategies in the anode loop. Typically, a purge strategy is characterized by the purge interval and the purge duration. A common purge strategy to determine the purge-interval under varying-current operation is current integration, which is regarded as a rather new approach [3]. This charge-dependent strategy requires neither a voltage drop nor a nitrogen concentration measurement. It is triggered when a certain integrated threshold value (e.g. given in Ampere-hours) is reached [3,4]. The determination of a suitable threshold may lead to unfavorable operating conditions

in which hydrogen starvation and thus carbon corrosion can occur. Carbon corrosion reduces the catalyst particles and leads to a permanent loss of the fuel cell performance. This reality motivated our use of simulation in this project and enabled operating conditions that would be harmful to the stack to be determined beforehand and therefore avoided at the test rig. One aim of this study is to prove that the purge strategy for a MFCS system can be investigated and developed using a simulation model developed from Modelica and the TIL Suite [5].

Material, methods and results: A simulation model of a MFCS is developed in Modelica using the TIL Suite [5] and the Addon for Hydrogen Energy Systems. The image below shows the components, connections and fluid flow of the MFCS test rig. It is parametrized based on manufacturer data.

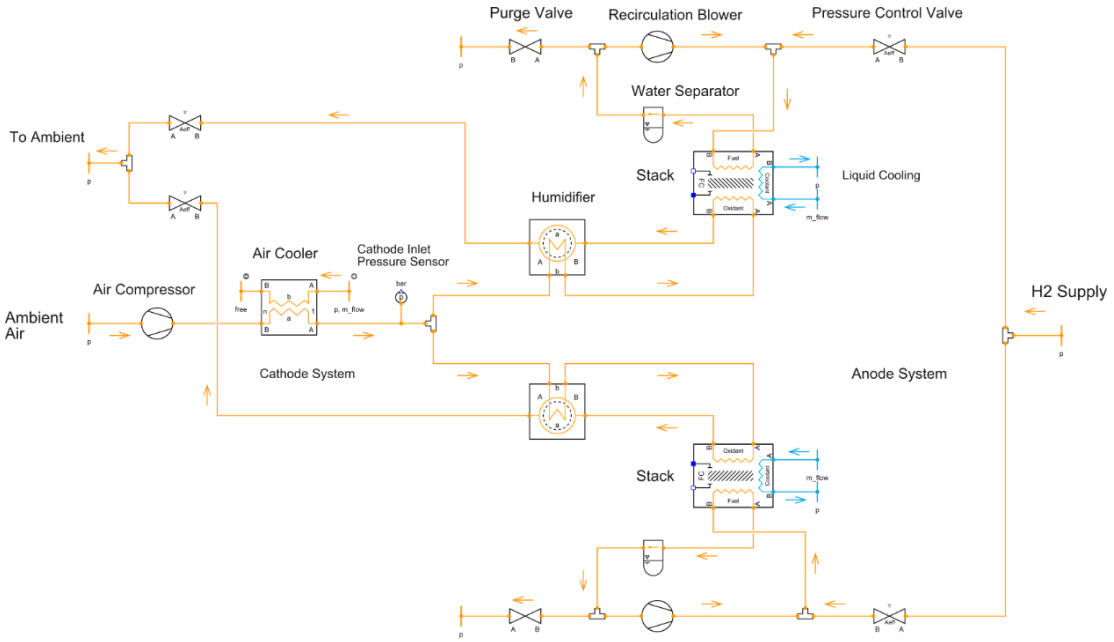


Figure 1: Flowchart visualization of the simulation model

The design of the anode subsystem is considered when analyzing the purge strategy. The anode gas is recirculated by a recirculation blower. Liquid water is separated using a water separator. Thus, the main purpose of the purge is to remove accumulated nitrogen. The crossover nitrogen molar flow rate $\dot{n}_{N2crossover}$ can be described the equation

$$\dot{n}_{N2crossover} = K_{N2} * A_{mem} * \frac{p_{N2cat} - p_{N2an}}{\delta_{mem}}$$

where K_{N2} is the nitrogen permeability in the membrane, p_{N2cat} and p_{N2an} the partial pressure of nitrogen on the cathode and anode side, A_{mem} the membrane area and δ_{mem} the thickness of the membrane.

The nitrogen crossover depends on the difference in partial pressure of nitrogen between the cathode and anode side. Instead of the current-integration strategy, which is commonly used with anode dead end configurations, here we propose to use the method of integrating the cathode inlet pressure $p_{CathodeInlet}$. The partial pressure of nitrogen and thus the partial

pressure difference between cathode and anode is directly proportional to the absolute pressure at the cathode inlet. Hence, the purge interval of the proposed method depends explicitly on the transport mechanism of the nitrogen crossover. In this MFCS configuration the air supply is combined for both stacks. The compressor controls the cathode inlet pressure $p_{CathodeInlet}$ at the junction splitting the flow to the separate stacks. Consequently, the cathode stack input pressure for both stacks is in a similar range, even with different loads on the stacks. In this way, a suitable value from the pressure integration determined by the simulation model can be used to calculate the purge intervals for both sides of the MFCS.

Conclusions: The work presents a system simulation model of a test rig of a multi-stack fuel cell system. A current-integration purge strategy known from the published literature was analysed and consequently a new pressure integration purge strategy was developed and investigated. This proposed strategy of pressure integration for MFCS applications with anode recirculation can be investigated using the system simulation model described.

Acknowledgment: The author would like to thank the Federal Ministry for Economic Affairs and Climate Action of Germany for the financial support for this work (research project number 20M2101 I/E/F).

References

[1] Zhiyang Liu, Jian Chen, Hao Liu, Chizhou Yan, Yang Hou, Qinggang He, Jiujun Zhang, Daniel Hissel, Anode purge management for hydrogen utilization and stack durability improvement of PEM fuel cell systems, Applied Energy, Volume 275, 2020, https://doi.org/10.1016/j.apenergy.2020.115110

[2] Cheng Bao, Minggao Ouyang, Baolian Yi, Modeling and control of air stream and hydrogen flow with recirculation in a PEM fuel cell system—I. Control-oriented modeling, International Journal of Hydrogen Energy, Volume 31, Issue 13, 2006 https://doi.org/10.1016/j.ijhydene.2006.02.031

[3] Khan, N.; Al-Sagheer, Y.; Steinberger-Wilckens, R. PEFC System Reactant Gas Supply Management and Anode Purging Strategy: An Experimental Approach. Energies 2022, 15, 288. https://doi.org/10.3390/en15010288

[4] Christoph Humer, Christoph Steindl, Peter Hofmann, Experimentelle Entwicklung einer H_2-Purge-Strategie zur Maximierung der Effizienz einer PEM-Brennstoffzelle, Diplomarbeit, August 2022

[5] TLK-Thermo GmbH, TIL Suite https://www.tlk-thermo.com/en/software/til-suite (accessed March 31, 2025)

EFCH2 2025 European Fuel Cells and Hydrogen
PIERO LUNGHI CONFERENCE
September 17th–19th 2025 Capri / Italy

Untreated vs. Treated Carbon Felt Anodes: Impacts on Power Generation in Microbial Fuel Cells

Abdelghani Ghanam*[a], Ambre Chabbert[a,b], Laurent Nicolas[a], Naoufel Haddour[a]

* corresponding author: abdelghani.ghanam@ec-lyon.fr

[a] Univ Lyon, Ecole Centrale de Lyon, INSA Lyon, Université Claude Bernard Lyon 1, CNRS, Ampère, UMR5005, 69130 Ecully, France

[b] Centre de Recherche sur la Biodiversité et l'Environnement, Université de Toulouse, CNRS, UPS, INPT, IRD, Toulouse, France

Keywords: Anode materials, carbon felt, electroactive bacteria, microbial fuel cell

Abstract: Microbial fuel cells (MFCs) offer a sustainable solution for simultaneous wastewater treatment and energy generation. This study evaluates the performance of pristine carbon felt (pCF) and acid-heat-treated carbon felt anodes, each functionalized with carbon nanofibers (CNFs), in MFC applications. While surface treatment reduced charge transfer resistance, it did not enhance power output. Notably, the untreated pCF anode promoted faster biofilm development and achieved a peak power density of 3.4 $W.m^{-2}$. These results highlight the potential of simple, low-cost electrode configurations for efficient MFC performance.

Introduction: MFCs are an emerging bioelectrochemical technology that enables direct conversion of organic matter into electricity through the metabolic activity of electrochemically active bacteria (EAB) [1,2]. The electrons released during substrate oxidation at the anode are transferred to the cathode, typically via an oxygen reduction reaction. Among the challenges impeding their large-scale application, low power output, which is primarily due to inefficient extracellular electron transfer (EET) at the anode—remains a key limitation. Carbon felt (CF), with its high conductivity, biocompatibility, and porous architecture, is widely used as an anode material, though its performance can be further enhanced via chemical and structural modifications.

Recent strategies have involved acid-heat treatments and CNF functionalization using surfactants or biopolymers to improve electrochemical properties and biofilm formation [3]. However, such approaches often increase material costs and complexity. This study evaluates the comparative performance of pristine CF and modified CF-based anodes to identify cost-effective configurations that support efficient EET and high power generation in MFC systems.

Objectives: This study aims to investigate the impact of surface treatment and CNF functionalization on the electrochemical performance of CF anodes in MFCs. Specifically, it evaluates and compares pristine CF and acid-heat-treated CF, each modified with CNFs dispersed in either SDBS surfactant or chitosan biopolymer. The goal is to determine whether complex modifications significantly enhance power output compared to unmodified anodes, and to identify cost-effective electrode configurations suitable for scalable MFC applications.

Material and methods

a) Pretreatment and Modification of Carbon Felt-Based Anodes

Six types of anodes were prepared by combining acid activation, heat treatment, and immersion in CNF dispersions, **Fig. 1**. The pCF was cleaned using ethanol, acetone, and water via ultrasonication,

then dried and cut into 1 cm^3 cubes. For the acid-heat-treated variant (A-CF), pCF was immersed in concentrated H_2SO_4, rinsed, dried, and heated at 450 °C. Both pCF and A-CF were subsequently modified by immersion in CNF dispersions prepared using either SDBS surfactant or chitosan (CS) biopolymer. The immersion-drying process was repeated thrice to enhance CNF loading. All anodes were then evaluated electrochemically in a KCl/$[Fe(CN)_6]^{3-}/^{4-}$ solution using cyclic voltammetry (CV) and electrochemical impedance spectroscopy (EIS).

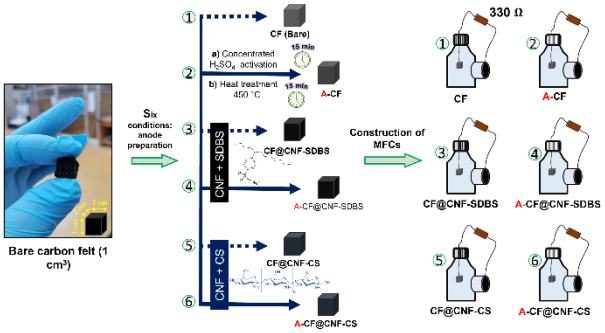


Figure 1. *Preparation of untreated and treated CF anodes.*

b) MFC configuration, inoculation, and operation

Single-chamber MFCs were assembled in 250 ml Wheaton bottles with Pt/C-coated CF air cathodes and 1 cm^3 CF cube anodes. Each reactor was filled with 250 mL of primary effluent and inoculated with anaerobic sludge (5 $g.L^{-1}$), source of EABs, and 1 $g.L^{-1}$ sodium acetate (NaAc) as the carbon source. Electrodes were connected via a 330 Ω resistor, and voltage was recorded at 1-min intervals to monitor biofilm development. The electrode spacing was maintained at ~2 cm.

c) Electrochemical characterization

Electrochemical tests (CV and EIS) were conducted using a three-electrode system in a redox probe solution to assess surface electron transfer. After biofilm maturation, polarization and power density curves were obtained via linear sweep voltammetry. The power density (P, $W.m^{-2}$) curves were obtained by multiplying the cell voltage by current density (J, $A.m^{-2}$) according to the fellowing equation.

$$P = V \times I/S$$

Where V and I represented the measured voltage and I denotes the current normalized to the projected anode surface area (S).

Additionally, CV analysis was performed in MFC reactors to evaluate the electroactivity of developed anodic biofilms, providing insights into EAB presence and redox behavior.

Results

a) Biofilm growth on CF-based anodes

Over an 11-day operation period, the MFC with pCF anode demonstrated the fastest biofilm development, reaching a stable voltage of ~300 mV by day four, as demonstrated in **Fig. 2**. Despite improvements in conductivity and hydrophilicity, acid-heat-treated and CNF-coated CF anodes showed slower biofilm kinetics. These results suggest that EABs more readily colonize hydrophobic surfaces like untreated CF, reinforcing the effectiveness of unmodified CF for rapid biofilm formation and stable operation.

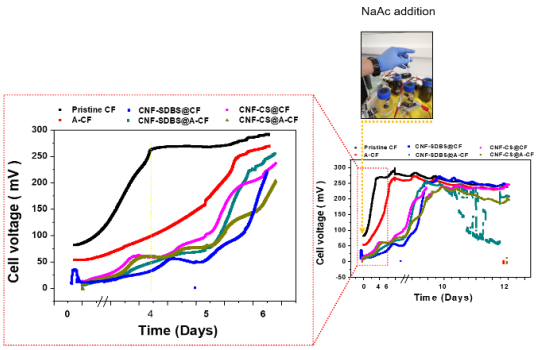


Figure 2. *Voltage outputs of MFCs with different anode materials across a 330 Ω external load.*

b) Power Generation at Biofilm Maturation

Polarization and power density curves (**Fig. 3**) at biofilm maturity revealed that the pCF anode outperformed all modified and treated ones, achieving a maximum power density of 3.4 ± 0.3 $W.m^{-2}$ and maximum Jmax of 26.2 ± 2.3 ± SD ($A.m^{-2}$) with an OCV of 550 mV. This value surpassed results from comparable studies, particularly those using more complex or dual-chamber MFC configurations. The high efficiency and simplicity of the unmodified CF anode highlight its potential for low-cost, scalable MFC deployment.

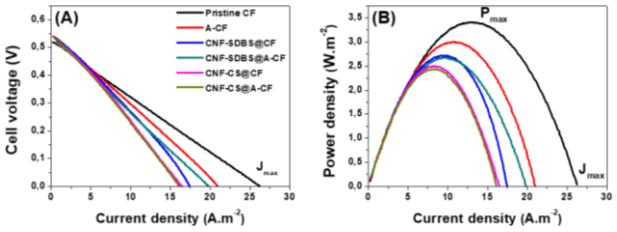


Figure 3*. (A) Polarization and (B) power density curves of MFCs with CF-based anodes after 11 days in wastewater with 10 mM NaAc.*

Conclusions: This study demonstrates that pristine CF anodes offer superior electrochemical performance and biofilm formation compared to their acid-heat-treated and CNF-coated counterparts. Despite modifications enhancing conductivity and surface morphology, they did not translate into improved power output. The pCF anode enabled faster biofilm growth and achieved the highest power density of 3.4 $W{\cdot}m^{-2}$, highlighting its strong interaction with electroactive bacteria and efficient electron transfer. Its simplicity, effectiveness, and low cost make it a promising candidate for scalable microbial fuel cell (MFC) applications

Acknowledgment : The authors would like to greatly acknowledge the financial support of funding from the “Hubert Curien Program” through the PHC MAGHREB Project N°19MAG23/41382WC and the BioPlant project for its support to the realization of this work.

References

[1] A. Ghanam, S. Cecillon, A. Sabac, H. Mohammadi, A. Amine, F. Buret, N. Haddour, Untreated vs. Treated Carbon Felt Anodes: Impacts on Power Generation in Microbial Fuel Cells, Micromachines 14 (2023) 2142.

[2] A. Godain, N. Haddour, P. Fongarland, T.M. Vogel, Bacterial competition for the anode colonization under different external resistances in microbial fuel cells, Catalysts 12 (2022) 176.

[3] M. Saadi, J. Pézard, N. Haddour, M. Erouel, T.M. Vogel, K. Khirouni, Stainless steel coated with carbon nanofiber/PDMS composite as anodes in microbial fuel cells, Materials Research Express 7 (2020) 025504.

EFCH2 2025 European Fuel Cells and Hydrogen PIERO LUNGHI CONFERENCE
September 17th–19th 2025 Capri / Italy

Innovative supported Pd@CeO_2-ZrO_2 catalysts for fuel cells applications

Alessio Occhicone*[a,b], Emmanuel De Gregorio[b], Valentina Naticchioni[c], Claudio Ferone [b], Viviana Cigolotti[d], Elio Jannelli [b], Oreste Tarallo[d], Giuseppina Roviello[b]

* corresponding author: alessio.occhicone@assegnista.uniparthenope.it

[a] Atena scarl, Via Vicinale Cupa Visconti, 77, 80147, Napoli.
[b] University of Naples Parthenope, Department of Engineering, Centro Direzionale Isola C4, 80133 Naples (Italy)
[c] ENEA—Italian National Agency for New Technologies, Energy and Sustainable Economic Development, Via Anguillarese 301, 00123 Rome (Italy)
[d] University of Naples Federico II, Department of Chemical Science, Complesso Universitario di Monte Sant'Angelo, 80126 Naples (Italy)

Keywords: Pd-based ORR catalysts; Ce-Zr mixed oxides; Pt-free PEMFC; metal–support interaction.

Abstract

Palladium nanoparticles supported on the fluorite-type mixed oxide $Ce_{0.6}Zr_{0.4}O_2$ (Pd@CeZr) were developed as platinum-free cathode catalysts for proton-exchange-membrane fuel cells (PEMFCs). A one-pot deposition–precipitation process followed by mild hydrazine reduction yielded a Pd loading of 7–20 wt% and uniformly anchored metallic crystallites with sizes between 3 and 7 nm onto the redox-active support. The Ce–Zr matrix supplies oxygen vacancies that promote self-healing of Pd and stabilize the dispersion, enabling complete redox PdO ↔ Pd cycling up to 1000°C without sintering. Carbon-ink electrodes prepared from the optimized batch delivered a specific electrochemically active surface area (ECSA) of 2.85 $m^2\ g^{-1}$ Pd, 15% higher than a commercial Pd/C benchmark despite the lower noble-metal loading with high resistance at also high temperature treatments. These results position Pd@$CeZrO_2$ as a cost-effective, durable alternative to Pt cathodes for next-generation hydrogen energy systems.

Introduction

Global deployment of proton-exchange-membrane fuel cells (PEMFCs) is presently constrained by the reliance on platinum-group metal (PGM) cathodes, whose scarcity, cost volatility and vulnerability to dissolution hamper the economic viability of large-scale hydrogen energy systems. The oxygen-reduction reaction (ORR) is intrinsically sluggish and accounts for ~80 % of the overpotential losses in state-of-the-art devices; hence, any reduction in PGM content must be coupled with materials capable of sustaining high turnover frequencies under acidic, high-potential conditions [1]. Palladium offers a d-band centre close to that of Pt and a markedly lower cost per mole of surface atoms, but its stability is undermined by oxidative passivation and particle growth during dynamic operation. Embedding Pd nanoparticles in an

oxide matrix endowed with fast oxygen storage/release is therefore a promising route to self-regenerating, Pt-free cathodes.

Mixed ceria–zirconia fluorite phases ($Ce_{1-x}Zr_xO_2$, $0.2 \le x \le 0.6$) display unparalleled oxygen-storage capacity (OSC) owing to the facile Ce^{4+}/Ce^{3+} redox couple and the lattice strain induced by Zr^{4+} substitution, which creates a high concentration of mobile anion vacancies [2]. When Pd is deposited onto $Ce_{0.6}Zr_{0.4}O_2$, these vacancies can shuttle lattice oxygen to and from metal sites, fostering strong metal–support interaction (SMSI) that (i) prevents nanoparticle sintering, (ii) promotes reversible PdO ↔ Pd transformations and (iii) protects the metal from dissolution by dynamically passivating it with a thin, reducible oxide adlayer [3]. Recent density-functional simulations and in-situ X-ray absorption studies corroborate that such Pd–CeZr interfaces stabilize oxygen-bridged configurations that lower the activation barrier for O_2 dissociation, an essential step in acidic ORR [4].

Despite these advantages, the scalable synthesis of highly dispersed Pd@CeZr catalysts and the quantitative correlation between OSC, Pd oxidation state and electrochemical activity remain underexplored [5]. The present work addresses this gap by developing a one-pot deposition–precipitation/hydrazine reduction route that yields ~5 nm Pd clusters crystalline structures well anchored on $Ce_{0.6}Zr_{0.4}O_2$, and by systematically linking structural descriptors (PdO/Pd^0 ratio, Ce^{3+} surface fraction, vacancy density) with ORR metrics under realistic PEMFC conditions.

Objectives

This study aims to (i) synthesize highly dispersed Pd@$CeZrO_2$ catalysts via scalable wet chemistry, (ii) elucidate structure–property relationships controlling Pd redox accessibility and OSC, and (iii) benchmark electrochemical performance against the commercial Pd/C under PEMFC-relevant conditions.

Materials & Methods

CeO_2 and ZrO_2 powders (molar ratio 6:4) were co-precipitated, calcined at 400 °C, impregnated with $Pd(NO_3)_2$, and reduced in hydrazine at 60 °C. Three batches (PdCZ_1–3) were produced by varying support pre-calcination and Pd/support ratios. Phase composition (Rigaku MiniFlex 600 XRD, Rietveld), redox stability (TGA up to 1000 °C), surface states (XPS) and morphology (SEM), were correlated with rotating-disk electrode (0.1 M $HClO_4$, 1600 rpm) metrics. Carbon-supported inks (40 wt.% catalyst, Nafion® binder) served as working electrodes.

Results & Discussion

XRD showed metallic Pd and minor PdO coexisting with a well-crystallised CeZr fluorite phase; optimized PdCZ_2 and PdCZ_3 displayed 3-5 nm Pd domains while PdCZ_1 suffered from larger crystallites (7nm) and amorphous nitrates. XPS revealed that an intermediate Pd loading maximizes the Pd^0/Pd^{2+} ratio (0.98) while increasing surface Ce(III), signaling enhanced OSC and SMSI.

TGA confirmed fully reversible PdO reduction and re-oxidation over repeated 25–1000 °C cycles with ≤ 1 % mass loss, evidencing remarkable thermal robustness (Fig.1). Moreover, most of Pd deposited on the surface could works also after the high oxidative thermal treatment, that's means a high resistance of the supported catalysts structure with no coalescence and migration of Pd also in strength conditions.

The SEM micrographs showed uniform Pd nodules (50–100 nm aggregates) decorating a meso-macroporous scaffold without pore collapse [6].

Electrochemically, carbonized PdCZ_1 delivered an ECSA of 2.85 $m^2\ g^{-1}$ Pd versus 2.52 $m^2\ g^{-1}$ Pt for commercial Pd/C, attributed to finer metal dispersion and superior electronic coupling through the oxide-derived carbon layer.

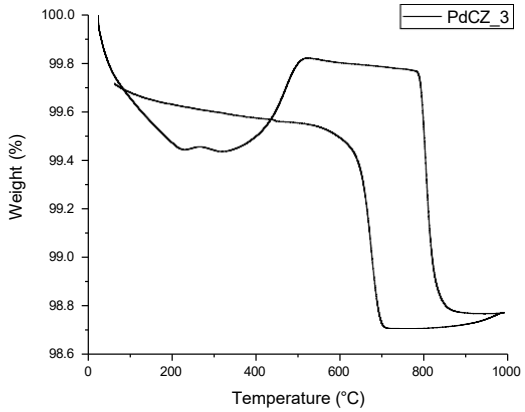


Fig.1: Thermogravimetric analysis of sample PdCZ_3, showing a usable Pd residue >85% after cycling at 1000°C.

Conclusions

A facile hydrazine route affords Pd@$Ce_{0.6}Zr_{0.4}O_2$ catalysts combining (i) sub-5 nm Pd dispersion, (ii) redox-buffered OSC that self-heals metal sites, and (iii) exceptional thermal and electrochemical stability. The best formulation narrows the activity gap with Pd/C while offering marked durability and cost advantages. Ongoing work targets MEA integration and single-cell validation to quantify full-device power gains.

Acknowledgment

The ENEA project WP3.1 – LA3.1.3 PNRR, Mission 2, Component 2, Investment 3.5, NEXT-GENERATION EU-CUP I83C220011700006 is gratefully acknowledged for financial support.

References

[1] A. A. Topalov, S. Cherevko, A. R. Zeradjanin, J. C. Meier, I. Katsounaros, and K. J. J. Mayrhofer, “Towards a comprehensive understanding of platinum dissolution in acidic media,” 2013, *Chem Sci*, vol. 5, pp. 631–638.

[2] A. Trovarelli and P. Fornasiero “Catalysis By Ceria And Related Materials (2nd Edition),” 2013, *Imperial college press*, vol 12.

[3] F. Fally, V. Perrichon, H. Vidal, J. Kaspar, G. Blanco, J. Pintado, S. Bernal, G. Colon, M. Daturi, J. Lavalley, “Modification of the oxygen storage capacity of CeO2-ZrO2 mixed oxides after redox cycling aging,” 2000, *Catalysis Today*, vol. 59, pp. 373–386.

[4] T. Wang, A. Chutia, D. Brett, P. Shearing, G. He, G. Chai, and I. Parkin, “Palladium alloys used as electrocatalysts for the oxygen reduction reaction,” 2021, *Energy & Environmental Science*, *14*(5), 2639-2669.

[5] X. Zhang, J. Wang, and Y. Zhao, “Enhancement Mechanism of Pt/Pd-Based Catalysts for Oxygen Reduction Reaction,” 2023, *Nanomaterials*, vol. 13, pp. 1275.

[6] I. Arsie, M. Battistoni, P. Brancaleoni, R. Cipollone, E. Corti, D. Di Battista, F. Millo, A. Occhicone, B. Paradisi, L. Rolando and J. Zembi, “A new generation of hydrogen-fueled hybrid propulsion systems for the urban mobility of the future,” 2023, *Energies*, vol 17, pp. 34.

European Fuel Cells and Hydrogen
PIERO LUNGHI CONFERENCE
September 17th–19th 2025
Capri / Italy

PVD and PECVD carbon based and nitride coatings for metallic bipolar plates

Miryam Gulino*[1], Claudio Larosa[2], Nicola Lisi[2], Francesco Bozza[2], Valentina Naticchioni[2], Danilo Zola[2], Anna Sytchkova[2], Alfonso Pozio[2], Marta Feroci[1], Maria Luisa Grilli*[2]

[1]*Department of Basic and Applied Sciences for Engineering (SBAI), University of Rome La Sapienza, Rome, Italy*

[2]*ENEA, Italian Agency for New Technologies, Energy and the Environment Department of Renewable Energies, Via Anguillarese, 301-00123 Rome, Italy*

**Corresponding authors: miryam.gulino@uniroma.it, marialuisa.grilli@enea.it*

Keywords: Bipolar plates, coatings, physical and chemical vapour deposition techniques, PEM fuel cells

Abstract:

Bipolar plates are key components of proton exchange membrane fuel cells because of their multiple functions in managing gas distribution, current conduction, and heat. To date, bipolar plates are made by carbon-based materials, metals and composites, each one having its own advantages and disadvantages. In this work, different carbon based and nitride coatings have been developed to coat polished and rough AISI 304 substrates by using different chemical and physical deposition techniques. The produced samples were analysed through physical and chemical characterizations to evaluate the best coating performances.

Introduction:

To convert chemical energy into electric energy, fuel cells are one of the best devices. They are constituted by a membrane electrode assembly, which is composed by a catalyst-coated membrane and gas diffusion layers, and bipolar plates. Bipolar plates are among the most important components in these systems [1]. Their role is to remove water and heat from the fuel cell, make uniform the distribution of reactive gases and collect the electrons generated during the electrochemical reactions in the membrane electrode assembly. In recent years, significant advances have been made in the production, storage and use of hydrogen but some limits still remain. In proton exchange membrane fuel cells (PEMFCs), substitution of graphite bipolar plates (BPPs) with metallic ones has great potential advantages owing to their

low density, high mechanical strength, very low hydrogen permeability and low cost [2]. To protect metal BPPs from electrochemical corrosion and passivation in PEMFCs operating environment, under acid, warm and humid conditions, coatings and surface modifications are necessary.

Objectives:

One of the main limitations present in fuel cells is the corrosion of the metal bipolar plates in the fuel cells environment work. This study aims to develop novel coatings by physical and chemical vapour deposition techniques to protect stainless steel BPPs against electrochemical corrosion in PEMFCs environment conditions.

Material and methods:

In this work, carbon-based and nitrides coatings have been developed to coat polished and rough AISI 304 substrates by radiofrequency sputtering, pulsed electron deposition (PED), and plasma enhanced chemical vapour deposition (PECVD) techniques. Figure 1 shows the images of the pulsed electron deposition apparatus and the inside of the deposition chamber during PED's operative conditions.

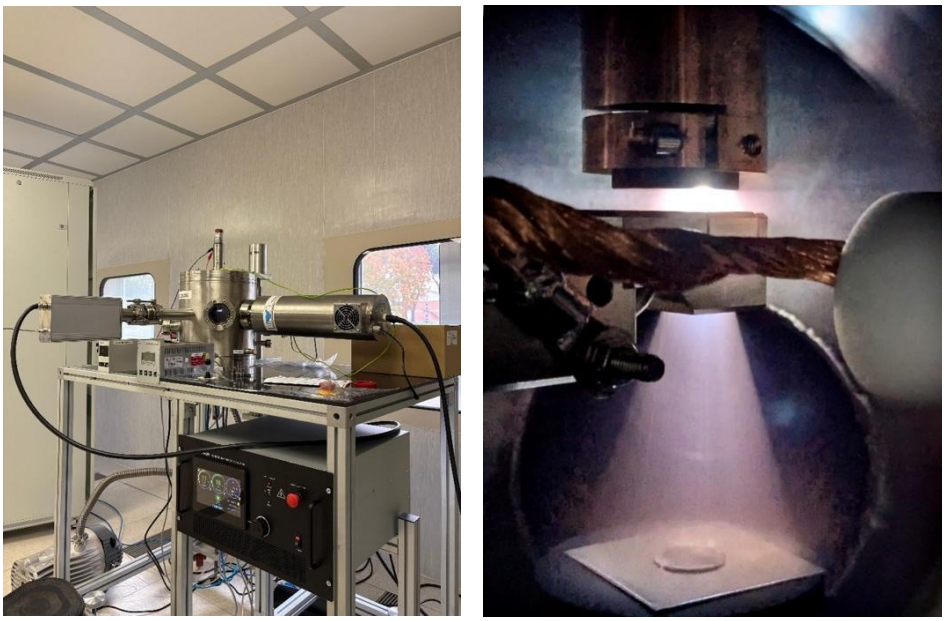


Figure 1: Pulsed electron deposition (PED) system used for depositions.

Thickness and surface roughness of the coatings have been obtained by stylus profiler and coatings were investigated for their physical and chemical characteristics by XRD, SEM and

Raman analyses. Interfacial contact resistance (ICR) and corrosion tests allowed us to evaluate the best coating performances for application in metal BPPs of PEMFCs.

Results:

Graphite and amorphous carbon coatings deposited, by PECVD and PED, respectively, showed the best ICR resistances. To guarantee the adhesion of the sputtered coatings to the AISI 3014 substrate, an interlayer was necessary both in case of carbon-based and nitride coatings. Cr served at best in both cases.

Conclusions:

Several carbon-based and nitrides coatings were deposited by radio frequency sputtering, PED and PECVD techniques. Coatings characteristics have been compared to explore their potential application in AISI 304 BPPs. Adhesion of coatings to the metallic substrate and coatings' conductivity resulted the main challenging issues. From this work, we conclude that the investigated coating materials have promising characteristics for application in PEM fuel cells.

Acknowledgment

ENEA - Italian National Agency for New Technologies, Energy and Sustainable Economic Development for funding (PNRR POR H_2 WP3.1 LA 3.1.2 "Sviluppo di rivestimenti a base di carbonio mediante tecniche di deposizione chimica e fisica da fase vapore e spruzzatura al plasma per applicazione in piatti bipolari in acciaio, titanio o leghe di alluminio).

References

[1] F. Madadi, A. Rezaeian, H. Edris, and M. Zhiani, "Improving performance in PEMFC by applying different coatings to metallic bipolar plates," *Mater Chem Phys*, vol. 238, Dec. 2019

[2] W. Tang *et al.*, "Research progress on coating and coating technology of fuel cell metallic bipolar plate," *Next Materials*, vol. 4, p. 100062, Jul. 2024.

EFCH2 2025
European Fuel Cells and Hydrogen
PIERO LUNGHI CONFERENCE
September 17th–19th 2025
Capri / Italy

Development and Characterization of Electrospun PBI Membranes for Enhanced Acid Uptake in HTPEMFC Applications

Emmanuel De Gregorio*[a,b], Carlo De Luca[b,c], Claudio Ferone[a], Viviana Cigolotti[b], Valentina Naticchioni[b], Elio Jannelli[a], Oreste Tarallo[c], Giuseppina Roviello[a]

* corresponding author: emmanuel.degregorio001@studenti.uniparthenope.it

[a] University of Naples Parthenope, Department of Engineering, Centro Direzionale Isola C4, 80133 Naples (Italy)

[b] ENEA—Italian National Agency for New Technologies, Energy and Sustainable Economic Development, Via Anguillarese 301, 00123 Rome (Italy)

[c] University of Naples Federico II, Department of Chemical Science, Complesso Universitario di Monte Sant'Angelo, 80126 Naples (Italy)

Keywords: PEM Fuel Cell, Non-fluorinated polymers, PBI, HTPEM, Electrospinning

Abstract

High-temperature proton exchange membrane fuel cells (HTPEMFCs), operating between 120 °C and 200 °C, benefit from the use of polybenzimidazole (PBI) membranes due to their excellent stability and ability to conduct protons when doped with phosphoric acid (PA). Recent advancements in electrospinning have made possible to produce fibrous PBI membranes with a 3D porous structure that greatly enhances their PA absorption capacity. In this work, electrospun PBI membranes were doped with PA under different experimental conditions. Compared to conventional dense membranes, the electrospun mats exhibited much faster adsorption kinetics, well described by a pseudo-second-order model, suggesting a chemisorption mechanism between PA and PBI's imidazole groups. Preliminary electrochemical evaluations indicated enhanced proton transport in the fibrous structures. Planned future work includes integrating these membranes into membrane electrode assemblies (MEAs) for practical fuel cell testing. Overall, the results support the potential of electrospun PBI membranes as a promising direction for improving HTPEMFC performance and advancing clean energy technologies.

Introduction

High-temperature proton exchange membrane fuel cells (HTPEMFCs), operating between 120 °C and 200 °C, offer key advantages over low-temperature systems, such as improved reaction kinetics, better tolerance to fuel contaminants like CO, and simpler water management due to their anhydrous operation. A critical component of HTPEMFCs is the proton exchange membrane, which must ensure thermal, chemical, and mechanical stability while maintaining high proton conductivity in dry conditions. PBI, when doped with phosphoric acid, meets these requirements through strong acid–base interactions that enable

effective proton transport without the need for humidification. Recent developments in electrospinning have enabled the fabrication of fibrous PBI membranes with high surface area and porosity, significantly enhancing PA uptake and diffusion. Current research focuses on optimizing fabrication parameters and post-processing to boost acid retention and conductivity. While early studies have investigated the structural and adsorption properties of these membranes, further work—especially involving membrane electrode assembly (MEA) integration and electrochemical testing—will be essential to assess their practical potential in real fuel cell environments.

Objectives:

The main goal of this study is to develop and analyze electrospun fibrous PBI membranes for use in HTPEMFCs. The work focuses on optimizing the electrospinning process by varying polymer solution concentrations and several processing parameters to control membrane morphology. After fabrication, membranes are doped with phosphoric acid, and the kinetic of acid uptake is studied at differenttemperature and by varying PA concentration. Kinetic modeling, and in particualr a pseudo-second-order model, is used to understand the chemisorption mechanisms involved. The study also includes detailed physicochemical characterization—such as porosity, surface structure, and stability—and preliminary electrochemical testing to assess proton transport properties. These findings are intended to support future integration of the membranes into membrane electrode assemblies (MEAs) for practical HTPEMFC applications.

Material and methods:

Fibrous PBI membranes were fabricated using the commercial S26 solution via electrospinning with a Fluidnatek® LE-100 system, allowing precise control over processing parameters. The membranes were characterized using SEM (FEI Nova NanoSEM 450) for morphology, FTIR (Anton Paar Lyza 7000) for chemical analysis, Instron testing for mechanical properties, and XRD (PanAlytical Empyrean) for structural assessment. Doping was performed by immersing the membranes in phosphoric acid solutions under different conditions. Acid uptake was measured gravimetrically, and kinetic modeling using in house MATLAB routines confirmed a pseudo-second-order mechanism. All experiments were conducted under controlled conditions to ensure data reliability for future HTPEMFC applications.

Results:

After optimizing electrospinning parameters, uniform and defect-free fibrous PBI membranes were successfully produced and thoroughly characterized. A custom doping protocol using progressively concentrated phosphoric acid solutions enabled controlled acid uptake under mild conditions. Kinetic analysis revealed a reaction order of 1.91, indicating a pseudo-

second-order chemisorption process driven by interactions between PA and the imidazole groups of PBI. Thermodynamic evaluation showed the process to be endothermic, with higher temperatures enhancing uptake. The Liu isotherm accurately described the adsorption behavior, suggesting a heterogeneous surface. These results confirm the potential of electrospun PBI membranes for efficient acid doping and support their suitability for HTPEMFC applications.

Conclusions:

This study demonstrated the successful fabrication of electrospun fibrous polybenzimidazole membranes optimized for high-temperature proton exchange membrane fuel cells. By fine-tuning electrospinning parameters, uniform and mechanically robust fibrous mats were produced, offering high surface area and porosity ideal for phosphoric acid uptake. A custom doping protocol using progressively concentrated acid solutions allowed controlled impregnation under mild conditions. Kinetic analysis indicated a reaction order of 1.91, consistent with pseudo-second-order chemisorption, while thermodynamic data confirmed the process to be endothermic and well-described by the Liu isotherm at 25 °C, 35 °C, and 50 °C. The combination of optimized morphology and controlled doping yielded membranes with enhanced functional performance, supporting their potential for future integration into MEAs and practical HTPEMFC applications.

References

[1] Li et al., 2003, Fuel Cells, 4(3), pp. 147-159.
[2] Savinell et al., 2005, Journal of Power Sources, 139(1-2), pp. 35-44
[3] Li et al., 2013, Journal of Power Sources, 223, pp. 20-27.
[4] Xing et al., 2004, Journal of Membrane Science, 229(1-2), pp. 95-106.

EFCH2 2025 European Fuel Cells and Hydrogen
PIERO LUNGHI CONFERENCE
September 17th–19th 2025 Capri / Italy

The importance of modifying anode materials for use in sofc fuel cells in the methane reforming process

Małgorzata Ruggiero-Mikołajczyk*[a], Grzegorz Mordarski[a], Piotr Michorczyk[b], Barbara Michorczyk[b], Małgorzata Zimowska[a]

* corresponding author: malgorzata.ruggiero-mikolajczyk@ikifp.edu.pl

[a] Jerzy Haber Institute of Catalysis and Surface Chemistry Polish Academy of Sciences, Niezapominajek 8, 30-239 Cracow, Poland;

[b]Cracow University of Technology, ul. Warszawska 24, 31-155 Cracow, Poland.

Keywords: fuel cells, LSCF perovskite, methane conversion, SOFC anode.

Introduction:

Solid oxide fuel cell (SOFC) operating at high temperature (600 - 1000 °C) is considered to be the most promising electrochemical power convertors. The high operating temperature of SOFC is advantageous due to the energy efficiency achieved under these conditions, but at the same time it is the cause of many technical and material difficulties related to their implementation. Oxide cells do not contain liquids, are dynamic and very durable and thanks to the high temperature it is possible to carry out fuel reforming (conversion to hydrogen) inside the cell, without the need to use additional external units with specific and expensive catalysts. This process takes place directly in the anode chamber of the cell. Moreover, due to the lack of gaseous such as NOx, SOx and dust pollutants, SOFC are one of the most environmentally friendly energy generators. The main advantage of these cells is the possibility of using various fuels, such as: natural gas, biogases from biomass gasification, pure hydrogen, hydrogen from coal gasification, gases obtained from liquid fuels, etc.

Objectives:

This work is related to the search for methods of improving the properties of anode material in SOFC devices powered by methane as a fuel. The SOFC anodes are used as various ceramic materials [1-3]. Ni-cermet based anodes are the most widely used anode materials in SOFCs due to their excellent electrochemical catalytic activity in the fuel oxidation reaction, high electrical conductivity, good stability and relatively low cost. In SOFC fuelled with the methane, anode is exposed to contamination by carbon deposited during the conversion reaction. The properties of the anode material largely determine the degree of conversion of methane to CO and H_2 and thus the efficiency and effectiveness of the cell in which it can be used.

This work presents the methods of modifying the anode material intended for use in SOFC devices. This modification concerns both, the choice of the modifying material and the surface modification technique. It is well known that both, different metals and ceramic composites can be used as elements modifying the anode structure. Therefore the obtained anode materials were gauged in the reaction of CH_4 reforming leading to the production of synthesis gas. Anode degradation occurs due to the deposition of carbon on the anode surface during the operation of the SOFC powered with hydrocarbon fuel.

The use of a nanocoating made of cathode material and applied to the anode material is an effective way to prevent such degradation. This is one example of the use of thin films applied to the anode as a form of its modification [4].

Material and methods:

In these studies, Ni/YSZ (i.e. 50-60% NiO + YSZ-Yttria Stabilized Zirconia) was used as anode material. This material was sintering in 1100 ^{o}C in a chamber furnace. The current research has been carried out in terms of the modification anode materials using of applying thin layers with PAD (Polymer Assisted Deposition) method. Thin layers made of composite materials such as: $La_{0.6}Sr_{0.4}Co_{0.2}Fe_{0.8}O_3$ (LSCF) and $La_{0.6}Sr_{0.4}Co_{0.2-x}Ir_xFe_{0.8}O_3$ (LSCFIr), as well as $La_{0.6}Sr_{0.4}Co_{0.2-x}Ba_xFe_{0.8}O_3$ (LSCFBa), $La_{0.6}Sr_{0.4}Co_{0.2-x}Bi_xFe_{0.8}O_3$ (LSCFBi), $La_{0.6}Sr_{0.4}Co_{0.2-x}Ca_xFe_{0.8}O_3$ (LSCFCa), $La_{0.6}Sr_{0.4}Co_{0.2-x}Mn_xFe_{0.8}O_3$ (LSCFMn).

The microstructural quality and morphology of the films were first characterized SEM method. Determination of the specific surface area (BET) and surface characteristics of samples, the pore size distribution were performed by nitrogen adsorption at 77 K. These materials were also examined using the XRD technique. EIS (Electrochemical Impedance Spectroscopy) have been performed in order to examine the selected cathode material such as: LSCF and LSCFIr, for reaction occurring in the SOFC. The aim of these measurements was to check whether the iridium addition facilitate oxygen reduction the reaction to oxide ion. The next stage of this work was checked the catalytic properties of the modified anode materials in the methane conversion reaction, leading to the obtaining of the most desirable products, i.e. to hydrogen and CO. Tests of anode material with thin layers were performed to check the degree of methane conversion at various temperatures in the range from 400 to 800 ^{o}C. These results were compared with tests obtained for unmodified anode material. The selectivity of the methane conversion reaction was also determined.

Results:

Deposition of LSCF thin layer coating on NiO-YSZ anode resulted in the formation of the particles with grain-like morphology. SEM images revealed the homogenous distribution of a thin layer of the LSCF coating on the NiO-YSZ anode, which exhibited a porous structure resulting from inter-grain spaces. Substitution of Co by Mn, Ca, Bi, Ba, and Ir brought about the recrystallization of parent LSCF structure and subsequent increase

of the particle size, the most pronounced for Bi, Ba, and Ir, respectively. All of the samples show low specific surface area (below than 1,5 m^2/g), which is typical for such materials. In the obtained isotherms very small hysteresis loop are observed corresponding to the presence of the inter-particle pores. The type of isotherms represents unrestricted monolayer-multilayer adsorption in the slit-shape pores. Analysis of the obtained EIS results indicates that iridium doped LSCF deposited on YSZ exhibits better oxidizing properties than the LSCF on YSZ without iridium. The measurements were made with use three electrodes: working, counter and reference and at four temperatures: 700, 750, 800, 850 °C. The obtained catalytic test results clearly indicate that the properties of the anode modified with applied thin layers do not expressively change in comparison to the unmodified anode. The largest differences can be observed for materials modified in layers: LSCFBi and LSCFMn, for which there is a slight decrease in the methane conversion rate.

Conclusions:

Morphology of the obtained LSCF anodes slightly differs in dependent of substitution. Anode containing Ir revealed the highly crystallized perovskite structure merging the small structures into larger ones accompanied by a highest decrease of BET surface area. From EIS measurements arises, that in reduction reaction of oxygen to oxide ion the cathode-iridium LSCF material has a better catalytic properties than the material of LSCF without iridium. Catalytic test results confirm the validity of the applied modification, because the ability of the anode material to catalyze the methane conversion reaction is only slightly impaired by the application of a thin layer. Additionally, the performed selectivity tests confirm the formation of the expected products of the assumed methane conversion reaction towards the formation of CO as an additional fuel component in the SOFC cell. These materials will be subjected to further tests to determine the degree of solid carbon deposition as an undesirable conversion product.

Acknowledgment

Małgorzata Ruggiero – Mikołajczyk, PhD, would like to acknowledge the support of the PROM Program – short-term academic exchange (contract number BPI/PRO/2024/1/00025 with NAWA Polish National Agency for Academic Exchange) co-financed by the European Union within the European Funds for Social Development.

References

[1] Liu Zhen Bian, Zhi Yuan Chen, Li Jun Wang, Fu Shen Li, Kuo Chih Chou, International Journal of Hydrogen Energy, 42, 2017, 14246-14252;

[2] Hyuk Kan Hyunjoo Lee; Applied Catalysis B: Environmental, 9, 2010, 108-114;

[3] Jiang Liu, Scott A Barnett; Solid State Ionics, 158, 2003, 11-16;

[4] Mirzababaei J. and Steven S. C. Chuang Catalysts 4, 2014, 146-161.

EFCH2 2025 European Fuel Cells and Hydrogen
PIERO LUNGHI CONFERENCE
September 17th–19th 2025
Capri / Italy

Dense electrolytes fabrication and innovative deposition technique for integration in Proton-conducting Fuel Cells

Freschi L.*[a, b], Novelli V. [a], Della Seta L. [a], Grilli M.L. *[a], Pumiglia D.[a], Monteleone G. [a], Di Bartolomeo E.[b]

* corresponding author: lorenzo.freschi@students.uniroma2.eu, marialuisa.grilli@enea.it

[a] Energy Technologies and Renewable Sources Department, Italian National Agency for New Technologies, Energy and Sustainable Economic Development (ENEA), Casaccia Research Center, Via Anguillarese 301, 00123 Rome, Italy

[b] University of Rome Tor Vergata, Department of Chemical Science and Technologies, Via Della Ricerca Scientifica, 00133 Rome, Italy

Keywords: PED, perovskite, proton conducting fuel cells, sintering optimization

Abstract

Within the manufacturing of Proton-conducting Fuel Cells (PCFCs), the fabrication of homogeneous, dense electrolytes such as electrolyte-anode integration is of great relevance. The work aims to investigate PED as an innovative technique for electrolyte deposition onto the anode using high-density electrolytes obtained by optimising the sintering process.

Introduction:

In recent years, fuel cells have attracted significant attention as a promising alternative for clean energy production in an ever-increasing global energy demand. Proton-conducting Fuel Cells (PCFCs) have several advantages over traditional Solid Oxide Fuel Cells (SOFCs), as the lower working temperatures (400-700 °C) which enables better performance and ease of integration for innovative applications [1]. Doping a $Ba(Ce,Zr)O_3$ perovskite structure with rare earth cations (such as Y or Gd) allows to achieve an optimal balance between high proton conductivity and chemical stability [2]. Various problems can be encountered during the electrolyte fabrication, especially during high temperatures sintering processes, which can lead to micro and macro structural defects, detrimental for the quality of the electrolyte (e.g. proton conductivity) and thus the entire cell [3]. It is of paramount importance to develop manufacturing techniques that improve integration between all cell components. Pulsed Electron Deposition (PED) technique, despite not yet extensively investigated , could represent a promising technique for electrolyte integration in complete cells. PED like Pulsed Laser Deposition (PLD), enables homogeneous materials thin film deposition with controlled thickness while maintaining same target stoichiometry. Key advantages of PED over PLD include lower equipment cost, higher energy efficiency and the capability to deposit all kinds of materials independently on their optical absorption coefficient. Moreover, PED avoids macroscopic discontinuities on the deposited film surface [4][5]. We, therefore, consider this technique very promising, especially for the deposition of complex ceramic stoichiometry as perovskite-based electrolytes onto anodic substrate, thus facilitating the integration of the half-cell.

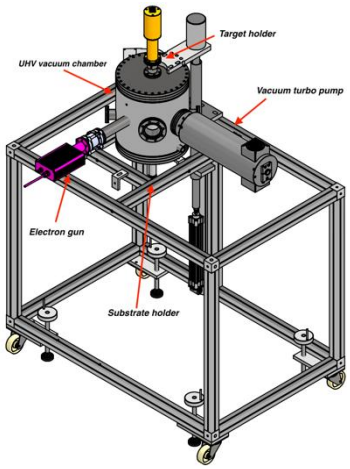
Objectives:

This work aims to study a dedicated sintering process to produce homogeneous, high dense and performing ceramic pellets of different $Ba_{1,1}Ce_{0,6}Zr_{0,2}M_{0,2}O_3$ (M = Y, Gd) ceramic electrolytes. Once their density is optimized, such pellets could be used as targets in PED

system to deposit electrolytes over commercial anodic substrate investigating the feasibility of this innovative technique within the PCFC manufacturing process.

Material and methods:

Ceramic powders with nominal composition of $Ba_{1,1}Ce_{0,6}Zr_{0,2}M_{0,2}O_{3-\delta}$ (M = Y, Gd) were synthetized by sol-gel modified Pechini process [6] and the pellet were obtained die pressing uniaxially. Sintered pellets were characterized by X-Ray Diffraction (XRD) and Scanning Electron Microscopy (SEM) to assess structural defects. The sintering process was adapted optimizing the parameters to reach dense ceramic electrolyte suitable for cells integration and to be used as PED target. Second type of pellets $BaCe_{0,7}Zr_{0,2}Y_{0,1}O_{3-\delta}$ with Cerpotech commercial powder were fabricated with same conditions and used as comparison. PED equipment assembled and tested includes (*Fig. 1*) a vacuum chamber (base pressure $4x10^{-6}$ mbar) with a rotating substrate (heated at about 300 °C) and rotating target holder (target-substrate distance about 50 mm). Deposition was carried out at Ar pressure of $1x10^{-3}$ mbar, pulsed frequency of 15-25 Hz and electron gun voltage in the range of 15-20 kV. The ablated perovskite ceramic target by pulsed electron beam is emitted in the form of highly ionized plasma plume and deposited onto the substrate (commercial anode Ni-YSZ of about 250 μm thickness). The deposition time was varied depending on the desired thickness of the electrolyte.



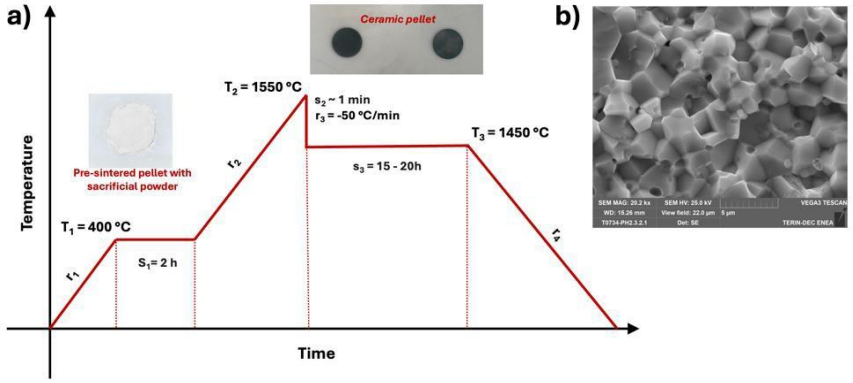


Fig. 2: sintering process ramp (a) and SEM image of BCZY pellet cross section after sintering process (b)

Results:

Dense ceramic pellets, with relative density > 92%, were obtained after optimised sintering process (*Fig. 2a*). A first step at 400 °C was introduced to let the binder decompose according to Thermogravimetric Analysis (TGA) results. The sample, covered by sacrificial powder, was slowly heated up to 1550 °C and then rapidly cooled (15 °C/min) to 1450 °C with a dwell time of 15 h. The as sintered pellets exhibited a cubic pm-3m structure and SEM images revealed high density and compactness (*Fig. 2b*).

First initial tests have been performed to evaluate the best ceramic target features and to study morphologically the quality of the deposition.

Conclusions:

A systematic study on the sintering parameters of $Ba_{1,1}Ce_{0,6}Zr_{0,2}M_{0,2}O_{3-\delta}$ (M = Y, Gd) ceramic electrolytes aiming at reaching maximum density of pellets has been carried out. Covering the pellet with sacrificial powder and using slow heating ramps is promising to avoid thermal stresses and Ba evaporation, thus reducing bending and macro cracks. Rapid quenching at 1450 °C was found fundamental to suppress grain-boundary migration, favoring exclusively grain-boundary diffusion and thus leading to high densification. This study demonstrates a successful process to obtain highly dense ceramic electrolytes without the need of sintering aids addition. Dense electrolytes can be used for inhouse target fabrication to be used in a PED system, highly potential for innovative manufacturing of anode-supported proton-conductive fuel cells.

Acknowledgment

This research was funded by the European Union - NextGenerationEU from the Italian Ministry of Environment and Energy Security, POR H2 AdP MEES/ENEA with involvement of CNR and RSE, PNRR - Mission 2, Component 2, Investment 3.5 "Ricerca e sviluppo sull'idrogeno", CUP: I83C22001170006

References

[1] S. Guo, L. Jiang, Y. Li, P.Zhong, S. Ismail, T. Norby, D. Han; Adv. Funct. Mater. (2024) 230-4729

[2] J. Jing, J. Pang, L. Chen, H. Zhang, Z. Lei, Z. Yang; Chemical Engineering Journal 429 (2022) 132-314

[3] S. Wang, L. Zhang, L. Zhang, K. Brinkman, F. Chen; Electrochimica Acta 87 (2013) 194-200

[4] M. Nistor, N. B. Mandache, J. Perrierre; J. Phys. D: Appl. Phys. 41 (2008) 165-205

[5] A. Liguori, C. Gualandi, M. L.Focarete, F. Biscarini, M.Bianchi; Coatings (2020) 10-16

[6] S. Barison, M. Battagliarin, T. Cavallin, L. Doubova, M. Fabrizio, C. Mortalò, S. Boldrini, L. Malavasi, R. Gerbasi;J. Mater. Chem. (2008) 18, 5120–5128

EFCH2 2025 European Fuel Cells and Hydrogen
PIERO LUNGHI CONFERENCE
September 17th–19th 2025
Capri / Italy

Bacterial cellulose-based ion exchange membranes for fuel cell applications

Maša Hren*[a], Selestina Gorgieva[a]

* Corresponding author: Maša Hren
[a] Faculty of Mechanical Engineering, University of Maribor, Slovenia

Keywords: bacterial cellulose, fuel cell, ion exchange membrane

Abstract: This work presents the fabrication of efficient anion exchange membranes (AEMs) based on bacterial cellulose (BC) for use in alkaline fuel cells. To overcome the limitations of uncharged but mechanically robust BC, BC was functionalized with quaternary ammonium groups and N-doped graphene oxide. The modified membranes showed a tenfold increase in ion exchange capacity over the neat BC and offer a promising, environmentally friendly alternative for low-cost, high-performance AEMs in fuel cell applications.

Introduction: Polymer electrolyte fuel cells efficiently convert chemical energy into electricity for various applications, but the high cost of components such as platinum catalysts limits their commercialisation. Alkaline fuel cells (AFCs) with AEMs offer a more cost-effective alternative as they allow the use of non-precious metal catalysts. However, existing AEMs lack the necessary performance for widespread adoption, emphasising the need for the development of new efficient, environmentally friendly and affordable alternatives. While the production of synthetic AEMs is often complex and environmentally unfriendly, naturally derived materials such as cellulose nanofibrils and BC are promising as they can be easily modified and can be produced in a sustainable way. Nevertheless, biopolymer-based AEMs lack ionic conductivity and good barrier properties, which can be overcome by functionalisation and the incorporation of suitable fillers enriched with charged moieties which act as long-range ion channels that can further accelerate ion transport. On the other hand, the addition of partially hydrophobic fillers can contribute to the development of hydrophobic regions in the AEM, which can limit the permeability of the fuel. [3]

Objectives: Fabrication of efficient ion exchange membranes based on the BC biopolymer functionalized with a quaternary ammonium group and N-doped graphene oxide to be used as anion exchange membranes in alkaline or microbial fuel cells.

Material and methods: Materials: BC films in a fully hydrated state with a wet thickness of ~0.05 mm and dimensions of 200 x 100 mm were purchased from Fzmb GmbH (Bad Langensalza, Germany). N-doped reduced graphene oxide nanoribbons (N-GO) were synthesised from commercially available multi-walled carbon nanotubes as described in detail in our previous publication [1]. Poly(diallyldimethylammonium chloride) (PDDA) solution (20 wt.% in H_2O, Mw: 400 000 – 500 000 g/mol, sodium hydroxide (NaOH), hydrochloric acid (HCl)

and potassium hydroxide (KOH) were purchased from Sigma-Aldrich, Darmstadt, Germany. All reagents and solvents were of analytical grade and were used as received. Preparation of membranes: Commercially available BC films were dried at room temperature and punched into 25 mm discs. A BC dispersion was prepared from a 200 × 100 mm wet film in 100 ml Milli-Q water using an IKA T25 ULTRA-TURRAX®. To form BC membranes, 100 µl of this dispersion was applied to a dry BC disc. For quaternisation, 50 µl of PDDA (0.1 or 1 wt.%) was added to the dispersion and applied to generate qBC_0.1% or qBC_1%. A 0.01 wt.% N-GO dispersion was sonicated and 50 µl was added to the BC dispersion and applied to form BC_N-GO, qBC_0.1%_N-GO and qBC_1%_N-GO membranes. All membranes were dried in air. Methods: ATR-FTIR spectra were recorded using a Perkin-Elmer Spectrum One FTIR spectrometer with a Golden Gate ATR (diamond crystal) in the 4000–650 cm^{-1} range. The XRD spectra of the membranes were recorded with a Bruker Siemens D5005 diffractometer using Cu-Kα radiation (40 kV, 40 mA) with a 2θ scan from 5° to 70° in 0.03° increments. The crystallinity degree was calculated from the ratio of the crystalline peak area to the total diffraction area. The ion exchange capacity (IEC) was measured by potentiometric titration. Membranes in OH^- form (pre-soaked in 1 M NaOH) were immersed in 40 mL of 0.01 M HCl for 24 hours and then titrated with 0.1 M KOH. Membrane samples were weighed before the assay and IEC was calculated using Eq1, where V_{blank} and $V_{membrane}$ are the consumed KOH volumes for the blank and sample (ml), c_{HCl} is the molarity of HCl (mol/l) and $m_{dry\ membrane}$ is the mass of the dry membrane (g).

$$IEC\ \left(\frac{meq}{g}\right) = \frac{(V_{blank} - V_{membrane}) \cdot c_{HCl}}{m_{dry\ membrane}} \quad \text{(Eq1)}$$

The water uptake (WU) and through-plane swelling ratio (SR_{TP}) were calculated using Eq2 and Eq3. The membrane samples were weighed (W_{dry}) and their thickness measured (T_{dry}) and then immersed in Milli-Q water for 24 hours at RT. After dabbing off the excess water, the wet weight (W_{wet}) and thickness (T_{wet}) were recorded.

$$WU = \frac{W_{wet} - W_{dry}}{W_{dry}} \cdot 100\ \% \quad \text{(Eq2)} \qquad SR_{TP} = \frac{T_{wet} - T_{dry}}{T_{dry}} \cdot 100\ \% \quad \text{(Eq3)}$$

Results: The FTIR spectra of all membranes (Fig. 1a) show a typical cellulose profile, with peaks detected at ~3600–3000 cm^{-1} (O-H stretching), ~2900 cm^{-1} (symmetric and asymmetric C-H stretching), ~1450 cm^{-1} (C-H bending), and at ~1162–1060 cm^{-1} (C-O and C-O-C stretching). The FTIR spectra of qBC_0.1%, qBC_1%, qBC_0.1%_N-GO and qBC_1%_N-GO exhibit peaks at 1639 cm^{-1}, which is attributed to C=C stretching, and at 1475 cm^{-1}, which is related to the quaternary ammonium group in the PDDA molecule and is attributed to C-H bending of the alkyl groups attached to the quaternary ammonium [2] which confirms the quaternization of the samples. The XRD spectra (Fig. 1b) show no change in spectrum profile after quaternisation and the addition of N-GO. However, the crystallinity of composite BC membranes was affected after functionalisation, with the addition of 1 wt.% PDDA reducing the degree of crystallinity of the qBC_1%_N-GO membrane by 6.1 % compared to the neat BC membrane. The addition of N-GO also reduced the degree of crystallinity by 4.5 %.

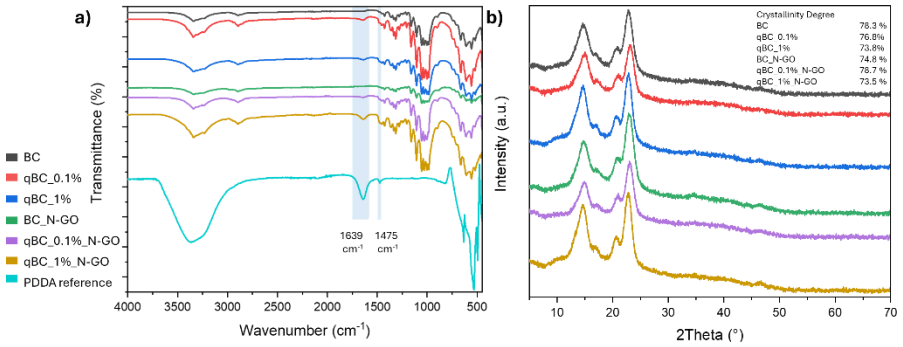


Figure 1. a) ATR-FTIR and b) XRD spectra of the BC-based membranes

Functionalisation with both N-GO and PDDA led to an increase in IEC, with the highest IEC of 0.1984 meq/g achieved for the qBC_0.1%_N-GO membrane, which corresponds to a significant, tenfold increase over the BC reference. The WU and SR_{TP} of all functionalized membranes containing PDDA increased due to the quaternary ammonium group of the reagent and decreased for the BC_N-GO, where the introduction of the GO sheets caused a decrease in WU and no effect on SR_{TP} due to the more hydrophobic nature of the two-dimensional N-GO.

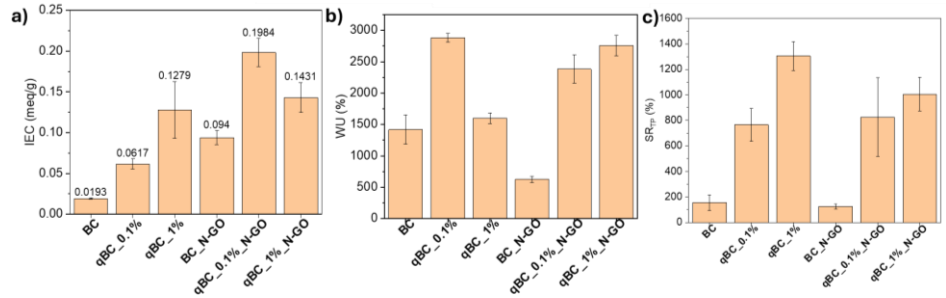


Figure 2. a) IEC, b) WU and c) SR_{TP} of the BC-based membranes

Conclusions: Robust BC-based membranes with N-GO fillers and quaternised by PDDA were successfully prepared. The functionalisation has been confirmed by FTIR and XRD and the resulting membranes have shown that such functionalisation increases the IEC by 10-fold and is an interesting approach to improve the properties of BC for its use as AEM in AFCs. In addition, experiments on ionic conductivity using the EIS technique are still pending.

Acknowledgment:

The financial support from Slovenian Research and Innovation Agency is received, in the frame of project "Efficient bacterial cellulose-based anion exchange membranes for alkaline fuel cell applications" (Z2-60175), "Nanofibrilar cellulose membranes in microbial fuel cells: material development for sustainable, high value-added applications" (J2-50086) and the Textile Chemistry and Advanced Textile Materials Programme (P2-0118). The N-GO sample was received from prof. dr. Boštjan Genorio, Faculty of Chemistry and Chemical Technology, University of Ljubljana.

References:

[1] S. Gorgieva et al., "Efficient chitosan/nitrogen-doped reduced graphene oxide composite membranes for direct alkaline ethanol fuel cells," Int. J. Mol. Sci., vol. 22, no. 4, p. 1740, 2021.

[2] M. Hren, M. Roschger, V. Hacker, B. Genorio, D. Fakin, and S. Gorgieva, "High performance chitosan/nanocellulose-based composite membrane for alkaline direct ethanol fuel cells," Int. J. Biol. Macromol., vol. 253, no. July, 2023.

[3] M. Hren, M. Božič, D. Fakin, K. S. Kleinschek, and S. Gorgieva, "Alkaline membrane fuel cells: Anion exchange membranes and fuels," Sustain. Energy Fuels, vol. 5, no. 3, pp. 604–637, 2021.

EFCH2 2025 European Fuel Cells and Hydrogen
PIERO LUNGHI CONFERENCE
September 17th–19th 2025
Capri / Italy

Machine learning based lifetime prediction of polymer electrolyte fuel cells for distributive power generation

Sukkee Um*[a], Jungrok Oh[b], Kyuhyung Park[b], Kwonwoo Yang[b], Sungjea Park[b]

* corresponding author: sukkeeum@hanyang.ac.kr
[a] Department of mechanical engineering, Hanyang university/South Korea;
[b] Graduated School of Hanyang university/South Korea;

Keywords: Machine learning, Lifetime prediction, Polymer Electrolyte Fuel Cells, Distributive Power Generation

Abstract

This study presents a multi-stage framework to estimate and validate degradation coefficients of internal resistances in proton exchange membrane fuel cells using macro-scale current–voltage data and electrochemical impedance spectroscopy. First, artificial intelligence is used to estimate the degradation of ohmic, charge transfer, and mass transport resistances from current–voltage curves. These estimates are then corrected and validated through impedance-based physical modeling. Finally, a machine learning model is trained to learn the correction behavior, enhancing predictive accuracy and physical consistency. This approach bridges data-driven estimation and physics-based validation to support resistance-specific degradation analysis.

Introduction:

Proton exchange membrane fuel cells (PEMFCs) are a promising clean energy technology [1] due to their high efficiency and low carbon emissions. However, their long-term durability is critically affected by component-level degradation within the cell. Unlike studies that focus solely on the total performance decay, recent research has emphasized the importance of understanding degradation at the level of individual internal resistances—namely, crossover, activation, ohmic resistance, electronic resistance, and mass transport resistance [2]. While current–voltage (I–V) curves provide a macroscopic view of cell performance, they do not directly reveal the evolution of individual internal components. In contrast, electrochemical impedance spectroscopy (EIS) enables decomposition of the total cell resistance into its constituent elements, offering a more detailed diagnostic perspective.

To address these limitations, this study proposes a three-stage framework: first, estimate resistance-specific degradation coefficients using artificial intelligence models applied to current–voltage data; Second, correct and validate these estimates using physically grounded resistance values obtained from electrochemical impedance spectroscopy, last, train a machine learning model to learn and replicate the correction process [3].

This work aims to develop a predictive model that integrates the data-driven modeling with the reliability of physics-based validation.

Objectives:

This study aims to estimate degradation coefficients for each internal resistance component individual internal resistances (i.e., crossover, activation, ohmic resistance, electronic resistance, and mass transport) based on current–voltage data through artificial intelligence modeling. These initial estimates are then physically validated and corrected using resistance values obtained from electrochemical impedance spectroscopy. Finally, the correction behavior is captured using a machine learning model that learns from the observed differences between AI predictions and physically derived references, enhancing the overall prediction accuracy and robustness.

Material and methods:

1. Resistance Degradation Estimation (AI-based)

Current–voltage curves [4] collected from proton exchange membrane fuel cells under controlled load conditions were used as input to an artificial intelligence model. The model was estimated degradation coefficient of the individual internal resistances using nonlinear regression and feedforward neural networks.

2. EIS-based Physical Correction

Electrochemical impedance spectroscopy was periodically conducted to obtain reference values for each internal resistance. These values were fitted using an equivalent circuit model. The differences between the AI-estimated coefficients and the EIS-derived measurements were computed and analyzed as correction offsets.

3. Learning the Correction with Machine Learning

The correction offsets served as the target output for a machine learning model, which was trained to predict these offsets from features extracted from the original current–voltage data. Random forest and gradient boosting methods were evaluated for their effectiveness in modeling nonlinear correction behavior [5].

Results:

1. The initial artificial intelligence model achieved moderate prediction accuracy ($R^2 \approx 0.82$) for degradation coefficients.
2. Electrochemical impedance spectroscopy revealed discrepancies in charge transfer resistance estimates, especially during the early degradation stages.
3. The machine learning-based correction model successfully reduced root mean squared error by approximately 50% of electronic resistances.

4. The corrected predictions closely matched EIS-derived resistance values, improving both physical interpretability and reliability.

Conclusions:

The proposed multi-step framework successfully combines current–voltage data analysis, physical validation, and correction learning to estimate internal resistance degradation in proton exchange membrane fuel cells. This approach enhances prediction accuracy while maintaining alignment with electrochemical principles, making it a valuable method for condition monitoring and diagnostic applications [6].

References

[1] Lyu, Z., Wang, Y., Sciazko, A., Li, H., et al. (2023). *Prediction of fuel cell performance degradation using a combined approach of machine learning and impedance spectroscopy*. Journal of Energy Chemistry, 87, 1–10.

[2] M. Jouin et al. (2016). *Degradations analysis and aging modeling for health assessment and prognostics of PEMFC.* Reliability Engineering and System Safety, 148, 78–95

[3] Liu, C., Zhang, X., Wang, Y., et al. (2024). *Accuracy improvement of fuel cell prognostics based on voltage degradation data and hybrid deep learning*. International Journal of Hydrogen Energy 58(5), 839–851.

[4] IEEE PHM Data Challenge 2014. (2021).

[5] Lv, Z., Wang, Y., Li, H., et al. (2024). *Diagnosis of PEM fuel cell system based on electrochemical impedance spectroscopy and deep learning method*. Journal of Power Sources, 575, 233–242.

[6] Zhao, Y., Liu, H., Deng, Z., et al. (2025). *Machine learning accelerates fuel cell life testing*. arXiv preprint arXiv:2504.18835.

European Fuel Cells and Hydrogen
PIERO LUNGHI CONFERENCE
September 17th–19th 2025
Capri / Italy

The green transition of the Maritime Sector through Fuel Cell Systems: analysis of an Italian case study

Michele Vincenzo Migliarese Caputi *[a], Manlio Pasquali[a], Carla Menale [a] Chiara Boccaletti [b], Stefano Elia [b], Francesco Vellucci [a], Giulia Monteleone [a]

* corresponding author: Michele Vincenzo Migliarese Caputi

[a] ENEA – The Italian National Agency for New Technologies, Energy and Sustainable Economic Development, Rome, 00193 Italy

[b] Sapienza University of Rome, Department of Astronautical, Electrical and Energy Engineering (DIAEE), Rome, 00164, Italy

Keywords: Hydrogen-fueled ship, Fuel cells, Zero-emissions maritime transport, Hybrid diesel-electric system.

Abstract

The maritime transport sector accounts for about 2.9% of global GHG emissions, with emissions rising due to growing trade. The IMO's 2023 Strategy aims to cut CO_2 emissions per transport work by 40% by 2030 and reach net-zero by 2050. The EU's "Fit for 55" and FuelEU Maritime regulation promote clean energy use on ships. This study compares conventional, hybrid, and fuel cell energy systems. It evaluates their emission reduction potential and efficiency through an Italian ferry case study [1].

Introduction

The IMO 2023 Strategy highlights that efficiency improvements alone are insufficient to meet 2050 decarbonization goals, requiring adoption of low- or zero-carbon fuels. In this context, the IMO is developing an integrated set of technical and economic measures, including mandatory requirements for the use of fuels with reduced greenhouse gas intensity and the implementation of global emission pricing systems, such as carbon taxes or emissions trading schemes, expected to come into effect around 2027. Maritime pollutants such as CO_2, SO_x, NO_x, and PM are increasingly regulated; the EU's FuelEU Maritime Regulation mandates a progressive reduction in marine fuel GHG intensity, aiming for an 80% cut by 2050. To address these environmental issues, Onshore Power Supp or zero-emission solutions will be required in EU ports. Despite technical and regulatory advances, international harmonization remains essential to protect industry competitiveness and ensure effective maritime decarbonization.

Objectives:

This study analyzes and compares three different onboard energy generation system configurations: conventional, diesel-electric hybrid, and fuel cell-based systems. The

application of a power generation system based on the use of fuel cells will be analyzed on board a 38-meter-long yacht used as a ferry. The aim of the study is to evaluate the vessel's energy consumption during a typical working day, which includes two round trips from the port of Naples to the island of Ischia and one round trip from Naples to the island of Capri.
The primary objective of this work is to assess the emission reduction potential and operational efficiency of zero-emission technologies, with specific reference to an Italian case study.

Material and methods

The method adopted in this study consists in identifying a reference vessel (a 38-meter yacht by manufacturer Rodriguez), developing its mathematical model, and considering three different propulsion system configurations: the original one, a hybrid version (with the addition of inline electric motor-generators and a battery pack), and a configuration based on PEM-type fuel cells, two battery packs, and PODs for propulsion.
The different weights, efficiencies, and performances of the three solutions are considered, taking as a reference the ferry routes currently operating between Naples, Ischia, and Capri. The vessel's propulsion system typically relies on two diesel engines, each delivering 1417 kW. Electrical loads are powered by two diesel generators rated at 55 kW each, with a maximum total electrical power of 104 kW. Instead of the conventional diesel engines and generators, the proposed system employs ten 200 kW PEM fuel cell modules, along with an additional 70 kW module. To support operations during transitory phases (such as start-up, docking, or load changes), two battery packs have been included in the design. Hydrogen is stored in high-pressure cylinders at 350 bar. A simulator was employed to model operational profiles [2]: the energy consumption of each power generation system has been assessed through a simulated journey. Considering the vessel's typical operational profile as a ferry, it completes three round trips per day: two between Naples and the island of Ischia, and one between Naples and Capri. These routes are used to establish the load profile necessary for accurately sizing the onboard power system components. The speed profile includes a constant speed of 1.6 knots during port manoeuvres, followed by gradual acceleration to a cruising speed of 16 knots, and a deceleration phase before entering the destination port. The electrical load associated with onboard auxiliary services is assumed to remain constant at 35 kW, corresponding to the power demand of the air conditioning system and other essential onboard utilities. For propulsion power estimation, approximately 20 nautical miles is considered for both the Naples–Ischia and Naples–Capri routes. The adopted speed profile is assumes of calm sea conditions. The safety and reliability of the power generation systems have also been assessed by considering potential issues that could arise during their operation, to identify any weaknesses and determine the necessary safety measures to prevent accidents. Finally, the costs associated with each energy generation system—

including component, maintenance, and operational costs—have been examined to evaluate their impact on the ship's overall operating expenses.

Furthermore, this study proposes a strategy aimed at determining hydrogen consumption as a function of both the number of fuel cells active at a given time and their operating power levels; two control strategies for the PEMFC system have been analysed:

- the first strategy involves starting the first fuel cell at 50 kW;
- the second strategy involves starting the first fuel cell at 80 kW, the point at which maximum efficiency is achieved.

Results and Conclusions:

This study compares three power systems for a 38-meter ferry: the conventional diesel system, the diesel-electric hybrid system, and an innovative hydrogen fuel cell system. After reviewing various fuel cell technologies, proton exchange membrane fuel cells (PEMFCs) were selected for their suitability. The analysis evaluated the systems based on energy consumption, size, weight, reliability, and safety.

A simulator was employed to model operational profiles, and two control strategies for the PEMFC system were tested. The strategy initiating fuel cell operation at the minimum power threshold (50 kW) demonstrated reduced fuel consumption. Overall, the PEMFC system exhibited significantly lower fuel consumption compared to traditional systems.

A key limitation of the PEMFC system is the increased weight and volume of hydrogen storage compared to diesel tanks. While liquid hydrogen offers higher storage density, it suffers from evaporation losses and currently faces immature distribution infrastructure. Continued research and development are essential to address these challenges.

In summary, the PEMFC system emerges as the most advantageous technology, offering lower fuel consumption, higher reliability, and long-term economic benefits. This work underscores the importance of adopting sustainable energy solutions in maritime transport to mitigate environmental impact and raise public awareness.

Acknowledgments

This research was funded by the European Union - NextGenerationEU from the Italian Ministry of Environment and Energy Security, POR H2 AdP MEES/ENEA with involvement of CNR and RSE, PNRR - Mission 2, Component 2, Investment 3.5 "Ricerca e sviluppo sull'idrogeno"

References

[1] Fourth Greenhouse Gas Study 2020 Available at: https://www.imo.org/en/ourwork/Environment/Pages/Fourth-IMO-Greenhouse-Gas-Study-2020.aspx, accessed May 2025.

[2] E. Rossi, M. Pasquali, S. Constà, “Programma AMICO, Automazione e Monitoraggio Intelligente dei Consumi”, ENEA, ottobre 2015

European Fuel Cells and Hydrogen
PIERO LUNGHI CONFERENCE
September 17th–19th 2025
Capri / Italy

Hydrogen Fuel Cell-Powered GPU for Zero-Emission Ground Power Supply in Aviation

Andrea Altomonte* [a], Elio Simeoni [a], Alessia Piccolo [a], Viviana Cigolotti [b], Elio Jannelli [a], M. Giampaolo[c], M. Corradi[c]

*Corresponding author: Andrea Altomonte
[a] University of Naples "Parthenope", Naples, Italy
[b] ENEA - Italian National Agency for New Technologies, Energy and Sustainable Economic Development, Naples, Italy
[C] SEA Milan Airports

Hydrogen Fuel Cell, Aircraft Charging, Off-Grid Power, Portable Energy Systems, Backup Ground Power

Abstract

The aviation sector's transition toward zero-emission operations requires innovative solutions to decarbonize ground handling equipment. This study presents a hydrogen fuel cell-powered Ground Power Unit (GPU) designed to deliver 400 Hz AC power to aircraft during turnaround operations. Starting from a commercial reference study, the project defines functional requirements, performs 3D component integration and thermal modeling, and develops a control strategy to optimize energy flows and operational autonomy. By replacing the diesel engine with a hybrid fuel cell-battery system, the GPU ensures silent, zero-emission performance while preserving operational reliability and compatibility with airport standards. Through simulation-based sizing and techno-economic assessment, the solution demonstrates its potential to reduce emissions, operational costs, and noise pollution on the apron.

Introduction

The global push for decarbonization is reshaping every segment of the aviation sector, including ground operations that have long relied on fossil-fuel-based equipment. Among the most impactful sources of emissions on the airport apron are GPUs, which provide essential 400 Hz power to aircraft during gate operations. These units, typically powered by diesel engines, generate considerable quantities of CO_2, NO_x, and particulate matter, contributing to poor air quality and increased greenhouse gas emissions at airports.

According to the European Union Aviation Safety Agency (EASA), ground support equipment (GSE) can contribute up to 20% of local apron emissions, with diesel GPUs being among the highest emitters due to prolonged idling and irregular maintenance cycles [1]. The exposure of personnel and passengers to such pollutants further reinforces the urgency of adopting clean and quiet alternatives.

In this context, hydrogen-powered systems, particularly those based on fuel cell technology, represent a promising solution. They offer zero local emissions, reduced noise, and high efficiency, aligning with the climate neutrality goals set by international aviation bodies. Replacing conventional diesel GPUs with hydrogen alternatives is a concrete step toward a more sustainable, silent, and health-conscious ground operation ecosystem. This work is innovative as it evaluates the feasibility of hydrogen-

powered GPUs using a detailed techno-economic and environmental assessment, a perspective that remains largely unexplored in existing literature and airport decarbonization roadmaps.

Objectives

The aim of this work is to introduce a concrete solution to support the decarbonization of airport ground operations through the deployment of a GPU powered by a hydrogen fuel cell system. The proposed unit is designed to replace conventional diesel-powered GPUs while maintaining the required performance in delivering 400 Hz electrical power to aircraft during ground handling phases. This follows the trend in recent literature of advancing GPU architectures capable of high-frequency output, low harmonic distortion, and compact integration for efficient power delivery [2].

As airports increasingly aim for climate neutrality, adopting zero-emission technologies has become a strategic priority. This study presents a hydrogen-powered GPU designed to operate autonomously, silently, and without local emissions, improving air quality, reducing noise pollution, and protecting the health of ground personnel.

Beyond its environmental advantages, the study investigates the technical, spatial, and energy requirements for integrating a fuel cell system into a compact GPU configuration. A detailed 3D model supports this evaluation by analysing the layout of hydrogen storage, power electronics, and thermal management systems within the unit. The model also acts as a design validation tool, assessing weight distribution, maintenance accessibility, and compatibility with existing airport infrastructure. The ultimate goal is to demonstrate how hydrogen technology can provide a reliable, sustainable, and scalable solution for electrifying apron operations without compromising performance or functionality.

Material and methods

To evaluate the feasibility of a hydrogen-powered GPU, a comprehensive approach is adopted, combining 3D modelling, load profiling, and system-level simulation. For the preliminary sizing in this analysis, an energy equivalence approach is applied, based on a review of currently available commercial units. A detailed CAD model verifies the spatial integration of key components: fuel cell stack, lithium-ion battery, hydrogen tanks, power electronics, and thermal systems within the dimensional limits typical of airport ground equipment.

Representative operating profiles are created based on standard aircraft turnaround procedures, accounting for load peaks, average power demand, idle phases, and ambient temperature variations. Input data come from GPU usage logs, technical specifications from airport equipment suppliers, and standardized duty cycles, ensuring that scenarios reflect typical apron operations for both narrow-body and wide-body aircraft.

An in-house simulation tool models the hydrogen powertrain under dynamic conditions. It simulates energy flows between the fuel cell, battery, and power electronics, and performs parametric optimization to define the optimal sizing of fuel cell power, battery energy and C-rate, and hydrogen storage capacity. The results are evaluated in terms of power availability, runtime, energy efficiency, and weight, ensuring that the hydrogen GPU matches the performance of conventional diesel and battery-electric systems.

Results

The comparison between diesel, electric, and hydrogen-powered GPUs highlights the advantages of the proposed fuel cell-based solution in terms of performance, autonomy, and environmental impact. Diesel GPUs, with power outputs between 48 kW and 144 kW, have high theoretical energy content (over 3,000 kWh), but due to engine inefficiencies, only around 25–30% is effectively usable. These units also emit significant pollutants and noise and require frequent maintenance. Electric GPUs offer zero local emissions and quiet operation, but their autonomy is limited. With battery capacities ranging from 132 to 176 kWh, they provide about 110–150 kWh of usable energy, often insufficient for longer operations without recharging.

The hydrogen GPU developed in this project combines a 45 kW fuel cell with a 25 kWh battery pack, supplying up to 94 kW of output power. With 40 kg of hydrogen on board, it stores approximately 1,330 kWh of energy, of which over 750 kWh are usable providing long autonomy, fast start-up, and consistent performance, all without local emissions or noise.

3D modelling confirmed the feasibility of integrating all components in a compact layout compliant with airport standards.

Conclusions

This work demonstrates the technical and operational viability of a hydrogen fuel cell-powered Ground Power Unit as a sustainable replacement for conventional diesel systems in airport ground operations [3].

The proposed configuration ensures equivalent power delivery, operational autonomy, and compatibility with existing apron procedures, while eliminating local emissions and reducing noise. Through simulation and 3D modelling, the system has been optimized to balance efficiency, compactness, and reliability.

Hydrogen-powered GPUs represent a concrete step toward the decarbonization of airport infrastructure, aligning with climate neutrality targets and improving the environmental quality of ground handling activities. Future developments will focus on prototype validation and integration into airport hydrogen ecosystems.

Acknowledgment

This project has received funding from the Clean Hydrogen Partnership under Grant Agreement No 101112098. The Clean Hydrogen Partnership receives support from the European Union's Horizon Europe Research and Innovation Program, Hydrogen Europe and Hydrogen Europe Research.

References

[1] [EASA, 2022] – European Union Aviation Safety Agency. Environmental Report 2022 – Aviation's Contribution to Sustainable Development. Luxembourg: Publications Office of the European Union.

[2] Rivera, M., Faundez, D., Kolar, J., Wheeler, P., Besoaín, F., & Riveros, J. A. (2018, June). A new ground power unit (GPU) supply for aircraft applications. In 2018 IEEE Biennial Congress of Argentina (ARGENCON) (pp. 1-6). IEEE.

[3] Testa, E., Giammusso, C., Bruno, M., & Maggiore, P. (2014). Analysis of environmental benefits resulting from use of hydrogen technology in handling operations at airports. Clean Technologies and Environmental Policy, 16, 875-890.

European Fuel Cells and Hydrogen
PIERO LUNGHI CONFERENCE
September 17th–19th 2025
Capri / Italy

Novel Dry Powder Processing Routes for Porous Anode Supports in Solid Oxide Electrochemical Cells

Dino Boccaccini *[a], Maria Cannio [b], Vincenzo Riva [b], Rosa Taurino [c,d], Cecilia Mortalò [e], Enrico Paradisi [a], Elisa Mercadelli [f], Angela Gondolini[f], Alessandra Sanson [f], Marcello Romagnoli [ag]

* corresponding author: Dino Boccaccini

[a] Dipartimento di Ingegneria "Enzo Ferrari", Università degli studi di Modena e Reggio Emilia

[b] Resoh Solutions SRL, Italy

[c] Department of Industrial Engineering, University of Florence, Italy

[d] National Interuniversity Consortium of Materials Science and Technology (INSTM), Italy

[e] Istituto di Chimica della Materia Condensata e di Tecnologie per l'Energia, Consiglio Nazionale delle Ricerche (CNR-ICMATE), Italy

[f] Institute of Science, Technology and Sustainability for Ceramic, Consiglio Nazionale delle Ricerche (ISSMC-CNR), Italy

[g] Centro Interdipartimentale di Ricerca e per i Servizi nel Settore della Produzione, Stoccaggio e Utilizzo dell'Idrogeno H2 – MO.RE. Università degli Studi di Modena e Reggio Emilia, Modena, Italy

Keywords: Solid oxide cells, anode support, digital deposition, dry pressing, ceramic processing, porous materials

Abstract

This research investigates fabrication of porous anode supports for solid oxide cells using yttria-stabilized zirconia (3YSZ) ceramics, seeking optimal compaction pressure by correlating microstructure with mechanical properties. Three formulations were studied: base 3YSZ with organic additives; 3YSZ with graphite as pore-former; and a complete anode support with 3YSZ, NiO, and graphite. Samples underwent uniaxial pressing (10-60 MPa) followed by sintering. Microstructure was analyzed via X-ray tomography to quantify porosity and connectivity, while mechanical properties were measured using ball-on-ring tests.

Results show higher compaction pressures reduce porosity and pore connectivity while improving mechanical strength. Graphite-based supports exhibited greater pore interconnectivity, beneficial for infiltration, whereas NiO-containing samples were denser even at lower compaction pressures. This study demonstrates how processing parameters influence the critical balance between gas permeability and mechanical integrity for optimized SOC components.

Introduction:

Solid oxide cells (SOCs), including fuel (SOFCs) and electrolysis (SOECs) types, are high-temperature ceramic devices known for high efficiency, fuel flexibility, and low environmental impact. Their elevated operating temperatures enhance reaction kinetics and allow direct internal fuel reforming. SOCs are also reversible, enabling hydrogen-based energy storage via steam electrolysis [1]. Anode-supported SOCs are widely adopted for their mechanical strength, thin electrolytes, and efficient mass transport. The anode acts both as an electrochemical component and structural support, making its porosity, strength, and connectivity critical to performance [2]. Designing porous anodes requires balancing gas permeability and mechanical integrity, i.e. excess porosity weakens the structure, while poor connectivity hinders diffusion [3]. Traditional powder-based processing remains standard, though optimization is ongoing. This study explores a novel fabrication method using digital dry powder deposition and uniaxial pressing to produce porous 3YSZ-based supports. Three formulations were tested: pure 3YSZ with additives, a 3YSZ/graphite mix for catalytic infiltration, and a NiO-

containing cermet. Compaction pressures from 10 to 60 MPa were applied to assess effects on microstructure and strength. X-ray tomography and mechanical testing were used to link porosity and connectivity to mechanical behavior, guiding improved anode design for next-gen SOCs.

Objectives:

This work aims to optimize the fabrication of porous 3YSZ-based anode supports for SOCs by enhancing mechanical reliability and microstructural performance. Three formulations were developed: base 3YSZ with additives, 3YSZ with graphite for future infiltration, and a NiO-containing cermet. The influence of compaction pressures (10–60 MPa) on porosity, densification, and strength was assessed using ball-on-ring testing, X-ray tomography, and SEM. The study establishes microstructure–mechanical property correlations and demonstrates the potential of digitally assisted dry powder deposition for scalable SOC production.

Material and methods:

The three formulations developed for porous ceramic anode supportsare reported in Table I:

Component	Formulation 1: 3YSZ + Additives (%)	Formulation 2: 3YSZ(additivated) + Graphite (%)	Formulation 3: 3YSZ(additivated) + NiO + Graphite (%)
3YSZ powder	67	-	-
Fluidizing agent	3	-	-
Plasticizer	17	-	-
Binder	13	-	-
3YSZ (additivated)	-	80	24
Graphite (pore former)	-	20	20
NiO	-	-	56

Processing Route

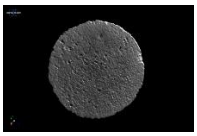
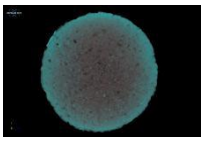
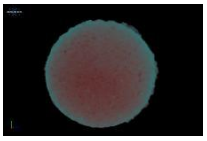
3YSZ powder was mixed with water, additives, and CMC in a ball mill for 5 minutes to form a homogeneous slurry (Table I), then dried at 120 °C for 4 hours. Formulation F1 was directly dry-milled, while Formulations 2 and 3, containing graphite and graphite + NiO respectively, were wet ball-milled again before drying. All dried materials underwent dry milling, were granulated with ~10% water, and sieved through a 300 µm mesh. The resulting granules were uniaxially pressed at 10–60 MPa to assess the effect of compaction pressure. Sintering involved heating to 900 °C at 1 °C/min with a 4-hour hold, followed by heating to 1315 °C at 2 °C/min with a 12-hour hold, and slow cooling over 13 hours. Post-sintering, samples were characterized by X-ray tomography for porosity and structure, and mechanical strength was evaluated using the ball-on-ring test and Weibull analysis.

Results:

Microstructure

SEM micrographs of the F2 formulation show a homogeneous porous backbone with well-distributed porosity throughout the ceramic matrix. Pores are uniformly dispersed with good interconnectivity, indicating effective graphite removal during thermal processing and ensuring adequate gas permeability for electrochemical applications. Figure 1 presents XR tomography images revealing detailed internal and surface microstructures of two compositions (pure 3YSZ backbone and 3YSZ-NiO composite) pressed at 10 MPa. The microstructural analysis reveals significant differences between sample compositions and pressing conditions, with 3YSZ samples at

10 MPa exhibiting higher surface texture and porosity (29.1%) compared to the denser 3YSZ-NiO counterparts (12.8%), while increased pressing pressure to 20 MPa consistently reduces roughness and porosity in both formulations (to 20.1% for 3YSZ and 11.4% for 3YSZ-NiO); cross-sectional tomography of samples pressed at 10 MPa shows internal architecture with slightly denser rings at edges, confirming that higher pressing pressure creates more homogeneous, denser microstructures throughout; detailed porosity analysis demonstrates that increasing pressure from 10 MPa to 20 MPa dramatically reduces both total porosity and pore interconnectivity in 3YSZ+Graphite samples (Euler number changing from -5065 to -505) and 3YSZ+NiO+Graphite formulations (Euler number rising from 6366 to 3265), with the understanding that these ceramic backbones will later undergo NiO infiltration followed by reduction to metallic Ni, which will further increase the final porosity of the structure.

XR surface microstructure	Porous 3YSZ samples pressed at 10 MPa (total p. 29.1%)	Porous 3YSZ-NiO samples pressed at 10 MPa (total p. 12.8%)
		

Conclusions:

This study developed an innovative ceramic processing method for SOFC anode supports, successfully demonstrating the feasibility of digital deposition and forming techniques. The research confirmed a clear correlation between controlled porosity and enhanced mechanical properties, with X-ray tomography providing crucial insights into porosity tailoring. Future work will focus on further optimizing these methods, employing a Design of Experiments (DoE) approach, and exploring microstructure-property correlations in greater detail.

References

[1] J. Wu, J.H. Myung, D. Ding, T. Zhu, Editorial: High Temperature Solid Oxide Cells, Front Chem 9 (2021) 719826. https://doi.org/10.3389/FCHEM.2021.719826/BIBTEX.

[2] D.N. Boccaccini, V. Gil, J. Gurauskis, R.I. Merino, A. Pellacani, C. Mortalò, S. Soprani, M. Romagnoli, M. Cannio, Influence of Porosity on R-Curve Behaviour of Tetragonal Stabilized Zirconia, Ceramics 2022, Vol. 5, Pages 533-549 5 (2022) 533–549. https://doi.org/10.3390/CERAMICS5030040.

[3] A.M. Martos, S. Márquez, R.S. Pavlov, W. Zambelli, S. Anelli, M. Nuñez, L. Bernadet, J.J. Brey, M. Torrell, A. Tarancón, 3D printing of reversible solid oxide cell stacks for efficient hydrogen production and power generation, J Power Sources 609 (2024) 234704. https://doi.org/10.1016/J.JPOWSOUR.2024.234704.



TOPIC 4 : HYDROGEN END-USE APPLICATIONS

European Fuel Cells and Hydrogen
PIERO LUNGHI CONFERENCE
September 17th–19th 2025
Capri / Italy

Numerical Analysis of Natural Gas-Hydrogen blending in Pipelines

G. Cortellessa*[a], F.Arpino [a], M. Dell'Isola[a], G. Ficco[a], G. Grossi[a],
V. Cigolotti[b], A. De Marco[b], P. Gislon[b], G. Monteleone[b]

* corresponding author: Gino Cortellessa

[a] Department of Civil and Mechanical Engineering, University of Cassino and Southern Lazio, Cassino, Italy
[b] Department of Energy Technologies and Renewable Sources, Agenzia Nazionale per le Nuove Tecnologie, l'Energia e lo Sviluppo Sostenibile (ENEA), Research Center Casaccia, 00123 Rome, Italy

Keywords: Thermal Mass Flow Meter, CFD, NG-H_2 blending, Power-to-Gas

Abstract

This study presents a Computational Fluid Dynamics (CFD) model developed to analyse the metrological performance of an insertion thermal flow meter in the case that it is employed for natural gas-hydrogen blending. The model was validated through an experimental campaign carried out at the Laboratory of Industrial Measurements (LAMI), using a real insertion-type thermal flow meter. Then, the validated numerical tool has been applied to study the thermal flow meter behaviour in the case it is employed with a Natural Gas (NG) - hydrogen blending. The results show that the thermal mass flow meter, calibrated for NG, is affected by measurement errors when used with a mixture of natural gas and hydrogen.

Introduction

The transition toward sustainable energy sources has increased interest in hydrogen as an alternative fuel. Maybe the most effective remedy for adding hydrogen into the energy stream is mixing it with natural gas and injecting it through the installed pipeline networks using the Power to Gas (PtG) technology [1,2]. But introducing hydrogen into natural gas grids poses a range of flow measurement, pipeline integrity, and system efficiency issues. Hydrogen differs from methane, the major component in natural gas, in having unique thermodynamic and transport characteristics. Such a non-homogeneous distribution leads to inaccuracies in flow measurement, particularly in meters that have been calibrated using pure natural gas. Also, hydrogen's increased thermal conductivity and reduced viscosity affect flow resistance, heat transfer rates, and turbulence behaviour. Accurate prediction of these effects is essential for ensuring the reliability of flow meters and optimizing pipeline operation. Traditional empirical correlations cannot describe complex phenomena present in hydrogen-natural gas mixtures, and thus Computational Fluid Dynamics (CFD) is a necessity to study such processes. This study aims to develop a CFD model capable of simulating the metrological performance of a real insertion thermal flow meter, validating it against experimental data, and applying it to analyse the effects of hydrogen blending. The insights gained from this study will improve the accuracy of flow measurement techniques, develop correction models, and support the transition to hydrogen-enriched gas networks.

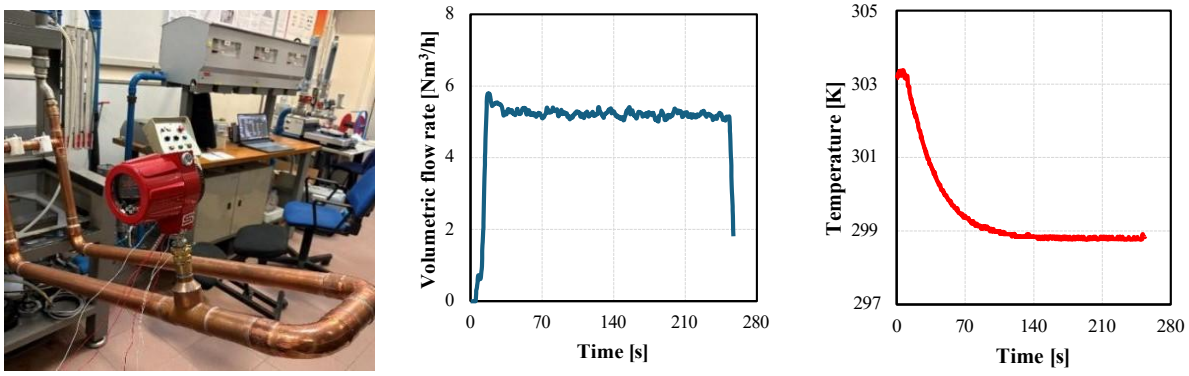
Governing Equations for CFD Modelling

The mathematical model is based on conservation equations of key physical quantities, describing the temporal and spatial evolution of variables in the computational domain. The mass, momentum, and energy equations are well-known in the literature and omitted for

brevity [3]. The species conservation equation is also solved to account for the balance of each chemical species in the fluid. The Unsteady Reynolds-Averaged Navier-Stokes (URANS) model was chosen to resolve turbulent flow, averaging turbulence effects over time and solving only the largest scales. After testing different turbulence models, the SST k-ω model was adopted for its suitability in highly turbulent flows and separation phenomena. The numerical implementation used Ansys Fluent, a CFD software based on the finite volume method [4].

Numerical model validation and results

An experimental campaign was carried out at the LAMI laboratory with the aim of validating the numerical model developed using air as the working fluid. The experimental tests were conducted using a SIERRA 640i thermal mass flow meter (Figure 1a), which was installed on a test bench and operated within a volumetric flow rate range from 3 Nm³/h to 26.6 Nm³/h.

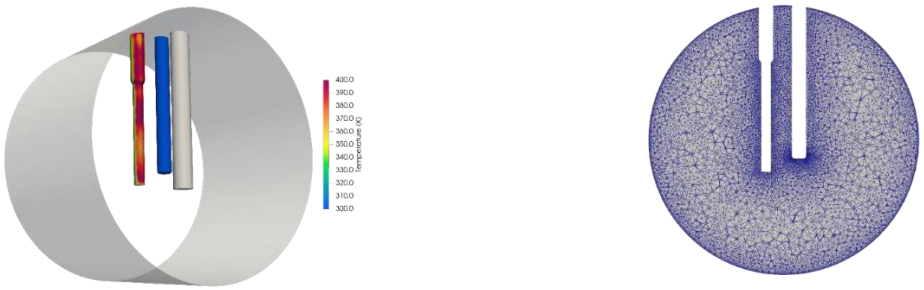


(a) (b) (c)

Figure 1. Image of the experimental setup showing the SIERRA 640i thermal mass flow meter mounted on the test bench (a); Examples of volumetric flow rate and temperature dynamic profiles selected among those investigated (b and c).

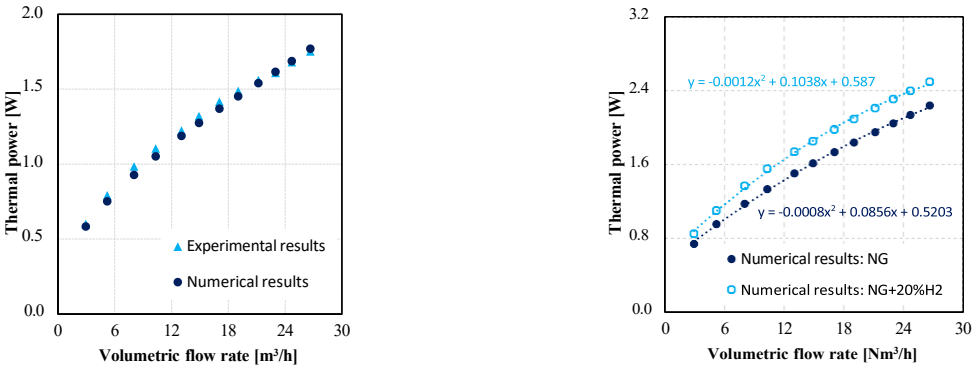
During the tests, the time trends of the volumetric flow rate (Figure 1b) and the gas temperature (Figure 1c) were recorded, waiting for the time necessary to reach steady-state conditions. Additionally, the electric current absorbed by the flow meter was monitored. After subtracting the background current required to operate the meter's electronic board and considering the supply voltage, it was possible to calculate the thermal power transferred to the fluid at each flow rate level in order to maintain a constant temperature difference (ΔT) of 50°C between the meter's surface and the fluid. The geometry of the SIERRA 640i flow meter was accurately reproduced, faithfully respecting all dimensions, with particular attention to the three elements immersed in the fluid: the heated velocity sensor, the gas temperature probe, and the protective stem (Figure 2a). In addition to the flow meter, the pipeline used in the experimental setup, featuring an internal diameter of 51 mm, was also numerically modelled. In Figure 2b, the adopted computational grid composed of 995030 elements is illustrated. The validation of the developed numerical tool is illustrated in Figure 3a, showing a good agreement between the numerical and experimental results with a maximum percent deviation of 5%. The validated numerical tool has then been applied to investigate the behaviour in NG and a blending of NG+20%H_2 (Figure 3b). For the blended

mixture, the deviation from the NG case ranged from a minimum of 11.33% to a maximum of 14.72% in terms of thermal power required.



(a) (b)

Figure 2. Detail of the computational domain showing the thermal flow meter immersed in the duct (a); adopted computational grid consisting of 995030 elements (b).



(a) (b)

Figure 3. Comparison between experimental and numerical results in terms of required thermal power as a function of the volumetric flow rate (a); application of the validated numerical tool with NG and a blending of NG-20%H_2 (b).

Conclusions

The CFD model developed in this study was successfully validated by experimental data in air. The numerical tool has been applied to investigate the metrological performance of an insertion flow rate in the case that it is employed with a blending of NG+20%H_2. The numerical results indicate that the thermal mass flow meter may overestimate the actual volumetric flow rate, potentially leading to significant billing inaccuracies. The validated model provides a valuable tool for analysing gas distribution systems, optimizing measurement techniques, and supporting the transition to hydrogen-enriched gas networks.

Acknowledgment

This work was funded by the Italian Ministry of Ecological Transition (MITE) through PNRR programme 2022-2025 Research and development on Hydrogen, Operative Plan for Hydrogen Research POR H2, Activity 2.5.1.

References

[1] P. Stephen, Renewable Energy: Power for a Sustainable Future, Oxford University Press, 4th ed., 2018.
[2] M. Lehner, R. Tichler, H. Steinmüller, M. Koppe, Power-to-Gas: Technology and Business Models, Springer Cham, 2014.
[3] J. C. Greenshields, H. G. Weller, Notes on computational fluid dynamics: general principles, CFD Direct Ltd, Reading, UK, 2022.
[4] J.E. Matsson, An Introduction to ANSYS Fluent 2022, SDC Publications, ISBN: 978-1-63057-569-4, 2022.

EFCH2 2025 European Fuel Cells and Hydrogen
PIERO LUNGHI CONFERENCE
September 17th–19th 2025 Capri / Italy

The impact of an economic green hydrogen supply on defossilized steelmaking and direct-reduced iron supply chains

Florian Scheffler*[a], Christoph Imdahl [a], Sabrina Zellmer[a,b], Christoph Herrmann[a,c]
* corresponding author
[a] Fraunhofer Institute for Surface Engineering and Thin Films IST
[b] Technische Universität Braunschweig, Institute for Particle Technology
[c] Technische Universität Braunschweig, Institute of Machine Tools and Production Technology
Keywords: Hydrogen-based steelmaking, Direct-reduced iron, Green iron export

Abstract

Introduction: In view of the European Union's target of achieving climate-neutrality in 2050, the EU's steel industry, responsible for around 5% of the EU's greenhouse gas (GHG) emissions (190 million tons), faces the challenge of achieving a defossilized and competitive production [1]. GHG-intensive primary steelmaking based on the blast furnace-basic oxygen furnace (BF-BOF) route using coking coal to reduce iron ore accounts thereby to around 60% of the EU's production [1]. European steelmakers, e.g. in Germany as the seventh largest steel producer worldwide, focus on implementing the direct-reduced iron-electric arc furnace (DRI-EAF) route utilizing solely renewable hydrogen (H_2) in the long-term as a reducing agent. The steel sector is currently a forerunner in shaping a demand for low-emissions H_2 with recently published tenders by German steel companies for off-take starting in 2027 [2]. Shaft furnace-based DRI plants, commercialized with the MIDREX and the HYL/Energiron technology, can be flexibly operated with H_2 and natural gas mixtures to overcome a shortage of an affordable H2 market supply until regional and cross-border H_2 supply chains are established [3,4]. Germany thereby is a prospective net importer of H_2 and power-to-x (PtX) products and thus dependent on developing international supply chains in line with a pan-European H_2 pipeline network and import infrastructure [5]. In addition, ambitions of potential global players in producing and exporting green H_2 like Australia, as the world's largest iron ore producer and exporter, are set on becoming a global supplier of green DRI products to domestic and global steelmaking markets alongside the development of other power-to-x value chains, which is reflected by multiple announced DRI projects [6,7]. DRI products can be exported as hot briquetted iron (HBI), a densified DRI form (≥ 5 g cm^{-3}) suitable for shipping solid bulk [3,8].

Objectives: The objective of this study is the evaluation of a potentially emerging green commodity market of hydrogen-based DRI (H_2-DRI) exports to low-emissions steelmaking countries in the EU. This affects the strategy of green H_2 procurement for integrated steel

sites investing in the DRI-EAF route, particularly in view of the current H_2 ambition and implementation gap [9]. In this study, prospective costs of PtX imports to Germany by ship and pipeline are compared to import costs of H_2-DRI. This can be reviewed with literature showing a long-term cost advantage for H_2-DRI exports from Australia to the EU [10].

Material and methods: The techno-economic assessment of a H_2-DRI export supply chain in 2030 is based on an annual DRI export of 2 million tons (Mt) by shipping and rail transport from Australia, Port of Hedland, to Germany via the Port of Wilhelmshaven. The results are compared to a H_2-DRI plant in an integrated German steel mill based on a H_2 supply mix of on-site production via electrolysis and H_2 supplied from ammonia imports. The main techno-economic parameters for the DRI supply chain are based on literature data, whereas a specific H_2 demand of 66 kg H_2 per ton DRI is applied for the H_2-DRI process [10,11]. DRI plants generally require the supply of higher-grade DR pellets (>67% Fe). DR pellet supply costs of 175 USD per t are assumed for both DRI locations [12]. H_2 supply costs are derived with renewable electricity prices of 40 and 80 € per MWh in Australia and Germany, whereas the H_2 import costs refer to an ammonia import from Canada to Germany [13].

Results: The H_2-DRI scenarios in Germany show additional levelized cost of 18-32% compared to the DRI import route from Australia (Fig. 1). The carbon abatement cost for H_2-DRI replacing a natural gas (NG) DRI plant operation (1.06 Mt CO_2) in Germany range between 667-806 € per t CO_2 for the German scenarios, while H_2-DRI in Australia achieves 40-49% lower abatement cost.

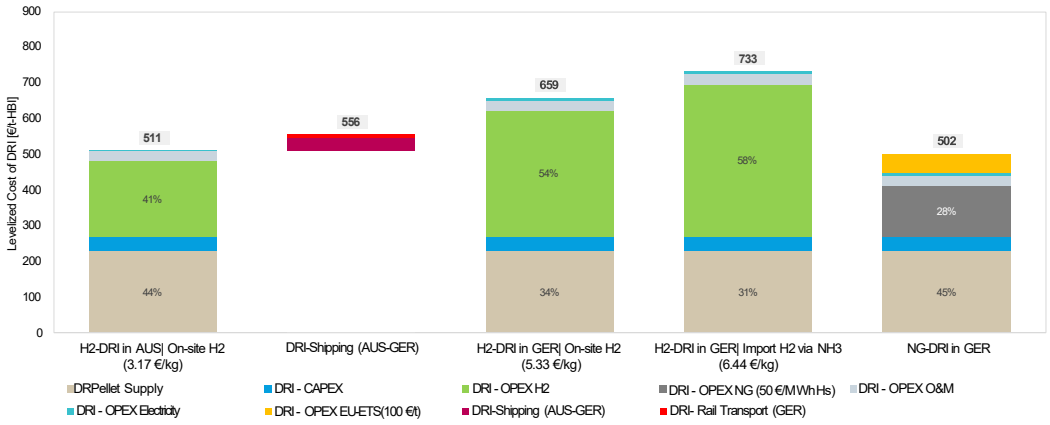


Figure 1: Levelized cost of H_2-DRI scenarios comparing an export route from Australia to Germany to a domestic H_2-DRI plant based on different H_2 supply cost and a DRI process fuelled by natural gas as a reference

The DRI import with a carbon footprint of 128 kg CO_2 per t DRI related to a fossil marine fuel for shipping still accounts for 11% higher cost compared to the NG-DRI process based on EU allowances cost of 100 € per ton CO_2.

Conclusions: The cost benefits and opportunities of global H_2-DRI supply chains could potentially accelerate the transition to low-emissions steelmaking in the EU. The predicted lack of an affordable green H_2 supply in countries like Germany can be addressed by establishing H_2-DRI exports from countries with low-cost H_2 production potentials and iron ore resources as shown for Australia. This could facilitate the transition to green steelmaking in the EU and solve the issue of low-cost H_2 supply options in the medium term.

Acknowledgment:

The Authors acknowledge funding from the German Federal Ministry of Education and Research under the "German-Australian Hydrogen Innovation and Technology Incubator" (HyGATE) for the project ScaleH_2, with grant number 03SF0711A.

References

[1] Somers J. Technologies to decarbonise the EU steel industry. Luxembourg; 2022.
[2] IEA. Global Hydrogen Review 2024. Paris; 2024.
[3] Midrex Technologies I. World Direct Reduction Statistics; Available from: https://www.midrex.com/wp-content/uploads/MidrexSTATSBook2023.Final_.pdf.
[4] Dorndorf M. Hydrogen use in Direct Reduction (DR) Plant – potentials for CO2 mitigation in steel works: Green Industrial Hydrogen via steam electrolysis; 2020.
[5] Federal Ministry for Economic Affairs and Climate Action (BMWK). Import Strategy for hydrogen and hydrogen derivatives; 2024.
[6] R. Daiyan, I. MacGill, P. Ellersdorfer, C. Wang, I. Canbulat, S. Saydam, T.C. Leung, M.H.A. Khan. Green Metals for Sustainable Steel from Australia and Germany: German-Australian Feasibility and Technical Study; 2024.
[7] DCCEEW. National Hydrogen Strategy 2024. Canberra; 2024.
[8] International Iron Metallics Association. Hot Briquetted Iron (HBI): A Guide to Shipping, Handling & Storage; 2020.
[9] Odenweller A, Ueckerdt F. The green hydrogen ambition and implementation gap. Nat Energy 2025;10(1):110–23.
[10] Ellersdorfer P, Wang C, Saydam S, Canbulat I, MacGill I, Daiyan R. Unlocking new export opportunities: An open-source framework for assessing green iron and steel supply chains. International Journal of Hydrogen Energy 2024;92:1366–74.
[11] Jacobasch E, Herz G, Rix C, Müller N, Reichelt E, Jahn M et al. Economic evaluation of low-carbon steelmaking via coupling of electrolysis and direct reduction. Journal of Cleaner Production 2021;328:129502.
[12] Altius Minerals Corporation. The Global Shift To EAF Steelmaking and the Implications for DR Grade Iron Ore Demand; 2024.
[13] Scheffler F, Imdahl C, Zellmer S, Herrmann C. Techno-economic and environmental assessment of renewable hydrogen import routes from overseas in 2030. Applied Energy 2025;380:125073.

EFCH2 2025 European Fuel Cells and Hydrogen PIERO LUNGHI CONFERENCE
September 17th–19th 2025 Capri / Italy

A Region-Specific European Analysis of SOEC-Based Green Ammonia Cost Competitiveness

Alessandro Magnino*[a], Paolo Marocco [a], Massimo Santarelli [a], Marta Gandiglio [a]

* corresponding author: alessandro.magnino@polito.it

[a] Department of Energy, Politecnico di Torino, Corso Duca degli Abruzzi 24, Torino, 10129, Torino, Italy

Keywords: Decarbonisation, Levelised Cost Of Ammonia, Mixed Integer Linear Programming, Solid Oxide Electrolyser Cells

Abstract Introduction:

Ammonia (NH_3) is essential for global food security as a key fertiliser component and is widely used in refrigeration, mining, water treatment, and as a potential energy carrier [1]. The transition from natural gas is driving research on integrating Haber-Bosch (HB) with electrolysers, moving toward EU targets of climate neutrality and energy and cost security [2].

Objectives:

This study develops a Mixed Integer Linear Programming (MILP) model for optimally sizing Solid Oxide Electrolyser Cell (SOEC)-based ammonia production plants powered by renewable and grid energy. By evaluating Levelised Cost of Ammonia (LCOA) under varying renewable potentials, the model explores both islanded and grid-connected setups.

This analysis provides a region-specific perspective on green ammonia production by integrating plant components and optimal operational strategies. It aims to guide cost-effective, sustainable ammonia production in Europe while examining the impact of new European directives on e-fuels production.

Material and methods:

The investigated plant is a SOEC-based ammonia production plant, as reported in Figure 1. The optimisation strategy involves modelling the electrical consumption and mass balances of all components, along with comprehensive heat integration between the HB and SOEC systems to minimise energy usage and satisfy a given annual NH_3 demand. Unlike most prior studies, this model includes a non-constant SOEC efficiency to accurately capture performance at partial loads, as well as heat consumption during off-periods to maintain a warm-standby state, preventing rapid cell degradation.

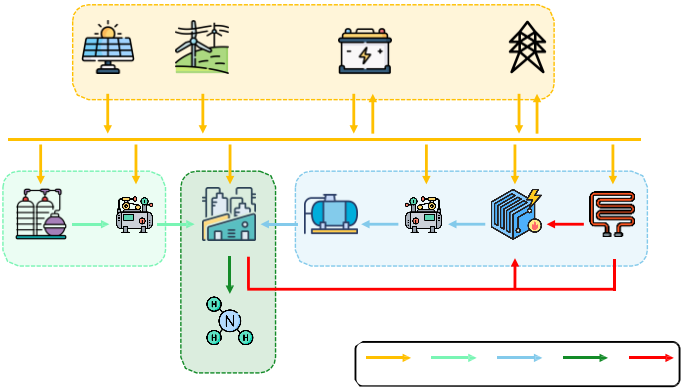


Figure 1. Ammonia production plant layout

Two main scenarios are analysed:

1. Scenario 1: ammonia as Renewable Fuel of Non Biological Origin (RFNBO) production, according to RED III requirements [3] imposing off-grid operation excepting in bidding zones where grid renewable share exceeds 90%.
2. Scenario 2: grid use is allowed in order to minimise ammonia production costs.

All European NUTS 2 regions are assessed to estimate the LCOA for each scenario, with PV and onshore wind as potential energy sources. In Scenario 2, national grid electricity prices are factored in [4].

The optimisation employs a MILP approach to minimise lifetime plant costs, determining the best plant configuration and operational strategy, including various energy storage options (as shown in Figure 1).

Results:

A summary of results can be observed in Figure 2, where the LCOA in each European region is evaluated.

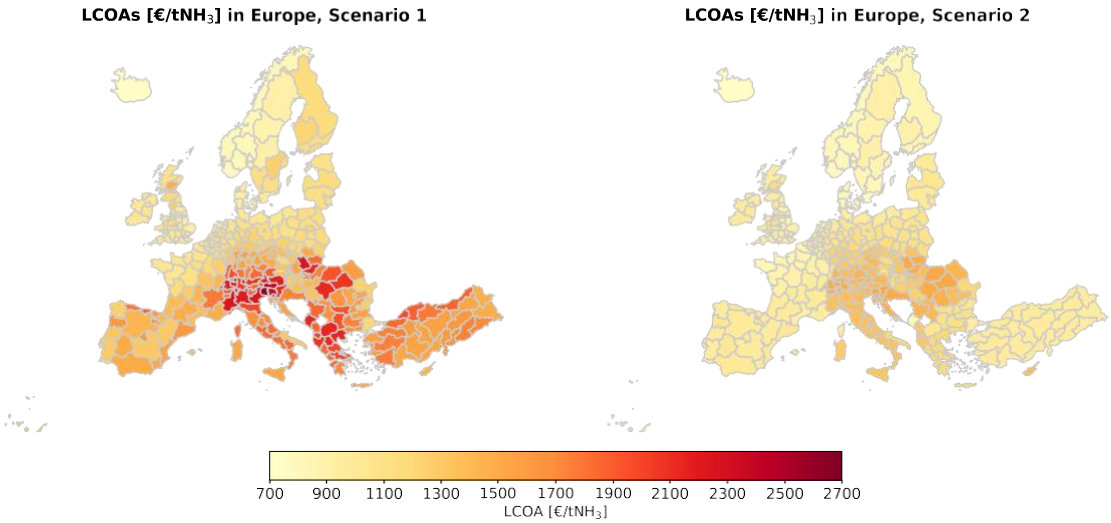


Figure 2. LCOAs [€/tNH3] in Europe, considering RFNBO production (Scenario 1) and up to 100% grid use (Scenario 2).

Regions with strong wind resources (e.g., Denmark, northern Germany, and parts of England) achieve lower LCOA values compared to solar-dominated regions (such as southern Italy, southern Spain, and Greece). Wind power, even if variable, has smoother fluctuations over time, making it more compatible with the continuous operation required for HB and SOEC systems. In contrast, solar-dominated regions require larger storage capacities to maintain overnight operations, driving up costs. However, regions allowed to use grid electricity (Norway, Iceland, and Sweden) reach the minimum LCOAs.

Allowing for grid electricity use in Scenario 2 notably reduces LCOA in less cost-effective areas (like northern Italy, Switzerland and Greece), highlighting that NH_3 production costs could be reduced if grid connection is present, while its effect on favourable areas is relatively limited.

Conclusions:

The analysis reveals that regions with abundant wind resources can achieve significantly lower LCOA values due to more stable power supplies, while solar-dominated regions need large storage systems to guarantee continuous operation. The flexibility to use grid electricity, as allowed in Scenario 2, notably lowers costs in less favourable regions. These findings support the case for region-specific ammonia production strategies, which can help advance Europe's transition to carbon-neutral, cost-effective green ammonia.

Acknowledgment

The work has been conducted in the framework of the AMPS (Automated Mass Production of SOC Stack) project (https://www.amps-project.eu/). The project is supported by the Clean Hydrogen Partnership and its members (GA: 101111882).

Project funded under the National Recovery and Resilience Plan (NRRP), Mission 4. Component 2 Investment 1.3 - Call for tender No. 1561 of 11.10.2022 of Ministero dell'Università e della Ricerca (MUR); funded by the European Union – NextGenerationEU. Project code PE0000021, Concession Decree No. 1561 of 11.10.2022 adopted by Ministero dell'Università e della Ricerca (MUR), CUP - E13C22001890001, Project title "Network 4 Energy Sustainable Transition – NEST".

References

[1] IEA. Ammonia Technology Roadmap Towards more sustainable nitrogen fertiliser production. 2021. https://doi.org/https://www.iea.org/reports/ammonia-technology-roadmap.

[2] European Commission. REPowerEU 2022. https://doi.org/https://ec.europa.eu/commission/presscorner/detail/en/ip_22_3131.

[3] European Parliament. Directive (EU) 2023/2413. 2023.

[4] Eurostat. Statistics | Eurostat. Electricity prices for non-household consumers 2024. https://ec.europa.eu/eurostat/databrowser/view/nrg_pc_205__custom_15713690/default/table?lang=en (accessed March 10, 2024).

European Fuel Cells and Hydrogen
PIERO LUNGHI CONFERENCE
September 17th–19th 2025
Capri / Italy

Preparation of European airports to operate with LH2

Maria Sol Rau*[a], Josef Kallo [a], Jan-Daan Maasland[b], Daan van Dijk[b]

* corresponding author: mariasol.rau@h2fly.de
[a] H2FLY GmbH
[b] Rotterdam The Hague Airport

Keywords: sustainable aviation, hydrogen, liquid hydrogen and fuel cells

Abstract Introduction:

The GOLIAT project, which is funded by the European Union under grant agreement n° 101138379, aims to advance sustainable aviation technologies by developing high-performance refuelling technologies and addressing gaps in hydrogen supply, infrastructure, and operations at European airports. The project focuses on preparing airports to handle liquid hydrogen (LH2) refueling and aircraft operations, with feasibility studies for these operations conducted at Stuttgart Airport, Rotterdam The Hague Airport, and Lyon Saint-Exupéry Airport.

Objectives:

The work that will be presented during the conference, aims to provide essential knowledge and practical insights to facilitate LH2 handling operations at EU airports, supporting the transition to hydrogen-powered aviation and fostering growth in the aviation sector.

Material and methods:

The study involves insights from three European airports and H2FLY GmbH, focusing on demonstration scenarios, concept of operations, logistics, safety, and regulatory aspects. Key aspects investigated in the feasibiliy study include:

- Definition of plan scenarios, logistics, and refueling procedures.
- Identification of mitigation actions.
- Analysis of infrastructural needs for LH2 aircraft operations and LH2 trailer handling.
- Execution of initial safety assessments on LH2 refueling and LH2 trailer handling

Results:

By integrating LH2 powered aircraft operations on three operational airports, GOLIAT provides tangible challenges and learnings. The feasibility study indicates that LH2 refueling

at the three airports is technically feasible. Operational integration requires coordination with local governments, civil aviation authorities, and community stakeholders to ensure compliance with regulations. The study highlights the need for specialized infrastructure, tailored regulatory approaches, comprehensive risk assessments, and environmental impact considerations.

The initial risk assessment gives a structured overview of the associated risks when transporting and staging a LH2 trailer and using this trailer to refuel a LH2-powered aircraft on airports. These risks, and other potential local risks, should be further classified at each demonstration airport in order to perform the demonstration in a safe manner.

Infrastructure and Logistics

- Establishing LH2 capabilities requires specialized infrastructure, including cryogenic trailers, refuelling devices, and venting systems.
- The logistical framework highlights the need for site-specific adaptations, from refuelling site layout to compliance with local ATEX (explosive atmospheres) zoning requirements.

Regulatory Considerations

- Airports must comply with European Aviation Safety Agency (EASA) regulations and national/local laws.
- Regulatory frameworks vary significantly among the demonstration locations, necessitating tailored approaches to permits, risk assessments, and safety measures.

Safety and Risk Mitigation

- LH2 presents unique risks due to its flammability, cryogenic nature, and low ignition energy.
- Comprehensive risk assessments are pivotal for ensuring safe demonstrations, including emergency protocols and mitigation strategies for potential hydrogen leaks or fires.

Environmental Impact

- Hydrogen propulsion aligns with the European Green Deal's objective of reducing transport emissions by 90% by 2050.
- The study emphasizes hydrogen's potential to revolutionize aviation, offering zero-emission solutions for short and medium-haul flights.

Demonstration Outcomes

- Each airport demonstration will provide critical data on operational challenges, enabling iterative improvements.

- Lessons learned will further define standards for infrastructure development, operational procedures, and certification processes for broader LH2 adoption.

Conclusions:

The GOLIAT project lays the groundwork for sustainable aviation by demonstrating the practicalities of LH2 operations at diverse European airports. The findings contribute to defining the operational framework and supporting the global transition to cleaner aviation. This project is a significant step towards achieving the European Green Deal's objective.

Acknowledgment

The GOLIAT consortium consists of 10 partners from eight countries: Airbus (France, Germany, UK), Chart Industries (Czech Republic, Italy), TU Delft (Netherlands), Leibniz University Hannover (Germany), Royal Schiphol Group (Netherlands), Rotterdam The Hague Airport (Netherlands), Vinci Airports (France, Portugal), Stuttgart Airport (Germany), H2FLY (Germany), and Budapest Airport (Hungary).

This research was carried out within the GOLIAT project, which is funded by the European Union under grant agreement n° 10113837



EFCH2 2025 European Fuel Cells and Hydrogen
PIERO LUNGHI CONFERENCE
September 17th–19th 2025 Capri / Italy

Comparative analysis of power-to-hydrogen energy storage system for residential applications

Pierpaolo Polverino*[a], Luigia Di Matteo[a]

*corresponding author: ppolverino@unisa.it

[a] Department of Industrial Engineering, University of Salerno, via Giovanni Paolo II 132, 84084, Fisciano (SA), ITALY.

Keywords: Power-to-Hydrogen; Energy Storge; Electrolysis; Fuel Cell; Renewable Energy.

Abstract

Introduction: Global energy consumption has been gradually increasing due to rising of population and living standards, resulting in a growth in global warming and environmental pollution, which makes the use of Renewable Energy Sources (RES) increasingly necessary [1]. Energy transition is one of the main challenges to mitigate CO_2 emissions from energy sector, and solar and wind energy seems to be the most promising alternatives for the future energy mix, with a target of 56% of total electricity generation from RES by 2050 [2]. However, these sources are inherently intermittent. As the voltage of electricity grids is strictly limited to ±10% of its nominal value, RES intermittent supply implies difficulties in feeding renewable electricity into existing infrastructures. Therefore, proper energy management and storage can enable continuous and extensive use of renewable sources. Among various solutions, hydrogen production and storage (P2H) stemmed out as promising solution for grid balancing: electricity surplus is converted into hydrogen through water electrolysis, stored as, e.g., compressed or cryo-compressed gas, and then fed to a fuel cell to produce electric power when needed [5]. P2H systems applies to many uses, such as power generation, heating, transportation, industrial and remote/off-grid applications [2]. However, their competitiveness compared to more mature technologies (e.g., batteries) is still limited due to lower durability and roundtrip efficiency: the latter is currently around 30%-40% but could reach 50% with more efficient technologies [6].

Objectives: This work provides a comparative analysis between P2H and battery energy storage and reuse systems, connected to an off-grid RES power plant for residential application. The user power request is taken from real historical data of average electricity consumption profiles, while the RES plant consists in a hybrid photovoltaic-wind turbine (PV-WT) system. The analysis is carried out in simulated environment to find a compromise between overall roundtrip efficiency and system cost.

Simulation framework: The user electricity request profile has been taken from ARERA

historical data [7] as average hourly consumption of a domestic customer with power class between 3 kW and 4.5 kW. The average profile covers a period of one year (8760 h), and the RES system components have been sized to cover the total annual energy demand of 2572 kWh/year. The PV system and the WT have been selected from the market, the former considering single modules each with surface of 1.67 m^2, nominal power of 335 W and rated efficiency of 20% [8], whereas the latter with a single horizontal rotor of 3.3 m^2 and nominal power of 1.50 kW [9].

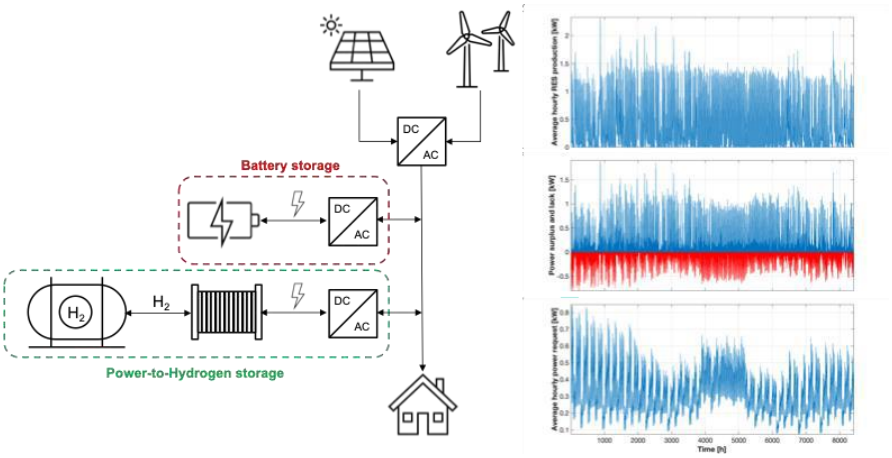


Figure 1. Case studies scheme with user power request and RES power generation profile.

Four PV modules are considered for the battery storage case, reaching a nominal power output of 1.34 kW. This choice represents a compromise between energy demand and production, to limit excessive energy surplus and plant cost. The Li-Ion battery storage system is modelled through its State-of-Charge (SOC), with charging and discharging efficiencies of 90%, DC/AC converter efficiency of 96.5%, and minimum and maximum SOC of 30% and 100%, respectively. For the P2H case, the PV modules are increased to seven to cope with user request and balance the losses related to electrolyser and fuel cell efficiencies. The WT is instead kept unchanged for the two cases. The P2H storage presents 2.75 kW PEM electrolyser (70% efficiency), 700 W PEM fuel cell (45% efficiency), and 550 L tank with maximum pressure of 300 bar [10]. The hydrogen storage is modelled through mass and energy balances, to account for transient operations.

Results: For the battery storage case, the Li-ion system was designed with a nominal capacity of 300 kWh, to ensure energy request satisfaction in off-grid conditions, applying a charge sustaining strategy (with initial and final SOC of 70%). The overall roundtrip efficiency considering charging, discharging and converter efficiencies is around 78%. The cost considered for the Li-ion storage system is 400 €/kWh [5], hence with a total cost of 120’000,00 €. Assuming an investment of about 4773.00 € for the RES plant [10], an overall investment cost of 124’773.00 € is achieved. A charge sustaining strategy is adopted also for

the P2H case, with an initial hydrogen mass of 7.5 kg (i.e., about 170 bar at 25°C). The roundtrip efficiency considering electrolysis, power generation, and converter efficiencies is about 30%. The average costs considered for the electrolyser, fuel cell and hydrogen tank are 2000.00 €/kW, 3947.00 €/kW, and 470.00 €/kgH2 [10]. Hence the overall investment, accounting also for the greater RES system cost (i.e., 6335.45 €), is 24'458.90 €, resulting five times lower than the reference case.

Conclusions: This work proposed a comparative analysis in simulated environment between P2H and battery energy storage systems connected to an off-grid RES (PV-WT) power plant for residential applications. For the battery storage, a great roundtrip efficiency is associated to a high investment cost, whereas the P2H system offers, on the one hand, a reduced efficiency (2.6 times less), but with a much lower investment cost (5.1 times less). Although higher losses, energy storage in the form of compressed hydrogen represents a long-term reserve with respect to battery storage. Hence, P2H is an economically feasible alternative for long-term energy storage coupled to RES sources.

References

[1] Kumar S.S., Himabindu V., Hydrogen production by PEM water electrolysis – A review, Materials Science for Energy Technologies 2 (2019) 442–454.

[2] Sánchez A., Zhang Q., Martín M., Vega P., Towards a new renewable power system using energy storage: An economic and social analysis, Energy Conversion and Management 252 (2022) 115056.

[3] Hu G., Chen C., Thuan Lu H., Wua Y., Liu C., Tao L., Men Y., He G., Gang Li K., A Review of Technical Advances, Barriers, and Solutions in the Power to Hydrogen (P2H) Roadmap, Engineering 6 (2020) 1364–1380.

[4] Maggio G., Nicita A., Squadrito G., How the hydrogen production from RES could change energy and fuel markets: A review of recent literature, International Journal of Hydrogen Energy 44 (2019) 11371-11384.

[5] Ban M., Yu J., Shahidehpour M., Yao Y., Integration of power-to- hydrogen in day-ahead security-constrained unit commitment with high wind penetration, Journal of Modern Power Systems and Clean Energy (2017) 5(3) 337–349.

[6] Abdin Z., Mérida W., Hybrid energy systems for off-grid power supply and hydrogen production based on renewable energy: A techno-economic analysis, Energy Conversion and Management 196 (2019) 1068–1079.

[7] arera.it/dati-e-statistiche/dettaglio/analisi-dei-consumi-dei-clienti-domestici.

[8] elfor.org/prodotto/panasonic-330.

[9] etneo.com/micro-eolico-orizzontale-1500w.

[10] Marocco P., Ferrero D., Lanzini A., Santarelli M., Optimal design of stand-alone solutions based on RES + hydrogen storage feeding off-grid communities Energy Conversion and Management 238 (2021) 114147.

European Fuel Cells and Hydrogen
PIERO LUNGHI CONFERENCE
September 17th–19th 2025
Capri / Italy

Green Hydrogen in Decarbonizing Hard-to-Abate Sectors: A Pathway for a Sustainable Steel Production

M. Minutillo[a], S. Lipardi [a], E. Jannelli[b], C. Bassano[c], S. Di Micco *[b]
* corresponding author: simona.dimicco@uniparthenope.it
[a] Department of Industrial Engineering, University of Salerno, Fisciano, Italy
[b] Department of Engineering, University of Naples "Parthenope", Naples, Italy
[c] ENEA - Italian National Agency for New Technologies, Energy and Sustainable Economic Development, Naples, Italy

Keywords: steel industry, decarbonization, green hydrogen, renewable sources

Abstract:

This study is focused on the use of green hydrogen for the decarbonization of the steel industry, one of the sectors classified as hard-to-abate.

Introduction: The iron and steel sector accounts for approximately 11% of global CO_2 emissions and requires a rapid transition to align with international climate mitigation objectives. In this context, green hydrogen represents a key solution for reaching these goals.

Objectives: This study aims to analyze the use of hydrogen (H_2) in blending with natural gas for supplying burners devoted to provide heat for the steel production process. The analysis is focused on the design and sizing of a H_2 production plant as well as on the evaluation of its economic feasibility in terms of levelized cost of hydrogen (LCOH).

Material and methods: The analysis is performed by using the numerical model based on an optimization algorithm that is able to identify the optimal size of a H_2 supply chain designed for producing green H_2 that can be used as an alternative zero-carbon fuel in a steel industry. A case study related to an industry located in the South of Italy is considered [1]. By analyzing the annual thermal energy demand (about 370 GWh/year), and by assuming that H_2 has to cover the 10% of this demand, the H_2 supply chain is designed and sized. A photovoltaic (PV) power plant and a wind farm (WT) are used as renewable energy sources (RESs) for supplying an alkaline electrolysis unit. To increase the exploitation of the RESs, a battery unit is integrated in to the system. The connection to the national grid is considered only to export the electricity surplus that is not used for the H_2 production. The layout of the proposed H_2 supply chain is shown in Figure 1. Different Scenarios (1-5) related to the percentage of power shares between the PV and WT plants are taken into account, as illustrated in Table 1.

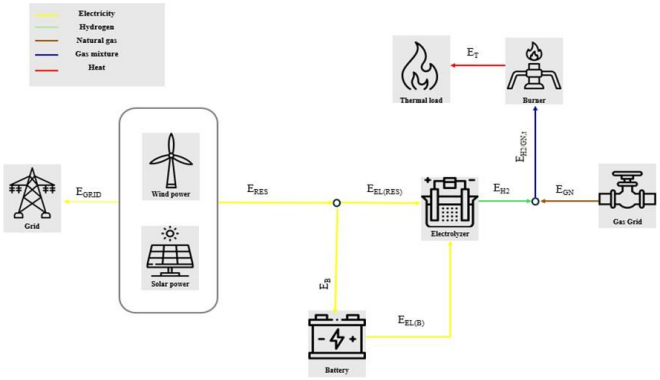


Figure 1- Layout of the proposed system

Table 1: Percentages of power shares between RESs.

RES Power Sharing	Scenario 1	Scenario 2	Scenario 3	Scenario 4	Scenario 5
WT	100%	0	50%	75%	25%
PV	0	100%	50%	25%	75%

According to these Scenarios the optimal configuration is identified as the one that assures the minimum LCOH. This economic parameter is calculated as [2]:

$$LCOH = \frac{CRF \cdot [CAPEX + \sum_{n=0}^{N-1}(C_{O\&M_an,n} + C_{rep_an,n=t} - R_{O_2_an,n} - R_{EL_an,n} - R_{CO_2_an,n})]}{m_{H_2}} \quad (1)$$

Where $CAPEX$, $C_{O\&M}$, C_{rep} and R are the investment costs, the operating and maintenance costs, the replacement cost and the revenues (due to the selling of oxygen, electricity and to avoided CO_2), respectively and m_{H_2} is the annual H_2 production. The subscript "an" means that the costs are calculated as annualized costs (they are calculated by considering the nominal discount rate and the inflation rate) [2]. The analysis considers a plant lifetime (N) of 20 years. The specific costs, used for the estimation of the LCOH, are listed in Table 2.

Table 2: Cost parameters

Components	Units	C_{inv}	$C_{O\&M}$	C_{rep}
PV plant	€/kW	440	1.5% C_{FC}	-
Wind farm	€/kW	1261	3% C_{FC}	-
Electrolyzer	€/kW	650	3% C_{FC}	43% C_{FC}
Battery	€/kWh	250	4% C_{FC}	C_{FC}

It is worth highlighting that the CAPEX in eq.1 are estimated taking into account the specific investment cost (C_{inv}) of each plant component. For the estimation of the revenues, 0.05 €/kg, 70 €/MWh and 70 €/ton$_{CO2}$ (according to the Emission Trading System) are assumed as prices for oxygen, electricity, and carbon dioxide, respectively.

Results: The size of each component of the designed hydrogen supply chain, according to the defined Scenarios, are summarized in Table 3. In Scenario 1 (only WT) and Scenario 2 (only PV), the size of the electrolyser is the highest as well as the battery size.

Table 3: Size of the components of the system for different Scenario analyzed

Components	Scenario 1	Scenario 2	Scenario 3	Scenario 4	Scenario 5
Wind turbine [MW]	43	-	29.5	40	18.5
PV plant [MW]	-	72	29.5	13	57
Electrolyzer [MW]	16.3	22.9	13.1	13.8	13.8
Battery [MWh]	48.9	68.6	39.2	41.5	41.4

With respect to the estimation of the LCOH, Figure 2 shows the obtained results for each Scenario. It is worth noticing that the highest value (3.87 €/kg) is obtained when 100% PV is used as RES (Scenario 1). On the other hand, the lowest LCOH (2.31 €/kg) is reached in Scenario 5 (25%PV-75%WT). For this Scenario the distribution of the electricity from RESs to supply the electrolyzer and the battery and the amount of electricity diverted to the grid are shown in Figure 3.

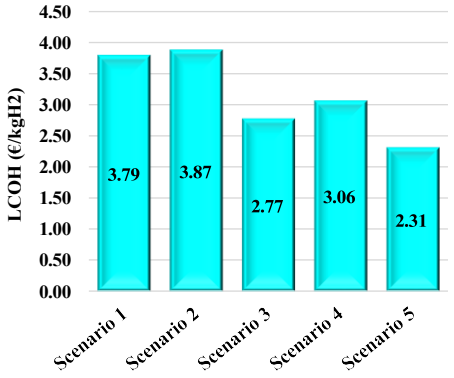


Figure 2- LCOH for each analyzed Scenario

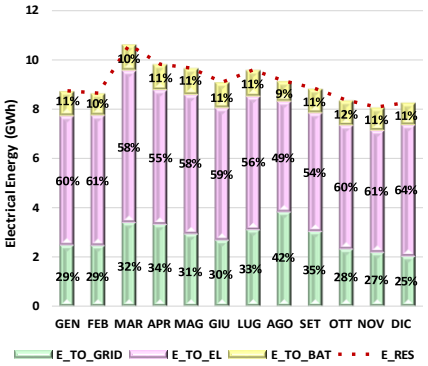


Figure 3- Electricity distribution

Conclusions: The system configuration that assures to cover the thermal annual demand of the steel plant with 10 % of H_2 while minimizing the LCOH (2.31 €/kg) is related to the Scenario 5, in which the power share between PV and Wind is 75% and 25%, respectively.

Acknowledgment

This research was funded by the European Union – NextGeneration EU from the Italian Ministry of Environment and Energy Security POR H2 AdP MMES/ENEA with involvement of CNR and RSE, PNRR - Mission 2, Component 2, Investment 3.5 "Ricerca e sviluppo sull'idrogeno", CUP: I83C22001170006.

References

[1] P.Marocco, M.Gandiglio, D.Audisio, M.Santarelli, *J Clean Prod*, 388, 2023, doi: 10.1016/j.jclepro.2023.135969

[2] A. Perna et al. "Designing, sizing and economic feasibility of a green hydrogen supply chain for maritime transportation," *Energy Convers Manag*, 278, 2023, doi: 10.1016/j.enconman.2023.116702.

European Fuel Cells and Hydrogen
PIERO LUNGHI CONFERENCE
September 17th–19th 2025
Capri / Italy

Hydrogen Valley Optimization: Integrating Sectoral Synergies for Decarbonization

Vincenzo Romano*[a], Paolo Marocco[a] , Marta Gandiglio[a], Massimo Santarelli [a]

* corresponding author: vincenzo.romano@polito.it

[a] Department of Energy, Politecnico di Torino, Corso Duca degli Abruzzi 24, 10129, Torino, Italy

Keywords: Hydrogen Valleys, Energy Hubs, MILP, PtX

Introduction:

This work explores integrated hydrogen-based energy hubs, commonly known as hydrogen valleys [1], through the development of a flexible and adaptable model. Designed to accurately represent these complex systems, the model is applicable across diverse case studies. Like most energy system models, its primary goal is to provide decision-makers with actionable insights for the design, deployment, and operation of hydrogen hubs. Its initial application focuses on a hydrogen valley under construction in Crete, developed within the EU-funded CRAVE-H2 project [2].

Objectives:

This work aims to bridge the gap in energy modelling literature by focusing on mid-scale energy hubs like hydrogen valleys, positioned between detailed component-scale and large-scale system models. Their smaller scope reduces computational demands, enabling greater component detail while optimizing multi-node, multi-vector energy flows.

The first step involves modelling the CRAVE-H2 hydrogen valley, leveraging the island's renewable potential to enhance its energy network and reduce reliance on mainland supplies. The model optimizes capacity planning and energy flow dispatch while assessing future expansion to additional demand sectors. Beyond this, the goal is to improve the replicability of hydrogen valley designs across diverse locations, maximizing cross-sector synergies.

Material and methods:

This work addresses the gap in energy modelling by focusing on mid-scale hydrogen valleys, balancing detail and computational efficiency in multi-node, multi-vector energy flows. The CRAVE-H2 hydrogen valley model, developed using PyPsa and SpineOpt, optimizes capacity planning and dispatch, leveraging the island's renewable potential to enhance its energy network and reduce reliance on mainland supplies.

The system supplies hydrogen and electricity for multiple applications, as depicted in Fig.1, including hydrogen buses, a touristic ship, grid balancing services, and cold-ironing at Heraklion port. Various CO_2 emission cap scenarios were explored, restricting grid electricity

use based on a national carbon intensity of 0.142 kgCO_2/kWh.

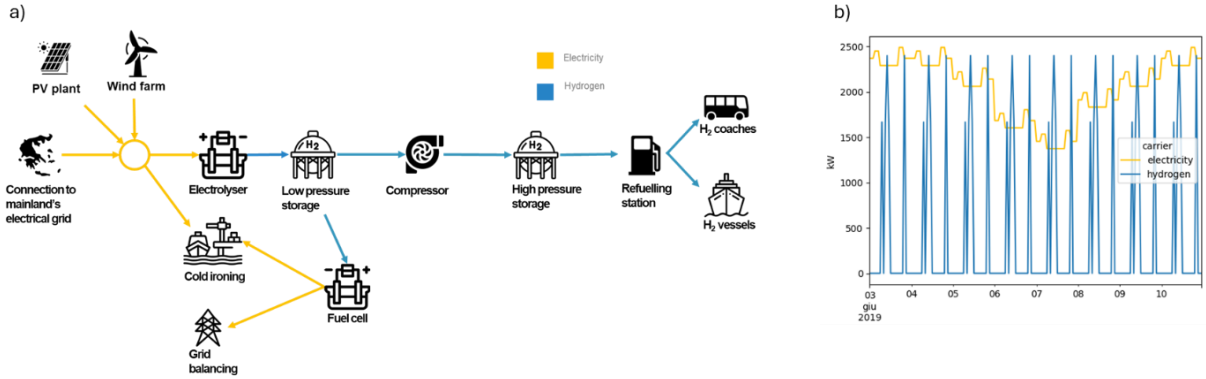
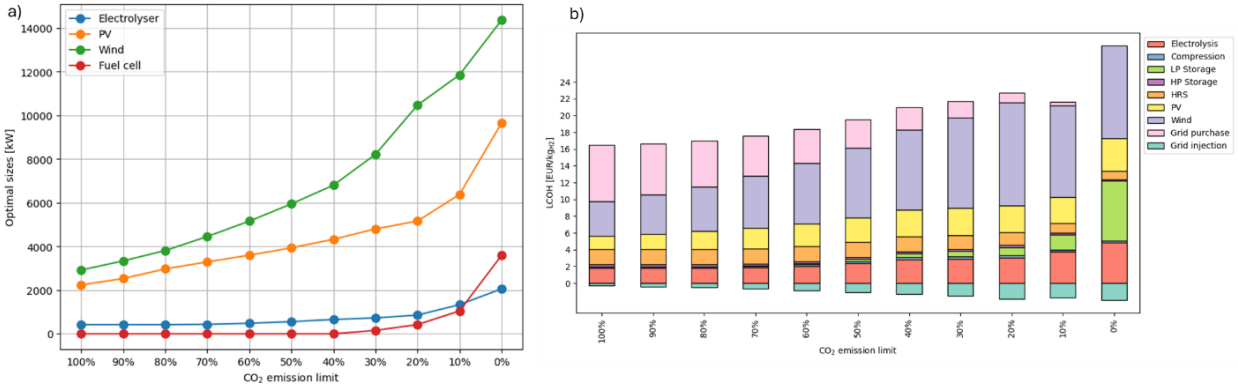


Figure 1: a) Scheme of the CRAVE-H2 valley. b) Weekly demand profile during touristic season.

Key performance indicators—LCOH, electrolyser utilization, renewable hydrogen share, and CO_2 savings—were analysed, alongside sensitivity studies on CO_2 limits and fuel cell electricity revenues to evaluate policy and incentive needs for hydrogen valley feasibility and expansion.

Results:

An initial simulation, run without emission limits, yielded 1.3 kt of CO_2 emissions. Of the total grid electricity consumed by the system, 34% was supplied to the electrolyser, resulting in 57% of its power input. This emission level served as a reference for the sensitivity analysis, where upper bounds on allowed emissions were progressively reduced by 10% until reaching



a zero-emission scenario.

Figure 2: Results from sensitivity analysis on total CO_2 emissions allowed by the system: a) Optimal components sizing. b) Levelized Cost of Hydrogen

As emission limits tighten, the model favours larger renewable generators, along with increased fuel cell and low-pressure storage capacity to support electric loads during shortages, driving up system costs (Fig. 2b). The electrolyser's cost impact remains moderate, while storage accounts for a significant share in low-emission scenarios. Notably, as emission

limits relax, storage costs decline and eventually vanish, as grid electricity replaces renewables, reducing fuel cell reliance to zero.

Conclusions:

When environmental constraints are not taken into account, the model relies on a large share of grid electricity for the supply of electrolyser and electric demands, as this results in substantial costs savings. In particular, the fuel cell remains unutilized when the system is allowed to cover the electric loads with energy from grid during renewable shortages. This reflects the needs for financial support through tariffs and incentives to exploit the great decarbonization potential of the valley while keeping it economically sustainable.

Further studies will have a focus on an in-depth look into aspects like transportation of the produced hydrogen and a more detailed interaction of the electrolyser and fuel cell system with the electric grid.

Acknowledgment

The project is supported by the Clean Hydrogen Partnership and its members (Project Crete Aegean H2 Valley, Grant Agreement No. 101112169).

References

[1] M. Bampaou and K. D. Panopoulos, “An overview of hydrogen valleys: Current status, challenges and their role in increased renewable energy penetration,” *Renewable and Sustainable Energy Reviews*, vol. 207, p. 114923, Jan. 2025, doi: 10.1016/J.RSER.2024.114923.

[2] CRAVE-H2, “CRAVE-H2 Project”, Accessed: Nov. 18, 2024. [Online]. Available: https://www.crave-h2.eu/

[3] D. Virah-Sawmy, F. J. Beck, and B. Sturmberg, “Ignore variability, overestimate hydrogen production – Quantifying the effects of electrolyzer efficiency curves on hydrogen production from renewable energy sources,” *Int J Hydrogen Energy*, vol. 72, pp. 49–59, Jun. 2024, doi: 10.1016/j.ijhydene.2024.05.360.

[4] P. Marocco, D. Ferrero, E. Martelli, M. Santarelli, and A. Lanzini, “An MILP approach for the optimal design of renewable battery-hydrogen energy systems for off-grid insular communities,” *Energy Convers Manag*, vol. 245, Oct. 2021, doi: 10.1016/j.enconman.2021.114564.

[5] E. Raheli, Y. Werner, and J. Kazempour, “A conic model for electrolyzer scheduling,” *Comput Chem Eng*, vol. 179, Nov. 2023, doi: 10.1016/j.compchemeng.2023.108450.

[6] “Electricity Maps.” Accessed: Mar. 12, 2025. [Online]. Available: https://app.electricitymaps.com/map/72h/hourly

EFCH2 2025
European Fuel Cells and Hydrogen
PIERO LUNGHI CONFERENCE
September 17th–19th 2025
Capri / Italy

Solar and wind energy integration with energy load and hydrogen production: the case of a large-scale airport in Italy

Gabriele Loreti*[a], Viviana Cigolotti [a], Navaid Ali [a], Giulia Monteleone [a], Martino Bosatra[b], Matteo Giampaolo[c], Leonardo M. Triaca[d] , Federica J. Giura[d], Stefano Terenziani[d]

* corresponding author: gabriele.loreti@enea.it

[a] Department of Energy Technologies and Renewable Sources (TERIN), ENEA C.R. Casaccia, 000123 Rome, Italy

[b] Maintenance Department, SEA Milan Airports, Milan Malpensa airport, Italy

[c] Environment and Funded Initiatives Department, SEA Milan Airports, Milan Malpensa airport, Italy

[d] ENAC, National Civil Aviation Authority, Rome 00185, Italy

Keywords: hydrogen production in airports, levelized cost of hydrogen, renewable energy sources integration, zero-emission hydrogen

Abstract

Airports are promising environments where hydrogen technologies have high unexpressed potential. In fact, in the same confined place there are many possible hydrogen off-takers (buildings, terrestrial vehicles, and planes) together with potential renewable energy production plants. Also, some preferential regulation patterns can be implemented in such places. The aim of this work is to quantify the Levelized Cost of Hydrogen (LCOH) of a local hydrogen production using excess Renewable Energy Sources (RES) with respect to the energy needs of the Milan Malpensa Italian airport. The LCOH is then compared with that attainable using a dedicated RES plant for hydrogen production. The comparison shows that the combined energy and hydrogen production in the airport reaches a lower overall cost for energy sourcing and hydrogen production, while having a LCOH slightly higher.

Introduction:

The production of hydrogen from renewable energy sources is a key factor to decarbonize industrial processes, heavy-duty transportation, and aviation. However, such process must be economically sustainable and several studies [1, 2] have quantified the LCOH when using dedicated renewable plants to hydrogen production. Literature results show that using optimal design ratios between renewable power and electrolyzer power, LCOH as low as 5 €/kg [1, 2] can be reached in Italy. However, there is a literature gap regarding the usage a renewable energy sources to sastisfy the energy loads of an airport and to also produce hydrogen.

Objectives:

The objective of the study is to quantify the economic viability of hydrogen production fed by a renewable energy source plant that primarily also serves the energy needs of an airport.

Material and methods:

All the components of the system are modelled with a lumped parameter approach. Yearly wind and photovoltaic are considered (Figure 1) for the average Italian scenario [3,4]. The electrolyzer is alkaline type with: minimum set-point 25% of maximum, maximum stand-by time 24h, specific consumption 51.9 kWh/kg H_2. We analyze five different scenarios with variable renewables composition photovoltaic-wind: 100%-0%; 75%-25%; 50%-50%; 25%-75%; 0%-100%

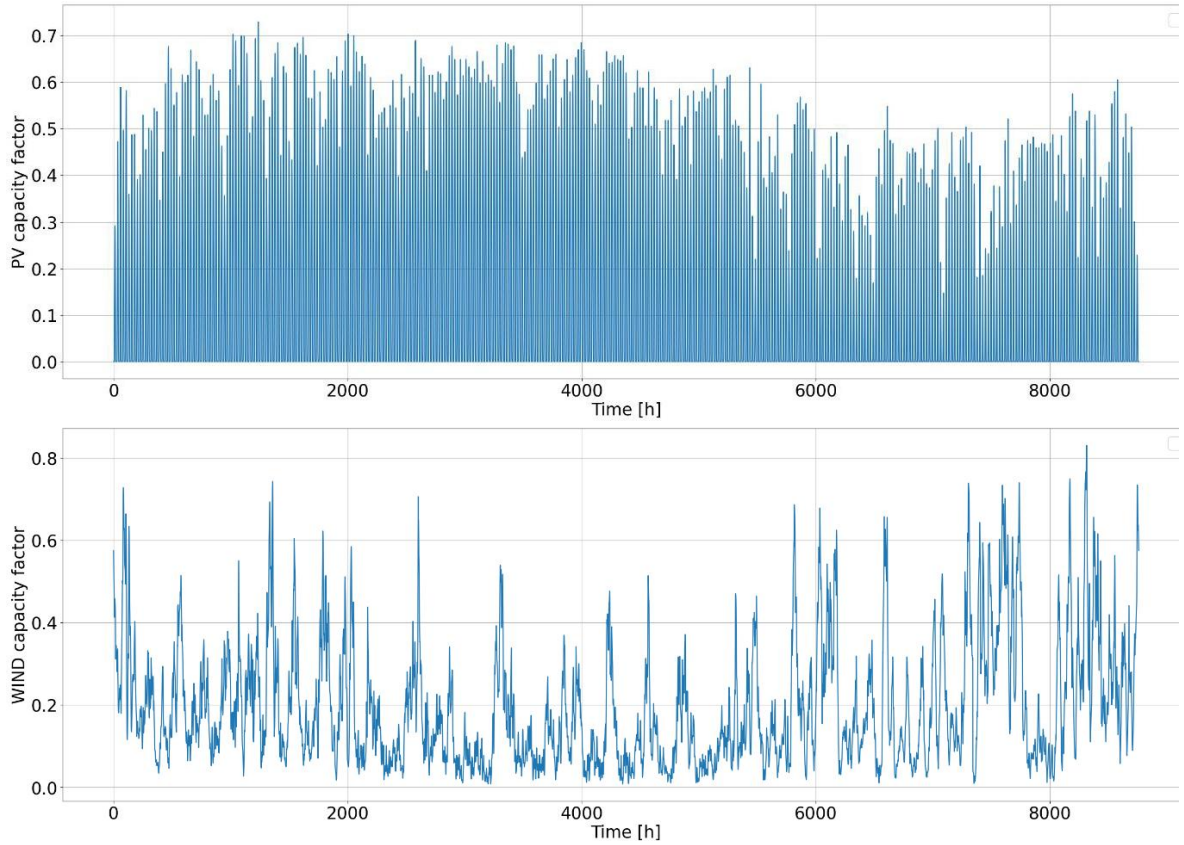


Figure 1: photvoltaic and wind capacity factors assumed on a yearly basis.

Results:

Results show that LCOH as low as 7 €/kg can be obtained when using the renewable energy to satisfy the energy requirements of the airport with priority to hydrogen production (Figure 2).

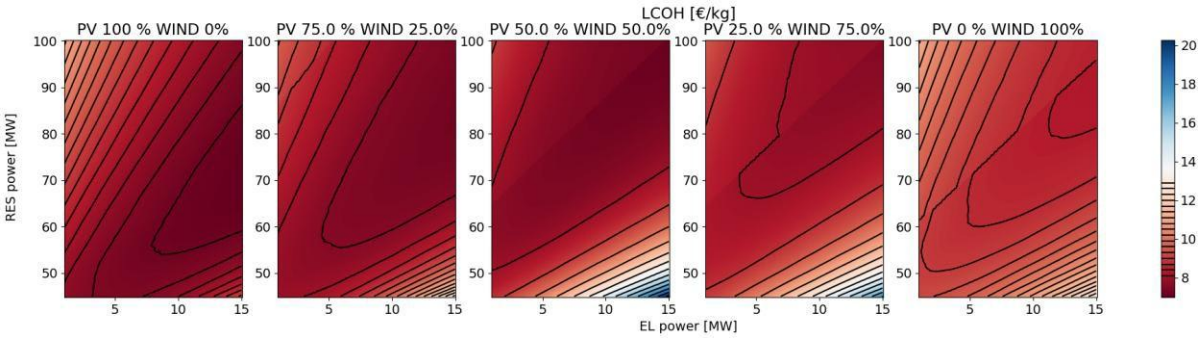


Figure 2: Levelized Cost of Hydrogen using renewable energy sources to satisfy energy loads of the airport and to produce hydrogen.

LCOH shows an optimal ratio between RES total power and electrolyzer power around 5 and such ratio is different from results in literature for dedicated system. Also, it seems that optimal RES mix is with higher PV composition. Finally, we note that the overall energy expenditure is lower when using the renewable plant for energy and hydrogen production

Conclusions:

The work shows that hydrogen production with renewable power production plants used also to satisfy energy loads of airports has a huge untapped potential that can help the diffusion of hydrogen technology in the transportation sector.

Acknowledgment

This work has been supported by the SAVES (Sustainable Aviation Vectors for Energy tranSition) project, founded by the Italian National Civil Aviation Authority (ENAC).

References

[1] Marocco, P., Gandiglio, M., Cianella, R., Capra, M., & Santarelli, M. (2024). Design of hydrogen production systems powered by solar and wind energy: an insight into the optimal size ratios. Energy Conversion and Management, 314, 118646.

[2] Franco, A., Carcasci, C., Ademollo, A., Calabrese, M., & Giovannini, C. (2025). Integrated Plant Design for Green Hydrogen Production and Power Generation in Photovoltaic Systems: Balancing Electrolyzer Sizing and Storage. Hydrogen, 6(1), 7.

[3] Pfenninger, Stefan and Staffell, Iain (2016). Long-term patterns of European PV output using 30 years of validated hourly reanalysis and satellite data. Energy 114, pp. 1251-1265. doi: 10.1016/j.energy.2016.08.060

[4] Staffell, Iain and Pfenninger, Stefan (2016). Using Bias-Corrected Reanalysis to Simulate Current and Future Wind Power Output. Energy 114, pp. 1224-1239. doi: 10.1016/j.energy.2016.08.068

European Fuel Cells and Hydrogen
PIERO LUNGHI CONFERENCE
September 17th–19th 2025
Capri / Italy

Impact of Subsidies on Hydrogen Refuelling Station Infrastructure Development

Muhammad Atif Mahmood*[a,b], Nicola Massarotti [a], Carlos Sanchez-Diaz[b], Laura Vanoli [a]

* corresponding author: muhammadatif.mahmood001@studenti.uniparthenope.it

[a] Department of Engineering, University of Naples "Parthenope", Centro Direzionale, Isola C4, 80143, Italy

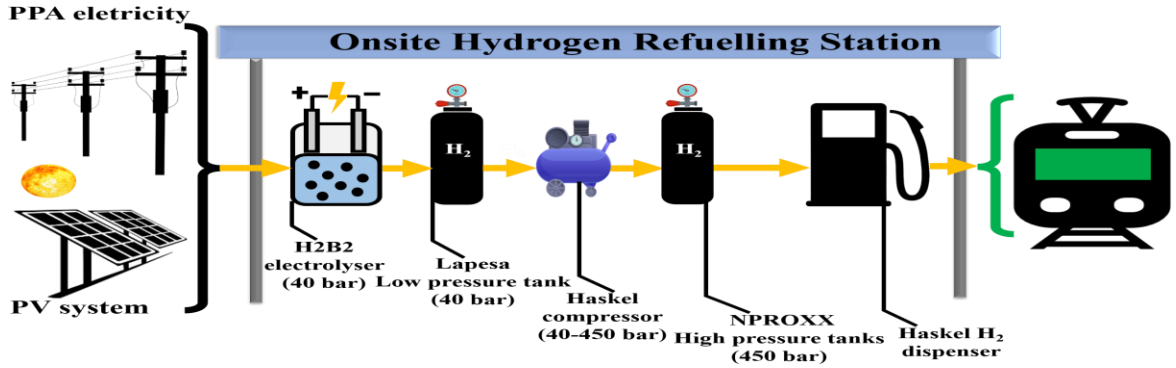
[b] Institute for Energy Engineering, Universitat Polit`ecnica de Val`encia, Camino de Vera s/n, 46022, Valencia, Spain

Keywords: Green hydrogen, Hydrogen Refuelling Station, Railway tram, Subsidies

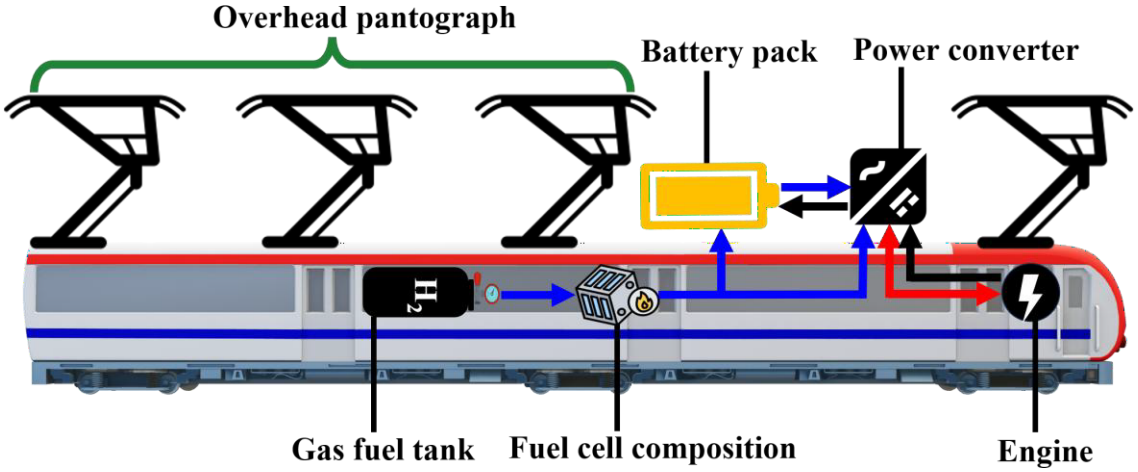
Abstract

Introduction: With global urgency in tackling environmental issues caused by enormous fossil fuel utilization, many countries positioning themselves to achieve climate neutrality goals through the ongoing EU 2050 decarbonization campaign. Reaching this target demands a paradigm energy shift favoring Renewable Energy Sources (RESs) throughout all economic sectors, especially for the transporting sector enabling renewable hydrogen fuel to light/heavy-duty vehicles (e.g., cars and trucks). The transportation sector relies heavily on fossil fuels, contributing 24% of CO_2 emissions from the energy sector [1]. Thus, this sector needs sustainability initiatives to promote modal shifts towards low-carbon traveling possibilities and lessen all existing transport modes' carbon intensity by properly considering technical and operational energy efficiency measures [1]. Developing RESs-powered Hydrogen Refuelling Station (HRS) infrastructure and distribution networks can boost hydrogen-fueled mobility [2], improving energy security, and advancing the future hydrogen industry for a greener future. This work economically evaluates RESs fed HRS to deliver 160.68 kgH_2/day to the Spanish heavy-duty railway tram running between the Benidorm-Denia route located in Alicante Province. After including various government subsidy values, final hydrogen cost is predicted to critically examine the economic viablity of proposed HRS facility.
Objectives: The study's primary objective is to perform a brief financial assessment of solar energy-powered onsite HRS by properly sizing components and considering all technical, economical aspects, and operational costs aimed at determining the end H_2 production cost for various Spanish subsidy values for empowering green hydrogen energy systems.
Material and methods: This economic study incorporated a 2.8 MW_P PV system for onsite electricity production along with a 515 kW capacity H2B2-EL100 N PEM electrolyzer to satisfy train fuelling needs (4 refuellings windows per day) of 160.68 kgH_2/day requiring 40.17 kgH_2 in single tank filling during 6:00 A.M. to 9:00 P.M. (train actual daily fuel requirements: 35.97 kgH_2 x 4 = 143.88 kgH_2) [1] running operation. The considered electrolyzer will produce 10.04 kgH_2/h at 40 bar and will be working 18 hours daily [1]. The necessary components for the

proposed HRS are shown in Fig. 1a. A Power Purchase Agreement (PPA) for buying green electricity at 65 €/MWh is made with the Spanish national grid for an uninterrupted power supply to the HRS facility. A schematic of a hybrid train propelled by H_2 fuel from RESs along a catenary system taking power from PPA contracts is shown in Fig. 2b.



(a)



(b)

Fig. 1. (a) HRS equipment configuration. (b) Schematic of H2 train.

Results: The equipment configuration in Fig. 1a was used to calculate green H_2 cost by considering subsidized financial costs alongside installation investments for Spain in HRS facilities. The Bank of Spain and the National Statistics Institute provided market discount rates (1.65%), interest rates (2.20%), and inflation rates (10.20%) for capital loan financial calculations. Employing financial costs in the HRS capital investment, an 80% loan is requested over 15 years (the useful life of components) leaving 20% assumed by the investor. As depicted in Fig. 2a, financial costs contribution to onsite HRS overall capital investment is 234,645 €, up 4.17% from 5,621,828 € in the base case scenario to 5,856,473 € in the present financial evaluation. Fig. 2b illustrates HRS costs over a 15-year lifespan with or without surplus energy sale income. Total cost varies from 5,634,656 € with 0% subsidies to 3,292,067 € with 40% subsidies, a difference of 2,342,589 € (58.42%) without subsidies. Hence, ensuring participation and dependence on government subsidies is vital, as they largely amortize

facility costs. Base case computed H_2 cost without considering excess energy sale revenue is 6.16 €/kgH_2; meanwhile, financial case cost adding said cost and without subsidies results in 6.43€/kgH_2 showing a difference of 0.27/€ kgH_2 or an increase of 4.19%.

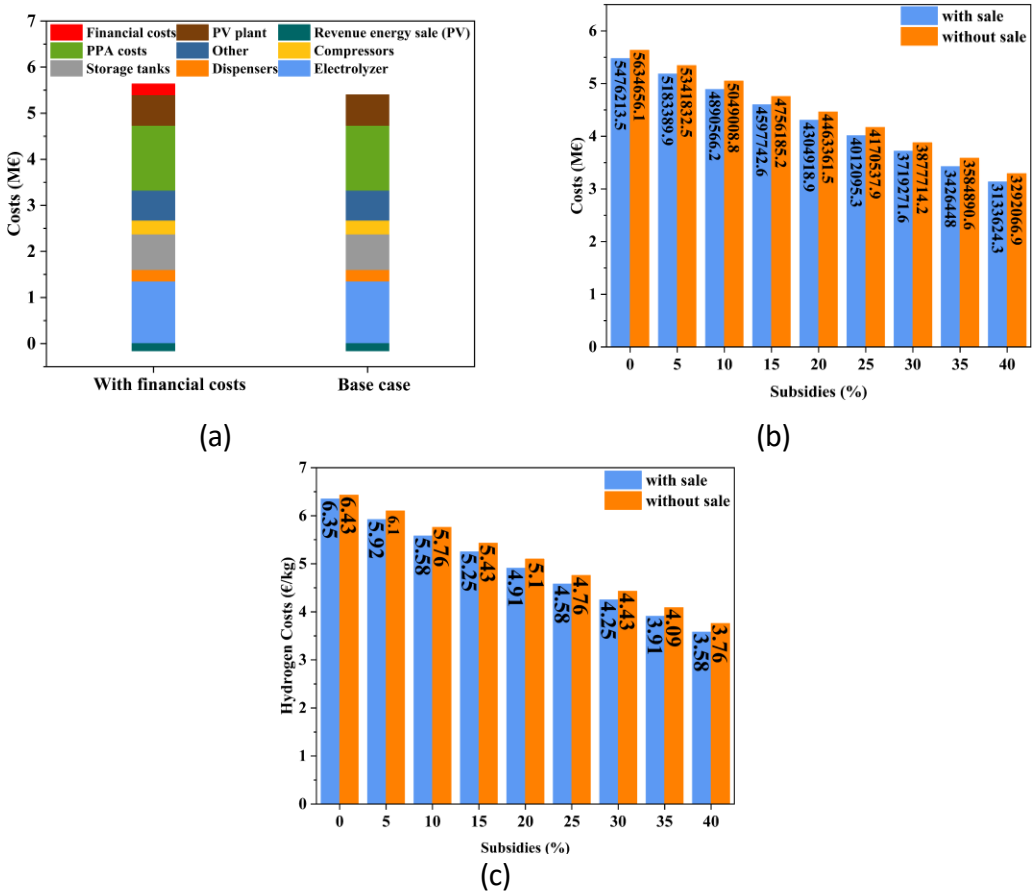


***Fig. 2**. (a) Economic analysis vs. base case investment breakdown. (b) Total costs after adding various subsidies value for economic analysis. (c) Final H_2 cost for various subsidies value.*

Conclusions: The financial analysis considering added Spanish subsidy values (0% to 40%) to the HRS facility results in end H_2 costs of 6.43 €/kg to 3.76 €/kg indicating subsidy funds provided by the government are essential to make green hydrogen technologies and infrastructure commercially competitive.

Acknowledgment

Work funded by Universitat Politècnica de València & Parthenope University of Naples.

References

[1] M. A. Mahmood, P. P. de la Calle, J. M. M. Zuluaga, N. Massarotti, and C. Sanchez-Diaz, "Techno-economic evaluation of hydrogen refuelling station with on-site electrolysis production powered by photovoltaic solar energy for the railway sector," International Journal of Hydrogen Energy, vol. 138, pp. 802-822, 2025.

[2] P. Zúñiga-Saiz, and C. Sánchez-Díaz, "Design of a Hydrogen Refueling Station with hydrogen production by electrolysis, storage and dispensing for a bus fleet in the city of Valencia," International Journal of Hydrogen Energy, vol. 104, pp. 651-664, 2025.

European Fuel Cells and Hydrogen
PIERO LUNGHI CONFERENCE
September 17th–19th 2025
Capri / Italy

Hydrogen Integration in Commercial Aviation: Technical and Operational Analysis at Malpensa Airport

A. Altomonte*[a], A.Piccolo [a], S. Di Micco [a], M.Minutillo [c], V. Cigolotti[b], E. Jannelli [a]

* corresponding author: andrea.altomonte@atenaweb.com
[a] University of Naples "Parthenope", Naples, Italy
[b] ENEA - Italian National Agency for New Technologies, Energy and Sustainable Economic Development, Naples, Italy
[c] Department of Industrial Engineering, University of Salerno, Fisciano, Italy

Keywords: Aviation decarbonization, Green Airways, Hydrogen, Sustainable airport

Abstract

The decarbonization of the aviation sector has become a central objective within global climate policies. Among the alternative energy carriers under evaluation, liquid hydrogen stands out as a promising solution for enabling zero-emission flight, particularly in short and medium-haul operations. This study provides a preliminary evaluation of hydrogen integration at one of Europe's busiest airports, that is Milano Malpensa airport. A dedicated simulation tool is developed for estimating liquid hydrogen requirements across different flight categories, taking into account the airport-level traffic data. A case study, referred to a short haul route is considered. Results addressing key aspects such as the operational feasibility and overall hydrogen demand, emphasizing the opportunities with the introduction of hydrogen-powered aviation in real operational settings.

Introduction

The aviation sector is under increasing pressure to transition toward sustainable energy carriers. Among the viable alternatives, liquid hydrogen has attracted growing interest due to its high energy content per unit mass and carbon-free combustion. However, the shift to hydrogen requires not only technological adaptation at the aircraft level but also robust planning at the airport infrastructure scale [1]. Milan Malpensa Airport has been identified as a relevant case study for evaluating hydrogen integration scenarios. Its diverse network of domestic, regional, and intercontinental routes enables detailed hydrogen demand estimates by flight segment: short, medium, and long-haul, supporting infrastructure design and strategic planning.

Objectives

This study aims at evaluating the operational feasibility of using liquid hydrogen as an alternative fuel for commercial aviation, focusing on short-haul operations. A representative flight of a conventional narrow-body aircraft is analysed to assess the impact of replacing kerosene with liquid hydrogen. In this purpose, a computational tool developed within the ALRIGH2T project is presented [2]. It is devoted at characterizing the Milano Malpensa traffic data in terms of number of most common operating aircrafts and of most common performed routes, with the aim of calculating for each of them the amount of hydrogen needed for replacing the kerosene.

Materials and Methods

To estimate the hydrogen amount needed to support all commercial departures, a structured algorithmic framework was developed.

This framework integrates detailed operational data and performs energy balance calculations to quantify hydrogen demand with high accuracy. Core variables include route distance, aircraft type, flight frequency, and passenger load, enabling a refined classification of hydrogen needs across short, medium, and long-haul operations. The process starts with the selection of representative aircraft models; each associated with specific fuel types and performance characteristics.

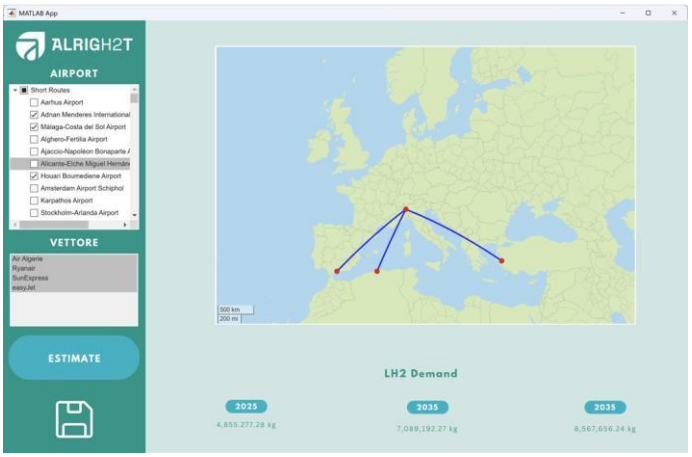


Figure 1: Developed Tool

Based on flight duration and distance, the algorithm calculates fuel consumption per segment. This data-driven, multi-variable methodology ensures a comprehensive and precise estimation of airport-wide liquid hydrogen demand, supporting strategic infrastructure design and optimal resource planning. Fig.1 shows an overview of the developed tool.

Results

Considering the potentiality of the developed tool, a specific case study has been selected. Table 1 summarized the aircraft type and the characteristics of its travelled common route.

Data	Value
Type of aircraft	Boeing 737-800
Rout Category	Short Houl
Distance [km]	1151

Distance [nm]	622
Travel Duration [hours]	1.51
Kerosene specific consumption [kg/km]	3.45
Kerosene total consumption [tons]	3.97

Table 1: Milano Malpensa - Madrid route Details

For the selected route, it is calculated a consumption of about 3.97 tons of Jet A1 fuel per flight, corresponding to an energy use of roughly 170.000 MJ. In the hypothesis of covering this energy requirement with hydrogen, about 1.41 tons of H_2 are needed. This represents a substantial reduction in fuel mass compared to kerosene, which has important implications for aircraft weight and fuel storage design. For context, similar calculations for other aircraft in the regional fleet, such as the Airbus A320 and the Airbus A321 neo, yield fuel consumption rates of 2.91 kg/km and 3.47 kg/km respectively, reinforcing the variability in demand depending on aircraft type and efficiency. However, the characteristics of the hydrogen storage technologies are fundamental issues to be taken into account since they can affect significantly the weigh and the volume of the hydrogen to be stored on board.

Conclusions

Aligning factors such as route types, flight frequency, and operational logistics to enable large-scale are fundamental parameters to consider for the adoption of hydrogen propulsion in airway sector. The developed analysis demonstrates the feasibility and benefits of hydrogen as an alternative fuel, while highlighting the need to address challenges related to liquid hydrogen storage and integration in existing aircraft configurations.

Acknowledgment

Funded by the European Union under grant agreement No 101138105. Views and opinions expressed are however those of the author(s) only and do not necessarily reflect those of the European Union (EU) or European Climate, Infrastructure and Environment Executive Agency (CINEA). Neither the EU nor CINEA can be held responsible for them.

References

[1] Oesingmann, K., Grimme, W., & Scheelhaase, J. (2024). Hydrogen in aviation: A simulation of demand, price dynamics, and CO2 emission reduction potentials. International Journal of Hydrogen Energy, 64, 633-642.
[2] alrigh2t.eu

European Fuel Cells and Hydrogen
PIERO LUNGHI CONFERENCE
September 17th–19th 2025
Capri / Italy

Experimental Evaluation of P2P for Long Duration Energy Storage

Bobby Laviguer[a*], Robert Flores [a], Jacob (Jack) Brouwer[a]

*corresponding author: Bobby Laviguer
[a] University of California, Irvine

Keywords: alkaline electrolyzer, dynamics, gaseous storage, PEM fuel cell

Abstract

Hydrogen based P2P systems enable long duration energy storage for meeting peak demand. This work evaluates an experimental P2P system of commercially available equipment, integrated and installed for evaluation at the University of California, Irvine. The P2P system features a 75 kW alkaline electrolyzer (AEC) system, compressor, storage system, 50 kW proton exchange membrane fuel cell (PEMFC) system, and balance of plant. Initial results and operational challenges focus on the AEC. Outcomes of this work include translating lessons learned from operation of a commercial AEC and verifying the dynamic capabilities from a systems perspective. Initially collected benchmarking tests of the system provide baseline data to compare against dynamic results including critical parameters of a P2P system like energy intensity and efficiencies.

Introduction

The P2P concept is still an emerging idea but continues to become more commercially viable as experimental systems are deployed. P2P is electrical energy storage where the principal steps are electrical energy generation, conversion of that electrical energy to hydrogen via water electrolysis, the storage of the produced hydrogen for a later time, and then reconversion of the stored hydrogen into electrical energy. Possible reconversion methods of the hydrogen include direct conversion back into electricity via stationary or vehicle fuel cells and the indirect conversion via hydrogen fired gas turbines. One application for P2P systems is meeting peak energy demand via long duration energy storage. The UC Irvine P2P system uses the commercially available equipment, detailed below in Table 1, which are referred to as subsystems in this work.

Table 1. Equipment specifications

Equipment	Specifications
AEC	Teledyne Energy Systems (TESI) HMXT-200 AEC rated for 1 kg/hr of 99.9998% H_2 at 150 psig
Electrolyzer and compressor chiller	Thermal Care NQA13 has cooling capacity of 55 kW with COP of 3.12

Hydrogen compressor	PDC-3-1250/7500 hydrogen compressor with a discharge pressure 350 bar
Hydrogen storage	Steelhead Composites Type 3 high pressure tanks with total capacity of 18 kg
PEMFC	Toyota GEN1 PEMFC has maximum continuous output power of 50 kW with a H_2 consumption rate of about 3.25 kg/hr
Fuel cell chiller	Thermal Care NQA25 has cooling capacity of 90 kW with COP of 2.8

Objectives

1. Integrate all P2P subsystems.
2. Complete individual sustained part load characterization of the AEC and PEMFC subsystem. This includes operation at steady-state and cold-hot start-up.
3. Experimentally evaluate the capability of the AEC to follow solar and wind energy resources.
4. Test the PEMFC dynamic response capabilities when operated to compliment renewable generators.

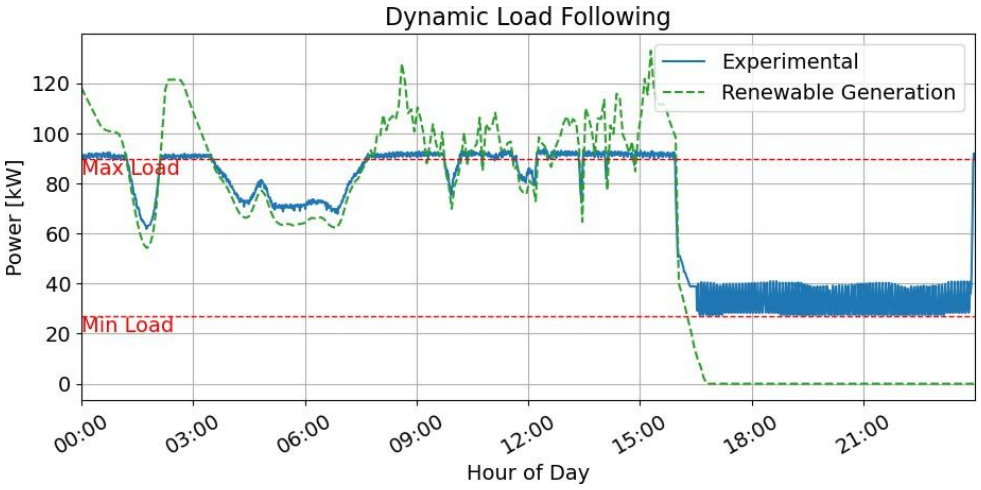
Material and methods

The two main areas of focus are the operation of the TESI HMXT-200 AEC and the Toyota GEN1 Mirai stationary PEMFC. AEC and PEMFC testing included full and part load system characterization, cold and hot start, and dynamic operation by changing the demanded production based on load following (electrolyzer) or load matching (fuel cell) of wind and solar profiles. Additionally, operation of the hydrogen compressor and storage tanks was conducted but with less formal structure because of their less significant impact on P2P system operations. Primary parameters of interest for each test scenario include power consumption/production of the whole subsystem, power consumption at each of the balance of plant (BoP) components, and the properties of fluids moving through system components.

Results

Operating Load	BoP Total Power [kW]	Stack Power [kW]	Power Supply Power [kW]	Chiller Power [kW]	Mains Power [kW]	Unbalanced Power [kW]
34.30%	1.85 (0.32)	20.25 (0.05)	24.05 (0.05)	10.26 (4.62)	35.22 (4.81)	0.91 (0.37)
50%	1.86 (0.32)	30.39 (0.48)	34.9 (0.39)	12.77 (1.36)	48.63 (1.52)	0.96 (0.34)

75%	1.87 (0.33)	48.81 (0.57)	54.5 (0.44)	12.84 (0.42)	68.24 (0.69)	0.91 (0.36)
100%	1.88 (0.33)	68.45 (0.34)	75.53 (0.29)	14.01 (0.73)	90.49 (0.96)	0.95 (0.36)



Conclusions

- Steady-state operation shows ambient temperature greatly affects chiller operation emphasizing the impact of temperature on seasonal energy storage at scale.
- Nominal operating parameters during steady-state operation include the following ranges
  - H_2 in O_2: 0.2 – 1.4%
  - DE-OX temperature: 40-85°C
  - Stack operating temperature: 60-65°C
- Cold start times to reach steady-state vary minimally between 11 and 13 minutes for minimum and maximum production rates, respectively.
- Cold-hot start times to reach steady-state for maximum production are equal because of the heat produced during ramping.
- The gas control system can sufficiently handle ramping of the emulated profile.

European Fuel Cells and Hydrogen
PIERO LUNGHI CONFERENCE
September 17th–19th 2025
Capri / Italy

Effect of hydrogen blending on odorant measurement

G. Cortellessa *[a], F. Arpino [a], M. Dell'Isola [a], G. Ficco [a], G. Grossi [a], V. Cigolotti [b], A. De Marco [b], P. Gislon [b], G. Monteleone [b], C. Imboccioli [c], A. Longato [c], D. Rossi [c]

* corresponding author: Gino Cortellessa g.cortellessa@unicas.it
[a] DICEM, University of Cassino and Southern Lazio, Cassino, Italy
[b] Department of Energy Technologies and Renewable Sources, ENEA Casaccia, Italy
[c] Pietro Fiorentini Spa, Via Enrico Fermi, 8/10 - 36057 Arcugnano (VI)

Keywords: odorization; accuracy, natural gas, gas chromatograph, hydrogen blending

Abstract

Blending hydrogen into natural gas networks offers a promising strategy to reduce carbon emissions, utilizing existing infrastructure without major modifications. However, this practice poses technical challenges, since hydrogen injection into natural gas changes the gas physical properties, potentially affecting odorant efficiency and the reliability of measurement devices. This requires careful selection of appropriate odorants, as some may react with hydrogen, influencing the mixture's properties [1, 2]. One key issue is maintaining reliable odorization, as both hydrogen and natural gas are odorless and colorless, making the detection of leaks essential for safety.

Introduction

In Italy, sulphur compounds like tetrahydrothiophene (THT) and mercaptans (such as ethyl mercaptan and tert-butyl mercaptan, TBM) are used to add a penetrating odor to natural gas, ensuring its detectability. While THT and TBM do not react with hydrogen and are thought to be effective for hydrogen-natural gas mixtures, the characteristics of these odorants and their concentrations are critical. UNI 7133-2 standard sets criteria for odorizing natural gas and methods for measuring odorant concentrations, ensuring that sufficient odor intensity is maintained. In addition to traditional gas chromatographic methods, new technologies like portable gas chromatography (GC) systems have emerged, allowing for field-based, rapid analysis of gas mixtures [3]. However, no studies are available in the literature on the reliability of the measuring system of odorant concentration when a NG-H_2 blend is delivered. In fact, as hydrogen concentrations increase, adjusting the odorant injection strategy may be necessary to maintain effective leak detection and cost efficiency.

Objectives

Recent studies suggest that odorants, such as THT and TBM, can be used effectively for natural gas and hydrogen mixtures without significant issues. Experimental results have shown that conventional odorant concentrations can be maintained even with hydrogen levels of up to 20%. Nevertheless, higher hydrogen concentrations may require adjustments. Therefore, this study addresses the gap in literature by investigating the reliability of odorant concentration measurement systems in hydrogen-blended gases and emphasizing the importance of accurate odorant measurement to maintain safety and minimize costs. The

study uses both laboratory and field experiments to assess odorant measurement systems, providing valuable insights for future network integration.

Material and Methods

The reliability of odorant measurement systems with hydrogen blends has been investigated at the Pietro Fiorentini Gas Chromatographic Analysis Laboratory [4], by using certified cylinders with methane-hydrogen blends and odorized natural gas from the city network. To this aim a two-phase experimental campaign was performed.

The first phase involved tests on certified cylinders at three odorant concentration levels (5, 30, and 100 mg/Sm^3) using both THT and TBM in three gas mixtures: 100% methane, 100% hydrogen, and a 20% hydrogen and 80% methane mixture. Tests with 100% methane served to validate the measuring process, with results compared to certified reference values provided by SIAD, an accredited laboratory. In Fig.1a the sketch of the test layout is reported. The second phase was carried out at the Hydrogen Innovation Lab of Pietro Fiorentini Spa (see Fig. 1b), where odorized natural gas (with THT) from the city distribution network is mixed with pure hydrogen produced on-site. The natural gas is pressurized to 5 bar and injected into a gas blender along with pure hydrogen at 2 bar. The odorant concentration of the produced mixtures with 5% and 20% hydrogen was measured downstream of the blending unit.

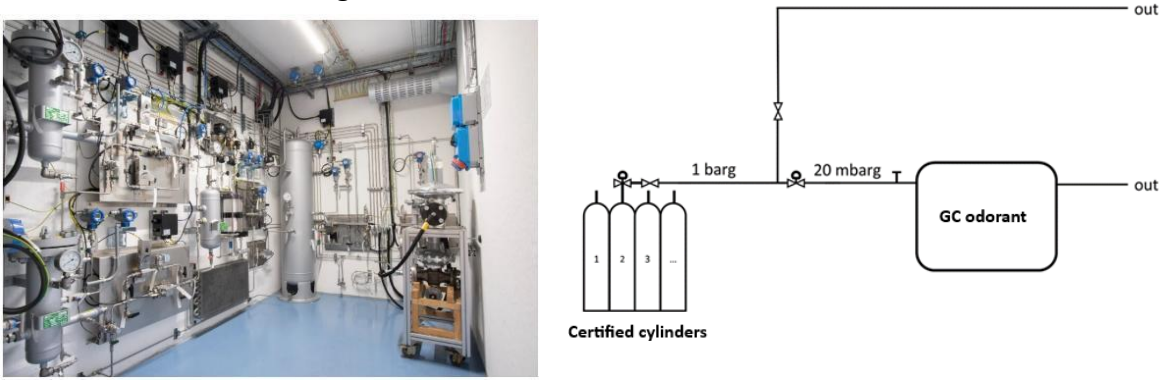


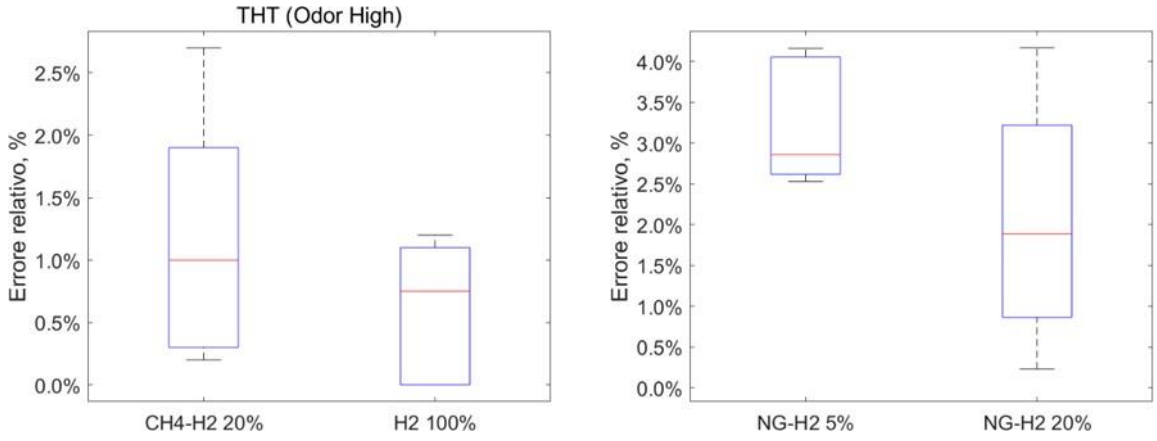
Figure 1: a) test layout for certified cylinders, b) Hydrogen Innovation Lab of Pietro Fiorentini

The relative error ($E_{\%}$) was calculated as the difference between the indication of the GC and the certified reference value. For tests with natural gas from the gas grid, however, since a certified reference value was not available, an expected reference value was estimated. To this aim, the mean measured values were used to derive a linearization function to obtain a $C_{GN,i}$ value interpolated at the exact time of measurement on the NG-H_2 mix. Consequently, the expected reference value C_{ref} of the THT concentration is estimated starting from the H_2%vol hydrogen content measured in the mixture.

Results

In Fig.2 the results of the tests have been reported in terms of box plot of the

measured relative error. For tests with 20% Hydrogen in CH_4-H_2 blend with THT, there was a tendency to overestimate the concentration at medium ($E_{\%}$=2.3%) and high concentrations ($E_{\%}$=1.2%), whereas for TBM no significant issues were observed at any of the tested concentrations, aswell as for THT at low concentrations. Finally, tests with 100% Hydrogen highlighted all positive errors generally within 0.6%, except for TBM at low concentration, where an error of $E_{\%}$= -3.4% was observed. Overall, the errors were consistent with the GC class 0.5 specifications, except for TBM at low concentration. Also, the normalized errors (E_n) were very low, ranging from 0.3 for TBM to 0.4 for THT, demonstrating the high reliability of the odorant concentration measurements even with hydrogen blends or pure hydrogen.



a) b)

Figure 2: a) Results for tests on certified cylinders, b) Results for tests on odorized gas

Conclusions

The results of tests indicated a tendency to overestimate the odorant concentration in both the 5% ($E_{\%}$=3.2%) and 20% hydrogen ($E_{\%}$=2.0%) blending concentrations. This overestimation was consistent with the data of the certified cylinder with 20% hydrogen mixture, demonstrating the reliability of the methodology used. However, overestimation of odorant concentration could pose potential risks, such as inadequate leak detection or unnecessary costs due to maintaining odorant levels higher than required.

Acknowledgements

This work was funded by the Italian Ministry of Environment and Energy Security through Ricerca di Sistema Elettrico Nazionale (RdS), programme 2022-2024 Integrated project 1.3: Hydrogen Technologies, GRANT number I53C22003020001.

References

[1] Dell'Isola, M.; Ficco, G.; Moretti, L.; Jaworski, J.; Kułaga, P.; Kukulska–Zaja¸c, E. Impact of Hydrogen Injection on Natural Gas Measurement. Energies 2021, 14, 8461.

[2] F. Arpino et al., Green hydrogen for energy storage and natural gas system decarbonization: An Italian case study. International Journal of Hydrogen Energy Volume 49,

Part D, 2 January 2024, Pages 586-600
[3] Huszal A., Jaworski J., Studies on the Impact of Hydrogen on the Results of THT Measurement Devices, Energies 2022, 15(1), 221; https://doi.org/10.3390/en15010221;
[4] https://www.fiorentini.com/en/about-us/expertise/hydrogen/pietro-fiorentinis- hydrogen-innovation-lab/, last accessed 2024-12-30

European Fuel Cells and Hydrogen
PIERO LUNGHI CONFERENCE
September 17th–19th 2025
Capri / Italy

Potential of retrofitting mgts to h2 and nh3: from combustion fundamentals to a techno economic prospective

Marcelo C. Rosário*[a], Ailton D. Gonçalves[a], Luciano Bueno[a], Shubham Das[a], Elena Surra[a], André Fonseca[b], Edgar C. Fernandes[a,c], Guilherme Gaspar[a]

*corresponding author: marcelo.rosario@hylab.pt
[a] HyLab - Green Hydrogen Collaborative Laboratory, Portugal
[b] Galp Energia SA., Portugal
[c] Instituto Superior Técnico - Universidade de Lisboa, Portugal

Keywords: Ammonia, Combustion Systems, Decarbonization, Hydrogen

Abstract:

Decarbonizing micro gas turbines (MGTs) through retrofitting strategies is essential for a cleaner and more reliable electrical grid system. This work surveys fuel fundamental aspects to converge towards guidelines to retrofit critical parts of such systems. By using a Capstone C30 MGT as a case study, simulations calibrated with experimental boundary conditions showed that the operation of the original injector and combustion chamber can be used with natural gas (NG) and hydrogen (H_2). However, it is limited to 25%/75% NG/H_2 whereas new design and fuel control strategies are needed. Sensitivity analysis to techno economic metrics is performed to show its viability for several operating combinations, namely H_2-NH_3 blends.

Introduction: Amid accelerating climate change and global targets like the Paris Agreement and the European Green Deal, forces the energy sector to rapidly shift toward decarbonization. MGTs are used in distributed generation and industry; however, they have a considerable carbon footprint due to the use of fossil fuels. Retrofitting MGTs to run on alternative fuels like H_2 and NH_3 offers a promising but complex path. Hydrogen enables low-emission combustion with its high flame speed, while ammonia, the world's second most used chemical, is a dense hydrogen carrier that's easier to store and transport. However, grey hydrogen and conventional ammonia are carbon intensive. Green hydrogen and green ammonia produced via renewable-powered electrolysis and cleaner Haber-Bosch processes can eliminate associated CO_2 emissions [1]. Hydrogen's appeal in power systems has grown, with MGTs emerging as compact, fuel-flexible options. Yet, hydrogen's high flame speed and combustion temperature increase risks like flashback and NO_x emissions, demanding system redesigns and advanced control [2]. Beyond technical aspects, economic viability hinges on

capital costs, fuel pricing, electricity market value, O&M expenses, and carbon pricing. Optimization models are needed to ensure a competitive return on investment.

Objectives: The goal is to demonstrate the viability of retrofitting a Capstone C30 MGT (30 kWe) installed at the combustion lab. It aims to enable the use of H_2 and NH_3 and their blends while controlling gas emissions. The focus of the retrofitting is the fuel injector, as it is a removable part of the burning system while it minimises the retrofit costs as soon as the design is in line with combustion fundamentals. A literature review of economic indicators is conducted to identify the most suitable metrics for evaluating the retrofit's feasibility and its outcomes, and for comparison with conventional MGT operation.

Material and methods: To perform the retrofitting, important combustion parameters were taken into consideration: Flammability limits, as CH_4 and NH_3 don't superimpose; energy density of the fuel, as for H_2 and NH_3 flowrate must be 3.3 and 2.5 times higher than natural gas, and its flame speed, to avoid flashback and blowoff (SL (m/s): CH_4=0.43, H_2=2.75, NH_3=0.07). CFD simulations were also performed with Ansys Fluent to evaluate the impact of using different fuel blends in the pollutant's emission. Economic indicators and other data of interest (e.g., fuel cost and investment per kW) were adapted from [1], [3] and further calculated for the case:

- Levelized cost of electricity (LCOE) calculates the average cost per unit of electricity generated over the lifetime of a project;
- Net present value (NPV) determines whether a project adds economic value;
- Internal rate of return (IRR) determines the project's expected rate of return;
- Discounted payback period (DPBP) determines the time needed to recover the investment, considering the time value of money.

Results:

- <u>System pollutant emissions</u>

Figure 1 shows that at the end of the combustion chamber, the concentration of CO and CO_2 decreases as H_2 content on the blend increases, most part due to H_2O production increase.

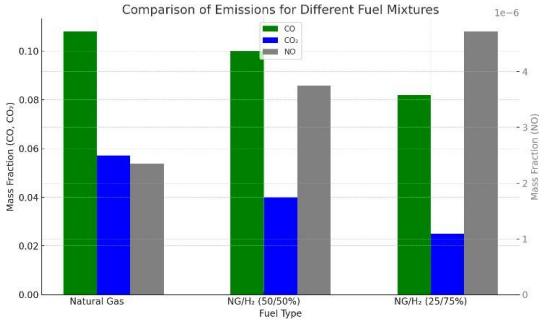


Figure 1 - Comparison of pollutant emissions at the outlet of a combustion chamber, using different fuel blend.

Also, NO species production almost doubles due to the increase on flame temperature (1577 K for 100% NG, 1687 K for NG/H_2 50/50% and 1750 K for NG/H_2 25/75%).

- Economic metrics

The initial investment for a system designed to operate on a ready-to-burn H_2-NH_3 blend is estimated at 960 €/kWh, with an O&M cost of 3 % of the initial investment per year [1]. In comparison, retrofitting NG-based MGTs to operate on H_2 or a H_2-NG blend is estimated to cost approximately 20% of the original investment [3]. The price of a MGT varies between 385-600 €/kW_{el}, while for a combined cycle power plant, costs range from 700 and 1100 €/kWel. The price of green H_2 and NH_3 is estimated to be between 3.50-5.30 €/kg [3], and 0.20- 1.80 €/kg [1], respectively. For reference, the cost of NG is approximately 0.50 €/kg [3]. The LCOE for systems using H_2-NH_3 blends ranges from 187 to 272 €/MWh, depending on the specific blend ratio [1]. These costs serve as a baseline to the developed techno economic models.

Conclusions: Simulation shows that pollutant production varies in different ways. Carbon based pollutants tend to decrease while nitrogen based tends to increase, due to thermal formation. Retrofitting the existing MGT to operate on hydrogen offers a more cost-effective alternative to new installations. Despite the current high costs of green hydrogen and ammonia, future price reductions could enhance their viability. Fuel choice plays a key role in overall system economics, particularly in determining the LCOE.

Acknowledgment:

The authors acknowledge funding provided by the Agenda Moving2Neutrality (reference 02/C05-i01.02/2022.PC644927397-00000038) managed by IAPMEI and funded by the call Aviso Convite nº 02/C05-i01/2022 of the Portuguese Recovery and Resilience Plan.

References

[1] A. M. Yazdani, M. Salimi, and M. Amidpour, "Techno-economic study of gas turbines with hydrogen, ammonia, and their mixture fuels," *Heliyon*, vol. 10, Dec. 2024, doi: 10.1016/j.heliyon.2024.e40727.

[2] R. Banihabib and M. Assadi, "A Hydrogen-Fueled Micro Gas Turbine Unit for Carbon-Free Heat and Power Generation," *Sustainability*, vol. 14, Oct. 2022, doi: 10.3390/su142013305.

[3] A. H. Samitha Weerakoon and M. Assadi, "Techno economic analysis and performance based ranking of 3–200 kW fuel flexible micro gas turbines running on 100% hydrogen, hydrogen fuel blends, and natural gas," *J Clean Prod*, vol. 477, Oct. 2024, doi: 10.1016/j.jclepro.2024.143819.

European Fuel Cells and Hydrogen
PIERO LUNGHI CONFERENCE
EFCH2 2025
September 17th–19th 2025
Capri / Italy

$LaNiO_3$ perovskites for ammonia decomposition: Kinetic Analysis at low temperatures

C. Italiano*, M. Thomas, G. Marino, M. Caporlingua, D. Maccarrone, A. Vita

* corresponding author: cristina.italiano@cnr.it
Institute of Advanced Energy Technologies of the National Research Council of Italy (CNR-ITAE), Via S. Lucia Sopra Contesse 5, 98126, Messina (ME), Italy

Keywords: Ammonia decomposition, Metal Exsolution, Perovskites, Reaction Mechanism

Abstract: Ammonia is a carbon-free hydrogen carrier with high potential for sustainable hydrogen production. This work investigates Mg-doped $LaNiO_3$ perovskite catalysts as a cost-effective alternative to Ru-based systems for ammonia decomposition. Catalysts were synthesized via sol-gel combustion and characterized by XRD, TEM, XPS, CO-chemisorption, CO_2-TPD, H_2-TPR, and in-situ DRIFTS. Mg doping modified the perovskite phase, forming a stable $MgNiO_2$ solid solution and promoting the exsolution of well-dispersed Ni nanoparticles. These features improved thermal stability, Ni dispersion, and surface basicity. H_2-TPR and XPS confirmed strong metal-support interactions and lower reducibility, while CO_2-TPD showed enhanced basic sites. Kinetic studies at 375-400 °C revealed that the $La_{0.1}Mg_{0.9}NiO_3$ catalyst performs efficiently, with results fitting the Temkin-Pyzhev model. In-situ NH_3-TPD indicated that the rate-determining step is the recombinative desorption of nitrogen species. These results highlight the potential of Mg-doped perovskites as effective catalysts for ammonia decomposition in compact, intensified systems for small-scale hydrogen production.

Introduction: *Ammonia, as a sustainable and carbon-free hydrogen carrier, plays a vital role* in the hydrogen economy. Developing new catalytic formulations with less critical materials is fundamental for improving both sustainability and energy efficiency [1]. Nickel-based perovskite catalysts are a promising and cost-effective alternative to Ru-based systems. The exsolution of Ni during reduction creates nanosized active metal sites with strong metal-support interactions. The incorporation of electron-donating alkali and alkaline earth metals into perovskites enhances the electron-rich environment around the Ni sites, boosting catalytic performance [2]. Therefore, Mg-doped $LaNiO_3$ perovskites were synthesized for hydrogen production by ammonia decomposition.

Objectives: *The main objective of this study is to synthesize Mg-doped $LaNiO_3$ perovskites* using a sol-gel combustion method and characterize them through various techniques to understand their structural and catalytic properties. The influence of Mg doping on the stability, formation of Ni particles, and catalytic performance for ammonia decomposition is investigated. The study also explores the reaction mechanism, specifically focusing on the rate-determining step. Additionally, the catalytic performance of the Mg-doped catalysts at lower temperatures is evaluated to improve efficiency and sustainability in hydrogen production.

Material and methods: *In this study, $Mg_xLa_{1-x}NiO_3$ (x=0,0.3,0.6,0.9) perovskites have been* synthesized via sol-gel combustion and characterized by N_2-physisorption, XRD, H_2-TPR, CO_2-TPD CO-chemisorption, TEM, and XPS. In-situ DRIFT spectroscopy was used for NH_3-temperature programmed desorption (TPD) experiments to gain insights into the reaction mechanism. Kinetic analysis was carried out at 375 and 400 °C by varying the partial pressure of NH_3, N_2, and H_2 at 60,000 $cm^3g^{-1}h^{-1}$. Power law model and Temkyn-Pyzhev models were utilised to calculate kinetic parameters.

Results: *The introduction of Mg led to a loss of the typical rhombohedral structure in all Mg-* doped catalysts. As the Mg content increased, the $LaNiO_3$ perovskite phase underwent modifications, resulting in the formation of the $MgNiO_2$ solid dilution, due to the size difference between La and Mg. After reduction, the appearance of a metallic Ni phase confirmed the exsolution of Ni onto the perovskite surface. The average crystallite size of metallic Ni was approximately 7 nm, indicating the presence of well-distributed, small-sized Ni particles. H_2- TPR peaks were shifted to higher temperature after Mg doping, indicating the formation of a more stable and less reducible $MgNiO_2$ solid solution. The addition of Mg also enhanced the amount of CO_2 desorbed for Mg-doped samples, which signifies improved availability of basic sites. CO chemisorption and XPS analysis further confirmed the formation well distributed Ni particles.

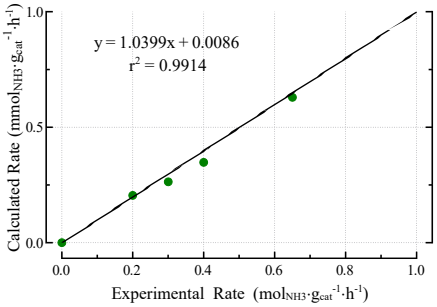


Fig. 1. *Correlation between the experimental and calculated reaction rates (derived from the Temkin-Pyzhev expression).*

Kin etic stu die s of the most effective $La_{0.1}Mg_{0.9}NiO_3$ catalyst

Mass Signal (a.u.)

demonstrated a satisfactory agreement between the experimental and calculated reaction rates based on the Temkin- Pyzhev expression (Fig. 1). In-situ NH_3-TPD analysis further confirmed the proposed mechanism (Fig. 2)

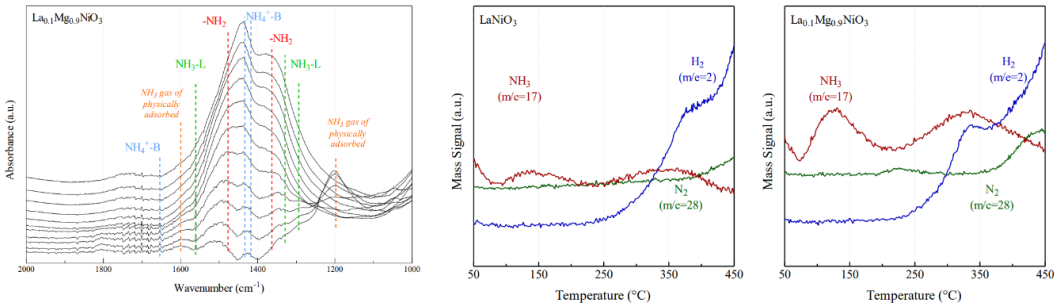


Fig. 2. *In situ DRIFT spectra over $La_{0.1}Mg_{0.9}NiO_3$ catalyst.*

Conclusions: *The results show that the $MgNiO_2$ phase enhances the stability of the* $La_{0.1}Mg_{0.9}NiO_3$ catalyst, as confirmed by TPR. Strong metal-metal interactions lead to the formation of small Ni particles during reduction without sintering, as demonstrated by XRD and CO-chemisorption. The electron-donor properties of Mg promote the dehydrogenation and N_2 desorption stages, as revealed by CO_2-TPD experiments. XPS analysis confirmed the partial reduction of Ni^{3+} to Ni^{2+}, consistent with XRD findings, and the presence of hydroxyl groups in the perovskite structure. Kinetic studies reveal that the reaction proceeds according to the Temkin-Pyzhev mechanism, where the recombinative desorption of N* is the rate- determining step.

Acknowledgment

Funded by the European Union

This work has received funding from the European Union's Horizon 2020 research and innovation program under grant agreement No. 101112118 (ANDREAH project). Views and opinions expressed are, however, those of the authors only and do not necessarily reflect those of the European Union or CHJU.

References

[1]. C. Italiano, G. Marino, M. Thomas, B. Hary, S. Nardone, S. Richard, A. Saker, D. Tasso, N. Meynet, P. Olivier, F. Gallucci, A. Vita, Processes, 2024, 12, 2663.
[2]. M. Pinzón, A. Sánchez-Sánchez, A. Romero, A.R. de la Osa, P. Sánchez, Fuel, 2022, 323, 124384.



TOPIC 5: HYDROGEN ECONOMY AND SUSTAINABILITY

European Fuel Cells and Hydrogen
PIERO LUNGHI CONFERENCE
September 17th–19th 2025
Capri / Italy

Life cycle assessement and life cycle cost addressing in developing solid oxide fuel cells

Sonia Sofi*, Massimiliano Lo Faro, Zahreddine Hafsi, Gaetano Maggio, Mauro Giorgianni, Agatino Nicita, Gaetano Squadrito

* corresponding author: Sonia Sofi: E-mail contact: sonia.sofi@itae.cnr.it

Affiliation: Consiglio Nazionale delle Ricerche: Istituto di Tecnologie Avanzate per L'energia "Nicola Giordano", Via S. Lucia sopra Contesse, n. 5, 98126, Messina, Italia.

Keywords: LCA; eLCC; SOFC; modular approach.

Abstract:

The aim of this study is to perform an in-depth Life Cycle Assessment (LCA) of a Solid Oxide Fuel Cell (SOFC) battery (stack) consisting of three cells with innovative materials, to quantify the environmental impacts whit a environmental Life Cycle Cost (eLCC), and to assess the economic feasibility with a Net Present Value (NPV) calculation by comparing with a commercial SOFC**.**

Objective:

The objective of this study is to focus the analysis on the production and assembly phases, deliberately excluding the use and end-of-life phases, as, given the innovative and experimental nature of this technology, it was deemed appropriate to assess the environmental impact and cost analysis.

Material and methods: The approach of this study is based on dividing the stack into functional modules to create a versatile and reproducible analytical unit. The basic module consists of the electrode-membrane assembly (MEA). The stack is completed by, the bipolar plate on the cathode side, where the bipolar plate refers to the cathode gas distributor, the electrical connection and the gas distribution anode, and two closing modules, one anode and one cathode. The base module is designed to provide greater flexibility in component design and to facilitate integration into different application contexts.


a

b

c

Fig. a, b, c: basic module of the cell built in the CNR ITAE laboratories.

The modularity allows easier management of the Life Cycle Inventory (LCI) phase, as each base module can be analysed in detail in terms of environmental impact, resource

consumption, improvement potential and cost incidence. This approach will enable more comparative studies to be carried out in the future, which are essential for identifying eco-design solutions and optimising the environmental impact of fuel cells.

The LCA method is applied according to the ISO14040-44:2006 standard (ISO, 2006a, 2006b) using the Simapro software (PRe' Sustainability, 2022). The eLCC is applied, using Simapro to estimate the monetization of externalities.

The functional unit used for the study stack of this SOFC with 3 cells is to be considered 1 kW nominal power.The system boundaries follow a cradle-to-gate approach. Otherwise, since third-party organizations supplied all the manufactured components, it was impossible to split the production costs into different phases. Therefore, the costs of each component include: purchased raw materials, transportation, production and taxes; these data have been considered in the processes already present in the database, therefore they are secondary data.

To harmonize the data modeling in both LCA and eLCC, the market datasets of the Ecoinvent 3 database are taken into account for the modeling of the background processes of each product involved in the technology.

The LCI is modeled using both primary and secondary data. These primary data concern the number, total weight and purchase costs of the primary components, as well as the percentage incidences of each material on the total weight. All other data are secondary data taken from ECOINVENT 3, and when missing, they were taken from previous literature studies. For the calculation of the environmental impact, the CML-IA baseline method was chosen, this method is used to evaluate 11 impact categories. In addition to what has just been described, the Cumulative Energy Demand (CED) method was also used, a method in which both the renewable primary energy (CEDr) and the non-renewable primary energy (CEDnr) consumed are calculated. These two methods are in line with the guidelines: Guidance Document for Performing LCAs on Fuel Cell and Hydrogen Technologies. As for the economic - environmental impacts a comparison was made with the eLCC. The "Carbon Footprint" was evaluated as impact category using a European model. The method is called "EP - Environmental Prices" and expresses the willingness to pay for less pollution (in euros per kilogram of pollutant). This method was developed by the Dutch research and consultancy company CE Delft in 2018 and is applicable to European countries. In order to compare the overall cost and affordability of the investment of commercial and innovative SOFC, the NPV was calculated, i.e. the discounted value at a discount rate, of all cash flows (negative and positive) generated over the life of the project.

Results: The modular approach used in this study not only facilitates the identification of the components with the greatest environmental impact, but also allows specific improvements in design and material selection to be suggested. This analysis model makes an important contribution to the field of eco-design by providing guidelines for the optimisation of fuel cell

technologies. An initial comparative analysis found that the use of the innovative materials led to a reduction in the consumption of critical materials, which translated into a reduction in production costs and costs in terms of environmental impact. The first results obtained do not include the energy used to assemble the various components. This data is difficult to obtain from the manufacturers. There is no primary data in the literature, and in the few cases where secondary data are reported, the sources are not indicated. The next step will be to derive the data from a direct laboratory analysis, scaling up to industrial production.
The results of the study, although positive, are limited by the lack of standardisation of production processes and the maturity level of the new SOFC technology.
Conclusions: The aim of the study is to verify the environmental and economic viability of a laboratory SOFC using innovative materials compared to a commercial. The comparative analysis carried out in the study was able to demonstrate that the innovative material developed within the reference project are suitable for reducing the impacts of the SOFC technology. The modular approach used in our methodology will allow to compare the further advancements in materials and production technologies in a simple way, reducing operators and machine working time, also in scaling up the prototype planned in the reference project. In this way facilitating the eco design of the SOFC technology and addressing the future research.

Acknowledgment:
This research was funded by the European Union – NextGeneration EU from the Italian Ministry of Environment and Energy Security POR H2 AdP MMES/ENEA with involvement of CNR and RSE, PNRR - Mission 2, Component 2, Investment 3.5 "Ricerca e sviluppo sull'idrogeno", CUP: B93C22000630006

References

1. Frischknecht, R., Jungbluth, N., Althaus, H.J., Bauer, C., Doka, G., Dones, R., Hischier, R., Hellweg, S., Humbert, S., Köllner, T., Loerincik, Y., Margni, M., Nemecek, T., 2007a.
2. Implementation of Life Cycle Impact Assessment Methods. Ecoinvent Report No. 3, v2.0. Swiss Centre for Life Cycle Inventories, Dübendorf.
3. Frischknecht, R., Jungbluth, N., Althaus, H.J., Doka, G., Dones, R., Heck, T., Hellweg, S., Hischier, R., Nemecek, T., Rebitzer, G., Spielmann, M., 2007b. Overview and Method- ology. Ecoinvent Report No. 1, ver.2.0. Swiss Centre for Life Cycle Inventories, Dübendorf, CH.
4. Masoni, P., Zamagni, A., 2011. FC-Hy guide – guidance document for performing LCAs on fuel cells and H" technologies. Available on. http://www.fc-hyguide.eu/.
5. UNI-EN-ISO 14040, 2006. Environmental Management — Life Cycle Assessment — Principles and framework
6. UNI-EN-ISO 14044, 2006. Environmental management — Life cycle Assessment — Requirements and guidelines.

European Fuel Cells and Hydrogen
PIERO LUNGHI CONFERENCE
September 17th–19th 2025
Capri / Italy

Sustainability assessment of PEMFC

Jure Gramc [a], Mitja Mori*[a]

* corresponding author: mitja.mori@fs.uni-lj.si
[a] University of Ljubljana, Faculty of Mechanical Engineering, Slovenia

Keywords: life cycle costing, life cycle sustainability assessment, proton exchange membrane fuel cell, social life cycle assessment.

Abstract

Introduction: Fuel cell and hydrogen (FCH) technologies are seen as an important part of the green transition. However, research usually focuses only on the environmental impact (often only on the carbon footprint), which does not provide sustainable information. Life cycle sustainability assessment (LCSA) is mostly used for holistic sustainability assessment. The first conceptual scheme for LCSA was proposed by Kloepffer [1]. It consisted of two approaches, namely: (i) LCSA as the sum of Environmental Life Cycle Assessment (E-LCA), Life Cycle Costing (LCC), and Social Life Cycle Assessment (S-LCA) without any formal weighting between them, and (ii) LCSA as a new assessment based on the same inventory. This means that additional impact categories are included in the LCIA step by incorporating LCC and S-LCA. The first approach (LCSA as the sum of E-LCA, LCC, and S-LCA) is most commonly used as the methods are already well established [2]. Its main advantage is transparency – the allocation of advantages and disadvantages of the indicators is clear, and there is no trade-off between the sustainability pillars. The main disadvantage is the lack of harmonization, which has been pointed out in several studies [2], [3], [4]. The problems with harmonization occur regardless of the definition of the United Nations Environment Programme (UNEP) LCSA guidelines [5]. Another problem is the lack of or non-transparent discussion of sustainability in LCSA studies [6].

One of the most advanced and commercially used FCH technologies is the proton exchange membrane fuel cell (PEMFC), which is currently the only FCH alternative to internal combustion engines in transportation [7]. Despite the high level of development and commercial applications, only one LCSA study on PEMFC has been made – the study by Mori et al [8].

Objectives: The goal of the study is to assess the sustainability of the manufacturing and End-of-Life (EoL) phases of the PEMFC using the LCSA methodology. The assessment is carried out for the reference case, defined in the study by Mori et al [8] and the prospective case defined in the study by Gramc et al [9] with a future optimistic implementation of Ecodesign Guidelines. However, the LCSA indicators do not evaluate sustainability holistically but each aspect of sustainability separately. For a holistic sustainability assessment, these LCSA indicators need to be integrated into a sustainability framework. The study addresses these issues and proposes important cornerstones on which the sustainable methodology linking the LCSA indicators should be defined.

Material and methods: As mentioned above, the LCSA consists of E-LCA, LCC, and S-LCA methods. The EU-funded project SH2E [10] defines guidelines for each LCSA method, specific for the FCH

technologies. The E-LCA method is also standardised by ISO 14040 [11] and ISO 14044 [12], while the (UNEP) [13] has established some guidelines for the S-LCA method. The functional unit of the LCSA analysis is a 48kWel PEMFC stack used in a light-duty transportation vehicle. The scope of the study includes the sourcing and processing of raw materials, the manufacturing processes and the EoL processes. The scope of the study, the system boundaries and the functional unit are the same for all methodologies. The environmental impacts are calculated using the Environmental Footprint 3.1 life cycle impact assessment methodology, while the social impacts are calculated using the PSILCA database.

Results: The results of the LCSA analysis are shown in Table 1. For the future development of PEMFCs with the implementation of ecodesign, significant reductions are foreseen for all LCSA indicators considered. However, for a holistic sustainability assessment, the LCSA indicators have to be combined within a framework methodology capable of providing a quantitative sustainability assessment.

Table 1: LCSA results for the reference case and the optimistic future case

LCSA indicator	Reference	Future
Acidification [Mole of H^+ eq.]	33.07	3.36
Climate Change [kg CO_2 eq.]	1206	319
Eutrophication, freshwater [kg P eq.]	0.0052	0.0035
Eutrophication, marine [kg N eq.]	1.53	0.24
Eutrophication, terrestrial [Mole of N eq.]	16.47	2.51
Resource use, fossils [MJ]	12737	3458
Resource use, mineral and metals [kg Sb eq.]	0.058	0.007
Total cost [€]	9813	6831
Child labour [med risk hours]	3446	293
Contribution to economic development [med opportunity hours]	176	64
Fair salary [med risk hours]	8038	3537
Forced labour [med risk hours]	0.77	0.34
Gender wage gap [med risk hours]	4284	886
Health expenditure [med risk hours]	652	116

Conclusions: The LCSA analysis carried out on the PEMFC is the basis for the holistic sustainability assessment. The indicators themselves do not provide sufficient information on sustainability. There is a lack of a holistic sustainability framework that links the indicators and enables a quantitative sustainability indicator of the PEMFC.

Acknowledgment

This work has been carried out within the framework of the projects eGHOST and GUESS-WHy. The projects have received funding from the Fuel Cells and Hydrogen 2 Joint Undertaking (now Clean Hydrogen Partnership) under Grant Agreement No. 101007166 and Grant Agreement No.101192392. Views and opinions expressed are however those of the author(s) only and do not necessarily reflect those of the European Union or the Clean Hydrogen Partnership. Neither the European Union nor the granting authority can be held responsible for them.

References

[1] W. Kloepffer, "Life cycle sustainability assessment of products," *Int J Life Cycle Assess*, vol. 13, no. 2, pp. 89–95, 2008, doi: 10.1065/lca2008.02.376.

[2] D. Costa, P. Quinteiro, and A. C. Dias, "A systematic review of life cycle sustainability assessment: Current state, methodological challenges, and implementation issues," *Science of The Total Environment*, vol. 686, pp. 774–787, 2019, doi: https://doi.org/10.1016/j.scitotenv.2019.05.435.

[3] T. E. T. Dantas and S. R. Soares, "Systematic literature review on the application of life cycle sustainability assessment in the energy sector," *Environ Dev Sustain*, vol. 24, no. 2, pp. 1583–1615, 2022, doi: 10.1007/s10668-021-01559-x.

[4] R. T. Fauzi, P. Lavoie, L. Sorelli, M. D. Heidari, and B. Amor, "Exploring the Current Challenges and Opportunities of Life Cycle Sustainability Assessment," *Sustainability*, vol. 11, no. 3, 2019, doi: 10.3390/su11030636.

[5] UNEP/SETAC, "Making informed choices on products."

[6] C. Wulf, J. Werker, C. Ball, P. Zapp, and W. Kuckshinrichs, "Review of Sustainability Assessment Approaches Based on Life Cycles," *Sustainability*, vol. 11, no. 20, 2019, doi: 10.3390/su11205717.

[7] A. Valente, D. Iribarren, and J. Dufour, "Life cycle assessment of hydrogen energy systems: a review of methodological choices," *International Journal of Life Cycle Assessment*, vol. 22, no. 3, pp. 346–363, Mar. 2017, doi: 10.1007/S11367-016-1156-Z.

[8] M. Mori *et al.*, "Life cycle sustainability assessment of a proton exchange membrane fuel cell technology for ecodesign purposes," *Int J Hydrogen Energy*, vol. 48, no. 99, pp. 39673–39689, 2023, doi: https://doi.org/10.1016/j.ijhydene.2023.05.255.

[9] J. Gramc *et al.*, "Ecodesign as a key concept for improving the life cycle environmental performance of proton-exchange membrane fuel cells," *Int J Hydrogen Energy*, 2024, doi: https://doi.org/10.1016/j.ijhydene.2024.08.020.

[10] E. Bargiacchi, G. Puig-Samper, F. Campos-Carriedo, D. Iribarren, and J. Dufour, "SH2E project, Deliverable 2.2 Definition of FCH-LCA guidelines," 2022.

[11] International Organisation for Standardisation, "ISO 14040: environmental management - life cycle assessment - principles and framework," 2006.

[12] International Organisation for Standardisation, "ISO 14044: environmental management - life cycle assessment - requirements and guidelines," 2006. [Online]. Available: www.iso.org

[13] United Nations Environmental Programme, "Guidelines for Social Life Cycle Assessment of Products and Organisations 2020," 2020.

European Fuel Cells and Hydrogen
PIERO LUNGHI CONFERENCE
September 17th–19th 2025
Capri / Italy

Hydrogen Ecosystem Development: A Case Study in California

Adam Z Weber*[a,b], Mohammed Tamim Zaki[b], Hanna Breunig[b]

* corresponding author: adam.weber@arches.org
[a] Alliance for Renewable, Clean Hydrogen Energy Systems (ARCHES), Irvine, CA USA
[b] Lawrence Berkeley National Laboratory, Berkeley, CA USA

Keywords: Analysis, Electrolysis, Hydrogen, Infrastructure, Innovation

Abstract

Key to enabling a hydrogen ecosystem is the deployment of various hydrogen technologies at scale in resilient and sustainable system. Recently, the Alliance of Renewable Clean Hydrogen Energy Systems (ARCHES), a collective representing the California region, was established as a hydrogen hub within the California Region. In this talk, an overview of ARCHES and its approach will be given. In addition, the need for innovation and specific research directions will be discussed in terms of both fuel cell and electrolyzer development in order to bring overall OpEx and CapEx costs down to reach market liftoff in the ARCHES ecosystem.

Introduction

To realize the hydrogen economy and unleash a new energy paradigm, the costs and inefficiencies of the core clean hydrogen technologies from production to end use need to be reduced. These technologies need to exhibit increased efficiency, (dynamic) performance, and durability to reduce costs and be commercially viable. Furthermore, to achieve market liftoff of hydrogen, not only cost reduction, but also a rational systems view is required. Such an approach is seen in various Hydrogen Valleys throughout the world. Critical is connecting upstream production with downstream demand through midstream infrastructure and ensuring that it is all synchronized temporally and geographically.

Objectives

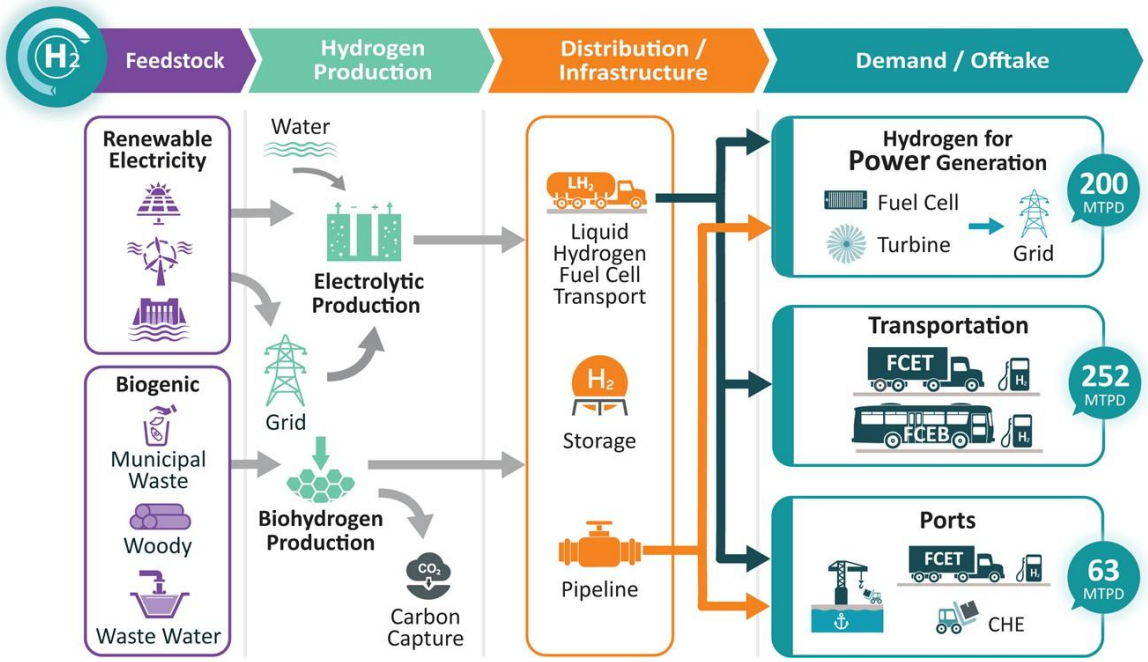
Key to enabling a hydrogen ecosystem is the deployment of various hydrogen technologies at scale in resilient and sustainable system. This approach is implemented by ARCHES using a combination of newly developed technoeconomic analysis and life-cycle assessment as well a systems approach towards connecting the various parts of an end to end hydrogen ecosystem. Identification of the critical barriers highlights the research and innovation needs by the various sectors.

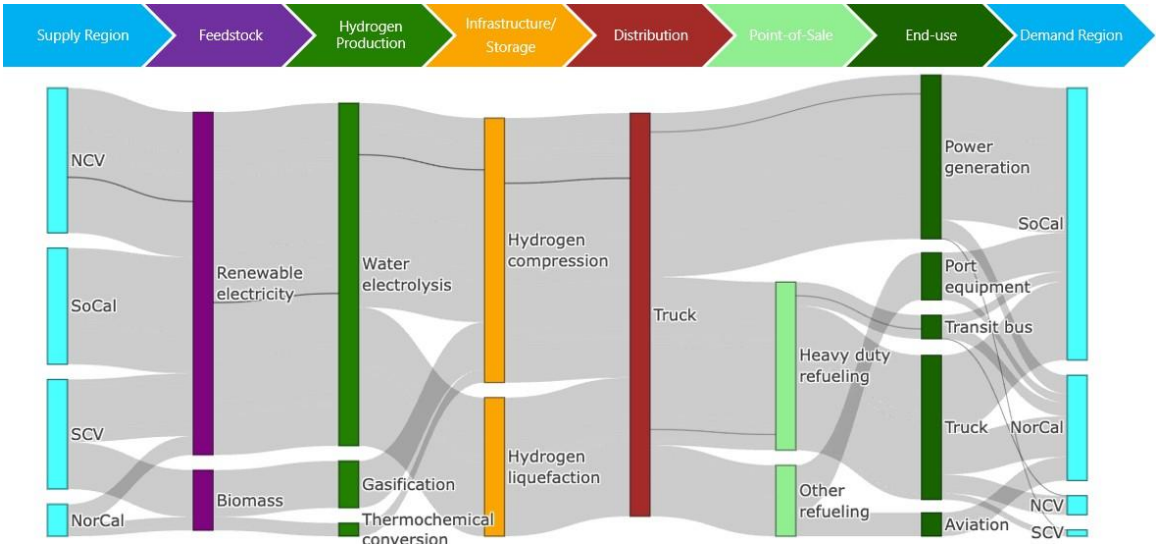
Material and methods

All mass and energy flows, as well as estimated emissions, are based on H2A process model designs and projections of technology performance, literature review, and LBNL process, economic and life cycle modeling. Life cycle phases associated with hydrogen production include feedstock preparation (water and biomass), energy production and consumption (renewable, grid, and combination of renewable and grid electricity), maintenance (chemical utilization in electrolysis and natural gas combustion in gasification), carbon sequestration, hydrogen storage (compression and liquefaction), and distribution (truck and pipeline).

Results:

The figure below shows the concept of the initial slate of ARCHES H2 Hub projects, with scenarios focused on green hydrogen production pathways using water electrolysis and biomass gasification. End-use applications included in the model are transit, medium and heavy-duty trucking, port authorities, and power and aviation companies that currently consume natural gas, diesel, and aviation fuel for their day-to-day operation. Representative locations for hydrogen production and end-use are based on recent projections of the hydrogen economy in California. A sample result is shown below in terms of a hydrogen Sankey diagram or flow of hydrogen from initiation to use. Example variations include: the inclusion of policy incentives or not, different representations of the electricity grid and source, electrolysis versus gasification versus combinations of both for production, liquefaction versus compression based on producer capacity cutoffs, transportation truck versus pipeline based on existing infrastructure, and ultimate end use.





Conclusions:

The cost-effective and sustainable deployment of hydrogen supply and demand networks, especially in large economic regions like California, can be challenging considering the spatial-temporal availability and variability of the different actors across the network such as production processes, distribution modes, and end-users. In this presentation, we provided an overview and demonstration of a modeling framework used to assess the various impacts of plausible hydrogen production and supply chain networks in California. Comparison of these different scenarios can help inform future projects by demonstrating the various trade-offs. In addition, there is a need to increase overall efficiency, performance, and durability of fuel-cell and electrolyzer systems through novel material deisgn, integration, and optimization.

Acknowledgment

This work is based on work done by the Systems Analysis Team in ARCHES including CRADAs with LBNL.

European Fuel Cells and Hydrogen
PIERO LUNGHI CONFERENCE
September 17th–19th 2025
Capri / Italy

A comprehensive assessment of hydrogen leakages along the entire supply chain: present and future scenarios

Davide Trapani*[a], Paolo Marocco [a], Marta Gandiglio [a], Massimo Santarelli [a]

* corresponding author: davide.trapani@polito.it

[a] Department of Energy, Politecnico di Torino, Corso Duca degli Abruzzi 24, 10129 Torino, Italy

Keywords: hydrogen-based economy, hydrogen leakages, hydrogen supply chain

Abstract

Low-carbon hydrogen is widely recognized as a key pillar of the global energy transition. However, since hydrogen acts as an indirect greenhouse gas, estimating its atmospheric leakages along the supply chain is crucial for an accurate evaluation of its overall environmental benefits. This study presents a comprehensive assessment of hydrogen leakages along the entire supply chain – including production, handling, storage, transport, and end-uses – under current conditions (2023) and projected scenarios for 2030 and 2050.

Introduction:

Low-carbon hydrogen and its derivatives can be effectively adopted in sectors where mitigating carbon dioxide (CO_2) emissions is particularly challenging, such as heavy industry, long-haul transport, aviation and shipping. While transitioning to low-carbon hydrogen is essential for achieving climate goals, it is equally important to consider the potential environmental trade-offs associated with its deployment. Hydrogen leakages along the supply chain represent a key concern as they could offset some of the anticipated climate benefits. Indeed, hydrogen acts as an indirect greenhouse gas as it can cause atmosphere perturbations leading to the increase in the concentrations of methane, ozone and water vapor [1]. Hydrogen emissions (both intentional and unintentional) may occur at various stages of the supply chain, with losses typically estimated below 10% of the transported hydrogen [2], [3]. However, the exact quantity of hydrogen released into the atmosphere remains unknown due to the absence of accurate hydrogen sensors capable of detecting concentrations with high sensitivity (i.e., ppb level) and fast response time [1].

Objectives:

The present work develops a thorough hydrogen leakage estimation framework, assessing hydrogen emissions across the entire hydrogen supply chain, encompassing hydrogen

production (i.e., steam methane reforming both with and without carbon capture and storage, electrolysis and coal gasification), handling (i.e., compression and liquefaction), storage, transport (i.e., transmission and distribution pipelines, compressed and liquid hydrogen delivery by trucks) and end-uses (i.e., industry, mobility, aviation and shipping, residential and power generation). To the best of our knowledge, this represents the first study providing a disaggregated, process-level quantification of hydrogen leakages along the entire supply chain under current and future scenarios (present, 2030, 2050).

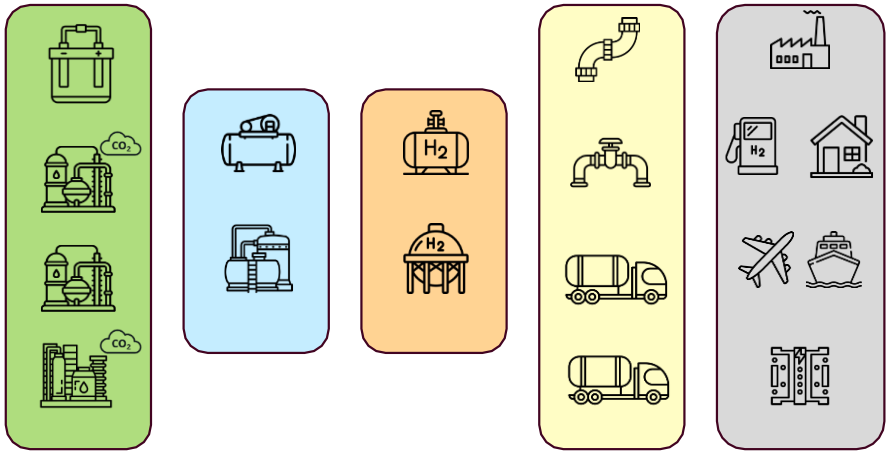


Figure 1. *Hydrogen supply chain.*

Material and methods:

Based on data available in literature (including peer-reviewed papers and technical reports [1], [4], [5], [6]) this study evaluates the average leakage rate for each stage of the supply chain and identifies a minimum-maximum variation range. Unlike previous studies that typically adopt single leakage values for each stage of the value chain, this study employs a complete dataset of hydrogen leakage rates and derived statistical values, accounting for uncertainties and variability in the available data. Building on this dataset of hydrogen leakage rates, several hydrogen-based scenarios are explored, considering projections from International Energy Agency (IEA), Hydrogen Council (HC) and International Renewable Energy Agency (IRENA) for 2030 and 2050. Ultimately, hydrogen emissions and overall supply chain leakage rates are assessed, with a detailed process-level breakdown computed to identify the most critical phases within the hydrogen infrastructure.

Results:

The results indicate that electrolysis is the most leakage-prone among the hydrogen production pathways, although its leakage rate is affected by high uncertainty. Moreover, liquid hydrogen is expected to emerge as a key contributor to hydrogen losses during

handling, transport and refueling operations. Annual hydrogen leakages currently amount to 1.3 Mt and are projected to nearly triple by 2030, followed by a sharp rise exceeding 22 Mt by 2050. The corresponding leakage rates of the hydrogen supply chain are estimated at 1.3% in 2023, rising to 2.2% in 2030, and reaching between 5% and 7% by 2050.

Conclusions:

These findings emphasize the importance of precise emissions quantification and effective mitigation strategies to ensure that hydrogen can achieve its intended climate benefits. By identifying the processes most susceptible to leaks, this analysis offers valuable insights for policymakers, researchers, and industry stakeholders aiming to minimize hydrogen losses and fully realize the environmental advantages of a hydrogen-based economy.

Acknowledgment

The work has been funded by the HYDRA (HYDrogen economy benefits and Risks: tools development and policies implementation to mitigate possible climAte impacts) project, project number: 101137758.

References

[1] S. Esquivel-Elizondo, A. Hormaza Mejia, T. Sun, E. Shrestha, S. P. Hamburg, and I. B. Ocko, “Wide range in estimates of hydrogen emissions from infrastructure,” 2023, *Frontiers in Energy Research*. doi: 10.3389/fenrg.2023.1207208.

[2] A. Alsulaiman, “Review of Hydrogen Leakage along the Supply Chain: Environmental Impact, Mitigation, and Recommendations for Sustainable Deployment,” Nov. 2024. Accessed: Apr. 02, 2025. [Online]. Available: https://www.oxfordenergy.org/wpcms/wp-content/uploads/2024/11/ET41-Review-of-Hydrogen-Leakage-along-the-Supply-Chain.pdf

[3] B. Van Ruijven, J. F. Lamarque, D. P. Van Vuuren, T. Kram, and H. Eerens, “Emission scenarios for a global hydrogen economy and the consequences for global air pollution,” *Global Environmental Change*, vol. 21, no. 3, pp. 983–994, Aug. 2011, doi: 10.1016/j.gloenvcha.2011.03.013.

[4] Z. Fan *et al.*, “Hydrogen leakage: a potential risk for the hydrogen economy,” 2022. [Online]. Available: https://energypolicy.columbia.edu/about/partners.

[5] Frazer-Nash Consultancy, “Fugitive hydrogen emissions in a future hydrogen economy,” Mar. 2022. Accessed: Apr. 02, 2025. [Online]. Available: https://www.gov.uk/government/publications/fugitive-hydrogen-emissions-in-a-future-hydrogen-economy

[6] A. Arrigoni and L. Bravo Diaz, “Hydrogen emissions from a hydrogen economy and their potential global warming impact,” Aug. 2022. doi: 10.2760/065589.



Robust design of green hydrogen production systems – Mitigating business risks from PPA power sourcing uncertainties

Jonathan Brandt*[a], Astrid Bensmann [a], Richard Hanke-Rauschenbach [a]

*Corresponding author: Jonathan Brandt brandt@ifes.uni-hannover.de

[a] Leibniz University Hannover, Institute for Electric Power Systems, 30167 Hannover, Germany

Keywords: Green hydrogen, PPA power sourcing uncertainties, robust design optimization

Abstract

Introduction: Following an episode of enthusiasm surrounding the opportunities of green hydrogen to achieve European emission reduction goals [1] and reduce dependence on energy imports [2], the implementation gap between announced and realised projects mirrors the slowed ramp-up of European green hydrogen production in recent years [3]. One reason is high and uncertain production and supply cost compared to hydrogen from alternative sources [4]–[7]. Among others caused by slower falling capital expenditures as expected [6] and regulatory requirements and uncertainties regarding power sourcing for electrolyser operation [5]. A second reason is a limited and uncertain green hydrogen off-take [8]. Both impair the profitability of green hydrogen production and thus hamper a European ramp-up, necessitating high project subsidies [3] to mitigate business risk for green hydrogen projects. As the European regulatory framework requires the primary usage of renewable power via power purchase agreements (PPAs) for green hydrogen production in most European countries and bidding zones [5], [9], [10], an additional business risk emerges as soon as power sourcing is due. PPA power sourcing does not only bring the challenge of matching the fluctuating feed-in of renewable energy sources to a relatively flat off-take of big industrial hydrogen consumers. In addition, the exclusive reliance on mainly long-term PPA contracts brings power supply risks due to the inter-year uncertainties regarding weather-reliant PPA power availability. This applies above all as long as short-term PPA contracts are not available and short-term power purchase via the electricity market for compensation is no option, as it is in the case of green hydrogen production [5], [9]. Here, the PPA or the electrolyser operator must bear the risk.

Objectives: In this work, we show to what extent green hydrogen production cost is affected by inter-year uncertainties of PPA power availability. Furthermore, we quantify possible hydrogen production cost increases when ignoring those uncertainties in the sizing and operation planning of green hydrogen production systems. To solve this issue, we present an optimisation approach to find a robust PPA, electrolyser and hydrogen storage design, considering the inter-year uncertainties, which helps to mitigate the risk of PPA power sourcing for green hydrogen production. In addition, the robust design considering

uncertainties gives a more differentiated picture of realistically achievable green hydrogen production cost.

Material and methods: The methodological base for our analyses is a linear optimisation model, minimising the installation and operation cost of the hydrogen production system shown in Figure 1 to meet a predefined hydrogen demand. Besides a water electrolyser including peripherals and compressor, the system contains various PPA and hydrogen storage options, which can be combined to create different power purchase scenarios and system configurations. The minimised cost allows a calculation of the specific hydrogen production cost, which is used to evaluate the economic viability of the different power purchase scenarios and system configurations. In addition, we use an extended version of our optimisation model that allows a robust design optimisation considering the uncertainties regarding PPA power availability. Historic feed-in time series in different European locations are used to map this uncertainty in PPA power availability.

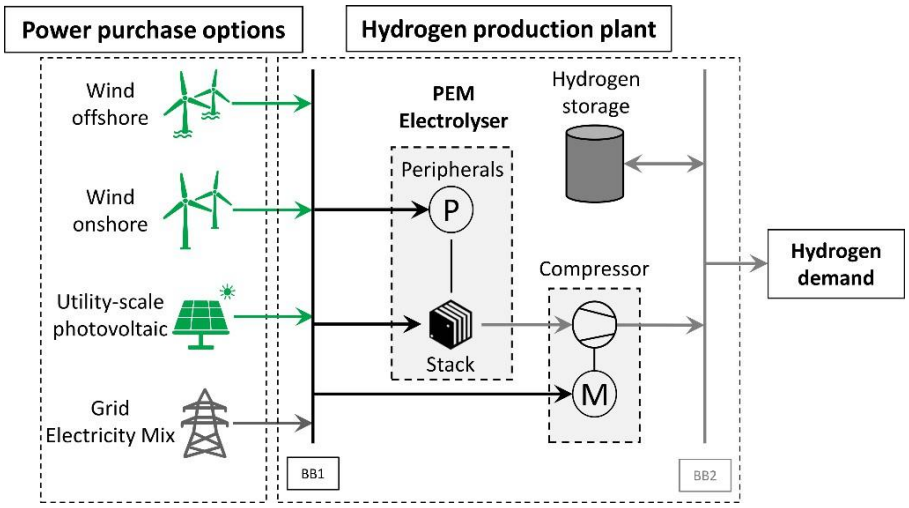


Figure 1:Considered hydrogen production system set-up.

Results: Our results show that the uncertainties regarding PPA power sourcing affect estimated green hydrogen production cost and the associated PPA, electrolyser and storage design. This applies to different European locations and especially at high hydrogen storage cost. Ignoring those uncertainties can lead to hydrogen underproduction, which could jeopardise the fulfilment of supply contracts with hydrogen off-takers. Resulting fines or hydrogen compensation purchases would increase green hydrogen production cost. The results of the robust optimisation show that considering the uncertainties not only prevents underproduction and thus mitigates the business risk but also provides clarity on the range of possible green hydrogen production cost. At the same time, the resulting cost-optimised and robust system design avoids costly PPA oversizing, which would also increase green hydrogen production cost.

Conclusions: Considering the inter-year uncertainties of PPA power purchase allows mitigating the business risk of green hydrogen production by avoiding costly PPA oversizing and fines for failed hydrogen delivery or hydrogen compensation purchases due to underproduction. In addition, a robust PPA, electrolyser and hydrogen storage design provides a differentiated picture of realizable hydrogen production cost. The presented model for robust design optimisation can be used to consider and evaluate further uncertainties potentially jeopardising the profitability of green hydrogen production. Those could be a changing hydrogen off-take characteristic or, if accessible via a local redispatch market, the fluctuating availability of otherwise downwards redispatched renewable power, another viable power purchase option for green hydrogen production.

Acknowledgment:

This work was funded by the Ministry of Science and Culture of Lower- Saxony (MWK) as part of the innovation laboratory H2-Wegweiser.

References

[1] European Commission, “Fit for 55 package,” 2021. https://ec.europa.eu/commission/presscorner/detail/en/IP_21_3541.

[2] European Commission, “REPowerEU Plan,” 2022. https://ec.europa.eu/commission/presscorner/detail/en/ip_22_3131.

[3] A. Odenweller and F. Ueckerdt, “The green hydrogen ambition and implementation gap,” *Nat. Energy*, vol. 10, no. January, 2025, doi: 10.1038/s41560-024-01684-7.

[4] Capgemini and EIT InnoEnergy, “Reducing low-carbon hydrogen investment and operating costs,” 2024. [Online]. Available: https://www.capgemini.com/insights/research-library/reducing-low-carbon-hydrogen-investment-and-operating-costs/.

[5] J. Brandt *et al.*, “Cost and competitiveness of green hydrogen and the effects of the European Union regulatory framework,” *Nat. Energy*, vol. 9, no. June, pp. 703–713, 2024, doi: 10.1038/s41560-024-01511-z.

[6] Ramboll, “What will it take to reduce CAPEX in green hydrogen production?,” 2023. https://www.ramboll.com/net-zero-explorers/what-will-it-take-to-reduce-capex-in-green-hydrogen-production.

[7] R. T. Shafiee and D. P. Schrag, “Carbon abatement costs of green hydrogen across end-use sectors,” *Joule*, vol. 8, no. 12, pp. 3281–3289, 2024, doi: 10.1016/j.joule.2024.09.003.

[8] BloombergNEF, “Hydrogen offtake is tiny but growing,” 2023. https://about.bnef.com/blog/hydrogen-offtake-is-tiny-but-growing/.

[9] European Commission, “Delegated regulation (EU) 2023/1184 on Union methodology for RFNBOs,” 2023. https://eur-lex.europa.eu/legal-content/EN/TXT/?uri=uriserv%3AOJ.L_.2023.157.01.0011.01.ENG&toc=OJ%3AL%3A2023%3A157%3ATOC.

[10] European Commission, “Commission sets out rules for renewable hydrogen,” 2023. https://ec.europa.eu/commission/presscorner/detail/en/IP_23_594.



Green Hydrogen and Wastewater Synergies: Cost-Effective Integra- tion of Electrolysis Oxygen in Wastewater Treatment Plants

Levin Matz[a], Lukas Koenemann[a], Steffen Brundiers[a], Inga Beyers[a], Arne Freyschmidt[b], Astrid Bensmann[*a], Richard Hanke-Rauschenbach[a]

* corresponding author: Astrid Bensmann

[a] Leibniz University Hannover, Institute of Electric Power Systems, Appelstraße 9A, 30167 Hannover, Germany

[b] Leibniz University Hannover, Institute of Sanitary Engineering and Waste Management, 30167 Hanover, Germany

Keywords: Green hydrogen, oxygen, sector coupling, wastewater treatment

Introduction:

This study examines the utilization of oxygen as by-product of green hydrogen production by water electrolysis in municipal wastewater treatment plant (WWTP) aeration. With increasing demand for green hydrogen, a significant expansion of water electrolysis is expected. Therefore, large amounts of oxygen will be generated during water electrolysis but usually remain unused. A promising application is its integration into WWTPs aeration of biological treatment, where oxygen is essential for microbial activity [1–3]. Conventional aeration employs air blowers to supply oxygen for the biological treatment stage [4]. WWTPs account for approximately 1% of global electricity consumption, of which 50-80% is used for aeration [5,6]. Supplementing aeration air blowers with electrolysis oxygen could substantially lower WWTP energy consumption and operating costs, thereby enhancing hydrogen's profitability. However, these benefits must be balanced against potential cost increases for oxygen integration in the aeration and extended hydrogen transport distances to demand sites.

Objectives:

This study assesses the total annual costs (TAC) of WWTP aeration systems incorporating electrolysis oxygen, comparing them to conventional aeration costs. Additionally, it evaluates how these savings impact hydrogen supply costs and whether they can offset transportation expenses for extended distribution distances.

Material and methods:

A holistic system model, implemented in OpenModelica, is used to analyze the integration of electrolysis oxygen into WWTP aeration. The models are characterized by quasi-stationary

energy and mass balances and incorporate non-linear performance models. The modelled system includes:

- The hydrogen supply chain: renewable electricity generation, electrolysis system, hydrogen compression, storage, and transport.
- The WWTP aeration system: conventional air blowers and required modifications for electrolysis oxygen, including piping, storage, retrofitting aeration diffusers, new additional diffusers and potential mechanical mixing.

The analysis covers a range of hydrogen supply amounts (which determines electrolysis oxygen availability) and WWTP sizes (which determines oxygen demand) to find economically and energetically viable ratios. Within this range, each system design is optimized via PyGMO parallel optimization library framework in Python aiming to minimize the entire system's TAC.

Results:

For a large scale WWTP with 500,000 population equivalents (PE), aeration TAC decreases by at least 68% (0.81 M EUR/year) when hydrogen supplies exceed 8 kt/year (oxygen production > 60 kt/year). Overall, operational savings from electrolysis oxygen outweigh capital expenditures for the optimized design of aeration system components that are necessary for electrolysis oxygen integration.

Results for WWTPs ranging from 100,000 to 2,000,000 PE all exhibit similar trends, indicating that aeration costs and system design scale linearly with PE. However, larger WWTPs, having greater oxygen demand, can accommodate higher hydrogen and electrolysis oxygen supplies.

Hydrogen supply costs decrease with scale, from 4.53 EUR/kgH_2 at 1 ktH_2/year to 3.47 EUR/kgH_2 above 16 ktH_2/year. Incorporating aeration cost savings leads to a maximum hydrogen cost reduction of up to 0.39 EUR/kgH_2, yielding minimum hydrogen supply cost of 3.27 EUR/kgH_2 for hydrogen supplies between 9–18 ktH_2/year.

Hydrogen transport costs via a 25 km long pipeline range from 0.81 EUR/kgH_2 (1 ktH_2/year) to 0.06 EUR/kgH_2 (>21 ktH_2/year). Aeration cost savings only offset transport costs if scaling effects in transport and aeration utilization align. For example, aeration cost savings achieved in WWTPs of above 500,000 PE can offset hydrogen transport costs of 25 km transport distance. Hydrogen transport costs for distances of 5 km can be offset by aeration cost savings in WWTPs above 100,000 PE.

Conclusions:

The integration of electrolysis-derived oxygen into WWTP aeration offers substantial cost reductions and enhances the economic viability of hydrogen supply. However, these benefits

depend on specific boundary conditions such as hydrogen production scale, WWTP size, and transport distance to yield overall economic viable systems. Further research can identify locations where these favorable conditions align, enabling targeted implementation and maximizing the benefits of electrolysis oxygen utilization in WWTPs.

Acknowledgment

The authors gratefully acknowledge the financial support by the federal state Lower Saxony in the project "SeWAGE PLANT H FuE" under grant no. ZW180159704. We appreciate the contributions of all project members with special thanks to the project partners from the Institute of Sanitary Engineering and Waste Management at Leibniz University Hannover: Arne Freyschmidt, Maike Beier focusing on the implementation of off-gas utilization at wastewater treatment plants and Sara Zahedi Nezhad and Dirk Weichgrebe for their work on LCA scenario evaluation.

The results were achieved by computations on the cluster system at the Leibniz Universität Hannover, Germany.

References

[1] Abdelfattah, A., Ramadan, H., Elsamahy, T., Eltawab, R., Mostafa, S., Zhou, X., and Cheng, L., 2023, “Multifaced Features and Sustainability of Using Pure Oxygen in Biological Wastewater Treatment: A Review,” J. Water Process Eng., 53, p. 103883. https://doi.org/10.1016/j.jwpe.2023.103883.

[2] Jentsch, M. F., and Büttner, S., 2019, *Dezentrale Umsetzung Der Energie- Und Verkehrswende Mit Wasserstoffsystemen Auf Kläranlagen*, ISSN 2366-9594

[3] Skouteris, G., Rodriguez-Garcia, G., Reinecke, S. F., and Hampel, U., 2020, “The Use of Pure Oxygen for Aeration in Aerobic Wastewater Treatment: A Review of Its Potential and Limitations,” Bioresour. Technol., 312, p. 123595. https://doi.org/10.1016/j.biortech.2020.123595.

[4] Fricke, K., 2009, *Energieeffizienz Kommunaler Kläranlagen*, Umweltbundesamt. [Online]. Available: https://www.umweltbundesamt.de/sites/default/files/medien/publikation/long/3855.pdf.

[5] Metcalf & Eddy, Inc, ed., 2014, *Wastewater Engineering: Treatment and Resource Recovery*, McGraw-Hill Education, New York, NY.

[6] IEA, 2016, *World Energy Outlook 2016*, IEA. [Online]. Available: https://www.iea.org/reports/world-energy-outlook-2016.

European Fuel Cells and Hydrogen
PIERO LUNGHI CONFERENCE
September 17th–19th 2025
Capri / Italy

Pre-normative research on hydrogen release assessment

V. Palmisano[a], A. Agostini [a], V. Troisi[b], M. Robino[b], V. R. Bescos[c], P. Pirras[d]
* corresponding author: V. Palmisano
[a] ENEA, Rome, Italy
[b] SNAM, Milan, Italy
[c] ENAGAS,
[d] FBK, .

Keywords: greenhouse effect, hydrogen emissions, hydrogen economy, mitigation strategies.

Abstract

Introduction: Hydrogen is set to play a supporting role in achieving climate neutrality by serving as an energy carrier for renewable sources. However, while hydrogen itself is not a direct greenhouse gas, its emissions can indirectly enhance the greenhouse effect with three main mechanisms [1,2]:

1 **Increase in atmospheric methane lifetime**: Hydrogen reacts with the hydroxyl radical (OH), which is the primary oxidant of methane (CH_4) in the atmosphere. The reduction of OH slows down the decomposition of methane, increasing its average lifetime and enhancing its climate-altering effect.

2 **Formation of tropospheric ozone**: Hydrogen radicals (H) resulting from the reaction with OH promote the production of ozone (O_3) in the troposphere, a greenhouse gas with a direct impact on global warming.

3 **Increase in stratospheric water vapor**: The reaction of hydrogen with OH leads to the formation of water vapor in the stratosphere, which has a net warming effect.

The resulting global warming potentials estimate of H_2 are remarkable: GWP100 is around 12 [3, 4] while GWP20 is as high as 40 [3, 5]. Consequently, minimizing hydrogen emissions is critical not only for enhancing the safety and efficiency of the hydrogen value chain but also for safeguarding the environment.

Despite its importance, the current understanding of hydrogen emissions across the value chain remains fragmented. Studies estimate that the rate of hydrogen dispersion can vary between 0.3% and 20% depending on the technologies used and operating conditions [6]. The uncertainty in hydrogen emission estimates is due to the current lack of direct measurements and most estimates are derived from analogies with natural gas and theoretical models. There is a lack of standardized, validated data on the amounts of hydrogen released during various processes, with existing studies often focused on accident scenarios rather than routine emissions. The absence of a comprehensive inventory hinders the ability to conduct reliable, scientifically validated research on hydrogen's climate impact and complicates the development of mitigation strategies. The NHyRA project addresses these challenges [7].

Objectives: The NHyRA project addresses the knowledge gap regarding the potential amount of hydrogen emissions expected along the entire H_2 value chain. The project is founded under the call HORIZON-JTI-CLEANH2-2023-05-03 with the following aims:

1. Prepare an inventory of H_2 emissions expected through the hydrogen value chain.
2. Identify the most critical archetypes in the H_2 chain in terms of emissions.
3. Develop and validate methods to gather data on H_2 emissions.
4. Create tools to simulate and quantify potential H_2 emissions under various scenarios.
5. Identify and develop solutions to mitigate H_2 emissions.
6. Provide recommendations for EU and international standards.

The project is aligned with the goals of the Horizon Europe Work Programme, aiming to support a sustainable and safe hydrogen economy. Thus, it is strongly connected to EU-projects funded under HORIZON-CL5-AWP23-D1-01-03: *Climate impacts of a hydrogen economy*, addressing the indirect forcing effect of H_2 emissions on the greenhouse effect.

Material and methods: As a first step, the project has defined the H_2 value chain, mapping its key components, operating conditions, and potential emission sources. This foundational work is being followed by the creation of an open-access inventory, which will aggregate data on hydrogen emissions from various processes and equipment. This inventory aims to serve as a vital resource for both the scientific community and industry, enabling consistent scenario analysis and informed decision-making. By welcoming contributions from external sources, the project aspires to continually expand and refine this database.

In addition to building the emissions inventory, the NHyRA project is advancing methodologies for detecting and quantifying hydrogen emissions. H_2 emissions can occur at any point along the supply chain, from production to end use, and can be intentional (venting and purging) or unintentional (leaks from pipelines, valves, tanks, and evaporation of liquid hydrogen). Three primary monitoring categories have been identified: 1) Detection of emissions at the component level; 2) Detection and quantification of emissions at the component level; 3) Surveillance and quantification of emissions at the area or site level.

The project leverages both existing and emerging techniques and instruments for these purposes. Furthermore, experimental, theoretical, and simulation-based methodologies are being developed and validated, allowing for accurate measurements in both laboratory and field settings. Critical elements of the hydrogen value chain will undergo experimental testing to assess their emission profiles. Looking ahead, the NHyRA project aims to provide a comprehensive understanding of hydrogen emissions by evaluating scenarios for the mid-term (2030) and long-term (2050) European hydrogen economy. These evaluations will help decision-makers quantify hydrogen's environmental impact, identify effective risk mitigation strategies, and prioritize actions for achieving a sustainable energy transition. Finally, the

project will formulate recommendations for standards and technical specifications to guide the hydrogen industry in minimizing emissions and ensuring safety.

Results: As the NHyRA project is approaching its mid-term, some results have been archived. A first version of the inventory of all the main archetypes involved in a hydrogen economy has been prepared. The main sources of hydrogen emission technologies to be assessed have been discussed and categorized, and an open-access, user-friendly tool to quantify emissions from the entire H_2 value chain is currently in development. The measuring campaign started. Sister projects focused on climate impacts of the H_2 economy have been individuated and collaborations were set up. Hydrogen release scenarios are being developed.

Conclusions: By addressing these knowledge gaps and fostering collaboration across scientific and industrial domains, the NHyRA project represents a critical step toward realizing hydrogen's potential as a cornerstone of the renewable energy landscape. The project is developing valid methods for assessing hydrogen releases to quantify the total hydrogen emissions under various scenarios. Critical points in the H_2 chain will be assessed and mitigation strategies will be recommended. Recommendations for EU and international standards will be provided.

Acknowledgments: This project has received co-funding from the European Commission and the Clean Hydrogen Partnership under Grant Agreement No 101137770. This Partnership receives support from the European Union's Horizon Europe Research and Innovation program, Hydrogen Europe and Hydrogen Europe Research.

References

[1] Arrigoni, A., and Diaz, B. L. (2022). Hydrogen emissions from a hydrogen economy and their potential global warming impact. Belgium, Germany: European Commission, JRC
[2] Ocko, I. B., and Hamburg, S. P. (2022). Climate consequences of hydrogen emissions. Atmos. Chem. Phys. 22, 9349–9368. doi:10.5194/acp-22-9349-2022
[3] Warwick, N.J., Archibald, *et al.* (2023). Atmospheric composition and climate impacts of a future hydrogen economy. Atmos. Chem. Phys. Prepr., doi:10.5194/acp-2023-29
[4] Sand, M., Skeie, R.B., Sandstad, M. *et al.* A multi-model assessment of the Global Warming Potential of hydrogen. *Commun Earth Environ* **4**, 203 (2023).
[5] Arrigoni, A., Dolci, F., *et al.* (2024). Environmental life cycle assessment (LCA) comparison of H_2 delivery options within Europe. Luxembourg: European Commission, JRC
[6] Esquivel-Elizondo, S.; Hormaza Mejia, A.; Sun, T.; Shrestha, E.; Hamburg, S. P.; Ocko, I. B. Wide Range in Estimates of Hydrogen Emissions from Infrastructure. Front. Energy Res. 2023, 11, 01–08
[7] https://nhyra.eu/

European Fuel Cells and Hydrogen
PIERO LUNGHI CONFERENCE
September 17th–19th 2025
Capri / Italy

Techno-economic feasibility study of an innovative proton conducting ceramic electrolysis system for hydrogen generation

M. Minutillo[a,d], F. Romano*[b], V. Cigolotti[c,d]

* corresponding author: fabiana.romano001@studenti.uniparthenope.it
[a] Department of Industrial Engineering, University of Salerno, Italy
[b] Department of Engineering, University of Naples Parthenope, Italy
[c] ENEA - Italian National Agency for New Technologies, Energy and Sustainable Economic Development, Italy
[d] ATENA Future Technology, Naples, Italy

Keywords: hydrogen, proton conducting ceramic electrolyzer, modelling, levelized cost of hydrogen

Abstract:

In this study, a preliminary techno-economic analysis (TEA) of an innovative electrolysis system based on the Proton-Conducting Ceramic Electrolysis (PCCEL) technology is carried out.

Introduction: Although the PCCEL technology is in an early stage of development, it can play an important role thanks to the production of pure, dry, and pressurized hydrogen. PCCEL can operate at intermediate temperatures with a higher efficiency than commercial electrolyzers, reducing cell degradation and allowing the use of inexpensive stainless-steel materials in pressurized systems [1].

Objectives: This study aims to estimate the Levelized Cost of Hydrogen (LCOH) for evaluating the economic feasibility of the hydrogen production by using the PCCEL technology.

Material and methods: In Figure 1, the model of the PCCEL system (1 MW), developed in the Aspen Plus™ environment, is illustrated. The Balance of Plant (BoP) mainly consists of heat exchangers needed to produce steam at the operating conditions required by the PCCEL unit. The electricity for assuring the system operation (electrolyzer and other components like the electric heater), is supplied by the electricity grid.

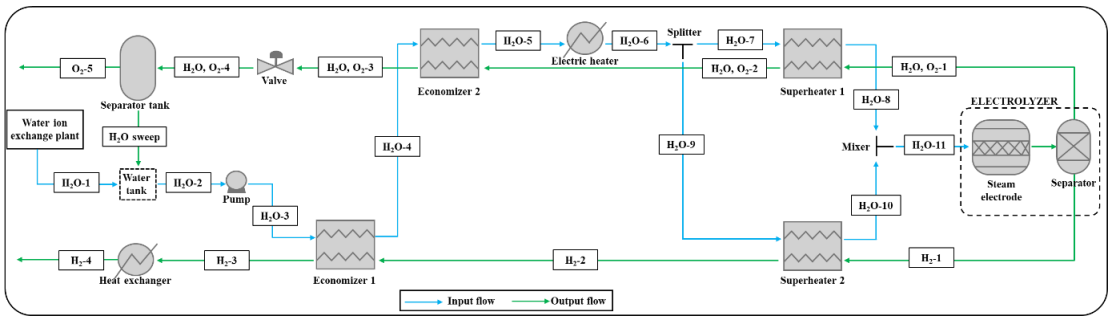


Figure 1- Flowsheet of the PCCEL system model

The calculated operating data and performance, as well as the investment costs ($CAPEX$), are listed in Table 1.

Table 1. Operating conditions, energy consumption and economic parameters

Operating data	Values	CAPEX (€)	Values
Operating Temperature (°C)	600	PCCEL	418,500 [2]
Operating pressure (bar)	15	Electric heater	12,645 [3]
System electrical consumption (kWh/kg)*	46.93	Separator tank	37,200 [4]
H_2O consumption (t/y)	1,792.50	Power converter	100,000
H_2 production (t/y)	200.56	Hotbox	482,695 [5]
O_2 production (t/y)	1,592		
Annual electricity consumption of system (MWh/y)**	9,412.7		

*Electrolyzer and electric heater consumption

**Considering 8,000 h/y operating hours

$CAPEX$ of the other components (i) of BoP can be calculated as follows:

$$CAPEX_i = a + bS^c$$

Where a and b are cost constants and c is a scaling exponent. They vary according to the type of equipment. S is the size parameter that differs according to the component and is calculated applying the equations illustrated in Table 2 [6].

Table 2. Calculation of the parameter S [6].

Component	Equation	Description
Water ion exchange plant, water tank, and pump	$S = \frac{m}{\rho}$	Ratio between the mass flows and their density in standard conditions.
Heat exchangers	$S = \frac{Q}{U \Delta T_{LMTD} F_t}$	Ratio between the heat transferred per unit time and the overall heat transfer coefficient, the log mean temperature difference and the correction factor.

Since $CAPEX$ of the BoP is referred to in 2012 and 2017, it is necessary to update these costs through the conversion factor inherent to Chemical Engineering Plant Cost Index ($CEPCI$) [7]. The economic parameters for estimating the operating and maintenance costs ($C_{O\&M}$) and the replacement cost (C_{rep}) are summarized in Table 3. The considered revenue (R_{O2}) is related to the oxygen that can be sold (0.13 €/m^3 [12]).

Table 3. Economic parameters for O&M estimation

Parameters	Value	Ref.
Electrolyzer $C_{O\&M}$	3% of C_{FC}/y	[8]
BoP $C_{O\&M}$	3% of C_{FC}/y	[8]
Deionized water $C_{O\&M}$	0.01 €/kg	[9]
Electricity $C_{O\&M}$	100 €/MWh	[10]
PCCEL membrane replacement C_{rep}	1,000 €/m^2 *	-

*Considering a stack area of 0.047 m^2

Thus, these calculated costs are used to estimate $LCOH$ taking into account the system's lifetime (N) of 20 years [11]:

$$LCOH = \frac{CRF \cdot [C_{FC} + \sum_{n=0}^{N-1}(C_{O\&M_an,n} + C_{rep_an,n=t} - R_{O_2_an,n})]}{m_{H_2,n}}$$

CRF is the capital recovery factor, i.e. the index used to calculate the present value of the annuity. It is calculated considering the real interest rate I_r (based on a nominal discount rate of 3% and an inflation rate of 2% [11]) and the system lifetime. The subscript "an" means that the costs are calculated as annualized costs [11]. C_{FC} is the total cost of the system ready for the start-up. This means that $CAPEX$ of electrolysis system must be increased by taking into account some cost factors (f) that refer to to the installation of the technical and engineering equipment [6]. It is calculated applying the following Equation:

$$C_{FC} = CAPEX \cdot [(1 + f_p) \cdot f_m + (f_{er} + f_{el} + f_i + f_c + f_s + f_l)] \cdot (1 + OS) \cdot (1 + D\&E + X)$$

Results: The estimated LCOH is 8.05 €/kg H_2 for the PCCEL system. The main contribution to this cost is due to the operating and maintenance costs, which have an impact of 76% on the LCOH value.

Conclusions: The preliminary results have highlighted the potential of this electrolysis technology, making it competitive with other technologies.

Acknowledgment:

PROTOSTACK project (n.101101504) has received support from the European Union's Horizon 2020 Research and Innovation Program, Hydrogen Europe and Hydrogen Europe Research.

References

[1] C. Herradon *et al.*, "Proton-conducting ceramics for water electrolysis and hydrogen production at elevated pressure," *Front Energy Res*, vol. 10, Oct. 2022, doi: 10.3389/fenrg.2022.1020960.

[2] R. J. Kee et al. "Perspectives on Technical Challenges and Scaling Considerations for Tubular Protonic-Ceramic Electrolysis Cells and Stacks," *J Electrochem Soc*, vol. 169, no. 5, p. 054525, May 2022, doi: 10.1149/1945-7111/ac6c4e.

[3] E. A. Harvego et al. "System Evaluations and Life-Cycle Cost Analyses for High-Temperature Electrolysis Hydrogen Production Facilities," 2012. [Online]. Available: http://www.inl.gov

[4] M. Ruth et al. "CEMAC-Clean Energy Manufacturing Analysis Center Manufacturing Competitiveness Analysis for PEM and Alkaline Water Electrolysis Systems Fuel Cell Seminar and Energy Expo CEMAC-Clean Energy Manufacturing Analysis Center 2," 2017.

[5] "https://www.bid-on-equipment.com/ovens-and-roasters/batch-ovens/410682~sahara-benko-10e04-cs-drum-hot-box-drum---tote-heater.htm".

[6] G. P. . Towler and R. K. . Sinnott, *Chemical engineering design : principles, practice and economics of plant and process design*. Butterworth-Heinemann is an imprint of Elsevier, 2022.

[7] S. Pratschner et al. "Techno-economic assessment of a power-to-green methanol plant," *Journal of CO2 Utilization*, vol. 75, Sep. 2023, doi: 10.1016/j.jcou.2023.102563.

[8] R. Hancke, T. Holm, and Ø. Ulleberg, "The case for high-pressure PEM water electrolysis," *Energy Convers Manag*, vol. 261, Jun. 2022, doi: 10.1016/j.enconman.2022.115642.

[9] D. Jang et al. "Techno-economic analysis and Monte Carlo simulation of green hydrogen production technology through various water electrolysis technologies," *Energy Convers Manag*, vol. 258, Apr. 2022, doi: 10.1016/j.enconman.2022.115499.

[10] "Electricity prices in Europe fell significantly in January 2023. https://gmk.center/en/posts/electricity-prices-in-europe-fell-significantly-in-january-2023/."

[11] A. Perna et al. "Designing, sizing and economic feasibility of a green hydrogen supply chain for maritime transportation," *Energy Convers Manag*, vol. 278, Feb. 2023, doi: 10.1016/j.enconman.2023.116702.



Electrosynthesis of Low-Carbon Olefins: A New Paradigm for Hard to Abate Industries

E.A. Nanaki[1,2], S. Kiartzis[1] , M. Papageorgiou[1] ,C. Athanasiou[3], A. Banti[4,5], V. Kyriakou[6], M. Konsolakis[7], G.E. Marnellos[4,5]

[1]Dept. New Technologies and Alternative Energy Sources, HELLENiQ ENERGY, Athens, Greece
[2]University of Aarhus, Dept. of Business Development and Technology, Herning, Denmark
[3]Department of Environmental Engineering, Democritus University of Thrace, Xanthi, Greece
[4]Chemical Process & Energy Resources Institute, CERTH, Thermi, Thessaloniki, Greece
[5]Department of Chemical Engineering, Aristotle University of Thessaloniki, Thessaloniki, Greece
[6]Department of Chemical Engineering, Engineering and Technology Institute Groningen (ENTEG), University of Groningen, Groningen, The Netherlands
[7]Technical University of Crete, School of Production Engineering and Management, Chania, Greece

* corresponding author: enanaki@helleniq.gr

Keywords: Light Olefins; Co-Ionic Electrochemical membrane reactors (ci-EMRs). Market Analysis ; Innovation;

Abstract

Low-carbon olefins, as important platform molecules, are generally produced by limited fossil energy, resulting in massive carbon emissions and intensive energy consumption inevitably. Therefore, it is necessary to develop clean and sustainable alternatives. With this in mind, the ECOLEFINS project was granted aiming to address these issues by introducing a new paradigm for the electrosynthesis of C_2-C_4 olefins using co-ionic electrochemical membrane reactors (ci-EMRs). This innovative approach captures and valorizes CO_2 to produce carbon-negative ethylene, propylene, and butylene, integrating anodic steam electrolysis for hydrogen production with cathodic CO_2 electrolysis and hydrogenation. Preliminary results indicate promising impacts on electricity requirements and economics, positioning the ECOLEFINS project to capitalize on the growing demand for sustainable chemical products and establish itself as a leader in the industry. This work presents preliminary findings from techno-economic analysis and life cycle sustainability assessment aiming to evaluate its feasibility and market potential.

Introduction:

The energy transition and emission reduction in the chemical industry are among the top global priorities in addressing climate change. As a significant energy-intensive sector, the chemical industry accounts for approximately 30% of global industrial energy consumption [1]. Its primary energy sources—oil and natural gas (NG)—serve both as energy carriers and as a feedstock for chemical production. Due to its heavy reliance on fossil fuels, the chemical industry is a major contributor to greenhouse gas (GHG) emissions, responsible for about 10% of global carbon dioxide (CO_2) emissions

and 14.5% of direct industrial emissions [2]. Low-carbon olefins (i.e., ethylene, propylene, and butylene) are essential building blocks for producing polymers, fibers, plastic, and other organic chemical materials in the petrochemical industry [3]. Generally, steam cracking and fluid catalytic cracking of fossil-based naphtha and petroleum are currently common processes for low-carbon olefins production [4]. However, the energy-intensive traditional processes produce considerable CO2 emissions, resulting in serious climate, environmental and ecological problems [5]. Thus, it is necessary to develop sustainable and clean alternatives for producing low-carbon olefins. In this direction, ECOLEFINS project was granted to originally put forward a new paradigm for C2-4= electrosynthesis in co-ionic (H+ and O2-) electrochemical membrane reactors (ci-EMRs). The proposed concept reverses the heavy CO_2 emissions associated to the petroleum-based light olefins production to massive CO_2 capture and valorisation for carbon negative ethylene, propylene and butylene. The concept introduces co-ionic ceramic membrane reactors and short-stacks/modules that merge the anodic steam electrolysis for hydrogen production with the cathodic CO_2 electrolysis and hydrogenation to light olefins, over tailored and nano-engineered electrodes; aiming to develop a substantially more effective technology, for the single-step, RES-powered artificial photosynthesis of CO_2 to valuable chemicals (**Figure 1**).

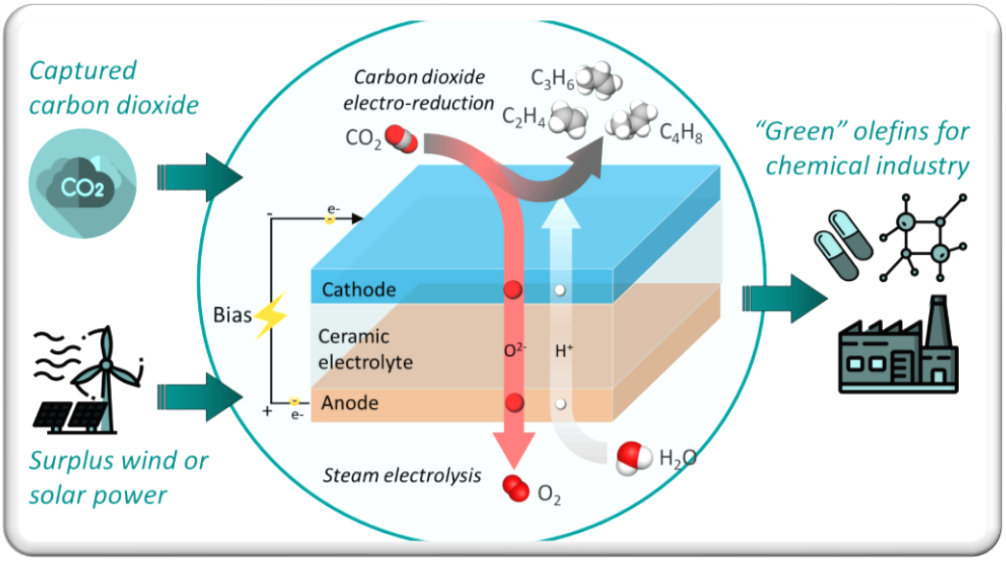


Figure 1. ECOLEFINS concept

The present work describes the ECOLEFINS concept and examines the impacts of the ci-EMRs' targeted performance on the electricity requirements and the economics of electrified C2-4=s, with respect to C2-4='s yields, ci-EMRs' specific resistance, electricity prices, carbon taxes and technology costs. A techno-economic analysis study is performed, in order to evaluate the technical and economic feasibility of the proposed process using different criteria: technical performance (carbon element efficiency and energy efficiency), environmental performance (emission CO_2-eq), and economic performance (unit production cost). In addition, major cost parameters are evaluated in sensitive

analysis study that identifies the key strategies to make the proposed process feasible. Business models are investigated for the market scale up.

Objectives:

- To assess the techno-economic and sustainability prospects of EMR industrial applications aiming to digital modelling of real-scale integrated ci-EMR plants. This will form the base for evaluation of the economic feasibility and overall sustainability profile of ECOLEFINS concept.
- To investigate the social acceptance and marketization prospects within the sectors of: (i) light olefins current producers (refineries) and end users (chemical industries of C2-4= utilization), and (ii) solid oxide cells materials, cells and stack/module prototypes, as well as ci-EMR systems and integrated processes.
- To develop coherent business models for market scale up.

Material and methods:

- Life Cycle Sustainability Analysis (LCSA) is going to be conducted. This includes Life Cycle Assessment (LCA), Life Cycle Costing (LCC) and Social Life Cycle Analysis (S-LCA). LCA takes into consideration the involved energy as well as ci-EMR (cells, stacks and modules) materials flows, with special emphasis to critical ones (e.g. Co, Gd, La, Ce), along with water resources (potentially grey or black) and wastes (including emissions) and by-products (CO, CH4, HCs etc.).
- Business plans, business canvas, scenario, PEST and SWOT analyses, competitive matrices and projected balance-sheets
- Stakeholder mapping and analysis.

Results: Results are under development as the project currently examines the impacts of the ci-EMRs' targeted performance on the electricity requirements and the economics of electrified C2-4=s, with respect to C2-4='s yields, ci-EMRs' specific resistance, electricity prices, carbon taxes and technology costs. Furthermore, preliminary results of Life Cycle Assessment (LCA), Life Cycle Costing (LCC) and Social Life Cycle Analysis (S-LCA) are under development.

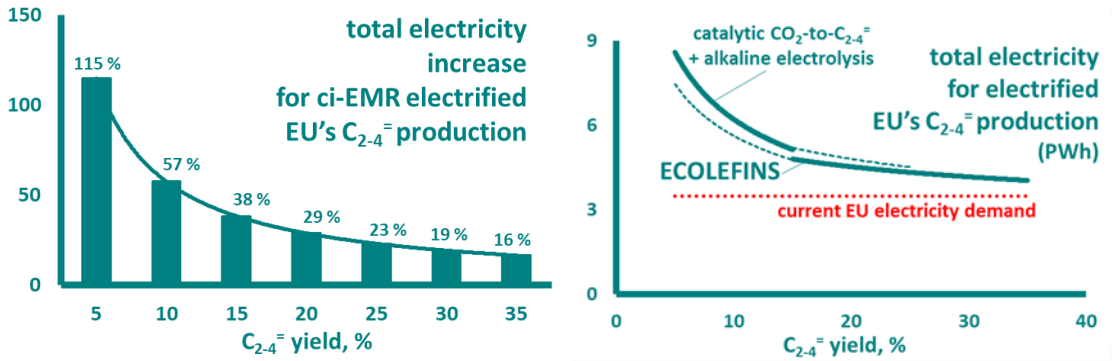


Figure 2. Total electricity increase for ci-EMR electrified EU's C2-4 production and comparison to ECOLEFINS

Conclusions: ECOLEFINS project is well-positioned to capitalize on the growing demand for sustainable chemical products. By adopting suitable business models and leveraging favorable market trends, the

project can achieve significant market penetration and establish itself as a leader in the sustainable chemical industry. Strategic partnerships, continuous innovation, and a strong focus on sustainability are key factors to its success.

Acknowledgment

This research has received funding from the European Union under grant agreement No 101099717 – ECOLEFINS project and UK Research and Innovation (UKRI) under the UK governments Horizon Europe funding Guarantee (10079292). Views and opinions expressed are however those of the author(s) only and do not necessarily reflect those of the European Union or European Innovation Council and SMEs Executive Agency (EISMEA) or UK Research and Innovation granting authorities. Neither the European Union nor the granting authorities can be held responsible for them.

Funded by the European Union

UK Research and Innovation

References

[1] IEA. Energy Technology Perspectives 2020; IEA: Paris, France, 2020; Available online: https://www.iea.org/reports/energy-technology-perspectives-2020

[2] IEA. Industry. Available online: https://www.iea.org/reports/industry

[3] T. Witoon, V. Lapkeatseree, T. Numpilai, C. Kui Cheng, J. Limtrakul CO2 hydrogenation to light olefins over mixed Fe-Co-K-Al oxides catalysts prepared via precipitation and reduction methods, Chem. Eng. J., 428 (2022), Article 131389, 10.1016/j.cej.2021.131389

[4] M.A. Alabdullah, A.R. Gomez, J. Vittenet, A. Bendjeriou-Sedjerari, W. Xu, I.A. Abba, J. Gascon, A viewpoint on the refinery of the future: Catalyst and process challenges. ACS Catal., 10 (15) (2020), pp. 8131-8140, 10.1021/acscatal.0c02209

[5] M. Fakhroleslam, S.M. Sadrameli, Thermal cracking of hydrocarbons for the production of light olefins; A review on optimal process design, operation, and control ,Ind. Eng. Chem. Res., 59 (27) (2020), pp. 12288-12303, 10.1021/acs.iecr.0c00923

EFCH2 2025 European Fuel Cells and Hydrogen
PIERO LUNGHI CONFERENCE
September 17th–19th 2025
Capri / Italy

Techno-economic assessment of large-scale hydrogen production via solid oxide electrolysis systems

Marco Ficili[a], Stefano Campanari[a], Paolo Colbertaldo*[,a]

* Corresponding author: paolo.colbertaldo@polimi.it
[a] Group of Energy Conversion Systems (GECoS), Department of Energy, Politecnico di Milano – Milan, Italy

***Keywords**: Low-carbon hydrogen, Solid oxide electrolysis, Techno-economic, Bottom-up.*

Abstract

Hydrogen is regarded as one of the main enablers of the decarbonisation process. Among production technologies, Solid Oxide Electrolysers (SOEs) operating at high temperature offer enhanced electric efficiency. Nonetheless, their diffusion is still limited by manufacturing scale and costs. This work, in the framework of the OUTFOX project, explores SOE-based hydrogen production systems under the techno-economic point of view. Results show a notable impact of hot recuperators and hydrogen compressor on CAPEX, whereas LCOH is strongly dependent upon the electricity supply costs.

Introduction

Hydrogen is expected to have a key role in the decarbonisation process of the upcoming decades. However, less than 1% of the current production uses low-emission technologies, and efforts are needed to increase this share by adopting large-scale efficient electrolysis systems coupled with renewable electricity generation [1]. Among electrolysis technologies, Solid Oxide Electrolysers (SOE) feature enhanced electrical efficiency thanks to high operating temperature (600-900°C). Nonetheless, manufacturing scale and costs are still limiting the diffusion of this technology.

In this context, the Horizon Europe project OUTFOX aims to overcome the challenge of scalability and to achieve ambitious goals in cost and life-cycle CO_2 emissions for hydrogen production [2]. This is pursued by manufacturing and testing cells with decreased thickness (<400 µm) and increased surface area (up to 900 cm^2), and by developing advanced solutions for stack and module assemblies. The validation will be achieved through 80 kW prototype testing for a total of 4000 h of operation.

Objectives

This work focuses on the techno-economic aspects of such plant. A process model of the modular SOE plant is developed, targeting large capacities (up to 100 MW_e). Building on the identified layout, a bottom-up CAPEX calculation is carried out. The levelized cost of hydrogen (LCOH) is then estimated, based on the plant's electricity and external heat needs as derived from process simulations.

Material and methods

The SOE system process model was developed in Aspen Plus®, serving as foundation for the techno-economic and life-cycle assessments. The plant layout (Figure 1) features liquid water as feed, and exploits internal heat recovery along both the air and fuel streams to reduce the external energy need for water evaporation/heating. The system operates at ambient pressure and includes

compression up to 30 bar, in line with reference technologies (steam reforming and low-temperature electrolysis).

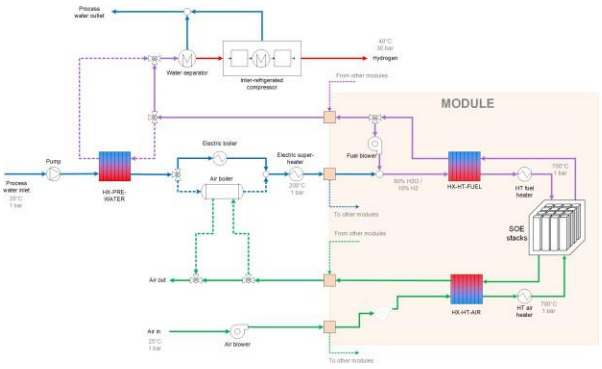


Figure 1. SOE plant layout.

Parameter	Value	Unit	Source
Electricity consumption (excl. boiler and compressor)	38.1	kWh/ kg_{H2}	Process modelling
Thermal consumption	7.02	kWh/kg_{H2}	Process modelling
Compressor consumption	2.31	kWh/kg_{H2}	Process modelling
Discount factor	8	%	Own assumption
Lifetime	25	y	Own assumption
EUR/USD conversion	1.08	-	Early 2024
Specific capex stack	72-306	€/$kW_{e,nom}$	[6]
Fixed O&M	6	%/y of capex	Including stack replacement [7]
Electricity cost	50	€/MWh_e	Own assumption

Table 1. Main techno-economic assumptions.

The model captures the inherent modularity of electrochemical systems and enables simulation at multiple levels: stack, high-temperature balance-of-plant (BoP), and low-temperature auxiliary components. The SOE stack is represented with a lumped model, calibrated against experimental polarization curves obtained from short-stack tests conducted within the OUTFOX project. BoP components such as heaters, heat exchangers, pumps, and compressors are modelled using standard unit operations. Capital expenditure (CAPEX) is estimated using a bottom-up approach that combines cost functions from chemical engineering handbooks [3,4] and outputs from Aspen Economic Analyzer®. The latter is particularly relied upon for complex components like the intercooled compressor, for which handbook-based estimates vary significantly [5]. Stack manufacturing costs are evaluated across different manufacturing scales [6]. The levelized cost of hydrogen (LCOH) is then calculated under diverse operational scenarios, hereby represented by plant capacity factor. The main process simulation results and techno-economic assumptions are summarised in Table 1.

Results

System CAPEX decreases by nearly one third when the stack manufacturing scale increases from 25 to 1000 MW/y. Despite this, SOE stacks contribute less than 20% on the total investment (Figure 2, left). The largest CAPEC shares are associated with hydrogen compressor (35%) and high-temperature recuperators (15%), with the latter requiring materials able to withstand hot conditions. The current estimation assumes one compressor serving four SOE modules of 1 MW each; this may benefit from substantial cost reductions through scale-up. In contrast, cost reductions for high-temperature recuperators are more challenging, as their size and number scale with the stack configuration. For these, ongoing developments such as larger stack and hot-box designs may help.

The LCOH is predominantly influenced by electricity supply cost, while CAPEX accounts for less than 20%. Notably, the energy required for steam generation (here assumed supplied as electricity) represents up to 13% of the final hydrogen cost.

Aiming to supply fully renewable electricity, the reasonable operation schedule inevitably reduces the capacity factor (unless massive electric energy storage is considered). Halving the capacity factor (as could be obtained via a balanced hybrid Photovoltaic+Wind+Battery system) yields a 10-20% increase in LCOH. A 40x increase in manufacturing scale appears to reduce the specific CAPEX by a third, and

this yields an LCOH reduction of 5-10%. Thus, these two effects may be taken into consideration for trade-off impacts (see first and last bars in Figure 2 right).

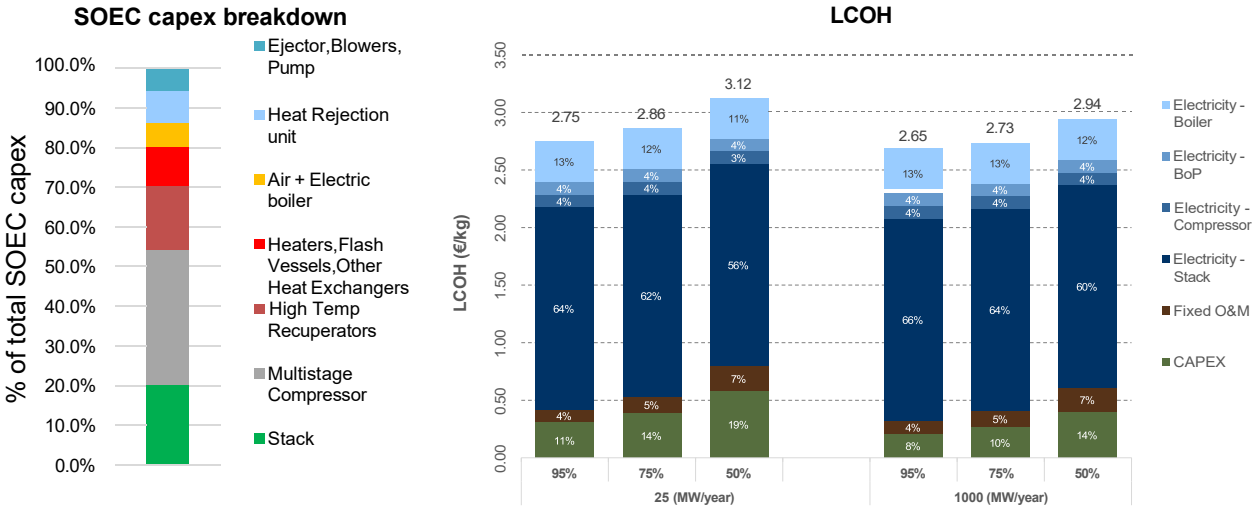


Figure 2. Capital expenditure (CAPEX) breakdown for a manufacturing scale of 1000 MW/y (left) and LCOH assuming two stack manufacturing scales under different capacity factor scenarios (right).

Conclusions

This work has analysed a modular SOE-based system for hydrogen production from liquid water. The estimated CAPEX is 400-600 €/kW, assuming mass manufacturing of stacks. The LCOH is primarily driven by electricity costs, with capacity factor and stack manufacturing scale playing secondary roles. CAPEX contributes less than 20% to the LCOH, highlighting that improving system efficiency, particularly through enhanced internal heat recovery, may offer more impactful cost reductions than capital cost alone. Future work will focus on optimizing system modularity to further reduce CAPEX and exploring integration strategies with renewable electricity sources to enhance operational flexibility and cost-effectiveness.

Acknowledgment

This work has been developed within the project OUTFOX (*Optimized up-scaled technology for next-generation solid oxide electrolysis*). The project has received funding from the EU under the Horizon Europe programme (GA n. 101101439).

References

[1] IEA, Global Hydrogen Review 2023, 2023. https://doi.org/10.1787/cb2635f6-en.
[2] OUTFOX project website. https://outfoxproject.com/.
[3] M.S. Peters, K.D. Timmerhaus, *Plant Design and Economics for Chemical Engineers*, McGraw Hill, 2003.
[4] W.D. Seider, D.R. Lewin, J.D. Seader, S. Widagdo, R. Gani, K.M. Ng, *Product and process design principles*, Wiley, 2017.
[5] W.L. Luyben, *Capital cost of compressors for conceptual design*, Chemical Engineering and Processing - Process Intensification 126 (2018) 206–209. https://doi.org/10.1016/j.cep.2018.01.020.
[6] J.H. Prosser, B.D. James, B.M. Murphy, D.S. Wendt, M.J. Casteel, T.L. Westover, L.T. Knighton, *Cost analysis of hydrogen production by high-temperature solid oxide electrolysis*, Int J Hydrogen Energy 49 (2024) 207–227. https://doi.org/10.1016/j.ijhydene.2023.07.084.
[7] Clean Hydrogen JU, *SRIA Key Performance Indicators (KPIs)*. https://www.clean-hydrogen.europa.eu/knowledge-management/strategy-map-and-key-performance-indicators/clean-hydrogen-ju-sria-key-performance-indicators-kpis_en (accessed November 18, 2024).

European Fuel Cells and Hydrogen
PIERO LUNGHI CONFERENCE
September 17th–19th 2025
Capri / Italy

Blue hydrogen can be a low-carbon hydrogen

Mehrshad Kolahchian Tabrizi , Caecilia R. Vitasari, Davide Bonalumi*, and Stefano Campanari

* corresponding author: Davide Bonalumi
Department of Energy, Politecnico di Milano, Milan, Italy

Keywords: Blue hydrogen, Carbon capture, Carbon footprint, Life Cycle Assessment

Abstract

Introduction: *Hydrogen is seen as one of the main players in the net-zero emission scenarios (NZE) [1]. For a NZE scenario in 2030, hydrogen production via the application of electricity and fossil fuels with Carbon Capture, Utilization, and Storage (CCUS) will reach 51.6 and 17.9 Mt, respectively [2]. In these strategies, hydrogen should be produced with low CO_2 equivalent emissions (low-carbon H_2). The current EU classification for sustainable activities (EU Taxonomy Regulation 2020/852) requires hydrogen production to remain below 3 kg CO_2 eq./kg H_2 [3]. According to DIRECTIVE (EU) 2024/1788, low-carbon hydrogen is produced from non-renewable sources and must reduce GHG emissions by at least 70% compared to the fossil fuel benchmark (94 g CO_2 eq./MJ) [4], equivalent to 3.38 kg CO_2 eq./kg H_2.*

Objectives: *The current study tries to address whether blue hydrogen meets the carbon footprint requirements and qualifies as low-carbon H_2. It investigates the techno-environmental performance of Auto Thermal Reforming (ATR) of natural gas and absorption-based CO_2 separation configuration, featuring the effect of the specific natural gas supply chain on the carbon footprint of blue hydrogen production.*

Material and methods: *ATR integrated with a chemical absorption unit based on MDEA (methyl diethanolamine) is simulated in Aspen Plus V14. Also, for comparison with literature, ATR coupled with carbon capture units from the absorption family, MDEA and Selexol (physical solvent), are included [5,6]. In simulated cycles, the CO_2 separation is only applied to the syngas (not flue gas), with the carbon capture rate (CCR) set to a minimum of 95%, while the configuration with Selexol is the only layout that also applies CO_2 separation from the flue gases. To meet the target hydrogen recovery of 98.5%, a recycle stream of PSA off-gases is used, as the PSA alone recovers 90% of the inlet hydrogen. The hydrogen output is 20,000 kg/h at 50 bar and 30 °C. CO_2 output is at 150 bar and 30 °C.*
The attributional LCA modeling is used to evaluate the carbon footprint of blue H_2 production. The LCA is performed following the principles of ISO 14040 and 14044 standards. GaBi

software and the library Sphera LCA database (2023.2) are used. Life cycle impact assessment is performed using the Environmental Footprint (EF) 3.1 characterization method, limited to GWP_{100}. The functional unit is 1 kg of gaseous hydrogen, with a cradle-to-gate (CTG) system boundary. In the part of the study analyzing the natural gas supply chain's impact on blue hydrogen's carbon footprint, the system boundary also covers CO_2 transport to the reservoir.

Results: *The configurations of ATR and MDEA with 95% and 99% CCR are compared. The slightly higher heat requirement for MDEA99 compared to MDEA95 results in 1 MW lower internal electricity production, leading to overall efficiencies of 76.19% and 76.23%, respectively. The carbon footprint of blue hydrogen production from the 4 selected ATR and carbon capture configurations is depicted in* ***Figure 1****. Using the natural gas in Italy based on GaBi, the carbon footprint of all the configurations is higher than the threshold of 3 kg CO_2 eq./kg H_2, assumed as a reference to qualify low-carbon fuels in the EU taxonomy [3], except for configurations with MDEA99 and Selexol with electricity supply from PV, resulting in GWP values equal to 2.87 and 2.56 kg CO_2 eq./kg H_2, respectively.*

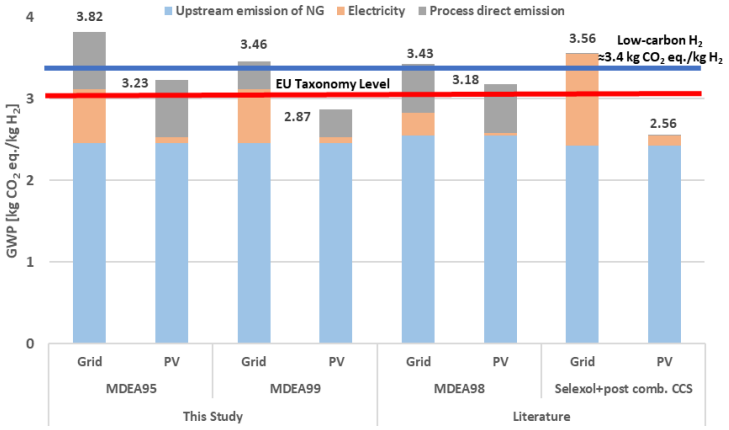


Figure 1. *The carbon footprint of blue hydrogen production via the 4 selected configurations*

Comparing the MDEA95 and MDEA99 cases shows that maximizing the carbon capture with only a limited increase in reboiler duty, which reduces the internal electricity production and raises the electricity import, is still beneficial in terms of carbon footprint performance, leading to a 9% and 11% GWP reduction for the grid and PV electricity supplied cases, respectively.

The contribution of natural gas to the carbon footprint of blue H_2 can vary depending on the natural gas supply chain, as shown in ***Figure 2****. The GWP value of blue H_2 based on Norway's gas is lower than 2 kg CO_2 eq./kg H_2 and can be as low as 0.87 kg CO_2 eq./kg H_2 for the CCR 99.5% configuration with PV electricity. For LNG from Qatar, the carbon footprint of the obtained H_2 can be less than 3 kg CO_2 eq./kg H_2 when renewable electricity is used.*

The average value of the estimated carbon footprint of all configurations is 3.3 kg CO_2 eq./kg H_2, while excluding the U.S. LNG dataset, the average carbon footprint of blue hydrogen powered by PV electricity is 2.6 kg CO_2 eq./kg H_2. These values are in the vicinity of the EU taxonomy level (3 kg CO_2 eq./kg H_2) and are lower than the low-carbon hydrogen definition

level based on EU directives (3.38 kg CO_2 eq./kg H_2). Blue hydrogen produced from a very low-emission natural gas supply chain, like Norwegian natural gas, can be competitive with wind-based green H_2 and may outperform the PV-based green H_2 (1 and 2 kg CO_2 eq./kg H_2 [7]).

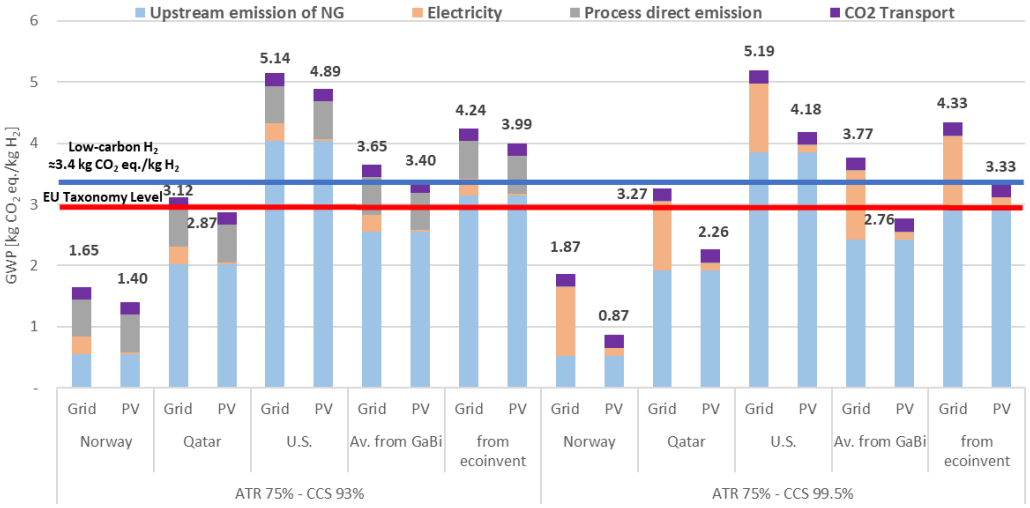


***Figure 2**. Carbon footprint of blue hydrogen produced from natural gas with different supply chains*

Conclusions: *The study presented the techno-environmental analysis of the reforming of natural gas coupled with carbon capture and storage (blue H_2). The findings show that for a proper blue H_2, partial electrification (for CO_2 separation unit to reduce the extra natural gas consumption due to CO_2 capture energy requirements), the use of renewable electricity, and maximizing the CCR rate can keep the carbon footprint below the EU taxonomy level or very close to it in most scenarios.*

Acknowledgment

This research was partly funded by the H2 JRP (Hydrogen Joint Research Partnership) at Politecnico di Milano (https://www.fondazionepolitecnico.it/en/initiatives/hyd)

References

[1] International Energy Agency (IEA). World Energy Outlook 2022. 2022.
[2] International Energy Agency (IEA). Global Hydrogen Review 2024. Paris: 2024.
[3] EU Commission. ANNEX 1 to the Commission Delegated Regulation supplementing Regulation (EU) 2020/852 of the European Parliament and of the Council: Manufacture of hydrogen 2021. https://doi.org/https://eur-lex.europa.eu/legal-content/EN/TXT/?uri=PI_COM:C(2021)2800.
[4] THE EUROPEAN PARLIAMENT AND THE COUNCIL OF THE EUROPEAN UNION. Directive (EU) 2024/1788 of the European Parliament and of the Council of 13 June 2024 on common rules for the internal markets for renewable gas, natural gas and hydrogen, amending Directive (EU) 2023/1791 and repealing Directive 2009/73/EC (recast) 2024. https://eur-lex.europa.eu/eli/dir/2024/1788/oj (accessed January 19, 2025).
[5] Antonini C, Treyer K, Streb A, van der Spek M, Bauer C, Mazzotti M. Hydrogen production from natural gas and biomethane with carbon capture and storage – A techno-environmental analysis. Sustain Energy Fuels 2020;4:2967–86. https://doi.org/10.1039/D0SE00222D.
[6] Zang G, Graham EJ, Mallapragada D. H2 production through natural gas reforming and carbon capture: A techno-economic and life cycle analysis comparison. Int J Hydrogen Energy 2024;49:1288–303. https://doi.org/10.1016/j.ijhydene.2023.09.230.
[7] Kolahchian Tabrizi M, Famiglietti J, Bonalumi D, Campanari S. How the boundaries of the supply chain affect climate profile: The case of renewable electricity and green hydrogen for Italy and the UK. Int J Hydrogen Energy 2025;106:156–70. https://doi.org/10.1016/j.ijhydene.2025.01.372.

EFCH2 2025
European Fuel Cells and Hydrogen
PIERO LUNGHI CONFERENCE
September 17th–19th 2025
Capri / Italy

Driving Energy Transition in Ports: Hydrogen-Powered Heavy-Duty Vehicles in Port Logistics

An economic and environmental assessment through Total Cost of Ownership analysis

Alessia Piccolo*[a], Andrea Altomonte [a], Elio Simeoni [a] ,Viviana Cigolotti [b], Elio Jannelli [a]

* Corresponding author: Alessia Piccolo - alessia.piccolo@atenaweb.com
[a] University of Naples Parthenope
[b] ENEA

Port logistics, Hydrogen, TCO, Sustainability, Heavy-duty vehicles

Abstract

In recent years, increasing focus on environmental sustainability has extended to the port sector, which, despite its crucial economic role, significantly contributes to local air pollution and associated public health concerns. Evaluating the economic and environmental sustainability of terminal trucks used for container handling through a Total Cost of Ownership (TCO) approach has become an essential tool for guiding strategic decisions aimed at achieving decarbonization targets. Results show that, supported by appropriate incentives and sustainable hydrogen production, fuel cell trucks represent a competitive and cleaner alternative for port operations.

Introduction

The maritime port sector is increasingly involved in the global effort toward climate neutrality. Ports, as strategic freight transport hubs, are undergoing significant transformation through the integration of sustainable technologies [1]. Among the most promising innovations is the use of hydrogen-powered heavy-duty vehicles, particularly 4x2 terminal trucks used for container handling and short-haul operations. These vehicles offer a clean alternative to traditional diesel-powered machinery, supporting decarbonization objectives while maintaining operational performance. With high energy density and zero tailpipe emissions, hydrogen represents a compelling energy vector for sustainable port logistics [2].

Objectives

Building on the outcomes and insights from the European H2Ports initiative, which promotes the integration of hydrogen technologies into port operations, this study independently evaluates the viability of 4x2 terminal trucks powered by hydrogen fuel cells. The analysis

compares three drivetrain configurations: diesel, battery electric (BEV), and fuel cell electric (FCEV), using a TCO approach over a 6-year operational period. The assessment considers both direct economic costs and environmental externalities, including CO_2 emissions. The cost associated with the EU Emissions Trading System (ETS) has also been incorporated into the Total Cost of Ownership (TCO) calculation. This comprehensive approach allows for a more accurate estimation of the overall cost of the diesel model, while simultaneously highlighting the comparative benefits of more sustainable alternatives. The analysis is intended to support port authorities and relevant stakeholders with evidence-based insights to inform the transition toward zero-emission logistics.

Material and methods

This study applies a mixed framework [3], integrating real operational data from the Port of Genoa, market costs, and techno-economic modeling for operating in port terminal yards. Inputs include annual energy consumption with different scenarios, duty cycles, maintenance, CAPEX, OPEX, system efficiency, and fuel prices sourced from industry data and literature. Three hydrogen supply scenarios are evaluated: green hydrogen, SMR-based hydrogen, and commercial hydrogen at a fixed market price. A 4% real discount rate and 5% inflation are applied, using 2024 energy prices as the baseline. Vehicle emissions are monetized with ETS costs and analyzed in the economic assessment.

The analysis assumes a nominal battery capacity of 236 kWh with 90% usable energy (~212 kWh). Under typical operating hours and consumption patterns, BEVs consume approximately 495 kWh daily. Diesel trucks consume about 196 liters per day, while FCEVs use 26 kg of hydrogen. Given the BEV's usable capacity, it can operate for roughly 8 hours per day. *To cover a 20-hour operational schedule, two BEVs are needed, effectively doubling the total costs.

Results

The diesel truck has the lowest purchase cost but incurs high fuel expenses, leading to a relatively high total cost of ownership, which rises significantly with fuel prices. BEVs have higher initial purchase costs but benefit from significantly lower energy expenditures especially when powered by renewable photovoltaic electricity, resulting in a substantially reduced TCO. FCEVs show mixed outcomes: green hydrogen provides a balanced profile with moderate costs and low emissions, while reforming-based hydrogen yields the lowest TCO thanks to its low fuel price, it comes with a higher environmental burden. Overall, FCEVs offer the most favorable trade-off between economic and environmental performance compared to diesel, especially when accounting for the social costs of pollutant emissions.

Type of Vehicle	MIN TCO with ETS value	MAX TCO with ETS value

ICE	735 K€	989 K€
BEV*	1.019 K€	1.192 K€
FCEV	439. K€	639 K€

Table 1: Total Economic TCO with ETS value over a 6-Year Lifetime

Conclusions

The study confirms that hydrogen-powered 4x2 terminal trucks, particularly FCEVs, are a feasible and strategic solution for sustainable port logistics. Compared to BEVs, FCEVs offer key operational advantages, such as faster refuelling times, longer range, and the ability to cover all of the vehicle's daily operational hours, a crucial factor in intensive, continuous-use port environments [4]. These characteristics make FCEVs especially suitable for high-duty cycles common in container terminal operations.

Inspired by the H2Ports initiative, this analysis explores the replicability of hydrogen-based solutions in other European ports, especially when supported by EU funding, scalable infrastructure, and renewable energy integration. The results highlight not only the economic and environmental viability of FCEVs, but also their potential to support broader sustainability goals, including emissions reduction, improved air quality, and enhanced operational resilience.

Future studies should explore progressive deployment scenarios, the integration with renewable hydrogen supply chains, and the social and environmental co-benefits of hydrogen technologies in the maritime sector.

Acknowledgment

This work was supported by the projects HyPOTT – Hydrogen hybrid Power unit for a 4x2 Terminal Tractor, funded by the European Union under the Italian National Recovery and Resilience Plan (PNRR), M4C2 – Investment 1.3, within the research program "Extended Partnership Network 4 Energy Sustainable Transition – NEST", and SPOTT – Smart Port Terminal Tractor for AI-Aided Logistics, funded by the European Union under PNRR MUR M4C2 – Investment 1.5, as part of the "Innovation Ecosystems – RAISE" initiative (Ministerial Decree No. 3277/2021).

References

[1] Holder, D., Percy, S. D., & Yavari, A. (2024). A Review of Port Decarbonisation Options: Identified Opportunities for Deploying Hydrogen Technologies. *Sustainability*, *16*(8), 3299. https://doi.org/10.3390/su16083299

[2] Zheng, Y., Zhao, J., & Shao, G. (2020). Port City Sustainability: A Review of Its Research Trends. *Sustainability*, *12*(20), 8355. https://doi.org/10.3390/su12208355

[3] Burnham, Andrew, Gohlke, David, Rush, Luke, Stephens, Thomas, Zhou, Yan, Delucchi, Mark A., Birky, Alicia, Hunter, Chad, Lin, Zhenhong, Ou, Shiqi, Xie, Fei, Proctor, Camron, Wiryadinata, Steven, Liu, Nawei, & Boloor, Madhur (2021). Comprehensive Total Cost of

Ownership Quantification for Vehicles with Different Size Classes and Powertrains. https://doi.org/10.2172/1780970

[4] De Wolf, D., & Smeers, Y. (2023). Comparison of Battery Electric Vehicles and Fuel Cell Vehicles. World Electric Vehicle Journal, 14(9), 262. https://doi.org/10.3390/wevj14090262

EFCH2 2025
European Fuel Cells and Hydrogen
PIERO LUNGHI CONFERENCE
September 17th–19th 2025
Capri / Italy

Hydrogen's impact on the environment in a net-zero plastics industry

Inga-Marie Lahrsen[a], Eleonora Bargiacchi[a], André Bardow*[a]

* corresponding author: abardow@ethz.ch
[a] ETH Zurich, Tannenstrasse 3, 8092 Zürich, Switzerland

Keywords: Life cycle assessment, prospective analysis, chemical industry, hydrogen demands

Abstract Introduction:

The plastics industry is a large greenhouse gas (GHG) emitter and will have to undergo a redesign to reach climate neutrality in the future. According to UNEP [1], plastics production could account for 19% of global GHG emissions by 2040. Achieving net-zero emissions in this sector by 2050 is expected to rely on clean hydrogen. However, the exact hydrogen demand needed for a net-zero plastics industry is unclear, along with its potential other impacts on the environment.

Objectives:

In our work, we apply prospective life cycle assessment (pLCA) to assess the importance of hydrogen in a plastics industry that targets minimum climate-change impacts. We calculate the required hydrogen and its supply technology and evaluate the plastic industry's footprint across various environmental impact categories.

Material and methods:

Our study is based on a model of the plastics industry, which is extended by a set of hydrogen production technologies, such as methane steam reforming, biomass gasification, and water electrolysis. The resulting model covers over 400 chemical processes, allowing to produce 90% of the global plastics production, including end-of-life treatment [2], [3]. The model represents both high and low Technology Readiness Level (TRL) technologies employing on biomass, CO_2, recycled plastic, and fossil feedstock. To account for the future development of environmental impacts, we use the premise tool [4] to generate pLCA data that builds on the ecoinvent 3.10 database. The datasets generated comprise three Shared Socioeconomic Pathways (SSPs) that range from moderate to optimistic future transitions in several socioeconomic sectors. The pLCA datasets are used to assess the life cycle impacts of the plastic industry according to the SSPs scenarios.

Results:

Our results indicate that the hydrogen demand in the plastics industry varies by one order of magnitude depending on the chosen technology mix for hydrogen supply and demand and on the SSP pathway (i.e., the policy framework). When we extend our assessment beyond climate change, we identify important environmental impact trade-offs arise for hydrogen production from water electrolysers and biomass gasifiers, highlighting the need for improvements.

Conclusions:

By applying prospective life-cycle assessment and an industry-wide assessment, this study provides valuable insights on hydrogen technologies, policymakers, and industry stakeholders engaged in the plastics sector and the development of the hydrogen market.

Acknowledgement

This work is funded by the European Union (Grant Agreement number 101070721). Views and opinions expressed are, however, those of the author(s) only and do not necessarily reflect those of the European Union or the European Innovation Council and SMEs Executive Agency (EISMEA). Neither the European Union nor the granting authority can be held responsible for them. This work is funded by UK Research and Innovation (UKRI) under the UK government's Horizon Europe funding guarantee grant number 10045035.
This work has received funding from the Swiss State Secretariat for Education, Research and Innovation (SERI) under grant number 22.00374.

References

[1] U. N. Environment, "From Pollution to Solution: A global assessment of marine litter and plastic pollution." Accessed: Feb. 18, 2025. [Online]. Available: https://www.unep.org/resources/pollution-solution-global-assessment-marine-litter-and-plastic-pollution

[2] R. Meys *et al.*, "Achieving net-zero greenhouse gas emission plastics by a circular carbon economy," *Science*, vol. 374, no. 6563, pp. 71–76, Jan. 2021, doi: 10.1126/science.abg9853.

[3] M. Bachmann *et al.*, "Towards circular plastics within planetary boundaries," *Nat Sustain*, vol. 6, no. 5, pp. 599–610, Mar. 2023, doi: 10.1038/s41893-022-01054-9.

[4] R. Sacchi *et al.*, "PRospective EnvironMental Impact asSEment (premise): A streamlined approach to producing databases for prospective life cycle assessment using integrated assessment models," *Renewable and Sustainable Energy Reviews*, vol. 160, p. 112311, May 2022, doi: 10.1016/j.rser.2022.112311.

EFCH2 2025 European Fuel Cells and Hydrogen
PIERO LUNGHI CONFERENCE
September 17th–19th 2025 Capri / Italy

A Flexible Methodology for Renewable Energy Integration: A PyPSA-Based Optimization Approach Applied to Northern Canada

Elia Perelli*[a], Elena Rozzi[a,b], Paolo Marocco[a], Marta Gandiglio[a]

* corresponding author: elia.perelli@polito.it

[a] Department of Energy, Politecnico di Torino, Corso Duca degli Abruzzi 24, 10129 Torino, Italy
[b] Energy Center LAb, Politecnico di Torino, Corso Duca degli Abruzzi 24, 10129 Torino, Italy

Keywords: Seasonal storage, Hydrogen, Energy system optimization, Renewable energy integration, Remote microgrids

Introduction

PyPSA stands for Python for Power System Analysis [1], is an open-access library for Python. It is currently coordinated by the Department of Digital Transformation in Energy Systems at the Technical University of Berlin. PyPSA is capable of simulating and optimizing energy systems, ranging from large-scale systems like global energy networks to smaller systems such as hydrogen valleys. It is able to optimize capacities for generation, storage, and transmission lines, minimizing economic costs, calculating emissions, and optimizing under various constraints, including economic, technical, and environmental factors. In addition, this study leverages PVlib [2], a Python library designed for modelling photovoltaic (PV) system performance. PVlib enables precise solar energy modelling by incorporating meteorological data, irradiation models, and system parameters. By coupling PVlib with PyPSA, it is possible to enhance the accuracy of renewable energy modelling, particularly in regions with variable solar potential. Due to their flexibility in modelling diverse energy scenarios, these tools are particularly well-suited for studying regions with challenging energy, environmental, and infrastructure conditions. The case study focuses of this analysis on Yukon, a remote region in Canada located in the northwest and bordering Alaska. Remote communities exist worldwide and often face significant challenges in electrification and reducing fossil fuel dependence. Studying these contexts allows us to explore renewable and feasible solutions under the most demanding climatic and socio-economic conditions. Yukon features an isolated electrical system disconnected from the North American grid, making it vulnerable to failures and energy deficits. Another major challenge is the existence of off-grid communities that lack connection to the main electricity network. Four off-grid communities rely on microgrids powered primarily by diesel generators. Currently, 92% of whole Yukon's electricity comes from renewable sources, predominantly hydroelectric, while 8% is generated through diesel-powered facilities [5].

Objectives

This study aims to evaluate PyPSA's effectiveness in optimizing energy systems in challenging environments such as Yukon, a region characterized by extreme climate conditions, vast distances between cities, an underdeveloped electricity grid, and low renewable energy potential. A key objective is to assess the feasibility of the ambitious 2030 goals set by the Yukon government in the Our Clean Future strategy, particularly the goal of producing an average of 93% of electricity from renewable sources and reducing diesel consumption for electricity generation in off-grid communities by 30% [6] . Additionally, we explore extreme scenarios where fossil fuel use is completely eliminated from the power sector, assessing the technical and economic feasibility of a 100% renewable-based energy system in Yukon. In these scenarios, we aim to analyze the role of chemical storage (hydrogen) and electrochemical storage (batteries) in managing energy supply fluctuations across daily and seasonal timescales in high-Renewable systems. At the same time, this research develops and explains a highly flexible methodology for energy system modeling, combining PyPSA, PVlib, and APIs (Application Programming Interface) connected to PVGIS [3] and Renewable Ninjas [4] databases. This approach first evaluates the renewable energy potential of a given region and then optimally designs an economically viable energy network based on that potential. The methodology also allows for the integration of existing infrastructures and the application of various technical, economic, and environmental constraints, making it adaptable to different regions worldwide.

Material and methods:

The proposed methodology follows a structured approach to optimize the energy system in Yukon using PyPSA, PVlib, API-based data retrieval, and clustering techniques. The first step involves collecting geographical, demographic, and energy-related data, including population distribution, power plants, energy consumption, and load profiles for different regions. To efficiently model the energy system, the k-means clustering method is applied to group areas, optimizing computational efficiency while preserving spatial representativity. The Elbow Method is used to determine the optimal number of clusters. However, off-grid communities are deliberately excluded from the clustering process to assess whether grid expansion could be a feasible solution for these isolated areas. Once the clustering is established, the methodology evaluates the renewable energy potential using API connections to PVGIS and Renewable Ninjas databases, which provide real-time meteorological data, irradiation levels, and wind potential. The capacity factor (CF) of photovoltaic systems is computed through PVlib, a Python library that processes meteorological inputs and system parameters to generate high-resolution solar energy predictions. This ensures accurate renewable resource

assessment before integrating energy sources into the model. After defining the spatial, demographic, and renewable energy characteristics, all gathered data including clustered bus locations, renewable resource potential, CFs and localized load demand are integrated into PyPSA. Finally, the model is executed to optimize the energy system, minimizing economic costs while considering technical, economic, and environmental constraints.

Results:

Preliminary findings highlight significant challenges in optimizing Yukon's energy system. Hydroelectric production fluctuates seasonally, dropping by up to 40% in winter, requiring large-scale storage solutions to balance supply. Solar potential is extremely low, especially in winter, while wind energy faces reliability issues due to extreme wind speeds, which can exceed turbine limits. Despite its high emissions, diesel remains economically competitive, especially in remote off-grid communities where transportation by helicopter further increases costs. A key insight from this study is the crucial role of storage, with hydrogen emerging as a key solution for both hourly and seasonal energy balancing. The methodology developed proves to be highly flexible and consistent, adapting well to different geographic and energy contexts. The combination of PyPSA, PVlib, and clustering techniques ensures an optimized energy mix based on local constraints, reinforcing the robustness and applicability of the approach.

Conclusions:

This study demonstrates the feasibility and challenges of optimizing Yukon's energy system using PyPSA, PVlib, and API-based data retrieval. The findings highlight the critical role of storage solutions, particularly hydrogen, in addressing seasonal fluctuations in hydroelectric output and the low availability of solar resources. Despite the economic competitiveness of diesel, its reliance in off-grid communities remains a logistical and environmental challenge. The developed methodology proves to be highly adaptable, offering a scalable framework for renewable energy integration in several geographic contexts.

Acknowledgment

I would like to express my sincere gratitude to Omar Najoui for his valuable support and collaboration throughout this work. His insights and contributions have been instrumental in the development and refinement of this study.

References

[1] PyPSA Website: https://pypsa.org/
[2] Pvlib Website: pvlib python — pvlib python 0.11.2 documentation
[3] Photovoltaic Geographical Information System (PVGIS) - European Commission: https://joint-research-centre.ec.europa.eu/photovoltaic-geographical-information-system-pvgis_en

[4] Renewables.ninja: https://www.renewables.ninja/
[5] Projects and Facilities | Yukon Energy
[6] Ensuring reliable, affordable and renewable energy | Government Of Yukon - Our Clean Future



Scenarios for Operational and Techno-Economic Analysis of the Hydrogen Value Chain for Aviation

Pieter-Jan Proesmans*[a], Sam Randeraad [a], Timo Schelm[b], Elise Bavelaar[a], Alexei Sharpanskykh[a], Astrid Bensmann[b], Finn Schenke[b]

* corresponding author: Pieter-Jan Proesmans (p.proesmans@tudelft.nl)

[a] Delft University of Technology, Faculty of Aerospace Engineering

[b] Leibniz University Hannover, Institute of Electric Power Systems

Keywords: Sustainable Aviation, Liquid Hydrogen, Techno-Economic Analysis, Airport Ground Operations

Abstract

Introduction: Hydrogen (H_2) is currently being investigated as a sustainable energy carrier for aircraft to decarbonise primarily short- and medium-haul aviation. Although hydrogen-powered aircraft can eliminate in-flight carbon dioxide and possibly reduce non-CO_2 effects [1], research is required to initiate and mature the hydrogen supply infrastructure and daily airport operations for such aircraft. The GOLIAT (Ground Operations of LIquid hydrogen AircrafT) project [2] seeks to overcome the current obstacles in technologies, regulations, processes, and economics to make widespread daily use of hydrogen at airports.

In the GOLIAT project, we will develop comprehensive liquid hydrogen (LH_2) demand and supply-matching models for air transport ground infrastructures. Future analyses will provide techno-economic insights by comparing forward-looking scenarios. To initiate the modelling and analyses, we first need to define the scope and develop new scenarios based on currently available literature and knowledge.

Objectives: This paper aims at **developing the multi-horizon scenarios** which can be used to perform operational and techno-economic analyses of the hydrogen value chain for aviation. The scenarios are built upon variations of factors, drivers, and barriers from several disciplines which impact the value chain of hydrogen. The goal of the scenarios is to analyse possible future situations, not to predict or impose the future of a hydrogen value chain. This paper elaborates upon the method for scenario construction and presents the scope and a set of five main scenarios for future operational and techno-economic scenarios.

Material and methods: Figure 1 presents the method employed for scenario development. In each of these five high-level steps, we use a combination of literature review and expert consultation to gain exhaustive insights. First, the problem is clarified and the scope if defined. Second, factors and drivers possibly impacting the value chain of hydrogen for aviation are gathered and categorized. We examine 51 factors from seven categories including policy, economics, airport infrastructure, hydrogen availability, air traffic growth, aircraft technology, and disrupting events. These factors are assessed in terms of their uncertainty and the impact they can have on demand, supply chain sizing and economics, and ground operations.



Figure 1 - Scenario Development Method

Key factors are selected based on the impact and uncertainty evaluation, with variations proposed for each. Eight conceptual scenarios are then constructed by combining these variations into logical narratives. The next step is to validate these scenarios by checking their plausibility, consistency, relevance, and novelty [3]. Additionally, we select the most relevant and novel scenarios. This validation and selection step is performed through a workshop with H_2 supply and operations experts, internal and external to the GOLIAT project. Figure 2 shows the expert's ranking of the conceptual scenarios in terms of relevance and novelty.

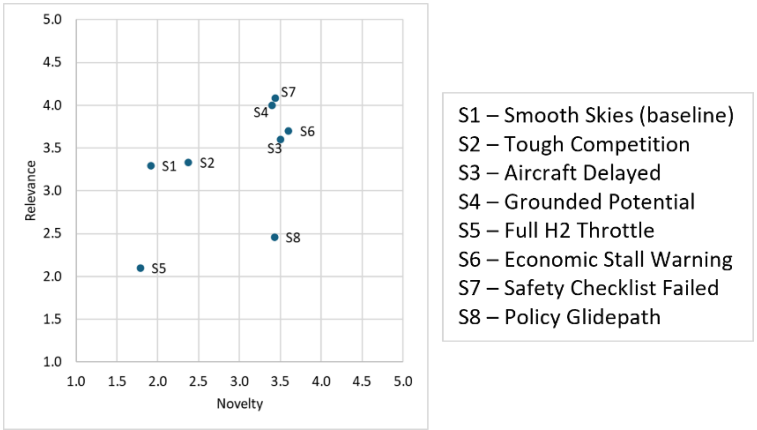


Figure 2 - Ranking of conceptual scenarios in terms of relevance and novelty (green indicates high levels of relevance and novelty, orange corresponds to low levels of relevance and novelty)

Results: The scope for the operational and techno-economic analysis is presented in Figure 3. Considering the scenarios, three key axes of driving forces are identified: 1) hydrogen availability and the energy market, 2) the readiness of airport infrastructure, and 3) the level of aircraft technology development. Furthermore, disrupting economic and safety forces should be considered in the techno-economic analysis. To capture varying levels of development along these three axes and these disrupting factors, the following five main scenarios are defined:

A. Smooth Skies – A baseline scenario with "mid-level" developments from literature.

B. Aircraft Delayed – This scenario considers delayed arrival of hydrogen aircraft which are expensive to operate (factor misalignment).
C. Grounded Potential – Many EU airports are not ready to support H2 refuelling operations, and H2 aircraft cannot be operated at full potential (factor misalignment).
D. Economic Stall Warning – After investments in infrastructure and aircraft technology, an economics crisis lowers the overall air travel demand (disruptive scenario).
E. Safety Checklist Failed – Major safety issues lower the social and regulatory acceptance of hydrogen aircraft and their operations at airports (disruptive scenario).

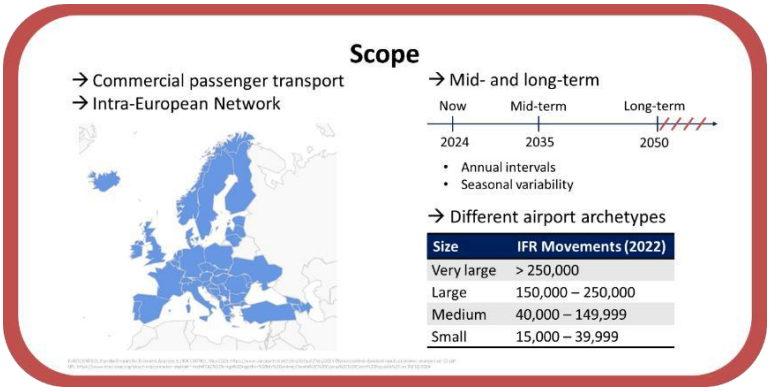


Figure 3 - Scope of techno-economic analysis

Conclusions: Based on literature review and expert consultation, five main scenarios are created for analysis of the future hydrogen value chain for aviation. The scenarios are based on variations in hydrogen availability, airport readiness, an aircraft technology, as well as economic and safety disruptions. These scenarios will be used to assess the demand, supply chain size and cost, and ground operations for hydrogen-powered aviation in Europe.

Acknowledgment

This research was carried out within the GOLIAT project, which is funded by the European Union under grant agreement n° 101138379. The authors would like to thank all the GOLIAT partners (GOLIAT | Airbus) for their contribution to this task, as well as all external participants involved in the workshop.

Funded by the European Union

References

[1] Adler, E. J., & Martins, J. R. R. A. (2023). *Hydrogen-powered aircraft: Fundamental concepts, key technologies, and environmental impacts*. In Progress in Aerospace Sciences (Vol. 141, p. 100922). Elsevier BV. https://doi.org/10.1016/j.paerosci.2023.100922

[2] Airbus. (16 May 2024). *Innovative aviation liquid hydrogen project launched* [Press release]. https://research.airbus.com/en/products-systems/goliat

[3] Amer, M., Daim, T. U., & Jetter, A. (2013). A review of scenario planning. In Futures (Vol. 46, pp. 23–40). Elsevier BV. https://doi.org/10.1016/j.futures.2012.10.003

European Fuel Cells and Hydrogen
PIERO LUNGHI CONFERENCE
September 17th–19th 2025
Capri / Italy

HyMantovalley – A Case Study from Italy

Marcello Romagnoli*[a], Nicola Galli[b]

* corresponding author: marcello.romagnoli@unimore.it
[a] H2 Research Centre MO-RE (Unimore), Via Università, 4, 41121, Modena - Italy
[b] AGIRE srl, Piazza Sordello, 43, 46100, Mantova - Italy

Keywords: Hydrogen Valley, Research and formation, Sustainable Development, Transportation

Abstract

Introduction: *The use of hydrogen technologies is vital for cutting emissions and tackling climate change. In Europe, demand for greener energy and lower greenhouse gases has led to focus on H2. The Po Valley in northern Italy is a good example: rich in industry but suffering from pollution and environmental challenges. The HYMANTOVALLEY project [1] aims to drive the move to clean energy, improve air quality and boost eco-business. It focuses on research and education, including a new research centre for H2 technologies and training courses to prepare technicians, essential for the growth of a local H2 economy.*

This summary shows how HYMANTOVALLEY fits into Europe's push for clean mobility and alternative fuels. The project shows how local H2 production, distribution, and use can be part of wider solutions for different sectors, like maritime transport and public mobility, while promoting innovation, education, and stakeholder engagement.

Objectives: HYMANTOVALLEY's integrated approach to H2 production and use directly supports the acceleration of H2 research and education. In particular, the initiative:

- Encourages robust frameworks for the production, distribution and use of green H2 in hard-to-abate sectors such as marine, inland waterway and transportation.
- Catalyses collaborations among public institutions, private entities, and research organisations to foster scalable and replicable H2 valleys across Europe.

- Contributes to sustainable regional development by reducing pollution, particularly in the heavily polluted Po Valley, providing transferable lessons for other high-pollution regions across the continent.

Material and methods: Drawing on methodologies commonly employed in H2 valley initiatives, HYMANTOVALLEY's approach integrates both technical and stakeholder-focused strategies.

Technical Framework.

- Green H2 Production: The project leverages an existing H2 facility in Mantova, transitioning it from low-carbon (blue) H2 to renewable (green) H2 via an electrolysis unit powered by dedicated photovoltaic installations.
- Storage and Distribution Innovation: Novel, transportable high-pressure storage solutions enable safe and efficient distribution of H2 to refuelling stations for ships, trains.
- Infrastructure Adaptation: Strategies for pipeline construction and H2 refuelling stations in key logistics hubs (such as the Port of Valdaro) facilitate large-scale adoption in maritime and rail applications.

Socio-Economic and Organisational Framework.

- Public-Private Synergy: Under the coordination of the Province of Mantova and regional energy agencies (e.g., AGIRE), the project promotes stakeholder engagement, community acceptance, and local workforce training for handling H2 technologies.
- Education and Research: Collaboration with universities (e.g., University of Modena and Reggio Emilia and Polimi) and research centers (FBK), supports H2-specific academic programmes, bridging theoretical research and real-world applications.
- Business Models and Funding: A crucial element involves leveraging multiple streams of investment—grants, private funding, and venture capital—to ensure sustainable financing and commercial viability.

Environmental and Social Impact Assessments:

- Data Integration. Monitoring of air quality and emissions data using a digital twin approach, refined through continuous feedback to gauge the environmental benefits of H2 adoption.
- Community Outreach: Demonstration projects (e.g., use of zero-emission vessel, pilot-scale H2 heating/cooling in public buildings) foster public awareness and acceptance, vital for broadening the project's impact.

By melding technical rigour with socio-economic considerations, HYMANTOVALLEY provides a holistic blueprint for H2 valley development. This methodology serves as a replicable model for other regions keen on deploying H2 as a cornerstone of their green transition.

Results: Preliminary considerations suggest that integrating H2 in local transport and industry could cut carbon and nitroxide emissions. Further pilot tests are needed to validate these projections. Key areas for verification include:

- Maritime and inland shipping: The expected shift to H2-powered vessels along the Mantua-Venice corridor, which could reduce reliance on diesel, requires thorough quantitative assessments of emissions and operational performance.
- Rail and road transport: While H2 locomotives and mobile refuelling stations are under development, actual operational data needs to be collected to confirm the viability and scalability of these solutions.
- Production and storage: Although initial simulations of local H2 production coupled with renewable energy suggest stable operation, real-time measurements will be essential to validate energy yield, storage efficiency and cost effectiveness.

The next phase of the project will include systematic field measurements, stakeholder feedback and environmental impact assessments. These efforts will verify whether the predicted benefits match real-world outcomes and provide definitive insights into the potential of H2 to drive a sustainable energy transition in regions such as the Po Valley - and beyond.

Conclusions: The transition to H2 as a cornerstone of sustainable energy systems is an increasingly urgent priority, both at national and European levels. As demonstrated by the HYMANTOVALLEY Project, well-coordinated public-private partnerships, robust technical strategies, and proactive stakeholder engagement underpin the successful development of integrated H2 ecosystems.

Looking ahead, future work will focus on:

- Scaling Up current pilot demonstrations to larger fleets of H2-powered maritime vessels, trains, and heavy-duty vehicles.
- Refining Business Models to ensure sustained economic viability and broader stakeholder uptake in diverse regions.
- Enhancing Education and Research through expanded partnerships with international academic and industry partners, ultimately nurturing a new generation of H2 specialists and entrepreneurs.

References

[1] https://hymantovalley.agirenet.it/en/

Co-funded by the European Union

Funded by the European Union. Views and opinions expressed are however those of the author(s) only and do not necessarily reflect those of the European Union or EISMEA. Neither the European Union nor the granting authority can be held responsible for them.

EFCH2 2025 European Fuel Cells and Hydrogen PIERO LUNGHI CONFERENCE
September 17th–19th 2025 Capri / Italy

Techno-economic assessment of Methane, Methanol, Ethylene and Acetic Acid production from electrolytic hydrogen and recovered CO2 for one chemical industrial park in the Hesse region of Germany

Carlos Camacho Gamboa[1], Paloma Rebollo Marco[1], Guillermo Gómez Tellería[1], Christian Aragón Briceño[1], Andrés Yáñez Amador[1], Ignacio Martin Jimenez[1]

* corresponding author: ccamacho@fcirce.es

[1] CIRCE - Research Centre for Energy Resources and Consumption, Parque Empresarial Dinamiza, Ave. Ranillas 3D, 1st Floor, 50018 Zaragoza (Spain)

Keywords: Hydrogen Valleys, Methane, Methanol, Ethylene, Acetic acid

Introduction:

The European chemical industry is undergoing a transformation toward sustainability by integrating circular economy principles into industrial operations. A key challenge in industrial parks is waste disposal and resource efficiency, particularly in carbon-intensive sectors. To address this, industrial symbiosis—where waste from one industry becomes a resource for another—has emerged as a viable solution. However, fully leveraging this approach requires the integration of advanced technologies that facilitate waste revalorization and resource recovery.

One promising pathway is the utilization of residual carbon dioxide (CO_2) and hydrogen to produce valuable chemical products. Hydrogen, recognized as a key energy vector in the European Union's decarbonization strategy, can be generated via water electrolysis, while CO_2 can be captured from industrial processes or biogas purification off-gases. These gases can serve as feedstocks for synthesizing essential chemicals such as Methane, Methanol, Ethylene, and Acetic Acid, contributing to both emissions reduction and resource circularity. Within this framework, the IS2H4C project (Industrial Symbiosis to Hubs for Circularity) supports the development and implementation of circular economy strategies in European industrial hubs. The German Hub, located in the Hesse region, explores the feasibility of producing high-value chemicals from hydrogen and recovered CO_2 as part of its industrial symbiosis strategy.

Objectives:

This study focuses on conducting a techno-economic assessment to determine the feasibility of these processes. The main objective is to develop an economic model to calculate the Levelized Cost of Production (LCOX) for each molecule, providing insights into investment requirements (CAPEX), operational costs (OPEX), and overall economic viability. By evaluating available technologies and selecting those with the highest Technological Readiness Level (TRL), this work aims to provide a comprehensive economic analysis that supports decision-making for the integration of CO_2-based chemical production in the industrial hub.

Material and methods:

The available technologies for each molecule production are evaluated and the one with a higher Technological Readiness Level (TRL) is selected to perform the process simulation. The study will consider all the equipment necessary to produce the molecule with the quality required on the market. Process open-source simulator DWSIM©, will be employed to develop the simulation model.

The raw CO2 to produce the molecules is obtained from the off gas generated from further purification process of biogas production at the German Hub participating in the project. Hydrogen will be generated by water electrolysis. The study considers the impact on production cost of implementing a process to increase the CO2 and renewable hydrogen availability by converting organic matter to CO2 by using a Water Gas Shift process preceded by a gasification unit.

The levelized cost (LCOX) is a tool that allows to calculate the average cost of production over the lifetime of an asset. It helps determining whether a production plant will be profitable and take the decision to go ahead.

To estimate the investment cost (CAPEX) and operational costs (OPEX) required to calculate the LCOX a simulation of the production process for each of the molecules will be used as a basis. The material and energy balance will be obtained from the simulation previously developed. The costing evaluation tool, included in the Pro version of DWSIM© will provide the equipment cost of the selected processes.

The operating cost will be calculated based on the opportunity cost of the raw materials and the utilities cost will be obtained from public sources. The life of the asset is set at 30 years.

Results:

The results will show the final cost for each molecule at which production is attractive, the economic impact of the investment and the potential yearly production. Final decision needs to considers the reduction in the dependency of hydrocarbons supply, greenhouse gases emission reduction and the potential to reduce cost in purchase of the high value chemicals.

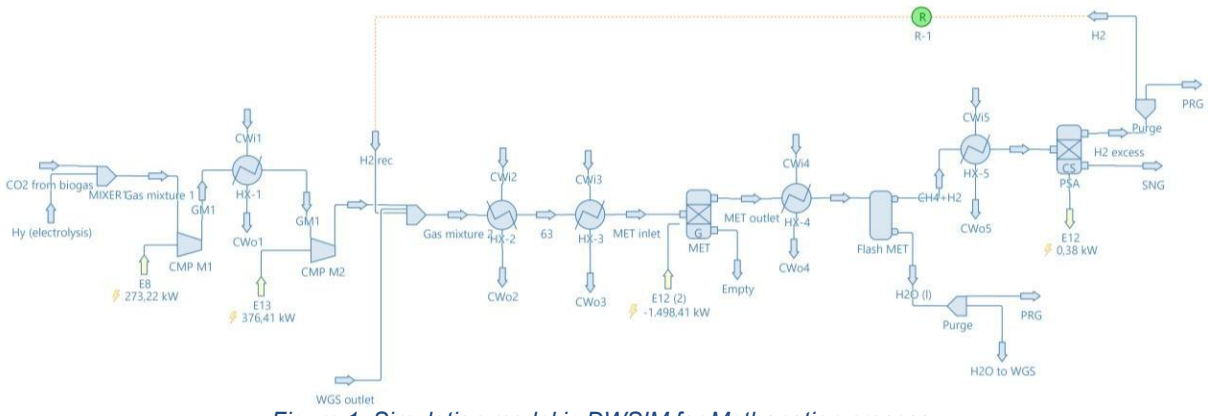


Figure 1. Simulation model in DWSIM for Methanation process.

Preliminary Conclusions:

This study will provide a techno-economic assessment of producing Methane, Methanol, Ethylene, and Acetic Acid from hydrogen and recovered CO_2 within an industrial hub in the Hesse region of Germany. By leveraging water electrolysis for hydrogen production and biogas purification off-gases for CO_2, the study will evaluate the feasibility of integrating these processes within a circular economy framework (Hub4Circularity).

Through process simulation in DWSIM and levelized cost of production (LCOX) calculations, will allow to determine the economic viability of these alternative pathways. The results will provide insights into the production costs, investment requirements (CAPEX), operational costs (OPEX), and potential annual outputs, helping decision-makers assess whether these processes are competitive and sustainable.

Beyond economic feasibility, the study also considers strategic benefits, including reducing dependency on fossil fuels, lowering greenhouse gas emissions, and enhancing local chemical production efficiency. The findings will be crucial in determining the attractiveness of these processes within the broader context of industrial symbiosis and decarbonization efforts in the European chemical sector.

Acknowledgment

The authors fully acknowledge the financial support from the European Union's Horizon Europe research and innovation programme under grant agreement No 101138473.

References

[1] https://is2h4c-project.eu/

European Fuel Cells and Hydrogen
PIERO LUNGHI CONFERENCE
September 17th–19th 2025
Capri / Italy

H2Start Teaming Project "Green Innovations in Hydrogen for Sustainable Energy Transition"

D. Vladikova*[a], G. Squadrito[b], M. Santarelli[c], D. Nozharova[d], M. Karabaliev[a], A. Nicita[b], P. Leone[c], E. Paolucci[c], E. Ilkova[d]

* corresponding author: d.vladikova@iees.bas.bg

[a] Trakia University, Students Campus, 6000 Stara Zagora, Bulgaria

[b] ITAE-CNR, Salita S. Lucia sopra Contesse, 5 - 98126, Messina, Italy

[c] POLITO, Corso Duca degli Abruzzi, 24 10129, Torino, Italy

[d] Bulgarian Hydrogen, Fuel Cell and Energy Storage Association, 10 Acad. G. Bonchev St., 1113 Sofia, Bulgaria

Keywords: Center of Excellence on Hydrogen, Hydrogen Valley, Rresearch infrastructure, Human resources strategy

Abstract

The H2START project aims to establish Bulgaria's first Centre of Excellence (CoE) in hydrogen, fostering the transition towards a low-carbon economy. By supporting Stara Zagora, where ZAHYR Hydrogen valley (Clean Hydrogen Partnership project) is to be developed, and other Bulgarian regions, the project will ensure sustainability in introducing innovative technological and economic approaches for renewable hydrogen production and utilization. This initiative aligns with national and EU strategies, promoting green hydrogen as a crucial component of energy transformation. The project commenced on January 1, 2025, with a duration of 72 months. As a transformative initiative, H2START will serve as a "lighthouse" for advancing Bulgaria's green transition and circular economy, positioning the country at the forefront of hydrogen research and innovation.

Project Background and Rationale

Hydrogen presents a crucial opportunity for the decarbonization of energy systems, particularly in regions with a high reliance on fossil fuels. The Stara Zagora region, characterized by a 3.6 GW power plant, extensive coal mining operations, and significant industrial hydrogen production facilities, offers a strategic setting for accelerating hydrogen deployment. The project capitalizes on Bulgaria's renewable energy potential, with projections indicating a capacity of 20 GW in renewable energy sources and 2-3 GW in

electrolysis by 2035. H2START aims to leverage these assets to enhance Bulgaria's hydrogen production and application capabilities.

Consortium

At the heart of H2START is a strong consortium of institutions, each playing a pivotal role in shaping Bulgaria's hydrogen future:

- Trakia University: As the project coordinator and a key member of Hydrogen Europe Research (HER), Trakia University leads national efforts in hydrogen and fuel cell research, leveraging its active participation in Horizon Europe projects.
- Bulgarian Hydrogen, Fuel Cell, and Energy Storage Association (BGH2A): This organization fosters collaboration between academia, industry, and policymakers, aligning efforts with Bulgaria's Clean Energy Transition (CET) Plan.
- Politecnico di Torino's Department of Energy: A leader in hydrogen education and research, coordinating an exclusive EU Master's program on hydrogen and maintaining strong ties with industry players.
- Institute for Advanced Energy Technologies - CNR: Representing CNR at the EU level in Hydrogen, managing hydrogen research infrastructure, and facilitating industry engagement.

Project Objectives

The primary objective of the H2START project is to elevate Bulgaria's research intensity in hydrogen technologies by building a robust and sustainable R&I ecosystem—the Center of Excellence H2START on Hydrogen Technologies. This initiative will serve as a beacon for Bulgaria's research landscape, integrating cutting-edge infrastructure, strategic governance, and a well-developed human resources framework.

To achieve this, the project focuses on several specific objectives:

- Establishment of a new R&I management and administrative ecosystem, implementing transparent and efficient coordination and governance models with autonomous decision-making frameworks.
- Development of strategic research and innovation agenda (SRIA): outlining a six-year roadmap with annual implementation plans to ensure that the CoE aligns with the European Hydrogen Research Area's scientific policies.
- State-of-the-Art research infrastructure: Equipping the Center with world-class research facilities while collaborating with advanced partners to go beyond the state-of-the-art, avoiding redundancy in existing infrastructure. The project team has prepared a survey on industry needs to inform the design of specialized testing laboratories.

- Human resources strategy and talent retention, following the principle of "*attract, retain, and empower scientific talent*" through a well-defined human resources strategy with transparent and open recruitment processes. A dedicated Human Resources Center will ensure a sustainable community of senior researchers. A specialized Master's program on hydrogen, developed in collaboration with leading European institutions, will be launched alongside extensive training, skilling and reskilling programs to build a highly competent workforce in Bulgaria and the region.
- Boosting Bulgaria's scientific output and global presence increasing research publications, patents, and participation in European projects through strong collaborations with international research institutions and industry leaders. Establishing a Knowledge and Technology Transfer Center and an Intellectual Property (IP) bureau will enhance visibility and attract complementary funding.
- Policy support and cross-cutting activities, promoting open science and international outreach through interactive platforms. A stakeholder forum will facilitate collaboration, while updates to the National Hydrogen Roadmap will drive regulatory improvements and support policymakers in shaping effective hydrogen policies. Engaging the public with innovative communication strategies based on the principle "*see, touch, use, understand, trust, wish*" will facilitate the sustainable market deployment of hydrogen technologies.

Securing Long-Term Sustainability and Impact

The H2START initiative is designed for longevity. With its strategic governance framework, advanced research facilities, skilled talent pool, and strong industry collaborations, the project will ensure long-term sustainability. By aligning with European research priorities and leveraging Horizon Europe funding of € 14,999,170 and 50 % additional Bulgarian funding (Program "Research, Innovation and Digitalization for Smart Transformation" 2021-2027), H2START is set to establish itself as a pivotal player in the European Hydrogen Research Area. This ground-breaking initiative will not only propel Bulgaria's hydrogen research capabilities but will also serve as a model for other emerging R&I ecosystems across Europe.

Acknowledgments

The authors acknowledge the support of the European Union under Horizon Europe (project 101136692).

European Fuel Cells and Hydrogen
PIERO LUNGHI CONFERENCE
September 17th–19th 2025
Capri / Italy

Hybrid Renewable Energy Systems with Hydrogen Storage: A Sustainability-Driven Optimization Approach

Elena Rozzi*[a], Paolo Marocco[a], Marta Gandiglio[a]
* corresponding author: elena.rozzi@polito.it
[a] Department of Energy, Politecnico di Torino, Corso Duca degli Abruzzi 24, 10129 Torino, Italy

Keywords: Hybrid energy systems, Life cycle assessment, Multi-objective optimization, Hydrogen utilization

Abstract

Renewable energy communities enable decentralized energy generation, enhancing self-sufficiency and reducing reliance on external utilities. This study presents a multi-objective optimization framework for designing and operating hybrid energy systems under both grid-connected and off-grid scenarios. The system integrates photovoltaic panels, solar collectors, battery storage, thermal energy storage, and hydrogen-based technologies - including electrolyzers for green hydrogen production and fuel cells for reconversion into electricity - to meet both electrical and thermal demands. The optimization problem considers economic and environmental objectives, incorporating life cycle assessment indicators. Implemented in PyPSA, the framework explores optimal configurations that balance cost, self-sufficiency, and environmental sustainability. Results highlight the benefits of coordinated multi-energy management in enhancing operational flexibility, reducing environmental impacts, and ensuring resilience in interconnected and autonomous configurations.

Introduction: Renewable energy communities (RECs) have emerged as a promising model for decentralized energy generation, enhancing local self-sufficiency and reducing dependence on centralized utilities. Hybrid energy systems offer a versatile solution to mitigate short-term fluctuations and address long-term seasonal variations, making them suitable for both grid-connected and off-grid configurations [1]. In particular, the integration of green hydrogen provides long-duration storage capability and reinforces energy autonomy. Recent studies have underscored the importance of multi-objective optimization frameworks in designing such complex systems. These frameworks simultaneously balance economic and environmental objectives, not only minimizing capital and operational costs but also integrating sustainability metrics through Life Cycle Assessment (LCA) indicators. The proposed framework co-optimizes system sizing and operational scheduling, evaluating trade-offs among cost, self-sufficiency, and environmental performance.

Objectives: The primary objective of this study is to develop and apply a multi-objective optimization framework for the design and operation of hybrid renewable energy systems

within both grid-connected and off-grid RECs. The framework aims to simultaneously minimize economic costs and environmental impacts while ensuring reliable coverage of both electrical and thermal demands. A key objective is the incorporation of LCA indicators into the optimization process, enabling sustainability-driven system design.

Material and methods: In this study, a comprehensive dataset of LCA indicators was compiled to inform both system sizing and operational scheduling within the proposed multi-objective optimization framework [3]. The dataset provides normalized environmental impact values per unit of technology capacity rather than per unit of energy delivered over the system's lifetime. This approach eliminates dependence on capacity factors, scheduling, and location, ensuring comparability across technologies. Only operational CO_2 emissions remain expressed per unit of energy delivered, as they directly reflect usage and performance. The dataset encompasses key indicators such as CO_2, mineral and metal depletion, water consumption, and land use. Data were collected from an extensive literature review of peer-reviewed LCA studies, international reports, established databases, and industrial sources.

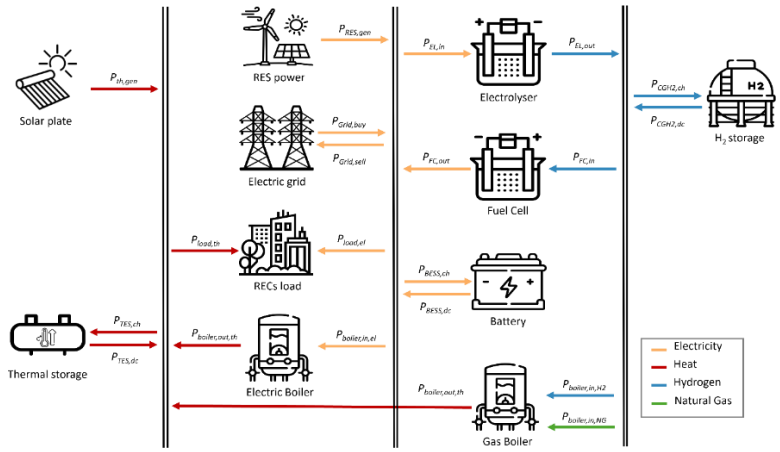


Figure 1. Renewable energy community layout.

The proposed energy system integrates multiple renewable and storage technologies to meet both electrical and thermal demands while balancing economic and environmental objectives (see Figure 1). Solar thermal collectors supply heat to a thermal storage unit, ensuring a stable heat supply despite daily and seasonal fluctuations. Simultaneously, photovoltaic panels generate electricity that can be directly consumed, stored in a battery energy storage system, or diverted to an electrolyzer for hydrogen production. The produced hydrogen is compressed and stored for later reconversion into electricity via a fuel cell, ensuring long-term operational flexibility. A backup boiler addresses any residual heating needs and can be powered by electricity, natural gas, or a blend of CH_4 and H_2, with the capability to operate on up to 100% hydrogen. Additionally, surplus electricity may be exported to the grid when available.

Operational variables determine the real-time dispatch of each component while ensuring that energy balances are satisfied at each time step (Eq. 1-3).

$$P_{RES,gen}(t) + P_{Grid,buy}(t) + P_{BESS,dc}(t) + P_{FC,out}(t) = P_{load,el}(t) + P_{EL,in}(t) + P_{BESS,ch}(t) + P_{Grid,sell}(t) + P_{boiler,el}(t) \quad (1)$$

$$P_{EL,out}(t) + P_{CGH2,dc}(t) = P_{FC,in}(t) + P_{CGH2,ch}(t) + P_{boiler,in,H2} \quad (2)$$

$$P_{th,gen}(t) + P_{boiler,out,th}(t) + P_{TES,dc}(t) = P_{load,th}(t) + P_{TES,ch}(t) \quad (3)$$

By integrating sustainability metrics derived from LCA with economic objectives, the model identifies configurations that minimize costs while mitigating environmental impacts. This comprehensive approach provides a robust methodological basis for designing RECs that are efficient, affordable, and ecologically responsible

Results: The results highlight the effectiveness of the proposed optimization framework in enhancing self-sufficiency and sustainability through the coordinated use of battery, hydrogen, and thermal storage. In particular, the integration of green hydrogen - produced via electrolyzers and reconverted into electricity through fuel cells - proves essential for addressing long-term energy balancing and seasonal variability. By optimizing the operation and sizing of hydrogen infrastructure alongside other storage systems, the model improves overall system flexibility and maximizes the utilization of renewable resources. Furthermore, the inclusion of LCA indicators ensures that the resulting configurations are not only economically viable but also environmentally responsible. The results demonstrate that incorporating LCA-based sustainability metrics into the optimization process facilitates significant reductions in greenhouse gas emissions, resource depletion, and other environmental impacts. Achieving these outcomes, however, requires balancing trade-offs between capital investment in emerging technologies, system synergies, and broader ecological considerations.

Conclusions: This study presented a multi-objective optimization framework for designing and operating hybrid renewable energy systems in both grid-connected and off-grid RECs. The results highlight the effectiveness of integrating battery, hydrogen, and thermal storage to enhance self-sufficiency, operational flexibility, and sustainability. The framework successfully balances economic and environmental objectives by incorporating LCA indicators into the optimization process, leading to reduced greenhouse gas emissions and resource depletion.

Acknowledgment: This research has been funded by the EU – Next Generation EU, Mission 4, Component 1, CUP E53D23004020006, project title “Smart Energy in Cities and Communities for 2050” (Prot. 2022ZM87LR).

References

[1] M. Tangi, A. Amaranto, Designing integrated and resilient multi-energy systems via multi-objective optimization and scenario analysis, Applied Energy 382 (2025) 125281. https://doi.org/10.1016/j.apenergy.2025.125281.

[2] T. Brown, J. Hörsch, D. Schlachtberger, PyPSA: Python for Power System Analysis, JORS 6 (2018) 4. https://doi.org/10.5334/jors.188.

[3] E. Rozzi, P. Marocco, M. Gandiglio, Life cycle inventory dataset for energy production and storage technologies: Standardized metrics for environmental modeling, Data in Brief 60

(2025) 111666. https://doi.org/10.1016/j.dib.2025.111666.

EFCH2 2025
European Fuel Cells and Hydrogen
PIERO LUNGHI CONFERENCE
September 17th–19th 2025
Capri / Italy

Environmental and Circularity Insights for the Design of Sustainable TiFe-based Alloys for Hydrogen Storage

Giuseppe Di Florio*[a], Francesca Garelli[b], Claudio Carbone[a], Jacopo Bindi[a], Erika Michela Dematteis[b], Mauro Palumbo[b], Viviana Cigolotti[a], Marcello Baricco[b], Alessandro Agostini[a], Paola Rizzi[b]

* Corresponding author: giuseppe.diflorio@enea.it

[a] ENEA: Italian National Agency for New Technologies, Energy and the Environment, via Anguillarese 301, 00123 Roma, Italy

[b] Department of Chemistry and NIS, INSTM, University of Turin, Via Pietro Giuria 7, 10125 Torino, Italy

Keywords: Environmental dissipation, Materials sustainable production and processing, Metal alloys for hydrogen storage, Responsible resource consumption and materials circularity

Abstract

Introduction: Over the past century, the diversity of materials employed in everyday products is enormously increased. This materials complexity is closely tied to technology specialization and advancement [1]. It is also well known that our societies will be in urgent need of large amounts of several raw materials, should the shift of energy production from fossils to renewables takes place. This challenge poses concerns about the availability of many materials in the near future, thereby threatening the real possibility to attain such a technological revolution. Green hydrogen represents a valuable solution to store and transport energy. Handling it by hydrogen carriers stand out as a promising option, due to their ability to achieve high volumetric densities (>80 Kg/m³). TiFe-based alloys are particularly promising for hydrogen storage due to their substantial capacity. However, challenges remain concerning activation and plateau pressure stability. TiFe is the most well-known AB compound for hydrogen storage applications, where A is an element form hydrides, while B is an element non reacting with hydrogen. Added advantages are that its properties can be tuned by substituting Ti or Fe with other metals and that incorporation of B-type elements (e.g., Cu, Ni, Co, Mn, Al) at the Fe site can enhance electrocatalytic activity, thereby improving the activation process. Nonetheless, for TiFe-based compounds to become a viable solution for hydrogen storage, it is important to correctly assess the economic and environmental sustainability of the current production methods. In this context, exploring strategies to recycle and recover raw materials like Ti and Fe is essential to reduce costs and environmental impact, supporting the sustainable development of TiFe alloys for large-scale hydrogen storage applications.

Objectives: This study investigates the environmental impacts of producing $TiFe_{0.80}$-$X_{0.20}$ (X = Co, Cu, Cr, Al) alloys. The selected elements are well known as substituents of the TiFe [2] and they reflect those commonly found when synthesizing the alloy from widely available scrapyard materials, such as

stainless steels, Ti grade 2 or Ti6Al4V, and Co, Al, and Cu alloys. This research provides valuable insights into the design of TiFe-X alloys for hydrogen storage, emphasizing the role of recycled materials to promote sustainability. In order to evaluate the selected substituents, the TiFe-X alloys were previously produced at laboratory scale through arc melting of high-purity raw materials in a vacuum environment, followed by appropriate annealing processes [3]. The goal of the study is to evaluate the sustainability of TiFe-X alloys production, and to quantify the potential benefits of increasing the share of recycled inputs, by combining a set of complementary methods, like LCA analysis, scenario analysis, circularity, environmental dissipation and social impacts analysis. This study aligns with the innovation principles of the Safe and Sustainable by Design framework, which advocates responsible and eco-friendly production methods for chemicals and materials.

Material and methods: The composition of alloys considered for the large-scale production are: $TiFe_{0.80}Al_{0.20}$, $TiFe_{0.80}Co_{0.20}$, $TiFe_{0.80}Cr_{0.20}$, $TiFe_{0.80}Cu_{0.20}$. A cradle-to-gate Life Cycle Assessment was conducted, covering the entire production chain from raw materials extraction to alloys synthesis. The system boundaries of the LCA were set to include the alloys production process, with a possible second annealing step. The functional unit selected for this analysis was the quantity of alloy required to store 1 kg of hydrogen, which depends on the specific storage capacity of each alloy. The LCA was performed using the software SimaPro 9.5 with the Ecoinvent 3.8.1 database. The impact assessment method employed was the Environmental Footprint (EF 3.1). The potential benefits of adopting recycled metals for production of alloys were analyzed based on several scenarios, derived from the use of different scrap inputs, along with a sensitivity analysis on the proportion of recycled content. The circularity potential was evaluated with the aid of *Circular Footprint Formula* (CFF). Additionally, resources consumption of various alloys production was evaluated through the perspective of the emerging concept of *environmental dissipation*, using the model developed by van Oers et al. and described in [4]. Finally, a Social Life Cycle Assessment (S-LCA) was conducted to examine the social impacts associated with alloy production, utilizing the PSILCA database.

Results: The most relevant impact categories identified for the production of all TiFe-X alloys are *Acidification*, *Climate change*, *Freshwater eutrophication*, *Particulate matter*, *Resource use - fossils*, and *Resource use - metals and minerals*. In all these categories, the impact can be attributed to the mining and processes at the raw materials extraction stage. Among the various inputs, titanium plays a particularly critical role in determining the environmental performance of all alloys production. The third alloying element shows a considerable contribution only in the case of cobalt, especially in the *Resource use - metals and minerals* category. As a result, despite the TiFeCo alloy has a large hydrogen storage capacity, in the case of cobalt inclusion, the third alloy element undermines the overall environmental performance of the system. Among the various alloys studied, a decisive factor results to be the amount of material needed to store the functional unit of 1 kg H_2: indeed, the alloys with larger gravimetric densities are the ones with lowest impact in all categories, at first place TiFeCr, followed by TiFeCu. On the other hand, both alloys containing aluminium – regardless of whether an annealing step is included - show the poorest environmental performances in all categories except *Resource use of metals and minerals*. The analysis of different scenarios incorporating recycled

materials demonstrates the potential gain for improving sustainability, particularly when high share of titanium scrap is attained in alloys production. Further, the possibility of sourcing chromium directly from steel scraps enhance the circularity potential of TiFeCr alloy. Recycling of cobalt, that can derive from Li-ion battery recovery, could markedly improve the sustainability of TiFeCo alloy. Finally, the environmental dissipation analysis proved more effective than traditional resource depletion metrics in highlighting inefficiencies in processes and resource management.

Conclusions: The study assessed the environmental impact of a class of materials, designed for hydrogen storage technologies, uncovering the strong interplay between materials properties, functional performance, and the specific environmental burden associated with the elements employed. The effect of replacing primary raw materials with widely available recycled or secondary materials was evaluated and the improvement in the sustainability of the production process was demonstrated.

Acknowledgment

This research was funded by the European Union – NextGeneration EU from the Italian Ministry of Environment and Energy Security POR H_2 AdP MASE/ENEA with involvement of CNR and RSE, PNRR - Mission 2, Component 2, Investment 3.5 ”Ricerca e sviluppo sull'idrogeno", CUP: I83C22001170006 and from Horizon Europe research, grant agreement No. 101192503.

Dr. Giuseppe Di Florio thanks the National Recovery and Resilience Plan (NRRP), Mission 4 Component 2 Investment 1.3—Call for tender No. 1561 of 11.10.2022 of Ministero dell’Università e della Ricerca (MUR); project funded by the European Union—NextGenerationEU. Award Number: Project code PE0000021, Concession Decree No. 1561 of 11.10.2022 adopted by Ministero dell’Università e della Ricerca (MUR), CUP I53C22001450006, according to attachment E of Decree No. 1561/2022, Project title “Network 4 Energy Sustainable Transition—NEST”.

References

[1] Graedel T. E., Harper E. M., Nassar, N. T., Reck B. K. “On the materials basis of modern society”, 2015, *PNAS*, **112**, 6295-6300

[2] Dematteis E. M., Berti N., Cuevas F., Latroche M., Baricco M. “Substitutional effects in TiFe for hydrogen storage: a comprehensive review”, 2021, *Mater. Adv.*, **2**, 2524-2560

[3] Garelli F., Dematteis E. M., Stavila V., Di Florio G., Carbone C., Agostini A., Palumbo M., Baricco M., Rizzi P. “Enhancing TiFe Alloy Activation for Hydrogen Storage Through Al, Cr, Co, and Cu Substitutions as a Step Towards Future Recycling”, 2025, arXiv:2504.0699ov2

[4] van Oers L., Guinèe J. B., Heijungs R., Schulze R., Alvarenga R. A. F., Dewulf J., Drielsma J., Sanjuan-Delmas D., Kampmann T. C., Bark G., Garcia Uriarte A., Menger P., Lindblom M., Alcon L., Sevilla Ramos M., Escobar Torres J. M. “Top-down characterization of resource use in LCA: from problem definition of resource use to operational characterization factors for dissipation of elements to the environment”, 2020, *Int. J. Life Cycle Assess.*, **25**, 2255-2273

EFCH2 2025 European Fuel Cells and Hydrogen
PIERO LUNGHI CONFERENCE
September 17th–19th 2025
Capri / Italy

Techno-economic-environmental analysis of hydrogen production technologies using domestic wastewater

Mendes T[a], Felizardo F[b], Silva R[b], Novais MH[b,c], Iten M*[a],

*muriel.iten@fraunhofer.pt
[a]Fraunhofer Portugal AWAM. , Régia Douro Park, Vila Real, 5000-033 Portugal
[b]University of Evora, SOL4R - Applied Research in Solar Energy for the Energy, 7000-083 Nossa Senhora da Tourega, Portugal
[c]University of Evora, Water Laboratory, 7005-345 Evora, Portugal

Keywords: hydrogen production technologies; domestic wastewater, Techno-economic-environmental analysis

Abstract

In this paper, green hydrogen production using urban wastewater is investigated, comparing the most suitable electrolysers presented in the literature review. The relevant technologies include Alkaline Electrolysis- AEL; Proton Exchange Membrane -PEM; Solid Oxide Electrolysis- SOEC, and Microbial Electrolyser Cell- MEC. These are compared from the technical, economic, and environmental points of view. At first, the technical criteria are established (e.g. system energy consumption, system energy efficiency and hydrogen generation rate from wastewater), following the economic criteria (i.e. investment costs, annual operating costs, plant lifetime, levelized cost of hydrogen-LCH) and the environmental criteria (i.e. global warming potential-GWP), acidification potential-AP), eutrophication potential-EP). This analysis is useful for a pre-feasibility analysis of hydrogen electrolysis, enabling comparisons from different perspectives. It is found that SOEC presents better performance on a technical perspective, due to its high efficiency (>85%) and hydrogen generation from wastewater (reaching up to 3000 m3/day). While on the economic side, the AEL presents more attractive values, namely on investment cost (due to its technology maturity), but the LCH is higher compared to other technologies. MEC technology presents the lowest environmental impacts.

Introduction:

Four main electrolysis technologies with different characteristics are presented in the literature review, as presented in Table 1.

Table 1- *Electrolysis Technologies Characterisation [1]*

Technology	Electrolyte	Ion Transport	Operating Temp (°C)
Alkaline Electrolysis (AEL)	Liquid KOH/NaOH	OH^-	~80
Proton exchange membrane (PEM Electrolysis)	Solid polymer	H^+	~50–80
Solid Oxide Electrolysis (SOEC)	Ceramic (YSZ)	O^{2-}	700–1000
Microbial Electrolyser Cell (MEC)	Liquid (e.g., wastewater)	H^+ or OH^- (depending on setup)	~20–40

Objectives:

Hydrogen can be produced from several technologies, making it a crucial source in the energy transition to low or zero carbon societies. Hydrogen production can be based upon renewable sources, urban or agricultural wastes, etc. A comprehensive analysis of technologies for hydrogen production fed by urban wastewater is still required. The key criteria, ranging from technical, economic and environmental aspects are presented, enabling

to perform a comparative analysis from these three perspectives. Hence, this study intends to compare the main four electrolysis technologies for hydrogen production considering the use of urban wastewater.

Material and methods:

This study follows the Preferred Reporting Items for Systematic reviews and Meta-Analyses 2020 (PRISMA 2020) methodology. PRISMA 2020 was employed to screen articles relevant to the study of hydrogen production through the electrolysis of urban wastewater. The bibliographic search was conducted using SCOPUS database for peer-reviewed literature. The search used the following keywords: ("wastewater" OR "wastewater treatment" OR "treated wastewater" OR "municipal wastewater") AND "electrolysis" OR "electrolyser" OR "electrolyzer" OR "electrochemical water splitting" OR "water electrolysis") AND ("hydrogen production" OR "hydrogen generation" OR "green hydrogen") Following the initial search, predefined inclusion and exclusion criteria were applied to screen and select studies [2]. Articles were then subjected to detailed analysis to extract data related to hydrogen production through electrolysis with urban wastewater as feed. This methodology enables the article selection as the basis for the techno, economic and environmental analysis. The technical criteria include system energy consumption (kWh/m3H2); system energy efficiency (%), and hydrogen generation rate from wastewater (Nm3/day/m2). For the economic analysis, the following criteria have been established: investment costs of electrolysis (M€); annual operating costs (k€/year); Plant lifetime (year); and levelized cost of hydrogen (€/kg). While for the environmental analysis includes the Global warming potential (GWP) (kgCO2 eq.); Acidification potential (AP) (kgSO2 eq.), and Eutrophication potential (EP) (gP eq.).

Results:

From the literature review, a total of 517 articles (limited to research articles and reviews) published between 2020 and 2025 were retrieved. Tables 2-3 present the summary of the technical, economic and environmental parameters. On a technical point of view, the most advantageous solution is the SOEC. Even though its energy consumption is higher than the MEC, the overall system presents higher energy efficiency and higher hydrogen generation from wastewater. From the economic perspective, the investment costs and annual operating costs are lower for the AEL, this is due to the maturity of this technology compared to others. The plant lifetime is similar for all technologies, while the levelized cost of hydrogen (e.g. the total expenses involved in producing hydrogen throughout its entire lifecycle, CAPEX and OPEX) is significantly lower for the MEC technology. On the environment perspective the SOEC presents the highest environmental loads, mainly related to the production chain of the electrolytic cell.

Conclusions:

Overall, the AEL present higher TRL, lower costs but require liquid electrolyte handling. The PEM electrolyser is more compact and presents fast response, but their costs are higher due to expensive catalysts. The SOEC present high efficiency and may use waste heat, however there is material degradation with high temperature operations and high environmental loads. The MEC presents simultaneous wastewater treatment and H2 production, but it presents slow kinetics and scale-up challenges.

Acknowledgment

This work was supported by European funds: H2tALENt project (Grant agreement ID: 101137611). DOI: 10.3030/101137611

References

[1] M. F. Ahmad Kamaroddin *et al.*, "Membrane-Based Electrolysis for Hydrogen Production: A Review," *Membranes*, vol. 11, no. 11, Art. no. 11, Nov. 2021, doi: 10.3390/membranes11110810.

[2] M. J. Page *et al.*, "PRISMA 2020 explanation and elaboration: updated guidance and exemplars for reporting systematic reviews," *BMJ*, vol. 372, p. n160, Mar. 2021, doi: 10.1136/bmj.n160.

Table 2 - Technical Parameters, literature survey

Electrolyser	System energy consumption (kWh/m^3_{H2})	System Energy Efficiency (%)	Hydrogen generation rate from wastewater (m^3/day)
Alkaline (AEL)	3.486 ; 3.96	66	448 ; 4.60
Proton Exchange Membrane (PEM)	4.482	62 ; 59	2.58*
Solid Oxide (SOEC)	3.154	**88 ,** 85	**3199.9**
Microbial Electrolysis Cells (MEC)	0.5 **; 0.08**	60 ; 78 ; 64 ;	0.3 0.8

*No area units

Table 3 - Economical Parameters, literature survey

Electrolyser	Investment costs electrolysis (M€)	Annual operating costs (k€/year)	Plant lifetime (year)	Levelized Cost of Hydrogen (LCH) (€/kg)
Alkaline (AEL)	**0.1 - 0.18**	**2 - 4 %* - 345**	**20**	6.28
Proton Exchange Membrane (PEM)	0.17 - 0.26	3 - 5 %* - 700		-
Solid Oxide (SOEC)	0.24 – 0.31	3%* - 675	**20 ; 20**	**2.70**
Microbial Electrolysis Cells (MEC)	0.22 ; 1.58 ;	768.33 ; 464.18	10 ; **20**	4.78

*Relation with the investment costs (M€)

Table 4 - Environmental Parameters, literature survey

Electrolyser	Global warming potential (GWP) ($kgCO_{2eq.}/kg_{H2}$)	Acidification Potential (AP) ($kgSO_{2eq.}$)	Eutrophication Potential (EP) ($gP_{eq.}$)
Alkaline (AEL)	3-7	0-0.010	0-0.0017**
Proton Exchange Membrane (PEM)	2.4	-	0.0032
Solid Oxide (SOEC)	3-5	**~0**	**~0****
Microbial Electrolysis Cells (MEC)	0.17 -10.0* **; 0.17** ; 0.22	0, 0023	0.002 – 0.016

* Per H_2 produced

** Units $g_{PO4eq.}/kg_{H2}$

European Fuel Cells and Hydrogen
PIERO LUNGHI CONFERENCE
September 17th–19th 2025
Capri / Italy

University–Business Collaboration in Transnational Hydrogen Valley

Marinella Favot*[a], Alberto Soraci [a,b], Fabio Morea[a], Barbara Monaco[a]

*corresponding author: Marinella Favot
[a] Area Science Park, Padriciano 99, Trieste (Italy)
[b] Department of Economics, University of Messina, Messina, Italy

Keywords: Hydrogen economy, Hydrogen Valley, Innovation Ecosystem, University-Industry Collaboration (UBC).

Abstract

This study examines university–business collaboration (UBC) within the North Adriatic Hydrogen Valley (NAHV). Surveying key stakeholders across Italy, Slovenia, and Croatia, it identifies shared goals, funding, and relationships as main enablers, while limited awareness and time mismatches remain key barriers. Public actors are most positive about UBC, firms more critical. Social acceptance of hydrogen hinges on regulatory clarity and public engagement. Aligning "hard" infrastructure with "soft" enablers is essential to realizing NAHV's innovation potential.

Introduction.

Hydrogen Valleys are integrated regional platforms where the full hydrogen value chain is tested in real conditions. Their success relies not only on technological solutions but also on effective collaboration among universities, companies, and public institutions. While university–business collaboration (UBC) is widely seen as crucial to innovation, specific insights for the hydrogen sector—and especially for Hydrogen Valleys—are still limited. This study focuses on the North Adriatic Hydrogen Valley (NAHV), involving Italy, Slovenia, and Croatia, to explore how different stakeholders perceive UBC dynamics, including enablers, barriers, and social impacts. The aim is to support policies that align infrastructure investment with collaboration and community engagement.

Objectives

Hydrogen Valleys are emerging as spatially integrated testbeds where hydrogen production, storage, distribution and multi-sector end use are piloted in real operating conditions. Some studies already address the UBC [1;2] but understanding of how university–business collaboration operates inside such complex ecosystems like hydrogen valleys is still limited. This study addresses that gap by profiling companies, universities and research centres, and public administrations plus business-support organisations (PA/BSOs) - perceive core dimensions of UBC. Particular attention is paid to the concrete enablers and barriers that, in the view of each group, accelerate or inhibit cooperation along the hydrogen value chain. The ultimate goal is to generate evidence that NAHV policymakers can use to synchronise "hard"

technology pillars with “soft” enablers such as regulation, education programs, shared labs and testbeds, as well as invest in the UBC collaboration and in social engagement to promote knowledge and acceptance of this technology.

Material and methods

Three structured online questionnaires were developed, each containing up to 50 items. Following pilot testing with ten external reviewers, the surveys were open from November 2024 to February 2025. The wording was adjusted to suit each respondent group, but the question sets were kept as closely aligned as practicable; group-specific items were added only where strictly necessary. The instrument contained different sections: a profiling block that captured geography, size, respondent position etc.; the section on current engagement and future interest in the hydrogen sector; the core section exploring the breadth and depth of co-operation across the hydrogen value chain including barriers and facilitators, motivational factors, support mechanisms; the fouth section investigating social acceptance of hydrogen; last section on the perceived level of collaboration addressed by 6 likert-scale questions to rate the overall intensity and quality of their collaboration with other actors.

The survey was disseminated via NAHV partners, regional business associations and incubators to cover all NAHV area. The questionnaires were hosted on Microsoft Forms, and the raw responses were collected in Microsoft Excel files. Using Power Query we cleaned, normalised, and reshaped the dataset, while the descriptive statistics and figures were produced with Excel’s built-in charting functions.

Results

The total number of valid filed questionnaires were 210 from which we select the 163 ones from the NAHV area respondents. The main perceived barriers to UBC identified across stakeholders include lack of awareness about university offerings, limited government funding for cooperation, and differing time horizons. The most cited facilitators of UBC were the existence of funding for cooperation, mutual interest and shared goals, and pre-existing relationships. From the likert replies we discovered that public actors hold the most positive views on UBC, while companies are more critical and universities remain in between. Firms see academic research as slow and insufficiently market-oriented, unlike public bodies who view it favorably. Universities doubt industry’s interest in collaboration, while public actors remain optimistic. Collaboration is widely seen to depend on funding, shared goals, and personal relationships. Barriers differ by group: firms cite time and funding gaps, universities point to firms limited absorptive capacity, and public actors stress bureaucratic inertia. Firms report strong needs for technical expertise, confirming high reliance on academic collaboration. Other questions addressed the perceived social impacts: the most significant perceived ones include public acceptance and its perception as a safe energy source, decarbonisation of energy production, and climate change mitigation. Respondents also highlighted job creation and contributions to energy independence, while concerns such as

water use and energy intensity were noted but considered less critical. To achieve positive social acceptance of hydrogen technology, respondents emphasized the need for clear and consistent regulatory frameworks as the most crucial factor, followed by calls for public education and awareness campaigns. Other important elements included transparent communication on climate contributions, hands-on public engagement through test beds, and early involvement of local communities in planning processes. Economic arguments and job transition support were seen as less central to social acceptance.

Conclusions

This study provides a comprehensive view of UBC within the North Adriatic Hydrogen Valley (NAHV), revealing both structural and perceptual gaps that influence cooperation along the hydrogen value chain. While all stakeholders acknowledge the critical role of UBC, their perspectives diverge significantly: public actors are the most optimistic, companies the most critical, and universities hold a moderate stance. Collaboration is widely perceived to depend on dedicated funding, shared goals, and existing relationships, yet barriers such as time mismatches, funding shortages, limited absorptive capacity, and bureaucratic inertia persist. The findings also highlight that for hydrogen technology to gain broad social acceptance, stakeholders prioritize regulatory clarity, safety communication, and inclusive engagement strategies over purely economic arguments. Public perception of safety, climate benefits, and energy independence stand out as key social drivers, while concerns over resource intensity remain secondary. These insights underscore the importance of aligning “hard” infrastructure investments with “soft” enablers—policy design, institutional cooperation, and social dialogue—to fully realize the innovation potential of hydrogen valleys like NAHV.

Acknowledgment

Grant information: This project has received funding from the European Union’s Horizon Europe research and innovation programme under grant agreement No [101111927](North Adriatic Hydrogen Valley [NAHV]). The funders had no role in study design, data collection and analysis, decision to publish, or preparation of the manuscript. Views and opinions expressed in this paper are however those of the author(s) only and do not necessarily reflect those of the European Union or the Clean Hydrogen Joint Undertaking. Neither the European Union nor the granting authority can be held responsible for them. The funders had no role in study design, data collection and analysis, decision to publish, or preparation of the manuscript.

References

[1] Evans, N., Miklosik, A., & Du, J. T. (2023). University–industry collaboration as a driver of digital transformation: Types, benefits and enablers. Heliyon, 9(1), e21017. https://doi.org/10.1016/j.heliyon.2023.e21017

[2] Ballesteros-Ballesteros, V.A.; Zárate-Torres, R.A. Mapping the Conceptual Structure of University–Industry Knowledge Transfer: A Co-Word Analysis. Publications 2025, 13, 8. https://doi.org/10.3390/publications13010008

European Fuel Cells and Hydrogen
PIERO LUNGHI CONFERENCE
September 17th–19th 2025
Capri / Italy

Cradle-To-Use Life Cycle Assessment of an Alkaline Electrolyzer

Sari Alfreijat*[a], Giovanni Cinti [a]

* corresponding author: sari.alfreijat@studenti.unipg.it
[a] Università degli Studi di Perugia, Department of Egineering, Via Duranti 93, 06122 Perugia

Keywords: Alkaline, Electrolysis, Life Cycle Assessment, Hydrogen

Abstract

In the coming years hydrogen will increasingly become a significant alternative to fossil fuels, which are widely used today in transportation, energy generation, and heating sectors. Hydrogen is essential in sectors such as metallurgy and chemical industry. A technology usually adopted for hydrogen production in these fields is water electrolysis, where systems called electrolyzers split water in its components: oxygen and hydrogen. However, only a few types of electrolyzers can be considered technologically mature -among them- the alkaline electrolyzers. This article presents an environmental Life Cycle Assessment (LCA) of an alkaline electrolyzer. This LCA follows a Cradle-to-Use approach, considering the extraction of raw materials, system production, and subsequent hydrogen generation. The results of the analysis are then referenced to one kilogram of hydrogen gas produced over the product lifetime, making this the functional unit. The results show that, in the manufacturing phase of the system, the highest contributions come from the BoP with a lower contribution from the stack.

Objectives: The objective of this study is to evaluate the environmental impact of an alkaline system for water electrolysis, highlighting the contributions of the production phase of the various components and the subsequent gas production phase. This analysis aims to provide more data to support future decisions for product improvement, including considerations of environmental impact.

Material and methods: The method used in this study is Life Cycle Assesment (LCA), procedure standardized by the International Organization for Standardization (ISO) in its 14000 series of standards [1]. In particular, the ISO 14040 subfamily focuses on product life cycle assessment, providing guidelines for conducting such assessments. The data used in this study come from the product company, which provided the machine's catalog, drawings and Bill of Materials. This data was supplemented with information from literature and online

catalogs, as well as on-site measurements, calculations, and estimates. All the results are referred to one kilogram of hydrogen produced, making this the functional unit of the assessment.

The system boundary is Cradle-to-Use: the supply chain leading to the assembled and ready-to-use product is modelled with a certain degree of approximation. Each component of the machine is analyzed starting from the extraction of raw materials, including transportation and all other processes leading to the assembly of the electrolyzer. The analysis then continues by considering the material and energy flows associated with the hydrogen production phase for 32000 h (other cases in the complete thesis). The end-of-life phase of the machine is excluded from the system boundary. The assessment is conducted using the SimaPro software [2], while the impact data come from the ecoinvent database [3]. For the LCIA part the Environmental Footprint 3.0 [4] method is used.

Results: Figure 1 (left) shows the impacts of the life cycle of alkaline electrolyzer considering a usage of 32000 h (six stacks). Considering that the stack represents more than a half of the weight of the system, the materials and processes involved in its production are not particularly critical from an environmental perspective, being the percentual contributions always under 50%. The usage phase represents the most significant share of the impacts, being considerably more impactful than the construction phase. As seen in Figure 1 (right) the largest contribution comes from the electricity required for the active electrolysis phase, while the demineralized water consumed often contributes less than 1% of the impacts caused by hydrogen production. A sensitivity analysis on energy source effects is reported in Figure 2, important results are achieved if photovoltaic energy is used, with the “Climate change” indicator reduced by 80%. Electrolyzer efficiency have a big impact on greenhouse gas emissions, with those reduced by 2% with a 1% efficiency improvement (benefits reach 12% with a 10% improvement in efficiency).

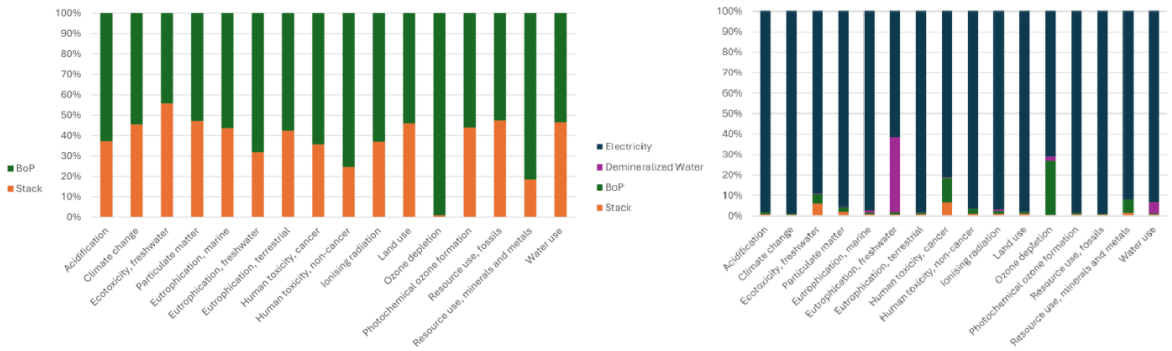


Figure 1: (left) Environmental Impacts Distribution for the Manufacturing Phase. (right) Total Life Cycle Impact Assessment results.

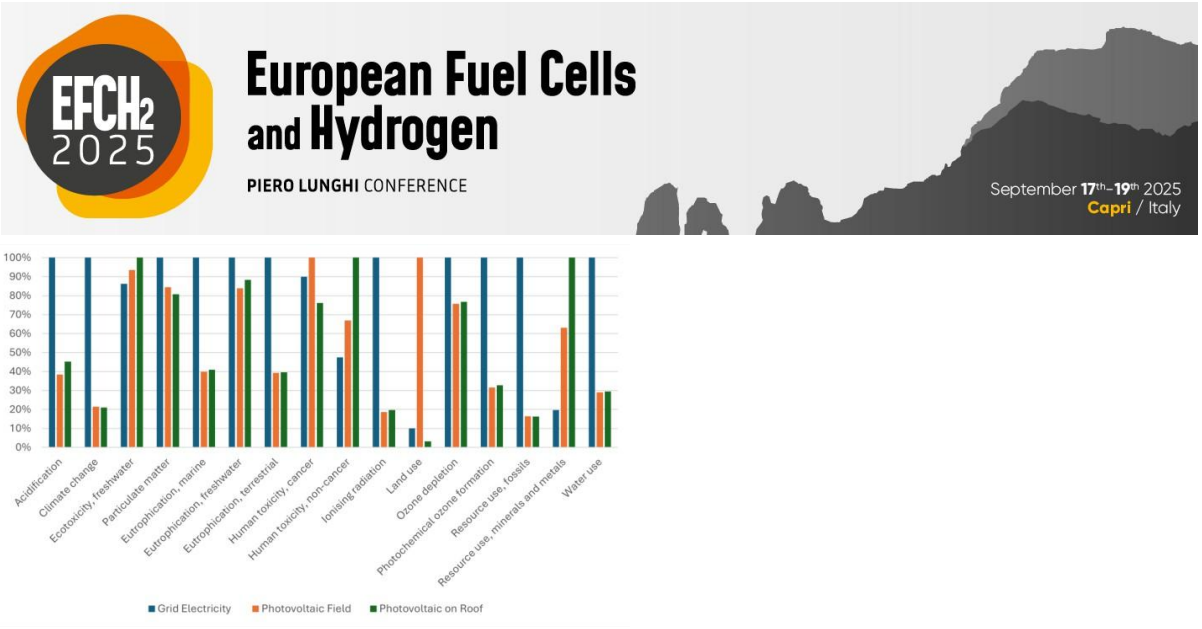


Figure 2: Comparison between use of grid and photovoltaic electricity.

Conclusions: The phase responsible for most of the impacts is the hydrogen production phase, with electricity being the main contributor. This is due to the significant electricity consumption during the product's life. Therefore, to achieve meaningful results in impact mitigation, the focus should be on the power source of the electrolyzer, as well as its efficiency. This means that efforts should focus on reducing the energy consumption of the electrolyzer by improving materials and technology, keeping in mind that the promising results from the sensitivity analysis can be achieved with small efficiency improvements.

Acknowledgment

This research was co-funded from the European Union and the Clean Hydrogen Partnership under Grant Agreement No. 101192392 (GUESS-WHy).

References

[1] "ISO 14000 family. Environmental management." Accessed: Jan. 26, 2025. [Online]. Available: https://www.iso.org/standards/popular/iso-14000-family

[2] SimaPro, "LCA software for informed changemakers." Accessed: Jan. 27, 2025. [Online]. Available: https://simapro.com/

[3] Ecoinvent, "Ecoinvent Webpage." Accessed: Jan. 27, 2025. [Online]. Available: https://ecoinvent.org/

[4] European Commission, "European Platform on LCA | EPLCA." Accessed: Jan. 27, 2025. [Online]. Available: https://eplca.jrc.ec.europa.eu/



Spatial assessment of the impact of hydrogen production on European freshwater resources

Julien BOLARD*[a], Lara KURZ[a], Alberto PISTOCCHI[a], Marco SERAFINI[a]

* corresponding author: julien.bolard@ec.europa.eu

[a] European Commission, Joint Research Centre

Keywords: hydrogen production, European freshwater resources, spatial assessment, hydrological modelling

Abstract

We assessed the water abstraction and consumption of current and future hydrogen production assets across 3 different climate change scenarios. We coupled data on water intake for plants with the JRC LISFLOOD hydrological model and analysed the total and relative impact of the hydrogen production at river-basin level. We conclude that the deployment of large-scale hydrogen production is likely to have a relatively minor impact compared to actual water stress up until 2030 and becomes significant in more than 10% of planned assets after 2030.

Introduction: Renewable hydrogen production requires high-quality water at the production site, both as a feedstock and as cooling agent for the electrolyser. Several studies address water consumption of an emerging hydrogen economy by focusing on aggregated volumes of water available and/or consumed at the global (Newborough et al., 2021) (IRENA, 2023), European (Beswick et al., 2021) or national level, such as in the United States (Lee et al., 2019). To the best of our knowledge, there is no assessment at river-basin level covering the European Union territory considering the relative impact of hydrogen production compared to other industrial and non-industrial users of water under different climate change scenarios.

Objective: As water stress and shortages are expected to increase across Europe in the mid- and long-term (Bisselink et al., 2020), a better understanding of the regional water availability for hydrogen production is needed to prevent unintended environmental consequences. This study will provide estimation of water consumption for hydrogen production in 2030 and 2050 in Europe as well as the relative impact of hydrogen assets against other local consumers of water under different climate change scenarios.

Material and methods: We collected data on the level of water abstraction and consumption of fossil-based and electrolytic hydrogen production processes. We compiled, cleaned, harmonised commercial and public datasets on current and future hydrogen production projects and validated

using GIS and remote sensing technologies. We evaluated water stress at basin-level for all plants by spatial joining with the World Resources Institute Aqueduct dataset (Kuzma et al., 2023) using the Water Stress Indicator. We compared the outcomes of this extraction using the LISFLOOD hydrological model developed by JRC (Van Der Knijff et al., 2010). We generated water basin-specific Water Exploitation Index + (WEI+) values (Casadei et al., 2020) for the years 2023, 2030, 2040, 2050 under three different climates scenarios. One scenario served as a baseline and is based on the statistical extrapolation of historical climate trend, two scenarios are based on the IPCC RCP4.5 and RCP8.5 scenarios (Calvin et al., 2023). We then conducted a statistical analysis of this data to estimate the share of hydrogen projects under potential water stress, meaning a WEI+ above 40%. We also compared project impacts between Aqueduct and LISFLOOD methodology.

Results: The model implementation returns 12 series of Water Exploitation Index at asset level for each year (2023, 2030, 2040, 2050) under 3 different climate scenarios. In total, 1 319 locations were assessed including 64 assets that were removed from the list because they were located on the coastline and had no WEI+ values. Preliminary results show that in 2023, 18 projects out of 776 (2.3%) had a WEI+ higher than 40% solely imputable to the production of hydrogen and 331 projects out of 776 (43%) were located in river basins already under water stress with a WEI+ greater than 40%. Only 3 hydrogen production assets are identified where the production of hydrogen specifically drove the WEI+ in water stressed range and where counterfactual scenarios showed no water stress without the production of hydrogen and its consumer, a refinery. In 2030, 35 assets out of 1233 (2.8 %) had a hydrogen specific WEI+ greater than 40%. In 2040, 128 assets out of 1231 (10.4 %) had a hydrogen specific WEI+ greater than 40%. This number increased to 164 out of 1204 (13.6 %) for 2050. Across all years, the values increased under higher climate stress.

Conclusions: Preliminary results show that the deployment of large-scale hydrogen production has a minor impact compared to actual water stress up until 2030 and becomes significant in more than 10% of planned assets after 2030. Most of the projects to be deployed before 2030 are also deployed in large-scale industrial hubs and are expected to rely on industrial water treatment systems.

Acknowledgment: Authors are grateful to the EIGL team and Ignacio HIDALGO GONZALEZ in particular for the data analysis and harmonisation.

Reference

Beswick, R. R., Oliveira, A. M. and Yan, Y. (2021), 'Does the Green Hydrogen Economy Have a Water Problem?', *ACS Energy Letters*, Vol. 6, Issue 9, pp. 3167–3169, https://doi.org/10.1021/acsenergylett.1c01375.

Bisselink, B., Bernhard, J., Gelati, E., Adamovic, Guenther et al. (2020), *Climate change and Europe's water resources - JRC PESETA IV project – Task 10*, *Publications Office of the European Union*, https://doi.org/10.2760/15553.

Calvin, K., Dasgupta, D., Krinner, G., Mukherji, A., Thorne, P. W. et al. (2023), 'IPCC, 2023: Climate Change 2023: Synthesis Report. Contribution of Working Groups I, II and III to the Sixth Assessment Report of the Intergovernmental Panel on Climate Change [Core Writing Team, H. Lee and J. Romero (eds.)]. IPCC, Geneva, Switzerland.', First, 25 July, Intergovernmental Panel on Climate Change (IPCC), https://doi.org/10.59327/IPCC/AR6-9789291691647.

Casadei, S., Peppoloni, F. and Pierleoni, A. (2020), 'A New Approach to Calculate the Water Exploitation Index (WEI+)', *Water*, Vol. 12, Issue 11, p. 3227, https://doi.org/10.3390/w12113227.

European Environment Agency (ed.) (2021), *Water resources across Europe: confronting water stress: an updated assessment*, EEA report, No no. 2021, 12, Publications Office of the European Union, Luxembourg, https://doi.org/10.2800/320975.

IRENA (2023), 'Water for hydrogen production', https://www.irena.org/Publications/2023/Dec/Water-for-hydrogen-production.

Kuzma, S., Bierkens, M. F. P., Lakshman, S., Luo, T., Saccoccia, L. et al. (2023), 'Aqueduct 4.0: Updated decision-relevant global water risk indicators'.

Lee, U., Xu, H., Daystar, J., Elgowainy, A. and Wang, M. (2019), 'AWARE-US: Quantifying water stress impacts of energy systems in the United States', *Science of the Total Environment*, Vol. 648, Elsevier B.V., pp. 1313–1322, https://doi.org/10.1016/j.scitotenv.2018.08.250.

Newborough, M. and Cooley, G. (2021), 'Green hydrogen: water use implications and opportunities', *Fuel Cells Bulletin*, Vol. 2021, Issue 12, Elsevier Ltd, pp. 12–15, https://doi.org/10.1016/S1464-2859(21)00658-1.

Van Der Knijff, J. M., Younis, J. and De Roo, A. P. J. (2010), 'LISFLOOD: a GIS-based distributed model for river basin scale water balance and flood simulation', *International Journal of Geographical Information Science*, Vol. 24, Issue 2, pp. 189–212, https://doi.org/10.1080/13658810802549154.

EFCH2 2025 European Fuel Cells and Hydrogen
PIERO LUNGHI CONFERENCE
September 17th–19th 2025
Capri / Italy

Comparative life cycle analysis of green hydrogen production

Caecilia Vitasari*a, Paolo Perico a, Davide Bonalumi*a

* corresponding author: Davide Bonalumi
a Department of Energy, Politecnico di Milano, Milan, Italy

Keywords: carbon footprint, Green hydrogen, greenhouse gas emissions, solid oxide electrolysis cell

Introduction

The environmental impact of water electrolysis for hydrogen production has been studied for more than one decade. Although it is useful to identify the major cause of environmental burden as well as to guide technology development, many literature has pointed out that the lack of data limits the assessment. As an example, the impact of an unknown component is usually assumed to be zero or the same as that of a similar material [1], which may lead to under- or overestimation.

In the OUTFOX project, solid oxide electrolysis cell (SOEC) technology was chosen to produce green hydrogen due to its higher temperature operation, which leads to lower electricity consumption. It is being developed to achieve 1 MW hydrogen production by using an optimised SOECs. The technology is designed and assessed based on the economic feasibility and environmental impact. Considering the common LCA limitation, we strive to use as much as primary data as possible. If there is still missing data, it will be estimated based on existing knowledge or literature.

Objectives

This study aims to calculate the greenhouse gas (GHG) emissions of SOEC and then compare them to the more mature technologies, namely Proton Exchange Membrane (PEM) and Alkaline Electrolysis Cell (AEC), in the European context.

Material and methods

The scope of this LCA study includes two stages: the manufacturing of stacks and Bill of Materials (BOM) units, and hydrogen production. Three electrolysis technologies were compared: PEM, AEC, and SOEC.

GREET® 2024 was used to calculate GHG emissions. The inventories of the electrolyzer (based on the BOM) were taken from the literature [1]. The missing primary data was estimated using the literature. The geographical location was set to the EU, using three different electricity sources: the EU grid, solar, and wind energy.

Results

For each studied electrolyzer, the material-related GHG emission somewhat corresponds to the major constituents of the stack and/or BOM, in which steel has the highest embodied emission. For all studied technologies, steel, the major component used in the stacks and BOPs, causes the highest embodied emissions.

Hydrogen production is the main source of total GHG emissions, which is attributed to the source of electricity used, with grid electricity having the highest impact, followed by solar and wind power. In fact, the total GHG emission could be reduced by one order of magnitude by using solar- or wind-generated electricity, leading to a more significant share of embodied GHG emissions of the manufacturing process (in the range from about 10% for PEM and SOEC to approximately 30% for AEC). The total GHG emissions of SOEC are the lowest among the electrolyzers, regardless of the electricity source. When wind-generated electricity is employed, the total GHG emission for SOEC is roughly 0.4 kg $CO_{2\text{-eq}}$/kg H_2, followed by PEM and AEC with approximately 0.65 kg $CO_{2\text{-eq}}$/kg H_2 and 0.8 kg $CO_{2\text{-eq}}$/kg H_2, respectively.

Conclusions

To minimise GHG emissions, renewable energy is preferred for producing green hydrogen by electrolysis. Introducing the primary data of stack and BOM manufacturing gives a starting point to further minimize GHG emissions and use critical raw materials.

Acknowledgment

The work is financed by the OUTFOX project (https://outfoxproject.com/), which is supported by the Clean Hydrogen Partnership and co-funded by the European Union (Grant Agreement no. 101101439).

References

[1] Iyer RK, Prosser JH, Kelly JC, James BD, Elgowainy A. Life-cycle analysis of hydrogen production from water electrolyzers. Int J Hydrogen Energy 2024;81:1467–78. https://doi.org/https://doi.org/10.1016/j.ijhydene.2024.06.355.



TOPIC 6: HYDROGEN POLICY, MARKET AND BUSINESS MODELS

EFCH2 2025
European Fuel Cells and Hydrogen
PIERO LUNGHI CONFERENCE
September 17th–19th 2025
Capri / Italy

Techno-economic evaluation/analysis of different applications for the direct utilization of imported ammonia

Gapinski, M.[a,b], Scheffler, F.[b], Munte, C.[a], Schulz, M.[b], Imdahl, C.[b] Zellmer, S.[a,b]
* corresponding author
[a] Technische Universität Braunschweig Institute for Particle Technology TU Braunschweig
[b] Fraunhofer Institute for Surface Engineering and Thin Films IST

Keywords: ammonia, decarbonization, systemic hydrogen carrier

Abstract

Introduction: Ammonia (NH_3) is emerging as a systemic transport vector for intercontinental hydrogen trading. The first large-scale exports from Egypt and Morocco are expected as early as 2027, even before suitable cracking plants are available. Therefore, ecologically viable supply options and cost-efficient approaches for direct utilization of ammonia must be identified and developed at an early stage. It is expected that green hydrogen can be imported cost-effectively at a price of 4.50 €/kg, and green ammonia of 800 €/t, respectively. [1–3]

Objectives: Green ammonia can easily replace fossil-based ammonia as feedstock in the chemical industry, while it is not cost-effective, costing approximately 3 times its fossil counterpart [3]. However, in the early stages, the allocation of limited green hydrogen resources must be carefully balanced against the need for immediate carbon reduction strategies [4, 5]. To address this gap, this research evaluates innovative applications and scenarios for the direct utilization of ammonia, considering techno-economic and environmental aspects.

Material and methods: This research models entire NH_3 value chains based on real import data on an annual ammonia import of 1 million tonnes and literature sources. The methodology combines both qualitative and quantitative analyses. The study focuses on several applications, including the direct combustion of NH_3 for energy generation, its conversion into electrical energy via ammonia fuel cells, the substitution of grey NH_3 in industrial processes and the direct reduction of iron ore. The techno-economic evaluation is conducted using cost-benefit analysis, while the ecological impact is assessed based on the specific CO_2 reduction potential of different applications paths.

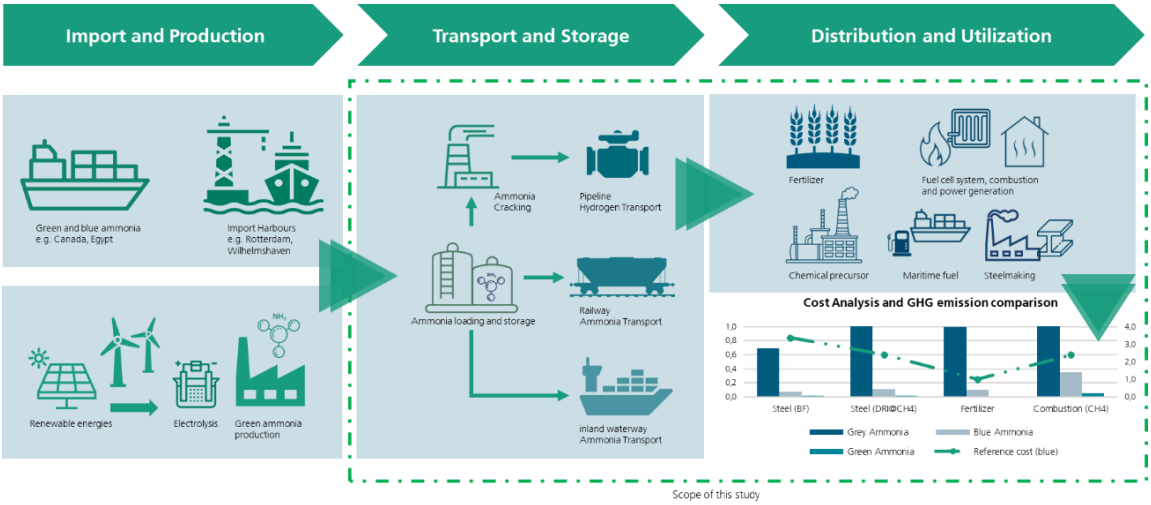


Figure 1: Graphical abstract and focus of the study on the techno-economic assessment of the direct use of ammonia in various sectors

Results: The analysis of direct ammonia utilization provides insights into efficient market mechanisms for decarbonization, highlighting their environmental benefits and economic feasibility. Although the largest CO_2 reduction potential resides in the production of direct reduced iron (4.7 t CO_{2eq}/ t NH_3), implementation in existing market structures such as the chemical industry is feasible in the short term with a CO_2 reduction potential of approx. 2 t CO_{2eq}/ t NH_3. Identifying and prioritizing specific application pathways support climate targets, contributing to discussions on NH_3's role in the future hydrogen economy and optimizing technical decisions from a techno-economic perspective.

Conclusions: The study demonstrates that ammonia is not only a viable hydrogen transport vector, but also offers significant potential for CO_2 reduction. The findings provide a comprehensive economic and ecological evaluation of short-term market-ready applications for the direct use of ammonia, particularly in the absence of large-scale cracking plants or optimized processes.

Acknowledgment

This publication was created as part of the research program "Transforming the Energy System Lower Saxony" (TEN.efzn) at the Energy Research Center of Lower Saxony (efzn).

Funded by zukunft.niedersachsen, the joint science funding program of the Lower Saxony Ministry of Science and Culture and the Volkswagen Foundation.

References

[1] German Federal Ministry for Economic Affairs and Climate. 2024. *Important step for global hydrogen ramp-up – Germany will work with H2Global to import green hydrogen products on a large scale from 2027*, Berlin.

[2] Ong, C. W., Chang, N., Tsai, M.-L., and Chen, C.-L. 2024. Decarbonizing the energy supply chain: Ammonia as an energy carrier for renewable power systems. *Fuel* 360, 130627.

[3] Scheffler, F., Imdahl, C., Zellmer, S., and Herrmann, C. 2025. Techno-economic and environmental assessment of renewable hydrogen import routes from overseas in 2030. *Applied Energy* 380, 125073.

[4] Tonelli, D., Rosa, L., Gabrielli, P., Parente, A., and Contino, F. 2024. Cost-competitive decentralized ammonia fertilizer production can increase food security. *Nature food* 5, 6, 469–479.

[5] Trinca, A., Vilardi, G., and Verdone, N. 2025. Towards carbon neutrality: The ammonia approach to green steel. *Energy Conversion and Management* 326, 119482.

EFCH2 2025 European Fuel Cells and Hydrogen PIERO LUNGHI CONFERENCE
September 17th–19th 2025 Capri / Italy

HyAcademy.eu: Building a Pan-European Hydrogen Skills Ecosystem for Climate Neutrality

Marcello Romagnoli*[1], Tiziana Altiero [1], Enrico Giliberti [1], Chiara Puecher[1], Hana Bartkova[2], Karel Bouzek[2], Robert Steinberger-Wilckens[2]

* corresponding author: Marcello Romagnoli

[1] H2 Research Centre MO-RE (Unimore), Via Università, 4, 41121, Modena - Italy

[2] University of Chemistry and Technology Prague, Technicka 5, Prague 166 28 – Czech Republic

Keywords: Hydrogen Education, Workforce Development, EU Green Transition, Hydrogen Technology Training, Multi-Stakeholder Collaboration

Abstract

Introduction: *Hydrogen is increasingly recognised as a pivotal element in the global transition towards a low-carbon economy, offering dual benefits of reducing greenhouse gas emissions and enhancing energy security. By integrating renewable energy sources with hydrogen storage, countries can mitigate reliance on fossil fuels and ensure a more resilient energy system [1,2]. Nevertheless, the large-scale implementation of hydrogen technologies is dependent on overcoming significant technological and economic challenges, including scaling up production while maintaining quality and safety standards. [3,4]. A critical barrier to achieving these objectives is the current shortage of skilled professionals equipped to handle the complexities of hydrogen technologies. HyAcademy.eu addresses this gap by developing high-quality educational materials, accessible to students and educators alike, to foster a well-prepared workforce capable of driving the hydrogen sector forward.*

Objectives: HyAcademy.eu seeks to bridge the skills gap in Europe's hydrogen economy by:

1. Building a **Network of 100 universities** offering accredited qualifications in hydrogen technologies.
2. Engaging over **500 schools** to integrate hydrogen topics into STEM curricula.
3. Establishing **5 hands-on training laboratories** for practical skill development.
4. Providing **multilingual, open-access educational materials** for educators.
5. Launching a **centralised portal** to connect trainees with programmes and career pathways.

6. Ensuring long-term sustainability through a viable business model post-funding.

Funding and Duration: Funded by the Clean Hydrogen Partnership Joint Undertaking, and the Swiss and British governments, the project leverages a multi-million-euro grant to consolidate outputs from prior EU hydrogen education initiatives. Active since 2024, it operates towards key milestones targeted by 2025, and full implementation by 2026.

Participants: Co-ordinated by: Prof. K. Bouzek and Prof. Steinberger-Wilckens (VŠCHT Praha-Czechia)), it involves 17 partners including: 12 academic and industrial from the EU and 5 partners from Associated Countries, as shown in Fig. 1.



Fig.1- Hy.Academy.eu participant map.

Strategic Impact: By harmonising fragmented educational efforts, HyAcademy.eu directly supports the EU's REPowerEU Plan and Green Deal objectives. Its focus on standardised curricula, teacher training, and public engagement ensures a pipeline of skilled workers for emerging hydrogen industries while promoting societal acceptance of clean energy transitions.

Conclusions: HyAcademy.eu represents a pivotal initiative in addressing the critical skills gap in Europe's hydrogen sector. By developing and disseminating high-quality educational materials, fostering a pan-European network of educational institutions, and promoting

public awareness, HyAcademy.eu plays a crucial role in aligning Europe's workforce with the demands of a rapidly evolving hydrogen economy. This project not only supports the EU's climate neutrality objectives but also enhances energy security by ensuring a well-prepared workforce capable of driving innovation and adoption in hydrogen technologies. Ultimately, HyAcademy.eu's efforts will be instrumental in facilitating a seamless transition towards a low-carbon future, where hydrogen technologies are integral to achieving sustainable energy systems.

Acknowledgment

This project gratefully acknowledges the funding received from the Clean Hydrogen Partnership Joint Undertaking under grant agreement No. 101137988, as well as from UK Research & Innovation (UKRI) and the Swiss State Secretariat for Innovation (SERI). The Joint Undertaking receives support from the European Union's Horizon Europe research and innovation programme, and from Hydrogen Europe and Hydrogen Europe Research.

Any opinions expressed in this text are solely those of the authors and neither of the funding organisations, nor the European Commission or its representatives.

References

[1] https://www.iea.org/energy-system/low-emission-fuels/hydrogen

[2] https://www.irena.org/Digital-Report/Geopolitics-of-the-Energy-Transformation

[3] https://www.europarl.europa.eu/RegData/etudes/ATAG/2021/690599/EPRS_ATA(2021)690599_IT.pdf

[4] https://www.fch.europa.eu/sites/default/files/Hydrogen%20Roadmap%20Europe_Report.pdf

EFCH2 2025 European Fuel Cells and Hydrogen PIERO LUNGHI CONFERENCE
September 17th–19th 2025 Capri / Italy

Business models and policy support for LH_2 supply infrastructure for H_2-powered aviation

Finn Schenke[a], Lukas Koenemann[a], Timo Schelm[a], Astrid Bensmann[a], Richard Hanke-Rauschenbach[a]

[a] Leibniz Universität Hannover, Institute for Electric Power Systems, 30167 Hannover, Germany

Keywords: H2-powerd aviation, liquid hydrogen infrastructure, business models, hydrogen policy, government support

Introduction:
The subject of this study are the business models and financing strategies for liquid hydrogen (LH2) supply infrastructure in hydrogen (H2)-powered aviation. Alongside sustainable aviation fuels, H2-powered aviation holds promise for reducing emissions, including non-CO2 emissions [1]. However, the recent decision by Airbus to delay the development of an H2-powered aircraft due to slower-than-expected technological advancements underscores the challenges associated with both the technology and the acceleration of H2 infrastructure implementation [2]. As the main challenge, the development of a hydrogen ecosystem is identified, encompassing infrastructure, production, distribution, and regulatory frameworks. This study builds on prior research in the techno-economic analysis of LH2 supply infrastructure [3–6] and investigations into financing and business models for the hydrogen sector [7–10]. It compares archetypal business models and examines potential government support mechanisms for the transition phase of H2-powered aviation.

Objectives:
This study aims to evaluate future business models for LH2 supply in H2-powered aviation. Three archetypal business models are identified, representing viable supply infrastructure strategies. Additionally, five potential government support mechanisms are assessed to facilitate the transition phase of LH2 infrastructure deployment and make these business models more attractive for investors.

Material and methods:
To derive the archetypical business models and government support mechanism, a literature study is conducted. To evaluate these business models and analyze the impact of the support mechanisms, a bi-level cash flow optimization approach is applied for the design and dispatch of the LH2 supply infrastructure.

Results:
Three archetypal business models are derived:

- **Single-source supply chain:** A joint venture of airports, airlines, ITPs, H_2 industry, and renewable energy producers owns and operates the entire supply chain, suited for early ramp-up.
- **Dyadic supply chain:** Similar to jet fuel supply, the ITP manages airport infrastructure, while a large oil and gas company oversees upstream LH_2 infrastructure.

- **Supply chain network:** Stakeholders focus on their domain—ITPs handle airport infrastructure, H_2 players manage production and liquefaction, and renewable energy producers supply power.

Stakeholders face varying financial conditions, such as access to financing, equity, and risk tolerance, which influence their weighted average cost of capital (WACC) and return on invested capital (ROIC) after the payback period. The cash flow analysis reveals that the dyadic supply chain results in the lowest LH2 supply costs due to the stakeholders' lower WACC.

To address the high initial costs of LH2 infrastructure and establish long-term economic viability, several government support mechanisms are identified, categorized into five clusters:

- **Direct financial support:** Grants, such as CAPEX funding under the IPCEI scheme can offset high upfront costs and provide non-repayable funds to early adopters. However, these mechanisms require significant government budgets.
- **Loan-based support:** Instruments such as low-interest loans and government-backed guarantees help mitigate financial risk. These are particularly beneficial for LH2 supply infrastructure as they lower long-term costs without requiring direct government expenditure, enhancing scalability.
- **Market-based instruments:** Mechanisms such as contracts for difference and carbon pricing can help bridge the cost gap between conventional fuels and LH2, making investments in LH2 infrastructure more attractive. These instruments create financial incentives for early adopters without requiring direct government subsidies.
- **Tax incentives:** Measures such as accelerated depreciation schemes can make investments more attractive and lower LH2 supply costs with relatively low fiscal impact.
- **Regulatory and policy support:** Essential for ensuring long-term market stability and stimulating demand.

Most support mechanisms risk market distortion, as they selectively benefit specific stakeholders.

Conclusions:

This study analyzes future business models for LH2 supply in H2-powered aviation and compares government support mechanisms that could facilitate these models. The analysis highlights that WACC is the primary cost driver for LH2 supply costs, with large stakeholders benefiting from better financing access and higher risk tolerance. While a single-source supply chain is likely during initial deployment, dyadic or networked supply chains offer lower supply costs in the long term.

Direct financial support and contracts for difference effectively reduce initial supply costs but require substantial government budgets. Loan-based support and tax incentives provide cost reductions in the long-term with lower fiscal impact. A combination of these mechanisms, alongside regulatory and policy support, can enhance market stability, attract investors, and stimulate demand for LH2-powered aviation.

Acknowledgment

The authors gratefully acknowledge the financial support by the Federal Ministry of Education and Research of Germany in the framework of HyNEAT under grant no 03SF0670A. The results presented were achieved by computations carried out on the cluster system at the Leibniz Universität Hannover, Germany.

References

[1] Clean Sky 2 JU and Fuel Cells and Hydrogen 2 JU, 2020, *Hydrogen-Powered Aviation A Fact-Based Study of Hydrogen Technology, Economics, and Climate Impact by 2050*. [Online]. Available: https://cleansky.paddlecms.net/sites/default/files/2021-10/20200507_Hydrogen-Powered-Aviation-report.pdf.

[2] Reuters, 2025, "Airbus Postpones Development of New Hydrogen Aircraft," Reuters. [Online]. Available: https://www.reuters.com/business/aerospace-defense/airbus-postpones-development-new-hydrogen-aircraft-2025-02-07/. [Accessed: 30-Mar-2025].

[3] Hoelzen, J., Koenemann, L., Kistner, L., Schenke, F., Bensmann, A., and Hanke-Rauschenbach, R., 2023, "H2-Powered Aviation – Design and Economics of Green LH2 Supply for Airports," Energy Convers. Manag. X, 20, p. 100442. https://doi.org/10.1016/j.ecmx.2023.100442.

[4] Schenke, F., Hoelzen, J., Bredemeier, D., Schomburg, L., Bensmann, A., and Hanke-Rauschenbach, R., 2024, "LH2 Supply for the Initial Development Phase of H2-Powered Aviation," Energy Convers. Manag. X, 24, p. 100797. https://doi.org/10.1016/j.ecmx.2024.100797.

[5] Hoelzen, J., Silberhorn, D., Schenke, F., Stabenow, E., Zill, T., Bensmann, A., and Hanke-Rauschenbach, R., 2025, "H2-Powered Aviation – Optimized Aircraft and Green LH2 Supply in Air Transport Networks," Appl. Energy, 380, p. 124999. https://doi.org/10.1016/j.apenergy.2024.124999.

[6] Schenke, F., Koenemann, L., Hoelzen, J., Schelm, T., Bensmann, A., and Hanke-Rauschen, R., 2025, "Planning LH2 Infrastructure for H2-Powered Aviation: From the Initial Development to Market Penetration."

[7] OECD, 2023, *Financing Cost Impacts on Cost Competitiveness of Green Hydrogen in Emerging and Developing Economies*, 227. https://doi.org/10.1787/15b16fc3-en.

[8] World Economic Forum, 2023, *Financing The Airports Of Tomorrow: A Green Transition Toolkit*. [Online]. Available: https://www3.weforum.org/docs/WEF_Financing_The_Airports_Of_Tomorrow_2023.pdf. [Accessed: 21-Nov-2023].

[9] Oxford Institute for Energy Studies, 2023, "Financing a World Scale Hydrogen Export Project."

[10] Staiger, R., and Tanțău, A., 2020, *Geschäftsmodellkonzepte mit grünem Wasserstoff: Wirtschaftliche und ökologische Auswirkungen für H2 als nachhaltiger Energieträger*, Springer Fachmedien Wiesbaden, Wiesbaden. https://doi.org/10.1007/978-3-658-30576-5.

EFCH2 2025 European Fuel Cells and Hydrogen
PIERO LUNGHI CONFERENCE
September 17th–19th 2025
Capri / Italy

The Impact of GH2 Infrastructure and Market Development on Optimal LH2 Supply Strategies for Aviation

T. Schelm*[a], F. Schenke [a], A. Bensmann [a], R. Hanke-Rauschenbach[a]
* corresponding author: schelm@ifes.uni-hannover.de
[a] Leibniz Universität Hannover, Institute for Electric Power Systems, 30167 Hanover, Germany

Keywords: Hydrogen-powered aviation, Liquid hydrogen infrastructure, Energy system optimization, Hydrogen supply

Introduction:

The subject of this study are optimal supply strategies for liquid hydrogen (LH2) in aviation, particularly in the context of fluctuating gaseous hydrogen (GH2) market prices and the anticipated scale-up of GH2 infrastructure. This topic holds significance as the aviation sector seeks to achieve net-zero emissions by 2050, with LH2 being a potential fuel solution [1, 2]. The viability of LH2 hinges on economically competitive costs amid the substantial investments required for infrastructure development to supply airports [1]. Aviation presents a unique case for LH2 infrastructure, lacking synergy with other industries and requiring dedicated pathways [3]. The evolving GH2 market presents both opportunities and challenges; while synergies can offer cost reductions, the dependence on GH2 infrastructure and market prices may as well negatively influence LH2 supply strategy. Rising competition for GH2 resources may lead to increased market volatility and prices, affecting the cost-effectiveness and reliability of LH2 supply for aviation.

Objectives:

This study aims to bridge two research areas: the economic analyses of GH2 supply costs and trade networks, and the previously isolated modelled LH2 aviation supply chain [4-6]. The primary objective is to provide new insights into optimizing LH2 supply strategies in aviation by incorporating the influence of dynamic GH2 market prices and infrastructure expansions on supply costs. Through a hybrid sourcing framework that combines internal GH2 production with external procurement from established markets. The study evaluates how uncertainties in GH2 pricing affect cost synergies, infrastructure scaling, and operational strategies. These analyses aim to guide the design of cost-efficient and resilient LH2 supply chains supporting sustainable aviation futures.

Method:

An optimization model was developed to evaluate the LH2 supply chain, integrating external GH2 supply options. With this framework a range of scenarios, emphasizing uncertainties in GH2 market pricing and their impact on cost synergies and operational strategies was examined. Key parameters include the assessment of supply routes, airport selections based on geographic and economic factors, and the integration of renewable energy sources.
The model is formulated as a linear mixed-integer programming problem, leveraging Python with Gurobi, to solve the optimization problem addressing operational and design variables across supply components.

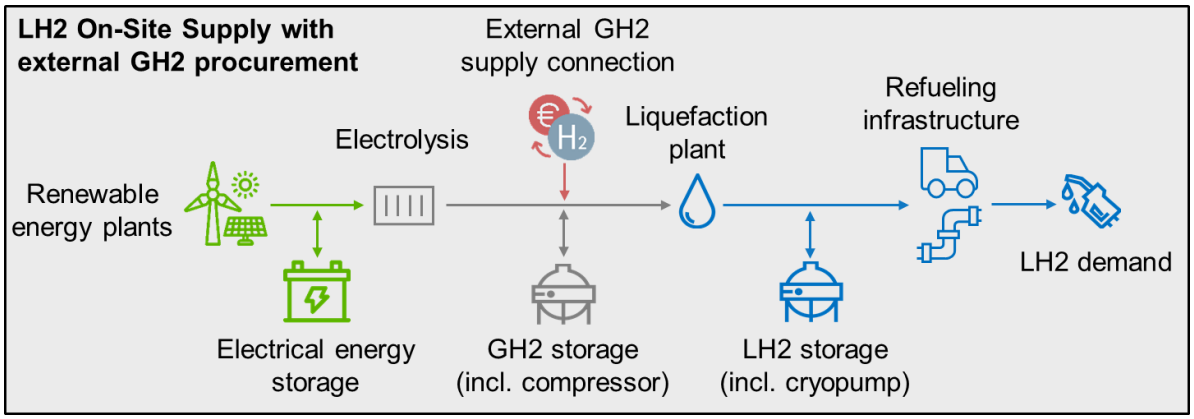


Figure 1: LH2 supply chain with the option of external GH2 procurement

Results:

Within the analysis a detailed cost and infrastructure evaluation is conducted, comparing stand-alone LH2 supply chains with integrated grid and market approaches. This comparison highlighted potential cost reductions derived from synergies with broader energy system infrastructures, contrasted against additional costs stemming from price-cost gaps and market premiums for GH2.
Exploration of varying GH2 price levels unveiled distinct supply strategies. Three optimal strategies emerged:

- Pure external GH2 procurement: only optimal when GH2 prices are extremely low
- Pure internal GH2 production: dominant at high GH2 prices, where reliance on internal production prevails, matching an islanded system for LH2
- Mixed/Hybrid strategy: a combination of external procurement and internal production is best for most external GH2 prices

Conclusion

This study underlines the relevance of integrating GH2 procurement in the planning of future LH2 supply chains for aviation. Decision makers need to consider market fluctuations in infrastructure planning in order to achieve cost-efficient and resilient supply strategies.

- **Hybrid Sourcing Benefits:** Combining internal GH2 production with external procurement reduces dependency during high market prices
- **Infrastructure Planning:** Scalable infrastructure that adapts to market conditions mitigates costs, and integrated development leverages existing and planned GH2 networks
- **Research Contributions:** The study offers a model for future exploration of GH2 dynamics in LH2 supply strategies, encouraging collaboration across disciplines and fostering policy innovation.

As efforts towards net-zero emissions intensify, integrating dynamic GH2 markets presents both challenges and opportunities, requiring coordinated action from the research community and industry stakeholders.

Acknowledgment

This research was carried out within the GOLIAT project, which is funded by the European Union under grant agreement n° 10113837

GOLIAT GROUND OPERATIONS OF LIQUID HYDROGEN AIRCRAFT

Funded by the European Union

References

[1] Scott, Mark. „Analysing the Costs of Hydrogen Aircraft“. *Final Report*, 2023.

[2] McCausland, Richard. „Net Zero 2050: Sustainable Aviation Fuels“, o. J.

[3] Hoelzen, J., L. Koenemann, L. Kistner, F. Schenke, A. Bensmann, und R. Hanke-Rauschenbach. „H2-powered aviation – Design and economics of green LH2 supply for airports“. *Energy Conversion and Management: X* 20 (1. Oktober 2023): 100442. https://doi.org/10.1016/j.ecmx.2023.100442.

[4] Schenke, F., J. Hoelzen, D. Bredemeier, L. Schomburg, A. Bensmann, und R. Hanke-Rauschenbach. „LH2 supply for the initial development phase of H2-powered aviation“. *Energy Conversion and Management: X* 24 (1. Oktober 2024): 100797. https://doi.org/10.1016/j.ecmx.2024.100797

[5] Makepeace, Robert William, Abbas Tabandeh, M. J. Hossain, und Md. Asaduz-Zaman. „Techno-economic analysis of green hydrogen export“. *International Journal of Hydrogen Energy* 56 (22. Februar 2024): 1183–92. https://doi.org/10.1016/j.ijhydene.2023.12.212.

European Fuel Cells and Hydrogen
PIERO LUNGHI CONFERENCE
September 17th–19th 2025
Capri / Italy

An agent-based analysis of hydrogen penetration in the South Africa energy system

PM. Koshikwinja, M. Cavana, P. Leone*
* corresponding author: pierluigi.leone@polito.it
Department of Energy, Politecnico di Torino

Keywords: Africa, agent-based modeling, hydrogen pathways, energy systems.

Abstract Introduction:

South Africa stands out as one of the most promising hubs for hydrogen systems development in Africa. The country possesses vast natural resources essential for manufacturing hydrogen technologies, including substantial reserves of platinum and iridium critical for electrolyzers and fuel cells [1]. Moreover, it has exceptional renewable energy resources, notably solar and wind, offering competitive conditions for green hydrogen production, with projected production costs ranging from 1.4$/kg to 3.5 $/kg[2]. Despite this potential, South Africa currently faces power shortages primarily due to ageing generation plants, with its energy supply heavily dominated by coal. As a pioneering nation on the continent, South Africa has proactively established comprehensive hydrogen policies and a clear roadmap for its hydrogen economy [3], [4]. Numerous initiatives are already underway, particularly within the mining sector, demonstrating the practical applicability and benefits of hydrogen technology [4]. Additionally, existing infrastructure projects, including pipeline connections with neighboring countries like Namibia, underscore the strategic importance of regional integration [2]. Recognizing the high domestic demand for decarbonization in hard-to-abate sectors such as heavy transport and industry, the country emphasizes the necessity for regional and international synergy and cooperation to advance its hydrogen ambitions [5]. Assessing potential local applications of green hydrogen within industrial and transportation sectors is vital for enabling higher penetration of renewable energy sources, ultimately contributing toward full energy access across the region.

Objectives:

The main objective of this study is to develop an agent-based energy system model for the Republic of South Africa to analyze hydrogen systems development pathways with a particular focus on domestic hard-to-abate industries and the transport sector. The specific objectives of this study are as follows:

- Identification and modeling of existing and possible future technologies, including hydrogen technologies, for the decarbonization of the energy system.
- Defining the investment decision metric for different groups of agents (population, industries, utilities, etc.) based on the socioeconomic situation of the country.
- Analyzing and comparing scenarios for hydrogen systems development by comparing existing policies, implications, and model output insights.

Material and methods:

The general methodology applied for this study is based on an innovative modeling technique that considers the human dimension in energy system development. To develop our model, we used an Agent-Based modelling tool named MUSE (Modular Energy Systems Simulation Environment). MUSE is a complex bottom-up, technology-rich, agent-based Integrated Assessment Model (IAM) designed to simulate long-term scenarios across all energy sectors at various scales, from country to global levels whose general scheme is reported in Figure 1. MUSE is a partial equilibrium, microeconomic model that replicates real decision-making processes in each energy sector. It uses a modular approach to represent energy sectors, tailoring investment drivers to reflect the unique characteristics of each sector. Using an agent-based method, MUSE simulates investment and operational decisions within each sector. [6].

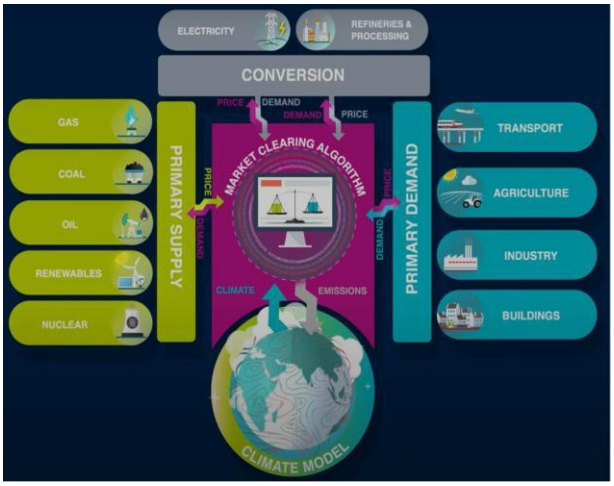


Figure 1. MUSE model architecture [6]

Results:

The analysis provides a comprehensive evaluation of the South African energy system, particularly highlighting hydrogen production and utilization across multiple key sectors, including iron and steel, heavy-duty land transport, mining, high-temperature industrial processes such as cement production, maritime, and aviation sectors. Importantly, agents within the iron and steel sector demonstrated notable potential in adopting green hydrogen technologies, closely followed by the mining industry. This early adoption in mining is facilitated by pre-existing hydrogen technologies, specifically hydrogen-powered dumper trucks [7], which serve as a viable entry point for broader technology adoption.

Furthermore, the study reveals significant emission reduction opportunities, especially within coal-based chemical production processes and refineries. Although green hydrogen prices are higher, in the longer term, it becomes increasingly competitive with traditional production processes. A critical finding is the role of early adopter agents. Initial adoption by these agents creates market confidence, encouraging subsequent agents to bear higher initial costs due to the perceived benefits of transitioning to sustainable technologies. This leads to the overall reduction of hydrogen price.

Government incentives targeted specifically at early adopter agents appear indispensable. The model also indicates additional demand for green hydrogen in maritime transportation sector. However, further detailed analysis is necessary to identify specific agents' decision drivers in the sector to transition towards hydrogen-powered ships.

Regarding green hydrogen production, preference goes for distributed systems, particularly when production sites are located near final users. This proximity enhances logistical efficiency, reduces transportation costs, and simplifies adoption processes. Further studies can therefore identify and analyze potential hydrogen clusters for a strategic planning approach.

Conclusions:

In today's world, global warming presents a critical challenge requiring urgent action. As fossil fuels continue to decline, renewable energy emerges as a key pillar for achieving decarbonization; however, electricity alone cannot effectively address emissions from all sectors. Hydrogen and hydrogen-based synthetic fuels stand out as viable solutions to decarbonize particularly hard-to-abate sectors and support grid management by balancing intermittent renewable sources such as solar and wind. This study significantly contributes to understanding potential pathways for hydrogen production and usage in South Africa, and provides policymakers and investors insights into agent motivations, enabling more effective policy design and strategic investments tailored towards achieving sustainability targets.

References

[1] K. Imasiku, F. Farirai, J. Olwoch, and S. N. Agbo, "A Policy Review of Green Hydrogen Economy in Southern Africa," *Sustainability*, vol. 13, no. 23, p. 13240, Nov. 2021, doi: 10.3390/su132313240.

[2] P. M. Koshikwinja, M. Cavana, S. Sechi, R. Bochiellini, and P. Leone, "Review of the hydrogen supply chain and use in Africa," *Renew. Sustain. Energy Rev.*, vol. 208, p. 115004, Feb. 2025, doi: 10.1016/j.rser.2024.115004.

[3] B. G. Pollet *et al.*, "Hydrogen South Africa (HySA) Systems Competence Centre: Mission, objectives, technological achievements and breakthroughs," *Int. J. Hydrogen Energy*, vol. 39, no. 8, pp. 3577–3596, Mar. 2014, doi: 10.1016/J.IJHYDENE.2013.11.116.

[4] D. Bessarabov, F. van Niekerk, F. van der Merwe, M. Vosloo, B. North, and M. Mathe, "Hydrogen Infrastructure within HySA National Program in South Africa: Road Map and Specific Needs," *Energy Procedia*, vol. 29, pp. 42–52, 2012, doi: 10.1016/j.egypro.2012.09.007.

[5] IRENA, *Geopolitics of the energy transformation: the hydrogen factor.* 2022.

[6] S. Giarola, J. Sachs, M. d'Avezac, A. Kell, and A. Hawkes, "MUSE: An open-source agent-based integrated assessment modelling framework," *Energy Strateg. Rev.*, vol. 44, p. 100964, Nov. 2022, doi: 10.1016/J.ESR.2022.100964.

[7] "Anglo American unveils a prototype of the world's largest hydrogen-powered mine haul truck - a vital step towards reducing carbon emissions over time | Anglo American." https://www.angloamerican.com/media/press-releases/2022/06-05-2022 (accessed Apr. 01, 2025).

EFCH2 2025 European Fuel Cells and Hydrogen
PIERO LUNGHI CONFERENCE
September 17th–19th 2025
Capri / Italy

Exploring the role of hydrogen infrastructure in the energy transition

Matteo Catania[a], Paolo Colbertaldo*[,a], Fabrizio Fattori[b], Mario Motta[a], Stefano Campanari[a]

* Corresponding author: paolo.colbertaldo@polimi.it
[a] Department of Energy, Politecnico di Milano - Milan, Italy
[b] Dipartimento di Scienze Teoriche e Applicate, Università degli studi dell'Insubria - Varese, Italy

Keywords: Hydrogen; Energy transition; Infrastructure; Long-term energy system modelling.

Abstract

The transition towards a decarbonised energy system entails profound modifications in how energy is generated, exchanged, and converted. Hydrogen can provide support in each of the phases, as energy vector as well as storage means. Through long-term energy system model, the exploration of scenarios spanning from 2025 to 2050 allows to identify synergies and impacts. This work focuses on the infrastructural aspects, that shows how south-to-north flows are likely to be expected, and how the combination of investments on electricity and hydrogen networks with a flexible use of the natural gas grid favourably impact the total system costs.

Introduction

Hydrogen is expected to play a critical role in the energy transition, with a supporting action in various sectors, such as heavy-duty transport and industry, as well as energy storage and sector coupling [1]. Exploring this role along the pathway towards a net-zero emission system is essential to understand the cross-impact of different technological solutions and their synergies [2]. Observing the interaction between energy vectors and their infrastructures also provides insights into preferential pathways.

Objectives

This work analyses the 2025-2050 energy transition of the Italian energy system towards a decarbonised structure, considering all end-use sectors (industry, transport, civil) and integrating multiple energy vectors (electricity, fossil and biogenic methane, hydrogen, biomass). Results and discussion focus on the role of infrastructure, aiming to explore the relation between investment in different or multiple networks.

Material and methods

The analysis adopts the *Future Energy traNsition multI-seCtor modEl* (FENICE), a bottom-up long-term energy system model developed on the open-source framework *oemof* with a Multi[4] approach: the representation is multi-node, multi-vector, multi-sector, and multi-period. Accurate tracking of CO_2 flows allows to account for fossil and biogenic contribution and close the balance, with progressively smaller annual CO_2 emissions until a 2050 condition that can be repeated identically afterwards.
Model runs adopt years as representative periods, with a dual clustering level that enables the identification of 24 typical days per year and a 5-year gap between representative years. Several assumptions are required, which can be grouped into (i) system operation data in each node and representative period (comprising hourly profiles of renewable power generation, and quantities and

hourly profiles of energy vectors consumption – elaborated from historical data by Terna, GSE, Snam, and other national datasets), and (ii) techno-economic assumptions for each technology, varying in each representative period, according to recent forecasts by IEA, IRENA, etc.

Results

Hydrogen proves crucial along the energy transition of the Italian energy system, progressively increasing its presence and relevance throughout the 2025-2050 time horizon. The deployment of Power-to-Hydrogen technologies extends the decarbonisation potential of renewable electricity to sectors that are difficult to electrify, such as high-temperature process heat generation, chemicals production, primary steelmaking, heavy-duty road transport, aviation, and shipping. The possibility of blending hydrogen and natural gas to progressively decarbonise end uses that rely on a gaseous fuel further enhances its significance, as it helps to reduce methane consumption.

In absence of particular constraints, domestic hydrogen production appears able to supply most of the demand, largely relying on installations in southern regions that feature high availability of renewables and low local demand. Hydrogen transport across the country may rely on a pure hydrogen network (assumed as pipelines) or on the existing natural gas grid (as H_2-NG blend). Figure 2 shows the evolution of the pure H_2 network, which appears valuable to transport large quantities across the country, particularly from southern to northern regions, where demand is concentrated.

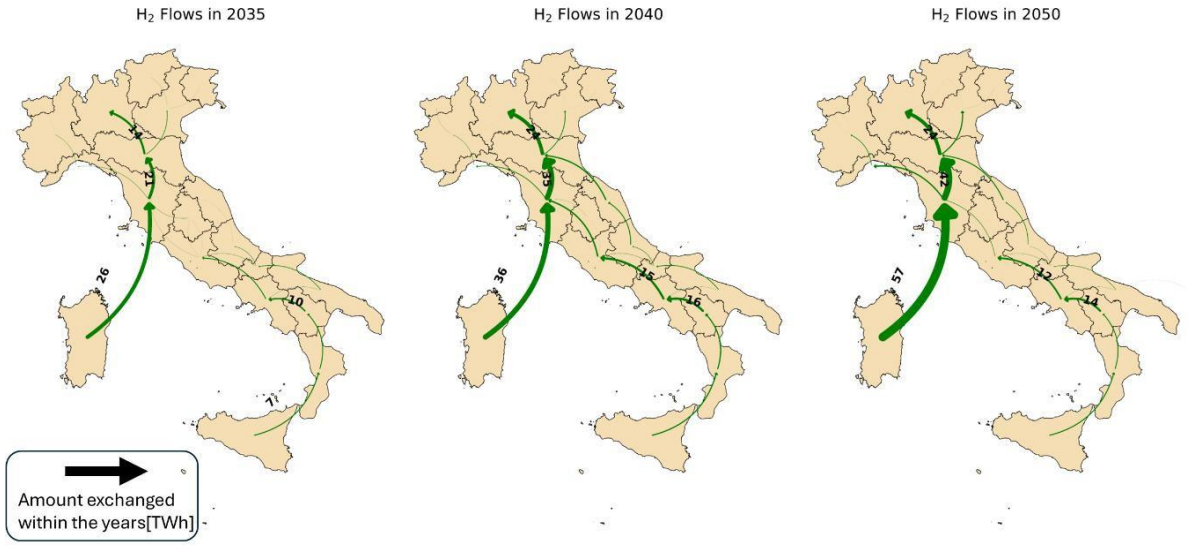


Figure 1. Evolution of the hydrogen infrastructure in different years of the investigated time horizon. The line thickness of the lines is proportional to the cumulative annual transit.

To further explore the possible evolution of the Italian energy system, diverse scenarios are compared looking at the impact of enabling investment in energy vector connections (electricity exchange, pure hydrogen exchange, hydrogen injection in the natural gas grid). Figure 2 summarises the resulting total system costs in the different scenarios. The order of magnitude is comparable to the annual Italian gross domestic product (GDP, averaging at 1,828 billion € over the past five years [4]), but to be split over 25 years.

Enabling investment in infrastructure development proves beneficial to the system economics, as increased interconnections between regions yield cost reductions up to 5.2%. The scenario with highest flexibility (expansion of both electricity and hydrogen networks and large H_2 share in the natural gas grid) results in the lowest total costs. The increase of the maximum allowed H_2 percentage in the natural gas pipelines is particularly significant in the case where investment in networks is disabled, when it becomes the only available means for hydrogen transport across the country. Accordingly, when only one of the networks can be expanded (e.g., due to policy or regulatory constraints), the investment in a hydrogen grid appears more impactful in case of low max H_2 percentages in the natural gas grid, whereas improvements in the electricity network have larger benefits when H_2 can be transported as part of a H_2-NG blend.

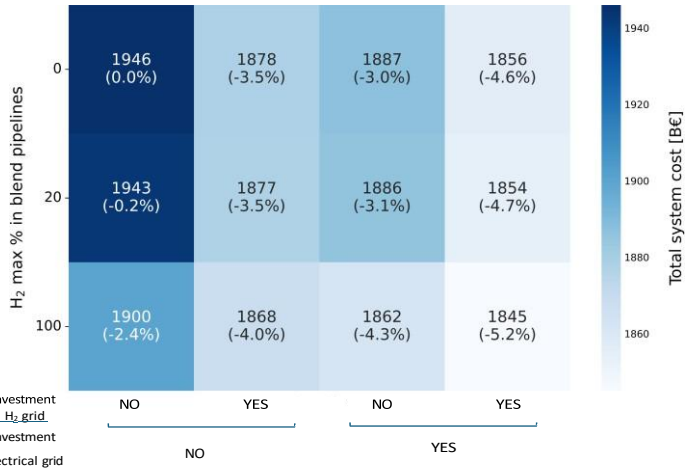


Figure 2. Total system cost, expressed in billion euro (B€), among the analysed scenarios.

Conclusions

This work provides insights on the role of hydrogen and hydrogen networks in the context of long-term decarbonisation pathways. The analysis, which investigated the case of Italy, shows the favourable effect of a progressive expansion of a pure H_2 network, and the positive impacts from electrical grid expansion and increasing allowed H_2 share in the natural gas grid, which all help decreasing the system total cost. Further assessments will investigate into the additional impacts from technological switch, implementing an endogenous optimised selection of end-use technologies.

Acknowledgments

This work has been partly funded by the Hydrogen Joint Research Partnership (H_2JRP) of Politecnico di Milano [5].

References

[1] IEA, *Global hydrogen review 2024*, 2024.
[2] M.G. Prina, G. Manzolini, D. Moser, B. Nastasi, W. Sparber, *Classification and challenges of bottom-up energy system models - A review*, Renew. Sustain. Energy Rev. 129 (2020) 109917. https://doi.org/10.1016/j.rser.2020.109917.
[3] M. Catania, G. Muliere, F. Fattori, P. Colbertaldo, *The impact of temporal clustering on long-term energy system models*, submitted to Applied Energy, under second-stage review.
[4] Istat, *Annuario statistico italiano*, 2024.
[5] Hydrogen Joint Research Partnership, https://www.fondazionepolitecnico.it/progetti/hydrogen-jrp/.

EFCH2 2025 European Fuel Cells and Hydrogen PIERO LUNGHI CONFERENCE
September 17th–19th 2025 Capri / Italy

Global Deployment and Commercial Roll-Out of Electrolyzers and Co-Electrolyzers: Technology Pathways, Market Projections, and Industrial Integration Strategies

Mariya E. Ivanova*[a], Suraj Reddy Chamakura[b], Asrar Sheikh[a], Kwati Leonard[c], Daria Vladikova[a], Blagoy Burdin[d]

* corresponding author: mariya.e.ivanova@takia-uni.bg
[a] Trakia University, Students Campus, 6000 Stara Zagora, Bulgaria
[b] University of California, Berkeley, Berkeley Graduate Division, Sproul Hall Rm 318, MC 5900, Berkeley CA 94720, USA
[c] Center for Energy System Design, International Institute for Carbon-Neutral Energy Research (I2CNER) Kyushu University, 744 Motooka, Nishi-ku, Fukuoka, 819-0395, Japan
[d] Institute of Electrochemistry and Energy Systems – Bulgarian Academy of Sciences, 10 Acad. G. Bonchev str., 1113 Sofia, Bulgaria

Keywords: Electrolysis, Co-Electrolysis, Hydrogen Economy, Industrial Decarbonization

The transition to a hydrogen-based economy is accelerating as governments and industries seek to decarbonize key sectors such as energy, chemicals, and heavy industry. Electrolyzers and co-electrolyzers play a pivotal role in this transformation by enabling the large-scale production of green hydrogen and synthetic fuels. The global electrolyzer market is experiencing rapid technological advancements, declining capital costs, and increasing policy support, driving deployment at unprecedented scales [1]. However, the commercialization of advanced electrolyzer technologies - such as solid oxide electrolyzers, which are transitioning from pilot to early commercial deployment, and proton-conducting ceramic electrolyzers - remains in relatively early stages, requiring further research and industrial investment. This study offers a detailed analysis of deployment trajectories, technological advancements, and industrial integration strategies for key electrolyzer and co-electrolyzer technologies with a special emphasis on the role of co-electrolyzers in sustainable syngas production [2].

The primary objectives of this study are to analyze the deployment trends of key electrolyzer technologies, including alkaline (AEL), proton exchange membrane (PEMEL), anion exchange membrane (AEMEL), solid oxide (SOEL), and proton-conducting ceramic (PCCEL) electrolyzers, as well as co-electrolyzers for syngas production. A key focus is to evaluate market projections and the techno-economic factors influencing the large-scale commercialization of these technologies. Additionally, the study aims to identify the leading regions in electrolyzer deployment, assessing their policy frameworks, renewable energy integration, and industrial synergies that drive adoption. Another crucial objective is to examine the role of electrolyzers within industrial ecosystems, particularly in sectors such as steel manufacturing, ammonia synthesis, and direct integration with renewable energy sources. Finally, the study seeks to provide strategic recommendations for policymakers, industry stakeholders, and researchers

to accelerate the scale-up of electrolyzers and co-electrolyzers, ensuring their widespread adoption in the global energy transition.

This study employs a multi-method approach to analyze the deployment and commercialization of electrolyzers and co-electrolyzers. A comprehensive market analysis is conducted, reviewing hydrogen production forecasts, investment trends, and policy initiatives from major economies, including Europe, North America, and the Asia-Pacific region [3]. The study also includes a detailed technology assessment, comparing different electrolyzer architectures such as anode-supported, electrolyte-supported, and metal-supported designs, with a focus on efficiency, durability, and scalability. To understand real-world applications, industrial case studies are examined, highlighting successful integration strategies in chemical parks, refineries, and hydrogen hubs. Furthermore, this study analyzes deployment trajectories through 2050 by examining cost reduction trends, energy demand growth, and policy commitments. By integrating these methodologies, the study provides a comprehensive evaluation of the factors shaping the future of electrolyzer technologies.

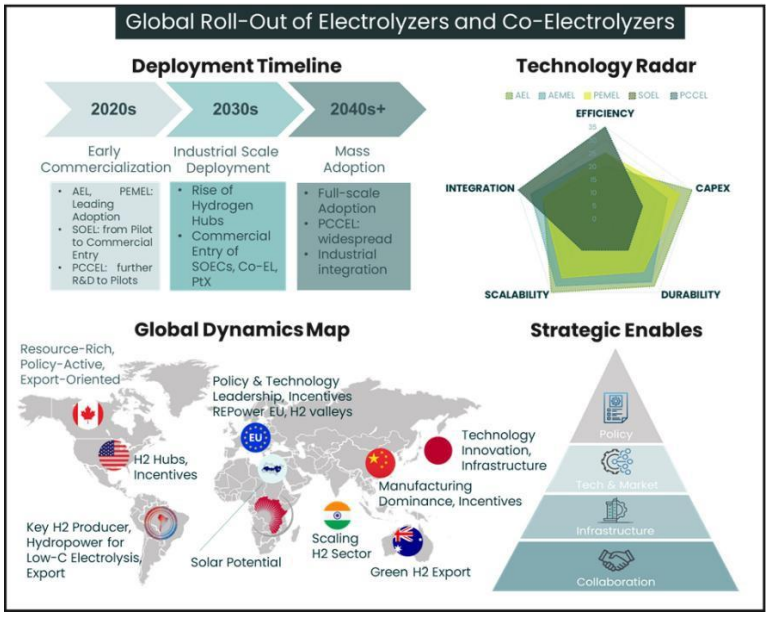


Figure: *Global Roll-Out of Electrolyzers and Co-Electrolyzers: Deployment, Performance, and Strategic Enablers*

The analysis identifies three distinct phases of electrolyzer deployment. In the 2020s, the market is characterized by early commercialization, with alkaline and PEM electrolyzers leading adoption, driven by strong policy incentives in Europe, the USA, and China. Meanwhile, SOEL and PCCEL technologies remain in pilot trials. Moving into the 2030s, the sector transitions to industrial scale-up, with the emergence of large-scale hydrogen hubs that integrate electrolysis with industrial clusters and renewable energy storage. During this period, SOEL and co-electrolysis begin commercial deployment, particularly in Power-to-X applications. By the 2040s and beyond, electrolyzer deployment reaches full-scale adoption, with advanced technologies like PCCEL achieving widespread commercialization due to their

superior efficiency and compatibility with circular hydrogen economies. By this stage, global electrolyzer capacity surpasses 1 terawatt, with more than 100 gigawatts dedicated to co- electrolyzers.

Regional analysis highlights Europe's leadership in policy-driven hydrogen deployment [4], China's dominant role in electrolyzer manufacturing, and the USA's investment in hydrogen hubs. Additionally, Australia is emerging as a key green hydrogen exporter, while India is rapidly scaling its hydrogen sector through government initiatives and industrial demand. The MENA region and Africa, leveraging their abundant solar potential, strategic locations, and increasing investment, are positioning themselves as major global hydrogen suppliers. South America is poised to become a key producer, utilizing its vast hydropower resources for low- carbon electrolysis. Meanwhile, Japan continues to drive hydrogen technology innovation and infrastructure development, reinforcing its role as a leader in fuel cell adoption and hydrogen imports. These findings underscore the accelerating pace of hydrogen deployment and the shifting global landscape in electrolyzer commercialization.

This study underscores the critical role of electrolyzers in enabling a global hydrogen economy. Key findings indicate that electrolyzer capital expenditures (CAPEX) are projected to decline by 50% by 2035, significantly enhancing the cost competitiveness of green hydrogen [3]. Industrial applications, particularly in ammonia production, steel manufacturing, and refineries, are expected to be the primary drivers of electrolyzer deployment, aligning with global decarbonization efforts. Additionally, co-electrolysis presents significant advantages for synthetic fuel production and carbon recycling, yet its widespread commercialization requires further technological advancements and cost reductions.

To accelerate deployment, policy measures such as Hydrogen Contracts for Difference (H_2- CfD), streamlined permitting processes, and sector-specific hydrogen mandates will be essential in bridging cost gaps and de-risking investments. Beyond policy, strategic actions must focus on strengthening supply chains, expanding hydrogen infrastructure, and fostering international collaboration to scale up the commercialization of electrolyzer and co- electrolyzer technologies. The findings of this study provide a clear roadmap for policymakers, industry leaders, and researchers, outlining the necessary steps to accelerate hydrogen adoption and establish it as a cornerstone of future energy systems.

Acknowledgment

MEI, AS and DV acknowledge the support of: (i) the Bulgarian Ministry of Education and Science through the Bulgarian National Recovery and Resilience Plan, Component "Innovative Bulgaria", Project № BG-RRP-2.004-0006-C02, titled "*Development of research and innovation at Trakia University in service of health and sustainable well-being*", and (ii) the European Union under Horizon Europe, Project No. 101136692 - *H2Start: Green Innovations in Hydrogen for Sustainable Energy Transition*.

References

[1] International Energy Agency (IEA) (2023). The Role of Electrolysis in Decarbonizing the Global Energy System.
[2] Hydrogen Council (2023). Hydrogen Insights: Scaling Up Electrolysis Technologies.
[3] BloombergNEF (2024). Global Hydrogen Market Outlook 2024.
[4] European Commission (2023). REPowerEU: A Plan for Reducing Dependency on Fossil Fuels.



TOPIC 7: HYDROGEN INNOVATION AND FUTURE TRENDS

EFCH2 2025 European Fuel Cells and Hydrogen PIERO LUNGHI CONFERENCE
September 17th–19th 2025 Capri / Italy

Design of Experiment (DOE) for Optimising Automated 3D Printing of Proton Exchange Membrane Fuel Cell (PEMFC) Electrodes

Luca Zannini*[a], Veronica Testa [a,b], Martina Iaia[a], Marcello Romagnoli[a,b], Fabrizio Roncaglia[b,c]
* corresponding author: luca.zannini@unimore.it

a Dipartimento di Ingegneria "Enzo Ferrari", Università degli Studi di Modena e Reggio Emilia, Modena, Italy

b Centro Interdipartimentale di Ricerca e per i Servizi nel Settore della Produzione, Stoccaggio e Utilizzo dell'Idrogeno H2 – MO.RE., Università degli Studi di Modena e Reggio Emilia, Modena, Italy

c Dipartimento di Scienze Chimiche e Geologiche, Università degli Studi di Modena e Reggio Emilia, Modena, Italy

Keywords: Automated electrodes production, Design-of-experiments (DOE), 3D printing, Proton Exchange Membrane Fuel Cells (PEMFCs)

Abstract

Introduction: Recent advancements in additive manufacturing, specifically in 3D printing, have introduced innovative approaches to PEMFC electrode fabrication. These advancements provide precise control over material deposition, enabling the creation of complex geometries and uniform layers at a lower cost compared to traditional manufacturing methods. Additionally, they facilitate customization and scalability, making 3D printing an ideal technique for fabricating conductive inks and thin-film electrodes for PEMFCs [1]. This study presents the experimental relationship between 3D printing parameters and electrode features for PEMFCs through a Design of Experiments (DoE) approach. Starting from carbon-based ink composition [2], the deposition of conductive layers is carried out with varying values of printing offset, nozzle diameter, and "filament diameter". The authors highlight their effect on some final Membrane Electrode Assembly (MEA) characteristics, such as: printing thickness and layer homogeneity, providing valuable insights for process control and identifying optimal printing conditions. Following optimization, the ink was directly printed onto Nafion® membranes to produce Membrane Electrode Assemblies (MEAs). Moreover, a prototype of an automated MEA production line will be presented.

Objectives: Demonstrate the feasibility of 3D printing for electrode production; enhance the deposition quality of electrodes, which directly influences cell efficiency, while ensuring scalability, reduced production time, and cost-effectiveness; optimize key printing parameters; Present an example of an automated printing line for MEA anode and cathode.

Material and methods:

Commercial carbon black powders (VULCAN XC-72, 30 nm) were chosen as the conductive filler due to their stability and electrical conductivity. The microstructure was acquired by SEM (Scanning Electron Microscopy, Quanta 200 ESEM FEG - FEI) and XRD pattern acquired by X-ray diffraction (XRD, X'Pert PRO and Empyrean - Malvern PANAlytical). Ink formulations consisted of carbon black (10%), ethanol (60%), and distilled water (30%). Inks were deposited onto a polymeric substrate. The viscosity of the Vulcan-based inks was carefully measured using an Anton Paar MCR 102 rheometer.

The DoE approach was chosen to identify significant interactions among multiple printing variables to provide a structured approach and find optimal conditions. Average thickness, thickness uniformity, covered area, and layer weight were defined as response variables.

Image analysis of printed layers was performed through MATLAB software. Images of the samples were captured under controlled lighting conditions using a high-resolution camera. To ensure consistency in analysis, each image was standardized to include only the 5x5 cm electrode area.

In the end, the first prototype of an automated production line was developed using Computer-Aided Design (CAD) software.

Results:

The study revealed that specific combinations of nozzle diameter, "filament diameter", and offset are critical for achieving the desired electrode characteristics. For example, a nozzle diameter of 1 mm paired with a "filament diameter" of 2 mm yielded the most uniform thickness. Additionally, offset settings significantly influenced layer uniformity. Optimal conditions were observed at a higher offset setting of 0.5 mm combined with the minimum filament diameter, which maintained the layer thickness at approximately 4 µm—below the target of 10 µm but within acceptable performance limits. PoE graphs highlighted the optimal levels for nozzle diameter, filament diameter, and offset that maximized electrode uniformity and minimized variability. DOE analysis indicated that a 0.5 mm nozzle diameter, 1.4 mm filament diameter, and 0.1 mm offset produced the best results, balancing precision and flow rate without compromising adherence.

Conclusions and future perspectives:

The results emphasize the potential of DoE-driven optimization in inkjet 3D printing: precise control over electrode thickness and uniformity reduces material requirements and improves scalability and sustainability within PEM fuel cell manufacturing. To further advance the industrial applicability of this method, efforts are directed towards the development of a fully automated production line. This integration aims to standardize the manufacturing process, ensuring reproducibility and high-throughput fabrication of PEMFC electrodes, ultimately contributing to the widespread adoption of hydrogen-based energy solutions.

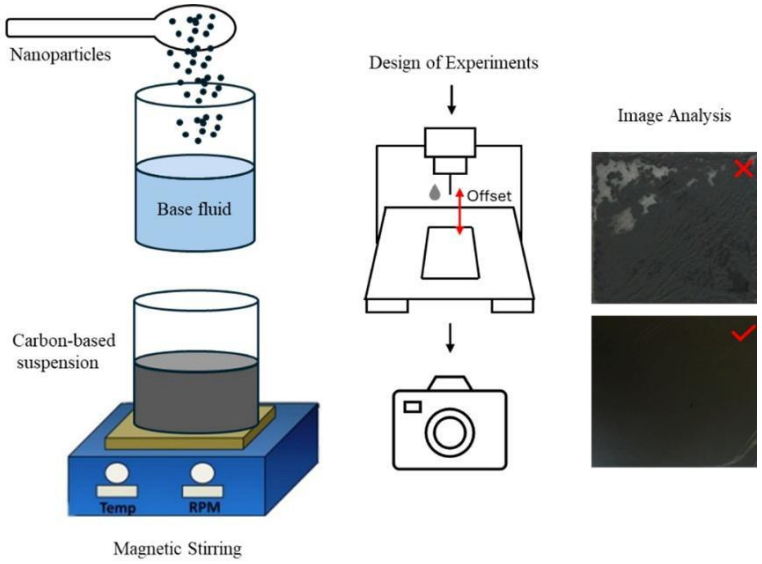


Figure 1: Schematic representation of the proess.

Acknowledgment

This project was funded under the National Recovery and Resilience Plan (NRRP), Mission 04, Component 2, Investment 1.5 – NextGenerationEU, ECS00000033, call for tender n. 3277 dated 30/12/2021, award number: 0001052 dated 23/06/2022.

References

[1] C. Li, F. Bu, Q. Wang, X. Liu, Recent Developments of Inkjet-Printed Flexible Energy Storage Devices, Adv Mater Interfaces 9 (2022) 2201051. https://doi.org/10.1002/ADMI.202201051

[2] M. Cannio, S. Righi, P.E. Santangelo, M. Romagnoli, R. Pedicini, A. Carbone, I. Gatto, Smart catalyst deposition by 3D printing for Polymer Electrolyte Membrane Fuel Cell manufacturing, Renew Energy 163 (2021) 414–422. https://doi.org/10.1016/j.renene.2020.08.064.

European Fuel Cells and Hydrogen
PIERO LUNGHI CONFERENCE
September 17th–19th 2025
Capri / Italy

On the relevance of the para- to orthohydrogen conversion for the exergy utilisation of liquid hydrogen in liquid hydrogen regasification

Magnus Lenger*[a], Steffen Heinke[a], Wilhelm Tegethoff[a], Jürgen Köhler[a]

*corresponding author, m.lenger@tu-braunschweig.de

[a] Technische Universität Braunschweig, Institut für Thermodynamik,
Hans-Sommer-Str. 5, 38106 Braunschweig, Germany

Keywords: LH_2, power generation, regasification, waste heat recovery

Abstract:

The para- to orthohydrogen conversion exergy can be utilised in liquid hydrogen regasification. It is largely contained at temperatures below 100 K. For example, the conversion exergy is 15 % of the exergy of equilibrium hydrogen at the normal boiling point (1.7 % of H2's lower heating value) for a reservoir at normal temperature, normal pressure and equilibrium hydrogen composition at normal temperature. In the conference presentation it will be discussed what conversion exergy share could be recovered in selected power generating liquid hydrogen regasification processes from the recent literature.

Introduction: The work required by a chain consisting of hydrogen (H_2) liquefaction and H_2 regasification can be reduced (i) by improving liquefaction processes and (ii) by utilising the reversible liquefaction work (the liquid hydrogen (LH_2) exergy) in LH_2 regasification [1]. Example: If liquefaction corresponds to a change of state from a state *A* (gas) to a state *B* (liquid) and if it is assumed for simplification that regasification represents the exact opposite change of state (*B* to *A*) given some thermodynamic reservoir, then the work *w* required for liquefaction and regasification (*A* to *B* to *A*) per unit H_2 mass is

$$w(\eta_{\mathrm{LIQ}},\eta_{\mathrm{REG}}) = e_{\mathrm{LH_2}} \cdot \left(\frac{1}{\eta_{\mathrm{LIQ}}} - \eta_{\mathrm{REG}}\right) \quad \text{with} \quad w_{\mathrm{LIQ}} = \frac{e_{\mathrm{LH2}}}{\eta_{\mathrm{LIQ}}} \quad \text{and} \quad w_{\mathrm{REG}} = e_{\mathrm{LH_2}}\,\eta_{\mathrm{REG}}.$$

Here $e_{\mathrm{LH_2}}$ is the specific exergy of LH_2 in state *B* and η_{LIQ} and η_{REG} are the exergy efficiencies of the liquefaction and regasification processes. The priority in the endeavour to reduce the energy demand *w* should be to improve the liquefaction processes, as $w_{\mathrm{LIQ}} \sim \eta_{\mathrm{LIQ}}^{-1}$ while $w_{\mathrm{REG}} \sim \eta_{\mathrm{REG}}$. For instance, 1/40 % - 40 % = 2.5 - 0.4 = 2.1. Improved liquefaction processes, however, have already been proposed in the recent past [2]. They achieve an efficiency of around $\eta_{\mathrm{LIQ}} = 44\ \%$ [1] and are yet to be technically implemented. LH_2 regasification with exergy utilisation has not yet been technically implemented ($\eta_{\mathrm{REG}} = 0$, or $\eta_{\mathrm{REG}} < 0$ if work is invested for regasification). In addition to the recovery of work, a previous study shows

synergies between power generating LH_2 regasification and the waste heat management of mobile fuel cell systems [3]. Another previous study [4, 5] shows a comprehensive comparison of 94 processes (**Fig. 1**) for power generating LH_2 regasification and their operation for maximum power generation. The best process achieves $\eta_{REG} = 38\ \%$ by power generation.

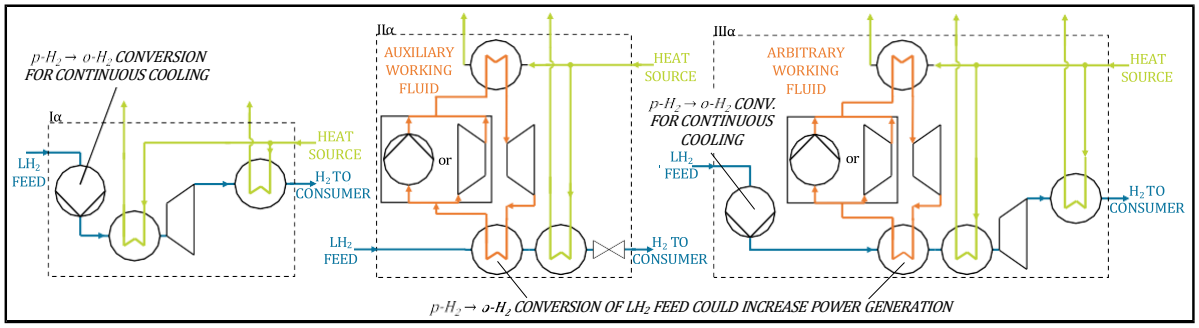


***Fig. 1**: Exemplary processes for power generating liquid hydrogen regasification, adapted from [4].*

For regasification processes shown in the previous study [4], however, the work that could be extracted from the para- to orthohydrogen conversion – the reversible spin conversion work, or spin conversion exergy – has not yet been considered. In H_2 liquefaction, the exothermic conversion of the two proton spin isomers of H_2 (para- and orthohydrogen, p-H_2 and o-H_2) is typically catalysed so that the two isomers are almost in equilibrium in LH_2. During liquefaction, the heat of conversion is removed by refrigeration through additional work input. The spin conversion exergy remains in the LH_2 as part of the LH_2 exergy and can be utilised in the regasification process. A currently technically feasible method for the exergy utilisation of the p-H_2 to o-H_2 conversion is the conversion catalysis in heat exchangers to increase the entropy sink of work extracting LH_2 regasification processes (cf. **Fig. 1**). Another, still theoretical method, is to use the conversion in H_2 compression devices for continuous cooling (cf. **Fig. 1**) to achieve higher compression pressure ratios for a given work input. The conversion exergy can then be extracted from downstream work extracting expansion.

Objective: The objective is to evaluate the relevance of the exergy utilisation of the p-H_2 to o-H_2 proton spin conversion in selected power generating LH_2 regasification processes from the recent literature [4]. It is therefore examined what share of the spin conversion exergy could be recovered (i) via heat exchangers and (ii) via compression devices.

Material and methods: Calculations are based on a mixture model for p-H_2 and o-H_2. The model utilises state-of-the-art Helmholtz free energy fundamental equations of state for p-H_2 and o-H_2 [6]. The mixture is considered ideal. Mixing entropy is considered in the ideal part of the Helmholtz free energy function. Reference entropy and reference enthalpy for p-H_2 and o-H_2 are set to the conversion enthalpy and conversion entropy [1, 7].

Results and conclusion: The spin conversion exergy is quantified for equilibrium H_2 by combining the first and second laws of thermodynamics to quantify its relevance:

$$e_{\mathrm{SPIN}} = \int_{T}^{T_{\mathrm{RES}}} \left(\frac{T_{\mathrm{RES}}}{T} - 1\right) \cdot \left(\frac{\partial h_{\mathrm{H_2}}(p,T,\xi)}{\partial \xi}\right)_{p,T} \cdot \frac{\mathrm{d}\xi(T)}{\mathrm{d}T} \cdot \mathrm{d}T\,, \qquad p = \text{constant}.$$

Here h denotes specific enthalpy, ξ the p-H_2 mass fraction in H_2, T the temperature, p the pressure and RES the reservoir state. For example, spin conversion exergy is 15 % of the exergy of equilibrium H_2 on the boiling liquid line at normal pressure for a reservoir at normal temperature, normal pressure and equilibrium H_2 composition at normal temperature. This corresponds to 1.7 % of H_2's lower heating value, or 2 MJ/kg_{H2}. The spin conversion exergy is mainly at temperatures of 100 K and below. The power output of LH_2 regasification can be increased by utilising the spin conversion exergy. To what extent this is possible via heat exchangers and H_2 compression devices depends on the regasification process and will be discussed in the presentation. It must be examined to what extent additional exergy losses reduce the surplus of generatable work or even result in a net loss.

Acknowledgment:

We would like to acknowledge the funding by the Deutsche Forschungsgemeinschaft (DFG, German Research Foundation) under Germany´s Excellence Strategy – EXC 2163/1 - Sustainable and Energy Efficient Aviation – Project-ID 390881007.

References

[1] M. Lenger, S. Heinke, W. Tegethoff, J. Köhler: On the importance of liquid hydrogen exergy utilisation for an energetically efficient hydrogen energy economy, *Int. J. Hydrogen Energy 89* (2024).

[2] U. F. Cardella: Large-scale hydrogen liquefaction under the aspect of economic viability, *Ph.D. thesis*, Technische Universität München (2018).

[3] M. Lenger, S. Heinke, W. Tegethoff, J. Köhler: Synergies of fuel cell system thermal management and cryogenic hydrogen exergy utilization, *Sci. Rep. 12* (2022).

[4] M. Lenger, W. Tegethoff: Liquid hydrogen regasification with exergy utilisation: pro-cesses and process operation for maximal power generation. *Int. J. Hydrogen Energy* (submitted February 2025)

[5] M. Lenger, S. Heinke, W. Tegethoff, N. Lemke, J. Köhler: Pump, compressor and expander requirements for power generating liquid hydrogen regasification, *14th International Conference on Compressors and Their Systems* (submitted March 2025)

[6] J. W. Leachman, R. T. Jacobsen, S. G. Penoncello, E. W. Lemmon: Fundamental equations of state for parahydrogen, normal hydrogen, and orthohydrogen, *Journal of Phys. and Chem. Ref. Data 38* (2009).

[7] R. J. Le Roy, S. G. Chapman, F. R. W. McCourt: Accurate thermodynamic properties of the six isotopomers of diatomic hydrogen. *J. Phys. Chem. 94* (1990).

EFCH2 2025 European Fuel Cells and Hydrogen
PIERO LUNGHI CONFERENCE
September 17th–19th 2025
Capri / Italy

Membrane engineering applications in hydrogen and CO_2 valorization under a greener energy scenario

Adolfo Iulianelli*[a,b], Henry B. Trujillo Ruales[a], Jan Veres[c], F. Galiano[a], A. Figoli[a]

* Corresponding author: Dr. Adolfo Iulianelli, a.iulianelli@itm.cnr.it, adolfo.iulianelli@cnr.it
[a] CNR-ITM, via P. Bucci 17C, Rende (CS), 87036, Italy
[b] International Agency for Green Energy, University of Waterloo
200 University Ave W. Waterloo, ON N2L 3G1
[c] VSB - Technical University of Ostrava - Energy and Environmental Technology Centre
Energy Research Centre, 17. listopadu 2172/15, 708 00 Ostrava-Poruba, Czech Republic

CO_2 valorisation, bio-polymeric membrane separation, hydrogen utilization, biomethane

Abstract

This work deals with a methanation reactor to produce synthetic methane from CO_2 and H_2 combined with a polymeric membrane separation stage. Overall, the proposed plant is able to recover over 80% of the produced synthetic methane as a biomethane stream (CH_4 > 97%, CO_2 < 1%).

Introduction:

The different challenges related to climate change and dependence on fossil fuels have led to the search for innovative and environmentally friendly solutions. To keep the global temperature rise below 2°C, global greenhouse gas emissions must be reduced by 50-75% by 2050 [1]. Batteries, renewable electricity, hydrogen, and the reduction of CO_2 reductions are the key factors for a net-zero world [2].

Within this approach, the production of biomethane by implementing integrated systems combining CO_2 and hydrogen under a methanation process with the eco-friendly membrane separation may represent a promising approach in the framework of negative CO_2 emission strategy. This context not only allows an energy transition but also aligns with the principles described by the circular economy, transforming wastes in valuable and sustainable resources [3]. CO_2 methanation process is a chemical reaction combining CO_2 and H_2 to produce CH_4 and H_2O. It is a strong exothermic reaction, which typically operates between 200 °C and 450 °C; therefore, it requires precise control of operating conditions to avoid unwanted by-products depending on catalyst and experimental conditions. Efficiency is improved by the use of advanced catalysts such as nickel (Ni) or ruthenium (Ru) supported by reducible oxides such as CeO_2, which increase selectivity and productivity.

Membrane separation is a new technology for purifying gas streams. The process allows for selective separation of the gaseous components according to their permeability properties through the active surface of the membrane. The usage of organic membranes, especially those based on bio-polymers is increasingly essential due to their gas purification efficiency, versatility, and low environmental impact.

PLA, a low-cost biodegradable polymer, offers good selectivity for CO_2 with respect to CH_4 and H_2, making it a promising material to improve the efficiency of biomethane purification by reducing the need for energy-intensive methods.

Objectives:

The main objective of this work focuses on the valorisation of CO_2 to respond to the urgent demand of CO_2 emissions depletion. Hence, here it is proposed an integrated system combining CO_2 methanation and membrane separation for the production of biomethane. The operational principles, process design, and results obtained are analyzed, with particular emphasis on biomethane recovery and negative CO_2 emissions. Figure 1 sketches the integrated system coupling a methanation reactor and a multi-stage polymeric system for biomethane recovery.

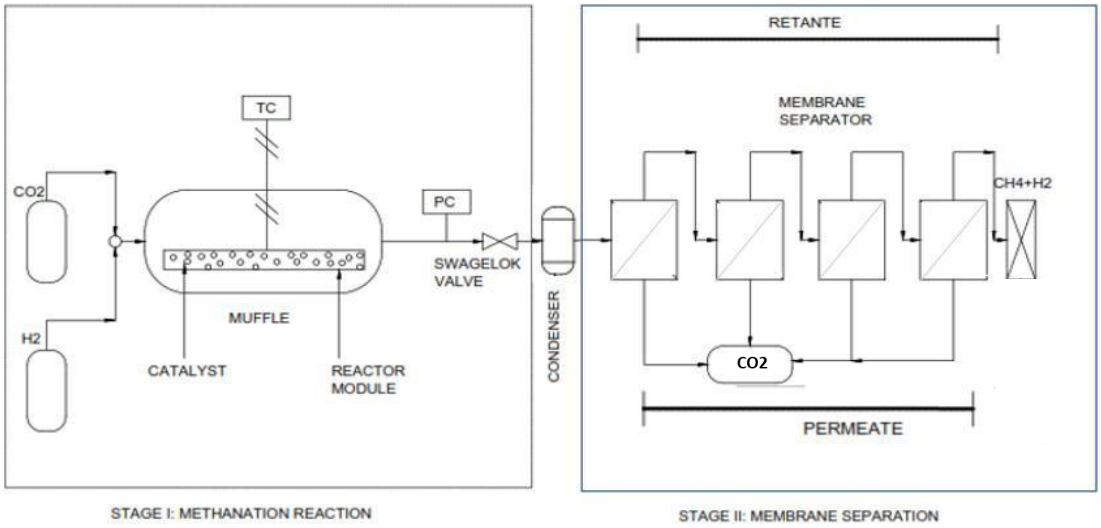


Figure 1. Combined Methanation and Membrane Separation System for High-Purity Biomethane Production

Material and methods:

3 g of a Ru/γ-Al_2O_3- 0.5% w/w catalyst have been inserted in the core of the methanation reactor. In such a configuration, reactor temperature and pressure can be assumed homogeneous without significant errors. Before starting reaction tests, the catalyst was reduced by passing pure hydrogen (15 mL/min) for 2 hours at 300 °C and atmospheric pressure. Permeation tests for each gas (H2, He, CO2 and CH4) were performed on various

samples of PLA membranes using an AISI 316L stainless steel cell (internal diameter: 4.0 cm). Each gas was supplied by mass flow controllers (Brooks Instruments, Hatfield, USA), controlled by software (Lira, Kiev, Ukraine). The permeate pressure was maintained constant at 1 bar while the transmembrane pressure between the feed side and the permeation side was varied in the range of 2-13 bar using a back pressure regulator, placed on the retentate side.

Results:

The experimental approach consisted of two main stages: the methanation of CO_2 in a fixed-bed reactor (PBR) and a second stage of biomethane separation using a series of polymer membrane separators based on PLA. The Ru-γAl2O3 catalyst used for the Sabatier reaction has shown an optimal balance between methane yield, resistance, and cost. Under operating conditions of 300 °C and pressures below 5 bar, a conversion of CO_2 between 70% and 80% was observed during the experimental phase, with an increasing trend in the reaction pressure. Regarding to the methanation reactor downstream treatment, a four-stage bio-polymeric membrane system operated at different transmembrane pressures and ambient temperature was used to obtain a biomethane stream. The first separation stage allowed us to achieve a methane concentration around 62%, with a significant reduction of CO_2 and H_2 content. The second stage reduced the CO_2 concentration to less than 0.003% molar, corresponding to a methane concentration of 76%. Finally, the fourth stage of separation allowed to obtain a biomethane stream (CH_4 > 97%, CO_2 < 1%).

Acknowledgment

This work was funded by the European Union – NextGeneration EU from the Italian Ministry of Environment and Energy Security POR H2 AdP MMES/ENEA with involvement of CNR and RSE, PNRR - Mission 2, Component 2, Investment 3.5 "Ricerca e sviluppo sull'idrogeno".

References

[1] C. Bataille, L. J. Nilsson, F. Jotzo, Industry in a net-zero emissions world: New mitigation pathways, new supply chains, modelling needs and policy implications, Energy Clim. Chang., vol. 2, p. 100059, Dec. 2021.

[2] M. Tommasi, S. N. Degerli, G. Ramis, I. Rossetti, Advancements in CO_2 methanation: A comprehensive review of catalysis, reactor design and process optimization, Chem. Eng. Res. Des., vol. 201, pp. 457–482, Jan. 2024.

[3] H. Bryan Trujillo Ruales, A. Spadafora, P. Fiore, J. Veres, A. Caravella, A. Iulianelli, Reformer + Membrane separator plant for decarbonized hydrogen production from Biogas/Biomethane: An experimental study combined to energy efficiency and exergy analyses, Energy Convers. Manag., vol. 315, p. 118748, Sep. 2024.

European Fuel Cells and Hydrogen
PIERO LUNGHI CONFERENCE
September 17th–19th 2025
Capri / Italy

A Simple and Field-Deployable Microbial Fuel Cell Architecture for Stable and Sustainable Energy Generation: A Comparative Study of Sediment- and Plant-based Systems.

Ambre Chabbert*[ab], Abdelghani Ghanam [a], Laurent Nicolas[a], Arnaud Elger[b]

* corresponding author: ambre.chabbert@ec-lyon.fr
[a] Laboratoire Ampère, Univ Lyon, Ecole Centrale de Lyon, INSA Lyon, Université Claude Bernard Lyon 1, CNRS, UMR5005, 69130 Ecully - France
[b] Centre de Recherche sur la Biodiversité et l'Environnement, Université de Toulouse, CNRS, IRD, Toulouse INP, UMR 5300, 31062 Toulouse - France

Keywords: Plant microbial fuel cell, sustainable energy, sediment, rhizodeposition

Abstract

Plant Microbial Fuel Cells (PMFC) offer a sustainable way to generate continuous electricity by harnessing plant rhizodeposition. This study compares the performances of sediment- versus plant-based MFC using a simple, field-deployable architecture. We tested two sediment types, showing that natural sediment supports stable electricity production, even in the absence of plants. With *Glyceria maxima*, PMFC maintained a stable power density of 6.0 ± 0.1 mW/m² over 130 days. These preliminary results highlight the PMFC's potential for sustainable energy, but further studies is needed to optimize its real-world performance.

Introduction

In the context of global environmental challenges and ongoing energy transition, PMFCs offer an innovative pathway toward sustainable energy generation. These electrochemical systems leverage the phenomenon of rhizodeposition, in which plant roots release organic matter into the soil, fueling electroactive bacteria that generate electrical current at the anode [1,2]. PMFC thus offer a continuous, renewable energy source by harnessing natural resources and biological processes [3]. Numerous studies have highlighted key factors influencing PMFC performance, such as soil type, plant species selection, and system configuration [4]. While significant progress has been made in optimizing certain parameters (e.g., electrode materials and system architecture), several scientific challenges remain. Particularly, achieving a stable and continuous electrical signal and enhancing performance to supply low-energy small electronic devices remain key unresolved issues [3].

Herein, the electrical performances of Sediment Microbial Fuel Cell (SMFC) and PMFC were compared, highlighting the impact of sediment and plant on the stability of the electrical signal. This will help assess the viability of PMFC as a sustainable energy source for environmental applications. Ultimately, the goal is to develop and deploy these fuel cells directly in situ.

Material and methods

A. PMFC architecture

The design of both SMFC and PMFC systems consists of a single chamber (**Fig. 1A**). The electrodes were made from an air cathode composed of carbon felt (CF) functionalized with platinum/carbon (10%) and a non-functionalized CF anode (**Fig. 1B**). Both electrodes have a 9.5 cm diameter. They were connected to each other via a stainless steel wire and an external 560 Ω resistor to trigger biofilm growth. A 3.6 cm hole was made in the air cathode to insert *Glyceria maxima*, a wetland plant suited for local conditions of the study area. Before PMFC setup, roots were rinsed and trimmed to 5 cm; electrodes were spaced 7 cm apart.

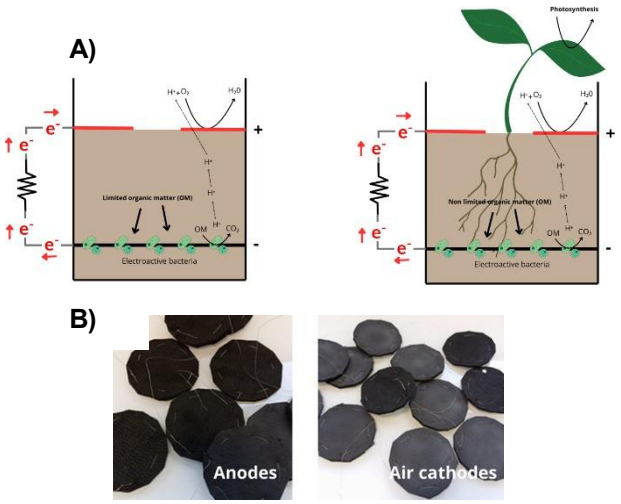


Figure 1: (A) SMFC-PMFC design. **(B)** Photographs of electrodes. The hole is not visible since it was made just before the cathodes were installed (i.e. after the photograph was taken).

B. Experimental conditions and characterization methods

Two types of sediment were tested in a SMFC configuration to determine which would be most suitable for plant insertion. The first, referred to as natural sediment, was collected from an *in situ* observation platform where *Glyceria maxima* could grow. The second, artificial sediment, is used to control soil in laboratory.
After selecting the optimal sediment, a second experiment was conducted to assess plant–sediment compatibility. This experiment compared the performance of sediment- versus plant-based MFC configurations. Power and polarization curves were regularly recorded throughout the experiment to monitor the electrical performance of the two systems. These curves help evaluate the maximum voltage, power and current produced by the fuel cells, offering insight into the efficiency and stability of the system over time. Additionally, biofilm electroactivity of the two systems was evaluated by cyclic voltammetry in a three-electrode system. Each condition was tested in triplicate and continuously watered to maintain optimal conditions.

Results

A. Impact of two sediment types

The biofilm growth kinetics were monitored throughout the experiment (**Fig. 2**). Regardless of the sediment type used, the biofilm reached maturation two days after electrodes connexion. However, notable differences were observed in the stability of the cell voltage generated, depending on the sediment type.
For the SMFC using artificial sediment, a drastic drop in voltage was observed by the fourth day, ultimately reaching a value of zero (**Fig.2**). This sudden extinction can be attributed to the compaction of the sediment when water was added, reducing electrode-sediment contact. This can limit ion diffusion through the system and electrochemical reactions, preventing current generation. In contrast, SMFC using natural sediment maintained a stable voltage ranging from 100 mV to 300 mV throughout the experiment (**Fig. 2**).

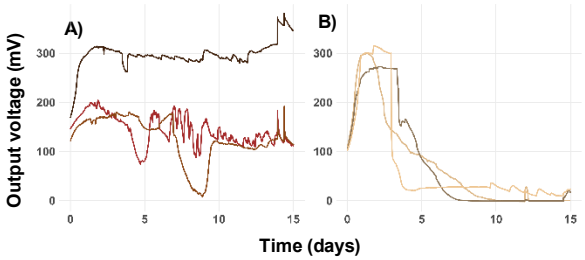


Figure 2 : Biofilm growth kinetics curves. Each color represents an individual. **(A)** Sediment from the natural pond. **(B)** Artificial sediment.

The maximum power density measured for natural sediment was 3.1 $mW.m^{-2}$. Whereas, the maximum current density measured was 57.14 $mA.m^{-2}$.
These results demonstrate that, although biofilm growth was similar in both sediments, artificial sediment is not suitable for efficient use in energy harvesting systems. Sediment compaction seems to be a limiting factor, highlighting the need to optimize the type of soil to ensure stable current generation. In contrast, natural

sediment offers better long-term energy stability, making it suitable for further tests with wetland plants like *Glyceria maxima*.

B. Plant-system integration

Both PMFC and SMFC were tested to compare their electrical performance, as well as to assess the integration of the plant and its growth, with the goal of sustaining the system through the phenomenon of rhizodeposition. Voltage output remained stable over time regardless of the condition tested (**Fig.3**).

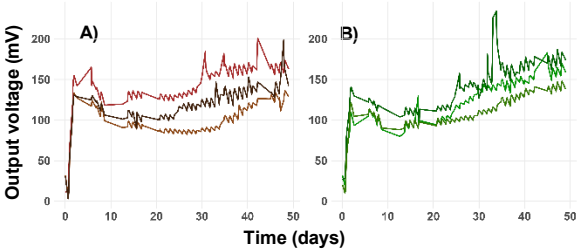


Figure 3 : Biofilm growth kinetics curves. Each color represents an individual fuel cell condition. **(A)** SMFC and **(B)** PMFC.

For the SMFC, the measured maximum power (P_{max}) and current (J_{max}) densities were 4.9 ± 0.3 mW.m^{-2}, 92 ± 70 mA.m^{-2} (day 4) and 5.8 ± 0.8 mW.m^{-2}, 49 ± 5 mA.m^{-2} (day 117). However, for the PMFC, the P_{max} and J_{max} were 3.6 ± 0.5 mW.m^{-2}, 355 ± 190 mA.m^{-2} (day 4) and 6 ± 0.1 mW.m^{-2}, 60 ± 0.7 mA.m^{-2} (day 117). It should be noted that while the P_{max} remained relatively stable over time, the J_{max} decreased. This suggests that, despite the initial higher current in the PMFC, the performance stabilized over the course of the experiment. The cyclic voltammetry indicated a higher anodic current for the PMFC (7.3 mA) compared to the SMFC (3.2 mA), indicating greater electrochemical activity of the biofilm. This difference suggests better microbial colonization, possibly due to a continuous supply of substrates from root exudates. These preliminary results indicate that the PMFC environment may promote the development of a more electroactive biofilm. This experiment yields promising results for the use of this architecture and sediment type as an energy source. The fuel cells have now been running for more than 130 days, maintaining stable voltage and power output throughout. Therefore, it is worthwhile to continue optimizing this system, especially by quantifying the impact of the plant on the electrical signal. This will help assess the potential energy production in environments where organic matter is scarce.

Conclusions

This study shows that a simple, field-ready PMFC can sustain stable energy production over long periods, highlighting its potential for environmental energy harvesting. Natural sediment was key to maintaining higher and more stable power output than artificial sediment, which is promising for real-world application. Future work should optimize plant–sediment–microbe interactions to boost energy yield and expand applications like environmental sensing. Further research will also refine design aspects, such as electrode spacing, electrode materials,and the impact of *Glyceria maxima* rhizodeposition, to enhance performance and long-term efficiency.

Acknowledgement

The authors acknowledge the CNRS BioPlant project for its support to the realization of this work.

References

[1] Chiranjeevi, P., Yeruva, D. K., Kumar, A. K., Mohan, S. V., & Varjani, S. (2019). Plant-microbial fuel cell technology. In *Microbial electrochemical technology* (pp. 549-564). Elsevier.

[2] Kabutey, F. T., Zhao, Q., Wei, L., Ding, J., Antwi, P., Quashie, F. K., & Wang, W. (2019). An overview of plant microbial fuel cells (PMFCs): Configurations and applications. *Renewable and Sustainable Energy Reviews*, *110*, 402-414.

[3] Bataillou, G., Ondel, O., & Haddour, N. (2024). 900-Days long term study of plant microbial fuel cells and complete application for powering wireless sensors. *Journal of Power Sources*, *593*, 233965.

[4] Rusyn, I. (2021). Role of microbial community and plant species in performance of plant microbial fuel cells. *Renewable and Sustainable Energy Reviews*, *152*, 111697.

EFCH2 2025
European Fuel Cells and Hydrogen
PIERO LUNGHI CONFERENCE
September 17th–19th 2025
Capri / Italy

Microbial Fuel Cells working as transistors: addition of 3rd and 4th "pins" for self-monitoring internal states

Daniela Zertuche Moreno[a], Ioannis Ieropoulos[a*]

* corresponding author: i.ieropoulos@soton.ac.uk

[a] Water & Environmental Engineering Group, School of Engineering, University of Southampton, Bolderwood Campus, SO16 7QF, UK

Keywords: self-sensing, microbial fuel cells, internal redox states, 3rd and 4th pins

Introduction:

Monitoring open circuit voltage in any power system, is a critical parameter in determining internal resistance and adjusting the load for maximum power transfer. In batteries and fuel cells, this is known as the current-interrupt method, which effectively disconnects the load for milliseconds to measure the open-circuit voltage and use the measured value to estimate the new (if different) internal resistance value and adjust the external load for maximum power transfer. In Microbial Fuel Cells (MFCs), the shortest time for reliably measuring the open circuit value, after disconnecting the load is ~30 minutes. If the internal redox state can be monitored in real time, then there is no need to interrupt the circuit. This is the purpose of introducing two additional smaller electrodes inside the anode and cathode respectively and using them as real-time monitors of the dynamic redox environment (Ieropoulos and Greenman, 2015*). It can help the operator to either manually or automatically using artificial intelligence/machine learning, to adjust operating conditions, such as external load, flow rate, pH, type of feedstock as well as to troubleshoot issues and better understand electrochemical limitations. (Gajda et al., 2021; Ieropoulos et al., 2018; Sánchez et al., 2022) In this study, 3rd and 4th electrodes or 'pins' inside a cuboid MFC, were studied at different maturation stages to monitor the redox potential between anode cathode and evaluate the stability and reliability of the pins at early stages of maturation.

Objectives:

1. Introduce two additional electrodes in the anode and cathode of MFCs, to act as floating references.
2. Independently measure the voltage across these 3rd and 4th pin electrodes in a Microbial Fuel Cell operating in continuous mode during polarisation.

3. Compare the findings from a mature vs a newly inoculated MFC, to evaluate the stability and hence the reliability of the process.

Material and methods:

Cuboid double chamber MFCs were used for the reported experiments. Each chamber had 29 mL and was designed to hold a working electrode (WE) and a pin electrode. The working electrodes, anode and cathode, were made of 270cm2 of carbon veil (CV) whereas the 3rd and 4th pins had a surface area of 27cm2 of the same material. The pins were not in contact with the working electrode (Ieropoulos et al., 2018). Each MFC was inoculated and enriched for three days with returned activated sludge (RAS) collected from Millbrook Wastewater Treatment Works (Hampshire, UK) and feedstock solution using 1% tryptone, 0.5 % yeast extract, 25mM sodium acetate, 2.5% sodium sulphate (% in w/v). Ferricyanide 0.1 M was used as catholyte. (Ieropoulos et al., 2005). After enrichment the MFC were connected in continuous mode.

A 'new' MFC, with 3 days of operation (new-MFC) and a 'old' MFC, with 153 days of operation (old-MFC) were polarised across a range of resistors (50,000-10Ω, 5 min step) using a resistance decade box (RDB) DR06 ELC connected to the WEs. The voltage (V) across the resistances (R) was continuously recorded using the PicoLogADC-24. In a different data logger channel, the voltage across the 3rd and 4th pin was recorded. The current (I) and the power (P) resulting from the polarization were calculated using I=V/R and P=IV. The resulting voltages and the power from the WEs were plotted against the calculated current.

Results and Discussion:

Figure 1. shows the polarisation results of the new- and old-MFC with 3rd and 4th.Despite the difference in maturation states, in both cases, a stable reading at OCV can be observed across the pins (grey line). The current study differs from previous studies in which pin electrodes show values close to half the starting open circuit voltage (Ieropoulos et al., 2018).

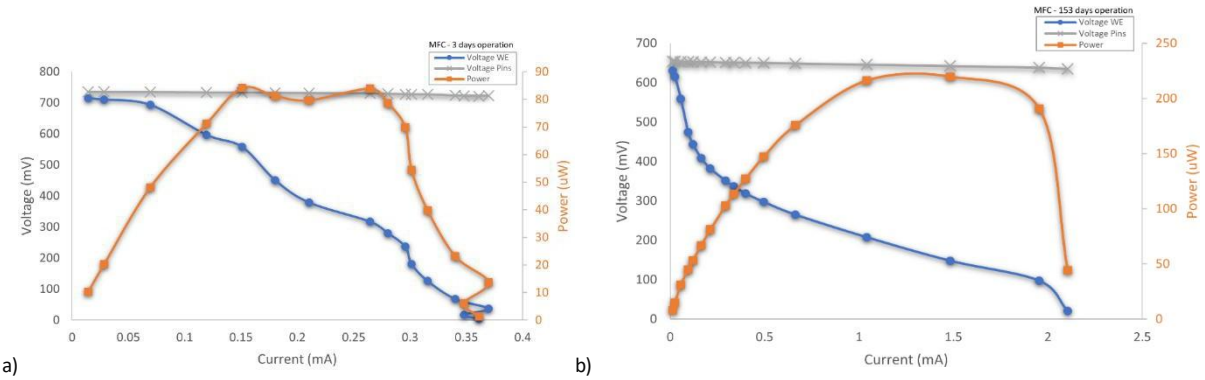


Fig 1. Polarisation of cuboid Microbial Fuel Cells (MFCs) with 3rd and 4th pins (grey line) to monitor OCV. a) MFC polarised at 3 days of operation. b)MFC polarised at 153 days of operation. Stable readings of the pins (grey line) at OCV level are observed.

The voltage level of the pin electrodes remained constant throughout the polarisation experiment and exactly at the level of the initial open circuit value, which is different from what was previously reported (Ieropoulos et al., 2018).

Conclusions:

The study revealed that the introduction of 3rd and 4th pins served as a real-time OCV monitoring tool that does not require interruption of the circuit, giving the end user more information about the redox potential value between the anolyte and catholyte. Assuming that the MFC internal environment is polarised during a polarisation run, one hypothesis may be that the MFCs were carbon-energy and oxidising agent (ferricyanide) replete, showing little change in internal, dynamic states. This clearly requires further investigation, which is part of the immediate research plans.

References

*National Center for Biotechnology Information (2025). PubChem Patent Summary for WO-2016120641-A1. Retrieved April 4, 2025 from https://pubchem.ncbi.nlm.nih.gov/patent/WO_2016120641-A1.

Gajda, I., You, J., Mendis, B. A., Greenman, J., & Ieropoulos, I. A. (2021). Electrosynthesis, modulation, and self-driven electroseparation in microbial fuel cells. *iScience*, *24*(8), 102805. https://doi.org/https://doi.org/10.1016/j.isci.2021.102805

Ieropoulos, I. A., Greenman, J., Melhuish, C., & Hart, J. (2005). Comparative study of three types of microbial fuel cell. *Enzyme and Microbial Technology*, *37*(2), 238-245. https://doi.org/https://doi.org/10.1016/j.enzmictec.2005.03.006

Ieropoulos, I. A., You, J., Gajda, I., & Greenman, J. (2018). A New Method for Modulation, Control and Power Boosting in Microbial Fuel Cells. *Fuel Cells*, *18*(5), 663-668. https://doi.org/https://doi.org/10.1002/fuce.201800009

Sánchez, C., Dessì, P., Duffy, M., & Lens, P. N. L. (2022). Gauging sediment microbial fuel cells using open-circuit auxiliary electrodes. *Journal of Power Sources*, *527*, 231216. https://doi.org/https://doi.org/10.1016/j.jpowsour.2022.231216

European Fuel Cells and Hydrogen
PIERO LUNGHI CONFERENCE
September 17th–19th 2025
Capri / Italy

N-integration in Ni-Fe-Cr-Ru-Mo High-Entropy Electrocatalytic Materials

Maryam Eslami *[a,b], Sandro Zorzi [a], Giulia di Gregorio [a], Gloria Gottardi [a], Matteo Testi [a], Luigi Crema [a]

*Corresponding author: meslami@illinois.edu

[a] Center for Sustainable Energy, Bruno Kessler Foundation, Trento 38123, Italy
[b] Applied Research Institute, The Grainger College of Engineering, University of Illinois Urbana-Champaign, Champaign 61820, Illinois, US

Keywords: Catalyst, Electrolysis, High-entropy alloys, Hydrogen

Abstract

Introduction: *Multi-principal element materials (MPEMs) also known as high entropy materials (HEMs) are regarded as essential electrocatalytic materials for high-performance electrochemical applications including hydrogen electrolysers.[1,2] MPEMs consisting of transition metal-based materials gained significant attention for their desired catalytic performance during oxygen evolution reaction (OER) and hydrogen evolution reaction (HER).[3,4] However, their long-term durability especially in acidic environments are yet to be improved and requires further investigation.[5] One of the latest approaches to improve the catalytic properties of MPEM is to incorporate small elements such as nitrogen (N) into the microstructure at different concentrations, aiming to induce defects and N to metal bonds to tune the surface energy or to form secondary phases with high catalytic activity. The influence of this method on catalytic activity and durability of MPEMs needs to be studied.[6]*

Objectives: *This work aims to synthesize Ni-Fe-Cr-Ru-Mo-(N) high-entropy alloy and high-entropy nitride thin films via RF/DC co-sputtering by systematically varying nitrogen-to-argon gas flow ratios and substrate temperatures to control nitrogen incorporation and nitride phase formation. The effect of these parameters on the electrocatalytic performance of the films is evaluated through detailed investigation of their hydrogen evolution reaction (HER) and oxygen evolution reaction (OER) activities in acidic and alkaline media.*

Material and methods: *The high entropy catalytic materials (with and without the incorporation of nitrogen (N)) were produced through a combination of RF/DC sputtering sources by co-sputtering the following target materials Ni-Fe-Cr, Mo and Ru on Ti plate*

substrate (previously cleaned with standard procedures). The targets' applied powers were optimized to obtain the desired elemental composition. During the depositions, the N_2 concentration in the atmosphere was varied to 0%, 6%, 13%, % in order to control nitrogen incorporation at different temperatures in the range of 250 to 450 °C. Electrochemical measurements were conducted using a potentiostat and a standardized 3-cell electrode. For HER measurements, 0.5 M of H_2SO_4 solution was used while for OER and overall water splitting (WS), 0.5 M KOH solution was used. Scanning electron microscopy (SEM) and energy dispersive X-ray spectroscopy (EDX) were performed on the films for microstructural and compositional analysis.

Results: *Preliminary results revealed the effect of temperature in promoting outstanding catalytic properties for the N-enriched catalytic coating (N-inc.) deposited with 6% of N_2 in the atmosphere with respect to HER in acidic media. In this regard, the incorporation of N at high temperature (the so-called N-inc. HIGH T. sample) showed kinetic and thermodynamic improvements after 16 h of stability test at 10 mA/cm^2 (N-inc. HIGH T (POST)). In fact, Tafel slope as well as the overpotential values measured at 10 mA cm^{-2} ($\eta_{@10mA/cm2}$) decreased from 50 to 37 mV/dec and from 150 to 50 mV, respectively, as shown in Figure 1a. While in the same media, the base alloy synthesized at high temperature (Base HIGH T) showed almost unvaried and inferior HER catalytic properties compared to those of the N-integrated samples with constant Tafel slope values of 58 mV/dec and $\eta_{@10mA/cm-2}$ varying from 110 to 70 mV, after 16 h of stability, as reported in Figure 1a. Although temperature was shown to enhance the catalytic properties in both the base and N-incorporated samples, the introduction of nitrogen clearly improved the activity as well as durability of the MPEM. This is evidenced by the SEM images in Figure 1b, which compare the base alloy (Base HIGH T) and the N-incorporated (N-inc HIGH T) catalysts synthesized at high temperature before and after 16 hours of stability test. Notably, the N-inc HIGH T sample resulted in strongly catalyzing both OER and HER in alkaline media, offering the possibility to build-up an overall WS catalyst. In this case, the N-integrated catalyst demonstrated valuable kinetics in HER and OER, with Tafel slopes of 100 and 44 mV/dec, and valuable overpotentials measured at -10 and 10 mA/cm^2 of 220 and 320 mV, respectively, during the overall WS in alkaline media. These results suggested the N-integration can effectively tune and enhance both the stability and electrocatalytic properties of MPEMs.*

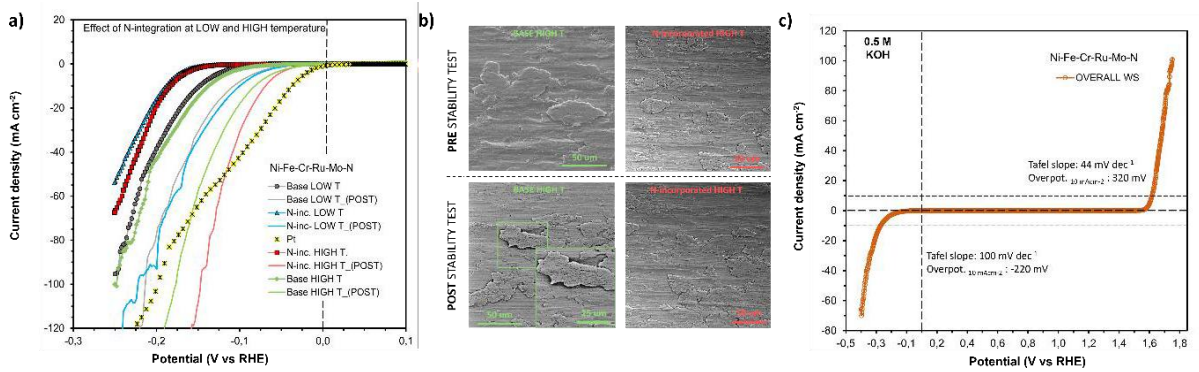


Figure 1. a) Polarization curves in acidic media (0.5 M H_2SO_4) and b) SEM images of the base alloys and N-inc. MPEM catalysts made at different temperatures collected before and after (POST) the 16 h stability test. c) Overall water splitting reaction of the N-inc. HIHG T sample measured in alkaline media (0.5 M KOH).

Acknowledgments

Maryam Eslami would like to thank Provincia Autonoma di Trento for sponsoring this research through the "Visiting Trentino 2024" grant.

References

1. A. Ahmad et al., *Small, **20*** (2024).
2. X. Huo, H. Yu, B. Xing, X. Zuo, and N. Zhang, *The Chemical Record*, **22** (2022).
3. S. Li et al., *Small*, **18** (2022).
4. S. Ahmad et al., *ACS Appl Energy Mater*, **6**, 10652–10664 (2023).
5. A. Asghari Alamdari et al., *ACS Appl Energy Mater*, **7**, 2423–2435 (2024).
6. S. Wang et al., *Applied Catalysis B: Environment and Energy*, **363**, 124791 (2025).

EFCH2 2025 European Fuel Cells and Hydrogen
PIERO LUNGHI CONFERENCE
September 17th–19th 2025 Capri / Italy

Green Hydrogen Innovation: A Patent-Based Analysis of Critical and Strategic Resource Use

Marinella Favot*[a], Riccardo Priore [a], Marco Compagnoni[b]

*corresponding author: Marinella Favot
[a] Area Science Park, Padriciano 99, Trieste (Italy)
[b] University of Milano-Bicocca, Milano, Italy

Keywords: Circular Economy, Electrolyser and Fuel Cell, Hydrogen Innovation, Critical Raw Material, Strategic Raw Material.

Abstract

This study investigates innovation dynamics and material criticality in the field of green hydrogen technologies, focusing on fuel cells and electrolysers. By analysing over 47 thousand patents from 2000 to 2023 using data from PATSTAT, the research explores global trends, national leadership, and the role of critical raw materials (CRMs[1]) essential for hydrogen production. China, Japan, and the United States emerge as dominant actors, with patent activity peaking in 2022. A text mining-based criticality analysis reveals that 12% of patents mention at least one CRM, with Nickel, Platinum, and Lithium being the most frequently cited (last one most likely used for lithium-ion batteries). These findings underline both the technological momentum of the hydrogen sector and its dependence on materials with potential supply constraints and price volatility, emphasizing the need for innovation in material reduction, substitution and recycling strategies to support the sustainable deployment of green hydrogen solutions.

Introduction

The global push towards net-zero emissions has intensified the development of green technologies, particularly hydrogen (H_2) production through water electrolysis. However, this process depends on Critical Raw Materials (CRMs), whose supply is concentrated and volatile, posing strategic challenges. With growing competition in innovation, especially in the green hydrogen field, understanding technological trends and material dependencies becomes essential. This study, initiated in the framework of the North Adriatic Hydrogen Valley project[2] involving the Friuli Venezia Giulia region (Italy), Croatia, and Slovenia, investigates the evolution of key hydrogen technologies—fuel cells (FC) and electrolysers—through patent

[1] CRMs defined according to the European Commission
[2] NAHV

data, identifying innovation leaders and assessing CRM reliance using text mining methodologies.

Objective

The research aims to identify global trends and national leadership in fuel cell and electrolyser technologies as H2 key technology using patent data from 2000 to 2023. A further objective is to conduct an initial criticality assessment of these technologies by analysing references to CRMs based on the EU Critical Raw Materials list.

Material and Methods

The analysis is based on the PATSTAT 2000–2023 dataset (autumn edition 2024). Four main datasets were created: the first pair includes patents with the keywords “Hydrogen & Fuel Cell” and “Hydrogen & Electrolyser” in the title or abstract; the second pair consist of subsets filtered for explicit mentions of CRMs. The methodological approach combines descriptive analysis—focused on patent time trends and national authority distribution—and a criticality analysis aimed at identifying and quantifying references to key raw materials.

Results

From 2000 to 2023, 47,143 patent applications were registered in the fields of fuel cells and electrolysers, with a peak in 2022 reaching 5,380 patents (Figure 1). China, Japan, and the United States emerged as leading countries in terms of innovation output, confirming their strategic investment in green hydrogen technologies.

Fig 1 *Patent trends for key H2 technologies: FC and Electrolyser (years 2000-2023)*

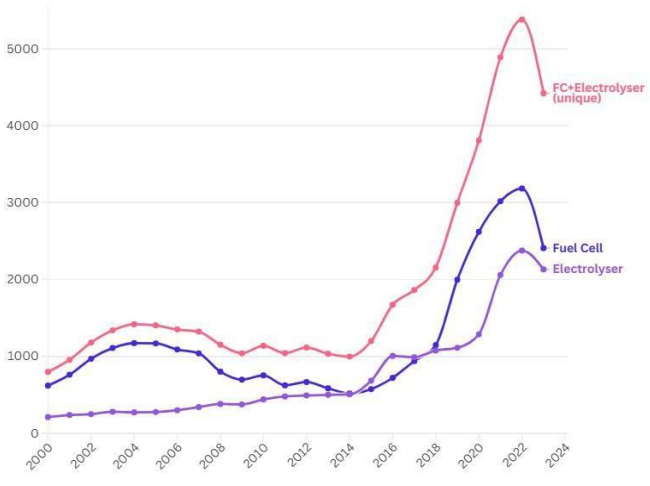
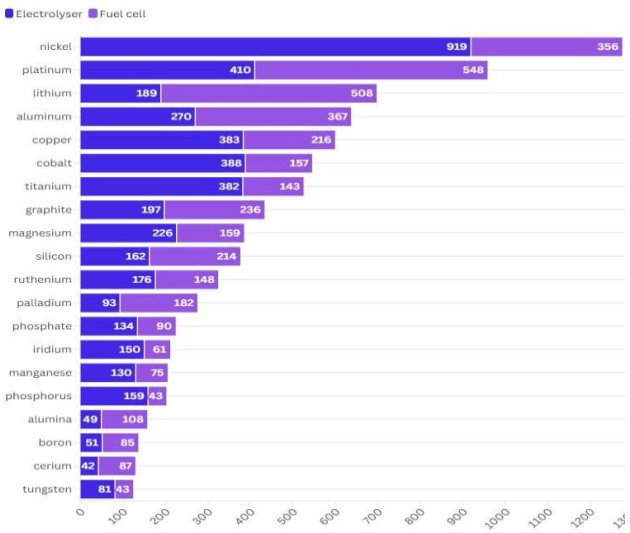


Fig 2 *Patens by top 20 CRM in Key H2 technologies (years 2000-2023)*



The total number of patent families for **electrolyser** are 18,015 with a strong presence of patents applications deposited at the Chinese authority (61.77%), while the subgroup of

patent applications that include at least one CRM are more than 17% (of which 74.98% filled in China). From a quantitative perspective, Chinese authority is the leader in this field, however when we apply a qualitative perspective (triadic patent families TPF[3]) the overall picture is radically modified with Japanese, Italian and US national authorities being the most important ones with 16 TPF for Japan and 9 for Italy and the US. Patent applications in the **fuel cells** are 29,128 with a strong leadership of automotive players (such as Toyota, Hyundai, Nissan and Honda). The subgroup of patent applications that cite at least one CRM is 8.5% with Toyota and Hyundai remaining important players while the leader applicant becomes the Chinese Academy of Sciences. Also, in this second set of patent applications, the TPF are dominated by Japanese and US applicants. In both groups of patent applications (electrolyser and fuel cells) the three-nation belonging to the NAHV area (Italy, Slovenia and Croatia) are scarcely represented so far, except for a company based in Italy.

Among the most frequently cited CRMs are nickel and platinum which appear to be essential across both technologies (Figure 2). Lithium is also cited even if it is not a primary material in fuel cells or electrolysers, but is extensively used in lithium-ion batteries, which may be cited as it is integrated with hydrogen technologies for energy storage purposes.

Conclusions

The rapid increase in patents for hydrogen technologies highlights a global push toward green hydrogen solutions, possibly peaking in 2022. The dominance of China, Japan, and the USA in hydrogen innovation reflects their strategic commitment to clean energy and market leadership. So far, NAHV countries are marginal in this overall picture. The reliance on Nickel, Platinum for both electrolysers and fuel cells raises issues related to supply risks, price volatility, and geopolitical dependencies. Similar lithium, used in battery storage. Future advancements in material alternatives or recycling strategies could help mitigate CRM dependency and ensure the sustainable growth of H_2 technologies.

Acknowledgment

Grant information: This project has received funding from the European Union's Horizon Europe research and innovation programme under grant agreement No [101111927](North Adriatic Hydrogen Valley [NAHV]). The funders had no role in study design, data collection and analysis, decision to publish, or preparation of the manuscript. Views and opinions expressed in this paper are however those of the author(s) only and do not necessarily reflect those of the European Union or the Clean Hydrogen Joint Undertaking. Neither the European Union nor the granting authority can be held responsible for them. The funders had no role in study design, data collection and analysis, decision to publish, or preparation of the manuscript.

[3] Triadic Patent Families (TPF) are patents taken at the European Patent Office (EPO), the Japanese Patent Office (JPO), and the US Patent and Trademark Office (USPTO) that share one or more priorities [2]

References

[1] Li, G. Y., Ascani, A., & Iammarino, S. (2024). The material basis of modern technologies: A case study on rare metals. *Research Policy, 53*(1), 104914. https://doi.org/10.1016/j.respol.2023.104914

[2] Dernis, H., Khan, M., 2004. Triadic patent families methodology. OECD Science, Technology and Industry Working Papers. No. 2004/02.



Techno-Economic and Environmental Assessment of Hydrogen Integration in Renewable Energy Communities in Italy

Silvia Ricciuti*[a], Michele Bolognese[a], Gionata Luca[a], Matteo Testi[a]

* corresponding author: sricciuti@fbk.eu

a Fondazione Bruno Kessler –Centro sustainable energy (SE)

Keywords: By products use, green hydrogen, Renewable energy community, Reversible solid oxide fuel cell

Abstract

The interaction and coexistence of hydrogen production and Renewable Energy Communities (RECs) form a critical nexus and a promising pathway toward sustainable energy systems [1]. As the world faces the twin challenges of climate change and energy security, hydrogen has emerged as a versatile energy carrier that facilitates the integration of Renewable Energy Sources (RES)[2]. In this study two RECs in Italy, based in Trento and in Naples, will be supported in the integration of a rSOC (reversible Solid Oxide Cell) for the first demo and a SOFC in the second demo. On one hand, exploring its use in SOFC (Solid Oxide Fuel Cell) mode allows to use biogas to produce incentivable electricity for the REC's self-consumption. On the other hand, the resulting green hydrogen produced in SOE (Solid Oxide Electrolyser) mode can serve to be blended with biofuels to reduce the fuel consumption; Indeed, H2 and CH4 blending represent an opportunity for industry decarbonisation. Moreover, using SOE mode in pick hours can contribute in generate incentive with shared energy. The cost of hydrogen production is a critical factor influencing the viability and competitiveness of hydrogen as a clean energy carrier, and the Levelized Cost Of Hydrogen (LCOH) for green hydrogen, produced via electrolysis with electricity from RES, can be competitive with that of blue hydrogen, produced from Steam Methane Reforming (SMR) and Carbon Capture and Storage (CCS) with low CO2 emissions, especially when carbon taxes are considered ([2][3]). The integration of hydrogen production systems, eventually in conjunction with RECs, can lead to reduce costs through economies of scale and improved operational efficiencies ([4][5]). Nevertheless, the integration of renewable energy into hydrogen production not only enhances the sustainability of the energy supply, but also contributes to addressing the intermittency issues typically associated with renewable sources ([6][7]).

Introduction: Integrating green hydrogen technologies into RECs represents a unique opportunity to develop sustainable and resilient energy systems, accelerating the global

energy transition to a low-carbon economy. By converting surplus renewable energy into hydrogen, the stored hydrogen can be blended with biogas to fuel industrial processes within companies. Moreover, beyond their high electrical efficiency, stationary fuel cells also generate heat, which can be exploited for use by local industries and small businesses. However, under the current REC regulations in Italy, integrating hydrogen into RECs remains challenging. While the use of hydrogen to produce electricity is not recognized as incentivable, there is no explicit restriction on the use of green hydrogen and the fact that an electrolyser can be a consumer within a REC, using excess PV-generated electricity to produce hydrogen. By exploring the implementation of a rSOC (reversible Solid Oxide Cell) in SOFC mode, in a REC, is possible to investigate the use of biogas in case of hydrogen unavailability to produce incentivable electricity for the REC. Indeed, in addition to reversibility, one of the advantages of rSOCs lies precisely in the possibility of accommodating different energy carriers in SOFC bundles[9]. Moreover, the resulting green hydrogen produced in SOE (Solid Oxid Electrolyser) can serve as a long-term energy storage solution, addressing the intermittency challenges of renewable energy sources.

Objectives: The main objectives of this study are to assess the feasibility of integrating green hydrogen into RECs, to analyse the technical performance of hydrogen production and utilization technologies into two demo cases, to evaluate the economic viability of hydrogen deployment, including cost and revenue analysis, to examine the environmental benefits and sustainability aspects of hydrogen integration in RECs, with the scope to identify key challenges and potential solutions for large-scale implementation.

Material and methods: The study is based on a combination of literature review, techno-economic analysis and environmental impact assessment. The integration of a rSOC is applied to two real case studies where productions and consumption are listed. An operation of one year is simulated to evaluate the performance and the economic advantages that hydrogen can bring to urban areas.

Results: The technical analysis led to the conclusion that rSOCs can offer a high-efficiency solution for hydrogen production and utilization within RECs. Environmental benefits include a 70–90% reduction in CO2 emissions compared to conventional fossil fuel-based systems. Hydrogen by-products such as heat, oxygen and demineralized water can enhance system efficiency by integrating with district heating or industrial processes.

Conclusions: The integration of green hydrogen technologies within REC represents a compelling strategy to enhance the sustainability and resilience of decentralized energy systems. The findings of this paper demonstrate that while regulatory directive is not

completely updated on the use of hydrogen in REC, particularly in the Italian context, the potential benefits of hydrogen-based solutions in RECs are significant and deserve further exploration. Both the case studies illustrate the current dynamics of energy production, consumption, and sharing within a REC. The analysis highlights the importance of optimizing the energy balance, ensuring maximum use of shared energy, and capturing the economic potential of self-consumed energy. With hydrogen technologies, particularly rSOC systems, it is possible to address energy gaps caused by the intermittency of renewable sources like solar power, ensuring a stable supply while enhancing the community's overall performance. These incentives, combined with the environmental benefits of green hydrogen, strengthen the business case for integrating advanced hydrogen technologies into RECs.

References

[1] T. S. Uyar and D. Beşikci, 'Integration of hydrogen energy systems into renewable energy systems for better design of 100% renewable energy communities', *Int. J. Hydrog. Energy*, vol. 42, no. 4, pp. 2453–2456, Jan. 2017, doi: 10.1016/j.ijhydene.2016.09.086.

[2] R. Bhandari and N. Adhikari, 'A comprehensive review on the role of hydrogen in renewable energy systems', *Int. J. Hydrog. Energy*, vol. 82, pp. 923–951, Sep. 2024, doi: 10.1016/j.ijhydene.2024.08.004.

[3] Q. Hassan, S. Algburi, A. Z. Sameen, and H. M. Salman, 'Assessment of industrial-scale green hydrogen production using renewable energy', *Proc. Inst. Mech. Eng. Part A*, vol. 238, no. 3, pp. 569–587, May 2024, doi: 10.1177/09576509231219339.

[4] Z. Kang and S. Liu, 'Research on Capacity Optimization Configuration of Renewable Energy Off Grid Hydrogen Production System Considering Collaborative Electrolysis', *Energies*, vol. 17, no. 8, Art. no. 8, Jan. 2024, doi: 10.3390/en17081962.

[5] A. M. Elshafei and R. Mansour, 'Green Hydrogen as a Potential Solution for Reducing Carbon Emissions: A Review', *J. Energy Res. Rev.*, vol. 13, no. 2, pp. 1–10, Feb. 2023, doi: 10.9734/jenrr/2023/v13i2257.

[6] A. Ciancio and L. De Santoli, 'Assessing the levelized cost of hydrogen production in a renewable hydrogen community in South Italy', Institute of Electrical and Electronics Engineers Inc. (IEEE), 2023. doi: 10.1109/EEEIC/ICPSEurope57605.2023.10194654.

[7] X. Guo, P. Kang, J. Zhang, P. Song, and G. Yang, 'Coordinated Control Strategy for System of Hydrogen Production from Renewable Energy Considering Regulating Characteristics of Electrolyzers', *J. Phys. Conf. Ser.*, vol. 2659, p. 012029, Dec. 2023, doi: 10.1088/1742-6596/2659/1/012029.

[8] K. Sayed *et al.*, 'Feasibility Study and Economic Analysis of PV / Wind-Powered Hydrogen Production Plant', *IEEE Access*, vol. PP, May 2024, doi: 10.1109/ACCESS.2024.3406895.

[9] M. Lamagna, D. Groppi, and B. Nastasi, 'Reversible solid oxide cells applications to the building sector', *Int. J. Hydrog. Energy*, vol. 48, no. 70, pp. 27033–27058, Aug. 2023, doi: 10.1016/j.ijhydene.2023.03.387.

European Fuel Cells and Hydrogen
PIERO LUNGHI CONFERENCE
September 17th–19th 2025
Capri / Italy

0D Modeling of Electrochemical Hydrogen Compressor

Federico Croci*[a], Francesco Russo[a], Alessandro d'Adamo [a]

* corresponding author: federico.croci@unimore.it

[a] *Dipartimento di Ingegneria "Enzo Ferrari", Università degli Studi di Modena e Reggio Emilia, Modena, Italy*

Keywords: analytical zero-dimensional methodology for the simulation of Electrochemical Hydrogen Compressor (EHC), optimization of the EHC electrical and flux efficiencies, evaluation of the optimal working zones, estimation of the series and parallel EHC stack configurations.

Abstract

Introduction: Electrochemical Hydrogen Compressors (EHC) represent an innovative and appealing technology to replace mechanical hydrogen compression in specific applications [1][2]. The absence of moving parts ensures a noise-free, low-maintenance component that can operate with high pressure ratios between anode and cathode. Furthermore, the materials employed for the creations of the cell do not suffer from hydrogen embrittlement, surpassing traditional compressors [3]. Moreover, a higher compression efficiency is possible, although this is limited to specific operating conditions, whose identification lies among the objectives of the present work. However, several disadvantages such as costs, hydrogen flowrate and back diffusion limit at present the application fields of this technology. For these reasons a deep investigation of EHC is needed in order to improve their performance, reduce the costs, and achieve a widespread application [4]. For this purpose comprehensive multi-physics (fluid and electrical) modelling can considerably assist and speed up the development of EHC.

Objectives: the presented analytical 0D steady-state EHC model has the aim to fill a knowledge gap in literature, studying all the main electrochemical and fluid-related processes developing inside the cell, providing an overview of the EHC behaviour at differ operating conditions and calculating the efficiency under multiple conditions. In this way it is possible evaluate the optimal working zones for maximum efficiency, thus guiding the operating mode of the EHC.

Material and methods: the model is implemented in a MATLAB® script divided into three different sub-models: electrochemical, mass flux and efficiency. The first sub-model takes into account all the equations needed to characterize the electrochemistry of the reactions taking place at the anodic and cathodic electrodes. The Nernst equation is implemented to define the open circuit potential under non-standard conditions. Tafel and Ohm's laws are applied to calculate the activations and ohmic overvoltages, respectively, where the membrane resistance is defined using the Springer formulation [5][6][7]. The second sub-model describes

all the mass fluxes: Faraday's law is implemented to define the hydrogen direct flow from low to high pressure compartment. Henry's law is employed for the diffusive species transportation across the Nafion® membrane, such as the hydrogen back-diffusion, and the Springer correlation is used to evaluate the electro-osmotic drag of water molecules [5]. The last sub-model calculates the total efficiency of the EHC as:

$$\eta_{Power}^{Steady} = \eta_{stack_{voltage}}^{Steady} \cdot \eta_{stack_{Flux}}^{Steady} = \frac{\frac{R*T}{2*F}*ln(\frac{P_{H_2out}}{P_{H_2in}})}{V_{stack}} \cdot \frac{\dot{n}_{ec} - |\dot{n}_{bd}|}{\dot{n}_{ec}} \quad (1)$$

This allows to consider both the voltage and hydrogen direct and back-diffusion fluxes contribution.

Results: the model was validated through the polarization curves reported in [8] showing excellent agreement between experimental and simulated data for current densities up to 0.7 A/cm^2 for three different operating temperature (35°C, 55°C, 75°C, see *Figure 1*). The linear trend of the curve is justified by relatively high values of exchange current density, which results in low activation losses. It is possible to notice that increasing the working temperature allows to work at higher current densities for the same cell voltage, as the ohmic overvoltage decreases.

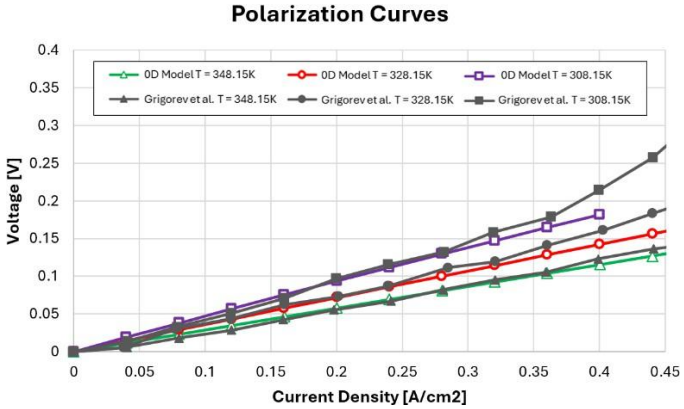


***Figure 1**_Polarization curves for model validation*

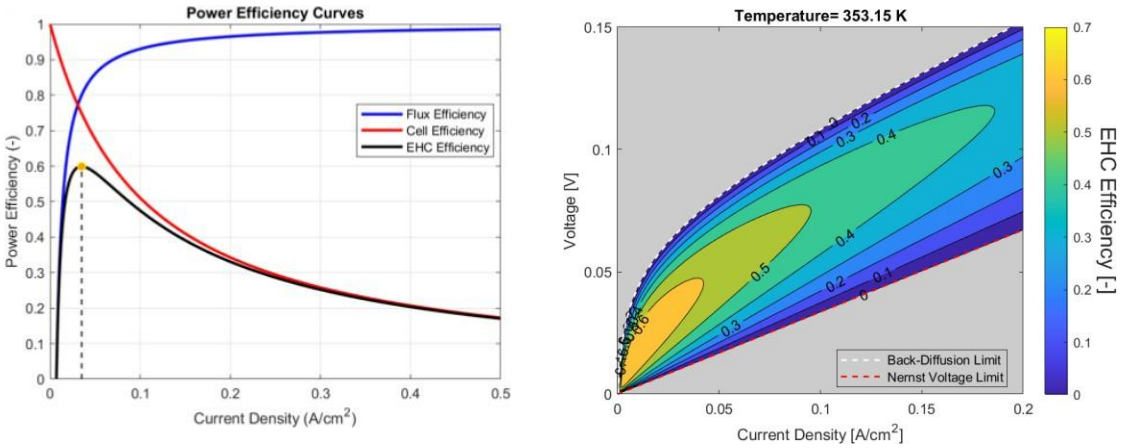


***Figure 2**_Power efficiency curves (left), iso-surface efficiency zones (right).*

Important results were achieved on the EHC efficiency and working conditions. As shown in *Figure 2,* electrical and flux efficiency have an opposite trend as the current density increases

forecasting important indication on operating points. The highest values of global efficiency are found for low voltages and current densities values. Similar evaluation were conducted for temperature, pressure ratios variations and different membrane thickness. Furthermore, a parametric optimization was performed to estimate advantages and disadvantages of series and parallel configurations of stack of EHC cells.

Conclusions: the maximum global efficiency operation for EHC is obtained at low voltages and current densities, as increasing current density improves the flux performance but decrease significantly the electrical efficiency, and vice versa is verified for high voltage operation. Low pressure ratios between anode and cathode ensure higher global efficiency while high temperature improve membrane proton conductivity and increase reactions rate. However, working at high temperature means a greater hydrogen membrane diffusivity and as consequence the back-diffusion phenomena are more relevant. Connecting EHCs in series allows a higher efficiency and reduces significantly the hydrogen diffusion towards the anode as the pressure step is divided between the cells.

Acknowledgment

The authors acknowledge the Centro Interdipartimentale di Ricerca e per i Servizi nel settore della produzione, stoccaggio ed utilizzo dell'Idrogeno (Centro H2 – MO.RE).

References

[1] G. Sdanghi, G. Maranzana, A. Celzard, and V. Fierro, "Review of the current technologies and performances of hydrogen compression for stationary and automotive applications," Mar. 01, 2019, *Elsevier Ltd*. doi: 10.1016/j.rser.2018.11.028.

[2] F. Barbir and H. Görgün, "Electrochemical hydrogen pump for recirculation of hydrogen in a fuel cell stack," *J Appl Electrochem*, vol. 37, no. 3, pp. 359–365, Mar. 2007, doi: 10.1007/s10800-006-9266-0.

[3] N. A. Burton, R. V. Padilla, A. Rose, and H. Habibullah, "Increasing the efficiency of hydrogen production from solar powered water electrolysis," Jan. 01, 2021, *Elsevier Ltd*. doi: 10.1016/j.rser.2020.110255.

[4] M. Aziz, U. R. Aryal, and A. K. Prasad, "Optimization of electrochemical hydrogen compression through computational modeling," *Int J Hydrogen Energy*, vol. 47, no. 78, pp. 33195–33208, Sep. 2022, doi: 10.1016/j.ijhydene.2022.07.256.

[5] T. E. Springer, T. A. Zawodzinski, and S. Gottesfeld, "Polymer Electrolyte Fuel Cell Model," *J Electrochem Soc*, vol. 138, no. 8, pp. 2334–2342, Aug. 1991, doi: 10.1149/1.2085971.

[6] A. D'Adamo, M. Haslinger, G. Corda, J. Höflinger, S. Fontanesi, and T. Lauer, "Modelling methods and validation techniques for CFD simulations of PEM fuel cells," Apr. 01, 2021, *MDPI AG*. doi: 10.3390/pr9040688.

[7] M. Bampaou, K. D. Panopoulos, A. I. Papadopoulos, P. Seferlis, and S. Voutetakis, "An electrochemical hydrogen compression model," *Chem Eng Trans*, vol. 70, pp. 1213–1218, 2018, doi: 10.3303/CET1870203.

[8] S. A. Grigoriev *et al.*, "Hydrogen safety aspects related to high-pressure polymer electrolyte membrane water electrolysis," *Int J Hydrogen Energy*, vol. 34, no. 14, pp. 5986–5991, 2009, doi: 10.1016/j.ijhydene.2009.01.047.

EFCH2 2025 European Fuel Cells and Hydrogen PIERO LUNGHI CONFERENCE
September 17th–19th 2025 Capri / Italy

An optimization algorithm for the integration of hydrogen into multi-carrier energy systems

Silvia Anna Cordieri*[a], Francesco Simmini [a]

* corresponding author: silviaanna.cordieri@rse-web.it
[a] Ricerca sul Sistema Energetico – RSE S.p.A. Milan, Italy

Keywords: Energy-Hub, hydrogen, multi-carrier energy systems, optimization algorithms.

Abstract

The electric sector currently plays an important role due to the maturation of renewable energy generation technologies and the progressive electrification of consumption. However, this also presents certain challenges, such as the need to balance production and consumption almost instantaneously and to manage short and intense production peaks. In this scenario, multi-carrier energy systems can convert energy from one form to another, providing the flexibility required to balance production and consumption. Additionally, the integration of Power To Gas plants in these systems can further enhance flexibility and enable the long-term storage of hydrogen.
In this work, we model a multi-carrier energy system that integrates multiple Energy-Hubs (EHs) connected through electrical, district heating, gas, and hydrogen networks. Each EH includes a Power To Gas system, which converts electrical energy into chemical energy via electrolysis, producing hydrogen. An optimization algorithm is developed for the long-term management of the EHs and the entire system. The results confirm efficient management of both the EHs and the overall system.

Introduction: The electrical sector currently plays a leading role due to the maturation of renewable generation technologies. Solar, wind, and other renewable energy sources have significantly become more efficient than in the past. This has positioned the electrical sector at the forefront of the global energy transition. However, this transition presents challenges, particularly in balancing production and consumption. Multi-carrier energy systems can convert energy from one form to another, providing the flexibility required. Within multi- carrier energy systems, Power to Gas (P2G) technology, particularly Power to Hydrogen (P2H2), is emerging as a complementary alternative to electrical storage. Unlike short-term electrochemical storage, hydrogen storage offers a potential solution for energy storage over weeks or months [1]. The adoption of hydrogen storage systems combined with a renewable

energy system appears to be a paradigm shift in the energy market, introducing new operational possibilities [2]. However, modelling and optimizing multi-carrier energy systems is not a trivial task, as they involve considering multiple criteria simultaneously. An overly simple model may miss key interactions, while a detailed one can be computationally demanding.

Objectives: This work studies an integrated multi-carrier energy system which includes Energy-Hubs (EH) interconnected via the electricity grid, district heating network, gas network, and finally, the hydrogen network. The latter is powered by electrolyzers in the EHs. The produced hydrogen can be reconverted into electricity using fuel cells. Then, the models of the resources of the considered carrier system are described, and a long-term optimization procedure is proposed. The optimization algorithm aims to minimize the system management costs while always ensuring compliance with operational constraints.

Material and methods: We expanded the algorithm proposed in [3]. Specifically, we separated the gas carrier (mixed with hydrogen) from pure hydrogen, to explore the hydrogen carrier in greater depth. Moreover, we added lower-level controllers to the optimization procedure. These controllers aim to follow the setpoints defined by the high-level planning while simultaneously compensating for disturbances based on the specific realization of random variables, such as loads and generation.

Results: The algorithm has been implemented using Julia [4]. The sample time is 1 h and the prediction horizon of the optimization procedure is one week. The tests were conducted using data on electrical, thermal, and gas demand from an industrial facility operating continuously, which utilizes the systems within the EH to meet its demand in a self-consumption framework. The battery energy storage and the thermal energy storage adapt to the operation of the renewable energy systems within the EH. Consequently, the optimization algorithm effectively maximizes the use of renewable resources by storing excess energy during periods of high production and utilizing it when solar energy availability is low. The hydrogen storage charges gas until reaching a peak around the middle of the week, after which it begins to discharge gas to make it available to the system. This suggests that the hydrogen storage system is effectively utilized to support the storage of excess electricity generated from renewable sources. Moreover, the energy fluxes are exchanged between the EHs to minimize transmission costs. This suggests an efficient energy exchange between the EHs. Finally, the lower lever controllers were tested considering fluctuations in renewable energy generation and in consumption, highlighting a good level of adaptation of the system.

Conclusions: We have developed an optimization algorithm for a multi-carrier energy system composed of interconnected EHs linked by the electrical carrier, the thermal carrier, and the gas carrier. The optimization algorithm aims to minimize the system's operational costs while always ensuring compliance with operational constraints. The results indicate efficient energy management of storage units, while ensuring efficient energy exchange between the EHs, with a good level of flexibility in fluctuations of demand and renewable generation.

Acknowledgment: This research was funded by the European Union – NextGeneration EU from the Italian Ministry of Environment and Energy Security POR H2 AdP MMES/ENEA with involvement of CNR and RSE, PNRR - Mission 2, Component 2, Investment 3.5 Ricerca e sviluppo sull'idrogeno.

References

[1] L. Li, X. Wang, Y. Han, Q. Li, S. Huo, and W. Chen, "Long-term optimization for multi-energy system of net-zero energy residential area with seasonal hydrogen storage," in 2023 10th International Conference on Power and Energy Systems Engineering (CPESE), 2023, pp. 395– 400, doi: 10.1109/CPESE59 653.2023.10 303 194.

[2] M. B. Abdelghany, V. Mariani, D. Liuzza, and L. Glielmo, "Hierarchical model predictive control for islanded and grid-connected microgrids with wind generation and hydrogen energy storage systems," International Journal of Hydrogen Energy, vol. 51, pp. 595–610, 2024, doi: 10.1016/j.ijhydene.2023.08.056.

[3] S. A. Cordieri and F. Simmini, "An Optimization Strategy for Energy Management of Multi- Carrier Energy Systems," 2024 IEEE International Humanitarian Technologies Conference (IHTC), Bari, Italy, 2024, pp. 1-7, doi: 10.1109/IHTC61819.2024.10855154.

[4] J. Bezanson, A. Edelman, S. Karpinski, and V. B. Shah, "Julia: A fresh approach to numerical computing," SIAM Review, vol. 59, no. 1, pp. 65–98, 2017, doi:10.1137/141000671.

EFCH2 2025

European Fuel Cells and Hydrogen

PIERO LUNGHI CONFERENCE

Capri, Gran Hotel Quisisana
17 > 19 September, 2025

ATENA FUTURE TECHNOLOGY

ENEA Italian National Agency for New Technologies, Energy and Sustainable Economic Development

Università degli Studi di Napoli Parthenope

CLEAN ENERGY INSTITUTE UNIVERSITY OF CALIFORNIA, IRVINE